THE SAN FERNANDO, CALIFORNIA, EARTHQUAKE OF FEBRUARY 9, 1971:

A preliminary report published jointly by the U.S. Geological Survey and the National Oceanic and Atmospheric Administration

U.S. DEPARTMENT OF THE INTERIOR U.S. DEPARTMENT OF COMMERCE

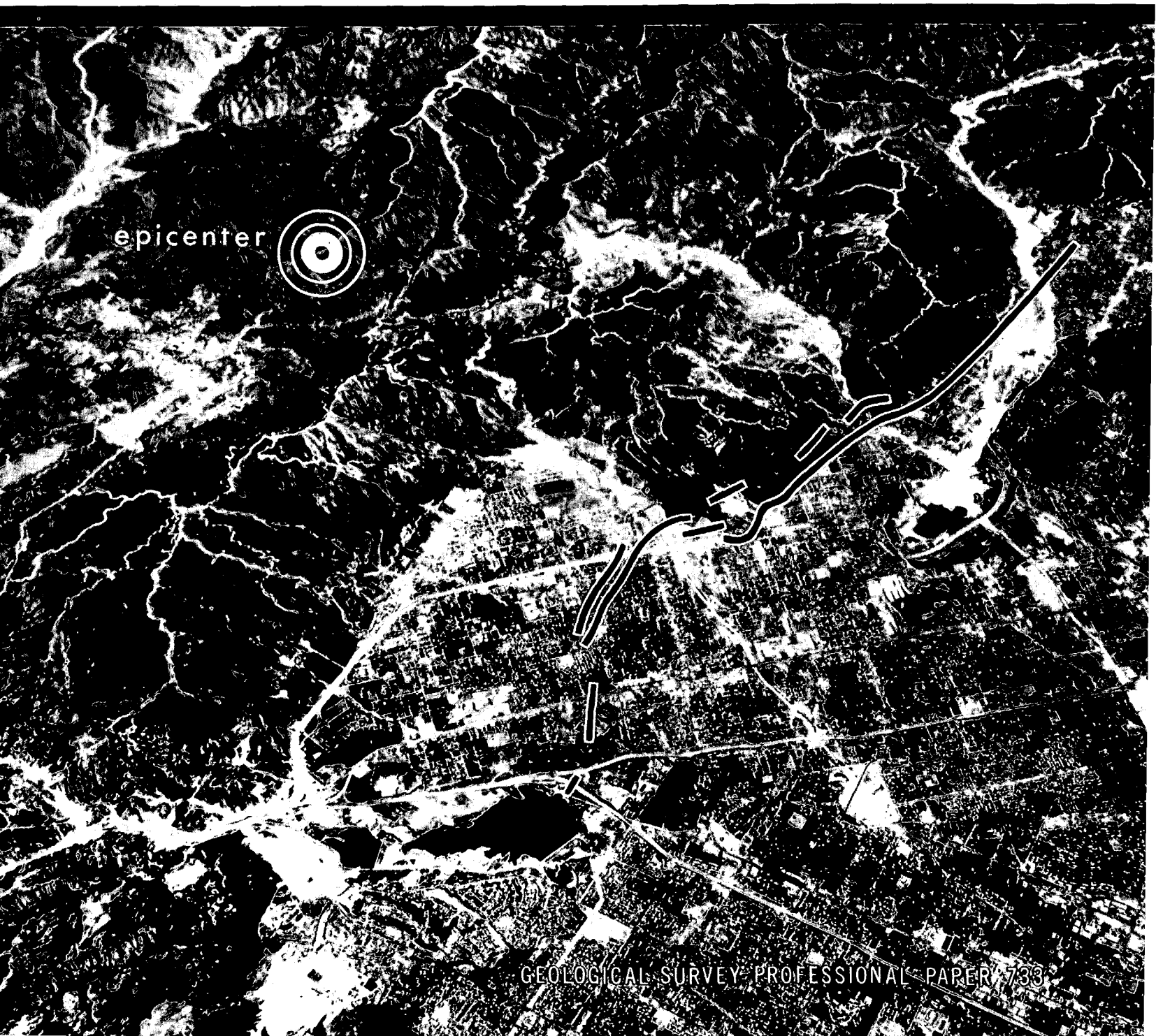

GEOLOGICAL SURVEY PROFESSIONAL PAPER 733

THE SAN FERNANDO, CALIFORNIA, EARTHQUAKE OF FEBRUARY 9, 1971:

A preliminary report published jointly by the U.S. Geological Survey and the National Oceanic and Atmospheric Administration

---

GEOLOGICAL SURVEY PROFESSIONAL PAPER 733

Contributions from:

California Division of Mines and Geology
California Division of Oil and Gas
California Institute of Technology
Earthquake Engineering Research Institute
H. J. Degenkolb and Associates, Engineers
Lamont-Doherty Geological Observatory of Columbia University
U.S. Department of Commerce, National Oceanic and Atmospheric Administration
U.S. Department of the Interior, Geological Survey

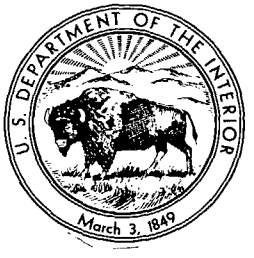

UNITED STATES GOVERNMENT PRINTING OFFICE, WASHINGTON: 1971

UNITED STATES DEPARTMENT OF THE INTERIOR
ROGERS C. B. MORTON, *Secretary*
GEOLOGICAL SURVEY
William T. Pecora, Director

UNITED STATES DEPARTMENT OF COMMERCE
MAURICE H. STANS, *Secretary*
NATIONAL OCEANIC AND ATMOSPHERIC ADMINISTRATION
Robert M. White, *Administrator*

For sale by the Superintendent of Documents, U.S. Government Printing Office
Washington, D.C. 20402 - Price $2.25 (paper cover)

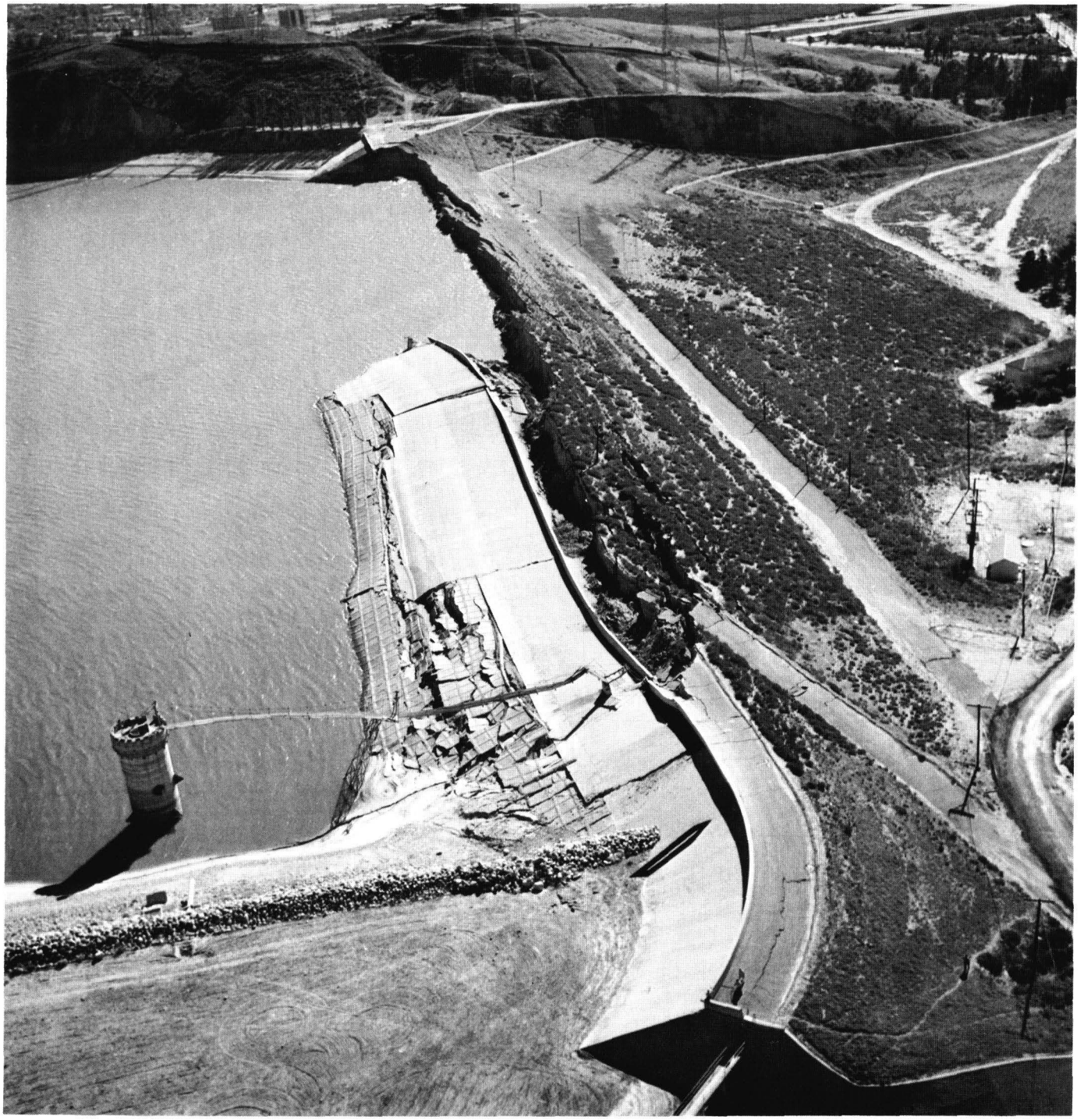

Lower Van Norman Dam in the Mission Hills, overlooking the heavily populated San Fernando Valley, was severely damaged and on the brink of catastrophic failure as a result of the San Fernando earthquake of February 9, 1971.

THE SAN FERNANDO, CALIFORNIA, EARTHQUAKE FEBRUARY 9, 1971

CONTENTS

	Page
Introduction, by Arthur Grantz, U.S. Geological Survey	1
An estimate of the damage, by Reuben Kachadoorian, U.S. Geological Survey	5
Geologic setting and activity of faults in the San Fernando area, California, by Carl M. Wentworth and R. F. Yerkes, U.S. Geological Survey	6
Main shock and larger aftershocks of the San Fernando earthquake, February 9 through March 1, 1971, by C. R. Allen, G. R. Engen, T. C. Hanks, J. M. Nordquist, and W. R. Thatcher, Seismological Laboratory, California Institute of Technology	17
Precise locations of aftershocks of the San Fernando earthquake 2300 (GMT) February 10—1700 February 11, 1971, by Thomas C. Hanks, Thomas H. Jordan, and J. Bernard Minster, Seismological Laboratory, California Institute of Technology	21
Aftershocks of the earthquake, by R. L. Wesson, W. H. K. Lee, and J. F. Gibbs, U.S. Geological Survey	24
Fault-plane solutions of the February 9, 1971, San Fernando earthquake and some aftershocks, by James H. Whitcomb, Seismological Laboratory, California Institute of Technology	30
Microearthquakes on the San Andreas fault and aftershocks of the San Fernando earthquake, by Christopher H. Scholz, Lamont-Doherty Geological Observatory of Columbia University	33
Preliminary source parameter determination of the San Fernando earthquake, by Max Wyss, Lamont-Doherty Geological Observatory of Columbia University	38
Pattern of faulting and nature of fault movement in the San Fernando earthquake, by Barclay Kamb, L. T. Silver, M. J. Abrams, B. A. Carter, T. H. Jordan, and J. B. Minster, Division of Geological and Planetary Sciences, California Institute of Technology	41
Surface faulting, by U.S. Geological Survey staff	55
Strains and tilts associated with the San Fernando earthquake, by Pierre Jungels and Don L. Anderson, Seismological Laboratory, California Institute of Technology	77
Preliminary measurements of tectonic movement, by R. O. Burford, R. O. Castle, J. P. Church, W. T. Kinoshita, S. H. Kirby, R. T. Ruthven, and J. C. Savage, U.S. Geological Survey	80
Repeated surveys of small scale figures established across surface fault ruptures following the earthquake, by John C. Lahr and Max Wyss, Lamont-Doherty Geological Observatory of Columbia University, and James A. Hileman, Seismological Laboratory, California Institute of Technology	86
Instrumental monitoring of post-earthquake fault movements (afterslip), by Robert D. Nason, Earthquake Mechanism Laboratory, National Oceanic and Atmospheric Administration	89
Preliminary results from recording aftershock ground motion on alluvial deposits, by Richard E. Warrick and William B. Joyner, U.S. Geological Survey	91
Shattered earth at Wallaby Street, Sylmar, by Robert D. Nason, Earthquake Mechanism Laboratory, National Oceanic and Atmospheric Administration	97
Seismically triggered landslides in the area above the San Fernando Valley, by Douglas M. Morton, California Division of Mines and Geology	99
Landsliding in the vicinity of the Van Norman Lakes, by T. L. Youd, U.S. Geological Survey	105
Ground failure on the San Fernando surface away from obviously tectonic rupture zones, by Robert V. Sharp, U.S. Geological Survey	110
Methane seep off Malibu Point following the San Fernando earthquake, by H. Edward Clifton, H. Gary Greene, George W. Moore, and R. Lawrence Phillips, U.S. Geological Survey	112
Oil and gas seepages and damage to oil field facilities related to the earthquake, by California Division of Oil and Gas	117
Water-resources aspects, by A. O.Waananen and W. R. Moyle, Jr., U.S. Geological Survey	119
Damage to constructed works associated with soil movements and foundation failures, by T. L. Youd and H. W. Olsen, U.S. Geological Survey	126
Preliminary structural lessons from the earthquake, by Henry J. Degenkolb, H. J. Degenkolb and Associates, Engineers	133

Page

THE FOLLOWING TECHNICAL REPORTS ARE FROM THE NATIONAL OCEANIC AND ATMOSPHERIC ADMINISTRATION, EARTHQUAKE ENGINEERING RESEARCH INSTITUTE

A preliminary report of near-field seismic monitoring of the San Fernando earthquake aftershock series, by A. F. Espinosa, E. R. Engdahl, A. C. Tarr, and S. Brockman, National Ocean Survey, National Oceanic and Atmospheric Administration ---- 135
Preliminary fault-plane solution for the San Fernando earthquake, by W. Dillinger and A. F. Espinosa, National Ocean Survey, National Oceanic and Atmospheric Administration ---- 142
Some observations of the San Fernando, California, earthquake with a laser strain meter, by Jon Berger, Institute of Geophysics and Planetary Physics, University of California, San Diego ---- 150
Preliminary report on felt area and intensity, by Nina H. Scott, National Ocean Survey, National Oceanic and Atmospheric Administration ---- 153
Ground motion amplification and vibration measurements, by Kenneth King, National Ocean Survey, National Oceanic and Atmospheric Administration ---- 155
Magnetic field survey of the San Fernando earthquake epicentral area, by J. E. O'Donnell and H. E. Kaufman, National Ocean Survey, National Oceanic and Atmospheric Administration ---- 157
Crustal-movement surveys and preearthquake strain analysis, by C. A. Whitten, National Ocean Survey, National Oceanic and Atmospheric Administration ---- 161
Preliminary strong-motion results from the San Fernando earthquake of February 9, 1971, by R. P. Maley and W. K. Cloud, National Ocean Survey, National Oceanic and Atmospheric Administration ---- 163
Evidence of record vertical accelerations at Kagel Canyon during the earthquake, by B. J. Morrill, National Ocean Survey, National Oceanic and Atmospheric Administration ---- 177
Introduction to the engineering study, by the Earthquake Engineering Research Institute Committee ---- 182
Soils and foundations, by L. LeRoy Crandall, L. LeRoy Crandall and Associates ---- 186
Damage to the Olive View Hospital buildings, by the Earthquake Engineering Research Institute Committee ---- 188
Damage to the Los Angeles County Juvenile Facilities, Sylmar, by James H. Thompson, Wilson and Thompson, Consulting Structural Engineers ---- 191
Damage to the Pacoima Memorial Lutheran Hospital, by William F. Ropp, Daniel, Mann, Johnson, and Mendenhall, Architects and Engineers ---- 193
Damage to the Holy Cross Hospital, by S. B. Barnes, S. B. Barnes and Associates ---- 195
Damage to the Indian Hills Medical Building, by James H. Thompson, Wilson and Thompson, Consulting Structural Engineers, and James J. Kesler, Karotis and Kesler ---- 198
Damage to the Union Bank building, by Paul Greenfield, Erkel-Greenfield and Associates ---- 200
Damage to the San Fernando Industrial Tract, by Earthquake Engineering Research Institute Committee ---- 201
Damage to the Sylmar Industrial Tract, by Earthquake Engineering Research Institute Committee ---- 203
Damage to a market, Glenoaks and Hubbard, San Fernando, by Walter Dickey, Consulting Structural Engineer ---- 204
Damage to a market, 13570 Eldridge, Los Angeles, by Earthquake Engineering Research Institute Committee ---- 206
Damage to two store buildings in the North Oaks Shopping Center, and one building in the Valencia Shopping Center, by James J. Kesler, Karotis and Kesler ---- 207
Damage to public school buildings, by J. F. Meehan, California Office of Architecture and Construction ---- 209
Damage to other buildings, by Walter Brugger, Research Engineer, Los Angeles City Division of Buildings and Safety ---- 213
Damage to building equipment and contents, by J. Marx Ayres, Ayres, Cohen, and Hayakawa ---- 220
Damage to water supply systems, by C. Martin Duke, University of California at Los Angeles ---- 225
Damage to transportation systems, by J. F. Meehan, California Office of Architecture and Construction ---- 241
Damage to energy and communications systems, by D. F. Moran, Consulting Structural Engineer ---- 245
Sociological aspects of the earthquake, by Earthquake Engineering Research Institute Committee ---- 251
Preliminary conclusions and recommendations based on engineering studies, by Earthquake Engineering Research Institute Committee ---- 253
Cooperating organizations ---- 254

THE SAN FERNANDO, CALIFORNIA, EARTHQUAKE OF FEBRUARY 9, 1971

INTRODUCTION

By ARTHUR GRANTZ
U.S. GEOLOGICAL SURVEY

The violent tremors that shook the San Fernando area (see fig. 1) at about 6 o'clock on the morning of February 9, 1971, are a painful reminder that earthquakes and the violent distortions and displacements of the earth's surface which commonly accompany them are a natural and permanent part of the environment in sizeable areas of the United States. The tremors also warn us that we must improve our ability to recognize those places where such potentially destructive distortions and displacements are likely to occur before we plan new cities or design buildings and structures in these areas. They also warn us that we must reexamine the criteria by which we judge the safety of older buildings and structures and the design of some types of new buildings and structures in the earthquake-prone regions. The reminder, however, cost 64 people their lives and created physical losses estimated at more than one-half billion dollars. The total loss may approach $1 billion when all the direct and indirect costs are tallied. If the earthquake had struck during the working day, when public buildings, businesses, and highways are crowded, the loss of life and the incidence of major injuries would have been greater. Had the Lower Van Norman Lake Dam, which was close to collapse when the earthquake ended, actually failed, the San Fernando earthquake might have become infamous as the deadliest in United States history.

It must be emphasized that the toll at and near San Fernando was exacted by an earthquake of only moderate size—as judged by its rating of 6.6 on the Richter magnitude scale. By comparison, the great San Francisco earthquake of 1906, which has been assigned a Richter magnitude of 8.3, radiated perhaps a few hundred times more energy and inflicted severe damage over a much greater area. If an earthquake like that of 1906 were to strike in or near one of coastal California's major population centers it is likely that the casualties and physical loss suffered at San Fernando would be exceeded manyfold.

On the other side of the ledger, many earth scientists and engineers are now convinced that the body of knowledge concerning earthquakes and their effects is at last sufficiently large and sophisticated that we can learn from this earthquake some important and very practical lessons by which we can alleviate and perhaps even forestall the damage that some types of earthquake will inevitably threaten. To this end, an impressive number of researchers and practitioners in the earth and engineering sciences immediately turned their attention to the San Fernando earthquake and its geologic, seismologic, and engineering effects.

A prompt response to the earthquake was critical, for both the public officials and the private persons who had to cope with the destruction had a great and immediate need for reliable information about the earthquake and its effects. In addition, past experience had shown that (1) monitoring of aftershocks and continuing distortions of the earth's surface must begin promptly because these phenomena die out quickly, (2) the field evidence from which the nature of earthquakes and their damaging geologic effects must be deduced is rap-

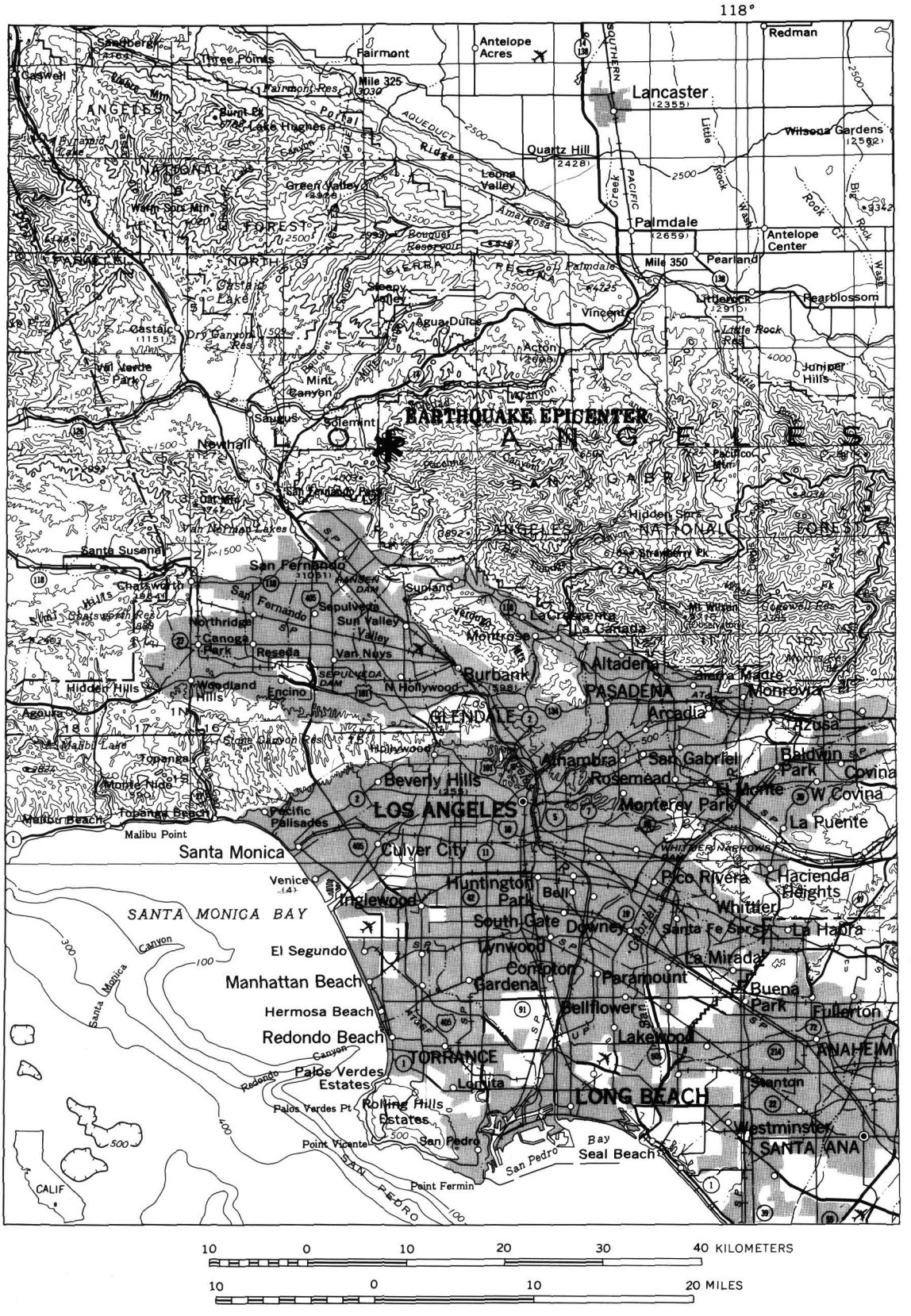

FIGURE 1.—Index map showing earthquake epicenter.

idly destroyed by even emergency repairs or heavy precipitation, and (3) hazardous geologic and engineering situations must be quickly identified and brought to the attention of public and private officials. Thus, although the San Fernando earthquake occurred at 6:00 a.m. local time, investigators from throughout California were in the stricken areas the same morning, and by the next day dozens of investigators were analyzing the engineering failures and were mapping and describing the surface fault ruptures, vertical and horizontal shifts in the land surface, landslides, and soil and foundation failures that caused much of the damage at San Fernando. Dozens of sensitive instruments were installed promptly to study the aftershocks and their effects on various kinds of geologic foundation materials and to monitor postearthquake fault movements and continuing distortions of the land surface. Fortunately for seismologists the epicenter fell within the permanent seismograph network of the Seismological Laboratory of the California Institute of Technology, and the character and location of the main shock and also of the early aftershocks were well determined even before the California Institute of Technology net was supplemented by the emplacement of portable seismometers from other institutions.

Damage in the San Fernando and Sylmar areas of Los Angeles County was severe because the epicenter lay only about 14 km (9 miles) north of the center of San Fernando and because the fault which broke to produce the earthquake was a thrust that extended beneath these communities from the epicenter and intersected and ruptured the surface of the ground in heavily built-up areas within them. Earthquakes have been associated with thrust faults before in California but not as commonly as with strike-slip faults of the San Andreas type. Accordingly, comparative studies of the seismic and geologic character, secondary geologic effects, and patterns of damage produced by these two types of earthquakes will receive careful attention. Examples of such comparisons are the relative widths of the zones of broken ground along the two types of fault ruptures and the relation of Richter magnitude and modified Mercalli intensity for the two types of earthquakes.

Relative uplift and warping of the land surface above the wedge of rocks overlying the northward-dipping thrust fault was a prominent feature of this earthquake, and one which the geologic record testifies has occurred repeatedly in the past. This indicates clearly that the San Fernando earthquake is not an isolated "freak" event, but one which we must presume will recur in the future. It is accordingly important that the recurrence interval and any relationship that may exist between the patterns of uplift and the patterns of damage will, it is hoped, be important aspects of the continuing studies of the earthquake.

The question of whether or not the location of the ruptures produced by the thrust fault zone where it emerged at the surface could have been predicted receives considerable attention in this report. Clearly, much of the damage could have been prevented had these zones been delineated, and zoned for open space or parks, before the San Fernando-Sylmar area was urbanized. It is encouraging for the future that many investigators feel confident that, armed with the knowledge gained at San Fernando, they can identify and delineate other similarly active thrust faults in this region and elsewhere in the Western United States.

Probably the most significant and certainly the most surprising body of data recorded during the earthquake is a unique collection of strong-motion accelerograms reported by Maley and Cloud in this report. These writers report that the ground accelerations produced by this moderate magnitude (6.6) earthquake ". . . were the highest ever recorded, that is, in the 0.5- to 0.75-g range with several high-frequency peaks to 1 g." These records will surely lead to a careful reassessment of earthquake-resistant design criteria because they indicate ground accelerations several times greater than those commonly assumed in building criteria for seismic regions. They will also provoke intensive study of the relation of these surprisingly high accelerations to local geologic or topographic conditions at the recording sites as well as to the characteristics of the earthquake and its associated thrust faulting.

The field and laboratory investigations of the earthquake were characterized, and materially aided from the very beginning, by unusually free interchange of information among the participating scientists and engineers. As a result, a preliminary understanding of the earthquake and its geologic and engineering consequences evolved and could be disseminated very quickly. This interchange was particularly gratifying to the participating investigators because it was apparent that a truly full and useful understanding of either the scientific or the engineering implications of the earthquake and its effects will require the integration of insights from many disciplines.

The present report is a preliminary evaluation of

data gathered by many groups of investigators during the first 3 weeks after the earthquake. A list of cooperating organizations is given at the end of the report. Though many of the papers are written for the specialist, most will be very useful to the general reader and to public officials wanting to learn about the earthquake and its effects. The report is published jointly by the Geological Survey of the U.S. Department of the Interior and the National Oceanic and Atmospheric Agency of the U.S. Department of Commerce in the conviction that early publication of these necessarily preliminary results will meet the following important and immediate needs:

—It will provide early geologic and engineer-guidance to private citizens and public officials engaged in reconstructing the damaged areas.

—It will alert private citizens and public officials to possibly dangerous geologic and engineering situations, such as landslide hazards, that were created by the earthquake.

—It will foster the early exchange of preliminary data and ideas among the many investigators studying the earthquake, particularly between workers in different disciplines and between scientists and engineers, to the end that knowledge of the utmost possible practical value to society will result.

—It will help to disseminate the preliminary results of the earthquake investigations and provide information on investigations in progress to the scientific and engineering communities. This should encourage the participation of additional investigators who might improve our understanding of the earthquake and its effects, and who might suggest additional measures that could be taken to reduce the risk posed by future earthquakes.

—It will inform the public about an event that directly affected hundreds of thousands of people and could be a preview of future events affecting millions.

—It will focus the attention of public officials and planners, while the memory of the earthquake is still fresh, on the multiplicity of ways in which earthquakes can destroy man's works and on some of the measures by which the hazards from future earthquakes might be reduced.

Rapid publication of preliminary results, while it meets many immediate needs, also inevitably results in some duplication, some lapses in data, and even a measure of disagreement among the various contributing investigators. Indeed, this report will serve to alert the participating investigators and others to the existence of these gaps and disagreements at an earlier stage than is usually possible, and we suspect that the final body of knowledge concerning the earthquake will be expedited and greatly improved thereby. Most of the investigations reported in preliminary form in this report are continuing, and most of the present papers will be followed by more complete accounts in the months and years ahead.

Readers of this report will find the following U.S. Geological Survey 7½′ topographic quadrangle maps useful for geographic details of the San Fernando area: Oat Mountain, San Fernando, and Sunland, Calif.

Published geologic source maps include the following—others are indicated in the reference citations:

California Division of Mines and Geology, 1969, Geologic map of California, Los Angeles sheet: scale 1 : 250,000.

Oakeshott, G. B., 1958, Geology and mineral deposits of San Fernando quadrangle, Los Angeles County, California: Calif. Div. Mines and Geology Bull. 172.

It would have been desirable to have used a single system of measurement units throughout this report, preferably metric. However, in the interest of timely publication of this report, conversion to a single system was impractical, especially as considerable redrafting of the illustrations would have been involved. To assist in making comparisons, the following table of equivalent metric and English units of length is provided:

1 millimeter (mm)	= 0.039 inch
1 centimeter (cm)	= 0.39 inch
1 meter (m)	= 3.28 feet
1 kilometer (km)	= 0.62 miles
1 inch	= 25.4 mm or 2.54 cm
1 foot	= 0.305 m
1 mile	= 1.609 km

AN ESTIMATE OF THE DAMAGE

By REUBEN KACHADOORIAN
U.S. GEOLOGICAL SURVEY

The San Fernando earthquake of February 9, 1971 lasted about 60 seconds. Within this brief span of time 64 persons lost their lives, and the Los Angeles area suffered damage estimated at $553 million (table 1). This estimate does not include the cost of emergency services, loss of employment, and loss of revenue from taxes and change in the tax base. The impact of the earthquake upon the economy of the Los Angeles area may reach three-quarters of a billion dollars when the damage analysis is completed and all factors are taken into consideration. The private sector suffered $253 million of the $553 million; the remaining $300 million damage was to publicly owned structures.

TABLE 1.—*Estimate of damage*

[Data supplied by the city of Los Angeles, city of San Fernando, county of Los Angeles, Los Angeles Unified School District, Corps of Engineers, Los Angeles Flood Control System, State of California, and region 7 of the Office of Emergency Preparedness]

Structure	Number damaged	Amount
Schools	180	$22,500,000
Hospitals	4	50,000,000
Residential:		
Homes	21,761	
Apartment houses	102	
Mobile homes	1,707	179,500,000
Commercial buildings	542	
Miscellaneous structures	250	
Highways and roads		27,500,000
Dams		36,500,000
Other public structures		145,000,000
Utilities		42,000,000
Personal property		50,000,000
Total		553,000,000

A total of 180 schools were damaged; of these, 35 received major structural damage and 18 had to be vacated. In the Los Angeles Unified School District, which includes the schools in the city of San Fernando, 131 of 617 schools received minor to major damage. The remaining 49 schools were not in the Los Angeles Unified School District. These schools received more than $1,000 damage each and were as far away as Whittier, about 40 miles southeast of San Fernando.

Two hospitals, the $34 million Olive View, only recently constructed, and the $15 million Veterans, sustained major damage and partial collapse. Reportedly, both facilities will have to be replaced. The Veterans Hospital was constructed during the 1920's prior to the establishment of earthquake codes in the State of California.

A total of 21,761 single family dwellings were damaged. Of these, 465 were declared unsafe. In addition, there were 62 apartment houses and 372 commercial structures so severely damaged that they were also declared unsafe.

Damage to highways and roads consisted of $22.5 million to the State Freeway system and $5 million to city and county roads. The chief damage to the freeway was the collapse of five overpasses and damage to an additional seven.

Five dams were damaged—the Upper and Lower Van Norman Dams, Pacoima Dam, Lopez Dam, and Hansen Dam. The Lower Van Norman Dam was damaged so severely that the estimated cost of replacement is $34 million. The gravity-arch Pacoima Dam suffered about $1.5 million damage at its abutments. Minor damage occurred at Lopez and Hansen Dams.

Public structures damaged, exclusive of dams, highways, and hospitals, include those owned by the city of Los Angeles, city of San Fernando, county of Los Angeles, State of California, and the Federal Government. About $73 million damage was done to structures owned by the city of Los Angeles.

Damage to utilities included $14 million to water, sewer, electrical and telephone facilities, and $28 million to the Sylmar electrical converter station.

GEOLOGIC SETTING AND ACTIVITY OF FAULTS IN THE SAN FERNANDO AREA, CALIFORNIA

By CARL M. WENTWORTH and R. F. YERKES
U.S. GEOLOGICAL SURVEY

With a section on

SEISMOLOGICAL ENVIRONMENT

By CLARENCE R. ALLEN
SEISMOLOGICAL LABORATORY, CALIFORNIA INSTITUTE OF TECHNOLOGY

The faulting associated with the San Fernando earthquake of February 9, 1971, occurred in the Transverse Ranges structural province, a region noted for its strong and relatively young tectonic deformation. This is, however, the first example of historic surface faulting within the interior of that province.

The Transverse Ranges structural province trends eastward across southern California (across the center of fig. 1) and constitutes a region of late Cenozoic north-south shortening that lies athwart the northwesterly regional trend of the dominant San Andreas fault system. In the past 30 million years the San Andreas fault, master fault of the system, has undergone about 200 km of right-lateral strike slip in southern California (Crowell, 1962). During historic time, surface faulting in southern California has largely been confined to this and related right-lateral strike slip faults in the San Andreas system. Notable exceptions are the historic ruptures of the east- and northeast-trending White Wolf and possibly Big Pine faults, and now the 1971 San Fernando faulting, all of which have displayed at least some component of left-lateral strike slip (fig. 1).

The Transverse Ranges province consists of numerous east-trending mountain ranges and valleys typified by late Cenozoic structural deformation and strike slip, reverse, and thrust faults of similar trend (Bailey and Jahns, 1954; Jennings and Strand, 1969). The most spectacular development of the structure of this province is in the Ventura Basin, where an immense Cenozoic syncline that includes a thickness of 1,500 m of marine Pleistocene sediments has both limbs overturned and overridden by thrusts (Bailey and Jahns, 1954, p. 92–96). Very young deformation in the Transverse Ranges is not restricted to the Ventura Basin, however, and late Quaternary faulting is known to occur from near Point Conception eastward to the San Andreas fault.

The February 9, 1971, faulting broke the ground surface near the north margin of the San Fernando Valley opposite the "great bend" in the San Andreas fault south of the San Joaquin Valley (fig. 1). The geometry of the crustal blocks in this region is such that the Transverse Ranges structural block southwest of the San Andreas fault is constrained and compressed against the bend as the block moves northwestward along the fault. During the past 5 to 10 million years' this compressive deformation has thrust the mountain blocks up over adjacent valleys to the south. The movement has occurred along north-dipping reverse or thrust-fault systems such as the Sierra Madre and Santa Susana, which trend west and northwest along the southern margins of the mountain blocks. The most impressive product of this uplift is the bold southern front of the San Gabriel Mountains, which stands some 1,500 m above the San Fernando and Los Angeles areas to the south. Additional horizontal shortening and uplift of one of the blocks occurred along the ruptures that accompanied the San Fernando earthquake.

Although segments of the surface traces of many of the Transverse Ranges faults have been mapped and interpreted in the context of regional structural history, the abundant but relatively unobtrusive evi-

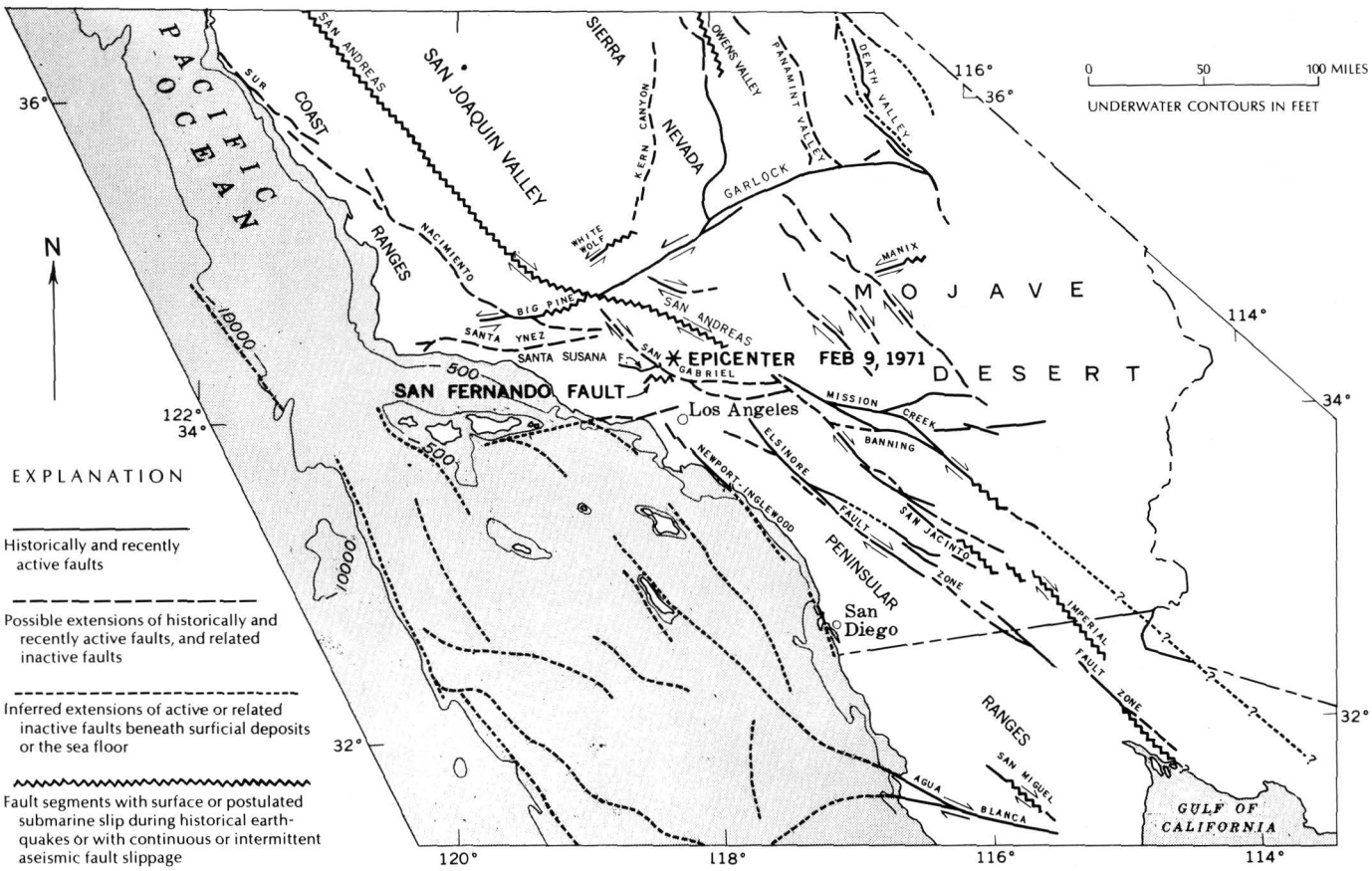

MAJOR HISTORICALLY AND RECENTLY ACTIVE FAULTS OF THE SOUTHERN CALIFORNIA REGION

FIGURE 1.—Major historically and recently active faults of the southern California region.

dence of their recent geologic activity has not been widely recognized or appreciated. Study of the 1971 San Fernando faulting should reinforce our confidence in using this geologic data to evaluate the future behavior of faults.

SEISMOLOGICAL ENVIRONMENT

In the years prior to 1971, the area of the San Fernando earthquake had been one of low to moderate seismic activity—not unlike that of many other parts of California. Indeed, the 1934–63 strain-release maps (Allen and others, 1965) indicated that the northern San Fernando Valley was seismically less active than most other parts of the greater Los Angeles area. Certainly there was nothing in the very recent seismic history to suggest that this area, more than any other area, was particularly likely to experience a magnitude 6.6 earthquake. It must be kept in mind, however, that an earthquake of at least this magnitude occurs somewhere in the southern California region on the average of about once every 4 years (Allen and others, 1965), and in this sense the earthquake itself was no great surprise. An earthquake of about this same magnitude occurred in 1968 in the Borrego Mountain area 220 km southeast of Los Angeles, but damage was small because—unlike the 1971 event—it occurred in a remote location.

Between 1934 and 1971, which is the interval during which epicentral locations of southern California earthquakes have been listed by the California Institute of Technology, only about 10 earthquakes of magnitude 3.0 and greater occurred within the area that corresponds to the epicentral region of the San Fernando earthquake. None of these was large, although a few were felt locally, such as the magnitude 4.0 shock of August 30, 1964, that was centered under southern San Fernando. Previous to 1934, two shocks are of special interest: the magnitude 5.2 earthquake of August 30, 1930, was probably much closer to San Fernando than the original assignment of the epicenter location in Santa Monica Bay suggests, and it is particularly noteworthy because it caused some minor damage to

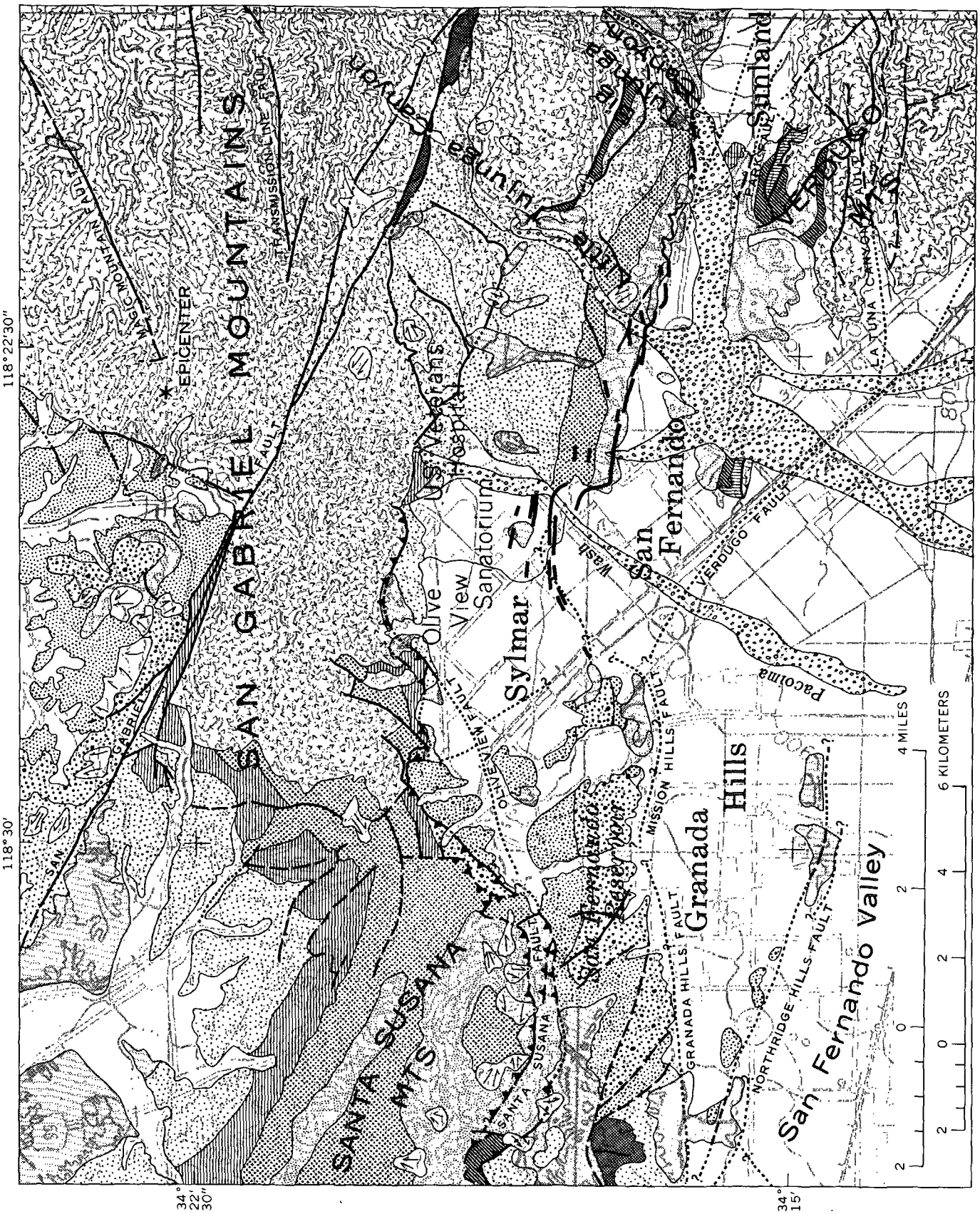
118°30'
118°22'30"
34°22'30"
34°15'
SAN GABRIEL MOUNTAINS
SANTA SUSANA MTS.
EPICENTER
SAN GABRIEL FAULT
MALIBU MOUNTAIN FAULT
TRANSMISSION LINE FAULT
Tujunga Canyon
Tujunga Valley
Olive View
Veterans Hospital
Sylmar
San Fernando
Wash
OLIVE VIEW FAULT
SANTA SUSANA FAULT
San Fernando
MISSION HILLS FAULT
GRANADA HILLS FAULT
Granada Hills
NORTHRIDGE HILLS FAULT
San Fernando Valley
VERDUGO FAULT
Pacoima
Simland
VERDUGO
LA TUNA CANYON FAULT
LA TUNA CANYON
4 MILES
6 KILOMETERS

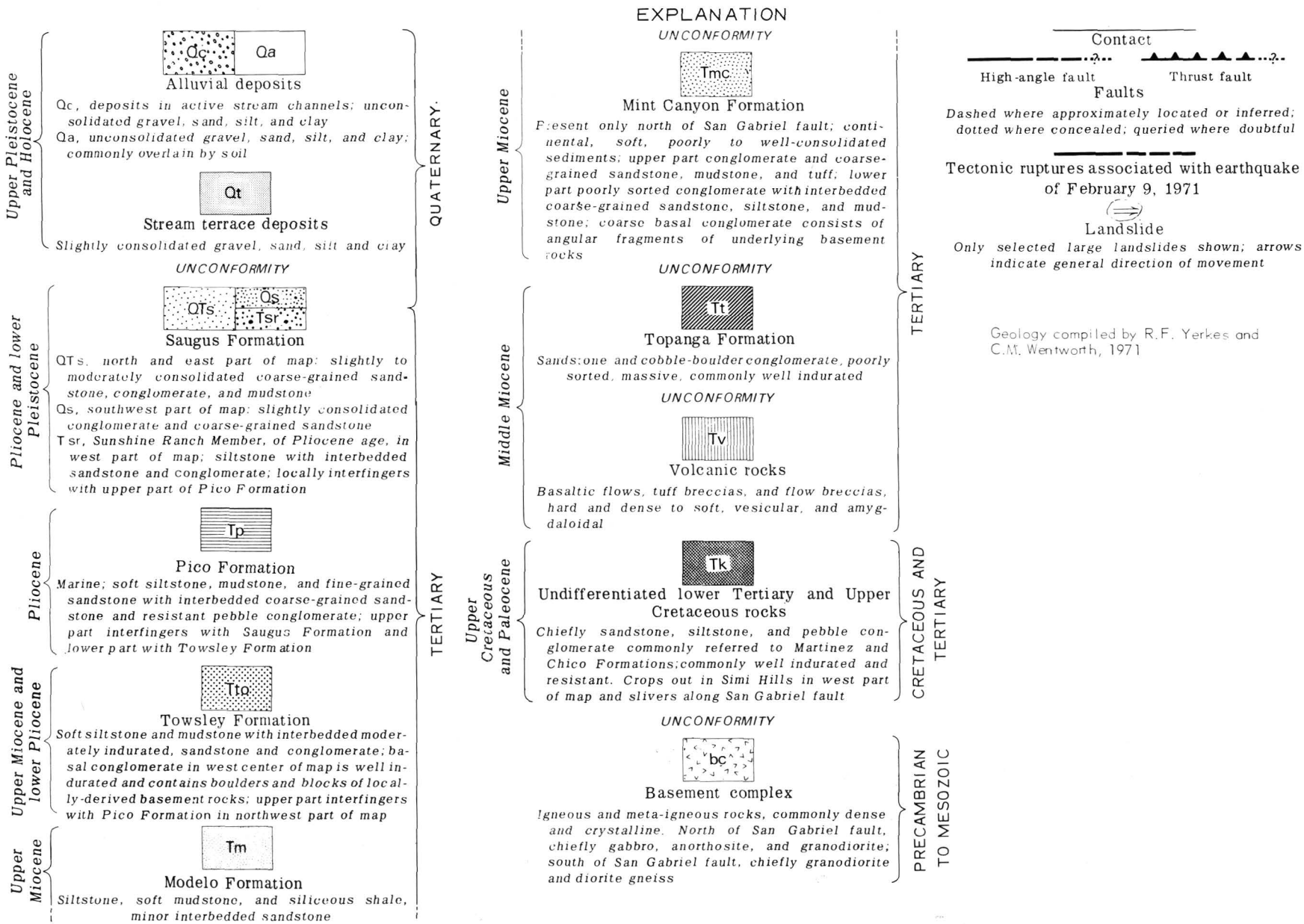

FIGURE 2.—Generalized geologic map of the San Fernando area, Los Angeles County, Calif. (Van Norman Lakes are called San Fernando Lakes on this map base.)

both Chatsworth Dam and Lower Van Norman Dam. Of much greater significance in terms of its similarity to the recent San Fernando earthquake is the so-called Pico Canyon earthquake of 1893; Pico Canyon is only 5 km west of Newhall, which was very heavily shaken by both the 1893 and the 1971 events. Townley and Allen's (1939) description suggests a magnitude of about 6, inasmuch as the shock was described as heavy in Mojave, Ventura, and San Bernardino, and was felt in San Diego. Numerous landslides and fissures were reported in the Newhall area, and aftershocks continued for some time. The contemporary report that "landslides from every peak in sight came tumbling down with huge boulders; the mountains appeared as if myriads of volcanoes had burst forth" might well have applied to the 1971 event in addition. It seems probable that the 1893 earthquake originated slightly west of the 1971 epicenter, but it certainly indicates that moderate earthquakes of this size are no stranger to the region.

STRATIGRAPHY

The San Fernando Valley is in the southeastern part of the Ventura Basin area, and its sedimentary rocks are similar to those described in the northwest by Winterer and Durham (1962). Oakeshott (1958) provides a description of the units at the north side of the valley, in the area of the main shock, aftershocks, and surface faulting that accompanied the earthquake.

In the central Transverse Ranges the crystalline basement rocks are overlain with great unconformity by Cretaceous and younger sedimentary rocks many thousands of meters thick. The San Fernando Valley itself (figs. 2, 3) is an asymmetric synclinorium developed chiefly in Miocene and younger rocks that have been deformed by late Cenozoic folding and faulting, especially at the northern margin by thrusting along the Santa Susana fault and its eastward equivalents. Based on a gravity-density model, Corbato (1963) estimates that approximately 4,500 m of sedimentary rocks are present in the central part of the valley.

None of the late Cenozoic sedimentary rocks are particularly hard, and the Saugus Formation especially is only partially indurated and difficult to distinguish from alluvium in drill holes.

Precambrian to Cretaceous crystalline rocks of the basement complex are exposed in the San Gabriel Mountains in the northeast part of the map area and in the Verdugo Mountains in the southeast corner. These dense metamorphic and igneous rocks

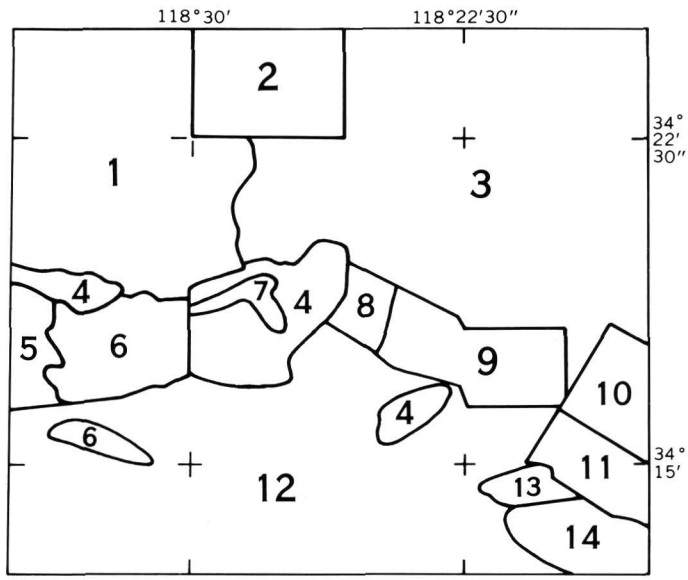

FIGURE 3.—Index to geologic map sources. 1, Winterer and Durham (1962); 2, R. B. Saul, 1970, California Division of Mines and Geology, work in progress; 3, Oakeshott (1958); 4, T. W. Dibblee, Jr., unpublished data; 5, Bishop (1950); 6, R. B. Saul, 1968, California Division of Mines and Geology, work in progress; 7, Merifield (1958); 8, Metropolitan Water District, 1968, unpublished geologic map L–1078; 9, Metropolitan Water District, 1968, unpublished geologic map B–20262; 10, Metropolitan Water District, 1968, unpublished geologic map L–1084; 11, Metropolitan Water District, 1968, unpublished geologic map L–1079; 12, R. F. Yerkes and C. W. Wentworth, generalized from California State Water Rights Board (1962), Corbato (1963), and Holmes (1919); 13, Johnston (1938); 14, C. W. Jennings and R. B. Saul, 1969, California Division of Mines and Geology, unpublished data. The unpublished maps of the Metropolitan Water District of Southern California are on file with the California Division of Mines and Geology.

constitute the terrane on which the sedimentary sequence was deposited. Cretaceous and lower Tertiary sedimentary strata are only exposed locally along the Santa Susana and San Gabriel faults, although to the west and south of figure 2 they crop out extensively. Within the map area south of the San Gabriel fault, the oldest sedimentary rocks overlying the basement are the middle Miocene Topanga Formation, which includes about 300 m of conglomerate, marine sandstone, and volcanic rocks.

As much as 1,500 m of marine upper Miocene Modelo Formation is exposed along the foothills of the San Gabriel and Verdugo Mountains, in the Mission Hills, and in the Santa Susana Mountains. The Modelo is overlain by, and locally interfingers with, the Towsley Formation of late Miocene–early Pliocene age. The Towsley ranges in thickness from zero where it is overlapped by the Pico Formation

just south of the San Gabriel fault zone to about 750 m in the east and west central parts of the map area.

The Pico grades upward and laterally into the late Pliocene–early Pleistocene Saugus Formation, a shallow marine to brackish-water unit that rims the north side of the San Fernando Valley. The Saugus Formation thickens westward from essentially zero at Big Tujunga Canyon to about 1,950 m at Lopez Canyon east of Pacoima Wash. An exploratory well drilled north of the Olive View fault and about 1½ km west of Olive View Sanitorium penetrated a minimum stratigraphic thickness of 1,200 m of Saugus Formation, and the California State Water Rights Board report (1962, v. I., p. 52) states that the formation exceeds 1,800 m in thickness in the syncline near Sylmar.

The "middle Pleistocene" Pacoima Formation of Oakeshott (1958) has been combined with the Saugus Formation on the map (fig. 2). This deformed fanglomerate-breccia unit is exposed north of Sylmar, where it unconformably overlies the Saugus and is unconformably truncated by stream-terrace and alluvial deposits.

Uplifted erosional remnants of stream-terrace gravel and sand are widely distributed in the San Fernando area, but only a few are shown on the generalized map. No direct evidence for the age of these deposits is available, although a late Pleistocene age is inferred on the basis of their stratigraphic position, lack of deformation, and unconformable relations with the underlying Saugus Formation. Oakeshott (1958) was able to distinguish five stages of terrace formation along Pacoima Wash and two in the Lopez-Kagel Canyon area 6½ km northeast of San Fernando. Some of the late Quaternary history of the mountain blocks can be obtained from such geomorphic features.

UNCONSOLIDATED SEDIMENTS

The relatively flat surface of San Fernando Valley is underlain by unconsolidated sand, gravel, and finer sediment ranging in thickness from zero at the valley edges to greater than 200 m in the east-central part of the valley near the south margin of figure 2. In the Sylmar area, alluvium is perhaps 6 m thick, except along Pacoima Wash (California State Water Rights Board, 1962).

Sediment west of Van Norman Lakes and along the southern part of the valley has been supplied by streams draining areas of sedimentary rocks, with the result that alluvium in these areas consists predominantly of clay. In contrast, larger streams at the north margin of the valley east of the Lakes drain crystalline rocks of high relief and have produced deposits of coarser materials with abundant gravel.

Additional information concerning the alluvial deposits in San Fernando Valley is available from California State Water Rights Board (1962): plate 6 (v. I) of that report shows contours on the base of the valley fill, or water-bearing sediments, and plate 30 shows ground-water contours as of 1958. The agricultural soil map of Holmes (1919) is also useful.

EVIDENCE FOR LATE QUATERNARY FAULTING

A number of faults in the San Fernando area follow prominent topographic breaks at the boundaries between the alluvial valleys and the adjacent hills and mountains. This relationship, combined with stratigraphic evidence, indicates that these faults were active in late Quaternary time and that they followed the general tectonic patterns established in late Tertiary time. The immediately available evidence concerning the late Quaternary history of these faults is cited in a following section on structure. This evidence is critical to the evaluation of possible future movements on these faults.

Unfortunately, the geologic record of the late Quaternary, which is the past few hundred thousand years of earth history, is incomplete and difficult to interpret. Few of the alluvial deposits that constitute the sole stratigraphic record of late Quaternary time in the San Fernando area are even approximately dated at present, and their stratigraphic relations are poorly known and difficult to decipher. Topographic features produced by faulting of the ground surface constitute the only other direct record of late Quaternary faulting but are often difficult to interpret. Most can form in more than one way, and their durability in various geologic and climatic situations, although relatively short in geologic time, is poorly understood.

Where late Quaternary faults are buried or obscured by alluvium, subsurface information is needed to evaluate their history. Particularly useful are data on the effects of such faults on the movement of ground water. These effects are essentially of two kinds: (1) clayey gouge seams can form along such faults, even in alluvium, and partly or completely block passage of water across them, or (2) faulting can also produce a step in the bedrock surface beneath the alluvium, which will impose a barrier to ground-water movements if the general direction of such movement is toward the upthrown block or the development of a ground-water cascade

if the direction is opposite. Although such steps could be formed by erosion or faulting prior to burial by alluvium, well-defined steps of significant length are more likely to form by postalluvium faulting. Erosion of a channel through a fault-gouge barrier could also result in the formation of a ground-water cascade. All hydrologic evidence cited in the following pages comes from a valuable study of ground water in the San Fernando Valley by the California State Water Rights Board (1962).

The age of the San Fernando Valley alluvium that is involved in faulting is unknown in detail. These deposits, however, are sufficiently young that it is prudent to consider any fault that has an observable effect on the movement of shallow ground water in the San Fernando Valley to have been active in late Quaternary time.

STRUCTURE

The structure of the San Fernando Valley area is dominated by two intersecting regional fault systems: the northwest-trending San Andreas system of right-lateral strike-slip faults, which includes the San Gabriel fault, and the east-trending system of north-dipping reverse and thrust faults along which much of the uplift of individual ranges has been accomplished. Among the latter are the Santa Susana–Sierra Madre trend and faults within the San Fernando Valley.

Although the older geologic history of the San Fernando Valley area is dominated by the San Gabriel fault zone, the present-day structure of the northern margin of the valley has been greatly modified by overthrusting on the north-dipping reverse faults. Uplift along these faults has created the large residual gravity gradients mapped by Corbato (1963, map 3) and are shown in figure 4 of this report. All of the foregoing fault trends exhibit evidence of late Quaternary displacement.

SAN GABRIEL FAULT

The San Gabriel fault resembles the San Andreas in many ways. It consists of a zone of imbricate steeply north-dipping faults and is characterized by deflected drainage courses, strike valleys, notched ridges, and largely dissimilar geology on opposite sides (Oakeshott, 1958).

The work of Crowell (1950, 1952, and 1962) indicates that the fault absorbed about 30 km of right strike slip and locally as much as 4.3 km of dip slip during Pliocene time. Oakeshott (1958) cites evidence for 2.5 to 6.5 km of right slip along the fault zone in late Pliocene-Quaternary time and shows the "middle Pleistocene" Pacoima Formation to be

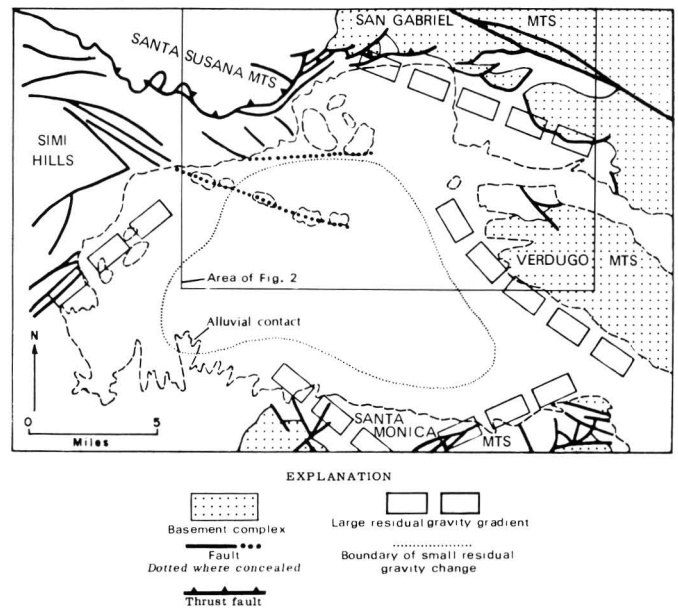

FIGURE 4.—Structure map of the San Fernando Valley area modified from Corbato (1963, fig. 7).

offset in an area northwest of figure 2. Late Quaternary stream-terrace deposits appear to be unaffected by the San Gabriel fault, although none lies completely across the fault zone. The displacement of Pleistocene deposits and deflected drainages along the fault warrant attention to the possibility of renewed movement along this fault.

SANTA SUSANA FAULT

The Santa Susana is a long east-trending fault zone characterized by low-angle thrusting, a sinuous trace, and a gentle north dip. Estimates of horizontal shortening and vertical separation across it range upward from 2.4 km (Hazzard, 1944; Oakeshott, 1958).

In the Santa Susana Mountains at the west side of figure 2, the fault consists of two parallel strands about 0.5 km apart. The northern strand is entirely within Tertiary rocks, whereas the southern strand forms a thrust contact on which Miocene strata on the north overrode Quaternary terrace deposits on the south (Bishop, 1950, p. 93–94).

More recent work east of Bishop's area by R. B. Saul (fig. 3) suggests that landsliding might account for some of Bishop's observations. In any case, late Quaternary faulting has occurred on the south face of the Santa Susana Mountains because the west-trending Devonshire fault of Bishop (1950) moved both during and after accumulation of the terrace deposits.

The two western traces of the Santa Susana fault

merge northwest of Sylmar and continue eastward to form a series of northeast-trending faults along which rocks of the basement complex have been thrust over sedimentary units as young as the Pliocene-Pleistocene Saugus Formation and the "middle Pleistocene" Pacoima Formation. The terrace deposits, however, do not appear to be affected (Oakeshott, 1958).

GRANADA HILLS-MISSION HILLS TREND

This trend of faults is a largely buried system of east-trending range-front faults along which the southeastern Santa Susana Mountains and the Mission Hills have been uplifted.

Existence of the Granada Hills fault is based on the straight south margin of the adjacent mountains, which suggests that the inferred fault had late Quaternary displacement.

The existence of the Mission Hills fault was postulated by Oakeshott (1958, p. 94, pls. 1 and 2) on the basis of topography, a geologic section in a test well, and analogy with faults in the mountains north of Sylmar.

The San Fernando fault zone, as used in this report, is defined as the zone of tectonic surface rupture of the 1971 San Fernando earthquake. It consists of the Mission Wells, Sylmar, and Tujunga fault segments and other scattered minor faults.

The Mission Wells and Sylmar segments extend generally eastward from the Granada Hills–Mission Hills trend and closely coincide with the surface trace of a known impediment to southward movement of ground water. This ground-water anomaly is shown in figure 2 as a northeast- and east-trending queried fault crossing the neck in the alluvial surface south of Sylmar. It is marked by a 15-m difference in ground-water levels, higher on the north, with ground-water cascades flowing southward through alluviated erosional notches at its east and west ends. Ground water north of the anomaly occurs in confined aquifers in steeply north-dipping Saugus strata that are truncated and covered by a thin veneer of alluvium; south of the anomaly ground water is unconfined and occurs in coarse alluvial gravels.

The California State Water Rights Board report (1962) relates the Sylmar ground-water anomaly to impermeable strata in the north-dipping Towsley (= Repetto in their report) and Saugus Formations. The trace of the ground-water anomaly, however, is at an oblique angle to the strike of beds in the Saugus-Towsley; this angle suggests that a structural discontinuity such as a fault could more reasonably explain it.

The ground-water anomaly is here concluded to be the product of a reverse fault that has raised northward-dipping Saugus Formation in the Little Tujunga syncline against alluvial gravels on the south, with progressive erosional planation maintaining only a thin veneer of alluvium over the Saugus strata in the rising northern fault block. Gouge along such a fault could account for the impediment to ground-water flow, and vertical displacement along it could account for the different thicknesses of alluvium north and south of the ground-water anomaly. Together, these factors could produce the resultant differences in ground-water habit across the anomaly. M. M. Clark has observed a rather subtle south-facing topographic escarpment, on aerial photographs taken in 1952, that extends nearly continuously along the approximate trace of the ground-water anomaly and which is thought to be a result of the latest movements on the fault postulated to have caused the anomaly. (See the section on "Surface faulting" by the U.S. Geological Survey staff in this report.)

The zone of faulting that approximately follows the base of the western San Gabriel Mountains eastward from San Fernando along the north side of Tujunga Valley is called the Tujunga segment of the San Fernando fault zone in this report.[1] Kamb and others (this report) note that the Tujunga fault segment as thus defined differs from that of Hill (1930) for a postulated fault in the central alluviated part of the Tujunga Valley and suggest that the older definition by Hill be dropped.

A number of unnamed fault traces had been mapped along the Tujunga fault segment prior to the new 1971 surface ruptures. One of these faults just west of Oliver Canyon dips northward 60° and thrusts Miocene strata southward over upper Pleistocene terrace deposits (Oakeshott, 1958). At the mouth of Little Tujunga Canyon a ground-water cascade of perhaps 30 m, which suggests late Quaternary displacement, is nearly coincident with the site of a 1971 rupture.

VERDUGO FAULT

The Verdugo fault lies at the southwest foot of the Verdugo Mountains (fig. 2, and Jennings and Strand, 1969) and is probably responsible for the 1,000 m of relief between the mountain crest and the base of the alluvial fill to the south. This conclu-

[1] R. J. Proctor of the Los Angeles Metropolitan Water District reports that tectonic ruptures associated with the February 9 earthquake roughly follow a north-dipping thrust fault which he had previously mapped and which he has named Lakeview fault. The scarps in Schwartz and Oliver Canyons coincide with this fault, which would be synonomous with the Tujunga fault segment as used in this report.

sion is supported by the steep residual gravity gradient found by Corbato (1963, map 3; fig. 4 of this paper) to extend along this trend from Burbank to west of the Pacoima Hills. The steep southwest face of the mountains, the presence of faulted stream-terrace deposits north of Burbank (California State Water Rights Board report, v.II., p. A-23) and a ground-water cascade at the mouth of Verdugo Wash led Wentworth, Ziony, and Buchanan (1970, pl. 1) to conclude that the southeastern end of the Verdugo fault had undergone late Quaternary displacement. Between the Verdugo Mountains and the Pacoima Hills, clayey gouge seams have been formed by fault movement in the alluvial fill along the trend of the Verdugo fault, and the resultant ground-water impediment has been used as the trace for the fault in figure 2. Topographic and gravity evidence for the Verdugo fault are lacking between the Pacoima Hills and the Mission Hills. Limited information indicates, however, that ground-water levels northeast of a reasonable extension of the fault are more than 60 m higher than southwest of it and therefore that a major ground-water cascade occurs there.

NORTHRIDGE HILLS FAULT

The Northridge Hills fault trends southeastward from the southeastern Santa Susana Mountains across the valley floor along the south side of the Northridge Hills. The eastward extent of the fault is unknown, although its easternmost topographic expression appears almost halfway across the valley. The fault forms a distinct though discontinuous topographic feature along its mapped length in the valley and is inferred to displace older late Quaternary deposits (Qt in fig. 2) and to raise Saugus Formation into low hills along its central part. Late Quaternary displacement on the Northridge Hills fault may be considerable, for cross sections in the California State Water Rights Board report (1962) show the base of the alluvium to be faulted downward by as much as about 300 m on its southwest side.

CHATSWORTH FAULT

Corbato (1963, map 3; and fig. 4 of this paper) shows a steep gravity gradient extending northeastward across the west end of the San Fernando Valley, which coincides in position with the northeastward trend of faults that juxtapose upper Miocene Modelo Formation against Cretaceous rocks at and southwest of Chatsworth Reservoir (Jennings and Strand, 1969). The bedrock surface beneath the valley alluvium has been dropped down on the southeast side to produce a 25-m ground-water cascade within the alluvium. Additional evidence of late Quaternary displacement may exist in the form of faulted terrace deposits at the northeast end of Chatsworth Reservoir (Conrad, 1949).

ACTIVITY OF FAULTS

A fault is active if, because of its present tectonic setting, it can undergo movement from time to time in the immediate geologic future. This active state exists independently of the geologists' ability to recognize it. A number of characteristics have been used to identify active faults, such as historic seismicity or surface faulting, crustal strain, geologically recent displacement inferred from topography or stratigraphy, or physical connection with a known active fault. Not enough is known, however, of the behavior of faults to assure successful discrimination of all active faults by such characteristics.

Of the faults discussed above, only the San Andreas fault and the San Fernando fault zone are known to be active on the basis of earthquakes or historic surface faulting, and the San Fernando fault was discovered to be active only when it ruptured the ground surface on February 9, 1971. It is evident, however, that more faults in the San Fernando Valley area may be active today than are now recognized. Study of the topographic and stratigraphic records of the past histories of these faults, in concert with studies of earthquake activity and crustal strain, can lead to important insights into their possible activity.

Agreement does not currently exist on the length of fault history that should be used in evaluating the future behavior of faults. The commonly used cutoff of 10,000 years (beginning of Holocene time) seems too short in the light of surface faulting in 1952 along the White Wolf fault, which was not previously recognized as an active fault and exhibited no obvious evidence of late Quaternary activity other than defining a steep mountain front (Oakeshott, 1955; Dibblee, 1955). The White Wolf experience, combined with the likelihood that only some fraction of the past movements of a fault will actually be evident in the geologic record, led Wentworth, Ziony, and Buchanan (1970) to suggest (p. 13 and 15) that faults with evidence of Holocene displacement probably should be considered active for most purposes and that it may be desirable to consider faults with late Quaternary displacement as active, at least for land uses requiring relatively high safety factors.

The addition of the 1971 San Fernando event to the experience of the 1952 White Wolf event strengthens the conclusion that, in the absence of proof to the contrary, demonstrated late Quaternary movement should be considered evidence that a fault is probably active. Thus, we would tentatively conclude that all the faults described above that have had late Quaternary displacement are probably active. Further work will be required to test and corroborate the conclusions of late Quaternary displacement and to evaluate the movement rates and characteristics of these faults.

In view of the foregoing, the location of the 1971 San Fernando faulting should not have come as a complete surprise because preearthquake information was sufficient to suggest the existence of faults having late Quaternary displacement along or near the positions of the main traces of the February 1971 ruptures. It would not, however, have been possible to predict, on the basis of present knowledge, that the next surface faulting in Southern California, or even in the San Fernando area, would occur either where or when it did.

CONCLUSIONS

The San Fernando Valley area is underlain by a depositional basin that dates from Miocene time and is bordered by pre-Cenozoic crystalline basement rocks. The basement rocks are unconformably overlain by an Upper Cretaceous-Cenozoic sequence of clastic sedimentary rocks that has been deformed by north-south compression, producing east-west folds and causing thrust faulting during late Cenozoic time along the southern margins of the mountain ranges. The thrust faulting—and the February 1971 rupturing—are continuations of long-established tectonic processes that have resulted in uplift of the mountainous parts of the Transverse Ranges.

The faulting of February 9, 1971, near San Fernando occurred on faults not previously recognized as active, although sufficient evidence was available to suggest that there had been movements along their main traces in late Quaternary time. The topographic and stratigraphic record of late Quaternary fault movements, including their effect on groundwater flow, must be given greater scrutiny, because late Quaternary displacement appears to be a sufficient criterion for probable activity of a fault in this area. Numerous faults in the San Fernando Valley area exhibit some evidence of late Quaternary displacement and in the light of the San Fernando faulting should be considered probably active until investigated in detail with both geologic and geophysical techniques.

REFERENCES CITED

Allen, C. R., St. Amand, P., Richter, C. F., and Nordquist, J. M., 1965, Relationship between seismicity and geologic structure in the southern California region: Seismol. Soc. America Bull, v. 55, p. 753–797.

Bailey, T. L. and Jahns, R. H., 1954, Geology of the Transverse Range Province, southern California, *in* Jahns, R. H., ed., Geology of southern California: California Div. Mines and Geology Bull. 170, p. 83–106.

Bishop, W. C., 1950, Geology of the southern flank of Santa Susana Mountains, county line to Limekiln Canyon, Los Angeles County, California: Los Angeles, California Univ. M.A. thesis.

California State Water Rights Board, 1962, The city of Los Angeles vs. City of San Fernando: California State Water Rights Board, Report of Referee, No. 650079, v. I, 258 p., 36 pls.; v. II, various pages.

Conrad, S. D., 1949, Geology of the eastern portion of the Simi Hills, Los Angeles and Ventura Counties, California: Los Angeles, California Univ. M.A. thesis.

Corbato, C. E., 1963, Bouguer gravity anomalies of the San Fernando Valley, California: California Univ. Pubs. Geol. Sci., v. 46, no. 1, p. 1–32.

Crowell, J. C., 1950, Geology of Hungry Valley area, southern California: Am. Assoc. Petroleum Geologists Bull., v. 34, p. 1623–1646.

———1952, Probable large lateral displacement on San Gabriel fault, southern California: Am. Assoc. Petroleum Geologists Bull., v. 36, no. 10, p. 2026–2035.

———1962, Displacement along the San Andreas fault, California: Geol. Soc. America Spec. Paper 71, 61 p.

Dibblee, T. W., Jr., 1955, Geology of the southeastern margin of the San Joaquin Valley, California, *in* Oakeshott, G. B., ed., Earthquakes in Kern County, California, during 1952: California Div. Mines and Geology Bull. 171, p. 23–34.

Hazzard, J. C., 1944, Some features of Santa Susana thrust, vicinity of Aliso Canyon field, Los Angeles County, California [abs.]: Am. Assoc. Petroleum Geologists Bull., v. 28, no. 12, p. 1780–1781.

Hill, M. L., 1930, Structure of the San Gabriel Mts. north of Los Angeles, California: California Univ. Pubs. Geol. Sci., v. 19, no. 6, p. 137–170.

Holmes, L. C., 1919, Soil survey of the San Fernando Valley area, California, *in* Field operations of the Bureau of Soils 1915: U.S. Dept. Agriculture, Bur. Soils, 17th rept., pl. 63, scale 1:62,500.

Jennings, C. W., and Strand, R. G., 1969, Geologic map of California, Olaf P. Jenkins edition, Los Angeles sheet: California Div. Mines and Geology, scale 1:250,000.

Johnston, R. L., 1938, The geology of a portion of the western Verdugo Mountains: Los Angeles, California Univ. M.A. thesis.

Merifield, P. M., 1958, Geology of a portion of the southwestern San Gabriel Mountains, San Fernando and Oat Mountain quadrangles, Los Angeles County, California: Los Angeles, California Univ. M.A. thesis.

Oakeshott, G. B., 1955, The Kern County earthquakes in California's geologic history, *in* Oakeshott, G. B., ed., Earthquakes in Kern County, California, during 1952: California Div. Mines and Geology Bull. 171, p. 15–22.

———1958, Geology and mineral deposits of San Fernando quadrangle, Los Angeles County, California: California Div. Mines and Geology Bull. 172, 147 p., map scale 1:62,500.

Townley, S. D., and Allen, M. W., 1939, Descriptive catalog of earthquakes of the Pacific Coast of the United States, 1769 to 1928: Seismol. Soc. America Bull., v. 29, p. 1–297.

Wentworth, C. M., Ziony, J. I., and Buchanan, J. M., 1970, Preliminary geologic environmental map of the greater Los Angeles area, California: U.S. Atomic Energy Comm., TID–25363, 41 p., map scale 1:250,000.

Winterer, E. L., and Durham, D. L., 1962, Geology of southeastern Ventura basin, Los Angeles County, California: U.S. Geol. Survey Prof. Paper 334–H, p. 275–366, map scale 1:24,000.

MAIN SHOCK AND LARGER AFTERSHOCKS OF THE SAN FERNANDO EARTHQUAKE, FEBRUARY 9 THROUGH MARCH 1, 1971 [1]

By C. R. ALLEN, G. R. ENGEN, T. C. HANKS, J. M. NORDQUIST, and W. R. THATCHER
SEISMOLOGICAL LABORATORY, CALIFORNIA INSTITUTE OF TECHNOLOGY

The purpose of this paper is to summarize the seismological information on the main shock of the San Fernando earthquake and its aftershocks that occurred within the subsequent three weeks, from February 9 through March 1, 1971. These preliminary data are based on records of the permanent stations of the California Institute of Technology seismographic array, with supplemental information from the U.S. Geological Survey station at Point Mugu and the California Department of Water Resources stations at Pyramid and Cedar Springs (both telemetered to Pasadena). During the first few hours of activity, these were the only nearby stations that were in operation, but portable seismographic units that were installed by various groups in the ensuing days will eventually allow much better hypocentral determinations for the late aftershocks than are presented in this preliminary report.

The main shock has tentatively been assigned the following parameters:

Magnitude (M_L)	6.6
Origin time	14:00:41.6, 9 February 1971 (GMT)
Location	34° 24.0′ N., 118° 23.7′ W.
Depth	13.0 km

It should be emphasized that the hypocenter of the main shock represents only the point of initial rupture. Breaking presumably then propagated southward and upward from this point at about 45°, reaching the ground surface in the Sylmar–San Fernando area (fig. 1). It is not surprising that the principal geologic and engineering effects were observed some distance south of the epicenter, where the fault plane was shallower and the fault displacement presumably was greater.

Station readings used in locating the main shock are given in table 1; all of these 11 stations are less than 200 km from the epicenter. The fact that three stations were within 40 km of the epicenter gives us reasonable confidence in the solution, although individual station corrections derived from accurately located aftershocks—and hopefully calibration explosions—will later be used to refine the hypocentral location. The x, y, and z standard errors for the tentative location of the main shock are 1.2, 2.0, and 2.5 km, respectively. The magnitude is based solely on the strong-motion (4X) record from Pasadena and will undoubtedly be modified when the more distant stations are considered; in the meantime it agrees well with the assignment of 6.5 by Berkeley

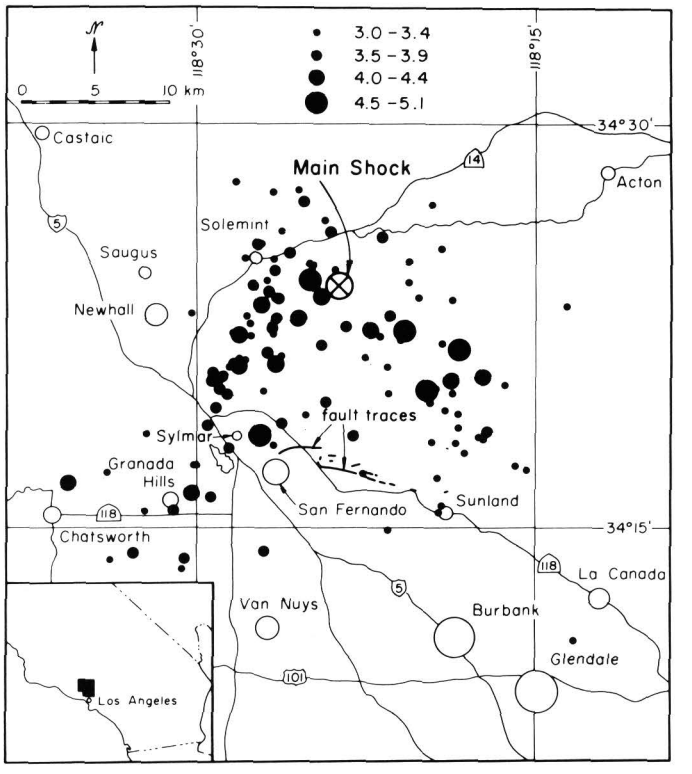

FIGURE 1.—Index map of study area, showing epicenters of the main shock and aftershocks of magnitude 3.0 and greater of the San Fernando earthquake for the first 3 weeks of activity, February 9 through March 1, 1971.

[1] Contribution No. 1990, Division of Geological and Planetary Sciences, California Institute of Technology, Pasadena, California.

TABLE 1.—*P-wave arrival times for the main shock at stations used in computing the hypocenter*

[DWR, California Department of Water Resources; USGS, U.S. Geological Survey]

Station symbol	Station name	Time h m s	Distance km
PAS	Pasadena	14:00:48.1	37.1
PYR	Pyramid (DWR)	14:00:48.0	39.5
MWC	Mount Wilson	14:00:48.3	39.5
SBLG	Pt. Mugu (USGS)	14:00:53.0	70.8
CSP	Cedar Springs (DWR)	14:00:57.1	97.0
RVR	Riverside	14:00:58.5	105.0
ISA	Isabella	14:01:04.5	140.2
SYP	Santa Ynez Park	14:01:05.0	146.2
CLC	China Lake	14:01:07.8	173.0
GSC	Goldstone	14:01:08.5	176.3
PLM	Palomar	14:01:09.2	183.3

(Bruce Bolt, personal commun.) and the range of 6.3 to 6.7 reported by the National Ocean Survey (Leonard Murphy, personal commun.).

There were no foreshocks or other obvious precursory activity, and a careful examination of the Mt. Wilson records indicates that no shocks exceeding magnitude 1.5 had occurred in the area in the preceding 8 days. No shock exceeding magnitude 2.5 had been identified in the area during the preceding 4 months, and it appears that the most recent identifiable event within the area of subsequent activity was a shock of magnitude 2.6 that occurred north of Sylmar (fig. 1) on September 28, 1970. In the years prior to 1971, the area of the San Fernando earthquake had been one of low to moderate seismic activity—not unlike that of many other parts of southern California (Allen and others, 1965). The only major historic shock originating within this specific area was the so-called Pico Canyon earthquake of 1893 (Townley and Allen, 1939), which was probably in the magnitude-6 range but clearly was not as large as the 1971 event. The San Fernando earthquake of 1971 again emphasizes the fallacy of assuming, for a given area, that the largest shock experienced in the past is necessarily typical of the largest shock to be expected in the future.

Table 2 is a preliminary list of all shocks of the San Fernando series of magnitude 3.0 and greater that occurred through March 1, 1971. The list, which includes some 200 events, is felt to be relatively complete following the first hour of activity, during which many small events cannot be discerned because of the frequent occurrence of larger shocks. Considerable use has been made of the 4X and 100X strong-motion instruments at Pasadena, Riverside, and Santa Barbara in studying shocks of the first hour, and we feel that most larger events have been recognized. With the exception of the main shock, locations of most of the earthquakes listed in table 2 have been determined with depths restricted to 8.0 km, which appears to be a reasonable average on the basis of the more accurate determinations using portable stations (Hanks and others, this report). None of the locations in table 2 has made use of portable stations; the objective has

TABLE 2.—*Shocks of the San Fernando series of magnitude 3.0 and greater, February 9 through March 1, 1971*

[Magnitude assignments, in particular, are very tentative. Depths are restricted to 8.0 km, except for the main shock, which is at 13.0 km]

Date	Time (GMT)	M_L	Lat (N.)	Long (W.)
Feb 9	1400 41.6	6.6	34°24.0′	118°23.7′
	1401	5.1	--------	--------
	1402	4.4	--------	--------
	1402	4.3	--------	--------
	1403	4.5	--------	--------
	1404	4.3	--------	--------
	1406	4.2	--------	--------
	1407	4.5	--------	--------
	1408	3.9	--------	--------
	1409	3.9	--------	--------
	1410 21.5	5.1	34°21.7′	118°18.4′
	1413	3.6	--------	--------
	1416	4.2	--------	--------
	1419	4.4	--------	--------
	1422	3.6	--------	--------
	1425	3.8	--------	--------
	1426 06.9	3.7	34°24.0′	118°27.5′
	1428	3.6	--------	--------
	1429 05.2	3.6	34°21.8′	118°24.6′
	1429	3.7	--------	--------
	1431	3.7	--------	--------
	1432	3.1	--------	--------
	1434	3.6	--------	--------
	1434	5.1	--------	--------
	1439	4.0	--------	--------
	1440	4.1	--------	--------
	1441	3.4	--------	--------
	1443	3.5	--------	--------
	1443 46.7	4.7	34°18.5′	118°27.2′
	1448	3.4	--------	--------
	1450	3.9	--------	--------
	1452 44.4	3.5	34°19.7′	118°24.3′
	1455	3.7	--------	--------
	1457 24.3	3.6	34°20.8′	118°29.4′
	1500	3.2	--------	--------
	1503 07.1	3.6	34°18.0′	118°28.6′
	1506	3.3	--------	--------
	1510 01.1	4.1	34°23.7′	118°24.5′
	1521 06.6	3.7	34°18.9′	118°30.5′
	1521	3.9	--------	--------
	1526 00.7	3.0	34°14.9′	118°21.6′
	1528 25.8	3.7	34°14.1′	118°27.0′
	1530 37.8	3.7	34°22.9′	118°21.6′
	1535 41.5	3.6	34°22.5′	118°23.4′
	1538 29.7	4.2	34°21.0′	118°28.1′
	1545 58.0	3.6	34°18.9′	118°26.2′
	1548 04.6	3.2	34°19.7′	118°19.7′
	1551 00.9	3.6	34°16.1′	118°29.4′
	1557	3.3	--------	--------
	1558 20.7	5.1	34°20.1′	118°19.8′
	1601 45.0	3.3	34°17.1′	118°15.3′
	1614	3.9	--------	--------
	1619 26.0	4.3	34°16.7′	118°35.7′
	1621	3.4	--------	--------
	1625	3.0	--------	--------
	1626	3.2	--------	--------
	1627	3.2	--------	--------
	1628 41.8	3.3	34°22.5′	118°20.6′
	1628	3.4	--------	--------
	1629	3.4	--------	--------
	1632	3.8	--------	--------
	1633	3.3	--------	--------
	1638	3.6	--------	--------
	1639	3.8	--------	--------
	1641	3.1	--------	--------
	1641	3.6	--------	--------
	1647 03.7	3.5	34°20.6′	118°29.3′
	1703 47.6	3.6	34°18.8′	118°29.6′
	1704	3.5	--------	--------
	1705	3.1	--------	--------
	1714	3.1	--------	--------
	1719 15.7	3.1	34°23.6′	118°26.5′
	1722	3.2	--------	--------
	1739	3.6	--------	--------
	1802	3.4	--------	--------
	1827	3.5	--------	--------
	1829 24.6	3.5	34°20.2′	118°29.0′
	1857 02.4	4.0	34°20.7′	118°17.3′
	1941	3.4	--------	--------
	1941	3.5	--------	--------
	2011 34.3	3.4	34°25.3′	118°19.1′
	2017	3.5	--------	--------
	2027	3.4	--------	--------
	2030	3.1	--------	--------
	2037	3.5	--------	--------
	2038	3.5	--------	--------

TABLE 2.—*Shocks of the San Fernando series of magnitude 3.0 and greater, February 9 through March 1, 1971*—Continued

Date	Time (GMT)	M_L	Lat (N.)	Long (W.)
	2043 24.9	3.4	34°21.3′	118°28.1′
	2046 11.9	3.5	34°23.6′	118°26.4′
	2053 34.2	3.4	34°24.7′	118°23.9′
	2056 02.1	3.1	34°23.6′	118°20.1′
	2128	3.4	----------	----------
	2129 08.1	3.4	34°20.1′	118°27.0′
	2248 37.3	3.7	34°21.1′	118°28.4′
	2344	3.1	----------	----------
Feb. 10	0013 55.1	3.1	34°18.8′	118°18.4′
	0016	3.3	----------	----------
	0107	3.3	----------	----------
	0116 12.0	3.0	34°19.4′	118°19.0′
	0138 15.6	4.0	34°16.3′	118°30.2′
	0228	3.3	----------	----------
	0230 13.5	3.5	34°19.6′	118°29.2′
	0312 11.9	4.0	34°20.5′	118°18.7′
	0314	3.3	----------	----------
	0402	3.2	----------	----------
	0410 11.6	3.3	34°22.1′	118°27.6′
	0415	3.5	----------	----------
	0416	3.4	----------	----------
	0506 35.8	4.6	34°22.4′	118°20.8′
	0518 07.0	4.6	34°24.3′	118°25.0′
	0533	3.4	----------	----------
	0541 41.7	3.1	34°19.3′	118°18.4′
	0624 49.8	3.3	34°22.1′	118°21.9′
	0654 33.0	3.3	34°22.2′	118°26.7′
	0700 45.3	3.2	34°15.8′	118°19.1′
	0714 57.4	3.4	34°18.1′	118°26.7′
	0727 03.2	4.1	34°21.1′	118°26.5′
	0736	3.3	----------	----------
	0830	3.4	----------	----------
	0923	3.2	----------	----------
	0933 24.3	3.2	34°17.3′	118°15.9′
	1000 06.3	3.6	34°25.6′	118°27.3′
	1129 25.2	3.4	34°26.0′	118°25.2′
	1131 34.5	3.5	34°21.6′	118°26.9′
	1145 53.1	3.5	34°20.0′	118°28.7′
	1153	3.2	----------	----------
	1210	3.5	----------	----------
	1227	3.2	----------	----------
	1242 19.1	3.1	34°18.4′	118°17.5′
	1349 53.6	4.2	34°22.8′	118°25.5′
	1435 26.5	3.8	34°20.7′	118°28.9′
	1511 25.5	3.0	34°24.8′	118°25.0′
	1522 10.7	3.2	34°23.0′	118°30.2′
	1548 11.3	3.5	34°18.7′	118°17.1′
	1738 54.9	4.3	34°22.4′	118°22.3′
	1854 41.5	4.1	34°23.4′	118°27.1′
	1906 06.0	3.4	34°21.9′	118°19.1′
	2342 28.5	3.3	34°22.0′	118°21.0′
Feb. 11	0030 01.0	3.4	34°22.5′	118°20.7′
	0343 11.9	3.3	34°24.9′	118°21.7′
	0407 17.0	3.2	34°21.0′	118°28.6′
	0733 59.5	3.1	34°27.9′	118°28.2′
	0924 38.8	3.2	34°21.4′	118°22.6′
	1132 56.3	3.1	34°20.3′	118°16.3′
	1421 20.6	3.3	34°18.2′	118°19.7′
	1643 31.8	3.4	34°13.6′	118°30.7′
	1935 08.2	3.5	34°26.0′	118°24.1′
	2328 21.1	3.1	34°27.5′	118°26.6′
	2335 47.8	3.5	34°18.5′	118°23.1′
Feb. 12	0809 31.3	3.0	34°23.5′	118°18.7′
	0920 53.8	3.1	34°25.0′	118°26.6′
	0952 20.7	3.2	34°17.4′	118°30.0′
	1502 43.7	3.5	34°25.8′	118°21.8′
	1622 44.6	3.6	34°25.2′	118°25.9′
Feb. 13	0256	3.0	----------	----------
	0645 55.6	3.2	34°18.6′	118°32.2′
	2230 18.9	3.0	34°26.4′	118°24.4′
Feb. 14	0338 39.9	3.2	34°19.2′	118°25.2′
	0732 54.3	3.0	34°10.8′	118°13.3′
	1208	3.1	----------	----------
	1344 49.2	3.6	34°15.7′	118°31.0′
	1753 58.9	3.2	34°18.3′	118°17.3′
Feb. 15	0110 50.4	3.3	34°21.2′	118°28.3′
	0804 49.7	3.9	34°27.1′	118°25.3′
	0846 54.8	3.5	34°23.8′	118°26.8′
	1303 42.3	3.3	34°24.2′	118°26.9′
	2333 12.0	3.0	34°17.1′	118°34.0′
Feb. 16	0437 04.4	3.5	34°14.1′	118°32.8′
	0708 26.0	3.4	34°22.3′	118°28.4′
	1439 19.1	3.2	34°18.2′	118°18.5′
	1654 39.3	3.0	34°24.8′	118°24.9′
Feb. 17	1008 06.2	3.0	34°21.3′	118°27.8′
	1015 40.5	3.3	34°20.0′	118°18.7′
Feb. 18	0921 52.8	3.1	34°20.0′	118°21.5′
	1545 22.5	3.1	34°24.0′	118°20.6′
	2209 41.2	3.0	34°22.6′	118°26.7′
Feb. 19	0245 11.2	3.4	34°17.4′	118°30.1′
	0807 57.1	3.4	34°27.0′	118°19.6′
	0808	3.7	----------	----------
Feb. 20	0809 27.4	3.3	34°26.0′	118°26.2′
	2315 57.9	3.3	34°15.7′	118°32.3′
Feb. 21	0242 12.0	3.2	34°13.9′	118°33.9′
	0550 52.3	4.0	34°22.2′	118°28.1′
	0715 11.5	3.9	34°22.5′	118°26.7′
	0743 03.1	3.5	34°22.8′	118°26.5′
	1050	3.0	----------	----------
	1406 05.1	3.3	34°22.6′	118°27.6′
Feb. 22	1813 13.0	3.0	34°15.6′	118°19.3′
Feb. 23	0624 43.8	3.0	34°16.9′	118°19.4′
Feb. 24	0531 38.0	3.0	34°21.5′	118°21.0′
	1518 01.4	3.0	34°27.6′	118°25.5′
	1604 14.8	3.5	34°24.6′	118°26.5′
Feb. 25	1127 33.2	3.1	34°22.9′	118°27.8′
	1425 51.8	3.2	34°25.0′	118°27.9′
	1554 06.1	3.0	34°20.2′	118°19.5′
	2027 58.5	3.4	34°17.0′	118°22.7′
Feb. 26	0210 24.9	3.0	34°23.2′	118°13.7′
	0333 01.0	3.3	34°21.4′	118°26.2′
	2122 34.9	3.3	34°25.5′	118°27.1′
Feb. 28	2251 34.7	3.0	34°17.8′	118°18.1′
Mar. 1	0428 20.9	3.3	34°21.3′	118°27.2′

simply been to get a rapid and homogeneous listing. Nevertheless, comparison of those epicentral locations in table 2 for which we have also obtained independent solutions based on the portable stations (Hanks and others, this report) suggests that most are accurate to within 2 km.

All the shocks in table 2 for which epicentral locations have been determined are shown in figure 1, which also shows their relationship to geographic features and to the traces of surficial fault movement associated with the earthquake (after Kamb and others, this report). The greatest concentration of aftershock activity lies roughly in the shape of an inverted U which has remarkable symmetry both with respect to the epicenter of the main shock and to the pattern of surface faulting. There appears to have been more aftershock activity on the southwest-trending west flank of the pattern, but the consistent outline is nevertheless striking; of particular note is the relative absence of aftershocks in the area just north of the surficial fault traces, where much of the heaviest shaking took place. It is interesting that the location of Pacoima Dam, where the extraordinary strong-motion record of the main shock was written (Maley and Cloud, this report; Housner and Hudson, 1971), is very nearly in the center of this aftershock-void area.

It is tempting to suggest that the aftershocks delineate the boundary of slippage on the north-dipping thrust fault, with the aftershocks concentrated in the areas of postearthquake stress concentration at the edge of the slippage. Since there is no stress concentration at the surface trace, few aftershocks would be expected here. The segment that slipped would then be visualized as a north-dipping thrust plate with the shape of an inverted U, extending north from the surface trace down to the hypocentral area 12 km north. The principal difficulty with this interpretation is that aftershock depths and focal mechanisms obtained to date do not portray

such a simple picture; instead, the aftershocks seem to fall into three distinct groups, each with its own characteristic depths and focal mechanisms (Hanks and others, this report; Whitcomb, this report). Much work remains to be done to synthesize the aftershock pattern and determine its tectonic significance. We nevertheless feel at this time that the aftershock epicenters of figure 1 do indeed tend to delineate the boundaries of the thrust displacement that caused the San Fernando earthquake, although many of the shocks of the western limb evidently represent deeper strike-slip events whose relationship to the main thrust fault is very complex.

Operation of the Caltech seismographic array has been made possible over the years by contributions by the Earthquake Research Affiliates, a group of industrial sponsors whose help is particularly appreciated at times such as this. We also appreciate the generosity and the spirit of free communication that has typified all the groups and individuals investigating this earthquake.

REFERENCES

Allen, C. R., St. Amand, P., Richter, C. F., and Nordquist, J. M., 1965, Relationship between seismicity and geologic structure in the southern California region: Seismol. Soc. America Bull., v. 55, p. 753–797.

Housner, G. W., and Hudson, E. E., 1971, Preliminary report on the engineering aspects of the San Fernando, California, earthquake of February 9, 1971: Seismol. Soc. America Bull. (In press.)

Townley, S. D., and Allen, M. W., 1939, Descriptive catalog of earthquakes of the Pacific Coast of the United States, 1769 to 1928: Seismol. Soc. America Bull., v. 29, p. 1–297.

PRECISE LOCATIONS OF AFTERSHOCKS OF THE SAN FERNANDO EARTHQUAKE 2300 (GMT) FEBRUARY 10–1700 FEBRUARY 11, 1971 [1]

By THOMAS C. HANKS, THOMAS H. JORDAN, and J. BERNARD MINSTER
SEISMOLOGICAL LABORATORY, CALIFORNIA INSTITUTE OF TECHNOLOGY

Forty-seven aftershocks of the San Fernando earthquake have been located using six portable seismograph units operated by the California Institute of Technology, a portable seismograph operated by the University of California, San Diego, and permanent stations at Pyramid (California Department of Water Resources) and Mount Wilson (Caltech). The locations of the seven portable units are shown in figure 1; station coordinates are listed in table 1. Both P- and S-wave readings have been the input data for an iterative, least-squares, half-space hypocentral location program similar to that described by Flinn (1960). A P-wave velocity of 5.58 kmps (kilometer per second) and an S-wave velocity of 3.26 kmps have been used for the hypocentral determinations given in figure 1.

TABLE 1.—*Location of stations used in hypocenter determinations*
[CIT, California Institute of Technology; UCSD, University of California, San Diego; CDWR, California Department of Water Resources]

Station	Agency	North lat	West long	Alt (m)
Mt. Wilson	CIT	34°13.4′	118°03.5′	1,730
Bouquet Canyon	CIT	33.5′	25.5′	890
Brown's Canyon	CIT	17.6′	35.4′	412
Indian Canyon	CIT	25.2′	16.2′	884
Soledad Canyon	CIT	26.1′	21.7′	575
Iron Canyon	CIT	23.3′	23.9′	588
Golden Oak Ranch	CIT	23.8′	28.3′	482
Little Tujunga	UCSD	17.7′	21.6′	396
Pyramid	CDWR	34.1′	44.5′	1,240

These aftershocks represent a reasonably complete sample of the locatable events occurring between 33 and 51 hours after the main shock. Most of these events have magnitudes in the range $1 < M_L < 3$; nine of them have $M \geq 3$. The epicentral distribution of these aftershocks (fig. 1) does not differ significantly from the general epicentral pattern of 120 larger aftershocks occurring up to 3 weeks after the main shock (Allen and others, this report). An exception to this is the absence of locations during the 18 hour sample considered here in the area 1–8 km (kilometer) north of Sunland. Generally, we believe that enough earthquakes have been located to sample reasonably well the aftershock region defined by the larger events. There is

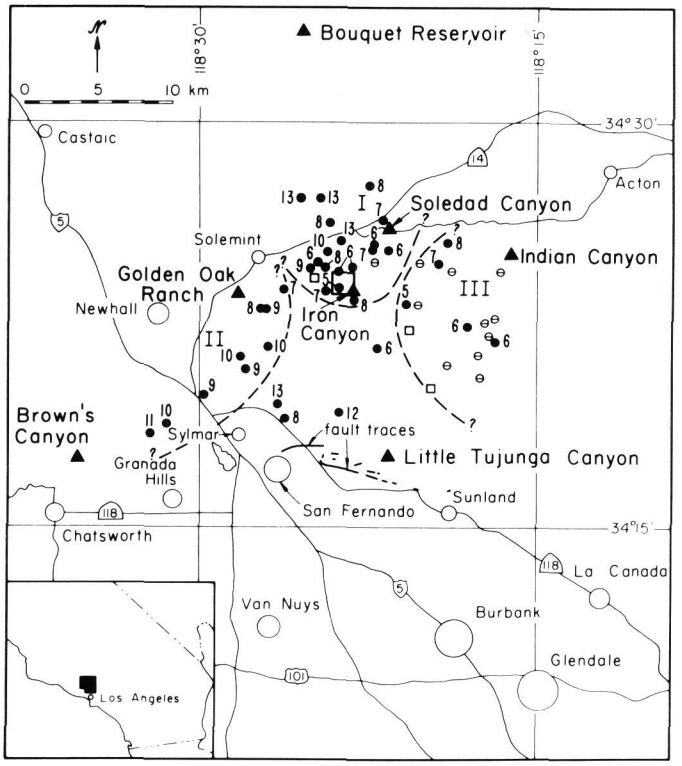

FIGURE 1.—Distribution of aftershocks of the San Fernando earthquake, in the time interval 2300 (GMT) February 10–1700 February 11, 1971. The larger open square is the main-shock epicenter; the three smaller squares are epicenters for three events $M_L > 4.5$. Solid triangles locate the portable seismograph stations. Numbered solid circles are aftershock locations with the depth (km) as indicated. Open circles with an interior line are shallow aftershocks ($h < 5$ km). Roman numerals denote groupings of aftershocks: I = epicentral group, II = Chatsworth segment, III = eastern group. Fault traces after the section by Kamb and others in this report.

[1] Contribution No. 1994, California Institute of Technology, Division of Geological and Planetary Sciences, Pasadena, California

no reason at this point to suspect that this 18-hour interval is anomalous. On the basis of their hypocentral locations, we have classified members of this sequence of aftershocks into three groups: the epicentral group, the Chatsworth segment, and the eastern group (fig. 1). We discuss the location characteristics for each group below.

THE EPICENTRAL GROUP

This group of 19 aftershocks is a cluster centered 3 km north of the main-shock epicenter (determined by Allen and others, this report, as 34°24.0′ N, 118°23.7′ W). Depths of these events range from 6 to 13 km, excluding one event at 5 km and one shallow event ($h < 5$ km). A typical location in this group is based on seven P- and three S-wave readings; the RMS (root mean square) travel-time residual is in general less than 0.2 sec. We consider the epicenters to be determined within 1 km and the depths to be determined within 1–2 km.

THE CHATSWORTH SEGMENT

This group of aftershocks lies within a linear zone extending southwest from the vicinity of the main shock to Chatsworth. The number of arrival times used and the RMS residuals computed are similar to those of the epicentral group. However, station proximity and azimuthal coverage are not so favorable as for the former group. We consider these epicenters to be determined within 1 km and the depths within 2 km. The depth range (7–11 km) of these events is narrower than that of the epicentral group, but this may only reflect the small number of locations. To our knowledge, there are no surficial tectonic features along this zone.

THE EASTERN GROUP

This group of aftershocks consists of 15 located events. All these have depths less than 8 km, and 10 are shallow ($h < 5$ km). More precise depth determinations for the shallow events have not been assigned because of inadequate control; the nearest stations are no closer than 5–10 km. The RMS residuals for events of this group are generally between 0.2 sec and 0.3 sec. An RMS residual of 0.23 sec for a typical event located at the surface increases only slightly (to 0.25 sec) if the aftershock is relocated at a depth of 5 km. Relocation of depths deeper than 5 km causes the RMS residual to increase rapidly, to 0.35 sec at 6 km and 0.53 sec at 8 km. The larger RMS residuals for these shallow events may reflect anomalous near-surface velocity structure, anomalous station residuals for rays traveling nearly horizontally, or both. Calibration of the array by an explosion in this area is necessary if hypocentral locations in this region are to be improved, especially for the shallower aftershocks. Six of the shallow events have $M_L > 3$. Thus, strain release in the aftershock zone is dominated by these shallow events during this period of time.

A fourth area of interest can be defined by the relative absence of aftershocks occurring within it. It is north of the observed surface-fault breakage and interior to the three groups discussed previously. Only four aftershocks are located in this region. This could reflect the limited time sample considered. All events in this region have local magnitudes less than 2, and they represent less than 10 percent of the data.

DISCUSSION

Recognizing the limitations imposed by the short time sample of aftershock occurrence discussed and the small number of events located, we believe that three groups of aftershocks can be tentatively identified on the basis of their hypocentral characteristics. These groupings can also be characterized by the type of focal-mechanism solution occurring within each. We will attempt a preliminary interpretation of these groupings and their relationship to each other, the observed surface faulting, and the main shock.

The deepest hypocenters of the epicentral group, with the exception of one event at 13 km depth, roughly define a plane which dips at 32° to the north. The strike of this plane is approximately east-west, which is consistent with fault-plane solutions for the main shock (Whitcomb, this report). The plane interesects the surface in the vicinity of observed ground breakage along the Sylmar and Tujunga fault segments (Kamb and others and U.S. Geological Survey staff, this report).

Recognizing the thrust characteristics of the surface faulting, the main shock, and aftershocks of the epicentral group, we will refer to this plane as the thrust plane, where the appellation is a matter of reference and interpretation. The tentative hypocenter of the main shock falls below this plane (Allen and others, this report), but its depth determination is probably reliable to only $\pm$ 4 km.

Focal mechanisms of aftershocks in this region are similar to that for the main shock (Whitcomb, this report). The shallower events of the epicentral group probably reflect readjustment of the upper thrust plate to the main-shock dislocation.

Events of the Chatsworth segment differ significantly from aftershocks of the epicentral group.

First, their epicenters define a linear seismic zone. Second, all hypocenters fall below the thrust plane. Third, the depth determinations for these events are relatively uniform. Fourth, fault-plane solutions for aftershocks in the Chatsworth segment are consistent with left-lateral strike-slip displacement in a direction parallel to the alignment of epicenters (Whitcomb, this report). While the amount of data in this group is limited, we feel that aftershocks of the Chatsworth segment reflect tectonic accommodation different from, although not unrelated to, that occurring in the region of the epicentral group.

Aftershocks of the eastern group constitute a third grouping, on the basis of the preponderance of shallow-depth determinations and the almost random orientation of compressional and tensional axes of fault-place solutions for aftershocks in this region (Whitcomb, this report). All the hypocenters of the eastern group aftershocks fall above the thrust plane defined by the epicentral group. It is not easy to relate this diffuse zone of shallow activity to the epicentral group, despite their proximity.

It is tempting to interpret these three groups of aftershocks as defining the boundaries of the upper thrust plate on the north (eipicentral group), the west-northwest (Chatsworth segment), and the east-northeast (eastern group). The south boundary is defined by the observed surface-fault breakage and zones of severe structural damage. The base of the upper thrust plate is defined by the thrust plane. However, this interpretation does not satisfy salient features of the aftershock sequence.

We have noted that all aftershocks of the Chatsworth segment lie below the thrust plane. We interpret this activity as defining northwest margin of the lower thrust plate. Displacement along this margin is left lateral as inferred from the fault-plane solutions. The absence of events along the Chatsworth segment above the thrust plane and the absence of surficial tectonic features along the zone suggest that the upper thrust plate remained competent across this demarcation. In contrast to the Chatsworth segment, the diffuse shallow activity of the eastern group does not define such an obvious boundary. Also Whitcomb has observed no consistent pattern in the fault-plane solutions for shocks in this region. Whether this constitutes a tectonic boundary is questionable. As yet we can offer no satisfactory explanation for the shallow activity of the eastern group.

ACKNOWLEDGMENTS

Geoffrey Davies provided an invaluable service by programming the hypocentral location program for the PDP–10. We gratefully acknowledge the efforts of J. Leonard Blayney, David Johnson, John Romo, Herrmann Spetzler, and Daniel Tanner in accomplishing a rapid emplacement of the portable seismograph units of the California Institute of Technology. James Brune made the University of California, San Diego records from Little Tujunga Canyon available to us. The tectonic interpretation presented in this work was developed in collaboration with James Whitcomb.

REFERENCE

Flinn, E. A., 1960, Local earthquake location with an electronic computer: Seismol. Soc. America Bull., v. *50*, p. 457–470.

AFTERSHOCKS OF THE EARTHQUAKE

By R. L. WESSON, W. H. K. LEE, and J. F. GIBBS
U.S. GEOLOGICAL SURVEY

Twenty-six hours after the San Fernando earthquake of February 9, 1971, teams from the U.S. Geological Survey were in the field in the epicentral area, establishing a network of 19 portable seismograph stations. The installation of this network was coordinated with other groups through the Seismological Laboratory of the California Institute of Technology. The purpose of studying the aftershock sequence is to determine the dynamics of the tectonic environment in the vicinity of the San Fernando earthquake and, if possible, to delineate the surfaces at depth along which movement occurred during and after the earthquake and to determine the nature of that movement. If this aftershock sequence follows the pattern of other sequences from earthquakes of a similar magnitude, as the present (March 1971) data suggest, the aftershocks may be expected to continue for more than 2 months.

This paper describes a preliminary analysis of 40 hours of recording from 0000 GMT, February 12, to 1600 GMT, February 13. A short-time sample such as this cannot give any detail of the temporal variation of activity, but by careful study of the earthquakes recorded in this period, we hope to obtain a picture of the spatial distribution of activity. The equipment, field operations, and data processing techniques are the same as those described by Eaton, O'Neill, and Murdock (1970). The seismometer output is recorded in the field on magnetic tape. The tape can later be played back slowly to give a conventional seismogram or at high speed for selected time periods.

The network is presently composed of 19 portable stations. The locations and recording histories of these stations are listed in table 1. During the time interval under discussion, a minimum of eight and a maximum of 14 portable stations were operational. Locations of these portable stations relative to the main shock are indicated in figure 1. Readings from the portable network were supplemented for some of the larger events by readings from permanent regional networks: California Institute of Technology (four events), California Department of Water Resources (four events) the University of Southern California (15 events) and the U.S. Geological Survey telemeter station near Point Mugu.

DATA ANALYSIS

Events were selected for timing and location by two methods. In the first case, high-speed playbacks were obtained for all earthquakes with signal duration longer than 25 seconds at the U.S. Geological Survey telemeter station near Laguna Peak (SBLG), some 70 km west of the active region. This duration corresponds to a local magnitude, M_L, of approximately 2.1. All these events were timed and located as were a few smaller events which happened to occur during the playback intervals. This process yielded 62 events. Secondly, to obtain a sample of the spatial distribution of smaller shocks, nine tapes were played back at high speed continuously for a 2¼ hour period from 0545 GMT to 0800 GMT February 12. All events that were thought to be locatable were timed. A total of 102 different events were located with local magnitudes as low as 0. Of course many of the smaller events could not be timed at all the stations, resulting in locations of lower quality.

The crustal velocity model used in computing the hypocenters is listed in table 2. It is a smoothed version of the model obtained by Healy (1963) on a reversed seismic refraction line from Santa Monica Bay to Camp Roberts. The velocity model was smoothed to avoid large velocity discontinuities which complicate focal depth determinations. The U.S. Geological Survey intends to conduct a seis-

mic refraction experiment to determine with preciseness the crustal velocity structure in the San Gabriel Mountains-San Fernando Valley region before the portable stations are removed. To make a first-order correction for lateral-velocity variations, the average arrival time residuals from the location of the 62 larger events were incorporated as station corrections. All 164 earthquakes were then located with the corrected model. This process tends to improve relative locations but does not correct for systematic bias. The quality of the resulting locations is described in table 3. The bases of the quality ratings are detailed in table 4. The locations were accomplished using the HYPO71 computer program written by W. H. K. Lee.

DISTRIBUTION OF HYPOCENTERS

The epicenters and focal depths of all the aftershocks with quality A, B, and C were plotted with the observed surface ground breakage in figure 2. The epicenters occupy a large inverted U-shaped area north of the surface breakage. The maximum focal depths generally increase toward the north from 5-7 km below the zone of ground breakage to 12-15 km at the northern limit of the activity. It is possible that there is a systematic error in the focal-depth estimates.

A projection of all these hypocenters onto a north-striking plane is shown in figure 3. The maximum focal depth along the section suggests the lower boundary of a wedge or slab-shaped area of activity dipping 30° to 40° to the north. The upper boundary is less clearly defined. The apparent alinement of hypocenters at 5 km depth is an artifact of the location computation and requires special comment. The program HYPO71 does not follow a straight-forward least-squares procedure, rather it utilizes a stepwise multiple-regression scheme described by Draper and Smith (1966). At each step in the iteration, the program examines the change in each variable for its statistical significance. If a change in a variable, say depth, is not statistically significant, the variable is eliminated from the regression for that step and remains unchanged. This means, in terms of the alinement of hypocenters at 5 km, (fig. 3) that no change in focal depth from the initial trial value of 5 km was statistically significant for the given set of arrival-time observations. Actually, many of the events shown at 5 km are probably more shallow, but there were no stations close enough to establish good control.

FOCAL MECHANISM SOLUTIONS

The line segments plotted at a few of the hypocenters in figure 3 indicate the apparent dip in the north-south plane of the approximately east-trending nodal plane resulting from preliminary focal mechanism determinations. During the last 16 hours of the sample interval, clear first motions were available for several earthquakes at as many as 16 stations. In several cases these readings were adequate to indicate a tentative fault-plane solution. Several types of mechanisms were observed. Solutions indicating thrust faulting were obtained at several different locations in the active region, although other types of solutions were also tentatively indicated. In particular, solutions for two shocks on the western limb of the U and two shocks on the northeastern edge indicated strike-slip faulting. Two solutions near the northern limit indicated normal faulting.

The generally dipping aftershock activity and the tentative results from aftershock focal-mechanism solutions are in general agreement with a fault-plane solution for the main shock determined from first-motions of P waves at both near-in and distant stations. First motions from 73 stations were used. The sources are National Ocean Survey (54), U.S. Geological Survey (8), California Institute of Technology (7), California Department of Water Resources (3), and University of Southern California (1). Ray paths to the near-in stations were computed using a local velocity model. The rest were computed using the P-velocity table of Herrin (1968). The solution is shown in figure 4.

The best fitting nodal planes are:

	Nodal plane		Slip direction	
	Strike	Dip	Trend	Plunge
Fault plane	N. 108° E.	50° N.	N. 56° E.	43°
Auxiliary plane	N. 146° E.	46° SW.		

The plane listed first is similar in strike and dip to fault surfaces mapped in the San Fernando area. The surface defined by the aftershocks is also similar in strike, but it dips at a more gentle angle to the north. The sense of movement is reverse and left lateral with a ratio of dip slip to strike slip of about 2. This is similar to the displacements observed in the field along well-exposed fault surfaces.

MAGNITUDES

The relationship of areal distribution to magnitude is shown in figure 5. The larger shocks are

concentrated around the periphery of the inverted U, while with few exceptions only smaller shocks occur in the interior. This concentration of large shocks on the periphery of the zone of activity is supported by the locations of the aftershocks magnitude 3.0 and above through February 23 obtained by the California Institute of Technology (1971). Therefore, this is not a bias in our time sample, but a true areal variation.

DISCUSSION AND WORK IN PROGRESS

It is hazardous at this point to speculate on the eventual conclusions of this study. The faulting associated with the San Fernando earthquake and its aftershocks is quite complex. We expect to locate several hundred more events to refine the spatial distribution of activity and to establish any temporal variations. Preliminary results suggest that focal-mechanism solutions will be extremely helpful in deciphering the complex pattern of faulting.

Despite the hazards, observations obtained thus far provide a firm basis for a working hypothesis. The inverted U-shaped pattern of activity, particularly the concentration of relatively large events on the periphery, and the ground breakage to the south seem to define the areal extent of a thrust sheet clearly. The distribution of focal depths and the nature of the focal-mechanism solutions indicate the principal plane along which slippage took place. This aftershock sequence provides a rare opportunity to study the three-dimensional character of a thrust sheet and the associated faulting.

ACKNOWLEDGMENTS

The authors wish to acknowledge the cooperation of the Seismological Laboratory of the California Institute of Technology, the California Department of Water Resources, the National Ocean Survey, and Professor Leon Teng of the University of Southern California. Ed Criley, John Coakley, and Steven Gallenthine of the U.S. Geological Survey installed and continue to operate the portable network. This research was carried out while one of the authors (R. L. W.) was pursuing an NRC-USGS Post-Doctoral Research Associateship.

REFERENCES

California Institute of Technology, Division of Geological and Planetary Sciences, 1971, Preliminary Seismological and Geological Studies of the San Fernando, California, Earthquake of February 9, 1971, Seismol. Soc. America Bulletin. In press.

Draper, N. R., and Smith, H., 1966, Applied regression analysis: New York, John Wiley & Sons, 407 p.

Eaton, J. P., O'Neill, M. E., and Murdock, J. N., 1970, Detailed study of the aftershocks of the 1966 Parkfield-Cholame, California, earthquake: Seismol. Soc. America Bull., v. 60, p. 1151-1197.

Healy, J. H., 1963, Crustal structure along the coast of California from seismic-refraction measurements: Jour. Geophys. Res., v. 68, p. 5777-5787.

Herrin, E., ed., 1968, Special number—1968 Seismological tables for P phases: Seismol. Soc. America Bull., v. 58, no. 4, p. 1196-1219.

TABLE 1.—*Portable station list—San Fernando earthquake, February 1971*

Station code	Location	Latitude	Longitude	Elevation (m)	Date and time of installation (PST)	
VAN	West of Van Norman Lake	34°17.66′	118°29.42′	358	2/10	15:23
OIL	Placenita Oil Field	34°23.78′	118°29.39′	588	2/10	15:30
AGD	Agua Dulce Canyon	34°26.65′	118°19.98′	622	2/11	13:05
BRD	Bear Divide	34°21.60′	118°23.85′	863	2/11	19:00
DOC	Doane Canyon	34°17.16′	118°18.88′	530	2/10	17:00
GRO	Griffith Park Observatory	34°07.08′	118°17.95′	344	In 2/11 out 2/13	17:05
GRG	Griffith Park-Girls Camp	34°07.65′	118°18.75′	244	2/13	
DUB	Dubois Farm	34°17.10′	118°22.83′	384	2/11	11:10
MAY	May Canyon-Sylmar	34°19.78′	118°25.73′	497	2/11	21:45
CHL	Charley Peak-Castaic	34°31.00′	118°34.94′	631	In 2/10 out 2/16	10:05
JOS	Josephine Peak Road	34°16.67′	118°08.59′	1335	2/12	
NIL	Niles Ranch-Aliso Canyon	34°24.91′	118°07.31′	1150	2/12	
TRP	Trippet Ranch-Topanga	34°05.43′	118°35.11′	421	2/12	
SUS	White Oaks Park-Santa Susanna	34°17.34′	118°39.75′	378	2/12	
TRC	Trail Canyon off Big Tujunga Canyon	34°18.94′	118°15.67′	945	2/12	
PIC	Pico Canyon, west of Newhall	34°22.42′	118°37.12′	532	2/15	
QAL	Quail Spring	34°23.85′	118°17.14′	1237	2/14	
SPL	Near Sierra Pelona Lookout, south of Bouquet Reservoir	34°33.76′	118°21.34′	1454	2/14	
CWC	Cold Water Canyon	34° 7.80′	118°24.25′	307	2/14	
OAK	Oak Spring	34°27.44′	118°23.44′	529	2/26	
HAS	Haskell Canyon	34°30.20′	118°28.75′	716	~2/16	

TABLE 2.—*Smoothed crustal model*

Velocity (km/sec)	Depth (km)
3.2	0.0
3.6	.5
4.0	1.0
4.4	1.5
4.7	2.0
5.1	2.5
5.4	3.0
5.6	3.5
5.8	4.0
5.9	4.5
6.0	5.0
6.4	14.5
6.8	15.0
8.2	32.0

TABLE 3.—*Quality of locations*

Quality (Q)	Number of locations
A	5
B	54
C	70
D	35
Total	164

TABLE 4.—*Bases of the quality ratings*

Q	*Epicenter*	*Focal depth*
A	Excellent	Good
B	Good	Fair
C	Fair	Poor
D	Poor	Poor

Q is based on both the nature of the station distribution with respect to the earthquake and the statistical measure of the solution. These two factors are each rated independently according to the following scheme:

Station distribution

	NO	*GAP*	*DMIN*
A	≥ 6	$\leq 90°$	$\leq$DEPTH or 5 km
B	≥ 6	$\leq 135°$	$\leq 2 \times$ DEPTH or 10 km
C	≥ 6	$\leq 180°$	≤ 50 km
D	Others		

Statistical measures

	RMS (sec)	*ERH (km)*	*ERZ (km)*
A	<0.15	≤ 1.0	≤ 2.0
B	<0.30	≤ 2.5	≤ 5.0
C	<0.50	≤ 5.0	
D	Others		

Q is taken as the average of the ratings from the two schemes, that is, an *A* and a *C* yield a *B*, and two *B*'s yield a *B*. When the two ratings are only one level apart the lower one is used, that is, an *A* and a *B* yield a *B*.

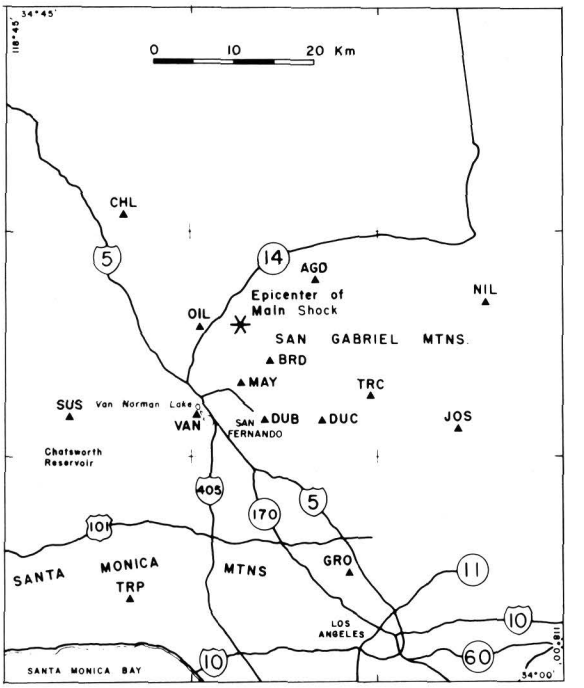

FIGURE 1.—Location of portable seismograph stations used for preliminary analysis.

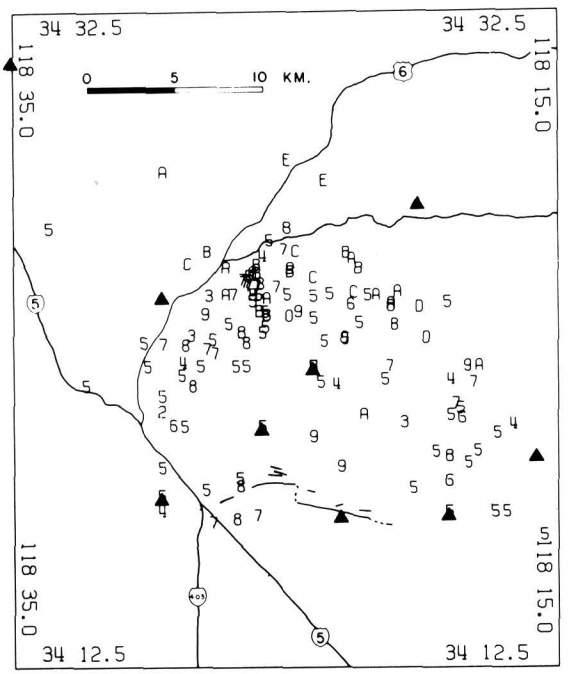

FIGURE 2.—Epicenters and focal depths of all A, B and C quality shocks. The symbols 0-9 and A-E indicate focal depths of 0 through 15 kilometers. Also indicated is the surface ground breakage. The maximum depths of the shocks generally increase to the north.

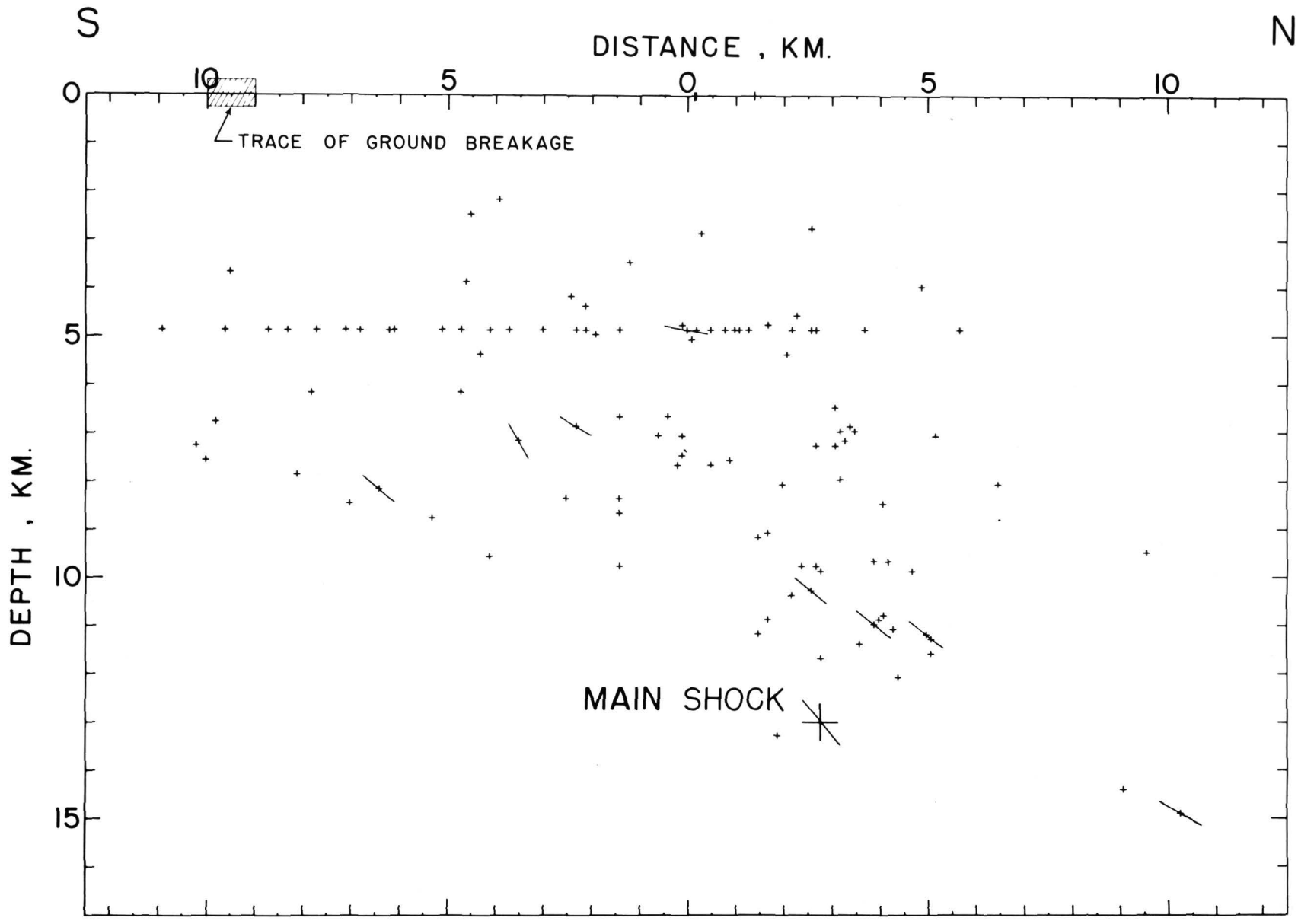

FIGURE 3.—Projection of all A, B and C quality hypocenters onto a north-striking vertical plane. Line segments indicate apparent dips in this plane of nodal planes from fault-plane solutions discussed in text. Also indicated are the trace of ground breakage and the hypocenter of the main shock as located by the California Institute of Technology (1971). The origin of the horizontal coordinates is 34°22.5′.

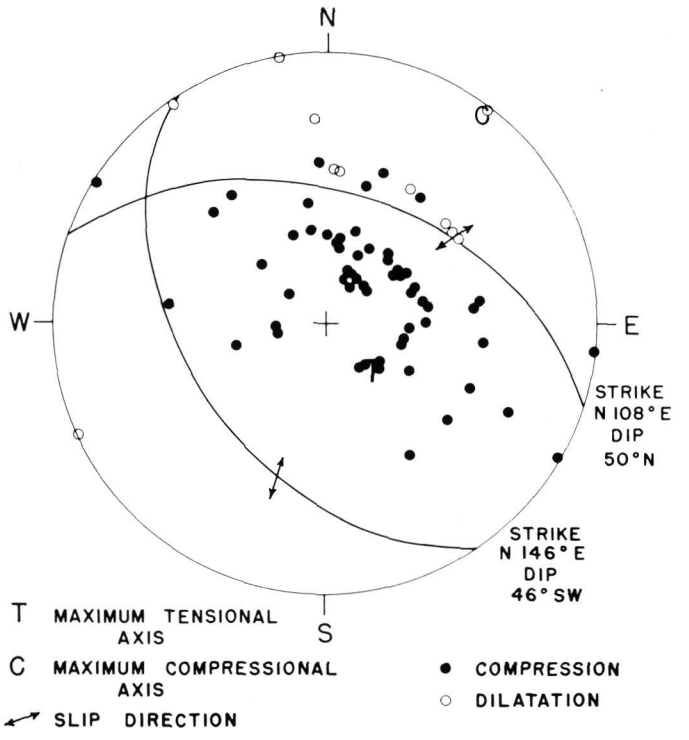

FIGURE 4.—Fault-plane solution from P-wave first motions of the main shock of the San Fernando earthquake. The plot is an equal area projection of the lower focal hemisphere.

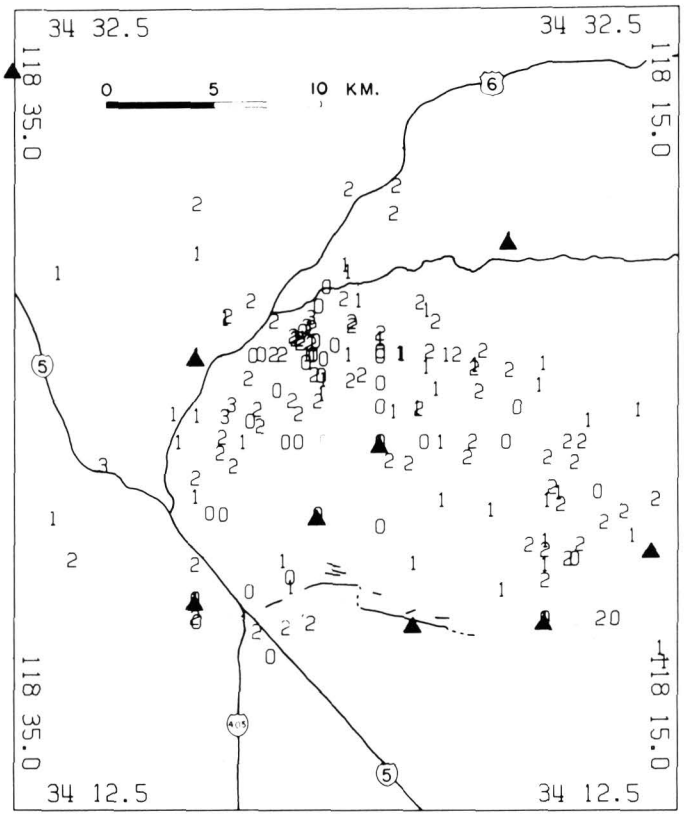

FIGURE 5.—Magnitudes of all located shocks. The larger shocks are concentrated on the periphery of the active zone.

FAULT-PLANE SOLUTIONS OF THE FEBRUARY 9, 1971, SAN FERNANDO EARTHQUAKE AND SOME AFTERSHOCKS [1]

By JAMES H. WHITCOMB

SEISMOLOGICAL LABORATORY, CALIFORNIA INSTITUTE OF TECHNOLOGY

This paper presents a preliminary look at the focal mechanisms of the February 9, 1971, San Fernando earthquake and 22 of the larger aftershocks during the first 3 days following the earthquake. (See table 1.) The location of the event was most advantageous for deriving first motions due to its occurrence in the midst of the seismic network of the California Institute of Technology in southern California. The only focal-sphere "hole" lay to the southwest in the Pacific Ocean, but fortunately this has not greatly limited the solution.

TABLE 1.—*Aftershocks recorded during first 3 days following the February 9, 1971, San Fernando earthquake*

[Focal-mechanism solutions are presented in figure 2. Depths are from Hanks and others, this report]

Aftershock	Date	Origin time		M_L	Depth km
		Hr	*Min*		
1	Feb. 9, 1971	15	10	4.1	
2	----do----	15	38	4.2	
3	----do----	15	58	5.1	
4	----do----	16	19	4.3	
5	Feb. 10, 1971	01	38	4.0	
6	----do----	03	12	4.0	
7	----do----	05	06	4.6	
8	----do----	05	18	4.6	
9	----do----	07	27	4.1	
10	----do----	13	49	4.2	
11	----do----	14	35	3.8	
12	----do----	17	38	4.3	
13	----do----	18	54	4.1	
14	----do----	23	42	3.3	<5
15	Feb. 11, 1971	00	30	3.4	<5
16	----do----	04	07	3.2	11
17	----do----	07	33	3.1	13
18	----do----	09	24	3.2	<5
19	----do----	11	32	3.1	<5
20	----do----	14	21	3.3	<5
21	----do----	19	35	3.5	
22	----do----	23	35	3.5	

The aftershocks were chosen mainly on the basis of magnitude and the availability of locations at the time this paper was written. All fault-plane solutions were constructed independently of each other without reference to their epicentral location. Only stations received by California Institute of Technology have been used thus far for the aftershocks. This limits the resolution of the dip of nodal planes somewhat, but it has been possible to determine quite well the general type and orientation of the focal mechanisms for most of the shocks above magnitude M_L=3.0.

MAIN EVENT

Figure 1 shows the fault-plane solution calculated from P-wave first motions plotted on the lower focal hemisphere. With the assumption of a double-couple mechanism, the two thrust planes derived have the following parameters: Strike = N. 26° W., dip = 44° SW. and strike = N. 64° W., dip = 52° NE. The latter is the preferred fault-plane choice based on the observed surface faulting. The northeast-dipping plane is well defined by a nodal line projecting through central California, Oregon, and Washington and by the dilatation at LASA. The strike of the secondary plane is fairly well defined by close-in stations. However, these stations, which plot near the rim of the projection, are expected to have more variability because they are most affected by lateral crustal-velocity discontinuities. Thus, the secondary plane, and in turn the slip-vector azimuth, are subject to the most error. The slip vector in the fault plane is shown in figure 1 and defines movement with a plunge of 45° and a rake of 64°. The ratio of throw or vertical motion to strike-slip is predicted to be about 1.6 to 1. A projection down the calculated fault plane from the observed surface faulting towards the epicenter yields a focal depth of about 15 km (kilometer) for the initiation of the main shock.

AFTERSHOCKS

Judging from their position with respect to the main epicenter and the observed surface faulting, most of the aftershocks seem to bound a thrust block along lines striking southwest and southeast

[1] Contribution No. 1991, Division of Geological Sciences, California Institute of Technology, Pasadena, California 91109.

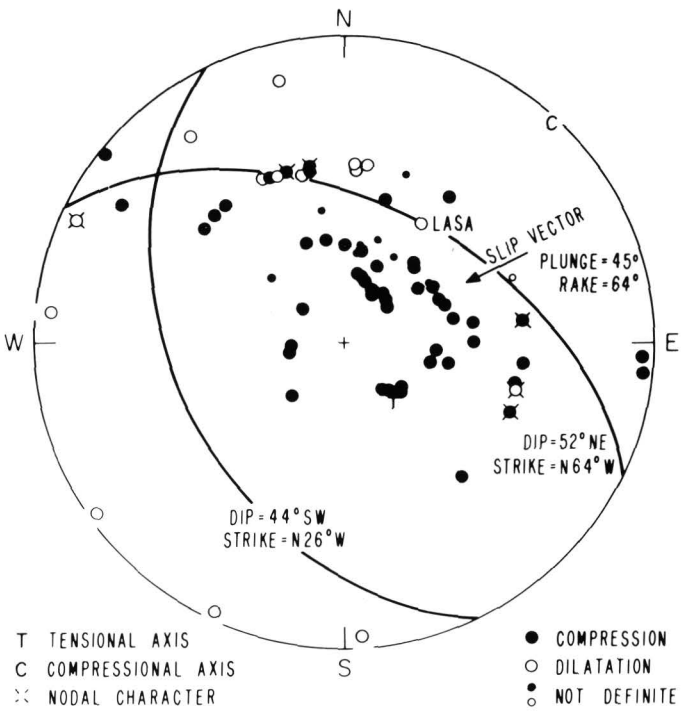

FIGURE 1.—Focal-mechanism solution for main shock of the February 9, 1971, San Fernando earthquake. Equal-area projection of P-wave first motions on lower focal hemisphere. Take-off angles were calculated using a crustal model with the CIT208 P-wave velocity model and a focal depth of 14 km. Readings were made by the author for southern California stations and were provided by various sources for the remaining stations. A complete listing of all readings is available on request.

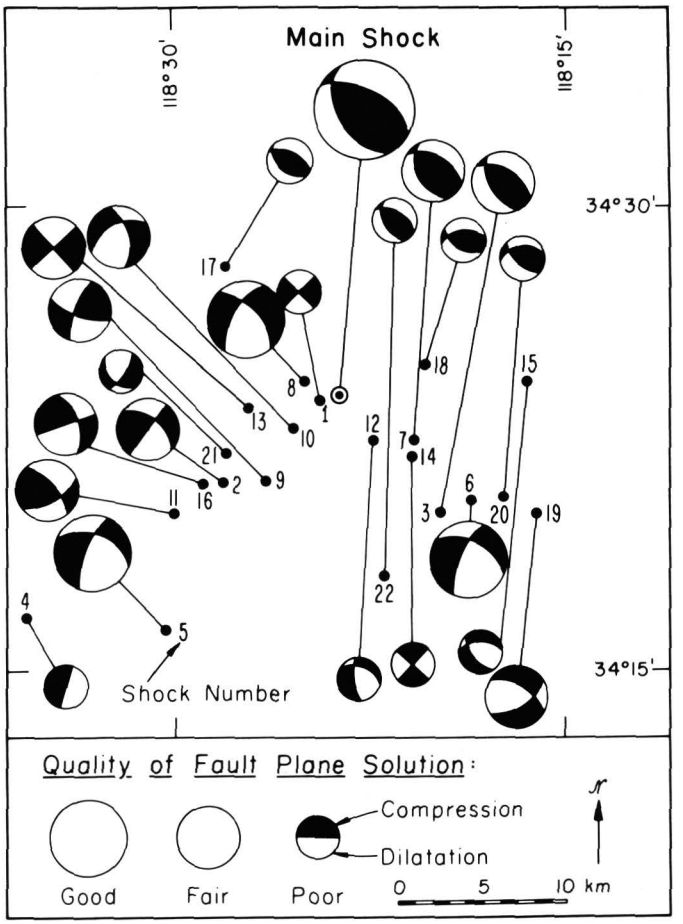

FIGURE 2.—Focal-mechanism solutions of 22 aftershocks of the February 9, 1971, San Fernando earthquake. The schematic solutions are on equal-area projections of the lower focal hemisphere. For a listing of the events see table 1.

from the main epicenter (Allen and others, this report). Figure 2 shows schematic diagrams of the focal-mechanism solutions (lower hemisphere) for the 22 aftershocks done thus far and given in table 1. Note that only six of the 22 aftershock fault-plane solutions have thrust mechanisms like the main shock and that three of these are separated from the main groups of aftershocks. Event 17 is northwest of the main epicenter and has a focal depth of about 13 km (Hanks and others, this report). Event 18 is east of the epicenter and has a shallow focal depth (<5 km). Event 22 is south of the main epicenter and presumably lies in the main thrust plane near the observed surface faulting. The remaining three thrust solutions, events 3, 7, and 20, are in the southeast-trending line of aftershocks.

Let us consider the hypothesis that the aftershock activity is a continuation of failure along the edges of the thrust plane associated with the main shock and with the same sense of motion—that is, a thrust plane dipping north-northeast. Events 3, 7, and 20 agree with this hypothesis. The last of these is about 10 km from the main epicenter and gives a shallow focus (<5 km, Hanks and others, this report) which would be expected. The southwest line of aftershocks, however, does not have a thrust focal mechanism in the events studied thus far. All the remaining solutions in figure 2 do not have more than small thrust components.

Now let us consider only motion of an overthrust block bounded by strike-slip faults along the two lines of aftershocks which strike southeast and southwest from the main shock. The edges of the overthrust block should then have right-lateral slippage along the southwest line and left-lateral slippage along the southeast line. There is only one solution in figure 2 that fits this picture; it is event 14 on the southeast line of aftershocks. A depth estimate for event 14 indicates a shallow (<5 km) focus (Hanks and others, this report) which is compatible with this hypothesis. The southwest line shows no solutions that are right-lateral, which is not compatible with the hypothesis that strike-slip

faults bound the upper thrust block. This does not preclude the possibility, however, that further investigation will find solutions of this type.

Another model to be considered would have the lower thrust block bounded by southwest- and southeast-trending strike-slip faults along the lines of aftershocks, with the upper thrust block immobilized by the crust to the north. By this hypothesis, the lower thrust block would have slipped along these strike-slip faults, resulting in left-lateral motion along the southwest line and right-lateral motion along the southeast line of aftershocks. The southeast line has only one solution, event 6, which is compatible with right-lateral strike-slip motion. Significantly, on the southwest line, all the solutions in figure 2 (except anomalous event 4) are compatible with left-lateral strike-slip on a nearly vertical southwest-striking fault plane. The only focal depth thus far determined for this group is 11 km for event 16 (Hanks and others, this report). These observations present a strong case for the hypothesis that the southwest-striking line of aftershocks represents motion of the lower thrust block against a block to the northwest along a left-lateral strike-slip fault. This mechanism also provides a convenient explanation for the aftershocks that extend more than 10 km southwest of the observed traces of surface faulting.

Three solutions near the southeast line of aftershocks show normal faulting with north or northeast-trending tension axes, events 12, 15, and 19. The last two have shallow focal depths (<5 km, Hanks and others, this report). These events may represent a local response to release of compressive stress in the upper thrust block by the main earthquake. This agrees with both the calculated and the observed response of the strain field to the main event in this direction (Junkels and Anderson, this report).

CONCLUSIONS

The overall tectonic picture of the main event and subsequent motions, based on the fault plane solutions obtained thus far, can be represented by a main thrust-fault plane striking N. 64° W., dipping about 52° to the northeast and having a left-lateral strike slip component. The upper thrust block is probably stuck to the crustal material to the northwest but is breaking up in a complicated pattern along the southeast aftershock zone. The lower underthrust block is actively slipping with left-lateral motion against the block to the northwest along a nearly vertical strike-slip fault which extends from the main-shock focus southwest along that aftershock zone to a point that lies at least 10 km south of the observed surface faulting.

The apparent asymmetry of the types of failure around the symmetrical aftershock pattern is probably due to the direction of the axis of maximum compression. Instead of a north-south compression symmetrical with the aftershock pattern and with the major strike-slip faults of the region, the axis of compression derived for the main shock trends northeast-southwest. This direction would favor a preexisting southwest-trending strike-slip fault and increase the normal stress on a southeast-trending strike-slip fault. This normal stress would promote complex failure, rather than simple strike-slip offset, on the southeast-trending fault zone after the thrust movement associated with the main shock.

ACKNOWLEDGMENTS

The first-motion data that was promptly provided by individuals and organizations too numerous to mention here is greatly appreciated. This work was aided by many discussions with Don Anderson, Clarence Allen, Peter Molnar, Thomas Hanks, Bernard Minster, and Thomas Jordan.

MICROEARTHQUAKES ON THE SAN ANDREAS FAULT AND AFTERSHOCKS OF THE SAN FERNANDO EARTHQUAKE [1]

By CHRISTOPHER H. SCHOLZ
LAMONT-DOHERTY GEOLOGICAL OBSERVATORY OF COLUMBIA UNIVERSITY

Summary

Within 36 hours of the San Fernando earthquake, four portable microearthquake stations were installed along the nearby San Andreas fault. The purpose of the study was to determine if the San Fernando earthquake produced an increase in microearthquake activity along that section of the fault. Instruments were located at a total of five sites evenly spaced from Gorman to Valyermo and operated for 4½ days at high magnification. Thousands of aftershocks were recorded, but only 16 events could be identified from S-P times as possibly originating from the San Andreas fault. To date, only two of these have been positively identified as local to the San Andreas. Even if all events are proved on further study to be local to the San Andreas, the rate of about one event per day at each site is not a significant increase over the activity observed in 1966 by J. N. Brune and C. R. Allen.

For the first 120 hours following the main shock, aftershock activity decayed exponentially with an exponent near −1, as is normal. The aftershock epicentral distribution was determined statistically from S-P time distributions at several stations. Most aftershocks fell within an area 25 km (kilometers) wide directly to the southwest of the main shock. The most intense activity occurred in a 5- to 10-km-wide band trending 15 km southwest from the main shock, with a secondary parallel zone of high activity 10 km to the southeast. First motions from the majority of aftershocks are consistent with thrust faulting with a left-lateral component on an east-west fault, similar to that observed from surface ruptures. This mechanism is compatible with the strain accumulation field in this region.

INTRODUCTION

The San Andreas fault zone lies approximately 20 km (kilometers) north of the epicenter of the San Fernando earthquake. That part of the San Andreas has not had a major earthquake since 1857 and therefore may be a likely site of high stress and possibly the site of the next great California earthquake (Allen and others, 1965). It therefore seemed important to monitor that region to determine if seismic activity had increased there as a result of the nearby San Fernando earthquake. This possibility did not seem unlikely because an earthquake of similar size, the Borrego Mountain earthquake of 1968, produced movement on faults as distant as 70 km from the epicenter (Allen and others, 1968).

MICROEARTHQUAKES ON THE SAN ANDREAS FAULT

On February 9, 1971, immediately after the San Fernando earthquake, efforts were initiated at the Lamont-Doherty Geological Observatory to prepare four portable high-gain microearthquake systems for this study. In spite of difficulties due to emergency restrictions around the epicentral region, three of these instruments were installed early the following day. The fourth station was installed 2 days later. These stations are shown on the map (fig. 1) and pertinent data are given in table 1.

The network was operated for 4½ days. On February 12, station LSV was pulled out and reinstalled at site BRC. All stations were within a few kilometers of the San Andreas fault, and the site distribution gave complete coverage along the 100-km-long segment from Gorman to Valyermo. The instruments were run at high gain (10^6 at 20 hertzes).

Thousands of aftershocks were recorded at each site. The records were carefully searched for events with anomalously low S-P times, and correlation between stations was attempted for such events. Of these, more than two-thirds were rejected as aftershocks not originating from the San Andreas region. To date, only 16 events have been recognized as possibly local to the San Andreas fault. These are listed in the table opposite the closest station and are grouped in three categories. The two events in category A were well recorded at two or more stations

[1] Contribution 1630, Lamont-Doherty Geological Observatory.

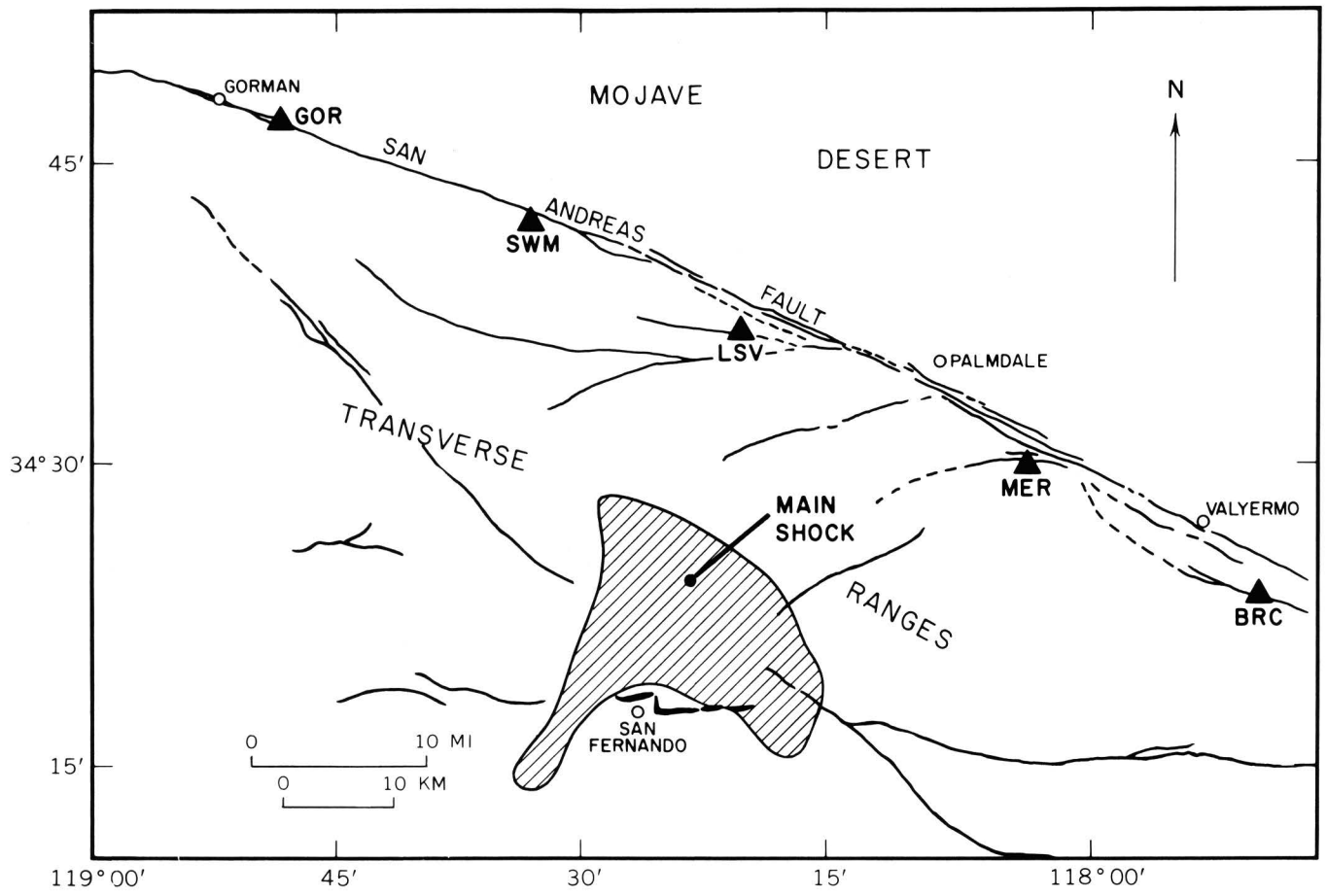

FIGURE 1.—Map of epicentral and adjoining regions, showing major faults. The triangles are temporary seismograph stations installed for this study. The crosshatched area gives the approximate distribution of aftershocks, and the heavy lines, surface ruptures of the San Fernando earthquake. Epicenter of main shock and area of aftershocks are from the section by Allen and others.

TABLE 1.—*Aftershocks originating from the San Andreas fault region during a 4½-day period following the San Fernando earthquake*

Station (fig. 1)	North latitude	West longitude	Date and time (GMT) installed	Recording hours	Events A	Events B	Events C	Rate of events per day this study	[1] 1966
GOR	34° 46.9′	118° 48.0′	2/10/71: 1200 hours	101	2	—	1	0.7	2.0
LSV [2]	34° 36.4′	118° 19.5′	2/10/71: 2100	49	—	—	2	1.0	.0
SWM	34° 42.1′	118° 32.1′	2/10/71: 1800	95	—	2	3	1.2	.0
MER	34° 29.8′	118° 02.4′	2/12/71: 1600	57	—	2	4	2.5	1.0
BRC	34° 23.0′	117° 46.3′	2/12/71: 2300	48	—	—	—	.0	5.0

[1] Rates measured by Brune and Allen (1967).
[2] Pulled out February 12, installed at site BRC.

A. Well recorded at two or more stations.
B. Well recorded at one station.
C. Doubtful.

and can definitely be considered local to the San Andreas fault. They occurred 4 minutes apart on February 13. The events in category B were well recorded at one station and are considered likely local events. Those listed under C are considered doubtful.

The resulting rates of seismic activity for the several sites ranged from 0 to 2.5 events per day. These are listed in the table with comparable rates measured in 1966 by Brune and Allen (1967). Three of the sites had slightly higher rates of activity than in 1966, but two were less active. One wonders, of course, how reproducible such low rates should be. Brune and Allen's four sites in the Carrizo Plains northwest of the present study area were reoccupied in 1968 with results that agreed completely with the earlier study (C. H. Scholz, unpub. data). On the other hand, a magnitude 3.4 earthquake on February 28, 1969, near Palmdale produced a considerable number of very local aftershocks (Max Wyss, unpub. data). Thus, in view of these uncertainties, plus the possibility that a number of the class C shocks noted above were misinterpreted aftershocks, it seems clear that no significant increase in seismic activity occurred on the San Andreas fault as a result of the San Fernando earthquake.

During the course of this work, numerous roads that cross the San Andreas fault trace were examined for possible cracking due to fault slip. No such cracking was observed.

AFTERSHOCKS OF THE EARTHQUAKE

As noted above, thousands of aftershocks were recorded at each site. Although the stations were not installed for optimum study of the aftershock sequence, it was of interest to see how useful a few rapidly installed portable stations could be in determining the characteristics of the sequence.

In figure 2 is shown the decay of activity recorded at SWM. The sequence obeys an exponential decay law. The solid line, for guidance, has a slope of -1, which is a normal decay rate for aftershock sequences. As can be observed, the actual decay rate is very close to this.

The spacial distribution of aftershocks was determined statistically by reading S-P times for a large number of uncorrelated events at several sites. Histograms of S-P times were then constructed for each site, giving the distribution of aftershocks with distance from site. Concentric rings corresponding to different S-P times could then be drawn on a map. Such rings from two stations intersect to define two alternative regions within which the relative activity can be determined, provided that it can be assumed that the aftershocks originated beneath one of the two alternative regions. Comparison of the area of aftershocks in figures 1 and 3 indicates that this is indeed a reasonable assumption.

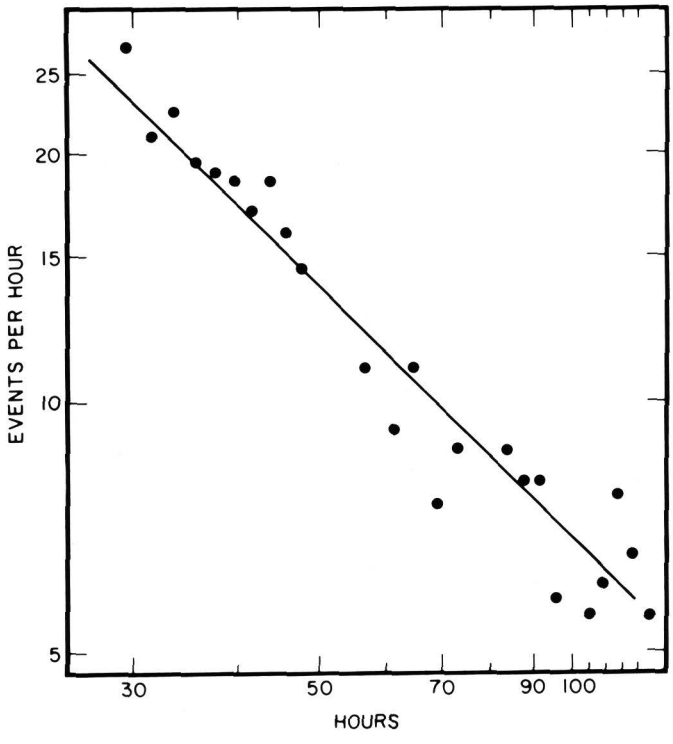

FIGURE 2.—Decay curve for aftershocks recorded at station SWM.

A map of the aftershock zone shown in figure 3 was constructed as noted above, using 200 events from stations GOR and MER. About 80 percent of our aftershocks occurred within both alternative regions, one of which corresponds with the area of aftershocks delineated in figure 1. The activity within each subregion of figure 3 is given as the percentage of the total number of aftershocks expected, on a statistical basis, to lie within that subregion.

The aftershocks appear to have been concentrated in a zone 25 km wide directly to the southwest of the main shock and north of the zone of surface faulting. The most intense activity formed a band 5-10 km wide trending 15 km southwest from the epicenter of the main shock. A secondary trend of activity parallels the most intense zone 10 km to the southeast.

First motions are dominantly up at stations GOR and SWM and down at LSV, MER, and BRC. These motions are consistent with thrust faulting with a left-lateral strike-slip component on an east-west

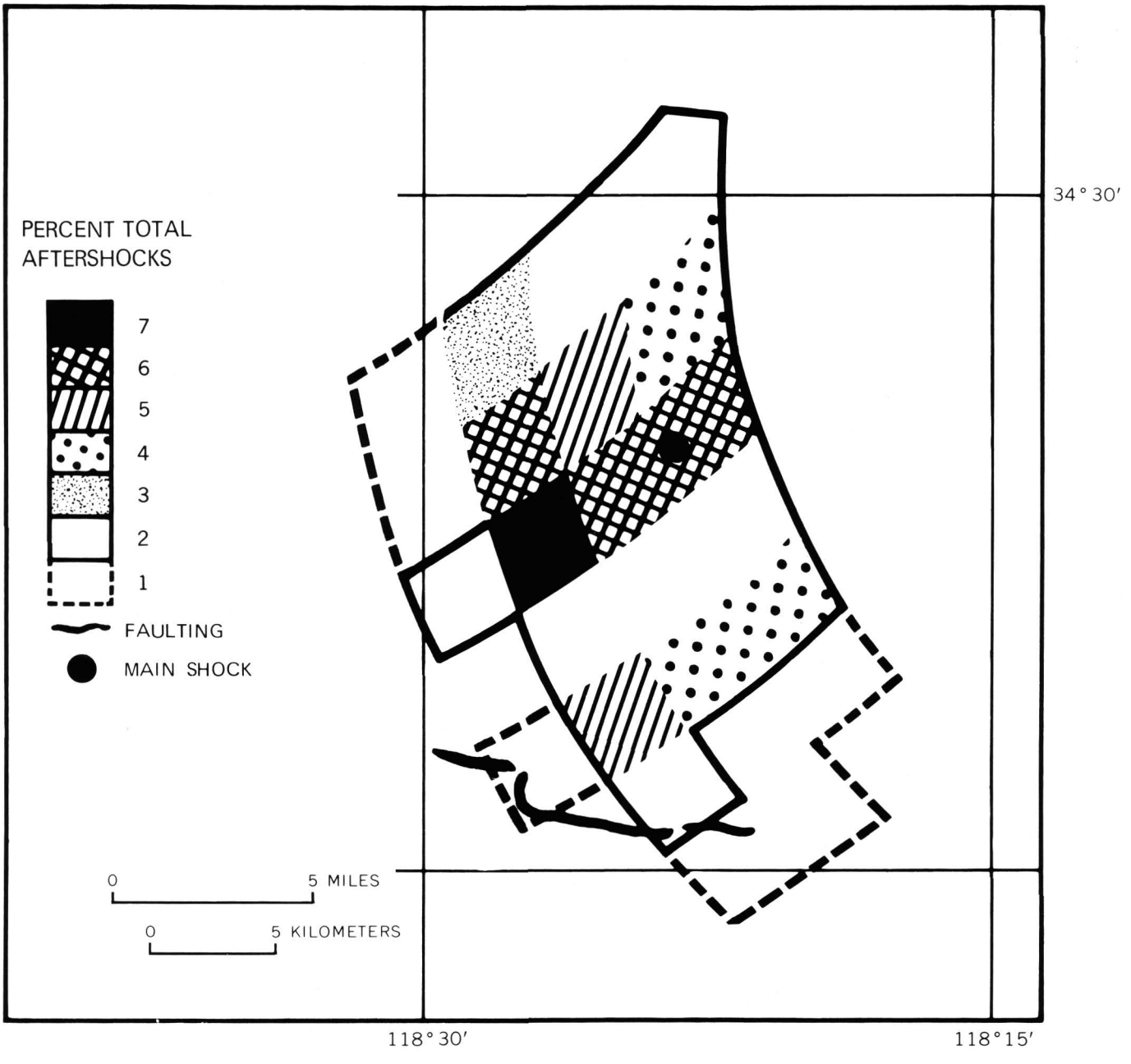

FIGURE 3.—Statistical distribution of aftershocks inferred from S-P time distributions at two stations (GOR and MER).

striking, north-dipping fault, that is, the motions are consistent with the evidence from surface rupturing. There appear to be enough exceptions, however, to suggest that a significant number of aftershocks have different mechanisms.

DISCUSSION

The San Fernando earthquake apparently occurred on one of the east-west-trending thrust faults of the Transverse Ranges, and involved thrusting to the south with some left-lateral movement. This seems to agree with the general state of stress for that region. Disregarding the poorly described 1857 earthquake, the only other major earthquake in the region of the east-west bend in the San Andreas fault system was the 1952 Kern County earthquake, which also involved thrust faulting with a left-lateral component. Both of these earthquakes thus

had slip vectors nearly perpendicular to the San Andreas fault. This agrees with geodetic evidence (Scholz and Fitch, 1969; Miller and others, 1969) which shows that strain accumulating in that region is nearly uniaxial compression perpendicular to the San Andreas fault.

The above also suggests that high shear stress is not now building up on that segment of the San Andreas. A lack of high shear stress now would explain why that region was unaffected by the San Fernando earthquake.

ACKNOWLEDGMENTS

I thank Max Wyss and John Lahr for their assistance in the fieldwork, and the enthusiastic group of colleagues and students who helped get us into the field quickly. This project was supported by the National Science Foundation under grant GA 22709.

REFERENCES

Allen, C. R., St. Amand, Pierre, Richter, C. F., and Nordquist, J. M., 1965, Relationship between seismicity and geologic structure in the Southern California region: Seismol. Soc. America Bull., v. 55, p. 753-797.

Allen, C. R., Grantz, Arthur, Brune, J. N., Clark, M., Sharp, R. V., Theodore, T., Wolfe, E., and Wyss, Max, 1968, The Borrego Mountain, California earthquake of 9 April 1968, A preliminary report: Seismol. Soc. America Bull., v. 58, p. 1183-1186.

Brune, J. N., and Allen, C. R., 1967, A microearthquake survey of the San Andreas fault system in Southern California: Seismol. Soc. America Bull., v. 57, p. 277-296.

Miller, R. W., Pope, A. J., Stettner, H. S., David, J. L., 1969, Crustal movements investigations—triangulations, Taft-Mojave area: U.S. Coast and Geod. Survey Operations Data Rept. DR-6, 85 p.

Scholz, C. H., and Fitch, T., 1969, Strain accumulation along the San Andreas fault: Jour. Geophys. Research, v. 74, p. 6649-6666.

PRELIMINARY SOURCE PARAMETER DETERMINATION OF THE SAN FERNANDO EARTHQUAKE [1]

By MAX WYSS
LAMONT-DOHERTY GEOLOGICAL OBSERVATORY OF COLUMBIA UNIVERSITY

Abstract

The seismic moment ($1.5 \cdot 10^{26}$ dyne cm) and the source dimensions ($8<r<21$ km) of the San Fernando, Calif., earthquake are estimated from teleseismically recorded P-waves and compared with the same parameters obtained from field observations. From the combined teleseismic and field data, the dislocation (100 cm) and stress-drop (30 bars) are estimated.

INTRODUCTION

The purpose of this paper is to supplement and improve by the use of teleseismic data the preliminary source-parameter estimates based on field observations.

Based on dislocation theory, the strength of a seismic source, the seismic moment M_0, can be estimated from the long period part of displacement spectra. To obtain the moment from P-waves, the theoretical results of Keilis-Borok (1959) and Ben-Menahem et al. (1968) were used. For surface waves the tabulated excitation functions of Ben-Menahem et al. (1970), which are based on earlier results by Ben-Menahem and Harkrider (1964), were used.

A second basic source parameter that can be estimated from body-wave spectra is the source dimension r. It has been recognized by several authors that the peak/corner frequency of the seismic spectrum must be a function of the source dimension (e.g., Kasahara, 1957, Berckhemer and Jacob, 1968; Archambeau, 1968). In the test case of the Borrego Mountain, Calif., earthquake, which produced a well-documented surface rupture and aftershock zone (Allen et al., 1968), it was found that the recent theory by Brune (1970) best predicted the source dimensions r from body-wave spectra. Brune's (1970) relation between corner frequency f_0 and the source area A is

$$A=\frac{1.1^2\,\alpha^2}{\pi f_0^2} \quad \text{or} \quad r=\frac{1.1\,\alpha}{\pi f_0} \tag{1}$$

where α is the P-wave velocity.

Aki (1966) showed that the moment M_0 was related to the product of fault area A times average dislocation across it D

$$M_0=\mu A D \tag{2}$$

where μ is the shear modulus. Combining the seismic moment and the source area, both determined from body wave spectra, with equation (2) one obtains the dislocation at the source D. Using the appropriate equation, one then can estimate the stress drop $\Delta\sigma$ from the ratio of D to r (Brune, 1970).

Since the moment determination is based on spectral amplitude, the error at any one station can be considerable. However, if several stations are used the errors are estimated not to exceed a factor of two. The determination of the corner frequency, and hence the source dimensions, can be reduced in accuracy by focusing effects due to a radiating source. However, if several stations at different azimuths are used, these effects will average out and the error of the final result for r will probably not exceed a factor of 2. In computing D and $\Delta\sigma$ from M_0 and A, somewhat larger errors could result. Particularly, the stress-drop critically depends on the estimated source dimension.

The accuracies with which the moment and source dimensions are determined from body-wave spectra are comparable to the accuracies of source parameters obtained from surface fracture observations. The fault-area estimate based on the aftershock distribution is more reliable than that based on teleseismic analysis. However, the relation of surface fractures to the area that ruptured during an earthquake is not always clear. In the present case, the San

[1] Contribution No. 1642, Lamont-Doherty Geological Observatory.

Fernando earthquake, the tectonic surface rupture seems to be shorter than the extent of aftershock activity, and the main zone of aftershocks appears not to be parallel to the surface break (Abrams et al., 1971). In such cases the accuracy of the source dimension and dislocation estimate based on teleseismic data and on field observations may be approximately the same. The moment determination from teleseismic data is considered superior to the field estimates because in the latter case the moment is obtained from the basic measurements by equation (2).

DATA

The seismic moment was computed from P-wave displacement spectra of four WWS stations and two high-gain instruments operated by Lamont-Doherty Geological Observatory. The moments together with the uncorrected long-period spectral amplitudes ($T>20$ sec) are given in table 1. For the moment determination the amplitudes were corrected for attenuation, geometrical spreading and the effect of the free surface at the receiver (Ben-Menahem et al., 1965). Both moment determinations based on the radiation pattern by W. H. K. Lee et al. (written commun., 1971) (USGS) and Abrams et al. (1971) (CIT) are given in table 1. Because of the more consistent results, the CIT solution is preferred. The USGS solution puts College, Alaska, on a node, which is inconsistent with our data. The average moment based on P-wave and the CIT fault-plane solution is $1.3 \cdot 10^{26}$ dyne cm.

The Rayleigh wave spectra from Stuttgart and Uppsala, at a period of 50 sec, furnished a moment of $0.8 \cdot 10^{26}$ dyne cm and $3 \cdot 10^{26}$ dyne cm, respectively. In this computation the tables published by Ben-Menahem et al. (1970) were used. The average moment obtained from surface waves is $1.9 \cdot 10^{26}$ dyne cm.

The preliminary corner/peak frequency f_0 is also given in table 1. For four stations an upper and a lower bound of f_0 was given. In the average the corner/peak frequency was found to be approximately 0.1 Hz.

The area outlined as possible fault area by the aftershocks was estimated from the aftershock data given by Abrams et al. (1971). The aftershocks occurred over an area of approximately 460 km^2. The average displacement as estimated from the surface rupture may be taken as 1. m (Abrams et al., 1971). These values for the source parameters are compared with the values obtained from P-wave analysis in table 2.

DISCUSSION AND CONCLUSIONS

The three independent moment determinations (P-wave, Rayleigh wave, field data) are in excellent agreement. Giving the three methods equal weight, the average moment of the San Fernando earthquake is $1.5 \cdot 10^{26}$ dyne cm.

The rupture area (source dimension) inferred from the P-wave spectra as compared with the aftershock area appears to be an overestimate when Brune's (1970) relation is used and an underestimate when Berckhemer and Jacob's (1968) results are used. Unlike the case of the Borrego Mountain earthquake, these preliminary data suggest that the method of Berckhemer and Jacob (1968) gives results which agree better than Brune's with the field observations (table 2). It appears that data from more azimuths are needed in order to decide which body-wave method, if any, furnishes the right source area for a thrust fault like the San Fernando earthquake. Preliminary limits for the radius of this earthquake are $21>r>8$ km.

Values for the average dislocation D are also given in table 2. They range from 31 to 220 cm. Because it is uncertain which equation should be used to compute the rupture area, the stress-drop is obtained from the moment and the dimensions of the aftershocks, rather than from body-wave spectra

TABLE 1.—*Spectral data*

Station	Distance (deg)	Azimuth (deg)	Long period amplitude (10^{-2} cm sec)	Corner frequency (Hz)	Moment (10^{26} dyne cm) USGS	Moment (10^{26} dyne cm) CIT
Umea (UME)	76.8	18	0.58	0.1	1.2	0.72
Stuttgart (STU)	85.0	32	.8	.07- .2	1.2	.86
Weston (WES)	37.0	63	1.8	.08	1.6	1.6
Georgetown (GEO)	33.3	70	2.4	.06- .08	2.0	2.1
Uppsala	78.			.1		
Clipper mine[1] (near COL)	35.3	339	1.3		7.7	1.5
Ogdensburg (OGD)	35.0	66	.7		1.0	1.0

[1] Murphy (1971).

TABLE 2.—*Source parameters*

	Moment (10^{26} dyne cm)	Source radius (km)	Area (km^2)	Displacement (cm)
P-Wave:				
(Brune)	1.3	21	1,400	31
(Berckhemer & Jacob).	1.3	8	180	240
Field Observations	1.4	12	460	100

alone. Using the average moment of $1.5 \cdot 10^{26}$ dyne cm and Starr's (1928) equation for stress-drop on dip-slip faults, we obtain approximately $\Delta\sigma = 30$ bars.

This preliminary result suggests that the San Fernando earthquake was another low stress-drop event. This supports the idea that stress-drop decreases with decreasing magnitude (King and Knopoff, 1968; Wyss, 1970). If the strength of the earth's crust is assumed to be on the order of 100 bars (Chinnery, 1964), the San Fernando earthquake relieved only approximately 30 per cent of the total stress that may have accumulated in the source region. This result suggests that the San Fernando area may not be considered immune to further earthquakes. However, it may take a very long time to accumulate the additional 30 bars necessary for another earthquake of the same size as the one on February 9, 1971.

ACKNOWLEDGMENTS

I wish to thank Mr. Modgling from the Environmental Data Service, NOAA, Dr. R. Schick, and Dr. M. Bath for furnishing data from their stations. Drs. P. Molnar, C. Scholz and B. Isacks critically read the manuscript and made helpful comments. This study was supported by the National Science Foundation NSF Grant GA-22709.

REFERENCES

Abrams, M., Allen, C., Anderson, D., Berkey, N., Carey, D., Carter, B., Davies, G., Engen, G., Foley, M., Hanks, T., Helmberger, D., Hileman, J., Jordan, T., Jungels, P., Kamb, B., Liu, H., Minster, B., Nordquist, J., Penrose, B., Silver, L., Smith, R., Thatcher, W., Thomsen, L., Whitcomb, J., and Wood, S., 1971, Preliminary seismological and geological studies of the San Fernando, California earthquake of February 9, 1971: Seismol. Soc. America Bull. [In press.]

Allen, C. R., Grantz, A., Brune, J. N., Clark, M. M., Sharp, R. V., Theodore, T. G., Wolfe, E. W., Wyss, M., 1968. The Borrego Mountain, California, earthquake of April 9, 1968. A preliminary report: Seismol. Soc. America Bull., v. 58, p. 1183-1186.

Aki, K., 1966, Generation and propagation of G waves from the Niigata earthquake of June 16, 1964, Part 2. Estimation of earthquake moment, released energy, and stress-strain drop from the G wave spectrum: Earthquake Res. Inst. Bull., v. 44, p. 73.

Archambeau, C. B., 1968, General theory of elastodynamic source fields: Rev. Geophysics, v. 6, p. 241.

Ben-Menahem, A., and Harkrider, D., 1964, Radiation patterns of seimsic surface waves from buried dipolar point sources in a flat stratified earth: Jour. Geophys. Research, v. 69, p. 2605-2620.

——— Smith, S. W., and Teng, T-L., 1965, A procedure for source studies from spectrums of long-period seismic body waves: Seismol. Soc. America Bull., v. 55, p. 203-235.

——— Rosenman, M., and Harkrider, D. G., 1970, Fast evaluation of source parameters from isolated surface wave signals: Part 1. Universal tables, Seismol. Soc. America Bull., v. 60, p. 1337.

Berckhemer, H., and Jacob, K. H., 1968, Investigation of the dynamical process in earthquake foci by analyzing the pulse shape of body waves: Final Scientific Report, AF61(052)-801.

Brune, J. N., 1970, Tectonic stress and the spectra of seismic shear waves from earthquakes: Jour. Geophys. Research, v. 75, p. 4997.

Chinnery, M. A., 1964, The strength of the earth's crust under horizontal shear stress: Jour. Geophys. Research, v. 69, p. 2085.

Kasahara, K., 1957, The nature of seismic origins as inferred from seismological and geodetic observations: Earthquake Res. Inst. Bull., v. 35, p. 473.

Keylis-Borok, V. I., 1959, On estimation of the displacement in an earthquake source and of source dimensions: Amali. Geofisica, v. 12, p. 205.

King, Chi-yu, and Knopoff, L., 1968, Stress drop in earthquake, Seismol. Soc. America Bull., v. 58, p. 249.

Murphy, A. J., 1971, High-gain, long-period seismograph station, Installation Report, Fairbanks, Alaska: ARPA Scientific Report. [In press.]

Starr, A. T., 1928, Slip in a crystal and rupture in a solid due to shear: Cambridge Philos. Soc. Proc., v. 24, p. 489-500.

Wyss, M., 1970, Observation and interpretation of tectonic strain release mechanisms: California Inst. Technology, unpub. Ph. D. thesis.

PATTERN OF FAULTING AND NATURE OF FAULT MOVEMENT IN THE SAN FERNANDO EARTHQUAKE [1]

By BARCLAY KAMB, L. T. SILVER, M. J. ABRAMS, B. A. CARTER, T. H. JORDAN, and J. B. MINSTER
DIVISION OF GEOLOGICAL AND PLANETARY SCIENCES, CALIFORNIA INSTITUTE OF TECHNOLOGY

PURPOSE AND SCOPE

In an effort to understand the mechanism of the February 9, 1971, San Fernando earthquake in relation to seismic observations and regional geology, we have gathered information on the occurrence and amount of ground displacement by surface faulting. Most of the field data were obtained within the first 4 days after the earthquake, because we wished to describe the fault features as much as possible in their pristine state. Systematic observations were made only in the area generally east of Sylmar and Olive View Hospital, that is, in the eastern part of the area strongly affected by the earthquake, where manifestations of surface faulting were particularly well developed. While our description of faulting is therefore limited to this area and while there doubtless are fault features that we have missed in the area studied, our results are presented here as a contribution to the general body of knowledge about the earthquake.

AREA STUDIED

Figure 1 shows the area of detailed study, and, in summary form, the results obtained. The geology of the area has been described by Oakeshott (1958). The San Gabriel Mountains, forming a steep escarpment at the northern edge of the area, are underlain by crystalline rocks thrust southward toward the San Fernando Valley along the north-dipping Hospital Fault, whose roughly east-west trace lies near the foot of the escarpment, about 0.7 km north of Veterans Hospital. The alluviated San Fernando Valley to the south is underlain by Tertiary sediments. These are exposed only at isolated places near the mountain front, being elsewhere deeply buried by Quaternary alluvium. East of Pacoima Wash, however, an area of foothills intervenes between the mountain front (here marked by the Lopez Fault, the apparent eastward continuation of the Hospital Fault) and the alluviated valley into which empties Big Tujunga Wash. These foothills, with relief of 90–180 m, are underlain by Tertiary sediments which, in the southern part of the hills, dip uniformly northward at about 65°.

In reconnaissance fashion we have searched for surface faulting in the San Gabriel Mountains northward from the area of figure 1 to Soledad Canyon, in the vicinity of the epcienter of the main shock.

FAULT PATTERN

Fault displacements of the ground surface that occurred in the earthquake are shown in figure 1, in as much detail as is possible at the map scale. Faulting extends almost continuously over a distance of 10 km from south of Sylmar eastward to the mouth of Little Tujunga Canyon, with small discontinuous manifestations continuing at least another 2 km farther east. This zone of faulting is here called the San Fernando fault zone. Its overall trend in the area studied is N. 72° W.

Some 2 km east of the easternmost fault feature shown in figure 1, there occurs a 1.0 m left-lateral offset of Oro Vista Avenue where it crosses Big Tujunga Wash. That this is not an isolated tectonic feature is shown by a number of indications of surface faulting in the intervening area (Perry Ehlig, personal commun.), which we have not studied. The San Fernando fault zone thus continues about 2 km beyond the eastern edge of figure 1. The total length of the zone of fault movement so defined is at least 12 km, and is comparable to the distance from the surface ruptures to the epicenter of the main shock, which lies about 13 km north of the mouth of Lopez Canyon (C. R. Allen, personal commun.).

Although the fault breaks that we studied die out westward as indicated in figure 1, other isolated manifestations of tectonic faulting, including the re-

[1] Contribution No. 1995, California Institute of Technology, Division of Geological and Planetary Sciences, Pasadena, California. Important contributions to the collection of field data for this report were made by N. Berkey, D. Carey, M. Foley, T. Hanks, D. Helmberger, H. Liu, B. Penrose, R. Smith, L. Thomsen, and S. Wood.

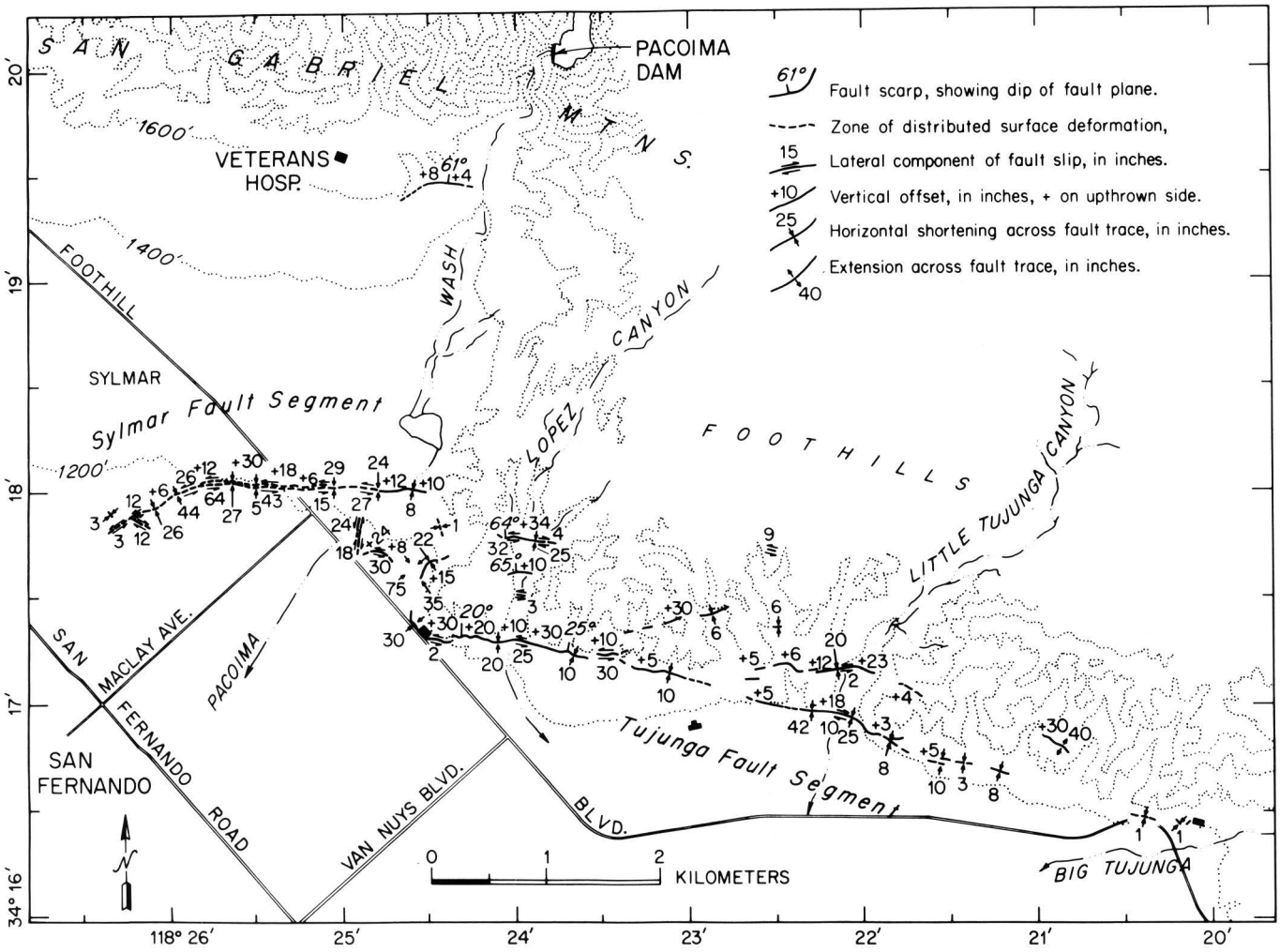

FIGURE 1.—Surface faulting in a portion of the area affected by the San Fernando earthquake. Base map from U.S. Geological Survey San Fernando and Sunland quadrangles, 1:24,000 original scale.

ported Mission Wells fault segment, may well be present west of the area of figure 1.

The fault breaks in the area studied can be conveniently placed in five groups: 1. A zone of breakage extending approximately westward from Pacoima Wash toward Sylmar, and here called the Sylmar fault segment. (See fig. 1.) 2. A fault line along the southern edge of the foothills, from Pacoima Wash eastward almost continuously to Little Tujunga Canyon and discontinuously farther eastward into the Big Tujunga; this is called the Tujunga fault segment. 3. A group of short faults within the foothills some 0.3–0.9 km north of the Tujunga segment, and trending subparallel to it. 4. A complex group of short breaks in the area between the west end of the Tujunga segment and the east end of the Sylmar segment. 5. A short fault just west of the mouth of Pacoima Canyon, which we will here call the Veterans fault, since it lies about 1 km east of Veterans Hospital (fig. 1). In the terminology used here and by the U.S. Geological Survey (this report), the Sylmar and Tujunga segments are a part of the San Fernando fault zone, which includes also the Mission Wells segment farther west. Fault groups 3 and 4 are also part of this zone, but the fault in group 5 is a separate feature.

The different groups of faults (with exception of group 5) have in common a generally east-west strike, northward dip, and combined thrust and left-lateral displacement. They differ in their relationships to the underlying bedrock, in the types of surface rupture produced, and in detailed features of attitude and displacement. The displacements along the Sylmar fault segment are generally larger than those in the other groups. The Sylmar segment reaches the surface in alluvium, and displacements along it tend to be distributed somewhat diffusely over a zone about 50 m wide, with few scarps,

"mole tracks," or other linear features of surface disruption that would allow discrete fault breaks to be traced continuously for distances of hundreds of meters. No direct observations of the fault attitude were possible. The Tujunga fault segment is for the most part a single clean break, forming a well-defined fault scarp that follows closely the topographic break at the base of the foothills. The scarp probably cuts bedrock near the surface over most of its length, but clean bedrock is rarely exposed in it because of its proximity to the bedrock-alluvium contact and because of a thick soil mantle derived by mass wasting from the slopes above. As judged from the trace where it crosses canyon mouths (for observations see fig. 1), the fault dips 20°–25° to the north and is a thrust. The faults of group 3 clearly cut and are controlled by the sedimentary rocks of the foothills. Where well exposed, the faults are seen to parallel bedding in the sediments and to dip about 65° N. They may be classified as bedding-plane reverse faults. The faults of group 3 have distinctly less lateral continuity than the Tujunga segment. The Veterans fault (group 5) is similar in having short lateral extent, and in being parallel to bedding in the enclosing Tertiary (Saugus) sediments. It dips about 60° N. Although it is a small fault, it is especially significant because it is the only definite tectonic displacement found in the zone along the foot of the San Gabriel Mountain escarpment, where the greatest recognized intensity of ground shaking occurred. Group 4 consists of a complex collection of breaks of various kinds, which do not fit the simple pattern of the other groups.

IDENTIFICATION OF TECTONIC FAULTING

The lines plotted in figure 1 represent either actual fault scarps or else zones of surface disruption that are definite and continuous enough to be considered the result of ground displacement by faulting. We avoid hypothetical interpolation between or extrapolation beyond observed features of surface faulting, even though in some examples, particularly along the Tujunga segment, the alinement of separate scarps is so good that movement along a single continuous fault surface at depth is clearly indicated.

We endeavor to omit from figure 1 any scarps or fissures caused by compaction of artificial or alluvial fill or by the motion of landslide blocks. In the Sylmar fault segment, there is relatively little possiblity of landslide motion because of the low relief; but in the foothill areas to the east, as well as in the San Gabriel Mountains to the north, very widespread landsliding took place during the earthquake. Numerous headwall fissures of landslide blocks, up to hundreds of meters in extent, are recognizable from their pattern and location on the affected slopes. A few of the scarps plotted in the foothill area of figure 1 have some attributes of such fissures but are retained in figure 1 because landslide blocks bounded by them are not recognizable as such and would have to be unexpectedly large. An example is the prominent scarp, about 1 m high located near lat 34°16.8′, long 118°20.9′. (fig. 1). If this scarp, which is accompanied by an extension crack about 1.2 m wide, were the head of a large landslide block, there should be a prominent toe somewhere lower on the slope, but none is found. It is possible that such scarps are in part tectonic in origin and have been accentuated and modified by down-slope movement, so that they take on some attributes of landslide fissures.

Scarps of the Tujunga segment have an attitude and sense of displacement appropriate to landslide toes and are consistently located near the base of the foothill front, where the toes of landslides on the steep south-facing slope of the foothills could be expected. However, the uniform northward dip of bedding in this area tends to inhibit landslide motion on these slopes. Recognizable landslides are relatively rare on the south-facing slopes, whereas they are abundant on eastward- and especially westward-facing slopes in the canyons that cut southward through the foothills. If the scarps along the southern foot of the hills were primarily toes of landslide blocks, one could expect that headwall fissures would be most prominent on the hill slopes above places where the scarps at the foot were largest. In fact, an inverse relationship is observed. The most prominent potential headwall fissure (at long 118°20.9′, fig. 1) is at a place where there is no scarp at the foot of the hills, and few indications of ground disruption there.

The scarp of the Tujunga fault segment is shown definitely to be tectonic in origin where it crosses the 0.5-km-wide mouth of Little Tujunga Canyon. In this locality there is no high ground to the north within 0.5 km of the scarp, and hence no source area for a landslide block of reasonable dimensions.

It is possible that in other places the scarps of the Tujunga fault segment contain some contribution from landsliding or general downslope motion along the front of the hills, but for the reasons given we believe that the displacements seen in these scarps are primarily tectonic in origin.

FAULT DISPLACEMENT

Figure 1 shows the slip, in inches, that occurred across the observed fault lines. In measurements repeated at given localities on different days, we found no change in displacement, and we therefore believe that essentially all the displacement occurred during the main earthquake.

In figure 1 the slip is given in terms of its vertical, lateral, and transverse components. Where the fault break has the more common form of a ramp several meters wide and where the ground surface is rough and irregular, the accuracy is as poor as ±5 inches or worse. The lateral slip component (horizontal component parallel to the fault strike) is measurable where preexisting straight features such as fences or curbs cross the fault line. In favorable situations the measurement is accurate to a fraction of an inch, but it is uncertain by 5 inches or more when the offset is distributed over many meters. Large errors arise if pre-existing jogs in streets or fence lines are not taken into account. The transverse slip component (horizontal component perpendicular to the fault strike) manifests itself either as extension or compression across the fault zone. Longitudinal shortening of street or sidewalk pavement is a very common feature of the San Fernando earthquake. Its usual form is a brittle failure of the pavement along a fracture perpendicular to the street or sidewalk and an overriding of the pavement from one side (the upthrown side, if any) over that on the other. In this situation the compression can be measured to an accuracy of about 1 inch. Compressional overthrusting along fault scarps in unpaved ground is also very common, and the amount of shortening can sometimes be determined to an accuracy of about 5 inches, particularly where turf overrides turf. Overall, the accuracy of the slip values given in figure 1 is ± 5 inches, although many values are more reliable than this.

The largest slip component in the San Fernando earthquake is left lateral and occurs near the middle of the Sylmar segment, where it reaches about 1.6 m (64 in). Left-lateral slip of up to 0.8 m (32 in) occurs in fault groups 2 and 3 but is not as consistently present as in the Sylmar segment. Vertical displacement, north side up, is shown by almost all faults. The maximum uplifts are comparable in fault groups 1 to 3 and amount to 0.8–0.9 m (30–34 in.). North-south compression across the generally east-trending faults is also a consistent feature. Transverse compressions of up to 0.8 m (30 in) are typical of fault groups 1 and 2, with a maximum of 1.1 m (42 in) recorded in Little Tujunga Canyon. Displacements are generally smaller in groups 4 and 5 than in 1 to 3.

The data in figure 1 indicate that the overall fault-displacement in the San Fernando earthquake involved nearly equal amounts of north-south compression, vertical uplift (north side up), and left-lateral slip and hence may be described as a thrusting of a northern block to the southwest over a southern block, along a fault surface dipping about 45° north.

A more detailed assessment of the fault motion is provided in table 1, which gives the displacement vector for faults of groups 1 to 3 at 13 locations where the slip components are relatively well determined. The vectors in table 1 are obtained from the slip components in figure 1 and are expressed in terms of the motion of the southern block relative to the northern. The directions of these vectors are plotted stereographically in figure 2. The grouping of the points in figure 2 reveals that in the central part of the San Fernando fault zone, from long 118°23′ to 25.8′, the displacement vectors tend to

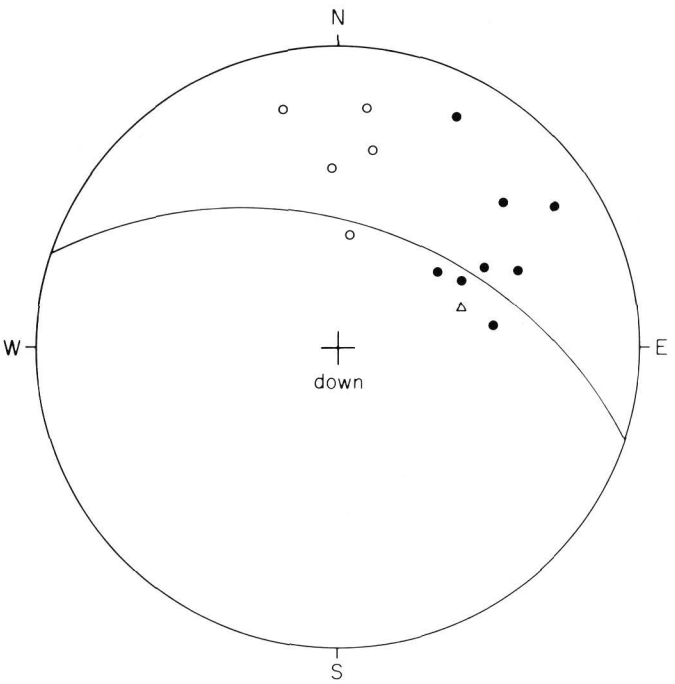

FIGURE 2.—Stereographic plot of fault displacement vectors at the localities listed in table 1. Vectors represent motion of south side of fault with respect to north side, and are plotted on the lower hemisphere. Solid circles refer to localities in the central part of the San Fernando fault zone, between longitude 118° 23′ and 118° 25.8′, open circles to localities outside this interval. The triangle is the plunge of slickensides at locality 13 in table 1. The great circle represents a fault plane striking N. 72° W. and dipping 45° north.

cluster about a plunge of 35° toward N. 60° E., whereas toward the ends of the zone the plunge azimuth swings northward. This behavior suggests that mechanical constraints require the lateral slip component to die out more rapidly toward the ends of the fault zone than the transverse component does. Relative to the overall S. 72° E. trend of the zone, the N. 60° E. plunge azimuth makes an angle of about 45°, implying equal components of lateral slip and transverse compression.

TABLE 1.—*Magnitude and direction of fault displacements*

No.	Fault group	Location		Fault slip vector (motion of south side relative to north side)				Dip of fault plane	
		Street(s)	Long 118°	Length in.	Length m	Azimuth	Plunge	Inferred	Observed
1	1	Glenoaks-Lucas	26.2′	30	0.8	N. 13° W.	12° N.	13° NW.	------
2	1	Phillippi-Chivers	25.9′	52	1.3	N. 7° E.	13° N.	15° NW.	------
3	1	Gridley	25.8′	72	1.8	N. 57° E.	9° NE.	?	------
4	1	Fernmont-Cometa	25.6′	74	1.9	N. 67° E.	24° NE.	48° N.	------
5	1	Adelphia-Harding	25.4′	53	1.3	N. 82° E.	35° E.	79° N.	------
6	1	Freeway 210	25.1′	34	.9	N. 27° E.	9° NE.	12° N.	------
7	1	Chippewa-Newton	24.8′	38	1.0	N. 49° E.	18° NE.	27° N.	------
8	2	Foothill (hospital)	24.5′	42	1.1	N. 53° E.	45° NE.	45° NE.	------
9	2	Lopez Canyon	24.0′	38	1.0	N. 61° E.	32° NE.	45° N.	25° N.
10	2	Little Tujunga (lower)	22.2′	46	1.2	N. 10° E.	23° N.	23° N.	------
11	2	0.25 km east of No. 10	22.1′	31	.8	N. 2° W.	29° N.	31° NE.	------
12	3	Little Tujunga (upper)	22.1′	31	.8	N. 6° E.	49° N.	49° N.	------
13	3	Lopez Canyon-Bailey	24.0′	53	1.3	N. 62° E.	40° NE.	53° N.	64° N.

The total fault displacements indicated in table 1 range from 0.8 to 1.9 m (31–74 in). The largest displacements are near the middle of the Sylmar fault segment. If we sum the displacements across faults of groups 2 and 3 in Lopez Canyon or in Little Tujunga Canyon, we see that the aggregate displacement across the Sylmar-Tujunga fault segments is as large or somewhat larger in the foothill area than it is farther west, amounting to about 2 m. The maximum aggregate uplift across the zone, calculated along a traverse in Lopez Canyon, is about 1.9 m (74 in), north side up.

The relative magnitudes of the vertical and transverse slip components provide a measure of the dip of the fault planes. Dips inferred on this basis are given in table 1 and are compared with dips measured directly on the fault planes at two locations where this was possible. The agreement is not close but suggests that individual inferred dip values are reliable to ± 20°. A similarly low reliability is implied by the scatter of the inferred dip values in table 1, if the actual fault planes of the zone have a nearly constant dip. At the level of accuracy of the inferred dip values in table 1, there is no clear distinction between overall fault-plane dips for groups 1 and 2, but there is a suggestion that faults of group 3 dip somewhat more steeply than those of group 2, in agreement with the available surface observations of fault attitude.

The average of the dip values in table 1 (omitting Nos. 1 and 2) is 42° north and may provide a measure of the overall dip of the master fault plane at depth. This dip is consistent with the observed hypocentral depth of 13 km for the main shock, in relation to the epicenter location about 13 km north of the zone of surface faulting (C. R. Allen, personal commun.).

DETAILED FEATURES OF THE SYLMAR FAULT SEGMENT

The representation of the Sylmar fault segment in figure 1 is based on the detailed observations of surface deformation shown in figure 3. The zone of fault movement is outlined by fractures in the paving of streets, sidewalks, and driveways. As indicated by the heavy solid lines in figure 3, with very few exceptions these fractures run either transverse to the streets or parallel to them along their margins. Because of this control of fracture orientation by the street pattern, the individual fractures do not generally give direct expression of the fault displacement in the Sylmar segment. Owing to the distributed character of the deformation, its effects in unpaved ground are generally too diffuse to be traced continuously. However, major structural damage to buildings is confined to the immediate zone of surface deformation outlined by the distribution of street fractures, even in places where deformation of unpaved ground adjacent to buildings is so diffuse as to be not clearly recognizable as the result of fault displacement. The zones of deformation indicated by the lighter lines in figure 3 were

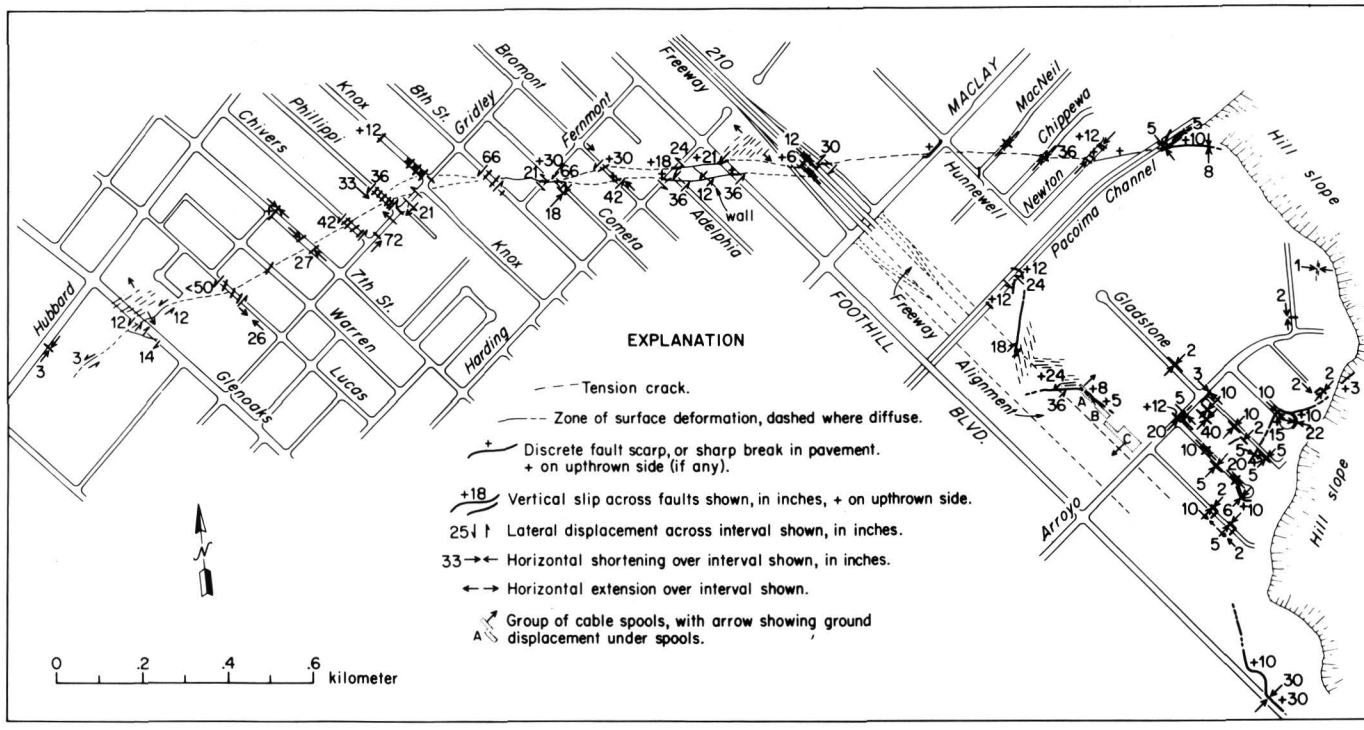

FIGURE 3.—Surface faults and street offsets in the Sylmar fault segment and in the area between the Sylmar and Tujunga segments. The Tujunga fault scarp terminates in the southeast corner of the map. Base map derived from aerial photography.

traced from one street crossing to the next by locating evidences of major structural damage to buildings in the intervening unpaved areas.

Most of the displacement figures given in figure 3 represent offsets across individual streets. Lateral components are in all such cases measured perpendicular to the street line, and longitudinal components (horizontal compression or extension) are parallel to the street line. Lateral and vertical displacements are generally distributed more or less diffusely over intervals of up to 50 m, and the figures given represent cumulative offset across the intervals marked by the arrow symbols. Longitudinal displacements, almost invariably compressional, are localized at individual fractures (overthrusts) or pressure ridges in the pavement; typically, several of these cross the street within the zone of fault deformation. Because of an apparent dynamic sliding of large, rigid pavement slabs during the earthquake, extensional cracks are occasionally found adjacent to compressional overthrusts crossing the same street. The best example of this is on Gridley Street between Chivers and Phillippi Avenues. The longitudinal displacements given in figure 3 are the net cumulative amounts over the intervals shown by the arrows, with any compensating extension taken into consideration.

To obtain displacements across the Sylmar fault segment from the street offset data in figure 3, some interpretation is necessary. In principle, the three perpendicular components of offset (vertical, longitudinal, transverse) across a single street completely determine the slip vector, which is obtainable by vectorial addition of these components. If the fault displacement is faithfully registered across each street crossed by the zone and if the south side moved as a rigid block with respect to the north side, then it follows that in a network of perpendicular streets the lateral offset across one street should in principle be equal to the longitudinal offset along nearly perpendicular streets nearby, the longitudinal offset being compressional or extensional as required by the sense of lateral offset and the trend of the fault with respect to the streets.

When this rule is tested against the street offset data of figure 3, it is found to be poorly satisfied. Examples of violation of the rule are found near intersections of the following streets: Chippewa and Gladstone, Harding and Adelphia, Cometa and Fernmont, Knox and Gridley, Gridley and Phillippi. The last of these is striking: the 21-inch left-lateral offset on Gridley between Knox and Phillippi requires 21 inches of longitudinal extension on Phillippi where the fault zone crosses it, but instead of

this, 33 inches of longitudinal compression is observed.

On some streets the lack of any recorded lateral offset, to correspond with longitudinal compression on perpendicular streets, may be simply a detection difficulty, if the original street alinement was not linear enough to allow observation of a distributed lateral offset. Inconsistent observations of longitudinal displacement may be due to the occasional operation of some mechanism of pavement sliding that distributes the longitudinal offset so widely as to be undetectable or that transfers it to seemingly inappropriate locations. Thus the 72-inch longitudinal compression on Gridley is more appropriate to a location near Knox than to its observed position between Phillippi and Chivers. The lack of longitudinal offsets on either Fernmont or Cometa near their intersection, in spite of the definite lateral offsets on these streets, argues clearly for some mechanism whereby the expected longitudinal displacements are redistributed elsewhere or masked.

To arrive at displacements across the Sylmar fault segment in the face of the problems discussed above, we adopt a somewhat arbitrary procedure. For each location listed in table 1, we select from figure 3 the street-offset observations considered representative, restricting the choice to streets in the immediate vicinity and ignoring any offsets that conflict in the sense discussed above. Where observations are compatible on adjacent streets, they are averaged. The selections are listed in table 2 in a format that shows also which offset observations are ignored at each location. Consistent with the previous discussion, the selections are made from the point of view that observed offsets are more significant than a lack of confirmatory offset observations on adjacent streets. Hence, the selections in table 2 give larger fault displacements than would be obtained if the offset observations on all streets crossed by the fault zone were simply averaged.

The fault vectors obtained in this way for the Sylmar fault segment are listed in table 1. The horizontal slip components shown along the Sylmar segment in figure 1 are obtained by projecting the vectors of table 1 onto the strike and the dip lines of the fault.

The street-offset data along the Sylmar fault segment in figure 3 show certain regularities that bear on the fault displacements derived in table 1. Lateral offsets are consistently left lateral, and on northwest-trending streets they are consistently larger than on northeast-trending streets. By itself this implies that across the generally east-trending fault zone there is some north-south compression in addition to left-lateral slip, but the lateral slip exceeds the transverse compression. This agrees with the displacement vectors found at locations 3 to 5 and at 7. If it were generally true, then longitudinal extension would be expected on northwest-trending streets crossing the fault, but, instead, these streets show only longitudinal compression. There are, however, indications of northwest extension in two areas of tension cracks, one between Foothill Boulevard and the 210 Freeway and the other between Glenoaks Boulevard and Lucas Street (figure 3). Both of these areas lie slightly northeast of the zone of fault deformation as indicated by breaks in street pavement. Indications of compression along northwest-trending streets are generally weak along the fault line east of Gridley Street, and in this portion we may conclude that, on balancing the indications from lateral and longitudinal street offsets, the overall fault displacement must have carried the south side approximately northeast relative to the north side and the lateral and transverse slip components on the west-trending fault must be approximately equal.

Near Gridley Street (long. 118°25.8′), the trend of the Sylmar fault segment swings rather abruptly from west to southwest. West of the bend, prominent longitudinal compressions on northwest-trending streets are found, which cause the indicated displacements to swing toward the north (locations 1 and 2, table 1). The approximate equality of longi-

TABLE 2.—*Selection of representative street offsets for determinations of displacement on the Sylmar fault segment*

Location No.	Streets	Offsets selected (+)		
		Vertical	Transverse	Longitudinal
1	Glenoaks		+	
	Lucas			+
	Warren			
	7th	+		+
2	Chivers		+	
	Phillippi		+	+
	Knox	+		
	Gridley			
3	Gridley		+	+
	Knox	+		
	Phillippi			
4	Fernmont		+	
	Cometa	+	+	
	8th		+	
5	Harding		+	
	Adelphia	+	+	
	Foothill		+	
	Bromont			
6	Freeway 210	+	+	+
	Maclay			
7	Chippewa		+	+
	Newton	+		
	MacNeil			
	Hunnewell			+

tudinal and transverse displacements across the fault is thus preserved west of the bend, but this requires that the rock masses north and south of the fault moved in a manner quite different from rigid blocks.

TUJUNGA FAULT SEGMENT

Because this fault is generally marked by a scarp or as a sharply localized zone of surface displacement, the components of slip across it can be measured directly, without the complications discussed above for the Sylmar segment. However, since the scarp traverses an unpaved and irregular ground surface over most of its length, the individual slip measurements cannot generally be made with the accuracy attainable along the Sylmar segment.

The fault scarp is most prominent at its western end and near Little Tujunga Canyon. Its detailed continuity is interrupted in several places between Lopez and Little Tujunga Canyons. The largest such interruption is at long 118°22.8′. Traced from the west, the scarp here decreases in height and separates into several small parallel scarps or fissures, which gradually become more diffuse and are replaced by parallel "mole tracks" in a zone about 15 m wide; finally this zone disappears in plowed fields.

Five-tenths km east of Little Tujunga Wash, the scarp enters an area of residential subdivision and becomes obscure. However, the line of faulting clearly extends 1 km farther east, as indicated by alined breaks in street pavement and in water mains. The displacement here is generally small (about 0.2 m of north-south compression, with little detectable vertical and no lateral movement), and there is relatively little major structural damage to houses along the fault line. Farther east the surface effects of faulting die out entirely, except for two broken water mains and some small north-south compressions in driveway pavement near long 118°20.4′.

Although the displacement on the Tujunga fault segment dies out toward the east edge of figure 1, substantial displacement reappears farther east, as mentioned earlier, along the segment of the fault in Big Tujunga Wash, where left-lateral slip of as much as 1.0 m is observed. This segment of the fault has a due-east trend and appears to turn toward the northeast near its eastern end, where it crosses Oro Vista Avenue.

Left-lateral displacement across the Tujunga fault segment is definite at Lopez Canyon, and a similar displacement vector is indicated at location No. 8 (table 1), where the fault reaches Foothill Boulevard and turns northwest (long 118°24.6′). The general lack of left-lateral offsets recorded elsewhere may be due in part to the scarcity of linear features crossing the fault line. However, at the Little Tujunga road there is definitely no lateral offset, and in an orange grove 250 m to the east there is a definite right-lateral offset of 25 cm.

FAULTS OF GROUP 3

The sharp, 0.8-m-high scarp in Lopez Canyon at lat 34°17.8′, 0.9 km north of the Tujunga fault segment, is one of the more striking fault features produced in the earthquake. It will be called here the *Oak Hill fault scarp* because it passes near Oak Hill School. Where the scarp cuts bedrock (Tertiary sediments) in the canyon bottom, it exposes the slickensided fault surface, dipping 64° N., in agreement with the dip indicated by the trace of the scarp on the west wall of the canyon. The plunges of slickensides, projected onto a vertical plane parallel to the fault strike, are in the range 40° to 55° E, indicating on the average about equal amounts of vertical and left-lateral offset across the fault. The average slickenside plunge vector is plotted as a triangle in figure 2.

The amount of clay gouge exposed in the fault scarp indicates that previous movements have occurred on the Oak Hill fault, but does not reveal their age.

Where the Oak Hill fault passes into alluvium in the canyon bottom, its scarp becomes diffuse. Although it reappears in the bedrock of the canyon walls, the scarp rapidly decreases in height as traced both east and west, and it disappears within 250 m of the canyon bottom on both sides. This behavior is peculiar, in view of the initial prominence of the fault scarp and the general absence of alluvial fill that might obscure its lateral continuation. Other scarps of group 3 are similarly restricted in their lateral extent. We believe that this is a real effect, although landsliding could in places obscure the faults and although our search was not thorough enough to rule out additional fault segments in some of the more remote parts of the foothill area.

The location, alinement, and displacement (table 1, location No. 13) of the Oak Hill fault might suggest that it represents an eastward continuation of the Sylmar segment, but there is definitely no connection between these two segments in terms of scarps or other recognizable features of surface faulting that formed in the San Fernando earthquake.

Lateral motion on group 3 scarps shows an inconstancy similar to that of group 2. Although the Oak Hill scarp 100 m west of Lopez Canyon Road shows an 0.8-m left-lateral displacement, the road itself is displaced right-laterally by 0.1 m along the same line. Small left-lateral displacements appear at several isolated places in the group 3 zone, including the northern scarp cutting the highway in Little Tujunga Canyon, but there are also examples of fault breaks with no lateral offset, such as the one in Lopez Canyon 300 m south of the Oak Hill scarp.

The northern fault break in Little Tujunga Canyon cannot be traced continuously eastward, and the only evidence of eastward continuation is an alinement of small scarps with reversed sense of vertical displacement (south side up), at long 118°21.8′. The prominent scarp at long 118°20.9′ lies on a continuation of the suggested S. 70° E. trend, but we found no evidence of fault continuity over the intervening distance of 1 km.

On the west side of Little Tujunga Wash, there is evidence, discovered by J. L. Smith (personal commun.), that the base of old terrace gravels is offset vertically 2.5 m, north side up, along the northern fault break. Since the displacement during the San Fernando earthquake was only about 0.6 m, this shows that previous displacements have occurred on this fault in Quaternary time.

Traced westward, the northern break in Little Tujunga canyon follows a number of discontinuous small scarps as far as long 118°22.7′. Its trend over this interval is due west and suggests that it might join the Tujunga fault segment farther west. Similar behavior is suggested for the rupture at long 118°22.9′, lat 34°17.4′.

If the dip observed for faults of group 3 (about 65° N) continues beneath the surface, these faults will meet the more shallowly-dipping Tujunga fault segment at depth. Since the 65° dip at the surface is controlled by bedding, it seems likely that at depth the faults will swing around into a tectonically-controlled orientation with an approximately 45° dip, as inferred for the fault zone as a whole. Thus, the faults of group 3 will tend to merge with the Tujunga fault segment at depth.

From their limited lateral extent and their relationship to the Tujunga fault segment, it appears that the faults of group 3 are secondary effects produced by fractures that splayed off from the main thrust fault and up into the overriding block. The tendency for secondary fracturing to affect the upper block is reflected also in the relatively shallow focal depths of the aftershocks, by comparison with the main shock (C. R. Allen, personal commun.). However, there is no evidence that any of the scarps of group 3 were formed during one of the aftershocks. Although the above interpretation identifies the Tujunga fault segment as the surface trace of the master thrust, it should be noted that the displacement across the zone of group 3 faults is comparable to that across the Tujunga fault segment itself. West of Pacoima Wash, the role of the master break is assumed by the Sylmar fault segment, but here there is no secondary faulting in the upper block, unless the Veterans fault is of this type.

FAULTS OF GROUP 4

These faults, shown in detail in figure 3, occupy the area between the eastern end of the Sylmar fault segment (northeast corner of fig. 3) and the western end of the Tujunga segment (southeast corner of fig. 3). They represent the mechanical connection between these two major fault segments during the earthquake. Viewed in general terms, the line of surface displacement along the Tujunga fault segment turns northward around the southwest corner of the foothill area and follows the western edge of the foothills north to the trace of the Sylmar fault segment, which then carries the displacement westward. In detail, however, this northward connection is complex. Instead of a single clear break, there is a maze of small ruptures.

As shown in figure 3, the scarp of the Tujunga fault segment disappears shortly after turning northward at Foothill Boulevard. On its projected trend to the north is an area of three city blocks southeast of Arroyo Street in which numerous small pavement ruptures indicate ground deformation. The fractures here are almost exclusively perpendicular or parallel to the streets, showing again, as in the Sylmar zone, that the pavement largely controls the individual fractures.

The style of deformation in this area is remarkable: there is little lateral or vertical displacement, but fractures of both northeast and northwest orientation show consistent shortening, which indicates a net loss of surface area. The aggregate compression (given in fig. 1) is, however, greater in the northeast direction than in the northwest, which is consistent with the relative motion indicated elsewhere for the blocks between which the deformed area lies.

In the northeast part of this area is a small scarp (maximum height 0.4 m, or 15 in.) that extends irregularly northeast, ignoring the street pattern, for

about 200 m. Landsliding from the nearby west-facing hill slope might be responsible for this scarp, but its configuration is not clearly that of a landslide toe, and the abundant other evidences of tectonic deformation in the immediate area make the appearance of a fault scarp plausible.

Although there are some small indications of surface deformation farther north, the main line of displacement appears to proceed westward across Arroyo Street to the roughly westward-trending fault scarp of maximum height 0.6 m (24 in.) that lies southwest of Gladstone Street. We shall refer to this feature as the Power Line scarp because it crosses a Southern California Edison Co. transmission line right of way at this point. It displaces a northwest-trending freeway fence line by 0.9 m (36 in.) left-laterally. From the Power Line scarp, the line of displacement goes northward to the Pacoima flood-control channel, following a north-trending break that shows definite right-lateral displacement where it crosses the freeway fence line. How the further connection northward to the Sylmar fault segment is made remains undetermined.

Some unique evidence as to ground displacements in the vicinity of the Power Line scarp is provided by an array of 173 large cable spools, each weighing about 6 tons, which stood in neat rows in the transmission-line right of way as outlined by the dotted rectangles in figure 3. The spools stood on their rims, like wheels, with the spool axes oriented northeast. The rims had pressed down as much as 10 cm into the sandy soil. Although the spools were oriented so as to roll northwest-southeast, during the earthquake very few of them rolled. Instead, most of them shifted 10–20 cm sideways, gouging out a track in the soil. The sideways (NE-SW) motions are plotted in figure 4, in a format which shows schematically both the displacement of each spool and also the position of the spool in the entire array. Figure 4 shows that some of the spools did not move and that some oscillated back and forth, but many moved in a consistent pattern to one side or the other. As a whole, the spools outlined in group A moved consistently toward the southwest, and those in group C moved toward the northeast, while those in group B showed no preferred direction of motion and represent a transition group between A and C. The actual positions of these groups on the ground are shown in figure 3.

The ground suface had little or no lateral slope in the area of the reels, and there was no consistent difference in lateral slope between groups A and C; hence, we believe that the reversal in response from

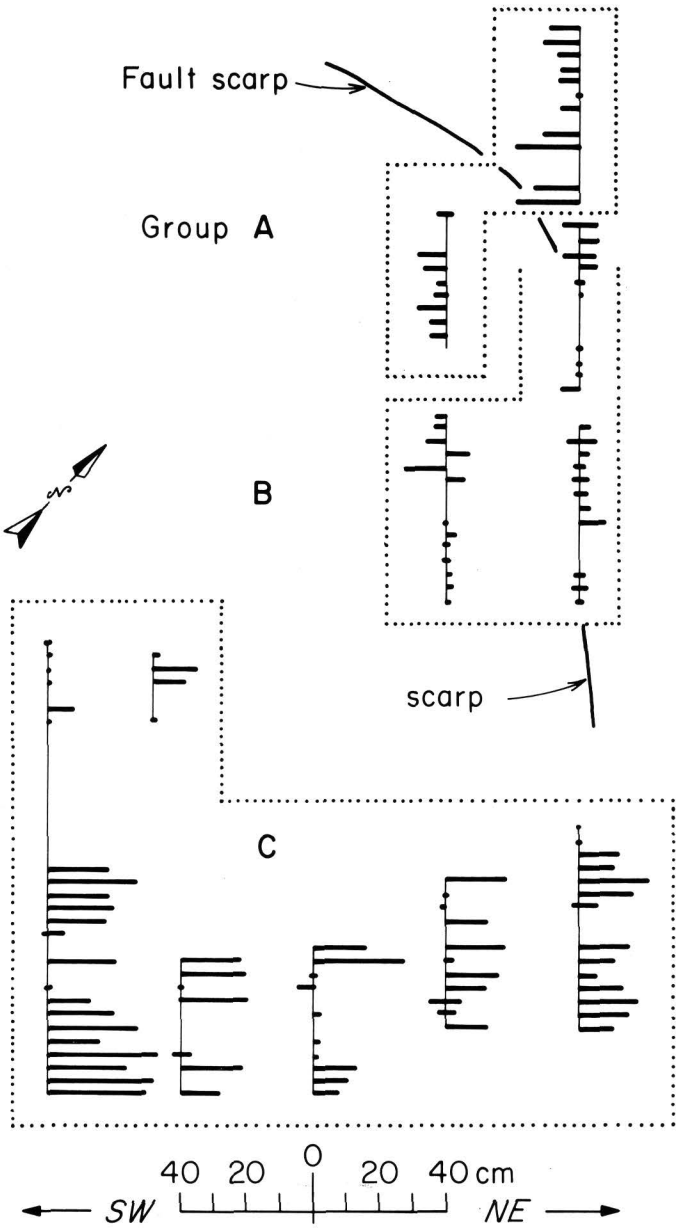

FIGURE 4.—Displacements of cable reels that moved in the earthquake. Fine lines represent rows of reels in their approximate original position on the ground, but foreshortened in the NW–SE direction. Heavy lines represent the amount of sideward displacement of individual reels northeastward or southwestward from their original positions, according to the scale at bottom. The actual position on the ground of the groups of reels, as outlined with dotted lines, is shown in figure 3. The location of the Power Line fault scarp is shown schematically in relation to the rows of reels.

group A to group C reflects a reversal in the sense of ground motion in the earthquake. Such a reversal is consistent with the geologic evidence that an important line of fault offset passed through the spool array. The Power Line scarp cut obliquely through the array, following a northwest trend along one of

the rows of reels for about 75 m before turning westward and out of the array, as shown schematically in figure 4. Although the reels that stood on or very near the scarp (which was here only 10 to 20 cm high) showed no preferred displacement, suggesting that the fault was a nodal line in the displacement field, the complete pattern of displacements in figure 4 indicates that the line of reversal in ground motion passed through the array along a roughly north-south line and did not follow the scarp.

The mechanics of the response of a 6-ton spool to the ground motion of an earthquake is a matter of some complexity that we must leave for future investigation. The simplest possible assumption is that the spools tended to remain stationary in space during the initial large ground displacement that occurred as nearby faults slipped. In this case the displacement pattern in figure 4 indicates that the west side of the nodal line, containing reel group A, moved northeast, and the east side southwest. The indicated type of displacement and fault orientation are the same as seen in the north-trending, right-lateral fault that lies northwest of the Power Line fault, as mentioned previously. We cannot explain the discrepancy between the fault pattern inferred from the reels and the pattern of fault displacement actually found on the ground surface in this area. Nevertheless, the fact that most of the reels moved sideways toward the northeast or southwest, whereas mechanically they could much more easily have rolled northwest or southeast, is strong evidence for a northeast-southwest polarization of the ground motion and a corresponding direction of fault displacement.

Although the faults of group 4 show, in aggregate, displacements comparable to those of the Tujunga fault segment at its western end, the detailed surface path by which the rupture on the Tujunga fault segment connected with the Sylmar zone was complex and remains obscure, as the preceeding discussion shows.

VETERANS FAULT

Because of its position 1 km east of Veterans Hospital (fig. 1), which was severely damaged in the earthquake, this fault has special importance. It lies at the east end of a zone along the base of the San Gabriel Mountain escarpment, where the greatest structural damage to buildings occurred. Within this zone, the Veterans fault is the only feature of ground disruption that has a direct tectonic origin, as far as we have been able to find. It is also the only tectonic feature produced during the San Fernando earthquake outside of the San Fernando fault zone, within the area studied by us.

The Veterans fault forms a low scarp, with maximum vertical offset of about 20 cm, extending for 350 m along a generally east-west trend. Some extension to the east beyond the visible scarp is indicated by a broken sewer pipe, but the scarp definitely does not cross Pacoima Wash or cut the paved road east of the wash. A southwestward extension of about 250 m beyond the recognizable scarp is defined by a zone of major structural damage to houses, but this zone cannot be traced to, or toward, the wing of the Veterans Hospital that collapsed in the earthquake.

The fault is clearly exposed cutting bedrock at several places. The fault plane dips consistently northward at about 61°. It is parallel to bedding in sediments of the Saugus formation (Plio-Pleistocene), which lie immediately north of the fault. Along the fault these sediments are brought into thrust contact with old (uplifted) Quaternary fan gravels. The total thrust displacement of Saugus over fan gravel amounts to at least 5 m, much larger than the displacement in the earthquake. This indicates a prior history of displacement on the fault in Quaternary (and possibly Holocene) time.

There was no detectable lateral component of displacement on the fault as a result of the earthquake.

The comparatively steep dip of the Veterans fault, and its relation to the underlying Tertiary sediments, is similar to the situation in faults of group 3 and by analogy suggests a relationship with the Sylmar fault segment. However, because of the proximity of the Veterans fault to the San Gabriel Mountain front and its accompanying thrusts, a mechanical connection with these important faults seems more likely.

RECONNAISSANCE SURVEY OF THE EPICENTRAL AREA

Previously mapped faults in crystalline rocks of the epicentral area between the north edge of figure 1 and Soledad Canyon, at the northern foot of the San Gabriel Mountains, were examined for indications of displacement in the earthquake. Where possible, the actual fault planes were examined. In most cases the faults could be located to within 10 m or better, so that even a small amount of displacement could have been recognized if present. The traverses for this purpose, which were made during the first 7 days following the earthquake,

also permitted a reconnaissance search for movements on previously unmapped faults.

The San Gabriel fault was examined near Bear Divide (long 118°23.8′ W., lat 34°21.5′N.) and near Dillon Divide (long 118°21.1′ W., lat 34°20.8′N.) and showed no evidence of displacement in either location.

In the area of the epicenter of the main shock near Soledad Canyon, three sets of faults can be distinguished, from oldest to youngest: (1) mostly east-west trending, probably right-lateral faults, with large vertical displacements (includes the Soledad fault); (2) left-lateral faults in a set trending about N. 35° E. and a slightly younger set trending about N. 55° E. with large displacements; (3) northwest-trending faults with small vertical and right-lateral displacements. All these are high-angle faults, with the exception of the Soledad fault, which dips at low angles to the north. None of these faults show evidence of Holocene activity, although all experienced movement in late Cenozoic time. The following faults of these sets were examined and showed no evidence of displacement: the Soledad fault at several places in Soledad Canyon in the vicinity of the originally located position of the epicenter near the mouth of Agua Dulce Canyon; north-northeast-trending fault which bounds part of the northwestern San Gabriel Mountains in upper Iron Canyon (long 118°23.8′ W., lat 34°23.6′ N.); the northeast-trending Magic Mountain fault in lower Sand Canyon (long 118°23.9′ W., lat 34°22.8′ N.) and Indian Canyon (long 118°16.3′ W. lat 34°25.7′ N.; and a northeast-trending fault in Bear Canyon (long 118°23.8′ W., lat 34°22.2′ N.), that is probably related to the Magic Mountain fault.

A small crack (2 cm wide and 15 m long) trends N. 55° E. along the trace of the Pole Canyon fault at long 118°23.0′ W., lat 34°25.0′ N. It cuts thin soil covering bedrock along the crest of a small ridge. It shows no horizontal offset, and might have been produced by differential settling of gravels on one side of the fault. The Pole Canyon fault showed no other evidence of movement at this location. In Soledad Canyon at long 118°21.4′ W., lat 34°25.7′ N., a zone of cracks in unconsolidated alluvium crosses the concealed trace of the Pole Canyon fault, which here trends N. 75° E. This zone is 2 to 3 m wide and about 300 m long, trends about N. 5° E. and consists of several tension cracks up to 4 inches wide. The cracks parallel the axis of the canyon and were probably caused by settling and compaction of the alluvium.

Several faults in Soledad Canyon near Ravenna (approx. long 118°14′ W., lat 34°27′ N.) were examined and show no evidence of breakage. However, there are cracks in road fill and asphalt in this area, which are noteworthy in that no comparable cracks occur along the Soledad Canyon highway for at least 10 miles to the west.

North of Pacoima reservoir, at lat 118°23.6′ W., long 34°21.2′ N. cracks were observed along several preexisting faults of unknown age and displacement. On the average, these faults strike N. 60° W. and dip 40° SW. Two examples showed dip-slip displacement of 1–2 cm, down to the southwest. This displacement could represent the movement of either tectonic or large landslide blocks downward toward the San Fernando basin. In view of the abundant other evidence of landsliding in the mountain area, the cracks in question cannot by themselves be taken as positive evidence of fault movement.

RELATION OF SURFACE FAULTING TO BEDROCK GEOLOGY

The overall fault motion that occurred during the San Fernando earthquake—combined left-lateral slip and thrusting across a north-dipping surface—is the type of motion expected in the Transverse Range structural province, on the basis of geological and seismological experience (Allen and others, 1965, p. 758). Faults along the southern edge of the San Gabriel Mountains have generally been interpreted as thrusts with predominantly dip-slip movement (Bailey and Jahns, 1954, p. 103), but faults elsewhere in the Transverse Range province, in particular the Malibu Coast fault and east-west faults of the Channel Islands, show definite left-lateral displacement (Lamar, 1961; Barbat, 1958; Kew, 1927; Rand, 1931).

The faults that actually moved during the earthquake, shown in figure 1, do not correspond closely with bedrock faults shown in recently published geologic maps (Oakeshoot, 1958; Jennings and Strang, 1969). However, an unnamed fault identical in surface trace with the Tujunga fault segment as defined here was indicated by Miller (1934) in a geologic map of the western San Gabriel Mountains. This fault was probably identified by Miller on the basis of the sharp topographic break at the south edge of the foothills. Miller represented the fault as turning abruptly northward at the southwestern corner of the foothill area, essentially at the point where the scarp of the Tujunga fault segment of the San Fernando earthquake turns northward toward the complex of group 4 faults described above. Although he did not individually discuss the partic-

ular fault in question, Miller (1934, p. 78) interpreted faults of this type as steeply northward-dipping reverse faults, which is in accord with our observations, except for the relatively shallow dip (about 25°) found here for the Tujunga fault segment.

The Tujunga fault segment as defined here is not the same as the Tujunga fault shown on the map of Hill (1930). Hill's fault, which was marked with a queried line, has a nearly east-west trend and lies 1.3 km south of the Tujunga fault segment as recognized here at the mouth of Little Tujunga Canyon. In defining the Tujunga in the way done here, we are proposing that the older definition introduced by Hill (1930) be dropped.

Near the south edge of the Little Tujunga foothills at long 118°20.9′, a short thrust fault dipping 60° N., and carrying Modelo (Miocene) sediments over Quaternary terrace gravels is identified by Oakeshott (1958, pl. 1). The fault is shown as extending with a N. 85° E. trace for a distance of about 0.8 km. If plotted on figure 1, it would pass just south of the observed scarp at long 118°20.9′, but with a distinctly different trend. No displacement was observed on this fault in the San Fernando earthquake. Its attitude and sense of movement are the same as observed for faults of group 3, and like these, it would joint the Tujunga fault segment if traced westward, according to the mapped trace shown by Oakeshott (1958). Its main significance is in establishing the prior occurrence of reverse faulting near the southern edge of the foothills.

No fault corresponding to the prominent Oak Hill scarp was recognized by Oakeshott (1958). The upper fault break in Little Tujunga Canyon would, if traced somewhat farther east than shown in figure 1, connect approximately with a fault of uncertain displacement and attitude shown by Oakeshott (1958). Further investigation is required to establish whether this bedrock fault does in fact connect with the fault that produced the scarp in Little Tujunga Canyon. As noted earlier, there is now evidence that both this fault and the Oak Hill scarp had a history of movement prior to the San Fernando earthquake.

Although published geologic maps do not show a fault along the trace of the Sylmar fault segment, it appears possible that this segment represents a northeastward continuation of the Mission Hills thrust, which was recognized by Oakeshott (1958) primarily from well data. If the southwest-trending western portion of the Sylmar fault segment is prolonged 1.6 km southwest, it connects approximately with the surface trace of the Mission Hills thrust as plotted by Oakeshott. Since the plotted trace of the thrust in this area was not based on specific geological control and was therefore marked with queries, the connection of the two fault segments is only hypothetical. Nevertheless, the Mission Hills thrust provides a reasonable example of the type of geologic and tectonic structure that probably underlies the trace of the San Fernando fault zone.

The Sierra Madre fault zone, a zone of major reverse faults and thrusts along which the crystalline basement rocks of the San Gabriel Mountains have been uplifted and thrust southward over Cenozoic sediments, is the most prominent tectonic element in the immediate vicinity of the region affected by the San Fernando earthquake. It extends east-west along the base of the mountain front near the north edge of figure 1. In that area, the main thrust contact between basement rocks and sediments is locally designated the Hospital Fault (Oakeshott, 1958). In view of the high intensity of ground shaking along the foot of the escarpment, as testified by the destruction at Olive View and Veterans Hospitals, and in view of the large thrust component of the overall fault motion that occurred, it would be reasonable to expect motion on the Hospital fault or other thrusts of the Sierra Madre zone. The only indication of such motion found by us is the small feature here called the Veterans fault. This fault lies 0.5 km south of the basement-sedimentary contact, which represents the major structural break and the probable trace of the Hospital fault, if it extends this far east (although it is not so shown by Oakeshott, 1958). The Veterans fault can be considered a part of the Sierra Madre fault zone, on the basis of its location near the basement contact, its attitude, and its sense of movement. Although the movement of the Veterans fault is thus a definite indication of activity on the Sierra Madre fault zone in the San Fernando earthquake, the fault feature involved was only a minor one and the extent and amount of displacement were small compared to what occurred to the south along the San Fernando fault zone. In a wider sense, however, the San Fernando fault zone can be considered an integral part of the same system of Transverse Range faults that includes the Sierra Madre fault zone, and in fact the two zones probably join when traced eastward to the vicinity of Sunland, about 5 km east of figure 1.

Geologic cross sections drawn from the San Fernando Valley northward across the San Gabriel

Mountains (Oakeshott, 1958) show faults of the Sierra Madre zone as dipping generally at angles of 60° and steeper northward. Although these relatively steep dips agree with the attitudes of faults of groups 3 and 5, they conflict with the previously discussed general indication that the active fault plane as a whole dips about 45° N.

CONCLUSIONS

The San Fernando earthquake was caused by movement on northward-dipping thrust faults that conform to a consistent pattern of such faulting in the Transverse Ranges. Almost all the fault movement in the area studied can be explained in terms of a single master fracture at depth, striking N. 72° W. and dipping about 45° toward the north. The individual fault segments that moved at the surface, forming collectively the San Fernando fault zone, strike more nearly east-west and bear an en echelon relation to the inferred master fracture. Although there are local divergences in displacements of individual faults, the overall fault motion was a thrusting of the north side approximately southwestward over the south side, with approximately equal amounts of vertical uplift, north-south compression, and left-lateral slip. This motion combines the types of displacement known to be characteristic of major faults of the Transverse Range province. The overall displacement was about 2 m.

Fault movement did not occur near the surface in the vicinity of the epicenter of the main shock. A reasonable model of the fault movement in the earthquake is initiation of fracture at a depth of about 13 km under the epicenter, followed by propagation of the fracture southward to the ground surface along a plane dipping about 45° N.

At the surface, only a small amount of localized fault movement took place along the Sierra Madre fault zone, the major tectonic feature in the immediate vicinity of the area most affected by the earthquake, and the most obvious candidate for movement of the type observed. Most of the fracturing reached the surface about 4 km farther south, along faults that are minor by comparison (the San Fernando zone). These faults nevertheless fit the general pattern of faulting set by the major faults, and they probably join the Sierra Madre fault zone a short distance to the east.

The tectonic model of the earthquake suggests that thrusts related to the Sierra Madre zone, which bound the San Gabriel range on the south, pass at depth entirely beneath the range to the north. Thus, they are not simply marginal reverse faults, as they are usually visualized. This model may apply to major Transverse Range thrusts generally.

None of the faults that moved in the San Fernando earthquake had been clearly identified in advance as active faults. There is now evidence that at least some of them had a prior history of movement. The Tujunga fault segment could have been suspected on the basis of its associated foothill topography. The Sylmar fault segment could have been recognized, if at all, only by subsurface investigations.

ACKNOWLEDGMENTS

We are grateful to the U.S. Geological Survey and to Woodward-Lundgren and Associates for supplying large-scale aerial photographs of the earthquake area, which helped materially in the mapping. We also wish to acknowledge the contributions to the collection of the field data made by the students and associates whose names are cited in the initial footnote. The material available for this report has been significantly improved by the generous exchange of information among many scientists studying the earthquake, whose names cannot be individually acknowledged here.

REFERENCES

Allen, C. R., St. Amand, P., Richter, C. F., and Nordquist, J. M., 1965, Relationship between seismicity and geologic structure in the southern California region: Seismol. Soc. America Bull. 55, 753.

Bailey, T. L. and Jahns, R. H., 1954, Geology of the Transverse Range Province, Southern California: California Div. Mines Bull. **170**, chap. II, p. 83.

Barbat, W. F., 1958, Los Angeles basin area, California, *in* Weeks, L. G., ed., **Habitat of Oil: Tulsa, Okla., Am. Assoc.** Petroleum Geologists p. 62.

Hill, M. L., 1930, Structure of the San Gabriel Mts. north of Los Angeles, Calif.: California Univ. Pubs. v. Geol. Sci. 19, No. 6. p. 137–170.

Jennings, C. W., and Strand, R. G. eds., 1969, Los Angeles sheet, Geologic map of California: California Div. Mines and Geology Map Sheet.

Kew, W. S. W., 1927, Geological sketch of Santa Rosa Island, Santa Barbara County, Calif.: Geol. Soc. America Bull. 38, 645.

Lamar, D. L., 1961 Structural evolution of the northern margin of the Los Angeles basin: Ph.D. Thesis, University of California, Los Angeles, 142 p.

Miller, W. J., 1934, Geology of the western San Gabrial Mountains of California: California Univ. Pubs., Los Angeles Math. Phys. Sci., v. 1, p. 114.

Oakeshott, G. B., 1958, Geology and mineral deposits of the San Fernando quadrangle: California Div. Mines and Geology Bull. 172.

Rand, W. W., 1931, Preliminary report of the geology of Santa Cruz Island, Santa Barbara County, Calif.: Calif. Div. Mines, Rept. State Mineralogist 27, 214.

SURFACE FAULTING

By U.S. GEOLOGICAL SURVEY STAFF [1]

Tectonic movements associated with the February 9, 1971, San Fernando earthquake produced a zone of surface breakage which partly follows the boundary between the San Gabriel Mountains and the San Fernando-Tujunga Valleys, and partly transects the northern salient of the San Fernando Valley. This latter zone of tectonic ruptures was specifically associated with some of the most extreme damage caused by the earthquake anywhere in the epicentral region.

The zone of surface breakage trends roughly east-west, is about 15 km long, and is slightly concave towards the south. A notable discontinuity occurs near the middle of the arc where the western half is offset about 1 km north of the eastern half. The sense of movement along the breaks is complex. Almost all scarps are south facing, with the mountain block up relative to the valley block. Most of the larger scarps consistently show a left-lateral sense of motion, but a broadly defined zone of smaller scarps and cracks, which parallels in part the main zone of breakage, shows right-lateral offsets. Within the entire 15 km length of the surface breakage, the maximum vertical offset measured on a single scarp is about 1 m, the maximum lateral offset about 1 m, and the maximum shortening (thrust component) about 0.9 m.

Almost all aftershocks recorded during the first weeks following the earthquake were located north of the main line of tectonic surface ruptures (fig. 1, and Wesson and others, this report). The aftershocks form a diffuse, but relatively well defined zone that dips about 40° to the north, which is about 15° less steep than the dip of the fault plane as measured at the surface. The calculated dip of the fault using the depth to the hypocenter and the distance between the epicenter and the tectonic ground breakage is about 45°, using data available on March 1, 1971. This is about 10° shallower than the most reliable dips measured at the surface.

Surface ruptures generated during the earthquake fall into two principal groups: tectonic and nontectonic. Although the two are vastly different in origin, they are commonly difficult to distinguish from one another in the field. Only scarps interpreted to be tectonic are shown in figure 2.

Surface ruptures that are known or suspected to be tectonic breaks created during the earthquake extend discontinuously from the San Diego Freeway just south of Lower Van Norman Lake to Big Tujunga Canyon. No such ruptures were found between the San Diego Freeway and the Osceola Street School or in the area from just east of San Fernando Road to just west of the intersection of Glenoaks Boulevard and Hubbard Street. The zone of breakage bends to the south about 0.4 km south of Lopez Dam, but some breaks may be continuous through the low hills into Lopez Canyon to the east. From the Foothill Nursing Home, eastward along the front of the mountains, the surface faulting is generally well defined, but locally discontinuous, to a point just east of Little Tujunga Canyon. East of this point, for a distance of about 2 km, no obvious surface faulting is found along the front of the range. About 0.3 km east of the Lakeview Terrace Sanitarium, surface breakage again is in evidence, with only a few interruptions, to a point about 0.3 km into Big Tujunga Canyon. About 0.4 km farther up the canyon, a 0.3 km scarp marks the eastern limit of surface ruptures. From approximately Lopez Canyon east to Little Tujunga Canyon, discontinuous, usually smaller, breaks occur north of the relatively through-going line of breaks along the front of the range. Two of these breaks are found in Lopez Canyon, two in Bartholomaus Canyon, four small breaks cross Kagel Canyon, and single breaks intersect Little Tujunga, Oliver, and Schwartz Canyons. A relatively short, presumably tectonic rupture characterized by a small south-facing scarp was recognized just east of the U.S. Veterans Hospital; it has no apparent continuity

[1] M. G. Bonilla, J. M. Buchanan, R. O. Castle, M. M. Clark, V. A. Frizzell, R. M. Gulliver, F. K. Miller, J. P. Pinkerton, D. C. Ross, R. V. Sharp, R. F. Yerkes, and J. I. Ziony.

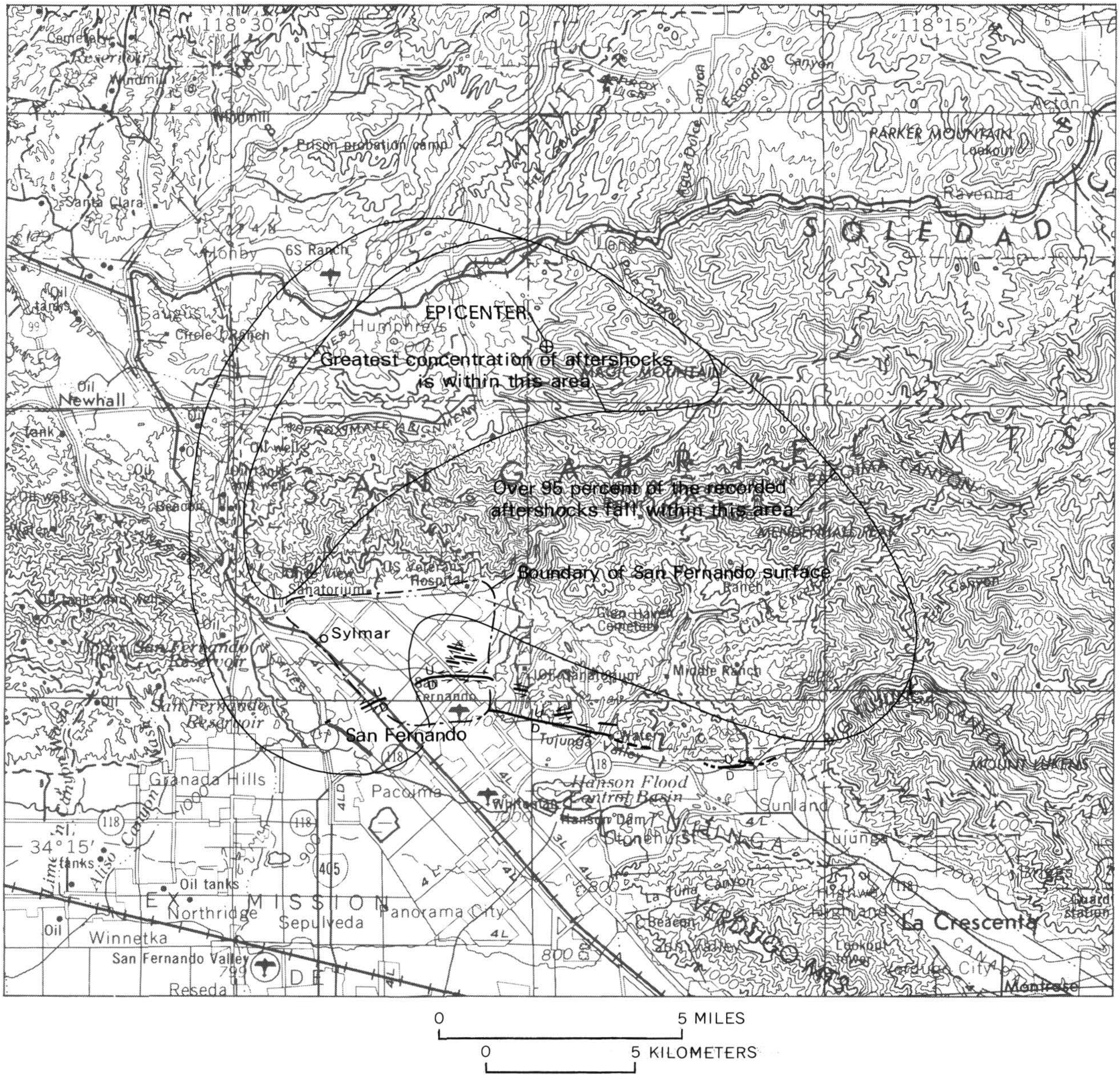

FIGURE 1.—Sketch map showing the relation of the surface faulting to the epicenter and the location of aftershocks.

with the main zone of breakage to the south.

The concentration of ruptures in some areas and their absence in others, and the apparent discontinuity near the middle of the breaks, allow a natural division into three segments. For convenience these segments are named as follows: (1) The surface faulting from the San Diego Freeway to just east of San Fernando Road is referred to as the Mission Wells segment of the San Fernando fault zone. (2) The ruptures from the intersection of Hubbard Street and Glenoaks Boulevard to the Foothill Nursing Home are referred to as the Sylmar segment of the San Fernando fault zone. (3) Some of the breakage that roughly follows the mountain front east of the nursing home is referred to as the Tujunga segment of the San Fernando fault zone.

Oakeshott (1958, p. 92) grouped several faults within the range front in the Sierra Madre fault zone; this zone extends from the northeastern end of the Santa Susana fault to the western end of the Rowley fault zone. Only the easternmost 0.3 km of the Tujunga segment of the February 9, 1971, surface faulting coincides with any of the faults shown on his geologic map, although the scarp formed east of the Veterans Hospital, identified provisionally as tectonic, may be part of the Sierra Madre zone. Oakeshott (1958, pl. 1) shows several faults in the Miocene and Pliocene sedimentary rocks in the foothills north of the Tujunga segment as mapped in figure 1 of this paper; but no movement was noted along them after the earthquake. Even though no movement occurred along any of the known faults composing the Sierra Madre fault zone, its importance should not be minimized. It is one of the major tectonic zones along which uplift of the San Gabriel Mountains has occurred (Oakeshott, 1958, p. 105), and the surface faulting of February 9 may be part of the same system.

DESCRIPTION OF SURFACE FAULTING

The tectonic ground breakage of February 9 is described segment by segment from west to east.

MISSION WELLS SEGMENT OF THE SAN FERNANDO FAULT ZONE

Near the Mission Wells historical monument, 1.5 km east of Lower Van Norman Lake, a small south-facing scarp 0.05–0.25 m in height trends about N. 60° E. (fig. 2). Surface cracks showing left-lateral offsets extend from just southwest of the northwest corner of Osceola Street School to about one block east of San Fernando Road. Cracks were also found in the concrete pavement of the Golden State Freeway along the strike of this zone, but these may have been caused by landslides. This segment has no surficial expression between the San Diego Freeway and the Osceola Street School, nor from a point about one block east of San Fernando Road to the intersection of Hubbard Street and Glenoaks Boulevard.

SYLMAR SEGMENT OF THE SAN FERNANDO FAULT ZONE

The Sylmar segment is a well-defined zone of tectonic fractures that extends eastward from the heavily damaged shopping center at the south corner of the intersection of Hubbard Street and Glenoaks Boulevard to the range front immediately south of Lopez Dam. Cumulative displacement across the central part of this zone consists of left-lateral, vertical, and horizontal-shortening components as great as 1.9 m, 1.39 m, and 0.6 m, respectively (fig. 3 and table 1). The maximum components of displacement across any individual break in the zone, however, are about half of these values, and they are far less across most breaks. This zone generally ranges from about 75 to more than 200 m in width, but virtually all the lateral movement and shortening caused by thrusting, together with about one-half of the vertical displacement, are concentrated in a narrow band along the southern border of the zone (fig. 2). The remainder of the vertical displacement is distributed across many small normal (extension) faults and a few small thrust faults that occupy the remainder of the zone and show minor left- or right-lateral displacement. Thus, the zone of fractures is divided into a narrow southern zone of shearing and thrusting and a wider northern zone of extension; vertical displacement occurs in both. This distribution of displacement is well shown by ruptured utility pipes beneath streets and by sidewalks, curbs, and streets (figs. 4 and 5).

The extension or compression of sidewalks and curbs with respect to the underlying ground provides a basis for estimating surface distortion. For example, all the northwest-southeast trending streets (Foothill, Eighth, Glenoaks) showed net extension across the fault zone, whereas the northeast-trending streets were shortened (fig. 6). Unfortunately, the large number of measurements required (commonly more than 100 in a block 400 m long) together with various uncertainties limits the accuracy of the determinations of net change across the fault zone to about $\pm$ 0.1 m. Our estimates were further hampered by street-repair crews, who swiftly removed sections of splintered or buckled sidewalks and curbs.

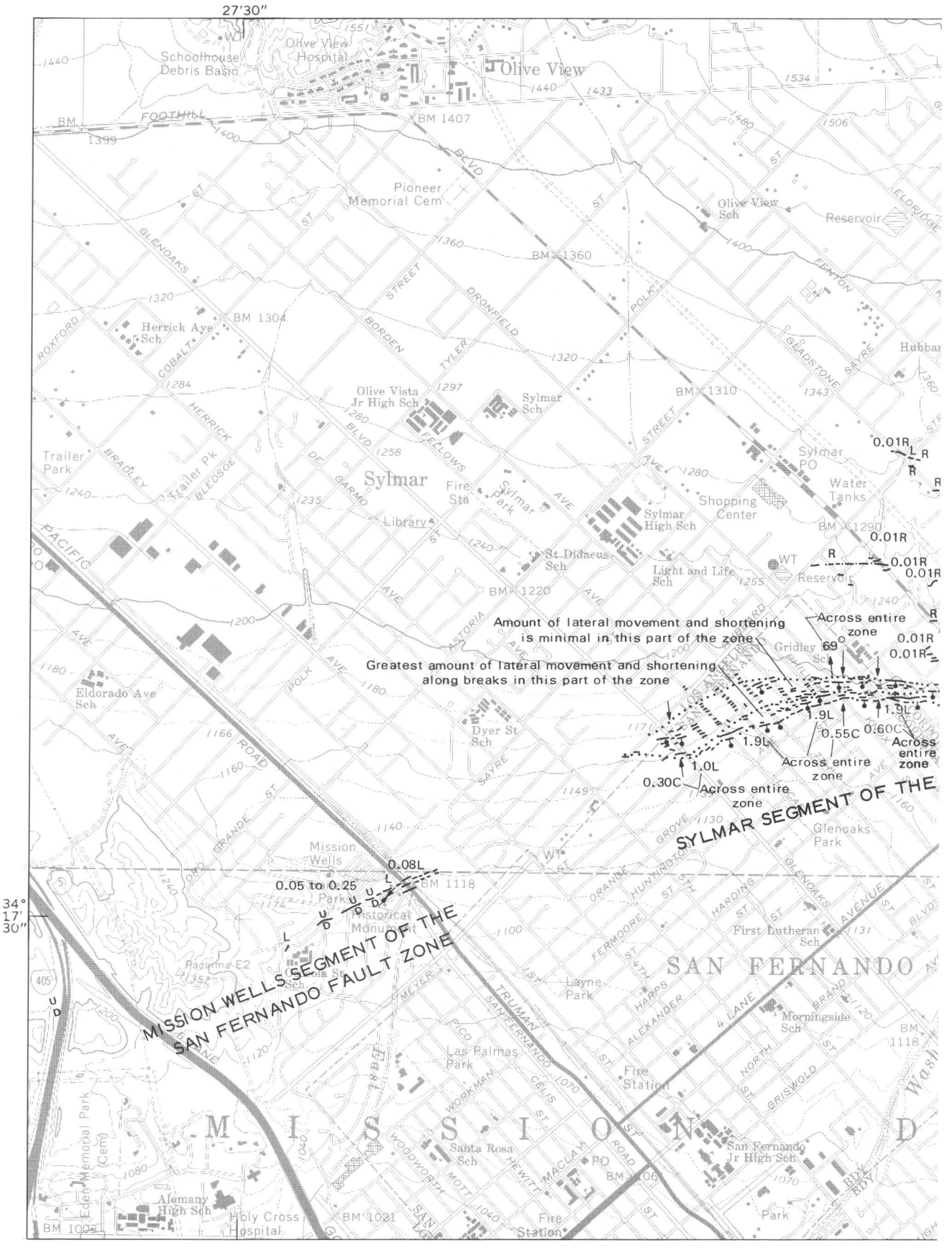

FIGURE 2.—Map showing tectonic ruptures formed during the San Fernando earthquake of February 9, 1971.
Figure 2 continues on following pages.

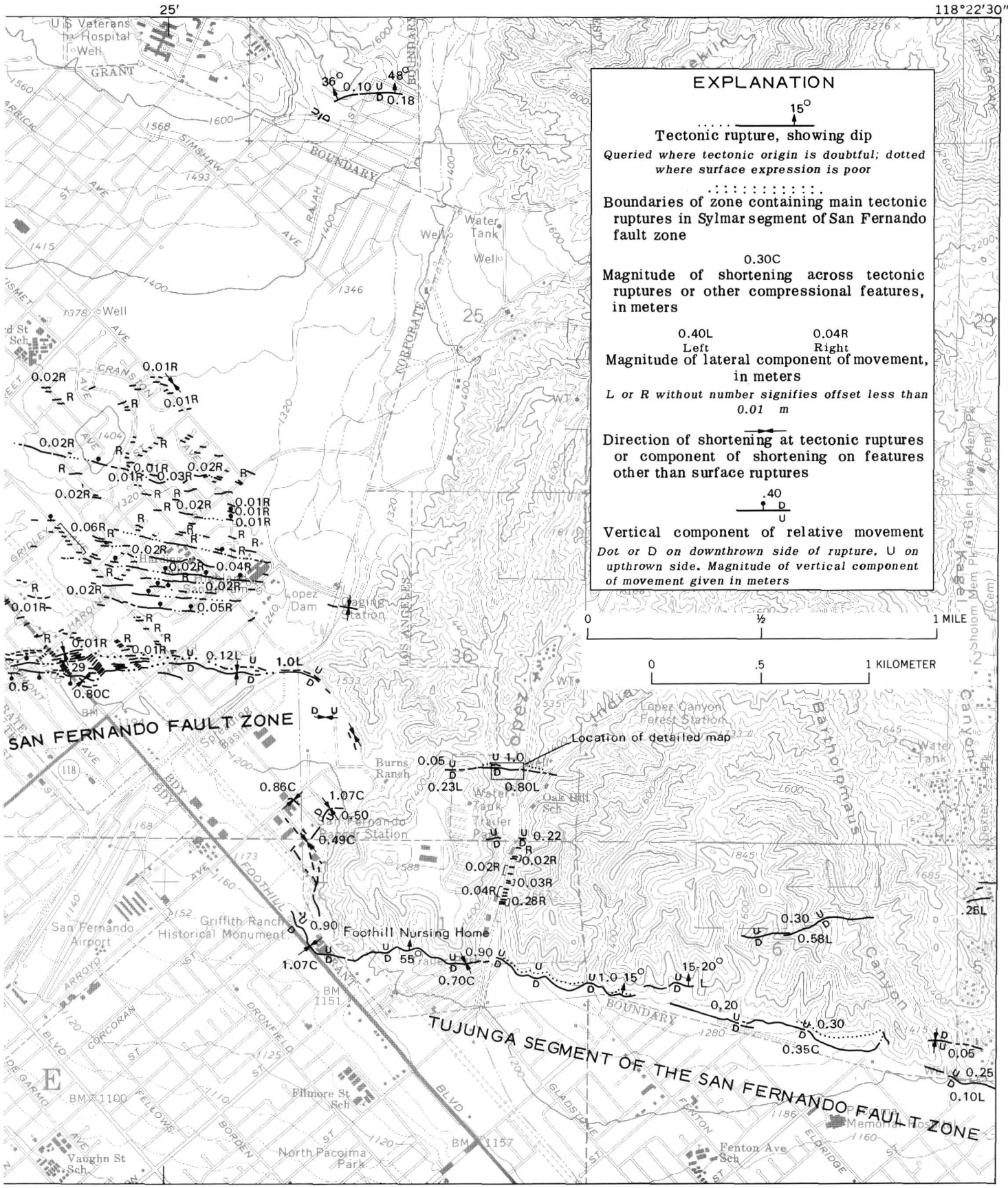

FIGURE 2.—Continued.

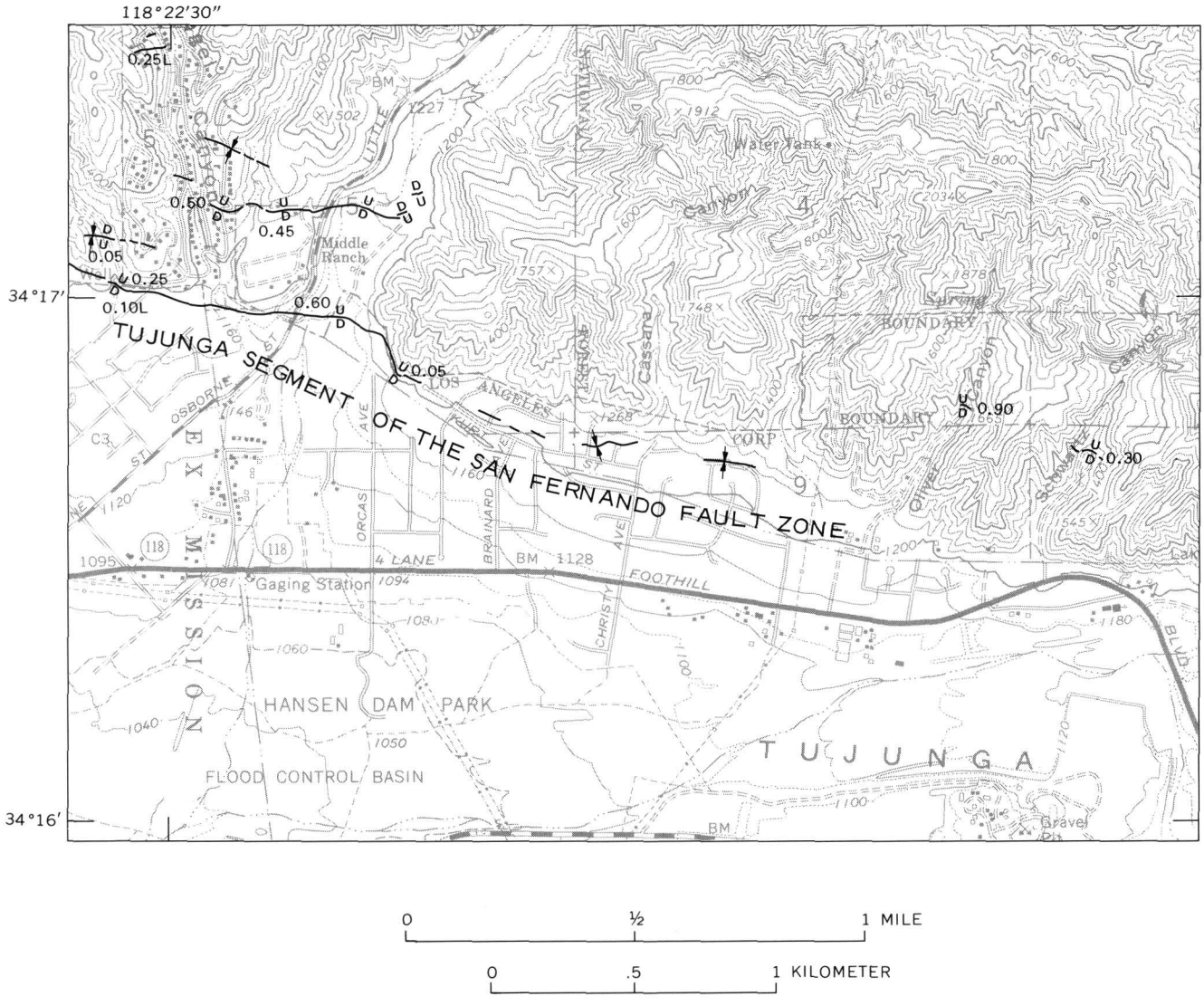

FIGURE 2.—Continued. See preceding pages for explanation.

Few fractures of the ground surface can be traced across streets, houses, and yards. Owing to their rigidity, streets (including curbs and sidewalks) tend to bridge the shear zone; this rigidity commonly allows compression to be transmitted to buckles and overthrusts in streets, curbs, and sidewalks as much as 100 m from the zone of ground breakage. On the other hand, extension is usually expressed in the overlying sidewalks and curbs at the closest construction joint (generally within a few meters) and in asphalt pavement by tensile failures normal to the length of the street (fig. 7) and apparently within a few tens of meters of the underlying ground extension. Houses commonly hide faults that pass beneath them unless displacement is large enough (about 50–100 mm) to visibly affect the house. Many fractures that are obvious on bare ground are completely hidden by cultivation or planting. However, the small number of fractures that have displacements greater than 0.1 or 0.2 m, such as those that cross Bromont Street and the street just west of it, generally maintain continuity across these features (fig. 8). The net result of these effects is that the shear zone is revealed, if not sharply bounded, by obvious left-lateral offset of each street that it crosses (fig. 9), whereas the zone of extension is marked by normal faults and extension fractures across each street within the zone.

The southern boundary of the zone of fractures is sharp, whereas the northern boundary is not. Obvious ground fractures cease a few tens of meters beyond the southern boundary of shearing and thrusting, whereas the zone of extension fractures has a diffuse boundary, marked by a gradual reduc-

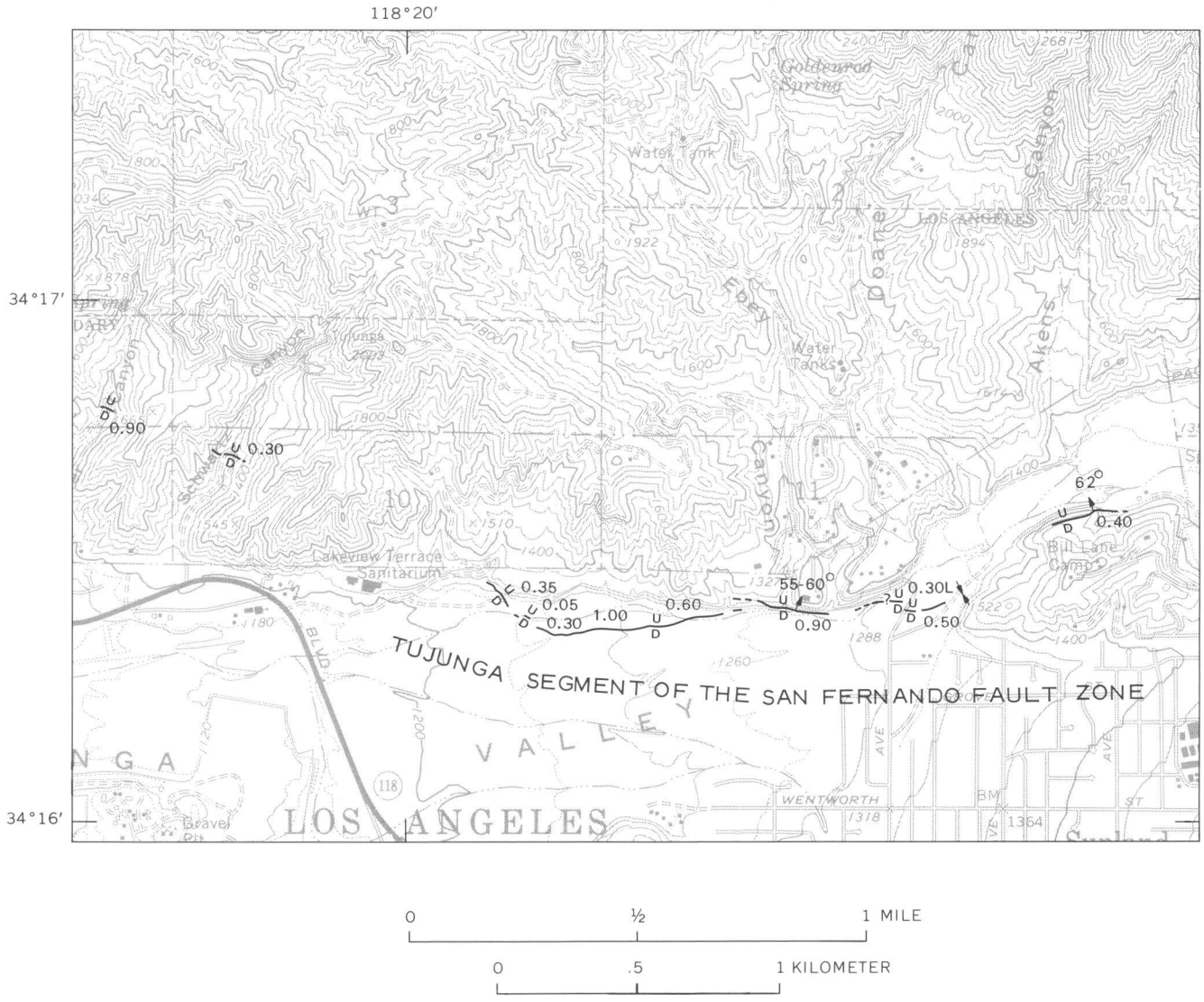

FIGURE 2.—Continued.

tion in the number of fractures and displacement across them. The northern boundary of the zone of extension shown in figure 2 roughly limits the area in which extension fractures are evident across bare ground.

The sharply defined main strand of the Sylmar fault segment changes northward into a broad area broken by numerous, relatively closely spaced faults which almost uniformly display small right-lateral offsets. The dimensions of the area showing fractures of this kind are about 1.8 km in the east-west direction, somewhat less than the length of the main part of the Sylmar fault segment, and about 1.3 km from north to south. The faults share the east-west trend of the left-lateral zone and generally show slight extensional gaping as well as right-lateral displacement. Where present, the sense of vertical components of movement is usually down on the north, or opposite to the direction of vertical offset in the belt of apparent right slip within the zone of the Sylmar fault segment. The right-lateral faults are usually simple, nearly linear fractures in the ground but have somewhat more complex traces where they break pavements, sidewalks, and concrete slabs of houses. Spacing of the faults ranges from a minimum of about 20 m to a maximum of about 100 m. Residents in the area state that many of the fractures showed only slight offsets immediately after the earthquake and that they continued to move for several days thereafter.

One of the most complex sectors of surface rupturing occurs northeast of San Fernando Airport in the area of apparent discontinuity between the Sylmar and Tujunga segments of the San Fernando

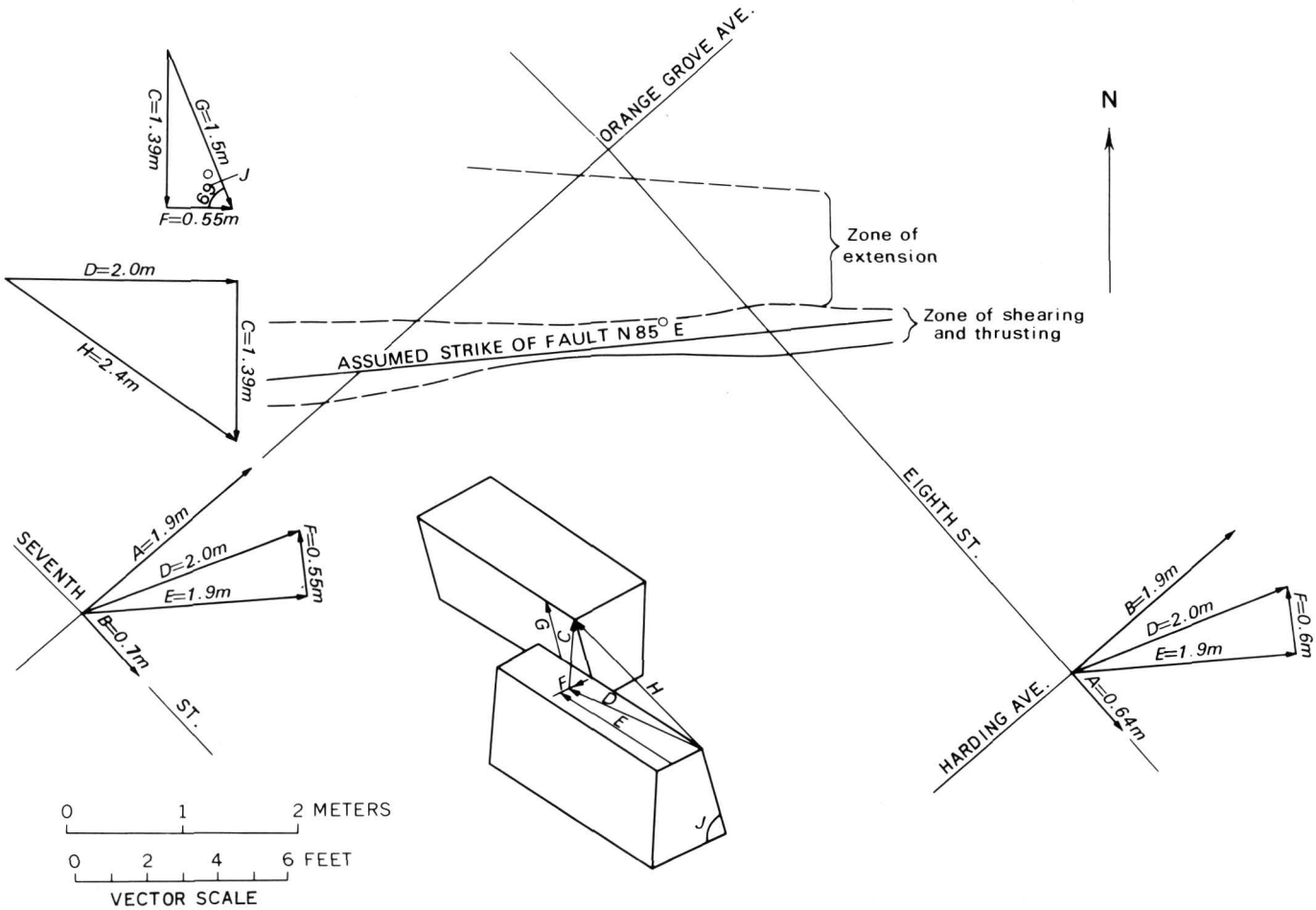

FIGURE 3.—Slip vectors along an assumed fault plane crossing Orange Grove Avenue and Eighth Street. Derived from post-earthquake changes (*A*, *B*, and *C*) in Orange Grove Avenue and Eighth Street (fig. 4). Vectors represent the movement of one end of each street with respect to the other end. Values are summarized in table 1. *A*, change in length of street; *B*, left-lateral displacement of street; *C*, vertical displacement of street; *D*, horizontal displacement of ground; *E*, strike slip; *F*, horizontal shortening; *G*, dip slip; *H*, net slip; *J*, dip of fault plane.

TABLE 1.—*Summary of measurements shown in figures 3 and 4*

	Orange Grove from 8th to 7th St. in meters and (ft) or degrees	8th St., from Orange Grove to Harding in meters and (ft) or degrees
A. Change in length of street	−1.9 (−6.2)	0.64 (2.1)
B. Left-lateral displacement of street	.7 (2.3)	1.9 (6.2)
C. Vertical displacement of street	−1.39 (−4.6)	----
D. Horizontal displacement of ground	2.0 (6.6)	2.0 (6.6)
E. Strike slip	1.9 (6.2)	.6 (2)
F. Horizontal shortening	.55 (1.8)	.6 (2)
G. Dip slip	1.5 (4.9)	----
H. Net slip	2.4 (7.9)	----
I. Strike of fault plane	N. 85° E.	N. 85° E.
J. Dip of fault plane	69°	----

fault zone. The complexity involves not only geometric irregularity of the fault strands but also loss of demonstrable continuity of the fault traces and possible variation in the sense of the lateral component of displacement.

Between Maclay Avenue and Pacoima Wash, the sense of horizontal separation on the Sylmar segment reverses from left- to right-lateral. The northern or northeastern side, however, is consistently the relatively upthrown block. On the first street southeast of Maclay Avenue, the break shows about 0.12 m of left-lateral separation of curbs; but one block farther southeast, no lateral separation is visible on curb lines, suggesting (from the angular relationship of the fault trace and street) a small left-lateral component of slip. One block farther east, curbs are separated right-laterally about 0.3 m, reflecting either a yet smaller left-lateral component combined with the vertical component of offset, or possibly a small right-lateral component of movement. Immediately east of Pacoima Wash, the

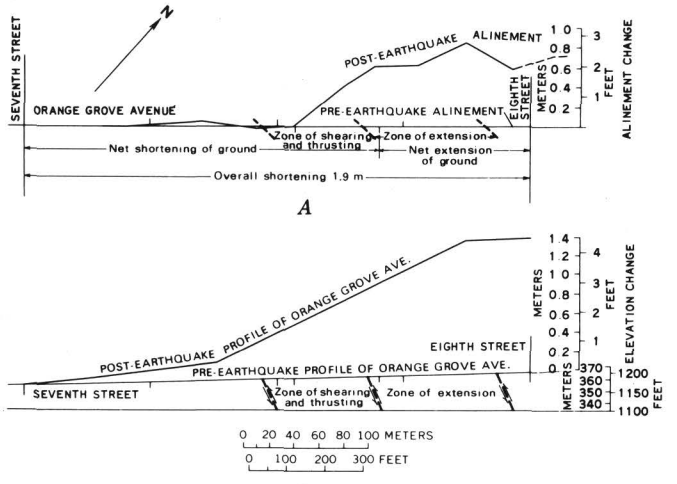

FIGURE 4.—Changes in level, length, and horizontal alinement along Orange Grove Avenue between Seventh and Eighth Streets, city of San Fernando. *A*. Changes in length and alinement (plan view). Left-lateral displacement of the street from the original alinement was measured by sighting along the northeast curb February 19, 1971. Change in length of the street was measured February 20, 1971, by R. T. Ruthven, U.S. Geological Survey. Localization of horizontal movement was determined by measuring compression and extension of curbs and sidewalks on both sides of Orange Grove Avenue. This figure shows that most of the shearing and thrusting is concentrated in the shear-thrust zone near the southern boundary of the break zone. *B*. Changes in elevation relative to leveling done in January 1962. The elevation of the intersection of Orange Grove Avenue and Seventh Street is assumed to have remained unchanged. Measured February 15, 1971, by R. E. Munn, Engineering Department, city of San Fernando. This profile shows that vertical displacement is distributed across the entire zone of breakage.

FIGURE 5.—Shortened section of gas pipe taken from the shear-thrust zone across Glenoaks Boulevard. This piece was shortened more than 0.1 m (4 in.); at least one other shortened section of the same pipe was removed from another place in this shear zone. Immediately north of the shear zone across Glenoaks Boulevard, but still in the fault zone, this pipe and adjacent water pipes were each broken in several places by extension of the ground combined with downward movement to the south. Despite the shortening in the shear zone shown by this photograph, the net change in the length of Glenoaks Boulevard and the pipes buried beneath it was an extension of 0.6 m between Hubbard and Orange Grove Avenues (measured February 20, 1971, by R. T. Ruthven).

FIGURE 6.—Shortened sidewalk. The slab resting on top of this sidewalk on the southeast side of Orange Grove Avenue near Phillippi Street has been thrust from left to right. Thrusting between Phillippi and Knox Streets shortened Orange Grove about 1.3 m (about 4 ft) and ejected the slab. The two corners at the ends of the block yielded little, forcing the sidewalk to buckle at this point.

Sylmar segment of the fault displaces an originally linear north-south fence about 1.0 m in a left-lateral direction. Because the trace of the ground rupture is almost exactly perpendicular to the fence line, there is no ambiguity as to the sense of the lateral component of offset at that point.

Eastward from the northern point of the spreading basin next to Pacoima Wash, the trace of the Sylmar segment of the fault curves abruptly to a southward trend and becomes approximately coincident with the base of the steep mountain front. The trace is visible only for a short distance at that location; however, despite the near absence of surficial breakage along the base of the slope southward to the reentrant canyons at the Burns ranchhouse, damaged water pipes excavated after the earthquake indicate at least 0.43 m of east-west shortening of the ground surface about 0.4 km northwest of the ranchhouse. The mountain block, furthermore, rose at least a few centimeters relative to the alluvial flat at that point. No obvious disturbance or cracking of the ground surface was evident at the shortened pipelines, raising the possibility that a

FIGURE 7.—Graben across Eighth Street in the zone of extension fractures. Foundering of the down-dropped block is exaggerated by the presence of a large (about 5 × 6 m cross section) flood-control conduit beneath Eighth Street. This conduit was severely damaged in the fault zone. The condition of the tie bars in the construction joint in the sidewalk in the foreground indicates at least one cycle of opening and closing of the sidewalk slabs with movement greater than the length of the exposed bars.

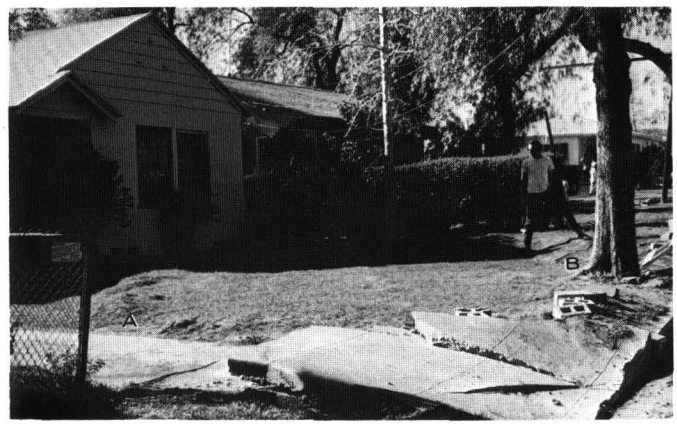

FIGURE 8.—Shear-thrust zone at Cometa Avenue (parallel to and northeast of Eighth Street). The two larger thrust faults (*A* and *B*) account for most of the strike slip and shortening of the shear-thrust zone, which is less than about 10 m wide at this location. The overthrust driveway and adjoining street span the shear-thrust zone and indicate roughly 1 m of shortening. The curb at the right is offset nearly 2 m left-laterally across these two breaks. Vertical displacement is about 0.5 m. The closest house has broken free of its foundation and shifted nearly 0.5 m to the right (north).

similarly imperceptible compression zone may continue southward to the vicinity of the San Fernando Ranger Station.

Near the San Fernando Ranger Station, the sidewalks and pavements at the southeast ends of two cul-de-sacs that run northwest-southeast were broken and shifted to the northwest; asphalt parking lots were disrupted; and two buildings were jammed together (fig. 10), causing severe structural damage to at least one of them. Their orientation indicates a strong component of northwest-southeast shortening. One of the cul-de-sacs, Montero Avenue, was shortened in a northwest-southeast direction by 1.07 m (the difference between the length measured by steel tape on February 14 and the length given in official records). A monument originally set on the projection of the centerline, and about 20 m southeast of the end of the street, was shifted about 0.2 m southwest of the centerline. The shortening buckled the sidewalk and flattened the circle at the end of the street and produced crescent-shaped openings between the curb and the sidewalk (figs. 11 and 12). The form of the ruptures both in the streets and in vacant lots indicates strong compression in the northwest-southeast direction and uplift of the southeast side, possibly combined with a minor right-slip component. Numerous landslide scarps up to 1 m high cut the flanks and ridges of the hill immediately to the east. Their presence suggests the possibility that settling and spreading of the bedded and jointed rock that constitutes the hill may have forced out a wedge of alluvium at the base of the hill, produced most of the compressional effects, and masked whatever tectonic displacements may have occurred.

The west end of the Tujunga fault segment may connect with the Sylmar segment along a hidden zone of compression near the base of the mountain slope in the vicinity of the San Fernando Ranger Station. It is furthermore possible that the Sylmar segment branches, and the eastern strand extends into the mountains along the line of the northernmost mapped faulting in Lopez Canyon. Demonstration of such a connection is not possible, however, because of the extensive landslides on the hill east of Burns Ranch.

FIGURE 9.—Left-lateral offset of the northeast side of Knox Street in the shear-thrust zone. Underthrusting of adjacent turf by both curb and sidewalk in the zone of offset indicates that they bridge a narrower shear zone in the ground.

TUJUNGA SEGMENT OF THE SAN FERNANDO FAULT ZONE

The Tujunga segment extends along the front of the hills on the north side of Tujunga valley in a discontinuous fashion from the vicinity of the Foothill Nursing Home, which lies on the northeast side of Foothill Boulevard, eastward into Big Tujunga Canyon.[1]

In front of the nursing home the curb is raised about 1 m above the street level (fig. 13). A transverse component of movement, shown by about 0.9 m of shortening, was measured along a fence trending N. 50° E. on the east side of the nursing home. East of the nursing home, a low, but well-defined fault trace continues with only a few interruptions to the mouth of Lopez Canyon. Where the surface ruptures transect the lower slopes of the hills just east of the nursing home, the scarps are low, but well defined. A conspicuous zone of tension cracks about 2–3 m wide formed about 10 m upslope from the base of the scarps. On the west side of Lopez Canyon, the scarp, which is about 0.85 m in height (fig. 14), is a hummocky, multistranded bulge at the leading edge of the overriding northern block. In a trailer park immediately west of Lopez Canyon, the fault appears to follow a shallow-dipping plane in Tertiary marine deposits. About 0.4 km west of Lopez Canyon and for approximately 200 m along strike, the fault plane has a rather uniform dip of about 55° N. Just east of the canyon, the fault zone is defined by many subparallel imbricate breaks.

Eastward from Lopez Canyon the fault zone is made up of many en echelon segments. About 0.8 km east of the mouth of the canyon, the dip of the fault appears to lessen to about 15° N., but tectonic scarps are difficult to distinguish from the toes of landslides in this area. At the mouth of Bartholomaus Canyon, the scarp is about 0.25 m high, up on the north side, and shows about 0.1 m left-lateral offset of the streambank. The frontal scarp is about 0.60 m high and well exposed in Little Tujunga Canyon (fig. 15). East of this canyon for about 1.5 km, the zone is marked by compressional buckles and lacks developed scarps.

A gap of 2.2 km, within which no tectonic breaks have been found along the range front, separates the breaks near Little Tujunga Canyon from a well-defined south-facing scarp on the north side of Big Tujunga Creek, about 0.4 km east of the Lakeview Terrace Sanitarium. The scarp is 150 m long and 0.35 m high, but it cannot be traced contin-

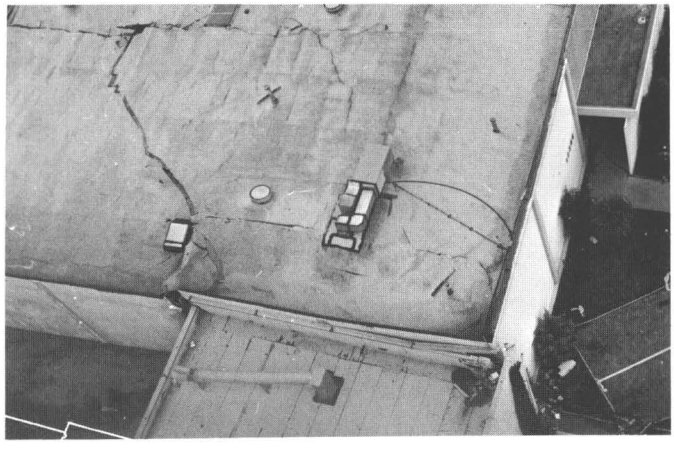

FIGURE 10.—Detail of interpenetration of two buildings caused by ground rupture. Edges of asphalt paving, outlined in lower left corner of photograph, overlap by 0.49 m. Near southeast end of Gladstone Avenue, near San Fernando Ranger Station.

[1] R. J. Proctor of the Los Angeles Metropolitan Water District reports that tectonic ruptures associated with the February 9 earthquake roughly follow a north-dipping thrust fault, which he had previously mapped and which he has named the Lakeview fault. The scarps in Schwartz and Oliver Canyons coincide with this fault, which would be synonymous with the Tujunga fault segment as used in this volume.

uously across the creek. The southeast end of this ground breakage is connected by a few discontinuous scarps to a well-developed line of surface rupture that is continuously traceable for about 0.9 km to the east. This line of ruptures is developed mostly in unconsolidated stream sediments which have been extensively churned by earth moving equipment, and the appearance and height of the fault scarp here varies considerably along strike. Several measurements of scarp height are shown in figure 2. About 1.5 km east of the Lakeview Terrace Sanitarium, this break cuts interlayered thin-bedded siltstone and conglomerate exposed on the north edge of Big Tujunga Wash. The fault plane here strikes about N. 70° W. and dips 55–60° N. Slickensides, which may or may not be related to the most recent movement, are developed in a thin zone of fault gouge and dip straight down the fault plane. The gouge indicates that the February 9 movement at this point occurred along a preexisting fault.

A few meters east of the faulted bedrock, the scarp, which is again in the stream sediments, becomes indistinct and cannot be distinguished from ridges formed by earth-moving equipment. Two disconnected scarps, each about 150–200 m long, continue en echelon to the east (fig. 2). The more easterly of these offsets the extension of Oro Vista Avenue about 0.3 m in a left-lateral sense. The height of this scarp is about 0.5 m, in the stream

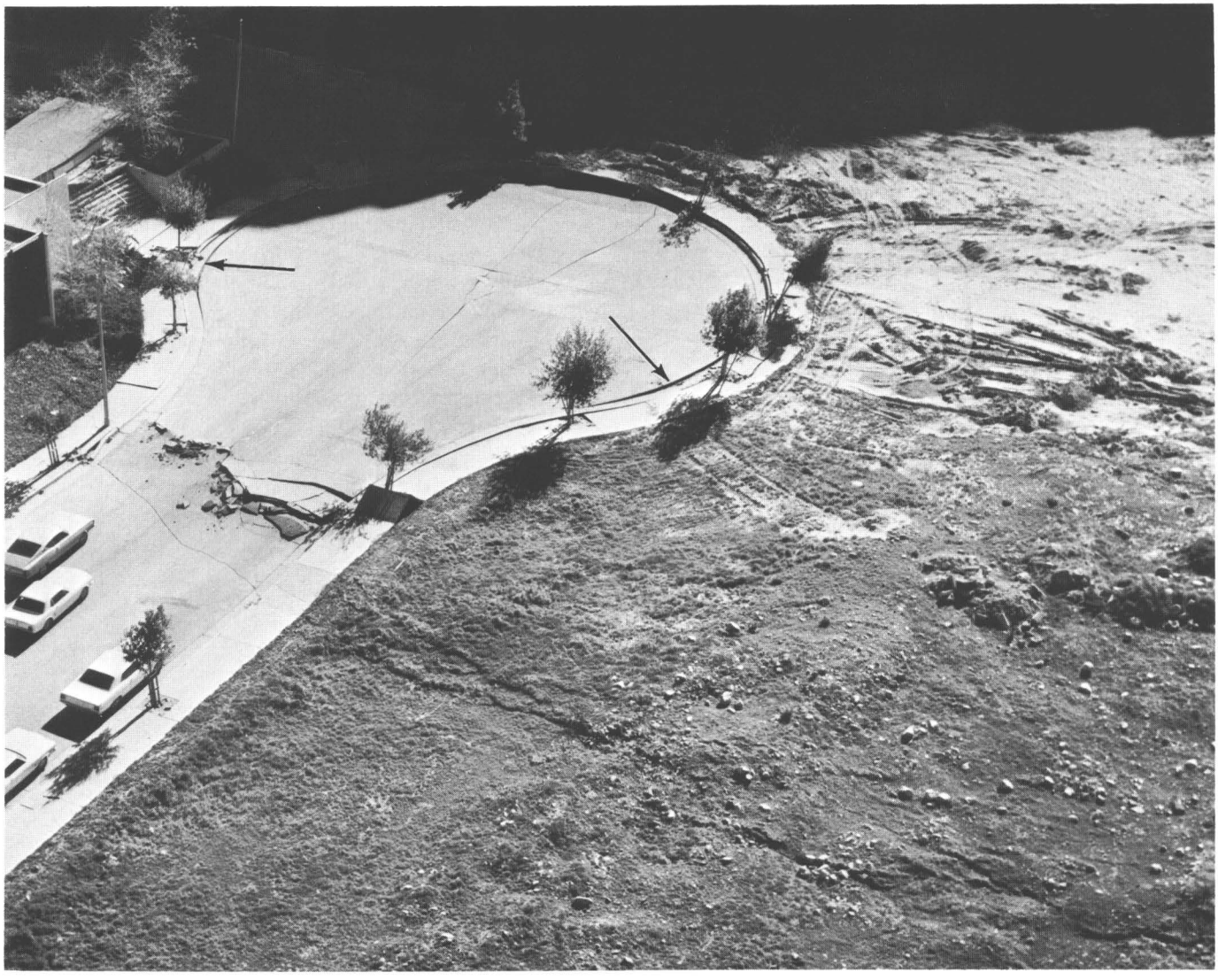

FIGURE 11.—Oblique aerial photograph of ground breakage on Montero Avenue near San Fernando Ranger Station. Note thrusting in open ground, compression of sidewalk and asphalt street, and crescent shaped openings near curbs (arrows).

FIGURE 12.—Detail of compression of sidewalk and asphalt street. The compressed sidewalk at left shortened 0.3 m. Note tree tilting southeast.

FIGURE 13.—Scarp formed near curb in front of Foothill Nursing Home. Scarp is about 1 m high here but is more subdued where it developed in unconsolidated sandy soil on either side of the nursing home. View looks northwest on Foothill Boulevard.

bottom below this street. About 0.4 km east of this break lies the scarp which marks the eastern end of the tectonic breakage. This scarp is 0.3 km long and strikes N. 75° E. Part of it is developed in thin-bedded siltstone and with the siltstone dips 62° N. Movement was up on the north, about 0.4 m. Four cracks that cross Mount Gleason Avenue about 0.7 km farther east show both left- and right-lateral displacements up to 0.02, m, and are probably not tectonic breaks.

SURFACE FAULTING IN THE MOUNTAINS NORTH OF THE TUJUNGA SEGMENT

In addition to the fault trace at the mouth of Lopez Canyon, other February 9 traces cross the canyon 0.6 km and 0.9 km north of its mouth. The northernmost of these occurred on an existing fault that was marked by gouge and shearing in the adjacent rock, but the earlier faulting apparently was not expressed in the modern topography. Where this trace extends westward from Lopez Canyon Road, it crosses a flat artificially graded surface underlain partly by bedrock and partly by alluvium (fig. 16). Figure 17 shows in plan and profile the very different expression of the fault in the two media. A distinct fault scarp about 1 m high formed in the bedrock (fig. 18), whereas a gentle monocline developed in the alluvium. The bedrock here consists of bedded friable sandstone, conglomerate, and thin shale, and it has about the same attitude (strike N. 80° W., dip 70° N.) on both sides of the fault. The fault strikes N. 80° W. and dips 65° N. at the surface (fig. 19), and this attitude continues to a depth of at least 10 m, where the fault was penetrated by a 36-inch borehole, visible

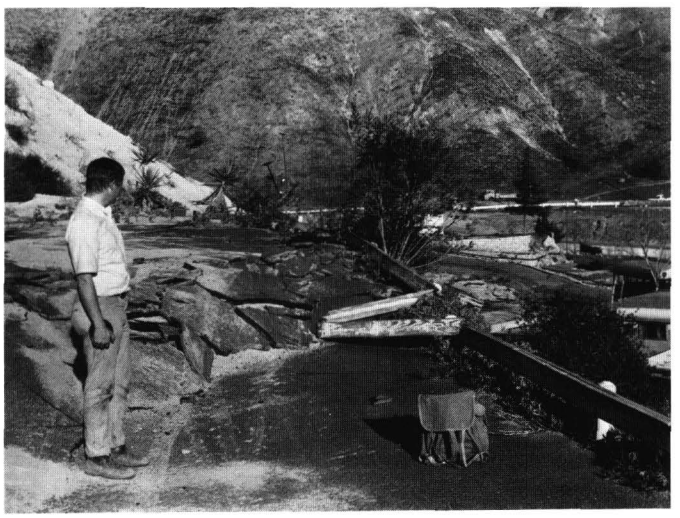

FIGURE 14.—Scarp in trailer court just west of the mouth of Lopez Canyon. Buckling of wood guardrail indicates considerable shortening, but the amount of shortening could not be precisely measured because guardrail posts on upper part of scarp detached from the ground. Height of scarp is about 0.85 m. View towards northeast. Mouth of Lopez Canyon in background.

in figure 16, drilled to install a wire extensometer. The gentle monocline that marks the fault in the alluvium is some 30–35 m wide (profile *B–B′* in fig. 17). Although the difference in height across the monocline is about the same as across the scarp, it would be difficult to identify this as a structural warp from the profile alone. Between S36 and S39

FIGURE 15.—Scarp in orange grove in Little Tujunga Canyon. Scarp is about 0.4 m high here, and about 0.6 m high in canyon bottom 80 m to west. View looks north.

on profile *B–B′*, the monocline is marked by a series of weakly developed pressure ridges trending east-southeast and tension fractures trending north-northeast. Some of the fractures show minor left-lateral displacement. Between S36 and S38, the monocline is characterized by generally east- or east-northeast-trending tension fractures that display small vertical movements (down on the south). These movements are accompanied by small left-lateral displacements between S36 and S37 and by small right-lateral displacements between S37 and S38.

Three linear features that were used to calculate the fault displacement in Lopez Canyon are marked I, II, and III in figure 17. These features, which were probably made by a bulldozer, consist of two ridges (I and II) and the edge of a shallow cut (III). The reverse-slip and left lateral slip components calculated from the field measurements are, respectively, 1.05 m and 0.80 m for I; 1.26 m and 0.85 m for II; and 0.88 m and 0.70 m for III. The average values of the components are about 1.05 m

FIGURE 16.—Oblique aerial photograph of fault scarp 0.9 km north of mouth of Lopez Canyon. Note gradation to monoclines at each end of scarp. Drill rig is setting casing in borehole that confirmed 65° dip of fault.

reverse slip and 0.80 m left-lateral slip, or 1.32 m oblique (net) slip.

Near the east end of the scarp, slickensides in the gouge are inclined 58° from the horizontal (fig. 20) which indicates a somewhat lower ratio (0.635) of strike slip to dip slip than was obtained from the displaced bulldozer features (0.76). It is uncertain, however, whether these slickensides formed on February 9 or during an earlier movement on the same fault plane. Both indicate that this was a left-reverse oblique fault according to the classification of Bonilla and Buchanan (1970, p 7–9).

About 0.6 km north of the mouth of Lopez Canyon, a small scarp bulges up the pavement of the Lopez Canyon Road, with the north side elevated about 0.2 m. A roadcut alongside the break exposes disturbed and somewhat slumped sandstone and siltstone, but no positive evidence or prior move-

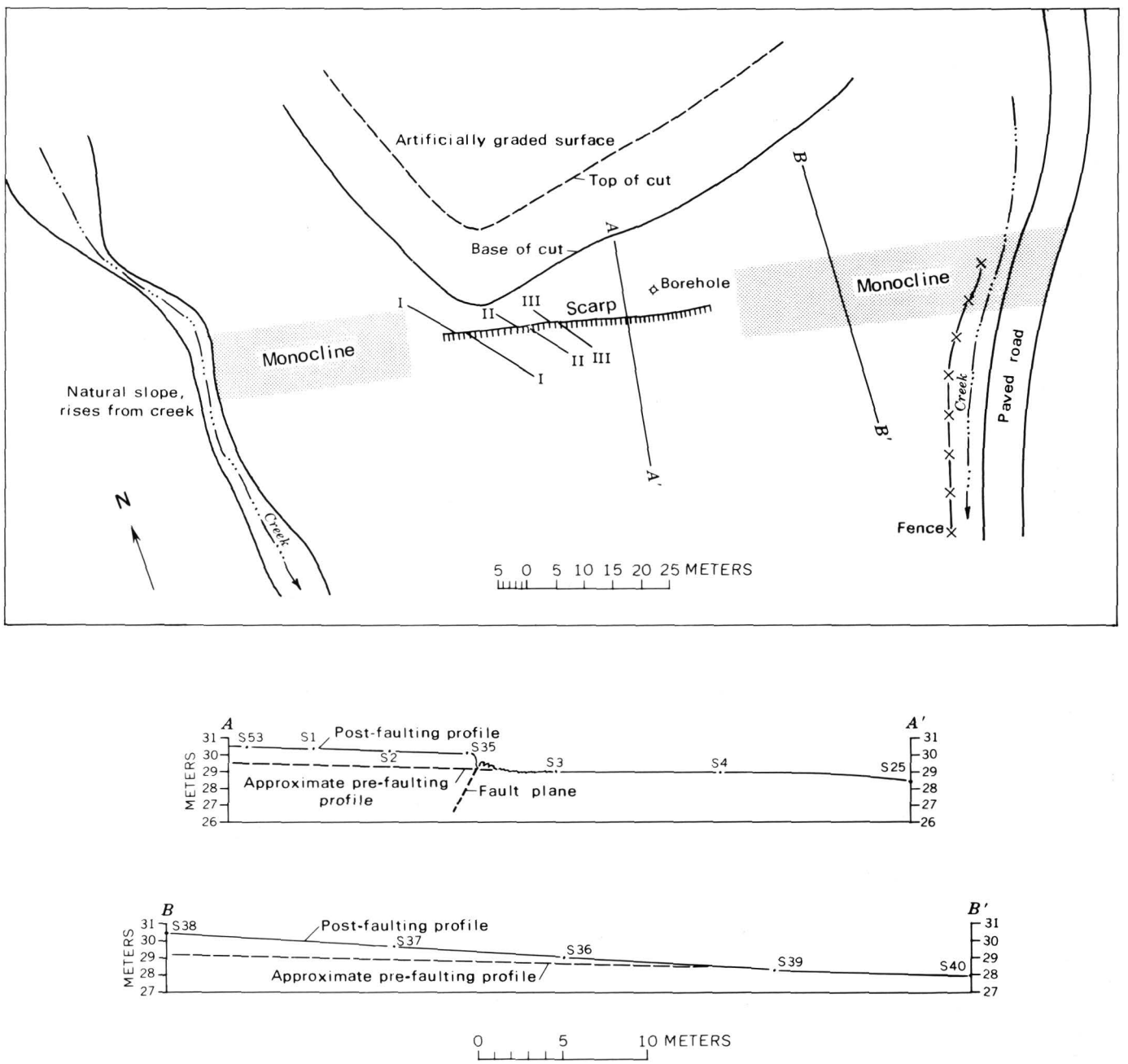

FIGURE 17.—Plan and profiles of trace of fault 0.9 km north of mouth of Lopez Canyon, based on planetable mapping. For location see figure 2. Elevations on profiles referred to local assumed datum. Numbers preceded by S are field survey stations. See text for details.

FIGURE 18.—Fault scarp in bedrock, Lopez Canyon. Note fault surface dipping under scarp, debris from collapsed hanging wall of fault, and thin layer of unconsolidated material over bedrock. Large divisions on horizontal rod are 12 inches (0.3 m).

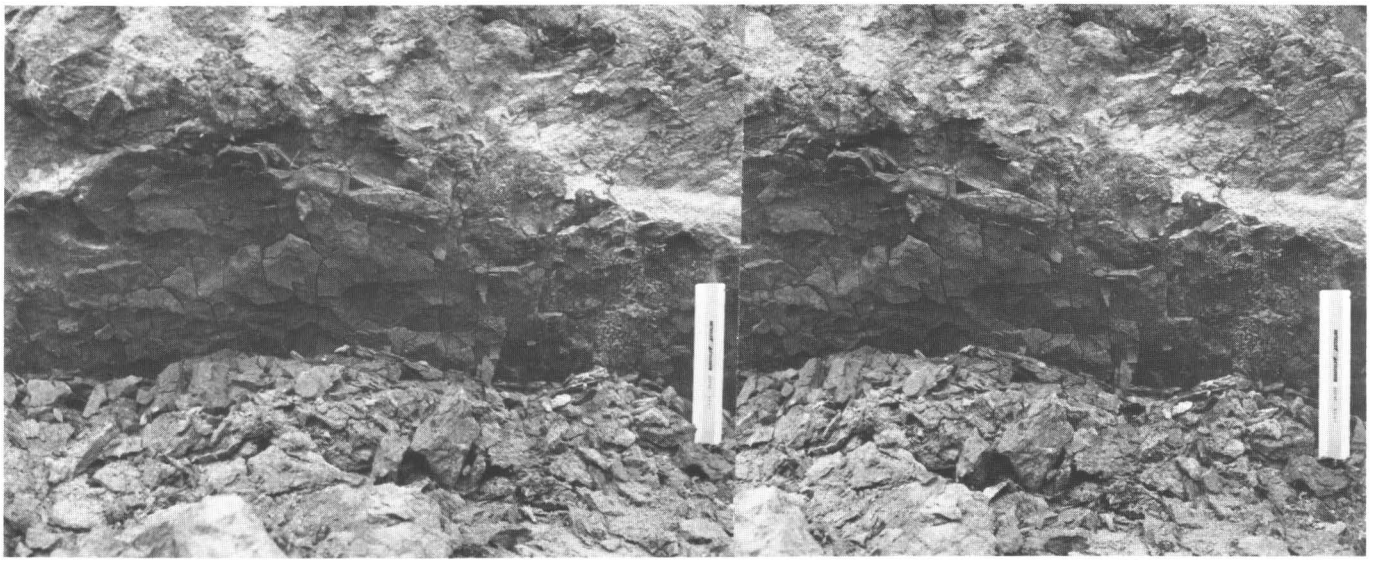

FIGURE 19.—Detail of dipping fault plane shown in figure 18, showing sloughing gouge; photographs mounted as a stereoscopic pair. The scale in the lower right, which is 170 mm long, is also shown at the same spot in figure 18.

ment such as a gouge zone or structural truncation of bedding is visible. About 110 m due west of this scarp, however, a northward-dipping fault surface is visible on a steep face cut in similar sedimentary rocks. Although preearthquake reference lines are not present across this break, a thrust movement of a few centimeters, possibly with a minor left-lateral component of slip is evident. In contrast to the cut at the road, the offset here appears to have occurred along a preexisting fault, as shown by gouge and the slight structural discordance of the underlying beds at the fault. The offset apparently dies out westward within the upper part of the cut, and no tectonic rupturing was found on a projected line at any point higher on the hill. Whether this fault joins the scarp to the east of Lopez Canyon Road is uncertain. Pavement and soil in the intervening sector are located on fill and are strongly fractured. This breakage, however, is probably nontectonic, and the continuity of the two offsets is in doubt.

Thirteen fractures exhibiting right-lateral offset break Lopez Canyon Road between 0.27 km and 0.53 km north of the Tujunga segment of the San Fernando fault zone. The net right-lateral offset across these breaks is about 0.5 m, of which about half is concentrated in a narrow zone at its southern edge. Although the breaks cannot be traced either west or east, it is likely that they are of tectonic origin. They appear to be similar to breaks within the broad zone of right-lateral rupturing immediately north of the Sylmar segment.

Another well-developed south-facing scarp lies about 0.4 km up Little Tujunga Canyon from the frontal scarp. This upper scarp is a hummocky bulge similar to those at the range front. It dies out about 0.3 km east of Little Tujunga Road, but it continues westward almost to Kagel Canyon. Just west of Little Tujunga Canyon, the scarp is 0.45 m high. Several small scarps cross Kagel Canyon, but cannot be traced for any distance outside the canyon. A small south-facing scarp extends westward from the bottom of Bartholomaus Canyon but cannot be traced east of it. Although the scarp is little more than a buckle in the bottom of the canyon, on the ridge 0.3 km to the west, it is about 0.30 m high and displays about 0.58 m of left-lateral offset.

Prominent scarps of probable tectonic origin cross the bottoms of Oliver and Schwartz canyons about 0.4 km north of their mouths. The scarp in Oliver Canyon is about 0.9 m high and that in Schwartz Canyon about 0.3 m. Although both are probably parts of longer structural features, they cannot be traced with confidence outside of the canyons through the extensive landslides which mantle the surrounding hillsides.

SCARP EAST OF THE VETERANS HOSPITAL

Although extensive damage to man-made structures occurred along a zone extending from Upper Van Norman Lake to the head of Pacoima Wash, there is only one scarp in this zone interpreted to be of possible tectonic origin. This scarp is about 300

FIGURE 20.—Detail of fault plane showing slickensides inclined 58° from horizontal; photographs mounted as a stereoscopic pair. Note apparent change of inclination of the striations over this length. Vertical groove near compass is artificial. These slickensides may have been produced by a fault movement previous to the one on February 9.

m long and is expressed as a small nearly east-west surface rupture. It is between the U.S. Veterans Hospital and Pacoima Wash and is well exposed in cuts and fills of a partly developed housing tract near Rajah Street (fig. 2). In the banks of cuts, the slip surface dips generally northward between 36° and 48°, parallel to bedding of sandstone and conglomeratic sandstone of the Pacoima Formation (included in Saugus Formation on the geologic map in the paper by Wentworth and Yerkes, this report). Displacement is apparently directly updip, and the maximum relative uplift of the northern slide is about 0.18 m. Westward the strike of the break gradually swings toward the southwest. A line joining the western end of the continuous fracture to a short scarp with vertical offset observed on Hubbard Street would have a southwesterly trend. Although the rupture has the appearance of a tectonic fracture, it conceivably could represent the bulged toe of an unexpectedly large landslide whose upslope limits have not been recognized.

The projection of the fault, is it continues along its last observed trend, passes well south of the Veterans Hospital. Although no further tectonic breaks were recognized west of the scarp, this does not preclude the possibility that the zone from west of Juvenile Hall to the Veterans Hospital was tectonically active during the earthquake. For example, left-lateral deformation may have occurred across the zone near the Juvenile Hall, as a postearthquake resurvey of San Fernando Road showed a small left-lateral and southward shift of a point due west of the Juvenile Hall with respect to a point at the corner of Roxford Street and San Fernando Road (Youd, this report).

COMPARISON OF RUPTURE DIMENSIONS TO MAGNITUDE OF THE EARTHQUAKE

Comparison of the maximum surface displacement and length of the February 9 faulting with other reverse-oblique-slip faulting is difficult because only about six examples of historic surface faulting of this sense are recorded in the world literature; furthermore, the data for this type of fault do not show a consistent relation between earthquake magnitude and fault displacement or length. Compared with historic surface faulting of all types, however, the February 9 faulting has a greater displacement and a smaller fault length than would be expected to accompany a magnitude 6.6 earthquake. Empirical data on all types of historic surface faulting treated as one group (Bonilla and Buchanan, 1970, figs. 2 and 3, set 1–140) indicate that the surface faulting accompanying a magnitude 6.6 earthquake is likely to have a maximum surface displacement of 0.8 m and a surface length of about 20 km, in contrast to the 2.4 m displacement and about 15 km length of the February 9 faulting.

PREEARTHQUAKE TOPOGRAPHIC EXPRESSION OF THE SAN FERNANDO FAULT ZONE

The San Fernando earthquake of 1971 shares many topographic similarities with the Arvin-Tehachapi earthquakes of 1952 (Oakeshott, 1955). Movements during both earthquakes combined thrusting with left-lateral strike slip, and both involved faults that were not widely considered, on topographic evidence, to be presently active.

Most of the 1971 breakage along the San Fernando fault zone followed scarps created by previous faulting. The Tujunga segment followed an obvious scarp along a range front, as recognized some time ago by Miller (1928 and 1934). Inspection of preearthquake vertical aerial photographs (1:24,000 scale from 1952 and 1:90,000 scale from 1964) reveals that the Mission Wells and Sylmar segments also followed a single, nearly continuous scarp, but this scarp becomes almost undetectable in its central part. Neither the Tujunga nor the Mission Wells-Sylmar scarps, however, could have been positively identified as scarps of presently active faults without supporting stratigraphic evidence.

The land forms created in the zone of breakage of a reverse fault contrast strongly with those that mark the most recently active traces of strike-slip faults such as the San Andreas, San Jacinto, and Garlock for example, Ross, 1969; Clark, 1970; Sharp, 1970; Vedder and Wallance, 1970. Thus although the scarp followed by the surface ruptures along the Tujunga segment is straight, in detail it lacks the striking continuity and abundant scarps across alluvium associated with known active strike-slip faults that follow range fronts. It also lacks the extensive, and in some places linear, scarps that characterize geologically young normal faults such as those along the eastern base of the Sierra Nevada (for example, Shelton, 1966, fig. 342). The geomorphic criteria of these other active faults indicate that the Tujunga segment might well be classified as less recently active than it evidently is.

The eastern end of the Sylmar segment follows the face of a prominent south-facing scarp that is 6–10 m high, but it diverges from this scarp to the west, near the Foothill Freeway. Farther west, the fault follows an increasingly wide and less well de-

fined scarp as far as Orange Grove Avenue, where the scarp becomes nearly indistinguishable from local variations in the regional slope. A distinct increase in slope occurs, however, where Glenoaks Boulevard crosses the fault zone, and the 1:90,000-scale aerial photographs show a broad (about 100–300 m wide) but definite south-facing scarp continuing westward to Mission Wells. There the scarp again becomes prominent along the Mission Wells segment of the 1971 breaks. The course of the Mission Wells segment farther west into the hills surrounding Lower Van Norman Lake follows no prominent topographic trend. These scarps and changes in slope along and between the Sylmar and Mission Wells segments are almost certainly tectonic, but they could not have been so identified before the earthquake without other corroborating geologic evidence as similar landforms could have been produced by other processes.

Thus, in marked contrast to many of the active strike-slip and normal faults of California, the active traces of the San Fernando fault cannot be identified by topography alone. Rather, topography along this thrust fault could serve to confirm identifications made from subsurface or other evidence. Were the fault identified by other evidence, however, the topography would indicate the sense of displacement across the fault. Where the scarps are distinct, the topography could also serve to define the position and character of displacement of the fault more closely.

If the San Fernando fault zone has a record of activity comparable to that of active normal and strike-slip faults in California, the generally poor topographic expression must be related to the nature of the surface ruptures and movements associated with thrusting. As shown in figure 2, displacement over most of the Sylmar segment extended across a wide zone, creating a broad, gentle scarp. Eastward from about Eighth Street, however, where displacement in 1971 was concentrated into a progressively more narrow zone, the old scarp becomes correspondingly narrower and steeper. This relation between width of the 1971 zone of breaks and the prominence of the old scarp suggests that previous movement on the Sylmar segment resembled that of 1971. If the present zone of breakage follows the course of prior recent movements on the Tujunga segment, much of the detailed topographic expression of these recent movements along the narrower zone of breakage of that segment probably was masked or destroyed by associated landsliding at the time of each earthquake.

The dip of a range-front reverse fault creates sinuous, rather than straight scarps or zones of surface breakage. The fault trace therefore lacks linear continuity, an important clue in the recognition of topography created by active strike-slip faults. Thrusting in alluvium or poorly consolidated sediments also seems to shatter the upthrown block more than do either strike-slip or normal faulting, presumably leading to more rapid destruction of the newly formed scarp.

COULD THE LOCATION OF THE FAULT SCARPS OF FEBRUARY 9, 1971, HAVE BEEN PREDICTED?

The recognition of active reverse faults has been shown above to be usually much more difficult than the recognition of active strike-slip and normal faults. As the recognition of such faults in seismic regions is critical to safe development, it is clearly important to ask whether a geologic investigation could have determined the location and youthfulness of the fault zone in which the surface ruptures of February 9 formed. The answer is yes.

Wentworth and Yerkes (this report) show that previous subsurface investigations revealed a groundwater anomaly along the trend of the Sylmar and Mission Wells segments of the San Fernando Fault that could reasonably have been interpreted as a very young fault. This interpretation would have been supported by the scarps discussed above; moreover, trenches across the fault zone would very probably have revealed lines of previous fault breakage. Similarly, subsurface investigations at critical locations along the Tujunga segment might have reinforced the limited data from surface features as to the recency of movement along the range front. For example, the newly exposed scarp in upper Lopez Canyon described in this paper contained abundant gouge of earlier episodes of movement, and the ground-water cascade further south in the canyon (Wentworth and Yerkes, this report) also suggests recent movement.

RELATION OF SURFACE FAULTING TO DAMAGE TO BUILDINGS

The Sylmar segment of the San Fernando fault is a zone of concentrated major damage to buildings. This fact is indicated by figure 21, which shows the location of buildings in parts of San Fernando and Los Angeles that were posted as unsafe as of February 24–March 1, 1971. Not only is there a greater concentration of such buildings within the mapped fault zone than in any other comparable area in the figure, but east of Seventh Street the

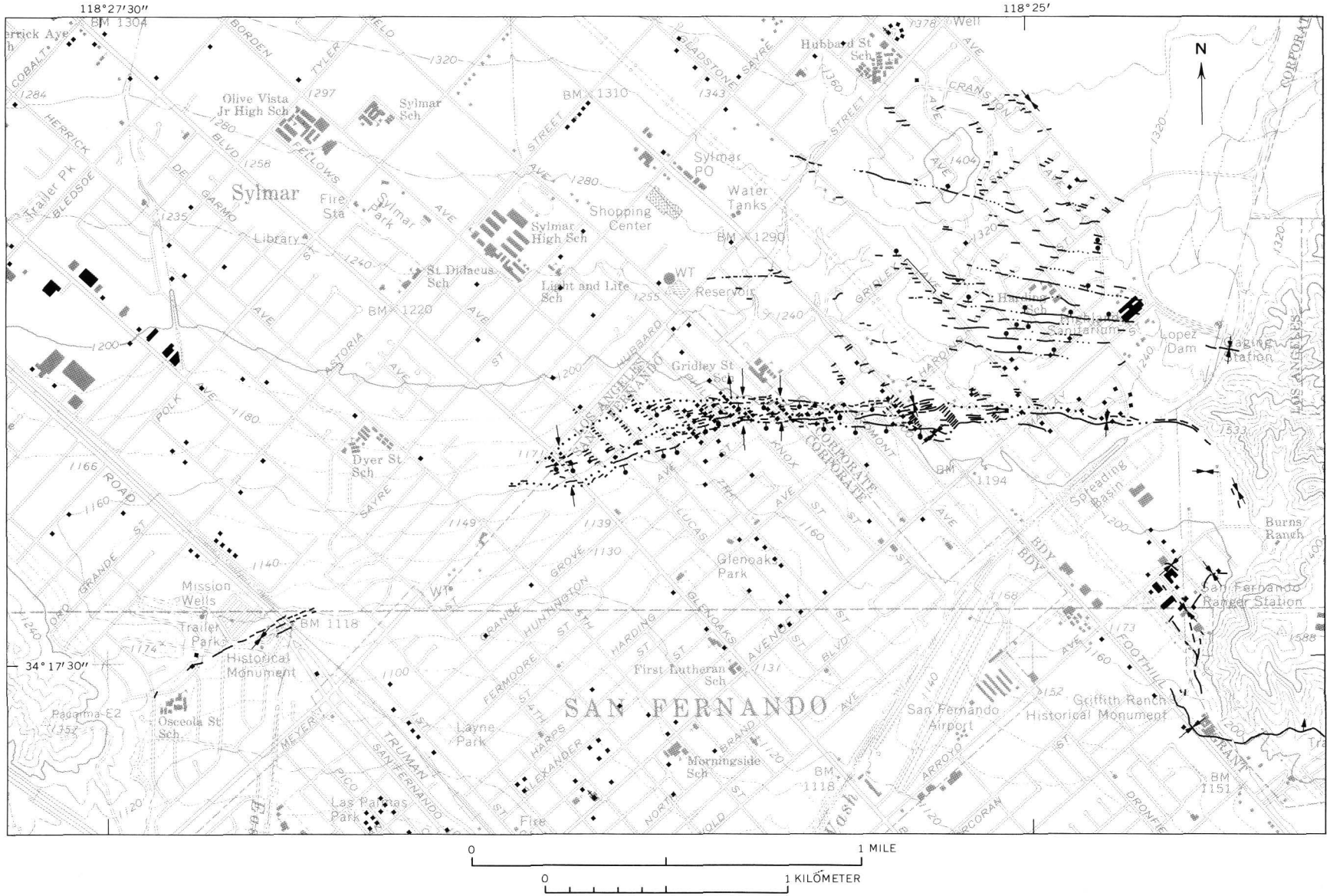

FIGURE 21.—Relation of surface faulting to the location of damaged buildings posted as unsafe (black squares) by officials of the cities of Los Angeles and San Fernando. From preliminary lists supplied by the Los Angeles Department of Building and Safety on February 24, 1971, and by the San Fernando Department of Building and Planning on February 24 and March 1, 1971. The lists were not necessarily complete and were subject to daily additions and deletions at the time they were sent. Many unsafe commercial buildings in the vicinity of San Fernando Road in San Fernando were not plotted because no street address was supplied. Most houses plotted along the Sylmar segment west of Foothill Boulevard are within 25 m of their correct position; elsewhere in San Fernando most houses are plotted within 50 m of their correct position; most of those on the remainder of the map are within 200 m of their correct position. Surface fault traces are from figure 2.

pattern of posted buildings closely conforms to the narrowing limits of the zone of breaks. Many additional buildings in the fault zone suffered severe structural damage, but were not classified as unsafe.

Table 2 compares the number of posted, damaged, and undamaged houses within the mapped fault zone between Seventh and Eighth Streets in San Fernando to the same categories of houses in bands of roughly comparable width adjacent to each side of the fault zone. The table shows some important differences between these zones. For example, 30 percent of the houses within the fault zone were posted as unsafe, as compared with only 5 percent of those on either side. Eighty percent of the houses in the fault zone suffered moderate or worse damage, but only 30 percent of those immediately beyond experienced such damage.

TABLE 2.—*Summary of damage to houses in San Fernando along the Sylmar segment of the San Fernando fault zone between Seventh and Eighth Streets* [1]

Type of damage	Within fault zone shown in figure 1		Within zones of comparable width on each side of the fault zone [2]	
	Number of houses	Percentage of houses in this zone	Number of houses	Percentage of houses in this zone
Total number of houses in zone	94	100	161	100
Undamaged or minor damage	21	20	110	70
Moderate to severe structural damage[3]	43	50	42	25
Posted as unsafe	30	30	9	5
Total, moderate damage or worse	73	80	51	30

[1] From preliminary house-by-house descriptions supplied by the San Fernando Department of Building and Planning, Feb. 24 and Mar. 1, 1971.
[2] Rounded to reflect uncertainties in the descriptions of damage.
[3] For example, cracked or broken foundation, house shifted on foundation.

The increased damage to houses in the break zone apparently resulted from the large horizontal and vertical displacements across ground fractures in this area (Youd and Olsen, this report). In contrast, the area north of the Sylmar segment and east of Foothill Boulevard has widespread surface fractures that show only small displacements. Significantly, this area was not associated with extraordinary damage to buildings, apparently in part because ground displacements were not sufficiently large.

Concentrations of "unsafe" houses shown in figure 21 beyond the limits of significant faulting may result from such causes as locally amplified seismic shaking, local surficial ground movement, undiscovered tectonic movement, or design and construction.

ABSENCE OF MOVEMENT ALONG KNOWN FAULTS IN THE EPICENTRAL REGION

Several faults in the epicentral region of the San Fernando earthquake were checked to determine if any movement occurred along them. No evidence of movement or cracks that might be related to tectonic movements were found. The following faults were examined:

1. Santa Susana thrust.
2. Mission Hills thrust where it is crossed by Woodley Avenue.
3. San Gabriel fault in Big Tujunga Canyon.
4. San Gabriel fault where it is crossed by Little Tujunga Road.
5. Unnamed fault trending west-northwest through downtown Sunland and Tujunga. This fault is entirely subsurface in the sections checked.
6. Park fault south of Foothill Boulevard and east of Green Verdugo Reservoir.
7. Hospital fault due north of U.S. Veterans Hospital (eastern extension of Santa Susana Fault on geologic map in paper by Wentworth and Yerkes, this report).
8. Northridge Hills fault at Balboa Boulevard.

TECTONIC AND ENGINEERING IMPLICATIONS

To recapitulate, mapping of the tectonic fracture zones shows that faulting associated with the San Fernando earthquake was characterized by left-reverse oblique slip of up to 2.4 m, along an approximately east-striking fault system that dips north about 55° at the surface. The sense of movement determined from surface measurements accords closely with that deduced from fault-plane solutions for the main shock. (See Whitcomb; Dillinger and Espinosa, this report.) Detailed mapping has also shown that the zone of tectonic fractures is defined on the south by a conspicuous major break or narrow shear zone; we identify virtually no tectonic fractures south of this boundary. The northern boundary of the breakage zone, however, is diffuse.

The gross relationship between earthquake damage and surface faulting is demonstrated by the remarkable concentration of major damage within the zone of surface breaks along the Sylmar segment. The gross relationship between damage and deformation in the thrust plate above the faults with surface breakage is shown, but more equivocally, by the great predominance of major damage in the upper plate. The occurrence of major damage along the mountain front between and beyond the Olive View and U.S. Veterans Hospitals suggests the possibility of faulting in that area. Tectonic fractures here could easily be masked by the abundant land-

slides; nevertheless, we have direct evidence of only one relatively short break along this zone that could be interpreted as tectonic.

REFERENCES

Bonilla, M. G., and Buchanan, J. M., 1970, Interim report on worldwide historic surface faulting: U.S. Geol. Survey open-file report.

Clark, M. M., 1970, Some characteristics of the most recently active traces of the Garlock fault [abs.]: Geol. Soc. America Abs. with programs, v. 2, no. 2, p. 82.

Miller, W. J., 1928, Geomorphology of the southwestern San Gabriel Mountains of California: Calif. Univ. Pubs. Geol. Sci., v. 17, p. 193–240.

———1934, Geology of the western San Gabriel Mountains of California: Calif. Univ. Los Angeles Pubs. Math and Physical Sci., v. 1, p. 1–114.

Oakeshott, G. B., ed., 1955, Earthquakes in Kern County, California, during 1952: Calif. Div. Mines Bull. 171, 283 p.

———1958, Geology and mineral deposits of San Fernando quadrangle, Los Angeles Co., Calif.: Calif. Div. Mines Bull. 172, 147 p.

Ross, D. C., 1969, Recently active breaks along the San Andreas Fault between Tejon Pass and Cajon Pass, southern California: U.S. Geol. Survey Misc. Geol. Inv. Map I–553, scale 1:24,000.

Sharp, R. V., 1970, Map showing recently active breaks along the San Jacinto fault zone between San Bernardino area and Borrego Valley, California: U.S. Geol. Survey open-file map, scale 1:24,000.

Shelton, J. S., 1966, Geology Illustrated: San Francisco, W. H. Freeman and Co., 434 p.

Vedder, J. G., and Wallace, R. E., 1970, Map showing recently active breaks along the San Andreas and related faults between Cholame Valley and Tejon Pass, California: U.S. Geol. Survey Misc. Geol. Inv. Map I–574, scale 1:24,000.

STRAINS AND TILTS ASSOCIATED WITH THE SAN FERNANDO EARTHQUAKE [1]

By PIERRE JUNGELS and DON L. ANDERSON
SEISMOLOGICAL LABORATORY, CALIFORNIA INSTITUTE OF TECHNOLOGY

The San Fernando earthquake of February 9, 1971, M=6.6, was well recorded on the quartz-strain seismometers and mercury tiltmeters at the Isabella facility of California Institute of Technol-

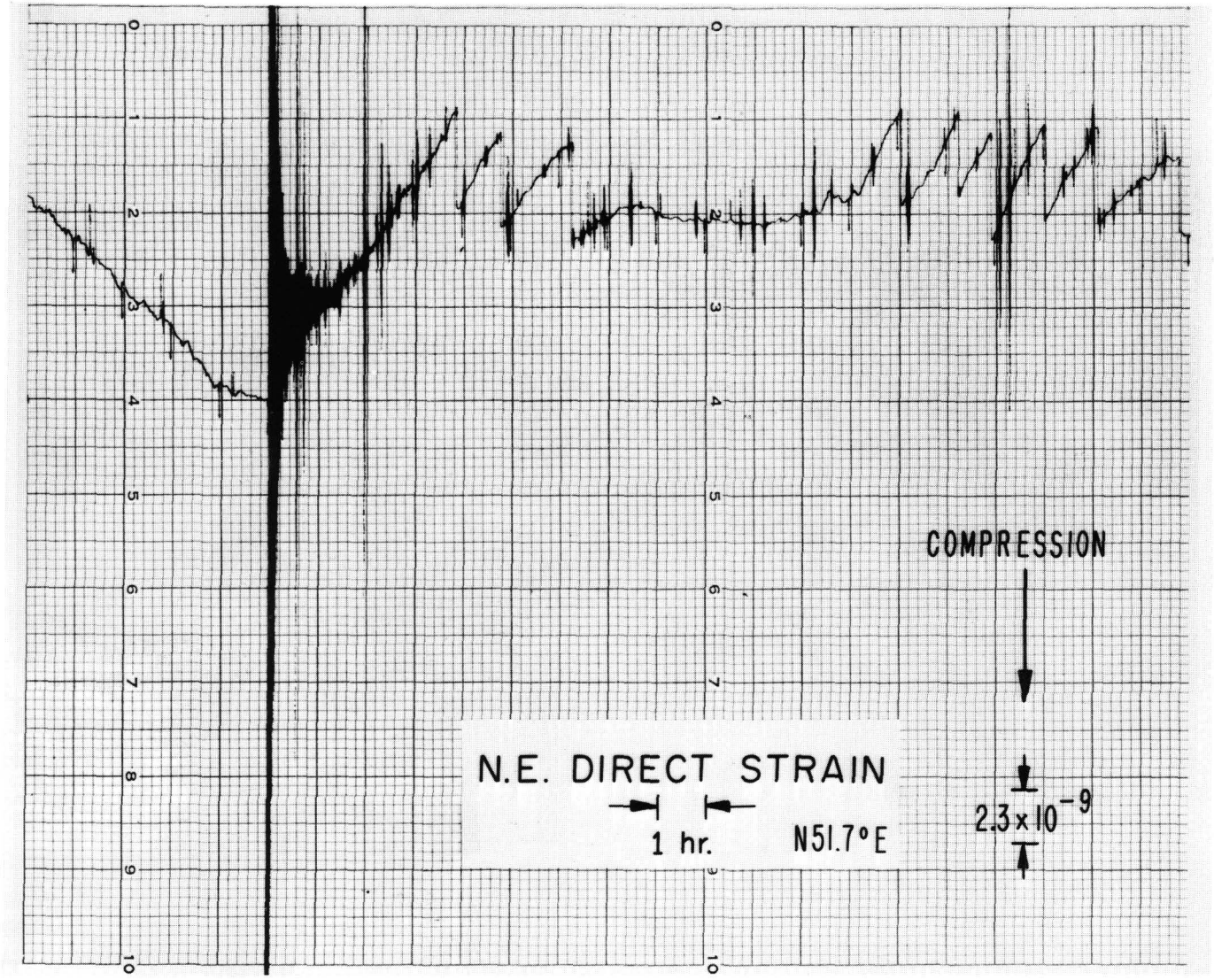

FIGURE 1.—Strain seismogram for the N. 51.7° E. component at Isabella from 0100 February 9 (left side of record) to 0100 February 10, 1971 (PST.). Note the "permanent" offset on the record at the superimposed very large amplitude deflections that mark the main shock at approximately 0601 February 9, 1971 (PST.). The vertical offsets, or steps, in the seismogram following (to the right of) the main shock are the result of automatic recentering of the trace.

[1] Contribution No. 1989, Division of Geological and Planetary Sciences, California Institute of Technology, Pasadena, California.

ogy. The facility is located 147 km (kilometers) north of the epicenter. Figure 1 shows the strain seismogram for the N. 51.7° E. component of strain from 0100 February 9 to 0100 February 10, 1971 (PST). The seismic waves from the main shock, which occurred at approximately 0601 on February 9 (PST), and aftershocks are superimposed on tidal strains. The "permanent" offset on this record corresponds to a net dilatation, or lengthening, of 4.19×10^{-9}. This represents a change in the static strain field that is associated with the earthquake.

The permanent offsets on the four instruments are:

N. 51.7° E. strain ——— -4.19×10^{-9},
N. 51.7° E. tilt ——— $<7 \times 10^{-3}\mu$ radians,
N. 38.3° W. strain ——— -13.6×10^{-9},
N. 38.3° W. tilt ——— 0.1μ radians.

The UCSD (University of California at San Diego) strain meter, southeast of the epicenter and oriented N. 45° E., exhibited an offset of $+1.6\times10^{-9}$, corresponding to a release of tension (J. Berger, personal commun.).

Two strain meters installed near the Nevada Test Site 380 km to the northeast of the epicenter exhibit offsets of the order of -3×10^{-10}, both dilatational.

From the fault-plane solution for the main shock, and from the field observations of surface faulting, Isabella should be in a compressional strain release quadrant, and the UCSD station should be in a tensional release quadrant. Both components of strain at Isabella and those of the Nevada Test Site exhibit tensional offsets, that is, release of compression. The UCSD strain meter indicates tensional release although we do not know, of course, if the net strain is tensional.

Both the fault-plane solution and the field observations of surface faulting indicate that overthrusting and left-lateral motion were associated with the faulting. The dip of the fault plane is 45° NE. at the surface and 52° NE. at the hypocenter. Unfortunately, solutions for the strain field associated with a dipping fault have not been published. Crude estimates of the expected strain field can be obtained by combining theoretical strains for strike-slip and dip-slip motion. For this purpose we use the graphs in Press (1965). Taking a fault length of 20 km, a fault depth of 10 km, a vertical movement of 1⅓ m (meters), and a horizontal movement of 1 m, we calculate for Isabella (147 km north of epicenter):

N. 51.7° E. strain ——— -12×10^{-9},
N. 38.3° W. strain ——— -10×10^{-9};

for the UCSD strain meter, $+1.4\times10^{-9}$; and for the Nevada Test Site we get an areal dilation of approximately -3×10^{-10}. This good agreement certainly provides us with the motivation to do the complete calculation. The results will be reported in a later paper.

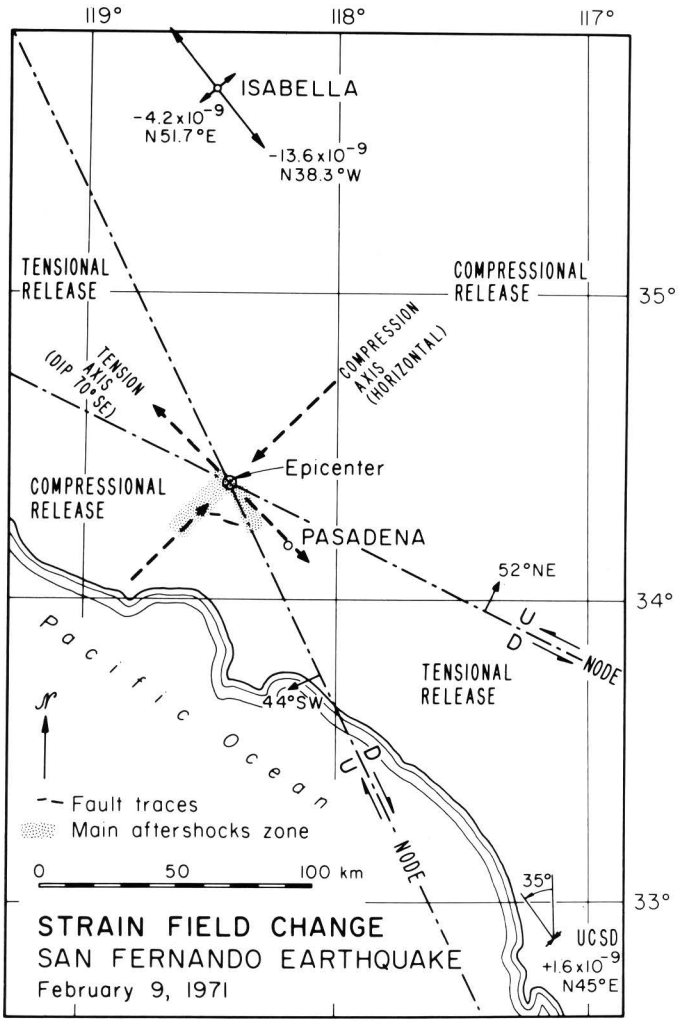

FIGURE 2.—Strain field changes associated with the San Fernando earthquake.

The theoretical tilts for the vertical fault are an order of magnitude greater than observed, and this probably is where the inadequacies of the model are most important.

The principal aftershocks mainly line up along the compression release axis and along the southeast nodal axis. It will be interesting to see if these two groups have different focal mechanisms.

The strike of the original break, as inferred from

the fault-plane solution, is closely parallel to the closest segment of the San Andreas fault some 30 km to the northeast. A simple calculation shows that the San Fernando earthquake decreased the elastic compressional stress across the San Andreas fault by 2×10^{-6}, which corresponds to a tensional stress of approximately 1 bar. Tension and shear strains calculated along the San Andreas are both about 5×10^{-7}, or a fraction of a bar.

As can be seen from figure 1, the earthquake occurred very close to the time of maximum tidal compressional strains. (A total lunar eclipse, associated with maximum tidal tension, occurred some 18 hours later.) Larger tidal compressions occurred during prior tidal cycles, 24 and 48 hours earlier.

ACKNOWLEDGMENTS

We acknowledge helpful conversations with Clarence R. Allen, James H. Whitcomb, David Harkrider, and Charles Archambeau. Auxiliary data was kindly provided by John M. Nordquist, Whitcomb, and John Berger. The Isabella facility is due to the efforts of Hugo Benioff, Stewart Smith, and William Gile. The station is supported by grants from the Advanced Research Projects Agency of the Department of Defense and was monitored by the Air Force Office of Scientific Research under contract Nos. F44620–69–C–0067 and AFOSR–70–1954. The Earthquake Research Affiliates, a private group of sponsors, has contributed greatly to our program in earthquake research.

REFERENCE

Press, Frank, 1965, Displacements, strains and tilts at teleseismic distances: Jour. Geophys. Research v. 70, p. 2395–2412.

PRELIMINARY MEASUREMENTS OF TECTONIC MOVEMENT

By R. O. BURFORD, R. O. CASTLE, J. P. CHURCH, W. T. KINOSHITA, S. H. KIRBY, R. T. RUTHVEN, and J. C. SAVAGE

U.S. GEOLOGICAL SURVEY

Instrumental measurements within an area surrounding the tectonic surface disturbance were begun almost immediately following the San Fernando earthquake of February 9, 1971. These measurements were designed to: (1) show such elevation and length changes as may have occurred at or about the time of the main shock, and (2) provide information on rate and amount of continuing tectonic movements (aftercreep), should any occur. A variety of measurement techniques were utilized for both preearthquake and postearthquake observations, including conventional leveling, triangulation, trilateration, vertical angle readings, and special instrumentation of the surface breaks.

PREEARTHQUAKE AND POSTEARTHQUAKE COMPARISONS

Results of comparisons between preearthquake and postearthquake measurements are summarized in figure 1. The general distribution of the tectonic surface fractures mapped during the postearthquake field investigation is also shown.

Preearthquake vertical control is generally good south of the frontal scarp of the San Gabriel Mountains; it extends into the mountains locally, notably along the Southern Pacific Railroad and up Lopez, Kagel, and Little Tujunga Canyons. Postearthquake level circuits were selected to determine the elevation changes across the zones of tectonic rupture discovered in reconnaissance of the area during the 2 or 3 days following the earthquake. Several assumptions exclusive of those associated with instrumental precision and surveying procedures are built into the elevation determinations leading to the vertical movements shown in figure 1.

1. Preexisting circuits of temporally separated levelings have been connected locally in order to provide a basis for the postearthquake comparisons. It has been assumed, in other words, that the connecting bench mark(s) remained stable between those levelings preceding the earthquake.
2. The elevation changes reported in figure 1 are in most cases based on a comparison between earlier adjusted elevations and postearthquake observed elevations. Owing to the relatively short circuits utilized in these comparisons, it is unlikely that the values given in figure 1 would be more than slightly modified if the comparisons had been between observed values only.
3. All the elevation changes shown in figure 1 are related to an arbitrarily selected separate control point within each one of the disconnected circuits.

Preexisting horizontal control has not yet been researched in detail; hence, we are limited at present to only a few meaningful comparisons. The triangulation networks of the National Ocean Survey and the Los Angeles County Department of County Engineer should provide a firm basis for the recognition of any regional length changes. Furthermore, survey traverses carried out in connection with freeway or other highway construction can be expected to provide fairly good local control. However, except for those areas in which horizontal changes have been dramatically large, remaining preearthquake horizontal control generally affords an inadequate basis for the recognition of significant earth movements.

Approximate length changes determined along several streets in the City of San Fernando depend on postearthquake resection of street intersections. The control points to which the 1938 surveying is referred have not been recovered; therefore, it is unlikely that these length changes are accurate to better than ± 0.1 m (meter). Length changes along those lines comprising the regional network represented in figure 1 are based on comparisons between preearthquake triangulated distances and 1971 geo-

dimeter measurements; changes over these distances are considered accurate to ±0.1 m, for lines up to 10 km (kilometers) long.

INTERPRETATION OF ELEVATION CHANGES

Level circuit 1 was deliberately routed through the unbroken area between the Mission Wells and Sylmar segments of the San Fernando fault zone. The elevation changes shown here are, nevertheless, compatible with those inferred from direct observations to the east and west of this circuit, where examination of the fractures indicates that the northern block was thrust upward and to the south relative to the southern block. That a substantial elevation change occurred between the northern and southern bench marks simply testifies to the existence of faulting that for reasons unexplained has not yet propagated to the surface.

Circuit 2 was so designed as to extend from a point well south of the zone of surface rupturing to a point at least a short distance beyond the base of the San Gabriel Mountains. This circuit was extended northward across the area of concentrated structural damage at the base of the San Gabriel Mountains in order to detect any earthquake-associated vertical uplift or faulting otherwise obscured by numerous landslides on the foothill slopes. The results indicate that there was no additional faulting along the base of the San Gabriel Mountains. A conclusion drawn from the elevation changes along circuit 2 is that the general uplift from south to north can be separated into three zones of distinct character: (1) northward tilt of the southern block between the railroad and the line of surface fractures, (2) pronounced upward arching of the leading edge of the upper plate with a peak uplift about ½ km north of the fracture zone, and (3) northward tilt of the northern block between the point of maximum uplift and the north end of the level line. The character of elevation changes along level circuit 2 is consistent in general with an elastic rebound model based on a reverse-slip or thrust interpretation of the observed phenomena. The lack of detail in preearthquake and postearthquake comparisons along level circuit 2 is a hindrance to a definite interpretation regarding elastic rebound, but a pattern consistent with the proposed rebound is more completely developed in the leveling along circuit 3.

The leveling network identified as circuit 3 in figure 1 is the most extensive and comprehensive of the circuits developed thus far in our operations. All the circuit 3 field elevations determined after the earthquake were related to a single bench mark (City of Los Angeles BM 5–M–22) at the corner of Foothill Boulevard and Eldridge Avenue. The vertical changes at recovered bench marks were entered on the map before closure errors on extended loops could be checked and distributed.

An area enclosed by the leveling loop through Kagel and Lopez Canyons contains the largest vertical displacements thus far documented. A profile of vertical displacement was constructed by projection of bench-mark data onto the line indicated in figure 1. Approximate locations for each even ½-m elevation change were determined by interpolation along the profile line, and the results are shown in figure 2.

Comparison of the elevation changes among the five or six bench marks clearly south of the fracture zone indicates a relatively slight northward tilt of the southern block compared to the prominent northward tilt of the upper (north) block from the point of maximum uplift up to Pacoima Reservoir. The leading edge of the upper plate was sharply arched or buckled in a similar manner to the upper plate north of the break in San Fernando. The south-facing flank of the upward warp contains at least three locally prominent but apparently discontinuous scarps. Total accumulated displacement across the known scarps accounts for only about 1.5 m of the uplift; the remaining 0.8 m could be distributed among smaller scarps or perhaps could be more smoothly distributed as a flexure in surface material overlying a cleaner break at some unknown depth.

The preliminary results of releveling are thought to be reasonably consistent with an elastic rebound model based on dislocation theory as presented by Savage and Hastie (1969). Although their work was an attempt to model a dip-slip (normal) fault with a right-lateral component, the resulting displacement values can be altered to predict the surface movements associated with a reverse or thrust fault with a left-lateral component by reversing all the signs and displacement vectors. The model thus altered suggests that the upper plate (north block) should rise near the leading edge by an amount approximately twice the amount of downdrop on the lower plate near the fault break. The apparent lack of complete agreement between the preliminary results of the releveling and the dislocation model might well be due to (1) the complex nature of the faulting indicated by the presence of several surface breaks, and (2) the relative nature of the preliminary data.

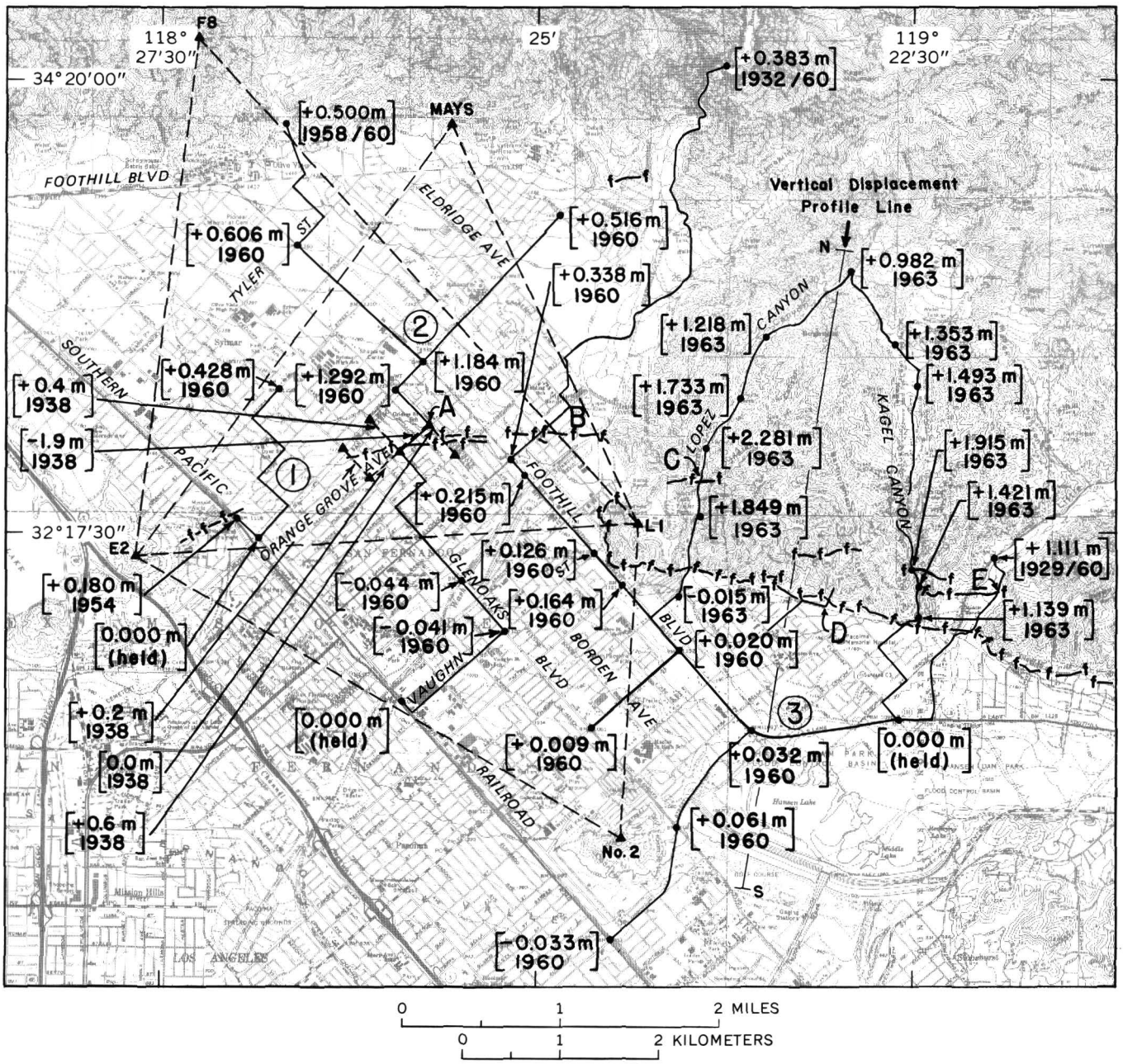

FIGURE 1.—Map showing elevation and length changes in meters derived through comparison of preearthquake and postearthquake measurements. Elevation changes along each of the three identified circuits are relative to arbitrarily selected control points to the south of main fracture zone. Based on unpublished data of the Geological Survey, Los Angeles County Department of County Engineer, Los Angeles County Flood Control District, City of Los Angeles Bureau of Engineering, and City of San Fernando.

A tentative tie between circuits 2 and 3, based on leveling underway by the Bureau of Engineering of the City of Los Angeles, indicates that the elevation changes along circuit 2 should be corrected by +0.057 m in order to compare them with changes recognized along circuit 3.

INTERPRETATION OF LENGTH CHANGES

Changes in horizontal lengths were measured on two different scales: a trilateration survey across the area of greatest damage involving lines of about 5 km length and a short traverse across the fault break in the City of San Fernando (near the corner

EXPLANATION

Level circuit showing locations of selected bench marks. (Change in elevation and date of original leveling shown in brackets).

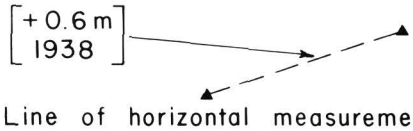

Line of horizontal measurement. (Change in length and date of original measurement shown in brackets; see Table 1 for long lines).

A through E

Approximate locations of creep arrays.

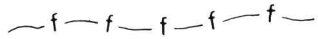

Approximate location of major tectonic fracture generated during earthquake.

FIGURE 1.—Continued.

of Borden and Orange Grove) involving lines shorter than 0.5 km. Both surveys showed significant changes between preearthquake and postearthquake data. The trilateration survey also indicated that measurable movement occurred after February 9, 1971.

A preliminary trilateration network consisting of stations PACOIMA L1, PACOIMA E2 ECC, SYLMAR F8, and MAYS 2 (designated L1, E2, F8, and MAYS, respectively, in fig. 1) was surveyed on February 11, 1971, with a Geodolite. A helicopter was flown along the line of sight at the time of observation to determine the refractivity. An expanded network consisting of 12 stations, including reobservation of the preliminary network, was surveyed by the same procedure 2 weeks later. At the present time, data are available to discuss only the preliminary network and one additional station (PACOIMA #2, designated No. 2 in fig. 1). Table 1

TABLE 1.—*Difference between preearthquake and postearthquake measurements*

Line	Length of line (meters)		Change in length (meters)
	Preearthquake	Postearthquake	
PACOIMA L1–PACOIMA #2	3,229.33	3,229.28	−0.05
PACOIMA E2 ECC	5,141.72	5,139.69	−2.03
SYLMAR F8	6,708.64	6,707.12	−1.52
PACOIMA E2 ECC–PACOIMA #2	5,728.76	5,728.57	−0.19
SYLMAR F8	5,354.90	5,354.94	+0.04

shows the line lengths determined before and after the earthquake. A mean date for the preearthquake surveys would be about 1935; thus, the changes in table 1 may include some strain accumulated in the 36-year period between surveys. The accuracy of the preearthquake data is probably accurate to 0.007 m. The uncertainty in the change of length is therefore of the order of 0.10 m. The simplest inter-

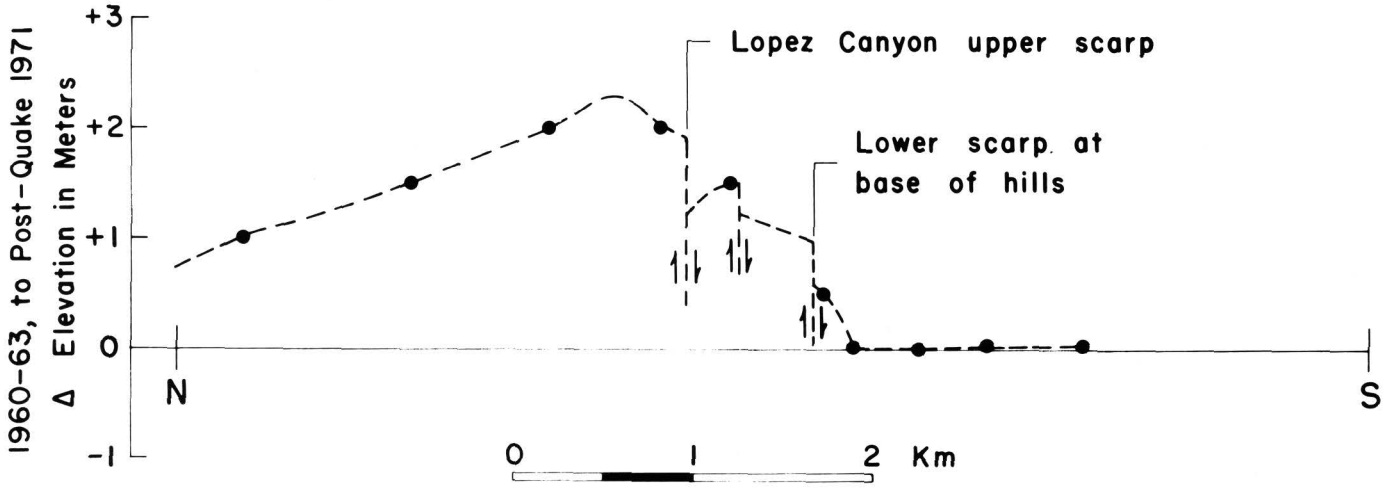

FIGURE 2.—Profile of interpolated relative vertical displacement along a line crossing the zone of surface breaks between Hansen Lake and Kagel Mountain. See figure 1 for location of profile line.

pretation of the data in table 1 is that stations PACOIMA #2, PACOIMA E2 ECC, and SYLMAR F8 have remained approximately fixed relative to one another (presumably lying south or west of the limits of the northern fault block), but PACOIMA L1 has moved 2.0 m to the west relative to those stations. This would suggest that PACOIMA L1 lies on the northern fault block. Superficially, it would appear to indicate pure left-lateral strike slip on the fault. However, dislocation models (for example, see Savage and Hastie, 1969) show that the motion near the toe of the hanging block of an oblique-slip fault of moderate dip is essentially parallel to the strike. Thus, the trilateration data are apparently consistent with reverse oblique slip (say 2 m reverse slip and 2 m left slip) on a fault plane dipping 50° to 60° N.

The resurvey of the preliminary trilateration network was undertaken to detect evidence for continued movement associated with either aftershocks or creep on the primary fault. The pertinent data are displayed in table 2. The uncertainty in

TABLE 2.—*Postearthquake length changes*

Line	Length of line (meters)		Change in length (meters)
	Feb. 11	Feb. 23	
PACOIMA L1–SYLMAR F8	6,707.12	6,707.07	−0.05
MAYS 2	4,510.51	4,510.47	−.04
PACOIMA E2 ECC–SYLMAR F8	5,354.94	5,354.96	+.02
MAYS 2	5,453.75	5,453.75	0.00
PACOIMA L1	5,139.69	5,139.65	−.04

each distance measurement is about 0.007 m, so that the uncertainty in the change in length is about 0.01 m. As can be seen from the table, additional movement has occurred in the 12-day interval between surveys.

Finally, a short traverse was carried across the fault break in the city of San Fernando to determine the displacement on the fault. Horizontal displacements were measured by changes in distances between street intersections. As can be seen in figure 1, a shortening of 1.9 m was observed in the northeast direction and a lengthening of about 0.4 m was observed in the northwest direction. Together these measurements imply a horizontal component of slip of about 2.0 m in the direction S. 57° W. Leveling data through this area suggest relative uplift of the northern block by about 1.3 m. Thus, the indicated fault movement is about 1.7 m left-slip and 1.7 m reverse-slip on a fault dipping about 50° N.

MEASUREMENTS FOR DETECTION OF CONTINUING MOVEMENTS

Tightly controlled creep arrays have been established in northern San Fernando, in Lopez Canyon, north of Pacoima Memorial Hospital, and in Little Tujunga Canyon. (See fig. 1.) In addition, selected segments of level circuits 1, 2, and 3 are being monitored for continuing vertical movements. Observations at each of the creep arrays include horizontal and vertical angle readings from a central point with a Wild T–3 theodolite, heights of instrument and targets measured to ±0.5 mm (millimeter), and indirect determination of two lengths per array by angle readings on subtense bars. All the lines along which these measurements were completed are between about 50 and 200 m in length. In general, two lines in each array cross a zone of surface breakage, and the remaining two are situated on the same side of the break as the instrument station.

The postearthquake movements detected thus far are mostly random. Some of these small displacements (on the order of a few millimeters) are definitely above the observational noise but might be associated with unstable marks or with continued landsliding or slumping of surface material.

VERTICAL WIRE EXTENSOMETER INSTALLATION AND PRELIMINARY RESULTS

A vertical exploratory hole was drilled through the buried surface of the prominent fault break in Lopez Canyon on February 19, 1971 (fig. 1, site C). The exposed slip surface of the fault on the hanging-wall scarp strikes about N. 81° W. and dips 65° N. Based on these data, the 3-foot (0.9-m) diameter hole was centered 4.6 m north of the projected lip of the bedrock scarp and was drilled to a depth of 11.3 m. The south edge of the hole intersects the buried fault-gouge layer at about 9.3 m below the surface. Following the emplacement of casing down to an 8.7 m depth, side-wall samples at 15-cm (centimeter) intervals below the casing were obtained, and slickensided gouge material abundant in the 8.90- to 9.35-m depth interval was examined. One slip surface in the gouge material which was exposed during sampling yielded a strike of N. 80° W. and a dip of 50° to 55° N.

Following examination and sampling in the hole, two invar wires were anchored to the bottom of the hole and were coupled to displacement-measuring devices at the top. One device is purely mechanical. It records with 10:1 amplification and ±0.02 mm resolution on a paper chart from which time can be read to about ±10 minutes. To date, the mechanical

recorder has operated continuously since 18:10 P.s.t. on February 19, 1971. Movement transmitted by the second wire is sensed by a precision electronic displacement transducer. Displacement signals are generated by movement of a ferrite core within the barrel of a linear variable differential transformer (LVDT). The LVDT output is recorded continuously on a portable strip-chart recorder. Optimum resolution for this system is about ±0.001 mm, and time can be read with resolution varying between ±1 and ±5 minutes depending on the chart-drive speed selected. The electronic system has produced about 75 percent complete coverage since the starting time given above. Sources of noise on both records are thought to be essentially limited to thermal expansion and contraction of the instrument table and steel support legs, aside from slight frictional drag in the mechanical system and thermally-induced drift in the various electronic components of the second system. The current maximum amplitude of the diurnal thermal drift on the sensitive displacement record does not exceed 0.005 mm.

The results obtained thus far suggest that slight downward movements of the hanging-wall block have occurred during certain of the larger aftershocks; these movements have produced a net lowering of the scarp by about 0.13 mm. These results are summarized in table 3. Two of the negative

TABLE 3.—*Vertical displacement episodes and net drift at Lopez Canyon extensometer site, February 1971*

[Pacific standard times. Displacement: negative entry denotes contraction]

Day	Time (±10 min)	Displacement (mm)	ϵ_z $\times 10^{-6}$	Comments
20	04:00	+0.04	+3.3	
	21:45	−0.09	−7.5	Mag. 4.0 aftershock at 21:51.
	23:15	−0.08	−6.7	Mag. 3.9 aftershock at 23:15.
21	08:00	+0.04	+3.3	
	14:00	+0.05	+4.2	
22	10:00	+0.03	+2.5	
19	18:10			
to		−0.13	−10.8	Net negative drift on mechanical record.
23	12:00			

(vertical contraction) events occurred as sharp steps of slightly less than 0.1 mm each on the mechanical record, and these were approximately coincident with the aftershocks of February 20 at 21:51 and 23:15 P.s.t. Several episodes of vertical extension (lengthening of the hole or upward movement of the hanging-wall block) were recorded on both instruments, but these show no obvious correlation with known aftershocks. The positive events are characterized by gradual onset of displacement over time intervals of about 1 hour; thus, they closely resemble episodic creep events recorded on certain strike-slip faults.

STRAIN MEASUREMENTS PROGRAM OF THE CALIFORNIA DIVISION OF MINES AND GEOLOGY

Twelve geodimeter lines within the State of California strain-monitoring network between Gorman and San Bernardino were remeasured within a few weeks following the San Fernando earthquake. Comparison of postearthquake lengths with those measured during the period 1963–66 shows that all lines examined are now longer, irrespective of their orientation. Preliminary appraisal of the changes suggests that areal dilation of about +2 to +3 parts per million occurred in a region surrounding the San Andreas fault and containing Gorman and Cajon Pass. The length changes do not suggest lateral slip on known faults or any significant shear, although a slight shear component might be detected following more rigorous analysis of the data (Roger Greensfelder, personal commun., 1971).

CONCLUSIONS

This brief summary of the preliminary results of instrumental observations shows that the moderate magnitude San Fernando earthquake has been associated with surprisingly large, if areally restricted, permanent crustal movements. Because the preexisting control is generally very good in the area of surface disturbance, the San Fernando earthquake may provide an almost unprecedented opportunity for detailed documentation of the tectonically induced surface movements associated with a failure along a reverse or thrust fault. The results of an expended study will doubtless contribute significantly to a much greater understanding of the general problems concerning surface expression of deep-seated tectonic processes.

REFERENCE

Savage, J. C., and Hastie, L. M., 1969, A dislocation model for the Fairview Peak, Nevada earthquake: Seismol. Soc. Am. Bull. 59 (5), p. 1937–1948.

REPEATED SURVEYS OF SMALL SCALE FIGURES ESTABLISHED ACROSS SURFACE FAULT RUPTURES FOLLOWING THE EARTHQUAKE [1]

By JOHN C. LAHR and MAX WYSS
LAMONT-DOHERTY GEOLOGICAL OBSERVATORY OF COLUMBIA UNIVERSITY

AND

JAMES A. HILEMAN
SEISMOLOGICAL LABORATORY, CALIFORNIA INSTITUTE OF TECHNOLOGY

ABSTRACT

Starting 36 hours after the February 9, 1971, San Fernando earthquake, four small-scale geodetic figures were established across the zone of surface-fault ruptures associated with the San Fernando earthquake. Each figure consists of one or two theodolite stations and about three reference points on each side of the fault. Two of the figures indicated no more than 2 millimeters of displacement. The data at the Middle Ranch figure, which spans the fault at the mouth of Little Tujunga Canyon, show that a small additional thrust with 2 mm uplift and 6 mm of compression may have occurred between two and four days after the main event. The displacements at the Aztec figure in Sylmar are consistent with left-lateral shear in the zone of the figure and range from 4 to 20 mm.

INTRODUCTION

Two recent California earthquakes with surface rupture were followed by substantial additional displacement across the related fault trace. During the 2 years following the Parkfield earthquake of June 28, 1966, a total of approximately 25-centimeter displacement was accumulated at an exponentially decaying rate (Smith and Wyss, 1968). Most of this displacement was aseismic (Scholz and others, 1969). During the days immediately following the main shock, the creep rate was so high that it was difficult to tell how much, if any, surface displacement was associated with the earthquake itself. In any event, the creep displacement was equal to, or exceeded, the initial offset (Smith and Wyss, 1968).

In the case of the Borrego Mountain earthquake of April 9, 1968, aftermovements were much less obvious. This earthquake produced two main branches of surface rupture which were offset in echelon (Allen and others, 1968). A small-scale geodetic network was established across the northern branch by Wyss only 12 hours after the earthquake. The position measurements across the fault were repeated at a rate of once per hour. However, no movement could be detected. A half year later, local residents suggested that the southern part of the fault was still active. Inspection of the fault trace indicated that additional displacement of the order of the initial offset on that part of the fault had accumulated.

It is evident that even the most basic questions concerning dislocations following an earthquake with surface breakage are still to be answered. Indeed it is not known whether aftercreep is the norm or the exception. Before one can understand the mechanism of aftercreep, one needs to know some of the basic properties of the phenomenon. Both the Parkfield and the Borrego Mountain surface traces lacked the extensive and dense network of measurements needed to determine the extent and propagation of creep events.

This study of small-scale geodetic networks across the surface trace of the faulting that accompanied the San Fernando earthquake of February 9, 1971, was undertaken with the hope of determining the extent of aftercreep at as many localities as possible. On February 10, 36 hours after the main shock, the first small-scale geodetic network has been installed across the fault trace. On February 11, three more networks were established.

DATA

The locations of the survey stations are given in table 1. The first three stations straddle the fault break that lies along the base of the foothills and is informally named the "Tujunga fault segment." (See maps showing tectonic ruptures in papers by Kamb and others and by U.S. Geological Survey

[1] Contribution No. 1631 Lamont-Doherty Geological Observatory; Contribution No. 1992, California Institute of Technology, Division of Geological and Planetary Sciences, Pasadena, California

TABLE 1.—*Location of surveys*

Station	North lat	West long	Date established (1971)	Date last measured (1971)
Middle Ranch	34°16′56″	118°22′13″	Feb. 11	Feb. 25
Lopez	17′15″	24′00″	11	24
Foothill	17′18″	24′31″	10	13
Aztec	17′58″	26′21″	11	Mar. 1

staff, this report.) The fourth station, Aztec, is somewhat west of the western end of the "Sylmar fault segment." This break appeared to stop or to branch out near the intersection of Hubbard Street and Glenoaks Boulevard in Sylmar. The Aztec station was set up beyond what appeared to be the end of the break in order to see whether the fault trace might propagate westward.

In establishing these stations, speed was considered to be of prime importance, because an exponential decay of possible creep as observed at Parkfield (Smith and Wyss, 1966) could be expected. Further it was felt that the number of stations was more important than accuracy at each station. Both at Parkfield and at Borrego Mountain, the accumulated creep displacement was large, but the number of stations deployed along the fault to record the displacement was insufficient.

For these reasons the theodolite stations consisted of 1-meter steel rods driven into the ground, while the other nearby points were nails in trees or telephone poles. More distant points were structures such as water towers or houses.

A Wild T–2 theodolite was used at station Lopez and for some of the later measurements at stations Aztec and Middle Ranch. All other measurements were made with a Kern DKM–3 theodolite.

The three figures at the base of the foothills were chosen in areas with as little relief as possible so that secondary slumping would not affect the measurements. Two of the figures, Lopez and Middle Ranch, are at the mouths of canyons and consist of one theodolite station and a number of points on both sides of the fault trace. At Lopez, two surveys indicated no more than 2 mm of lateral motion or compression across the Tujunga fault segment.

At the Middle Ranch figure, the changes in three angles which cross the fault zone are consistent with 6 mm of north-south compression and no lateral motion across the Tujunga fault segment. A conservative estimate of the error in this measurement is plus or minus 3 mm. This displacement occurred between February 11 and 13 and was combined with 2 plus or minus 1 mm uplift of the targets north of the fault.

The Foothill figure is at the western end of the Tujunga fault segment, just before the break turns north. It consists of two theodolite stations, three reference points on the south side of the fault and two points on the north side. The data indicate that no more than 2 mm of vertical, lateral, or compressive movement occurred across the fault zone at the Foothill station.

Between Pacoima Wash and Foothill Boulevard, the Sylmar fault segment trends east-west. Farther to the west it continues for 2 km as a zone curving to the south. The Aztec figure is somewhat to the north of the end of this zone over ground that experienced little apparent offset during the earthquake. The figure is set up in a field free from hardtop, and at the time of installation, no cracks, pressure ridges, or fault scarps could be detected. It was hoped that further lateral offset would extend with less curvature and pass through this figure. The network consists of two theodolite stations, three points within 200 m, and a distant water tower. Changes have been observed in all three short lines that are consistent with left-lateral motion both northeast and southwest of the theodolite stations. Between February 13 and March 1, a line to a garage on the southwest indicated about 2 cm of left lateral displacement, while a more distant telephone pole at the same azimuth indicated only 5 mm displacement. A telephone pole to the northeast showed 4 mm left lateral displacement. A conservative estimate of the errors is plus or minus 3 mm. This error estimate is rather large because some of the observed angles changed in an erratic fashion. We believe that these changes, however, could be real. In the field it was evident that streets and sidewalks acted as stress guides over long distances. The telephone poles could have been coupled to the pavement, which may react in a complex manner to ground deformation.

DISCUSSION

Very little displacement occurred along the predominant trace of the faulting that accompanied the San Fernando earthquake in the period from 1½ to 14 days after the main event. A number of explanations for the absence of much fault creep are possible. The creep after the Borrego Mountain and Parkfield earthquakes may have been exceptional, and many earthquakes may not produce significant creep. Only observations after future earthquakes can resolve this question. Perhaps the mechanism of aftermovements is more effective for strike-slip displacement than for thrusting. The aftershocks may have occurred predominantly within the upper block rather than on the thrust plane (California Institute

of Technology, 1971). This would in turn imply that the deformations occuring after the main event were within the upper block and would not result in additional significant displacement on the initial fault plane. Finally, it is possible that aftercreep has occurred at other locations or will occur in the future.

ACKNOWLEDGMENTS

We thank L. Sykes and B. Isacks for critically reading the manuscript. Ralph Gillman, Chris Scholz, and Peter Molnar helped establish and survey the figures. Our thanks also go to B. Kamb and to all those at the Seismological Laboratory, California Institute of Technology, for their aid in quickly locating the zones of surface faulting. This project was supported by the National Science Foundation under grant GA 22709 and by the Advanced Research Projects Agency of the Department of Defense and was monitored by the Air Force Cambridge Research Laboratory under contract F 19628–68–C–0341.

REFERENCES

Allen, C. R., Grantz, A., Brune, J. N., Clark, M. M., Sharp, R. V., Theodore, T. G., Wolfe, E. W. and Wyss, M., 1968, The Borrego Mountain, California, earthquake of 9 April 1968: A preliminary report: Seimol. Soc. America Bull., v. 58, p. 1183–1186.

California Institute of Technology, Division of Geological and Planetary Sciences, 1971, Preliminary seismological and geological studies of the San Fernando, California, earthquake of 9 February 1971: Seismol. Soc. America Bull. (In press.)

Scholz, C. H., Wyss, M., and Smith, S. W., 1969, Seismic and aseismic slip on the San Andreas fault: Jour. Geophys. Research, v. 74, p. 2049–2069.

Smith, S. W., and Wyss, M., 1968, Displacement on the San Andreas Fault subsequent to the 1966 Parkfield earthquake: Seismol. Soc. America Bull., v. 58, p. 1955–1973.

INSTRUMENTAL MONITORING OF POSTEARTHQUAKE FAULT MOVEMENTS

By ROBERT D. NASON
EARTHQUAKE MECHANISM LABORATORY, NATIONAL OCEANIC AND ATMOSPHERIC ADMINISTRATION

With many earthquake sequences it has been noted that surface movement continues on a fault for many days and even months. This shows a gradually increasing offset, but at a steadily decreasing rate, at the fault in the days following the main earthquake. The continuing postearthquake fault movement can be called "afterslip" in analogy to aftershocks.

Afterslip was well observed following the June 1966 earthquake at Parkfield, Calif. (Wallace and Roth, 1967; Smith and Wyss, 1968; Scholz and others, 1969), and has been noted from historic data for at least five other California earthquakes (Nason, 1969). But afterslip has apparently not occurred following some other earthquakes. The total number of known examples is small.

The cause of afterslip or its absence is not known, though there are several theories (Scholz and others, 1969; Nason, 1969). The relationship between afterslip and aftershocks is also unclear. But it is likely that the study of afterslip will provide many clues for better understanding of earthquake mechanism and aftershocks. It is even possible that the study of afterslip may help in estimating the probability of large damaging aftershocks following an earthquake.

The Earthquake Mechanism Laboratory of the National Oceanic and Atmospheric Administration has prepared a special program for the instrumental monitoring of afterslip following major earthquakes. The first instrumental installation was at Ocotillo Wells, Calif., immediately after the Borrego Mountain earthquake of April 1968. The prime objectives of the program are: (1) is afterslip occurring with a particular earthquake sequence; (2) if so, what are the time and spacial characteristics of the afterslip; and (3) how does the afterslip relate to the earthquake aftershocks.

SAN FERNANDO EARTHQUAKE MONITORING

Early field reports by many investigators indicated that sizeable transverse movement had occurred on faults in the northern part of the San Fernando Valley. We are particularly indebted to the geologists from the California Institute of Technology and the U.S. Geological Survey for these early reports. The thrust movement on the north-dipping faults caused both uplift and compression at the fault traces which approached 1 meter at many places. (See other sections in this report.)

Twelve creepmeters (instruments designed to monitor the slippage on faults) were immediately assembled and taken to the earthquake area the day after the earthquake; six were specially designed to measure horizontal (strike-slip) fault movement and six were designed to measure vertical (dip-slip)

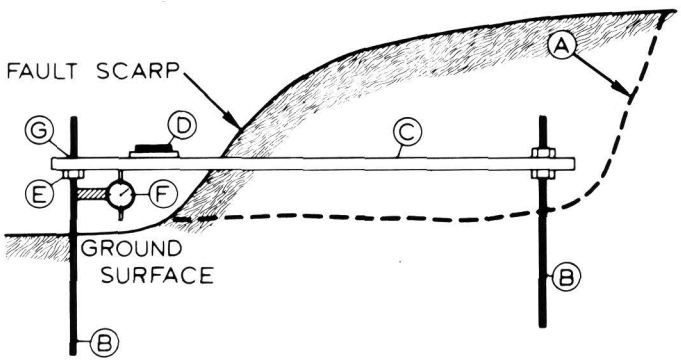

FIGURE 1.—Design of dip-slip (beam-tilt) creepmeter: (A) trench cut into upper wall of fault scarp, (B) ½-inch threaded rods driven into ground, (C) beam of rectangular cross section, with slotted holes, securely fastened to right-side rod, (D) precise 20-second spirit level, mounted, (E) nut on threaded rod to raise or lower end of beam until level, (F) machinists dial gauge, reading to 0.01 mm, to measure amount of raising of beam in any releveling, and (G) mark on beam to indicate any change of horizontal distance between threaded rods.

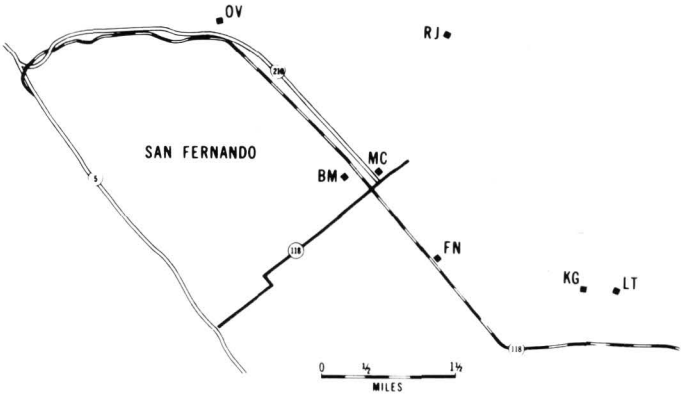

FIGURE 2.—Location of fault monitoring sites.

fault movement (fig. 1). Five of the dip-slip creepmeters were installed on the thrust faults (their first use in afterslip studies). The five instruments were installed at (1) Little Tujunga Canyon (site LT, fig. 2), (2) Foothill Nursing Home (site FN), (3) Maclay Street (site MC), (4) Bromont Street (site BM), and (5) Rajah and Tucker Streets (site RJ). In addition, small fault monitoring patterns of survey marks were established at Kagel Canyon (site KG), Rajah Street (site RJ), and Olive View (site OV).

The initial results indicate that there has been no change (no afterslip) at any of these sites.

ACKNOWLEDGMENTS

The author thanks the many geologists of the California Institute of Technology, U.S. Geological Survey, and the California Division of Mines and Geology for information on the location of the fault traces, and David Polanshek of San Francisco State College for assistance with the instrument installation.

REFERENCES

Nason, R. D., 1969, Continuing fault movement after earthquakes: Am. Geophys. Union Trans., v. 50, no. 1, p. 252.

Wallace, R. E., and Roth, E. F., 1967, Rates and patterns of progressive deformation, *in* The Parkfield-Cholame, Calif., earthquakes of June-August 1966—Surface geologic effects, water-resources aspects, and preliminary seismic data: U.S. Geol. Survey Prof. Paper 579, p. 23-37.

Scholz, C. H., Wyss, Max, and Smith, S. W., 1969, Seismic and aseismic slip on the San Andreas fault: Jour. Geophys. Research, v. 74, no. 8, p. 2049-2069.

Smith, S. W., and Wyss, Max, 1968, Displacement on the San Andreas fault subsequent to the 1966 Parkfield earthquake: Seismol. Soc. America Bull., v. 58, no. 6, p. 1955-1973.

PRELIMINARY RESULTS FROM RECORDING AFTERSHOCK GROUND MOTION ON ALLUVIAL DEPOSITS

By RICHARD E. WARRICK and WILLIAM B. JOYNER
U. S. GEOLOGICAL SURVEY

Six sensitive accelerographs were installed to record aftershocks from the San Fernando earthquake of February 9, 1971, to determine the relative ground response in different geologic environments. Sites were located on the Quaternary alluvium covering the San Fernando Valley and on both sedimentary and crystalline bedrock in the nearby hills. Several recordings were obtained through February 22, the last date records were collected before this report. All the usable recordings were from sites on alluvium; however, the instruments are still in place so future events may be recorded at both bedrock and alluvial sites.

The instruments are Kinemetrics type SMA-1 strong motion accelerographs equipped with vertical triggers and employing sensors designed for full scale deflection at ¼ *g*. These instruments have been modified by H. Mills, of the U.S. Geological Survey, National Center for Earthquake Research, to allow the recording of radio time signals from National Bureau of Standards station WWVB. The recording of any 1-minute segment of the radio time-signal permits identification of the day, hour, minute, and second of a seismic event. The complete station consists of the accelerograph, radio receiver with antenna, and a storage battery. The motion sensors are set for approximately 0.6 critical damping. Sensitivities and resonant frequencies of the instrument are listed in table 1.

The recordings were made in two phases. During the first phase, February 10-13, the emphasis was on fast deployment, and the instruments were not bolted down. They were placed on existing concrete slabs embedded in the ground, except for station LA-6, where the instrument was placed on a scraped surface of outcropping granite. During the second phase, which began on February 18 and is continuing, some changes of location were made, including adding a third bedrock station, and all the instruments were secured in place with bolts. Tilt calibrations were made on the instruments between the two recording phases.

TABLE 1.—*Instrument characteristics*

Instrument	Station assignment Phase I Feb., 10-13	Station assignment Phase II Feb., 19-22	Component	Average resonant frequency (Hz)	Average sensitivity (cm per g)
163	LA-2	LA-5A	L	11.8	7.8
			V	11.1	8.4
			T	13.5	5.8
171	LA-3	LA-2A	L	14.1	6.6
			V	13.2	6.4
			T	13.4	5.8
173	LA-4	LA-7	L	14.9	5.8
			V	11.9	7.7
			T	13.5	6.6
176	LA-5	LA-3	L	13.5	6.2
			V	13.6	6.1
			T	12.6	6.9
177	LA-6	LA-8	L	13.5	6.4
			V	13.8	6.2
			T	13.0	7.3
178	LA-1	LA-6	L	13.4	6.7
			V	13.0	7.0
			T	13.2	6.8

The index map (fig. 1) shows recording sites and the epicenters of two events selected for illustration. The times of operation and the data quality at the various stations are diagrammed in figure 2. The coordinates of the recording sites and brief geologic descriptions based on Oakeshott's (1958) map and our own field observations are given in table 2. The available subsurface geologic information has not yet been compiled, but maps and sections published by the California State Water Rights Board (1962) suggest that the valley sites are characterized by Quaternary alluvium up to 100 feet thick overlying Pleistocene or Pliocene sediments.

The two best recorded events occurred on February 21 at 0550 and 0715 GMT (figs. 3 and 4). The preliminary analysis of these records is limited to a simple reading of the period and peak amplitude

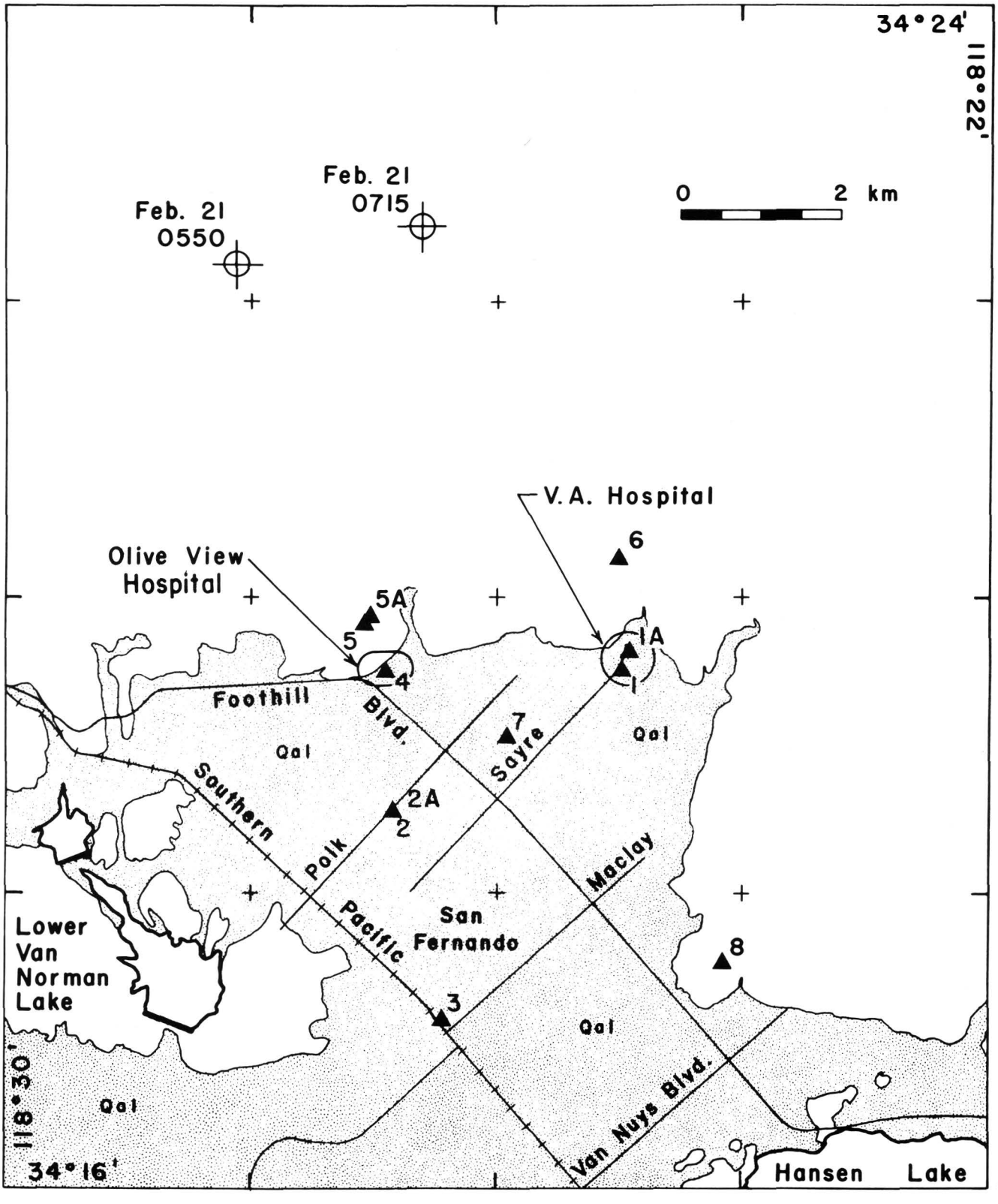

FIGURE 1.—Index map of recording stations and two selected epicenters. The thin line indicates the approximate contact between the recent alluvium and older material along the northern part of the San Fernando Valley (Oakeshott, 1958). Stations are indicated by triangles. Epicenters are indicated by circles and crosses.

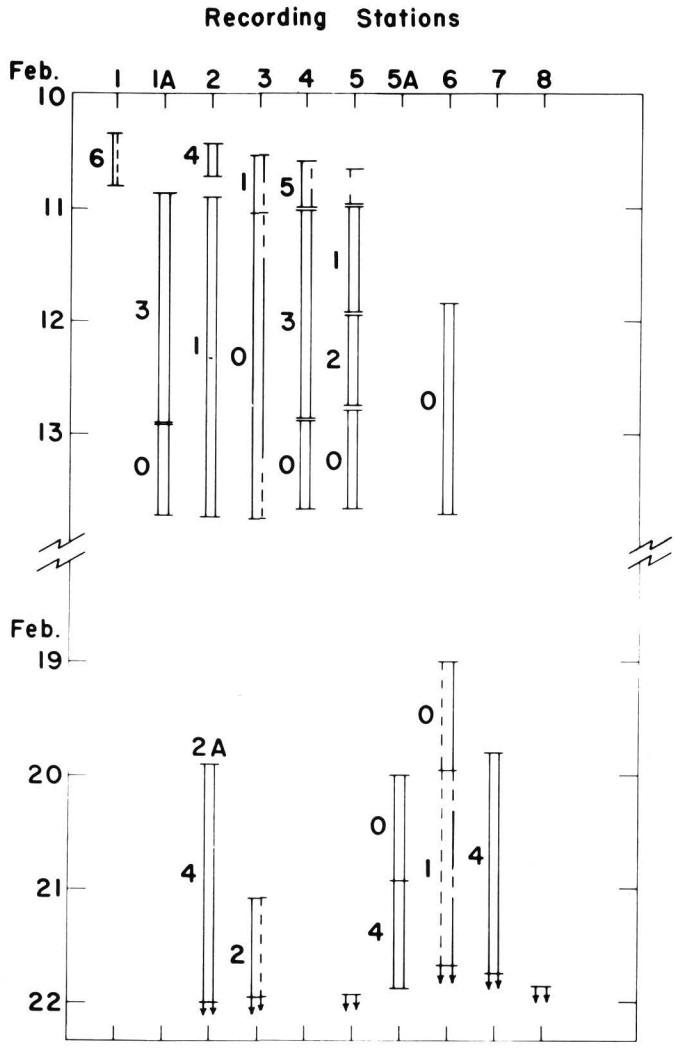

FIGURE 2.—Instrument operation and data-quality chart. The short horizontal lines note beginning and end of recording intervals. The numerals to the left of the recording interval bar give the number of events recorded in that interval. The left vertical line of the bar refers to data quality: solid when good, broken when questionable for any reason. The right side line refers to timing signals: solid when good, broken when absent or unreadable. The time scale shows the beginning of each day in Greenwich mean time.

of the maximum pulse recorded on any component. These data are given in tables 3 and 4 along with preliminary determinations of epicenter location and magnitude furnished by Wayne Thatcher of the California Institute of Technology.

Station LA-2A recorded somewhat greater amplitudes than the other stations and, from the visual appearance of the record, shows a somewhat greater emphasis on low frequencies. Further analysis will be required to determine the significance of these characteristics. Station LA-3 recorded lower amplitudes, which may be due to the greater distances from the epicenters. With the exception of station LA-3, there is no obvious relation between distance from epicenters and amplitude or frequency content.

Consistently higher ground accelerations were recorded for the 0715 event compared to the 0550 event even though the magnitudes and distances from epicenters for the two events are very nearly the same. This difference may be related to the nature of the source function or it may reflect uncertainty in the preliminary determinations of magnitude.

A more detailed analysis of the recordings is planned. The recording units will be left in place for as long as there is a significant chance for additional

TABLE 2.—*Station descriptions*

Station	North latitude	West longitude	Geologic unit (Oakeshott, 1958)
LA-1	34°19.50′	118°24.93′	Quaternary alluvium (at edge of alluvial basin).
LA-1A	34°19.63′	118°24.87′	Do.
LA-2	34°18.53′	118°26.82′	Quaternary alluvium.
LA-2A	34°18.53′	118°26.82′	Do.
LA-3	34°17.13′	118°26.39′	Do.
LA-4	34°19.49′	118°26.87′	Quaternary alluvium (at edge of alluvial basin).
LA-5	34°19.81′	118°27.04′	Sandstone of the Lower Pliocene Repetto Formation.
LA-5A	34°19.85′	118°27.02′	A local deposit of alluvial material at the foot of a hill composed of sandstone of the Lower Pliocene Repetto Formation.
LA-6	34°20.22′	118°25.00′	Granitic rock.
LA-7	34°19.01′	118°25.87′	Quaternary alluvium.
LA-8	34°17.53′	118°24.19′	Interbedded conglomerate and sandstone of the Lower Pliocene Repetto Formation.

TABLE 3.—*Event on February 21, 1971 (0550 GMT)*

[Origin time: 05:50:52.5. Location: 34°22.2′ 118°28.1′. Focal depth: Constrained to 8 km. Magnitude (M_L) 4.0. Data from California Institute of Technology]

Station	Epicentral distance (km)	Azimuth, station to epicenter	Maximum component of acceleration (g)	Approximate period (sec)	Direction
LA-2A	7.1	N. 16° W.	0.08	0.25	E
LA-3	9.7	N. 15° W.	.05	.14	N
LA-5A	4.7	N. 21° W.	.08	.15	N
LA-7	6.8	N. 30° W.	.06	.16?	S

TABLE 4.—*Event on February 21, 1971 (0715 GMT)*

[Origin time: 07:15:11.5. Location: 34°22.5′, 118°26.7′. Focal depth: Constrained to 8 km. Magnitude (M_L): 3.9 Data from California Institute of Technology]

Station	Epicentral distance (km)	Azimuth, station to epicenter	Maximum component of acceleration (g)	Approximate period (sec)	Direction
LA-2A	7.3	N. 2° E.	0.15	0.24	W
LA-3	9.9	N. 2° W.	.06	.22	E
LA-5A	4.9	N. 6° E.	.10	.20	N
LA-7	6.5	N. 11° W.	.12	.14	S

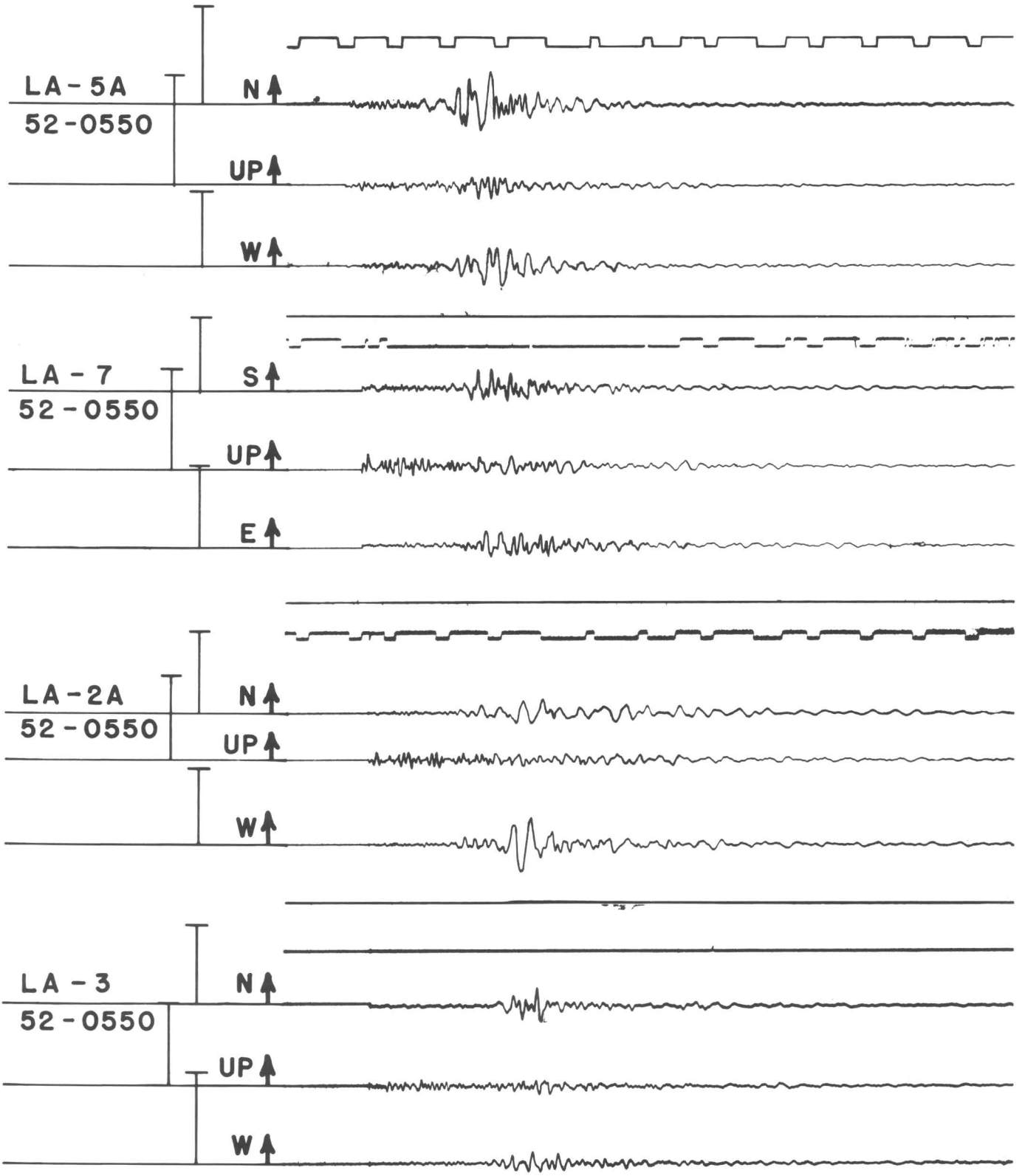

FIGURE 3.—Accelerograms of Feb. 21, 0550 event. The vertical capped bar indicates the 1/4g deflection as determined by tilt calibration. The direction symbol and arrow shows the sense of ground motion for deflections in the direction of the arrow.

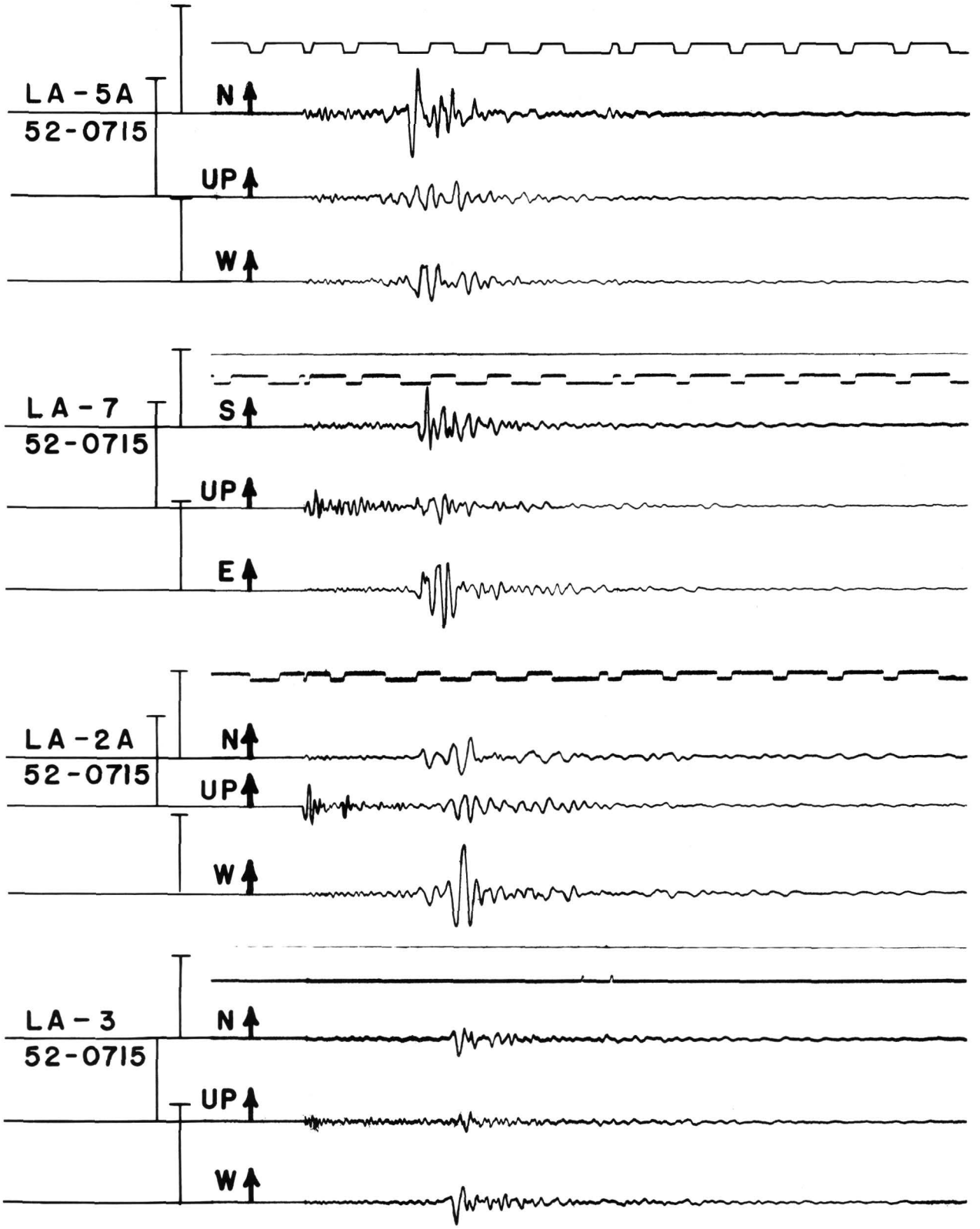

FIGURE 4.—Accelerograms of Feb. 21, 0715 event. The vertical capped bar indicates the 1/4g deflection as determined by tilt calibration. The direction symbol and arrow shows the sense of ground motion for deflections in the direction of the arrow.

events to yield data for comparing the response of bedrock and alluvial sites.

ACKNOWLEDGMENTS

We wish to express appreciation to the staffs of the U.S. Veterans Hospital and the Olive View Hospital and to the officers and men of the Los Angeles Fire Department, Station 91, and the San Fernando Fire Department, for their generous cooperation at a difficult time and for giving permission to install the recording instruments. Mr. Edward Arneson, President of the California Camellia Gardens, and Mrs. Hanna, manager of the trailer court on Lopez Canyon Road, gave permission to install instruments. We are indebted to Edward Roth, of the U.S. Geological Survey, who set up and maintained the instruments during the second phase of field operation and to Kinemetrics, Inc., of San Gabriel, which assisted with supplies and emergency repairs to the recorder.

REFERENCES

California State Water Rights Board, 1962, The city of Los Angeles vs. city of San Fernando: California State Water Rights Board, Report of Referee, No. 650079, v. I, 258 p., 36 pls.

Oakeshott, G. B., 1958, Geology and mineral deposits of San Fernando quadrangle, Los Angeles County, California: California Div. Mines and Geology Bull. 172, 147 p.

SHATTERED EARTH AT WALLABY STREET, SYLMAR

By ROBERT D. NASON
EARTHQUAKE MECHANISM LABORATORY, NATIONAL OCEANIC AND ATMOSPHERIC ADMINISTRATION

One of the most fascinating effects of the earthquake's shaking is found at a small area of "shattered earth" near Wallaby and Rajah Streets. This site is in the northeasternmost corner of Sylmar, and only 1 mile from the strong-motion instrument, which showed high seismic accelerations at Pacoima Reservoir. The shattered earth is on the narrow flat top of a low ridge parallel to Wallaby Street and north of Rajah Street. The ridge-top is about 20 feet higher than Wallaby Street and about 60 feet higher than a stream canyon to the east. (See approximate cross section, fig. 1.) The ridge-top consists of 10 feet of uplifted unconsolidated terrace

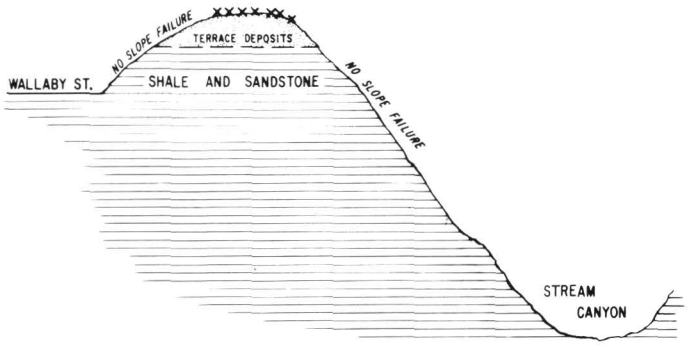

FIGURE 1.—Approximate northeast-southwest section across ridge with shattered-earth effects alongside Wallaby Street, Sylmar. XXX's indicate location of shattered earth.

deposits, which overlies consolidated Late Cenozoic shale and sandstone. The flat top is about 15 feet wide.

For 200 feet along flat ground at the top of the ridge, the soil was thoroughly broken and overturned by shaking during the earthquake, giving an impression of well-plowed land (figs. 2, 3, 4). Soil clods are shattered and overturned such that 90 percent of the surface is fresh mineral soil. The

FIGURE 2.—View of shattered earth on flat ridge-top, looking southeast. Wallaby Street on right.

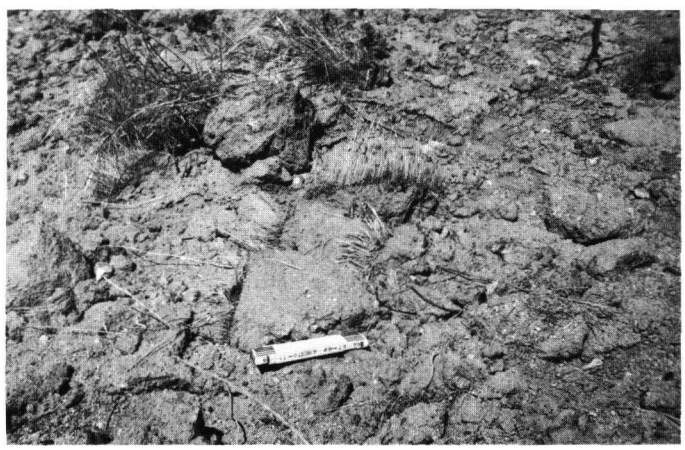

FIGURE 3.—Detail of shattered earth, with 6-inch folding rule for scale. Fine-grained material has been partially consolidated by a postearthquake rainstorm.

other 10 percent consists of the grassy tops of detached soil clods. Much of the soil has been pul-

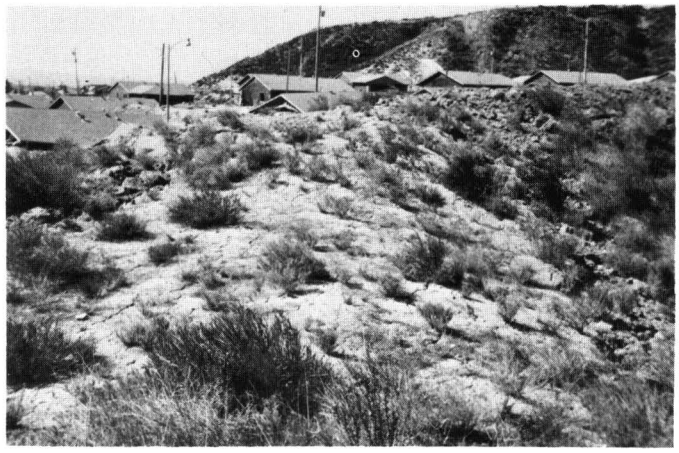

FIGURE 4.—View of fractured ground immediately southeast of shattered earth, which is on the ridge-top in upper right. Collapsed frames of uncompleted houses on far side of Wallaby Street.

verized into particles of sand-grain size. The surface was soft enough so that one would sink about 3 inches into the loose soil when the site was first observed 4 days after the earthquake. The soil had undoubtedly been hardpacked like nearby areas before the earthquake. A 30-inch-deep trench and probings with a stick showed that the soil is loose to a depth of 1 to 2 feet, becoming gradationally harder like the original soil with increased depth. No discontinuities or layers were evident in the trench.

The tossed-earth effect is confined to the 15-foot-wide flat top of the ridge for a length of 200 feet. To the north and south the ridge-top is wider, and the tossed-earth effect does not occur. The south end of the shattered-earth area is well defined with a transition from the thoroughly shattered earth to unshattered earth in a boundary only 10 feet wide. South of the boundary the flat ridge-top is crossed by many open fractures up to 1 inch wide and several feet apart, which might represent incipient shattering, but there is no overturning of dirt. Boulders on the ground outside of the tossed-earth area are somewhat dislodged but not shifted in any unusual manner. There are no boulders for special study in the tossed-earth area. The surrounding local countryside was searched, but no other region of tossed-earth effects was found.

The special features of this site are (1) the tossed-earth phenomenon of overturned soil, which may indicate a seismic shaking exceeding 1.0 g; the pulverization of the soil may mean that the high acceleration occurred over many wave cycles; (2) the localized nature of the shaking, with the tossed-earth effect occurring in an area only 200 feet long by 15 feet wide and a southern boundary only 10 feet wide; (3) the restriction of the tossed-earth phenomenon to the top of the ridge where the ridge is narrowest, with no significant slope failures on the sides of the ridge line. The very localized nature of the high acceleration indicated by the tossed-earth may result from unknown effects of constructive interference of seismic waves arriving along different paths and possible focusing or concentration of seismic wave energy at the narrowed-down ridge-top. This suggests that seismic wave interference effects are probably very important to the detailed distribution of strong shaking and earthquake damage. A local resident living on Tucker Street reports that the strong shaking lasted through many cycles. This agrees with the inference of many wave cycles because of the pulverized nature of the broken soil. The fact that the soil was thoroughly overturned is an indication of the strength of the shaking. It would appear that possible seismic wave interference and focusing patterns may be very important to the local distribution of strong seismic shaking and related damage.

ACKNOWLEDGMENTS

The author thanks John Pfluke and Glenn Converse of the National Oceanic and Atmospheric Administration Earthquake Mechanism Laboratory for their assistance in the field.

SEISMICALLY TRIGGERED LANDSLIDES IN THE AREA ABOVE THE SAN FERNANDO VALLEY

By DOUGLAS M. MORTON
CALIFORNIA DIVISION OF MINES AND GEOLOGY

Interpretation of aerial photographs taken a few days after the San Fernando earthquake indicates that the earthquake triggered more than 1,000 landslides in a 250 km^2 (square kilometer) area in the hilly and mountainous terrain north of the San Fernando Valley. The gross distribution of the slides was controlled primarily by the intensity of ground shaking, but important local variations in the density of landslides reflect variations in the character and structural history of local geologic formations. The earthquake also produced some areas of highly fractured rock, especially along ridge tops, that are likely to give rise to abundant landslides if they receive sufficient moisture.

This report summarizes a preliminary photointerpretive investigation of landslides triggered by the earthquake. The investigation used black-and-white aerial photographs taken for the U.S. Geological Survey on February 9, 1971 (American Aerial Surveys, Inc., scale 1:10,000), and color photographs taken on February 18, 1971 (U.S. Air Force, scale $\simeq$ 1:20,000). Photographic coverage was adequate for the area of interest (see fig. 1) with the exception of the northeast part, where cloud cover largely obscured the ground.

Landsliding was a direct and immediate response to the ground shaking of the earthquake, although some rock falls continued for several days along steep canyon walls (for example, Pacoima and Little Tujunga Canyons). Some of these rock falls may have been triggered by aftershocks. The landslides are concentrated south-southwest of the epicenter of the main shock, adjacent to the area of tectonic rupture at the surface, and within the area of principal aftershocks.

Approximately 1,000 landslides, ranging in length from about 15 to more than 300 m (meters) were mapped from the aerial photographs. Only a few were verified in the field. Rock falls, soil falls, debris slides and avalanches, and slumps were the principal types of landslides triggered by the earthquake. Surficial ($\simeq$ 0.2 to 1 m thick) debris slides (fig. 3) and avalanches were probably the most widespread and common types of failure and were especially pronounced in areas underlain by sedimentary rocks. Rock falls were common on steep-walled canyon faces cut in well-fractured basement rock, but also occurred in sedimentary rock where a particularly resistant bed cropped out on oversteepened slopes. Soil falls occurred mainly at the free face of recent stream terrace deposits along major drainages. Slumping (fig. 2) was found largely on reactivated, preexisting (preearthquake) slumps.

Landslide distribution was controlled primarily by the intensity of ground shaking, for most slides occurred in the area of surface rupture. Local variation in landslide density reflected the character of local rock units, degree of fracturing and faulting, and the existence of preexisting landslide deposits. Physiography controlled the density of landslides only in areas of extreme topographic steepness.

The relationship of landsliding to the intensity of shaking is particularly clear in the westward-striking Pico, Modelo, Towsley, and Saugus Formations west of San Fernando Valley. There, the number of landslides decreases markedly along strike westward from the valley, away from the area of aftershocks and most intense tectonic rupturing.

Landslide distribution controlled by rock type is best seen in the vicinity of Lopez and Bartholomaus Canyons (fig. 4*B*). Here, numerous landslides formed on outcrops of the Modelo and Towsley Formations, while relatively few formed on the immediately adjacent Saugus Formation. Free faces of stream terrace deposits were also especially slide

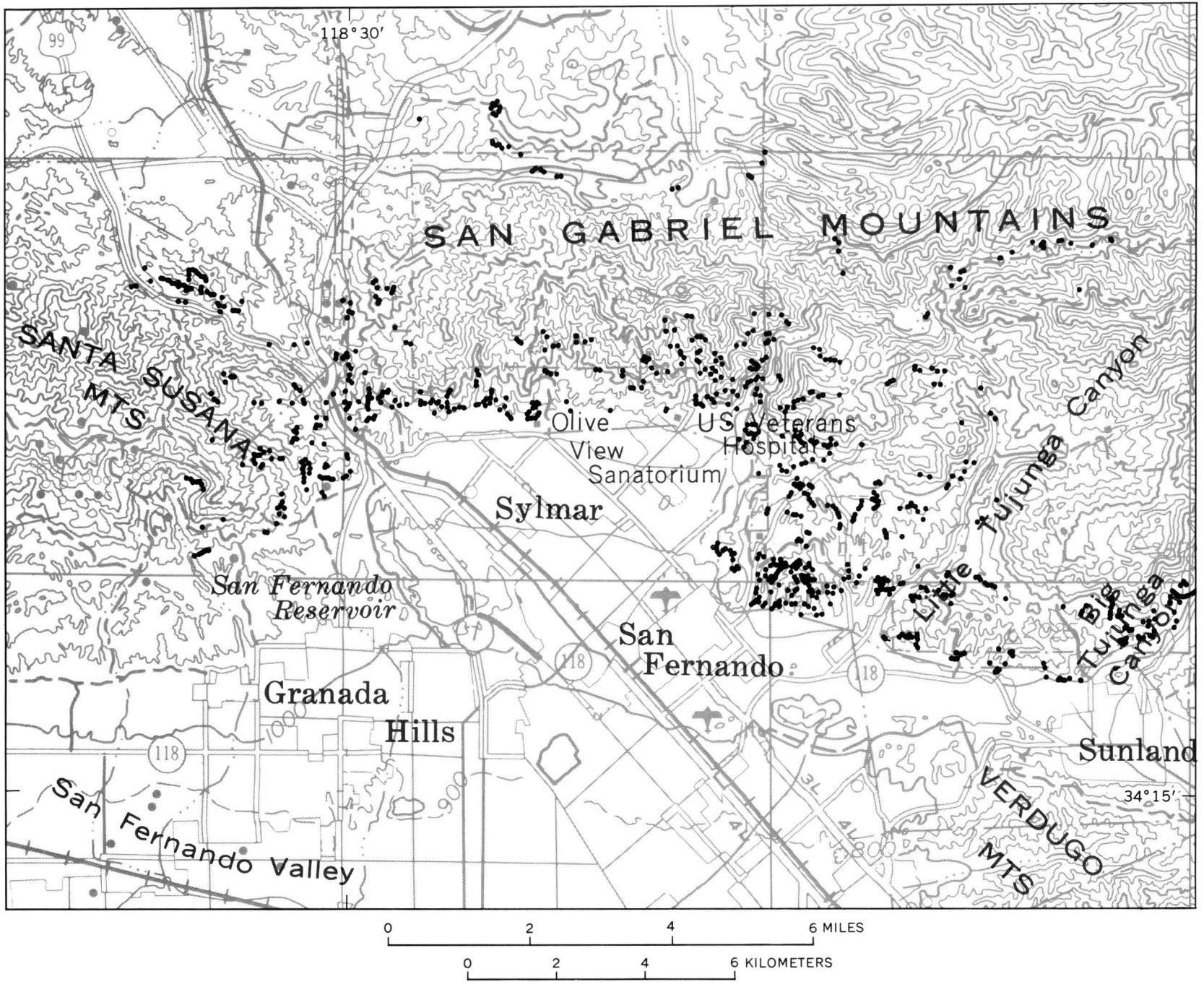

FIGURE 1.—Seismically triggered landslides in the San Fernando Valley area.

prone, giving rise to small soil falls over a considerably larger area than that of figure 1. Numerous rock falls also occurred where highly fractured basement rock is exposed on steep slopes, especially along the major drainages—Pacoima, Little Tujunga, and Big Tujunga Canyons. Rock falls at the mouth of Pacoima Canyon (fig. 4*A*) covered sizable areas, but apparently consisted only of surficial material.

Previously weakened rock showed a common tendency to fail. A number of old landslides were reactivated, as shown by fresh scarps from 0.25 to about 1 m high. Some small old scarps failed as debris slides. Parts of other large old slides failed as a number of small discrete new slides generally concentrated along the toe of the old slide (for example, in Pacoima Canyon, fig. 4*A*). Some landslides were localized by crushed rock along fault zones. Thus, the San Gabriel fault zone was the locus of a narrow band of landslides north of Placerita Canyon (fig. 5).

Landslides were also common in excavations, and many roads were blocked by failures in cut slopes. Innumerable minor rock falls occurred in roadcuts in the area of figure 1, and extended eastward throughout most of the San Gabriel Mountains.

Large rotational or complex landslides, which are characteristic of the San Gabriel and Santa Susana Mountains, did not form during the San Fernando earthquake. Apparently, such slides form under different circumstances—for instance, seismic shaking at times when the ground is saturated by prolonged or heavy rain, or by seismic shaking with longer period vibrations or of longer duration than the San Fernando earthquake. One possible incipient, large complex failure may be represented by features south and east of the San Fernando Ranger Station, which lies between the west end of the Tujunga segment and the east end of the Sylmar segment of the San Fernando fault zone. Northward, compressional surface deformation in the valley margin there may represent relatively large-scale landsliding related to numerous fractures which extend over an area 0.2 to 0.5 km wide in the hills above the ranger station (fig. 4*B*).

FIGURE 2.—Slump-type failure, east of Little Tujunga Canyon.

Widespread ground fracturing throughout much of the area of figure 1 is closely related to landsliding. This fracturing appears to be most pronounced along ridge tops, where, given sufficient rainfall, the highly fractured surficial materials may give rise to abundant debris slides and flows. These materials may now conceivably have the potential for generating as many (or even more) landslides as were triggered during the earthquake.

FIGURE 3.—Failure in roadcut, Balboa Boulevard, with small debris slide in ravine to the right of roadcut.

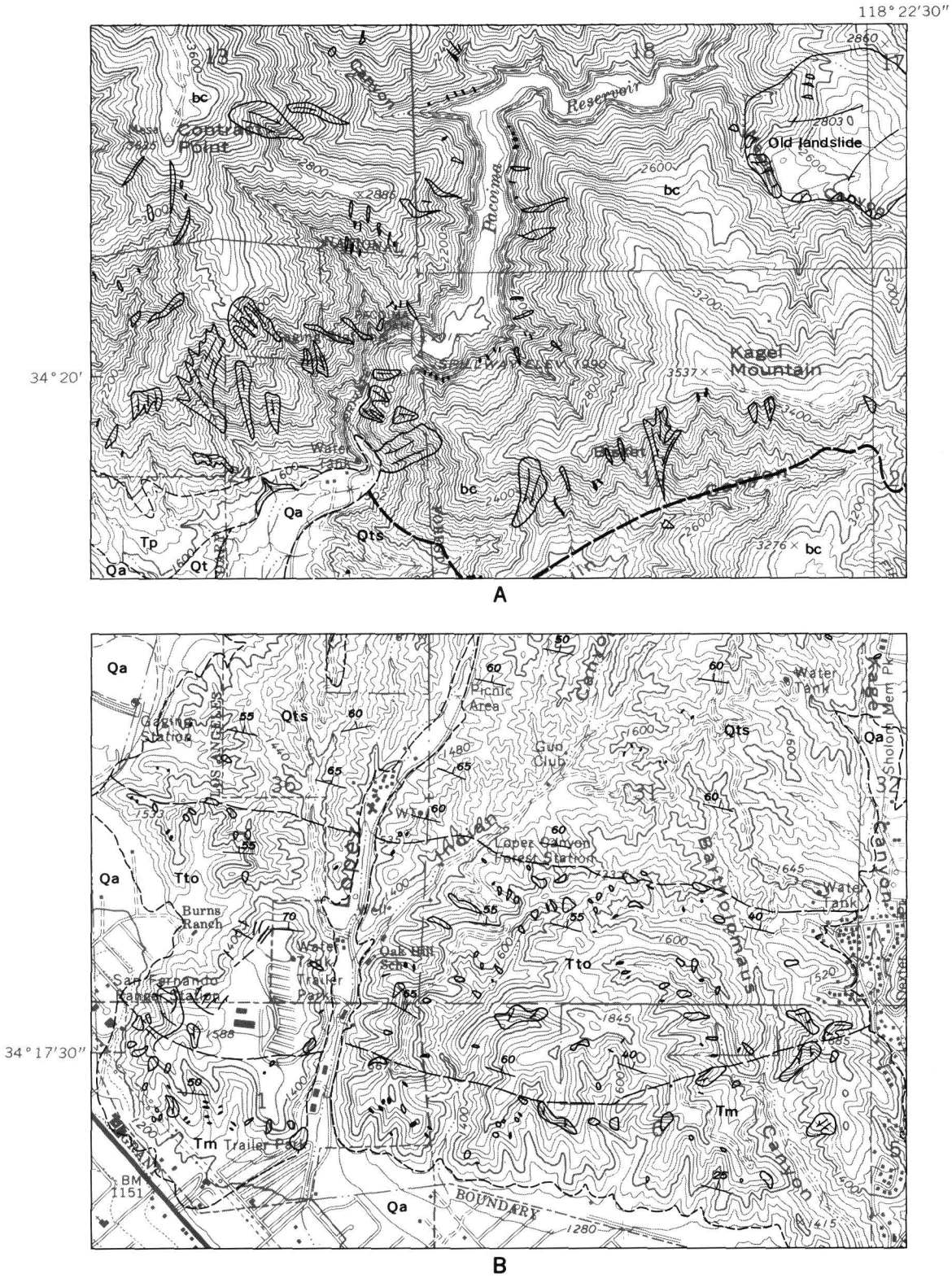

FIGURE 4.—*A*, Landslides in lower Pacoima Canyon area, San Fernando quadrangle, showing topographic control of some landslides and landsliding within older landslide deposits. *B*, Landslides in the Lopez Canyon area, San Fernando quadrangle, showing lithologic control of landslide distribution. See figure 5 for explanation of symbols.

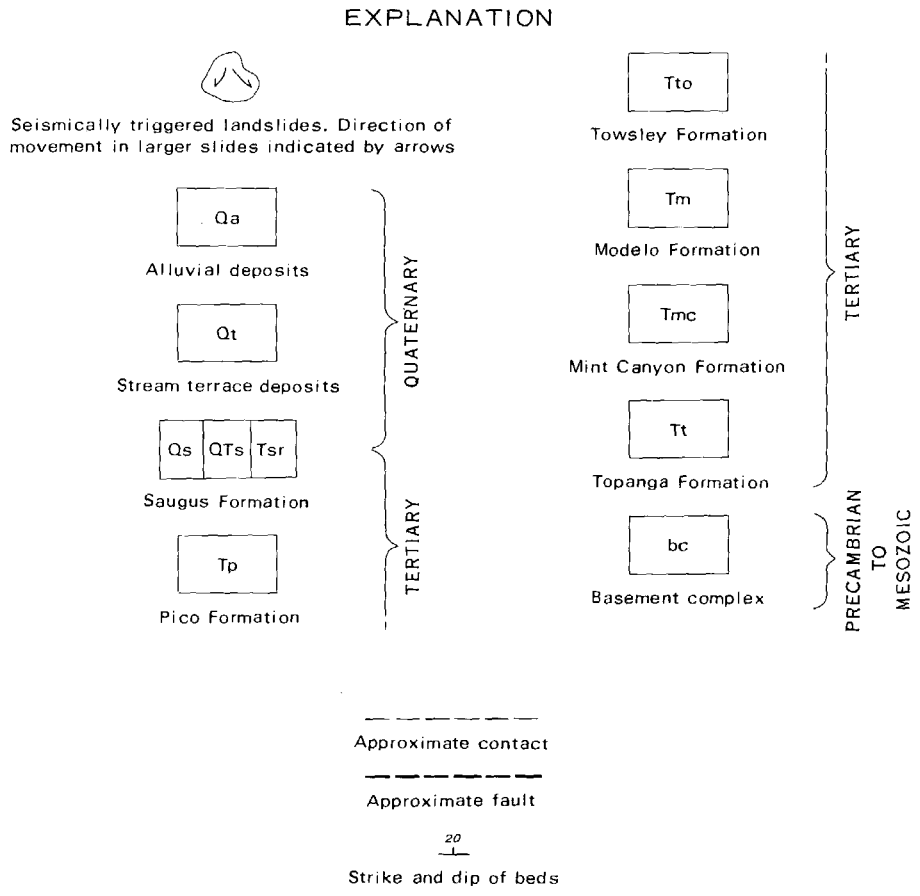

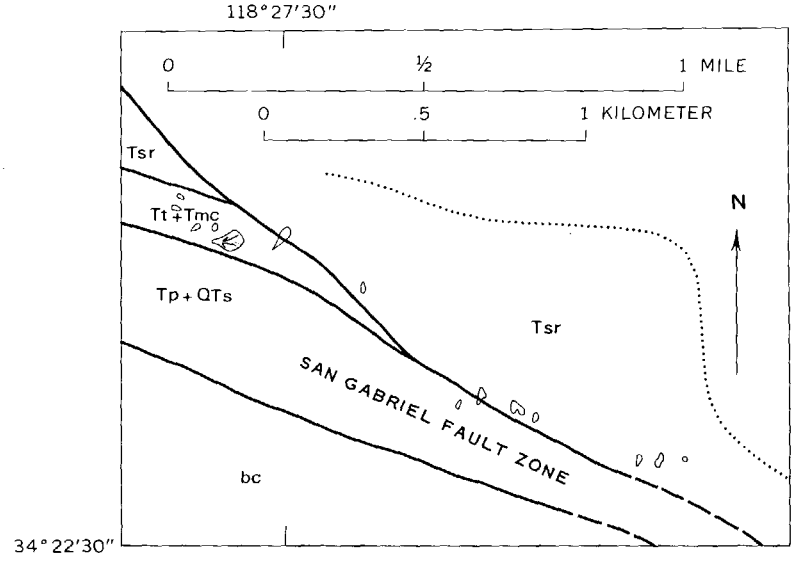

FIGURE 5.—Landslides in the Placerita Canyon area, Mint Canyon quadrangle, showing localization of landslides along the San Gabriel fault.

LANDSLIDING IN THE VICINITY OF THE VAN NORMAN LAKES

By T. L. YOUD
U.S. GEOLOGICAL SURVEY

This section focuses on the Van Norman Lakes area because the earthquake triggered a large number of landslides there and because some of these slides moved down very gentle slopes. An additional reason is the large amount of damage which occurred there.

The geology of the area has been described by Oakeshott (1958), Merifield (1958), and Wentworth and Yerkes (this report). The following information is from their reports. The Van Norman Lakes lie in a valley eroded in north-dipping strata of the Saugus and Modelo Formations. The lakes are impounded at their south ends by dams constructed across this valley. Both lakes are bounded on the southeast and southwest by slightly consolidated sandstones and mudstones of Pliocene and Pleistocene age. The rest of the lakeshore area is covered by recent alluvium. The principal structural features in the area are the Mission Hills thrust located south of the Mission Hills, the Olive View fault, which cuts northeastward across the area just north of the upper lake, and the Mission Hills syncline, which generally parallels the Olive View fault. (See fig. 1.)

Because of the reservoirs and a confined aquifer in the Little Tujunga syncline, the water table in the general area is at a relatively high level and intersects the surface at several locations. At the time of the earthquake, the water table was probably not more than a few meters below the surface at any point in the alluvial areas surrounding the lakes.

The soils in the area have been mapped by the Soil Conservation Service (U.S. Department of Agriculture, 1915). Sandy loams, commonly with components of gravel and silt, have formed on the alluvium. Clay loams and rough ground are the common soil types on the upland hills.

LANDSLIDES

A large number of landslides formed in the vicinity of the Van Norman Lakes in response to the February 9 earthquake. The most significant ruptures generated by these movements are plotted in figure 1. Only the slides in recent alluvium are discussed here. Slides in bedrock areas, including some in the subject area, are described by Morton (this report); and slope failures in constructed fills, including the nearly disastrous slump in the Lower Van Norman Dam, are described by Youd and Olsen (this report).

Extensive slumping occurred in the alluvium around the margins of both the Lower and the Upper Van Norman Lakes. In some places a nearly continuous line of scarps formed. The scarp on the west shore of the lower lake is more than 1 km (kilometer) long. Sand boils commonly formed below these scarps (fig. 1).

A recently filled and graded area west of the upper lake was broken up by numerous fissures, which generally tended to parallel the shoreline and the contour of the previous surface, shown by the contours on the map in figure 1. This area is considered here because of the likelihood that failure in the alluvium below the fill is reponsible for the sliding. Extensional and vertical displacements in the fill indicate movement toward the reservoir either in the form of block glides or in slightly rotated slumps. Sand boils erupted in the southern part of this fracture zone some 180 m (meters) from the lake and several meters above the water level at the time of the shock.

Many fissures formed in the area west of that described in the previous paragraph. Of those observed, the most notable were in a schoolyard in the mouth of Bee Canyon, nearly 1 km from the upper lake. These fissures were characterized by vertical displacements of as much as 50 mm (millimeters) and continuous lengths of perhaps 100 m. They seemingly formed the head of a landslide which had moved down the very mild slope (about 1.5° or 2.5 percent) eastward toward the upper lake.

The most damaging slide in the vicinity of the lakes formed a tonguelike feature (in plan) extend-

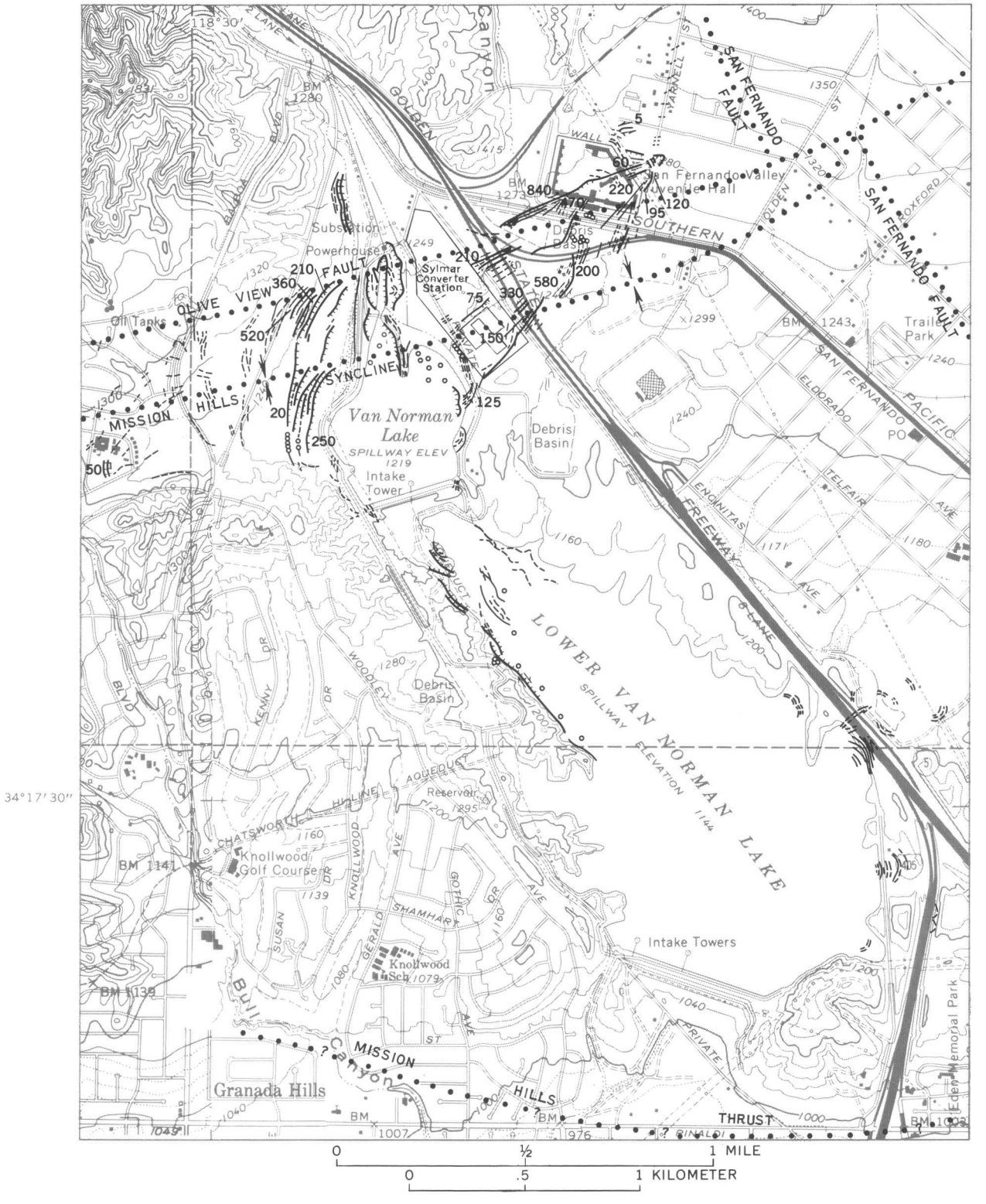

FIGURE 1.—Map of Van Norman Lakes vicinity, showing surficial ruptures associated with landslides activated by the earthquake.

EXPLANATION

Small surface crack

Large surface crack

120

Vertical displacement, in millimeters

95

Horizontal displacement, in millimeters

Sand boil

Structural feature

Geology from Merifield, 1958 and Oakeshott, 1958

FIGURE 1.—Continued.

ing northeastward from the upper lake for a distance of 1.2 km. Located on or crossing this slide, hereafter called the Juvenile Hall slide (fig. 2), are a major part of the San Fernando Valley Juvenile Hall, trunk lines of the Southern Pacific Railroad, San Fernando Boulevard, Interstate Highway 5, the Sylmar electrical converter station, and several pipelines and canals. (See Youd and Olsen, this report). Earthquake damage to these facilities will likely exceed $30 million.

The available evidence indicates that the displacements associated with this feature are of landslide rather than tectonic origin. The evidence includes: (1) the tonguelike shape of the feature and the fact that the rupture pattern did not extend beyond the bounds of the feature; (2) fissures with right-lateral displacements formed on the north margin, fis-

FIGURE 2.—Oblique photograph of San Fernando Valley Juvenile Hall area and approximate boundaries of the Juvenile Hall slide. View to east.

sures with an almost equal amount of left-lateral displacement formed on the south margin, and almost purely extensional cracks formed at the head; (3) Survey data generously supplied by the City of Los Angeles (L. D. Paulsen, Bureau of Engineering, city of Los Angeles, Oral Commun., Feb. 26, 1971) show that movements of the feature relative to the adjacent ground exceeded relative movements between survey points on opposite sides of the feature.

Resurvey of San Fernando Boulevard revealed that the distance across the slide from the survey point at the Interstate 5 overpass to a point near Olden Street had shortened 43 mm. Relative to the Roxford Street intersection with San Fernando Boulevard (southeast of the slide), the survey points near the Interstate 5 overpass (northwest of the slide) had moved south 300 mm and west 210 mm. These relative movements are considerably less than the total downslope movements of the slide, which ranged from 0.5 to 1.0 m (based on visual observation and cumulative measurements of displacements across fissures). Thus, it appears unlikely that the feature mapped as the Juvenile Hall slide had a tectonic origin, even though the southwest movement of the Interstate 5 overpass with respect to the Roxford Street intersection could have been produced by left-lateral tectonic displacement on a northeast trending fault or fault zone through the area of the slide.

The surface on which movement occurred has a very gently slope; it averages about 1.5° (2.5 percent) over its entire length assuming that the toe of the slide is at the shoreline of Upper Van Norman Lake. The maximum slope was about 3° (5 percent) near the head. Surprisingly, the average slope between the Juvenile Hall and the converter station, which appeared to be the minimum, was only 0.9° (1.5 percent).

Numerous sand boils erupted on the lake floor, presumably near the toe of the slide. These were exposed after the water level was lowered. Sand boils were also found at the following locations: Behind the converter station near the base of the graded fill, in a field south of Juvenile Hall (fig. 3), and along the north edge of the railroad grade in front of the Juvenile Hall Administration Building.

During the earthquake, the crest of the Upper Van Norman Dam subsided a maximum of 0.9 m and shifted downstream a maximum of 1.5 m with respect to its abutments (W. F. Hansen, Los Angeles Department of Water and Power, oral commun., Feb. 23, 1971). In light of this it would appear that a low-gradient slide, similar to the one described above, may have cut through the valley floor beneath the dam and caused these movements.

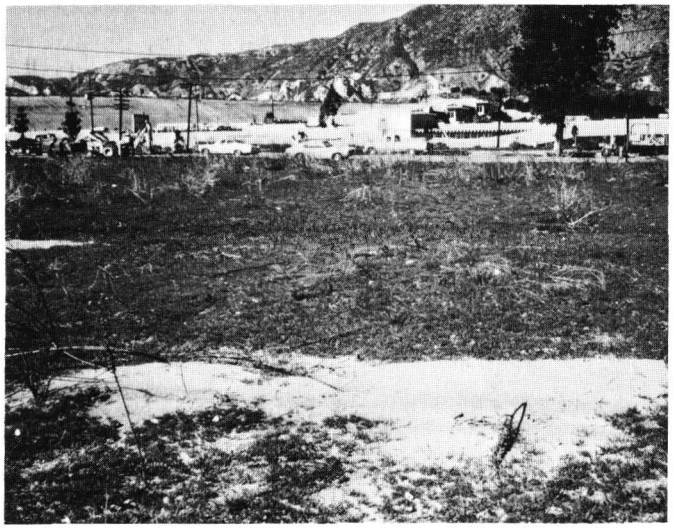

FIGURE 3.—Sand boils on Juvenile Hall slide. A damaged part of the Juvenile Hall is in the background.

EXPLANATION OF SLIDES ON LOW-GRADIENT SLOPES

The most reasonable explanation for slippage of the Juvenile Hall slide on a slope of such low gradient is that the underlying soils were partially or completely liquefied during the earthquake. The many sand boils observed on or near the slide are evidence that this occurred.

In addition to causing sand boils, the increased pore water pressures associated with the liquefied condition would reduce the shear strength of the subsurface soils. This strength would have to be reduced to a value less than the tangential component of the lithostatic stress for movement to occur on slides such as the Juvenile Hall slide, which is presumed to be very long compared with its depth. This reduction in strength can readily be explained by increased pore water pressure and the shear strength relationship for granular soils:

$$\tau = (\sigma_n - u) \tan \phi \qquad (1)$$

where τ is the shear strength of the soil, u is the pore water pressure, σ_n is the normal stress on the failure plane (essentially the lithostatic pressure for low-gradient slopes), and ϕ is the angle of internal friction of the soil. Thus, if the pore water pressure under the Juvenile Hall slide increased to a value

approching the lithostatic pressure during the shock, the soil strength would have been reduced to nearly zero, allowing the movement to occur. The field evidence indicates that this probably was the case.

It is also probable that movements on many, if not all, of the other slides in the alluvium surrounding the Van Norman Lakes were directly attributable to increased pore water pressures generated by the earthquake.

REFERENCES CITED

Merifield, P. M., 1958, Geology of a portion of the southwestern San Gabriel Mountains, San Fernando and Oat Mountain quadrangles, Los Angeles County, California: Los Angeles, California Univ. M.A. thesis (unpub.)

Oakeshott, G. B., 1958, Geology and mineral deposits of San Fernando quadrangle, Los Angeles County, California: California Div. Mines and Geology Bull. 172, 147 p., 5 pls.

U.S. Department of Agriculture, 1915, Soil map, California, San Fernando Valley sheet: Soil Conservation Service, Washington, D.C.

GROUND FAILURE ON THE SAN FERNANDO SURFACE AWAY FROM OBVIOUSLY TETONIC RUPTURE ZONES

By ROBERT V. SHARP
U.S. GEOLOGICAL SURVEY

The earthquake of February 9 produced widespread ground fracturing in the form of cracking, thrusting, and slumping across much of the surface on which the communities of San Fernando and Sylmar are built. The relatively smooth and flat surface, here termed the "San Fernando surface," is outlined in the generalized ground-rupture map by the U.S. Geological Survey staff. Fracturing on the San Fernando surface is particularly evident in pavements and sidewalks. The nature of displacement on many fractures hints at possible deeply rooted tectonic influence; yet most offsets can be explained satisfactorily by surficial slippage not involving tectonism. In view of previously published literature on the geologic evidence for faults projecting under the San Fernando surface from the neighboring mountainous area, fracturing was investigated throughout the surface to determine whether it reflected renewed tectonic movement along generally concealed faults.

Examination of the affected region revealed no definite tectonic zones other than those described elsewhere in this volume. Particular effort was made to identify persistent patterns or alinements of fracture zones that might be expected along through-going faults. Despite the negative evidence, however, it is conceivable that tectonic movement did alter the form of the San Fernando surface in a subtle way at unrecognized locations. Geodetic remeasurement of the horizontal and vertical positions of established points on the surface is now in progress. Detailed data of this kind will provide the critical evidence for or against tectonic dislocation outside of the San Fernando fault zone. The fracturing in the fault zone itself is described in accompanying sections by Kamb and others and by U.S. Geological Survey staff.

Where fractures resulting from landsliding, slumping, and lurching are developed near or within a zone of tectonic rupture, it is sometimes difficult to determine the origin of individual fractures. However, many fractures are readily attributable to nontectonic processes because of their localized distribution, orientation with respect to natural or artificial topographic features and constructed works, and the sense and pattern of the offset along them. Tectonic fractures are primarily recognized by their continuity and map pattern, pattern of displacement, and indifference to the position of overlying constructed works.

Three kinds of ground failure by fracturing were recognized outside of the major zone of tectonic movement on the San Fernando surface—ground breaks evident in both soil and overlying constructed works, cracks restricted to soil near built structures, and cracks in pavements and other thin structures resting on unaffected substrate. These all displace the ground surface in a manner that can be related to minor topographic features or constructed works, and they appear not to be related to through-going fracture systems. Nontectonic fractures were not mapped and are not illustrated in this preliminary report.

Ground breaks involving both constructed works and the underlying soil occurred on large and small scale. The larger failures of this type, such as the landslide under the San Fernando Valley Juvenile Hall, are discussed in the section by Youd. Small-scale failures and fractures that break both the soil and overlying works appear to be related chiefly to artificial cut or fill slopes on the ground surface. Parallelism between the free face and scarps developed at the upslope end of the fill indicate failure by small-scale downslope movement.

Failures in soil alongside structures or large fills

are a common result of shaking on the San Fernando surface. Both extensional cracks and compressional zones indicated by small-scale thrust faults have been produced by vibration and lurching of houses, concrete walls, curbs, sidewalks, and other heavy objects imbedded in the ground. Many of these fractures do not extend into even small structures, such as driveways, that may lie above them. In every case, the distribution of fracturing of this type is restricted to the immediate location of structures or larger fills, and consequently cannot be considered to be tectonic.

The most easily seen evidence for apparent ground breakage outside of known tectonic zones is the fracturing, thrusting, and buckling of pavements, curbs, and sidewalks. However, only in exceptional cases do the breaks extend across the adjoining ground surface as far as a meter, and most terminate at the edge of the slabs of pavement. The evidence thus indicates that fractures in pavement for the most part do not reflect displacement in the ground and hence are nontectonic. Even vertical offsets in pavement usually do not extend into the surrounding soil, suggesting that compaction of the roadbed or perhaps of fill over buried pipelines has occurred. At the time of strong shaking, slabs of pavement (including curbs and sidewalks) commonly decoupled from the underlying soil and were translated downslope along the lengths of the streets. Slight rotational effects resulting from small differences in the amount of translation of one side of such slabs relative to the other side are shown by lateral offsets at many of the open extensional cracks that broke pavements during the earthquake.

Distinguishing the various types of displacement produced by shaking from truly tectonic movement ultimately rests on whether there has been any net extension, shortening, or changes in elevation. The observation that compression may be transmitted along a street for several blocks before the appearance of overthrusts or buckled up blocks of pavement complicates the problem of locating minor ground displacements of possible tectonic origin. Attempts at quickly determining dimensional changes along streets by tabulating extensional openings and compressional overlaps have shown that errors which are comparable to the size of the offsets being sought are possible. In addition to the imprecision in measuring fractures, permanent dimensional changes in the form of compressional shortening and possibly tensile elongation of pavement and sidewalk slabs are known to have occurred. Other dimensional changes were presumably caused by myriad fractures that escaped detection because of their extremely small size. Apparently only relatively large offsets can be detected and roughly estimated by measuring fractures in sidewalks and pavement and that small but real tectonic offsets could easily be overlooked.

METHANE SEEP OFF MALIBU POINT FOLLOWING THE SAN FERNANDO EARTHQUAKE

By H. EDWARD CLIFTON, H. GARY GREENE, GEORGE W. MOORE, and R. LAWRENCE PHILLIPS
U.S. GEOLOGICAL SURVEY

At approximately 8 o'clock on the morning of the San Fernando earthquake, February 9, 1971, observers on the pier in Kellers Shelter near Malibu Point, Calif. (fig. 1), noticed a large volume of gas escaping from the ocean surface about 500 m (meters) from the shoreline. The seep probably began with the earthquake at about 6:00 a.m. but was unnoticed for 2 hours because coastal fog restricted the visibility around Malibu Point. The seep occurred in a linear zone that was oriented approximately east-west, parallel to the general trend of geologic structure in this area (Schoellhamer and Yerkes, 1961). Malibu Point lies approximately 50 km (kilometers) southwest of the earthquake epicenter, and some houses in the vicinity of the Point suffered minor structural damage during the earthquake. The probable coincidence of the seep with the San Fernando earthquake and the similarity of its trend to that of local faults (fig. 1) raised the possibility that the earthquake had triggered secondary faulting near Malibu Point.

To evaluate the geological significance of the seep, personnel of the U.S. Geological Survey conducted a brief investigation. The day after the earthquake George W. Moore visited the site and, with the aid of local diver Bill Farell, obtained samples of the gas for analysis. The following day the other authors of this section used scubas to investigate the sea floor at the seep and to collect additional samples of the gas. A surveying team from the Department of the Los Angeles County Engineer located the position and the trend of the seep by triangulation from onshore beach marks to marker buoys emplaced by the diving team.

We wish to acknowledge the generous assistance of Mr. Sam Miller, Regional Engineer, Department of the Los Angeles County Engineer. We also wish to thank Lt. Ted Davis and Mr. Roger Smith, Los Angeles County Lifeguard Patrol, who provided support for the diving operation.

SETTING

The seep occurred in 6-8 m of water east of Malibu Point, 400-500 m from the mouth of Malibu Creek. The area around Malibu Point appears to be at least in part a deltaic deposit at the mouth of the creek. Outcrops of bedrock occur, however, at the southernmost tip of the Point, and abundant boulders near the shoreline suggest that bedrock lies close to sea level on the east side of the Point.

Malibu Point lies on the south side of the Santa Monica Mountains. The rocks underlying the vicinity of the Point consist of marine shale, mudstone, siltstone, and sandstone of middle and late Miocene age (R. F. Yerkes, written commun., 1971). These strata lie in or near the east-trending Malibu Coast deformation zone, which includes the Malibu Coast fault (fig. 1). This zone is characterized by north-over-south compressive deformation and contains a number of north-dipping faults (R. F. Yerkes and C. M. Wentworth, unpub. data, 1965).

The sea floor in Kellers Shelter slopes evenly and gently seaward to a distance of about 6 km from the shore, where it abruptly increases in slope (U.S. Coast and Geodetic Survey Sheet 5101). In the vicinity of the seep, 400-500 m from the shore, the sea floor is nearly flat and an unknown thickness of relatively young sediment overlies the bedrock.

DESCRIPTION

Gas bubbles broke the ocean's surface in a zone approximately 12 m wide by 120 m long and oriented N. 78°E. (fig. 1). Two days after the earthquake the gas bubbles ranged in diameter from 0.5 to 2 cm (centimeters) at the surface and were escaping into the atmosphere at a rate of about 1-5 bubbles per second; some strings of bubbles were discontinuous. Eyewitnesses reported that a much greater volume of gas was escaping on the day of the earthquake and that a second zone of bubbles was present trending shoreward at an acute angle from the major seep.

The sea floor in the vicinity of the seep is composed of fine to very fine brown sand that contains abundant organic debris. Irregular sand ripples 1-4 cm high cover most of the floor. During the diving observations, the ripples were inactive and currents generated by the waves transported only fine organic matter. A few millimeters to several centimeters below the surface of the floor, the sediment is very cohesive and is black and fetid. Approximately 10 cm beneath the surface of the floor, the sand coarsens to medium grain size and is better sorted.

The gas emanated from small holes and craters in the sea floor. The smallest holes were only several millimeters in diameter, whereas the largest craters were up to 40 cm across and 10-15 cm deep. The craters were lined or rimmed with dark sand derived from the subsurface. Generally, a greater volume of gas issued from the larger craters, although some of the large craters seemed to be totally inactive. All the craters were sharply defined and showed no evidence of modification by waves or bottom currents. Many of the craters contained large amounts of grass and other organic detritus. The gas commonly emanated around tubes of an unidentified burrowing organism.

Many of the emanation sites seemed to be locally clustered and lay a few centimeters to 1 or 2 meters apart; outside such clusters the emanations occurred several meters apart. Some of the emanations occurred several meters apart. Some of the emanation clusters showed a linear trend approximately parallel to the general trend of the seep. Ripples within the clusters tended to be less pronounced than they were elsewhere, and detrital organic material, particularly grass, seemed to be more abundant in the areas of greatest emanation.

No ruptures or dislocations of the sea floor were observed during the dive. The cohesiveness of the sediment in Kellers Shelter probably is sufficient to preserve the expression of such features. Moreover, the state of preservation of the craters suggests that little or no sediment was transported by wave activity during the two days that elapsed between the earthquake and the time of underwater observation of the seep. Therefore, scarps or fissures that formed on the sea floor would probably have been discernible had they existed. An anchor chain lying on the sediment surface crossed one of the clusters of craters at an angle to the trend of the seep; this chain was lying in a shallow scour groove that was nowhere dislocated along its extent. The absence of dislocation precludes lateral faulting of the sediment, at least along the extent of the anchor chain.

Three box cores were taken through the uppermost 17 cm of sediment in one of the clusters of craters to look for possible earthquake disturbance of internal sedimentary structures. None of the cores was taken directly over an active gas emanation. X-ray radiographs of the cores identify a layer 5-6 cm thick at the top of the core consisting of finely cross-stratified sand. Within this layer no evidence exists of breakage or other disruption attributable to the San Fernando earthquake.

COMPOSITION OF THE GAS

The gas was sampled by inverting glass containers, filled with water, over bubble outlets. After the gas displaced the water, the containers were capped. The bubble outlets that were sampled were located in the center of small craters on the ocean floor at a depth of about 10 m. Precaution was taken to release pressure from the sample container on ascent to the surface.

Mass-spectrometer analysis by Motoaki Sato, U.S. Geological Survey, Washington, D. C., shows the sample of gas collected for Moore to have the following composition:

	Volume percent (with water)	Volume percent (without water)
Methane	90.0	93.3
Nitrogen	4.4	4.6
Water	3.6	--
Carbon dioxide	1.2	1.2
Oxygen	.75	.8
Argon	.08	.1

The ratio of nitrogen to argon is virtually that of air, but the ratio of nitrogen to oxygen is not. Oxygen is apparently deficient, whereas carbon dioxide is added (Motoaki Sato, written commun., 1971). Other samples of gas are being processed for radiometric dating.

DISCUSSION

Two possible origins exist for the methane that seeped from the sea floor near Malibu Point. Either the gas developed from decaying organic material in the marine sediment above the Miocene bedrock, or it formed and was trapped in the bedrock until its release following the earthquake. Presently, data are insufficient to eliminate either possibility. The composition of the gas suggests that it is marsh gas. Gas from the oil fields in the Los Angeles basin con-

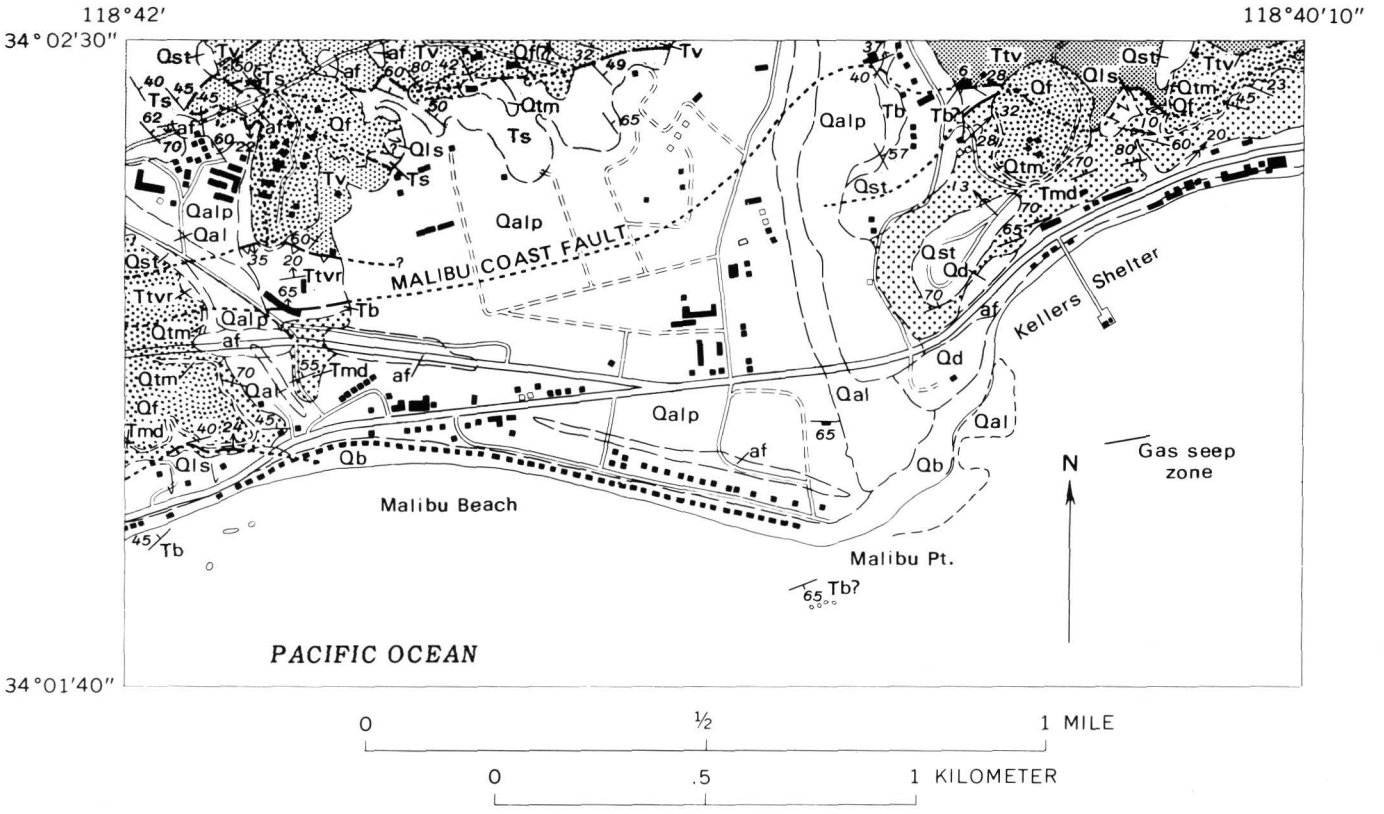

FIGURE 1.—Location of the gas seep that began off Malibu Point on February 9, 1971, and its relation to local geologic features. Geology modified from R. F. Yerkes (written commun., 1971).

tains about 9 percent ethane and 1 percent propane, both of which would have been detected in the seep gas had they been present. It is not known whether the sediment cover in Kellers Shelter contains sufficient organic material to generate the volume of methane that escaped in the seep. The bedrock exposures at sea level at Malibu Point and in adjacent sea cliffs suggest that the sediment thickness at the seep is not very great. No accurate data on thickness are available; the nearby pier is sufficiently old that no records remain of the depth to bedrock under its pilings (Sam Miller, oral commun., 1971).

If the gas originated in the unconsolidated sediment, three possible explanations for the seep exist: (1) compaction within an ancient linear channel incised into the bedrock, (2) release in a line controlled by bedding in the underlying Miocene strata, and (3) release in a line controlled by a fracture in the bedrock. If the gas originated within the Miocene strata, the seep could only have formed along a fracture in the bedrock. No dislocation or displacement of bedrock is necessarily implicit in either of the two possible explanations that postulate a fracture in the bedrock.

The orientation of the seep is consistent with all the foregoing possibilities. If it were alined along an ancient channel in the bedrock, it would imply that the channel was cut parallel to the slope contours. Such an orientation of a deeply eroded channel seems somewhat unlikely, but would not be impossible for short distances. The orientation is nearly parallel to bedding in the rocks exposed at Malibu Point and also parallel to the trend of faults mapped in this area (fig. 1). The eyewitness account of a second line of gas seepage extending shoreward at an acute angle from the primary seep suggests that the flow of gas is at least partly controlled by fractures in the bedrock.

The westward projection of the seep extends into a cove lying between two patches of abundant boulders. This cove could be interpreted as a channel cut in the past by Malibu Creek, as a less resistant stratigraphic layer in the bedrock, or as a sheared zone of faulting in the bedrock. The location of the cove along the projection of the seep therefore provides little evidence concerning the origin of the seep.

The roads leading out to Malibu Point and the alluvium on the delta of Malibu Creek were examined

EXPLANATION

SURFICIAL DEPOSITS

Holocene

af

Artificial fill

Chiefly fill for roadways; locally includes cut surfaces

Pleistocene and Holocene

Qal | Qalp | Qf | Qb | Qd | Qls

Alluvial, colluvial, fan, beach, dune, landslide, debris, and undifferentiated surficial deposits:

Qal, *alluvial sand, gravel, and silt; subrounded boulders locally exceed 5 feet, thickness locally exceeds 100 feet in Malibu Canyon*

Qalp, *alluvial and mudflow deposits underlying flood plains incised to depths as great as 25 feet*

Qf, *fan deposits in tributaries and below steep slopes along coast; thickness locally as great as 100 feet, but commonly less than 10 feet*

Qb, *beach deposits; fine- to medium-grained sand, rounded pebble gravel locally at base, thickness less than 25 feet*

Qd, *dune deposits; fine- to medium-grained loose sand; thickness locally exceeds 50 feet*

Qls, *landslide deposits; may include both bedrock and surficial materials*

Pleistocene

Upper Pleistocene

Qst | Qtm

Terrace deposits

Qst, *stream terrace deposits; interbedded gravel, sand, and silt, thickness locally as great as 100 feet*

Qtm, *marine terrace deposits; sand, silty sand, and gravel; sand, friable, well sorted, fine to medium grained, as thick as 20 feet*

QUATERNARY

BEDROCK UNITS

AREA SOUTH OF MALIBU COAST FAULT

Miocene — Middle and upper Miocene

Tmd

Monterey Shale

Marine shale and siltstone

Middle Miocene

Tb

Unit B

Marine mudstone, siltstone, and sandstone

AREA NORTH OF MALIBU COAST FAULT

Middle Miocene

Ttv / Ttvr

Middle and upper Topanga Formation of Durrell (1954) (Upper plate of Malibu Bowl fault)

Ttv, *volcanic rocks; andesitic and basaltic flows and flow breccias; locally includes mudflow breccia, pillow breccia*

Ttvr, *volcanic rocks of Ramera Canyon area; andesitic and basaltic breccias, tuff breccias, flows (?), and minor volcanic sandstone*

Miocene

Lower Miocene

Tv

Vaqueros Formation

Undivided sequences of chiefly marine sandstone, siltstone, and pebbly sandstone

Upper Eocene, Oligocene and lower Miocene

Ts

Sespe Formation

Nonmarine sandstone, pebbly sandstone, and mudstone

Eocene, Oligocene, and Miocene

TERTIARY

MAP SYMBOLS

Bedding

Contact or mapped horizon

Long dash where approximately located, short dash where inferred

25

Strike and dip of beds

30

Approximate strike and dip of beds determined from indirect evidence

25

Strike and dip of indistinct layering in volcanic rocks

65

Strike and dip of joint

Faults

Fault symbols; long dash where approximately located, short dash where inferred, dotted where concealed, queried where doubtful; ×, igneous rock intruded along fault

65 U D ×----?

High-angle fault, showing dip; U, upthrown side; D, downthrown side

Low-angle fault, sawteeth on upper plate
Relative displacement not determined

40

Malibu Coast fault, showing dip
Boxes on upper plate of reverse fault

Folds

60

Axis of complex fold, showing direction and amount of plunge, and dip of axial surface

25 Minor anticline 30 Minor syncline

Showing plunge and dip of axial surface

Landslides

Most landslides are complex; symbol may include more than one type and stage of movement; may include both bedrock and surficial materials

(?)

Landslide

Arrows show general direction of movement; queried where origin of feature doubtful

for fresh fractures that might be associated with the methane seep. Only one fresh joint or crack was found. This crack occurs in hard-packed alluvium on the west side of Malibu Creek well off the projection of the seep. No offset across the crack could be detected.

CONCLUSIONS

The methane gas that seeped from the sea floor following the San Fernando earthquake may have originated from the decay of organic material in Holocene or Pleistocene sediment, or it may be much older, having formed in the Miocene bedrock underlying this area. Radioisotope analysis of the gas, currently in progress, may establish its age and origin.

The trend and location of the seep may be controlled by either ancient channels incised in the bedrock, structural attitude of the underlying strata, or fractures through these strata. The report of a second line of gas seepage shortly after the earthquake suggests that fractures are at least in part responsible. If the age of the gas proves to be pre-Pleistocene, seeping of the gas along fractures in the bedrock would be indicated.

Regardless of its origin, the seep was not accompanied by active faulting on the sea floor. No detectable rupture or dislocation of the sediment surface occurred along the seep as a result of the San Fernando earthquake.

REFERENCE

Schoellhamer, J. E. and Yerkes, R. F., 1961, Preliminary geologic map of the coastal part of the Malibu Beach quadrangle: U.S. Geol. Survey open-file rept.

OIL AND GAS SEEPAGES AND DAMAGE TO OIL FIELD FACILITIES RELATED TO THE EARTHQUAKE

By California Division of Oil and Gas

OIL AND GAS SEEPAGES

SALT LAKE FIELD

Four oil and gas seepages have been reported within a 1-mile radius of the famous Rancho La Brea tar deposits following the earthquake of February 9. Historically, this area, like many other areas in Southern California, has been known for its high incidence of oil and gas seepages.

This area also marks the location of many oil wells that were abandoned between 1920 and 1935.

The exact relationship between the earthquake and the seeps is not known at this early date; however, there is a joint study under way by members of the oil and gas industry to determine the full nature of this phenomenon. The California Division of Oil and Gas is actively involved in this project.

MALIBU OFFSHORE

On February 9, 1971, bubbles of gas were discovered rising to the surface of the ocean approximately 200 yards off Malibu Pier. (See figure 1 of this report and also the map in the section by Clifton and others.) Lt. Ted Davis of the Los Angeles County

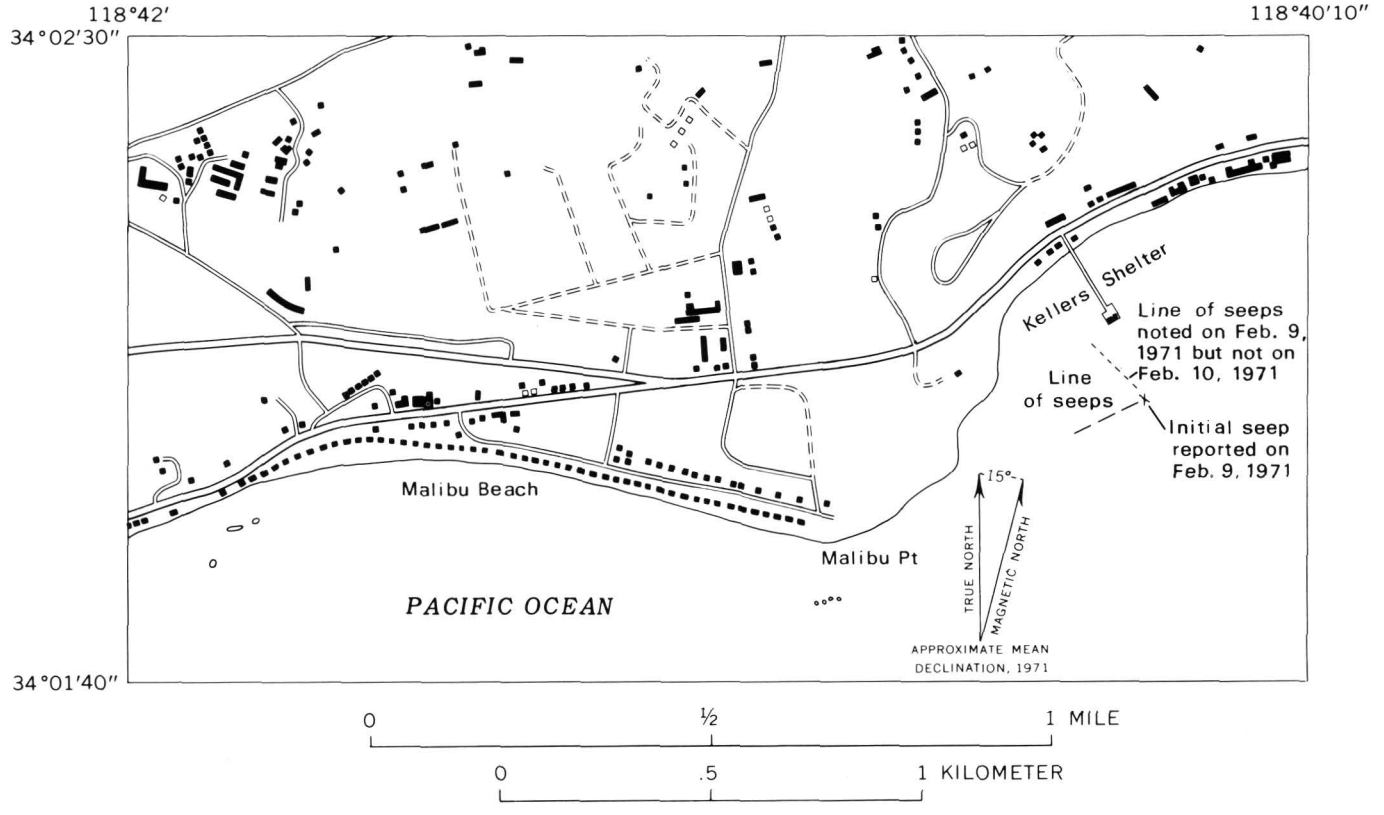

FIGURE 1.—Location of gas seeps off Malibu Point.

Lifeguard Patrol stated that the bubbles had appeared shortly after the earthquake.

On February 10 the seep was seen to consist of a series of small individual seeps occurring along a line extending at least 800 feet from a point 200 yards slightly southwest of the end of Malibu Pier, and approximately 600 yards northeasterly from Malibu Point.

Lt. Davis stated that another line of seeps was noted on February 9, originating at the easterly end of the previously noted seep line and extending northwesterly some 300 feet. However, by February 10 bubble activity along this line had declined to the point that it was no longer visible.

Scuba divers reported that the seeps appeared to emanate from the sea floor as individual columns of bubbles occurring along the previously described line. Plastic bags placed over individual seeps required about 20 minutes to recover approximately three-quarters of a cubic foot of gas.

In the opinion of those who were present on February 9, the seep activity had declined approximately 75 percent by February 10.

An analysis of the gas is presented in the section by Clifton and others.

DAMAGE TO OIL FIELD FACILITIES

Despite the severity of the earthquake of February 9, relatively little damage was sustained by facilities in the nearby oil and gas fields.

Division engineers making field checks after the earthquake reported minor damage to tanks, roads, and a few wells. Line breakage occurred in several fields; however, where breaks did occur, only minor spillage was noted.

Several fields lost electrical power and immediately shut down, but most of them were again operating normally within a matter of hours.

The Newhall Refining Co., Inc., refinery, 2 miles southeast of the town of Newhall and approximately 11 miles southwest of the earthquake's epicenter, was forced to shut down temporarily because of damage to storage tanks and pipelines. Estimated repair costs range from $8,000 to $12,000. The refinery is a 5,500-barrels-per-day unit that produces asphalt, road oils, and jet fuel.

A note of interest was the report that the Cascade field showed an increase in gas production after the quake.

WATER-RESOURCES ASPECTS

By A. O. WAANANEN and W. R. MOYLE, JR.
U.S. GEOLOGICAL SURVEY

Damage to hydraulic structures constituted the major impact of the San Fernando earthquake of February 9, 1971, on the water resources and the water supplies of the area principally affected by the seismic shocks. The effects on the water resources of the region included noticeable fluctuations in the stages of streams and reservoirs and water levels in wells, the roiling of water in water-supply systems, short-term changes in the flow of streams, and short-term changes in ground-water levels. The major damage was caused by the principal M6.6 shock that occurred at 0601 hours February 9. The full effect or effects of any additional damage that may have resulted from the lesser shocks have not been appraised in this preliminary account.

A normal and expected effect of earthquakes of magnitude 5.0 or greater is the development of hydroseisms—seismically induced fluctuations of water levels in wells, streams, lakes, ponds, and reservoirs. They are a common response of water bodies to seismic shock. Hydroseisms resulting from moderate and greater shocks have been recorded at streamflow measurement stations and ground-water observation wells over wide areas and have been reported by many investigators. The impact of the Alaska earthquake of March 27, 1964, for example, as reported by Vorhis (1967) was recorded at sites far distant from the epicenter.

Hydroseisms caused by the San Fernando earthquake on February 9 were recorded at gaging stations and observation wells over a wide area in California, and in Arizona and Nevada. The area extends more than 500 km (kilometers) from the epicenter near San Fernando, about 40 km northwest of Los Angeles. Responses were recorded as far north as Fresno, in the middle Salinas River basin, near the Mexican border in California, and as far east as Phoenix, Ariz. Selected sites in California that are indicative of the areal extent of the seismic shock effects are shown in figure 1. The data were obtained at gaging stations and observation wells operated by the U.S. Geological Survey and by state, county, and local agencies. The cooperation of these agencies in making the data available is gratefully acknowledged.

Fluctuations recorded at selected gaging stations are listed in table 1; the location of the stations is shown in figure 1. Similar fluctuations were indicated by the charts for many stations in the San Fernando Valley, Santa Clara River basin, and adjacent basins; most of the records indicate response only to the principal shock.

TABLE 1.—*Fluctuations in water level recorded at gaging stations, February 9, 1971*

Site (fig. 1)	Stream or reservoir and station	Fluctuations recorded as double amplitude (mm)	Net change, rise (+) or fall (−) (mm)
1	San Antonio Reservoir near Bradley	60	0
2	Santa Margarita Lake near Pozo	6	0
3	Arroyo Grande at Arroyo Grande	21	0
4	Santa Ynez River near Lompoc	24	+3
5	Sandyland Bridge at slough at Carpinteria	113	0
6	Matilija Reservoir at Matilija Hot Springs	54	0
7	Sespe Creek near Fillmore	34	+6
8	Los Angeles River below Sepulveda Dam	225	0
9	Arroyo Seco near Pasadena	67	+24
10	San Gabriel River below Santa Fe Dam, near Baldwin Park	100	+6
11	Deep Creek near Hesperia	12	0
12	Mojave River at Afton	6	0
13	Santa Ana River diversion near Mentone	9	0
14	Santa Ana River below Prado Dam	46	0
15	San Jacinto River near San Jacinto	8	0
16	San Luis Rey River near Oceanside	9	0
17	Sweetwater River near Descanso	3	0

Parts of recorder charts showing hydroseisms on February 9 at three selected gaging stations are reproduced in figure 2. The record for Los Angeles River below Sepulveda Dam (site 8) shows the effects of the principal shock and at least two of the lesser shocks. The record also indicates the effect

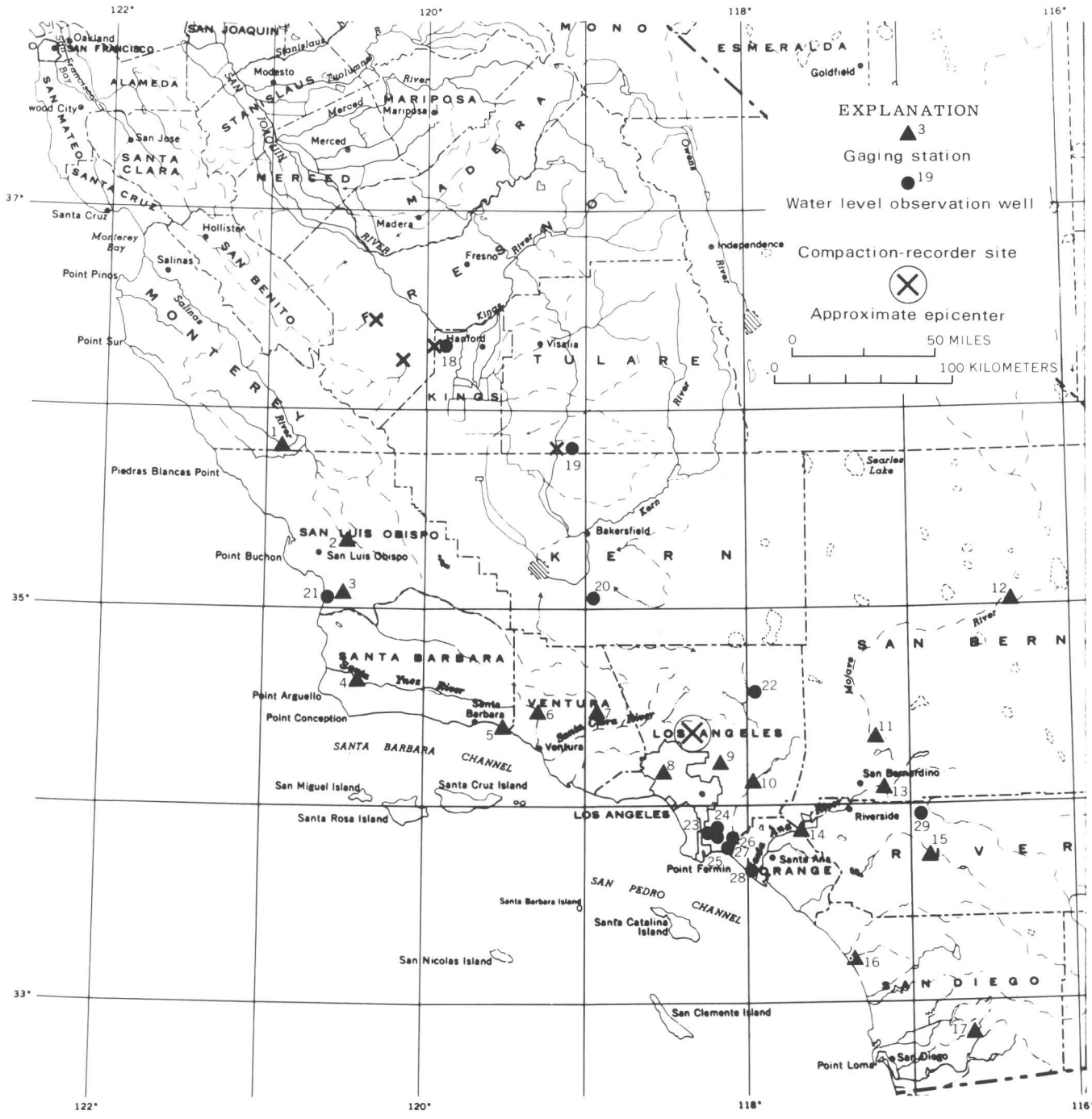

FIGURE 1.—Selected gaging stations, observation wells, and compaction-recorder sites that showed effects of the San Fernando earthquake, February 9, 1971. Gaging stations and observation wells are listed in tables 1 and 2, respectively.

of the release of water from Lower Van Norman Lake to Bull Creek and subsequent discharge to the Los Angeles River.

Change in streamflow—a common response of the water regimen to earthquakes—is indicated by the records for Arroyo Seco near Pasadena (site 9) and San Gabriel River below Santa Fe Dam, near Baldwin Park (site 10), though the changes are minor. The effect of the sequence of shocks that followed the principal seismic shock is shown by the Arroyo Seco record, and the discharge increased from 5.4 cfs (cubic feet per second), or 0.15 cubic meters

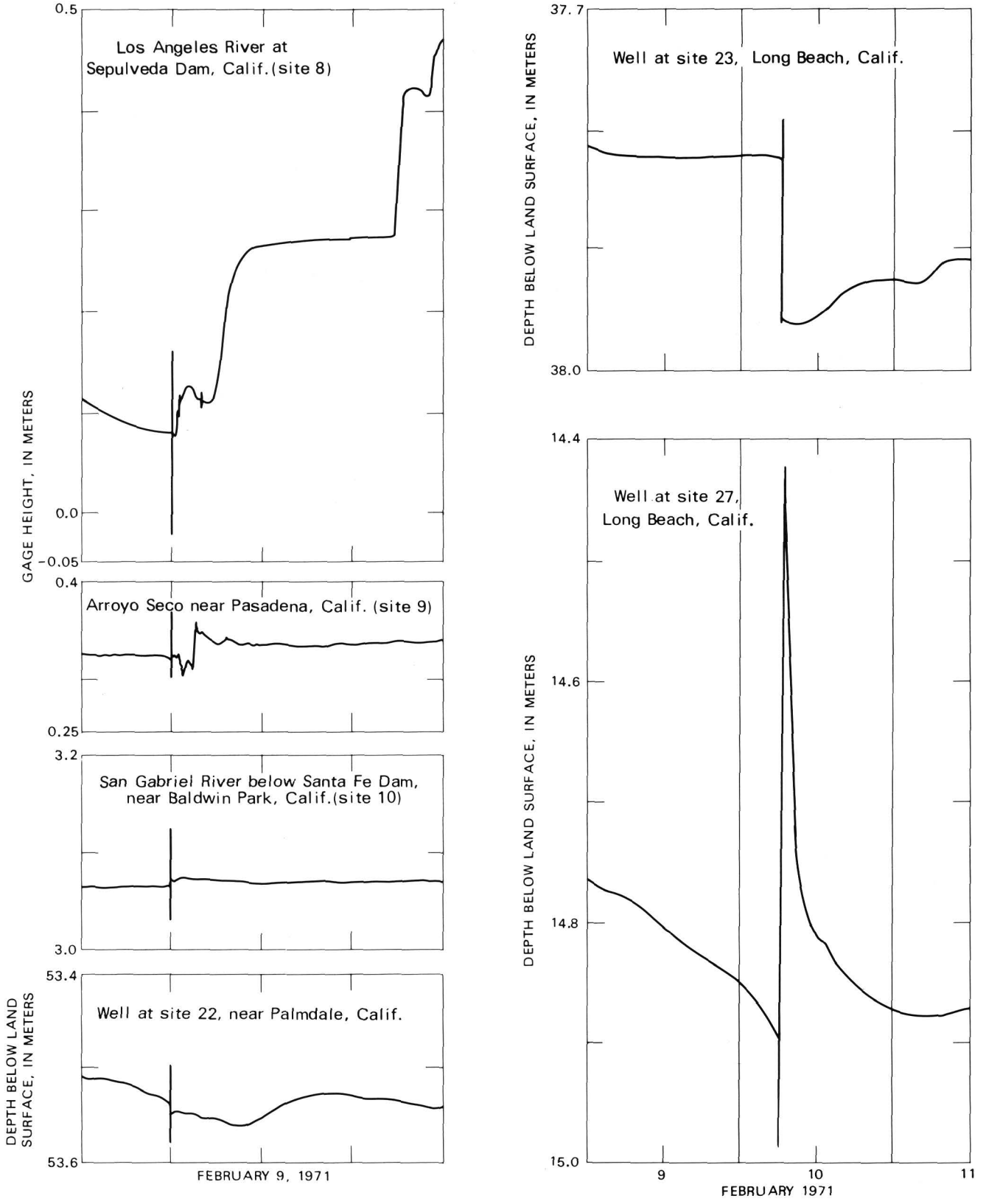

FIGURE 2.—Fluctuations recorded at selected gaging stations and observation wells in response to the San Fernando earthquake.

per second to 6.6 cfs (0.19 cubic meters per second). The San Gabriel River record reflects a minor increase in discharge. Gaging stations in the vicinity of the epicenter of the earthquake have not been accessible because of landslides and road damage; thus, the seismic effects on water flows in Pacoima Creek have not been determined.

The records for reservoirs such as San Antonio Reservoir near Bradley (site 1), Santa Margarita Lake near Pozo (site 2), and Matilija Reservoir at Matilija Hot Springs (site 6), though reflecting the principal seismic shock, do not show significant periodic water-level fluctuations (seiches). Santa Margarita Lake (Salinas Reservoir) previously had shown seiche-caused water-level fluctuations in response to the Alaskan earthquake of March 27, 1964, and the Borrego Mountain, Calif., earthquake of April 9, 1968.

Seiches, however, may be the most common surface-water effect attributable to the San Fernando earthquake. Countless swimming pools in the San Fernando Valley and in widespread adjacent areas in southern California were subjected to seiches and sloshing water. Many lost a substantial part of their contents through sloshing and spill. Pools as far away as Cypress, 30 km southeast of Los Angeles and 70 km southeast of the epicenter, were lowered as much as 30 cm (centimeters) by spill.

Abrupt and pronounced fluctuations of water levels in wells in response to the seismic shocks February 9, 1971, were shown by many recorders on observation wells. The records for several wells also demonstrated some postearthquake changes in water levels as a result of the shock. Compaction recorders in Fresno, Kings, and Tulare Counties showed movements at the approximate time of the principal shock.

Hydroseismic data for selected wells are given in table 2; the location of the wells is shown in figure 1. The wells listed are identified by both a site number and a well number. The well numbers indicate the location of wells according to the rectangular system for the subdivision of public lands. The numbers identify the township, range, section, location within the section, serial number of well in the section, and the baseline and meridian in accord with the standard practices in California and Arizona.

Parts of recorder charts showing fluctuations and water-level changes in response to the principal seismic shock at three observation wells are reproduced in figure 2. The records for the two Long Beach wells (sites 23 and 27) illustrate contrary effects, but records for other wells in the Long Beach area

TABLE 2.—*Fluctuations of water level in observation wells, February 9, 1971*

Site (fig. 1)	Well	County	Area	Depth of well below land surface (meters)	Double amplitude (mm)[1]	Net change rise (+) or fall (−) (mm)
18	18S/19E-20P1 M	Kings	Lemoore	55.23	24	−24
19	24S/26E-34F1 M	Tulare	Richgrove	62.40	152	−143
20	32S/28E-20Q1 M	Kern	Conner	48.04	140	−125
21	32S/13E-30K14 M	San Luis Obispo	Arroyo Grande	9.24	6	−6
22	6N/10W-20P1 S	Los Angeles	Palmdale	53.5	76	−9
23	4S/13W-12K1 S	do	Long Beach	37.82	174	−174
24	4S/12W-5H2 S	do	do	13.20	920	+46
25	4S/12W-21L1 S	do	do	17.13	880	−122
26	4S/12W-24M4 S	do	do	13.82	1070	+340
27	4S/12W-24M4 S	do	do	14.87	590	+150
28	6S/10W-6P S	Orange	Huntington Beach	1.5	244	−15
29	3S/1W-1N1 S	Riverside	Beaumont	107.8	85	0
—	B-2-9-7abb G	Maricopa, Ariz.	Harquahala Plains	92.7	107	−107
—	B-2-2-24cbb2 G	do	McMicken	117.4	30	0

[1] In some wells, water levels changed in one direction only.

(sites 24, 25, 26, and others) show effects that correspond with one or the other of these examples. The water-level rise of 1.07 m (meter) in the well at site 26, near Long Beach, was the greatest change observed; subsequently the level declined 0.74 m in 2 hours and an additional 0.24 m in the next 24 hours. The trace was quite similar to that for the well at site 27 (fig. 2). The well at site 22, near Palmdale, demonstrates a direct response to the principal shock and is representative of the records at many observation wells.

The most dramatic water-related effects of the seismic shocks were on hydraulic structures such as dams, reservoirs, water tanks, water mains, pipelines, and sewer facilities. Many incidents of destruction, rupture or other damage, and associated loss of water-supply services occurred in the San Fernando Valley and adjacent areas.

The Van Norman Lakes (fig. 3), a series of reservoirs at the head of the San Fernando Valley, suffered severe damage. The lakes are part of the Los Angeles Aqueduct water-supply system and provide part of the water supply to the local area.

The earthfill dams on both the Upper and the Lower Van Norman Lakes (sites A and B, fig. 3) were severely damaged by the earthquake. The dam at the upper lake moved about 2 m downstream and the crest slumped substantially. The dam on Lower Van Norman Lake, initially completed in 1918, was fractured, the crest slumped, and a large part of the upstream concrete facing of the dam slid into the reservoir. (See section by Youd and Olsen.) One of the two intake towers was destroyed. Fortunately the dam was not breached. At the time of the earthquake Lower Van Norman Lake (capacity, 20,500 acre-ft)

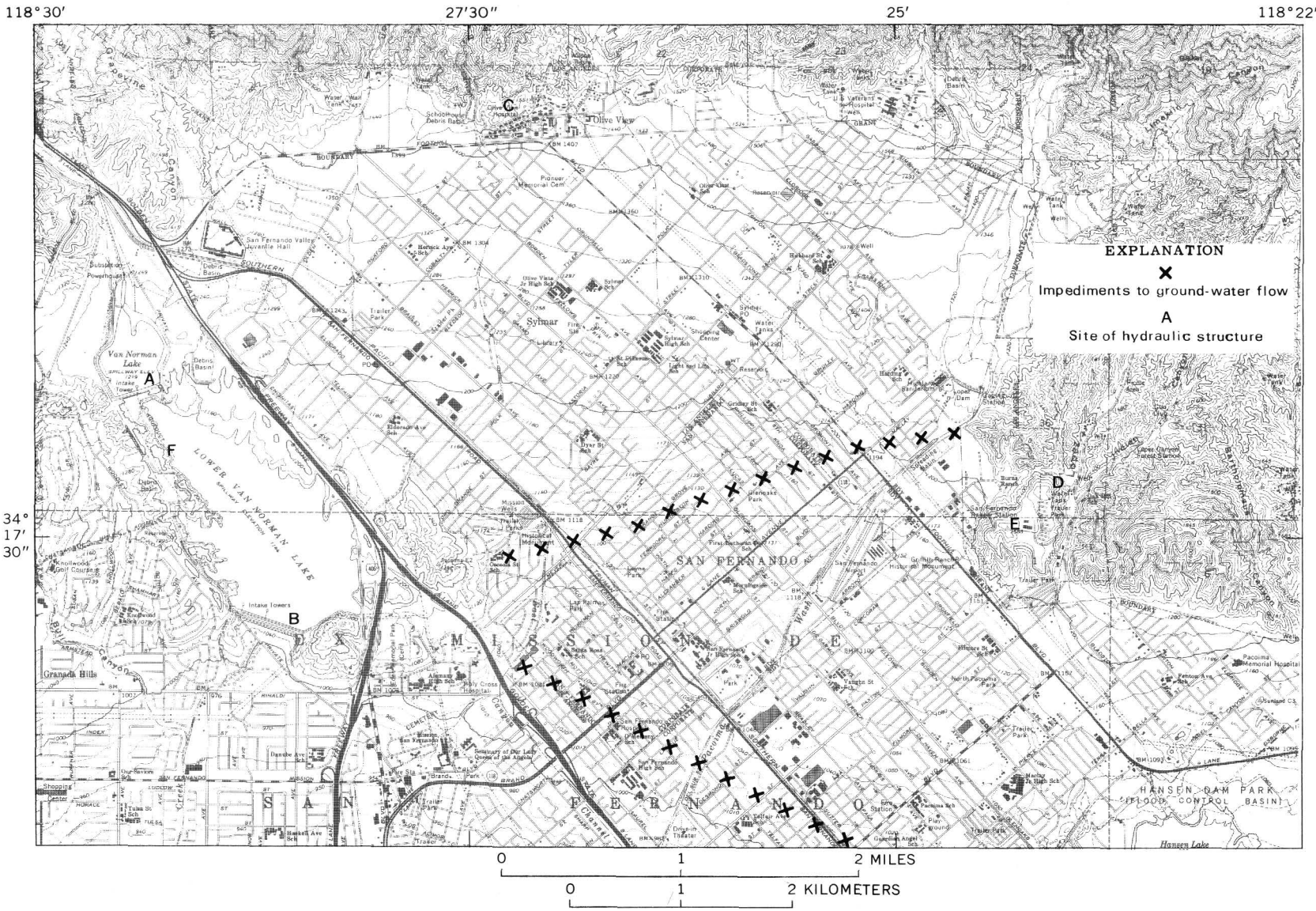

FIGURE 3.—Map showing location of hydraulic structures damaged by the San Fernando earthquake and of impediments to ground-water flow.

was being filled and contained about 11,000 acre-feet of water at a level 7.6 m below the spillway crest. A water-surface surge of 0.6 m was recorded at the time of the principal shock. The surge probably was caused by the shock, the destruction of the dam facing, and landslides near the spillway.

Prompt opening of the available discharge facilities at Lower Van Norman Dam started lake-lowering operations necessary to reduce the hazard of breaching the dam; by February 15 the levels had been lowered more than 6 m. The record for Los Angeles River below Sepulveda Dam (fig. 2), at a point 15 km downstream from Lower Van Norman Dam, illustrates the manner in which water discharged from Lower Van Norman Lake reached the Los Angeles River on February 9. Effective operations at the dam were expedited by prompt decisions by local authorities. The speedy evacuation of residents from the area downstream from Lower Van Norman Lake was based on the awareness of personnel of the city of Los Angeles of the potential extent of flooding if the dam were breached.

Other facilities of the Los Angeles Department of Water and Power also suffered heavy damage. Many water mains in the Sylmar and San Fernando areas were ruptured by the seismic shocks. The damage was particularly heavy along Foothill Boulevard (fig. 3) in the vicinity of the San Fernando fault. Damage to water-distribution facilities becomes evident readily through reduction or interruption of water service. Damage to sewer lines and systems is less obvious, however, and may not become evident for many months. Damage to two aqueducts cut off water service to nearly 10,000 homes in Los Angeles for a short period. Because of the damage to the Van Norman Lakes, the Los Angeles water supplies normally transported by the Los Angeles Aqueduct through the lakes were diverted to other reservoirs in the system after February 9.

In the city of San Fernando, damage to water wells interrupted water service to about 17,000 residents. Tanker trucks were put into service to supply basic needs pending the restoration of water-supply and distribution facilities.

Many water tanks were destroyed by the earthquake. Elevated tanks appeared to be particularly susceptible to damage. A short northwest-trending break of uncertain origin north of the Olive View Hospital at Sylmar passed under and apparently caused rupture of a large steel water tank (site C, fig. 3). An elevated water tank at a trailer park in Lopez Canyon (site D, fig. 3) was destroyed; in the process the tank was moved about 30 m northwest from its pad. The top and sides of a steel above-ground tank near the mouth of Lopez Canyon (site E, fig. 3) were severely battered by wave motion in the tank. An elevated fiberglass tank near the northwest shore of Lower Van Norman Lake (site F, fig. 3) literally exploded when it struck the ground, as shown by the shredding of the fibers. In contrast, a concrete tank set in the ground near the Sylmar Post Office (site G, fig. 3) was not damaged.

Studies of the ground-water resources of the upper San Fernando Valley by state, county, and local agencies, particularly by the California State Water Rights Board (1962) and the Los Angeles Department of Water and Power have indicated the presence of several impediments or barriers to ground-water flow. Two of these impediments are indicated in figure 3. The east-west impediment passing through the city of San Fernando closely parallels the San Fernando fault, the zone of ground rupture from the February 9 earthquake. This barrier marks the boundary between the Sylmar and San Fernando hydrologic subareas of the upper Los Angeles River valley-fill area. The investigations have indicated confined ground-water conditions in the Sylmar subarea.

Review of water-level altitudes in the Sylmar and adjacent San Fernando subareas in 1938, 1944, 1958, and 1970 indicates that changes in ground-water levels have not been great, generally less than 6 m, north of the San Fernando barrier and east of the northwest-trending barrier. Water levels on opposite sides of the barrier south of San Fernando, however, are markedly different, with the levels southwest of the barrier as much as 80-90 m lower.

Postearthquake data are being obtained by the Los Angeles Department of Water and Power as part of the regular monitoring program. These data should provide information significant to assessing the effects of the earthquake on the barriers and on ground-water flow. In the immediate postearthquake period, water-level rises could be expected in some areas following cessation of pumping as a result of power interruption and damage to wells and distribution facilities.

The quality of water in distribution systems was affected temporarily by the extensive disruption of the facilities, mains, and pipelines caused by the seismic shock combined with the rupture and damage to the mains. The sediment content of the water supplies remained high for a time following restoration of services.

Facilities of the California Water Project, notably the nearly complete Castaic Dam and powerplant,

near the epicenter of the earthquake, as well as the California Aqueduct and tunnels through the Tehachapi Mountains, experienced no damage from the shocks.

REFERENCES

California State Water Rights Board, 1962, Report of referee, city of Los Angeles vs. city of San Fernando, California Superior Court, County of Los Angeles, No. 650079: Calif. State Water Rights Board, v. 1, 258 p.

Vorhis, R. C., 1967, Hydrologic effects of the earthquake of March 27, 1964, outside Alaska: U.S. Geol. Survey Prof. Paper 544-C, 54 p.

DAMAGE TO CONSTRUCTED WORKS, ASSOCIATED WITH SOIL MOVEMENTS AND FOUNDATION FAILURES

By T. L. YOUD and H. W. OLSEN
U.S. GEOLOGICAL SURVEY

This report describes earthquake damage to dams and canals, transportation routes, utilities, and buildings in the northern San Fernando Valley that was caused by, or associated with, various types of soil movements and foundation failures. Because our reconnaissance was relatively brief and limited in scope, the information presented here is a preliminary and partial account of these types of damage.

DAMS AND CANALS

The February 9 earthquake severely damaged the Upper and Lower Van Norman Dams. The latter appeared to have been on the brink of failure, which would have created catastrophic inundation of the heavily populated area below. Eighty thousand people were forced to abandon their homes for 4 days while the water level in the reservoir was lowered to a level which would preclude flooding in case of further damage to the dam during strong aftershocks. On brief visits to the other major dams in the strongly shaken area, we observed only minor to negligible damage.

In the vicinity of the Van Norman Lakes, sections of several canals were badly damaged and rendered unusable until major repairs could be made. Several flood-control dikes also suffered slumping, but because they were not impounding water at the time of the shock, their failure presented no immediate hazard. The hydrologic effects of the shock and the disruption of water-distribution services and related facilities are discussed by Waananen in this report.

The principal damage to the Lower Van Norman Dam was a massive upstream slope failure which dislodged a major segment of the earthfill embankment and deposited it on the reservoir floor (fig 1).

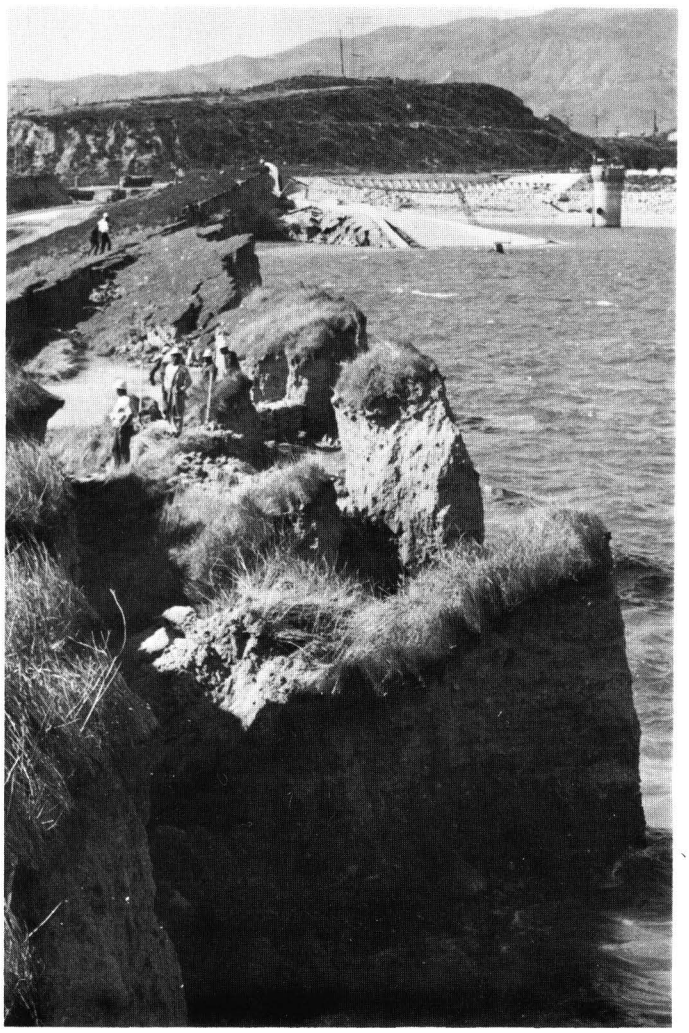

FIGURE 1.—Scarp of upstream slope failure in the Lower Van Norman Lake Dam.

The slide carried with it the upstream concrete lining and crest of the dam and moved along a rup-

ture surface which intersected the downstream face of the dam at an elevation only 1.5 meters above water level (John R. Teerink, Deputy Director, California Department of Water Resources; statement presented to the Special Investigations subcommittee of the House Committee on Public Works, in Los Angeles, Calif., on Feb. 24, 1971).

The Upper Van Norman Dam, immediately above the lower lake, subsided about 0.9 meter and shifted downstream about 1.5 meters during the shock (W. F. Hansen, Los Angeles Department of Water and Power, oral commun.). Extensive cracking and slumping disrupted the upstream concrete lining of this dam, and the downstream slope of the embankment also was cracked. The concrete lining around the Upper Van Norman Lake was cracked extensively near the high-water line.

Both the Upper and the Lower Van Norman Dams were constructed by the hydraulic-fill process. The lower dam was built in 1918 and enlarged several times since then. (Statement by J. R. Teerink cited above.) The upper dam was built in 1921. The

FIGURE 2.—Canal damage caused by the Juvenile Hall slide.

materials in the lower dam, exposed by the slope failure, are sandy in composition and distinctly layered.

A safety inspection of the Lower Van Norman Dam in 1964 led to an agreement between the State of California and the City of Los Angeles Department of Water and Power that the reservoir operations would be restricted so that the water level was maintained nearly 10 feet below normal. (Statement by J. R. Teerink cited above.) Because the quake reduced the height of the dam substantially below the previous normal water level, it is indeed fortunate that this additional margin of safety had been required.

The massive slope failure in the Lower Van Norman Dam may have been caused by seismically induced inertia forces alone or in concert with liquefaction of the embankment materials, tectonic deformation, or foundation soil failures. Tectonic deformation is considered because of the surface rupturing discovered on the Mission Hills segment of the San Fernando fault zone near the east abutment of the dam and because of the possibility that undetected movements may have extended into the vicinity of the dam. Foundation soil movements are considered because of the numerous slides observed in the reaches above the dam (Youd, this report).

Possible causes for the subsidence and downstream movement of the Upper Van Norman Dam include seismic compaction, lateral spreading of the embankment, and foundation movements associated with the landslides described by Youd (this report).

Damage to the canals in the vicinity of the Van Norman Lakes was generally in the form of cracked and broken concrete linings and displaced canal banks. In nearly all places this damage was related to slumping of the canal banks or displacement of the canal structure by an underlying landslide. For example, the lining of the canal between the Sylmar electrical-converter station and Interstate 5 was severely disrupted in the section located on the Juvenile Hall slide (Youd, this report), but suffered only minor damage beyond this area (fig. 2).

TRANSPORTATION ROUTES

Earthquake damage blocked several major transportation routes through the northern San Fernando Valley and severely disrupted many others. Interstate Highway 5 was blocked in both directions by collapsed bridges, as were also the main lines of the Southern Pacific Railroad, at the Foothill Interchange complex (fig. 3). A number of other highway bridges also collapsed or were damaged beyond use. Slope failures, subsidence at bridge approaches, and buckled and displaced pavements left other sections of freeway, main roads, and city streets disrupted in varying degrees.

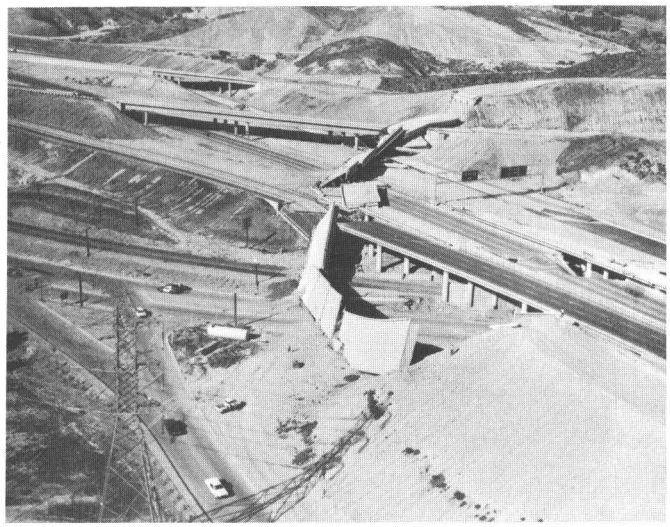

FIGURE 3.—Collapsed structures at the Foothill and Golden State Freeway interchange.

Tectonic displacements in the San Fernando fault zone were responsible for a large part of the pavement damage caused by the earthquake. Wherever structures such as roadways, curbs, and walks crossed zones of tectonic disturbance, they were cracked, buckled, or displaced. In some locations these disruptions blocked the streets; in others, where the magnitude of the tectonic displacement was less or spread over a wider zone, the pavement was cracked and distorted but posed only slight hindrance to traffic.

Thrust faulting was particularly destructive to pavements, leaving them fractured and vertically displaced at all places where fault ruptures were observed to cross them. Compression over finite zones, apparently caused by the thrust faulting, spectacularly buckled rigid pavement sections at vulnerable points and pushed walks over curbs at street intersections. Extensional cracks were common in the zones of tectonic rupture but were generally small enough to cause little hindrance to traffic; however, they will have to be repaired to protect the road base from water intrusion. Similar types of pavement damage were also produced by small gravitational downslope ground movements outside of the zones of tectonic rupture.

Landslides also caused severe highway damage. For example, in Weldon Canyon just north of the

heavily damaged Foothill interchange, a section of Foothill Boulevard located on a cut in the mountain side slipped down and blocked both northbound lanes of Interstate 5. Another landslide in a fill near the east shore of the Lower Van Norman Lake disrupted the southbound lanes of Interstate 5. The pavement was badly broken here by the landslide, and cracks extended into the fill to considerable depths—one fissure 4 meters deep was found in the embankment slope. Emergency repairs were made, and the grade was reopened to traffic within hours after the earthquake.

Where the Juvenile Hall slide crossed the Southern Pacific Railroad, San Fernando Boulevard, and Interstate 5, the rail and roadway embankments subsided appreciably in places and were laterally displaced generally more than 0.5 meter (fig. 4).

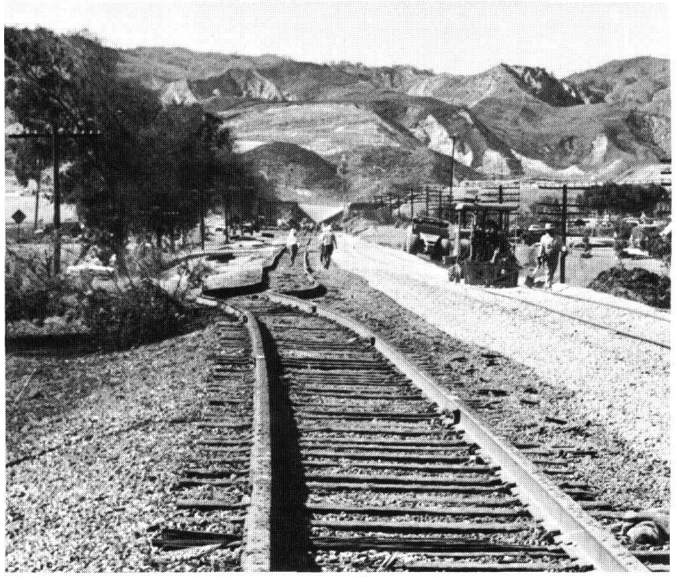

FIGURE 4.—Lateral and vertical displacement of the Southern Pacific Railroad on the Juvenile Hall slide. The lateral displacement of the rail exceeded that of the underlying embankment.

Substantial repairs had to be made to both the highways and to the railroad before normal traffic could resume.

Subsidence of the approaches to highway bridges was very common in the northern San Fernando Valley and probably resulted from seismic compaction or lateral spreading of the highway fills or underlying soils. Compaction and (or) lateral spreading also caused considerable differential subsidence in highway grades where fill sections adjoined cut sections. Examples of this type of damage were found in the Interstate 5 grade east of the Van Norman Lakes.

Seismic shaking rather than tectonic ground movement, landslides, or local bearing-capacity failures appeared to be the primary causes of the bridge damage we observed.

UTILITIES

Extensive damage was inflicted upon the telephone, power, gas, water, and sewer systems in the northern San Fernando Valley communities of Sylmar, San Fernando, and Pacoima. Buried pipelines were particularly hard hit where breaks, probably numbering in the thousands, disrupted essential services. Above-ground facilities also were damaged. It took at least 2 weeks to restore essential gas and water services throughout the area, even with the aid of temporary emergency measures.

The Sylmar electrical converter station was hard hit, with damage estimated at $28 million. This facility is particularly important because it ties southern California to the Bonneville electrical power system, and is the facility that converts the power from direct current to alternating current. The damage to this facility consisted mainly of overturned and broken elecrical equipment and ruptured underground conduits (fig. 5). Return of the facility to full service will probably take at least a year.

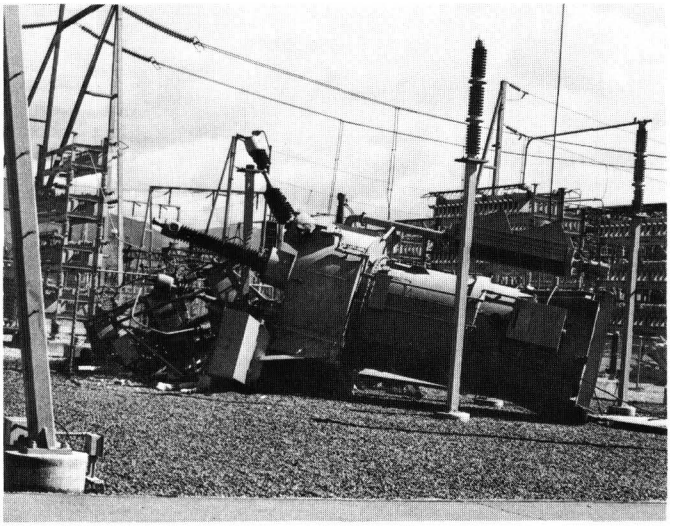

FIGURE 5.—Overturned equipment at the Sylmar electrical converter station.

A power-generating plant north of the converter facility was also heavily damaged and will likewise be out of service for some time. Substantial but less serious damage was sustained by substations, transmission poles and towers, and powerlines throughout the heavily shaken area.

The extensive damage to underground pipelines was due in large part to the location, size, and distributed nature of the surface ruptures generated by the tectonic movements in the San Fernando fault zone. The largest fault displacements had both thrust and left-lateral components. Nearly every pipeline crossing such ruptures was either fractured or badly distorted. Sketches illustrating thrust and left-lateral movements and their effects on pipelines and buildings are diagramed in figure 6. Zones of extensional cracking and zones of compression were associated with the tectonic ruptures. Extensional displacements were frequently large enough to pull apart or fracture pipelines. Displacements of this type are diagramed in figure 6D. In the compressed zones, many pipes were buckled and telescoped or thrust into manholes, commonly with relative displacements of as much as several tenths of a meter (illustrated in the section of "Surface faulting," by U.S. Geological Survey staff, this report).

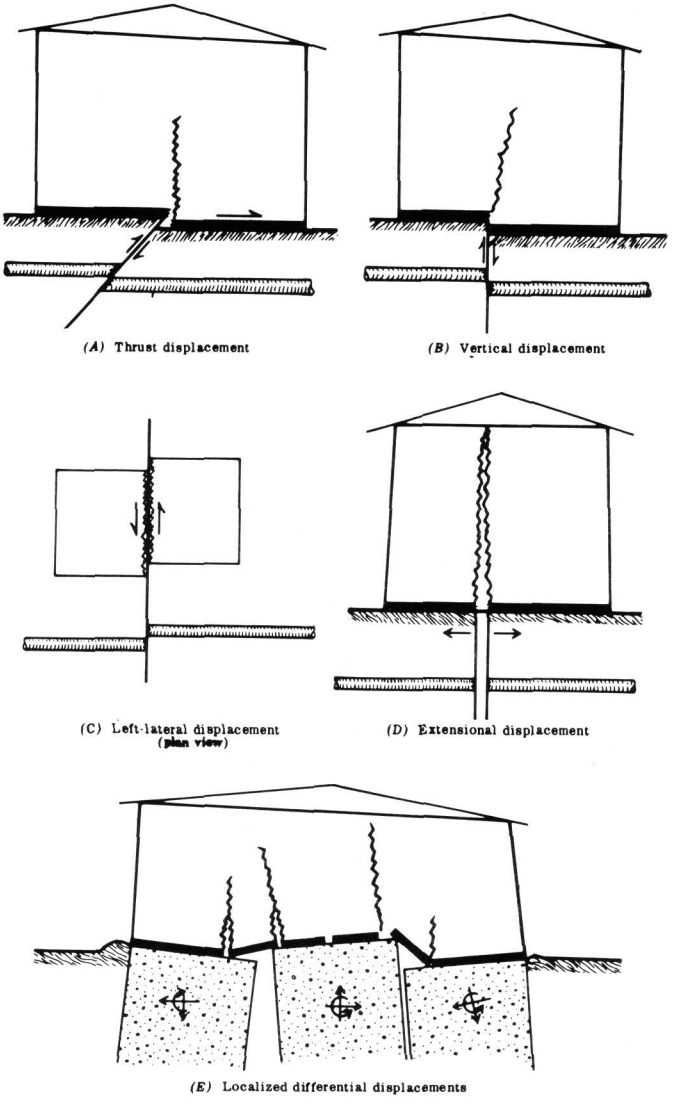

FIGURE 6.—Basic types of ground ruptures and associated pipeline and building damage in the northern San Fernando Valley.

Landslides and minor downslope gravitational movements also contributed substantially to pipeline damage. The associated differential horizontal and vertical displacements commonly marked locations of pipeline breaks. For example, several breaks were found along the margins of, at the head of, and in an area upslope from the Juvenile Hall slide. Lateral, vertical, and extensional pipe offsets were observed in these breaks, and the observed offsets were invariably consistent with the observed surface ground movements.

In the area upslope from the head of the Juvenile Hall slide, several extensional cracks, as much as 30 mm wide, were found in the vicinity of the pipeline breaks. These fissures indicate downslope movements similar to those discussed by Sharp (this report) and are probably expressions of a poorly delineated landslide.

The Sylmar electrical converter station sits astride the lower parts of the Juvenile Hall slide. Although this slide apparently caused no significant structural damage, many fissures were found within the surrounding graded yard. These fissures may have played an important part in the subsurface damage to the station.

Some pipeline breaks occurred in areas where no ground fractures were detected. Yield or fatigue fractures were detected. Yield or fatigue fractures could have caused these ruptures.

A common secondary effect of gasline and waterline breaks was disruption of the overlying surface, either by erosion from leaking water or in the form of a crater blown out by the pressurized gas. In a few places the gas was ignited, leading to spectacular fires.

Damage to overhead utilities, including telephone and power transmission lines, consisted of tightened and in some places broken wires, sagging lines, and downed or leaning poles. Shortening or lengthening of the distance between poles or towers by tectonic or landslide movements and disturbance of the pole foundations by surface rupturing appeared to be the principal causes of this type of damage.

BUILDINGS

Damage to buildings, ranging from minor cracking to total collapse, occurred throughout the Los Angeles area. But damage in the northern San Fer-

nando Valley communities of Pacoima, San Fernando, and Sylmar was by far the most severe and widespread. Major damage occurred to buildings of all types in these communities, including single- and multiple-family dwellings, light-commercial and industrial buildings, schools, and hospitals. There were no high-rise buildings in these communities. The hospitals were among the tallest buildings in the area, and their partial collapse produced most of the deaths and injuries, and the most dramatic damage of the earthquake. Part of the damage, including the collapses at the Olive View and Veterans Administration Hospitals, occurred in areas where no significant soil or foundation failures were evident.

A substantial part of the building damage observed in our reconnaissance was directly related to ground rupture beneath structures. Sketches of the basic types of ground ruptures observed, and simplified diagrams depicting the types of damage inflicted to buildings located athwart these ruptures, are illustrated in figure 6.

Almost all buildings overlying thrust faults, with or without accompanying lateral displacements, suffered severely. Figure 6*A* illustrates the type of distress such displacements induced in overlying structures. A house wrecked by a thrust fault is shown in figure 7. Commonly, buildings undercut by such rup-

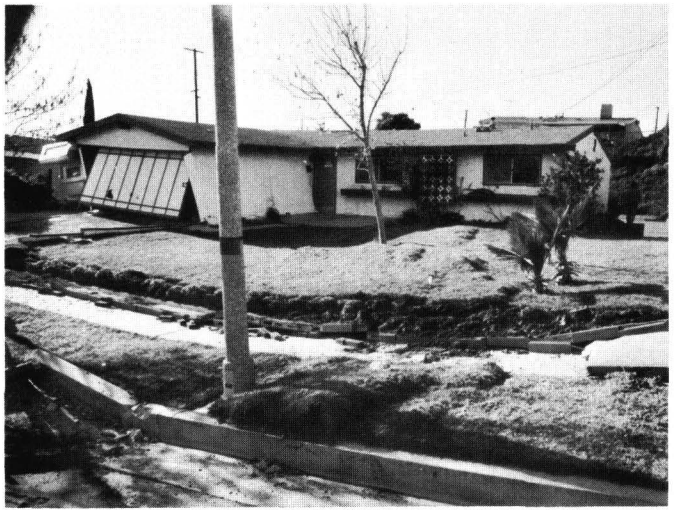

FIGURE 7.—House damaged by thrust-fault displacement.

tures were thrust horizontally, in some places being forced against adjacent buildings. (See photograph in section on "Surface faulting," by U.S. Geological Survey staff, this report.)

As previously mentioned, extensional cracks, accompanied to some degree by vertical and horizontal components of fault displacement, were common throughout the San Fernando fault zone. Similar cracks were also formed on slopes by weakly developed landslide movements. Where cracks of this character passed beneath light buildings, their foundations often fractured in tension, which in turn opened up cracks in the overlying structures (fig. 6*D*). An example of this type of damage was observed in a house on Tucker Avenue east of Rajah Street in the area sloping down toward Pacoima Wash. Downhill displacement of no more than a few tenths of a meter opened up a crack which broke through the street and walks, passed beneath the house (fig. 8), and continued on down the slope

FIGURE 8.—House damaged by tension crack.

behind. The slab foundation of the house was fractured by tension cracks as was the house itself. Damage was severe, and the house was designated as unsafe. Weakening of this house by foundation failure probably made the house more vulnerable to additional shaking damage.

The San Fernando Valley Juvenile Hall was severely damaged where it was underlain by the Juvenile Hall slide. The ground in the slide zone was ruptured in a complex manner, having components of vertical (fig. 6*B*), lateral (fig. 6*C*), and extensional (fig. 6*D*) displacement. In one part of the area, it appeared that the foundation and underlying soil had fractured into blocks which moved relative to one another in a manner illustrated by figure 6*E*. This behavior suggests that blocks of soil were temporarily supported by an underlying liquefied or partially liquefied layer. Evidence for this is the existence of sand boils nearby and the very low gradient down which the landslide moved.

SUMMARY

Soil movements and foundation failures were associated with much of the damage to structures in the northern San Fernando Valley. Tectonic movements of various kinds, including compressional (thrust), vertical, lateral, and extensional displacements, were particularly damaging to underground utilities and all types of overlying structures. Landslide movements on nearly level ground inflicted extensive damage to pipelines, canals, and light buildings such as the Juvenile Hall but caused little damage to heavier structures on massive foundations such as the principal building at the Sylmar electrical converter station. Small landslide movements in hilly areas generated minor cracks and displacements that caused heavy damage to overlying single-family dwellings. Massive landslides on steep natural slopes and constructed embankments blocked major highways at several locations, and nearly breached the Lower Van Norman Dam.

PRELIMINARY STRUCTURAL LESSONS FROM THE EARTHQUAKE

By HENRY J. DEGENKOLB
H. J. DEGENKOLB AND ASSOCIATES, ENGINEERS

It is always risky to try to anticipate lessons from a disaster before all of the data, studies, and research are available. In this particular earthquake there are certain complicating factors that may emphasize this fact. However, this very statement emphasizes one or two factors that greatly influence the structural engineer's attitude when approaching a structural design problem.

First and foremost, it is very clear that the ground motions and stability of the foundation greatly affect the performance of the structure situated thereon. It is clearly evident that certain structures situated within a very narrow band of great ground disturbance in this earthquake were affected much more than those outside of this band. There is a band, for example, going diagonally through the San Fernando Juvenile Hall, the Boy's Market at Glenoaks and Hagar, and certain industrial areas north of the San Fernando Airport where buildings of identical or similar construction were damaged much more than structures only 50 or 100 feet away. Some way must be found to locate precisely these areas of great ground deformation so that the structural engineer can either avoid these areas or provide suitable foundations so that the buildings can perform as a unit.

Secondly, there may be ground or rock configurations that will shake the superimposed structure to a greater intensity than anticipated from past records.

It is reported that the closest strong motion record of this earthquake, taken at or near the summit of a fractured rock formation, indicated ground accelerations of more than 100 percent g horizontal and 70 percent g vertical. For 12 seconds, the recurring motions were recorded at about 50 percent g. This would indicate that ground motions for even a moderate earthquake may be much greater than assumed by many engineers and that the required strength or ductility may be much greater than anticipated by many engineers and the current building codes. The very fact that such strong ground motions continued for such a long time would indicate that structural materials may have to undergo many more cycles of stress in the plastic range than many previous tests and research studies have assumed. While it may be argued that such conditions are highly unusual, many buildings, dams, bridges, towers, and so forth, may be and are located on these unusual sites and may be subjected to these extreme motions. At the very least, some method must be devised to recognize those unusual sites that are subject to such large forces for so long a time. It is interesting to note that these high concentrations of force, motion, or energy are on some form of rock rather than on saturated alluvium. They occurred with a smaller earthquake than the previous (El Centro 1940) maximum record on alluvium.

If it can be assumed that the damage caused by ground vibration as compared to ground permanent deformation would be typical or representative of the anticipated design earthquake, certain rather disturbing observations can be made even at this preliminary stage. However, these observations must be accepted with great caution, since at present there is no clear way of differentiating damage due to vibration from damage caused by permanent ground deformations.

Observation 1 concerns light industrial or warehouse structures using tilt-up concrete or reinforced masonry walls with plywood diaphragm roofs. Many walls pulled away from diaphragms at forces approximating or exceeding 100 percent g. It is not enough to rely on the plywood nailing to attach the walls to the roof diaphragm. The main framing members—girder, beams, and joists—must be anchored substantially to the walls in addition to the plywood nailing. Many roofs failed when the nails

pulled out of the diaphragms even though the plywood sheet splices were staggered.

Observation 2 concerns the horizontal reinforcing in reinforced concrete block walls. The 1952 Kern County earthquakes showed that horizontal reinforcing should not be concentrated only at foundations and bond beams but must be distributed throughout the height of the wall. Over the years this uniform distribution has been minimized to the point where only prefabricated wire ties are used at about 24 inches center to center vertically. Various failures in this last earthquake strongly indicate that this is not sufficient and that more substantial reinforcement is required, especially in stack bond construction.

Observation 3 concerns the use of frame action concrete framing (bending of beams and columns) to resist major earthquake forces. The October 1, 1969, Santa Rosa earthquake gave a preview of trouble to come when very well designed structures had large deformations causing much nonstructural damage in a comparatively small (Richter 5.6) earthquake and caused spalling in 80 percent of the columns. With the present somewhat larger (but not major or great) earthquake, the example of the Olive View Sanitarium main building and the smaller two-story building to the north, should give engineers and code-writing authorities nightmares. Even though the building remained standing, all but one of the exits were unusable, and the emergency power equipment was inoperative owing to building failure. A slightly longer earthquake with the same amplitude of motion or magnitude of accelerations would probably have caused collapse of the main structure with a greater loss of life. Some more stable method of framing must be devised.

Observation 4 concerns the use of nationally acceptable specifications for the use of structural materials. Most specifications are designed to yield certain minimum specified or reliable strengths. Strength alone is not enough in earthquake-prone areas. Both strength and ductility are required. Present specifications for concrete buildings in particular (probably also for other materials) permit details of steel reinforcing that are not appropriate in seismic areas although they are accepted in present building codes. Most California engineers use more column ties than required by national standards. The lack of sufficient column ties was probably a cause of much column disintegration as exhibited in this earthquake. Building codes must be reexamined to improve requirements relating to hooks, bonding, column ties, through reinforcing, bar laps, and other items.

Observation 5 concerns electrical and mechanical equipment. Some transformers, boilers, pumps, and panels were displaced and rendered unusable. Emergency power supplies in some cases were inoperative because of building failures. In future designs, it will be necessary to consider the effects of earthquakes on the equipment to a greater extent than at present. Equipment must be more adequately braced and anchored.

CONTRIBUTIONS FROM NATIONAL OCEANIC AND ATMOSPHERIC ADMINISTRATION, EARTHQUAKE ENGINEERING RESEARCH INSTITUTE

A PRELIMINARY REPORT OF NEAR-FIELD SEISMIC MONITORING OF THE SAN FERNANDO EARTHQUAKE AFTERSHOCK SERIES

By A. F. ESPINOSA, E. R. ENGDAHL, A. C. TARR, and S. BROCKMAN
NATIONAL OCEAN SURVEY, NATIONAL OCEANIC AND ATMOSPHERIC ADMINISTRATION

Two seismological field parties from the National Oceanic and Atmospheric Administration, National Ocean Survey, were dispatched to southern California immediately following the San Fernando earthquake of February 9, 1971 to monitor aftershock activity in the immediate vicinity of and near the epicenter. During the early morning hours of February 10, a four-man team from the Special Projects Party at Las Vegas, Nev., installed a continuously recording tripartite array (fig. 2) centered on, and at distances of 5 to 10 km from, the provisional epicenter. The total number of Special Projects Party stations was increased to 28 at the end of the first week. A three-man team from the Albuquerque Seismological Center installed five self-contained units between 20 and 35 km from the epicenter.

The instrumentation of the tripartite array consisted of two systems—a short-period vertical seismometer recording on smoked paper, and higher-gain, multilevel, three-component seismometers recording on magnetic tape. The near-field instrumentation consisted of self-contained, short-period seismometers recording on magnetic tape.

The locale of the Sen Fernando earthquake is shown in figure 1. Figure 2 is a topographic map centered on the section of the San Gabriel Mountains in which the tripartite array was deployed. The locations of the three stations were:

SCF	34°26.0′ N.	118°17.3′ W.
SGM	34°22.9′ N.	118°23.0′ W.
SHC	34°30.4′ N.	118°21.7′ W.

These stations were in operation 24 hours after the main shock. A sample smoked-paper seismogram is shown in figure 3.

Of the hundreds of aftershocks detected by these instruments, most were in the 2.0 to 3.0 magnitude range, many were larger than magnitude 3.0, and some were as small as magnitude 1.0. Aftershocks with magnitudes larger than about 3.0 show clipped amplitudes on the smoked-paper records. On the basis of the frequency of aftershocks, the zone of activity appears to be closest to station SCF. (See fig. 4.) Figure 5 depicts the decay of aftershock occurrence at station SCF; the frequency of occurrence falls quite rapidly from a maximum of 45 events per hour on February 10, and 15 events per hour on February 11, to 6 events per hour on February 15. On the basis of S-P times at station SCF, the aftershocks occurred over a range of 5 to 45 km from this station with a mode of about 15 km. Variations in signal character were clearly evident and wave frequencies ranged from 10 to 25 Hz. Variability in the sense of first motion at SCF is indicative either of the areal extent of the aftershock zone or of a change in the focal mechanism itself for individual aftershocks, or both.

Station LSM, at Little Skull Mountain, Nev., is a sensitive installation about 318 km from the aftershock zone; this station was capable of monitoring the principal aftershocks in the series. Operating gain at LSM is 2 million at 10 Hz, and 220,000 at 1.0 Hz. Figure 6 depicts the hourly counts of aftershock detection, which fell from 20 per hour at the beginning of the sequence to 4 per hour at 2400 GMT, February 10, 1971; a cumulative count for the period was 292 events.

The cooperation of the following individuals is acknowledged: W. K. Cloud, J. Hoffman, K. King, L. M. Murphy, J. Peterson, and C. Stepp of the National Ocean Survey, and C. Allen of the California Institute of Technology.

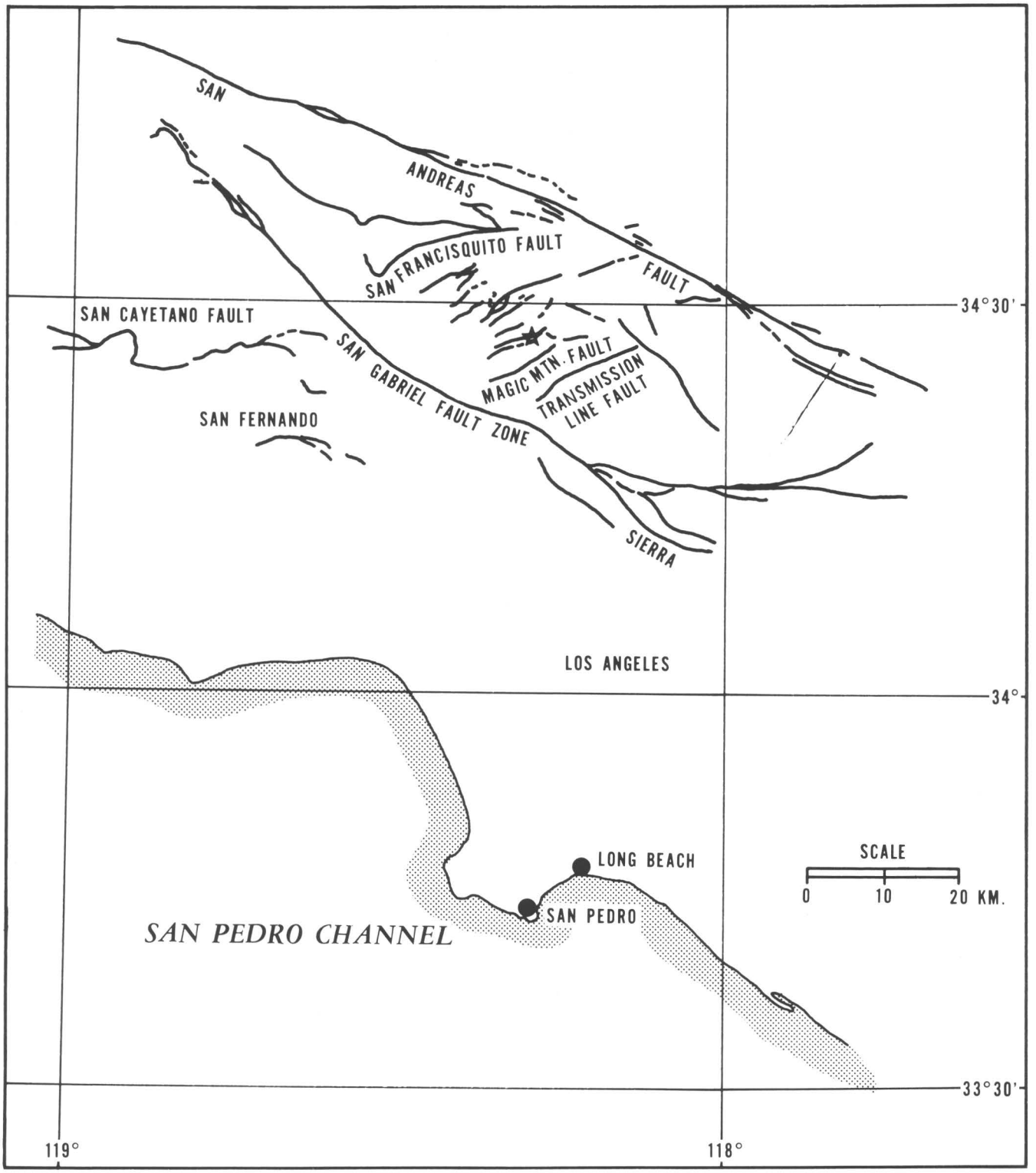

FIGURE 1.—Index map of part of Los Angeles County, showing some of the major fault systems in the epicentral area, place names, and the epicenter of the main shock (star).

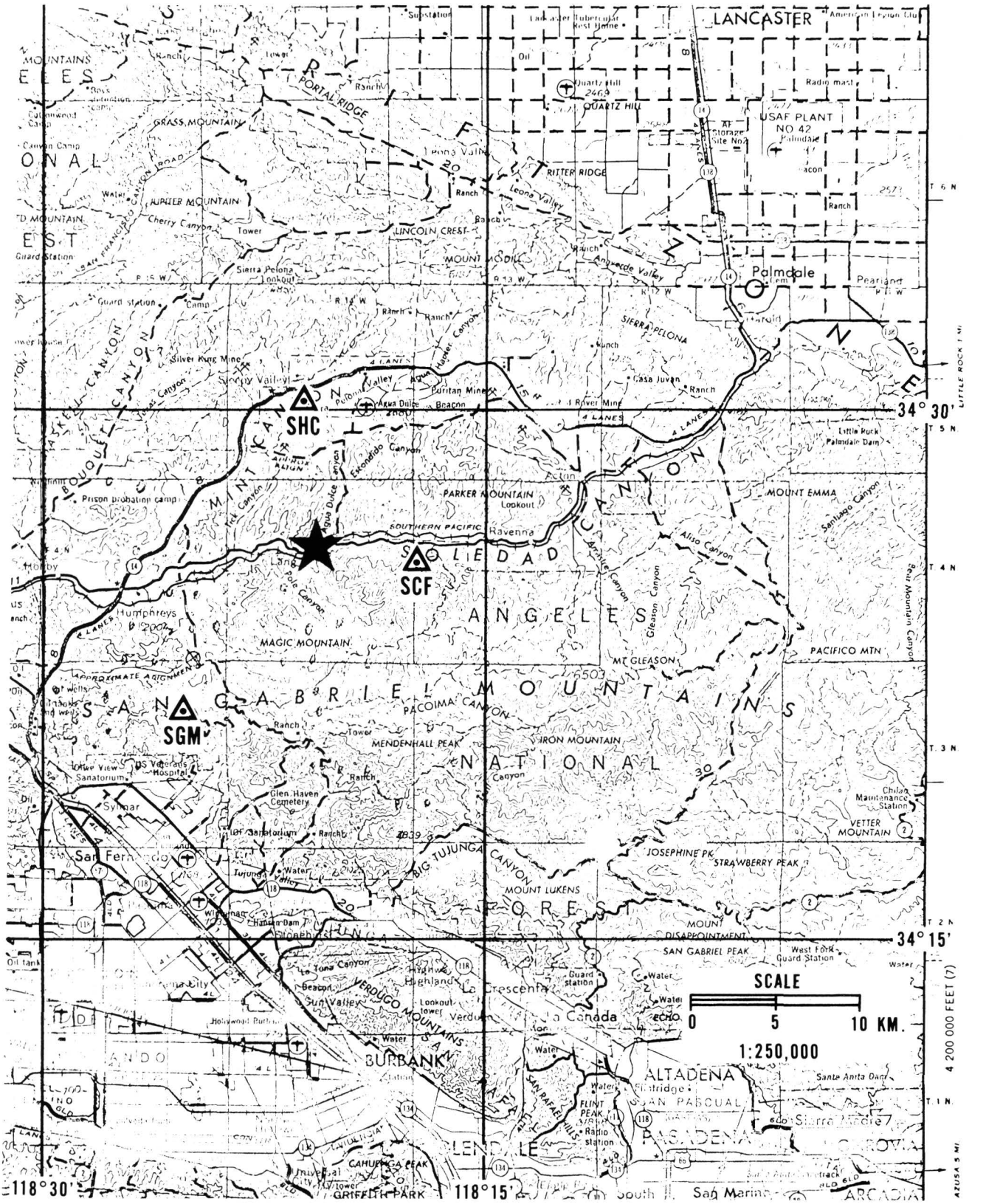

FIGURE 2.—A topographic map of San Fernando and the San Gabriel Mountains, showing the epicenter location (star). SCF, SGM, and SHC are the recording sites of the NOAA/NOS station locations.

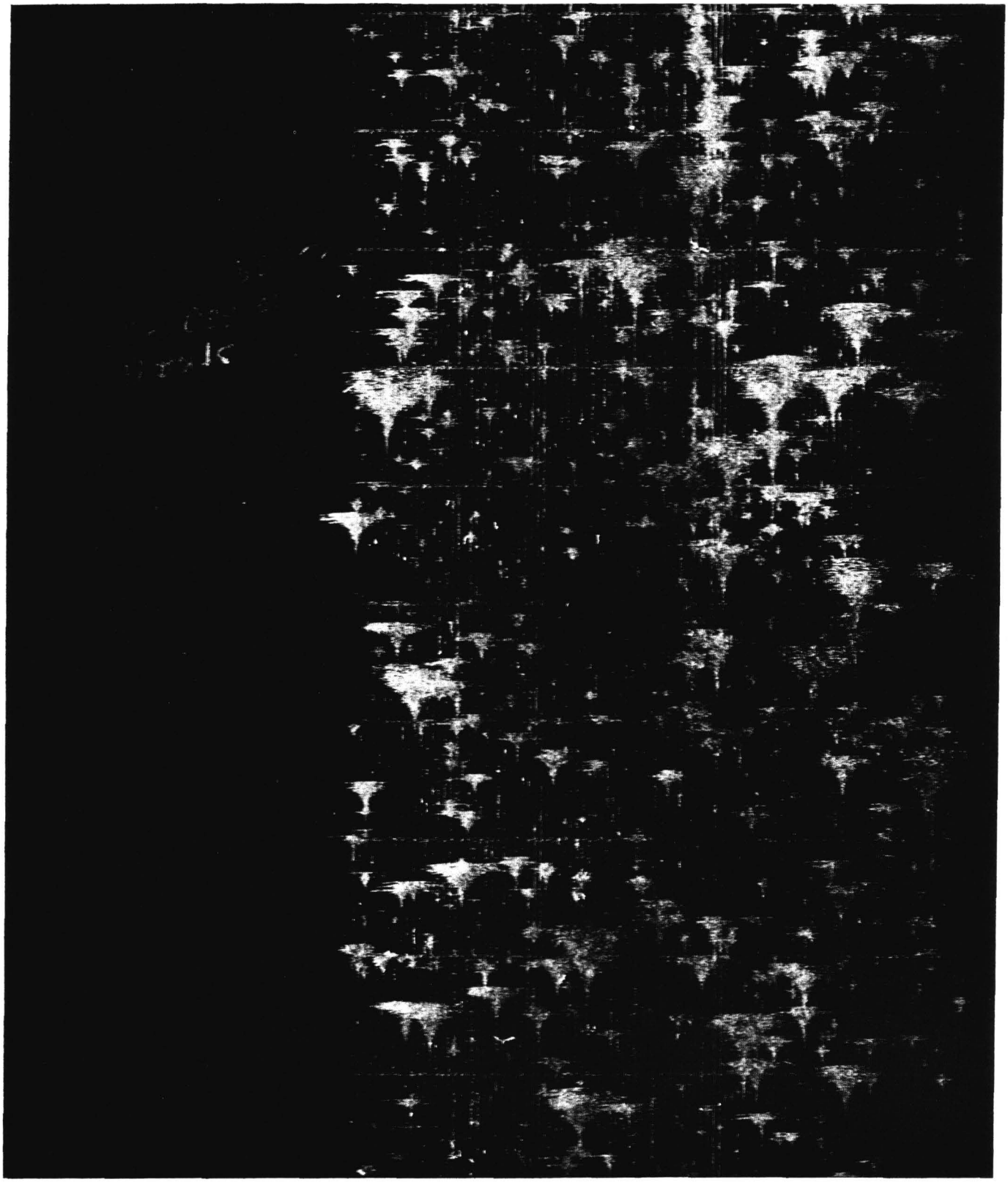

FIGURE 3.—Smoked-paper seismogram from station SCF. Installation was at 0800 GMT, February 10, 1971.

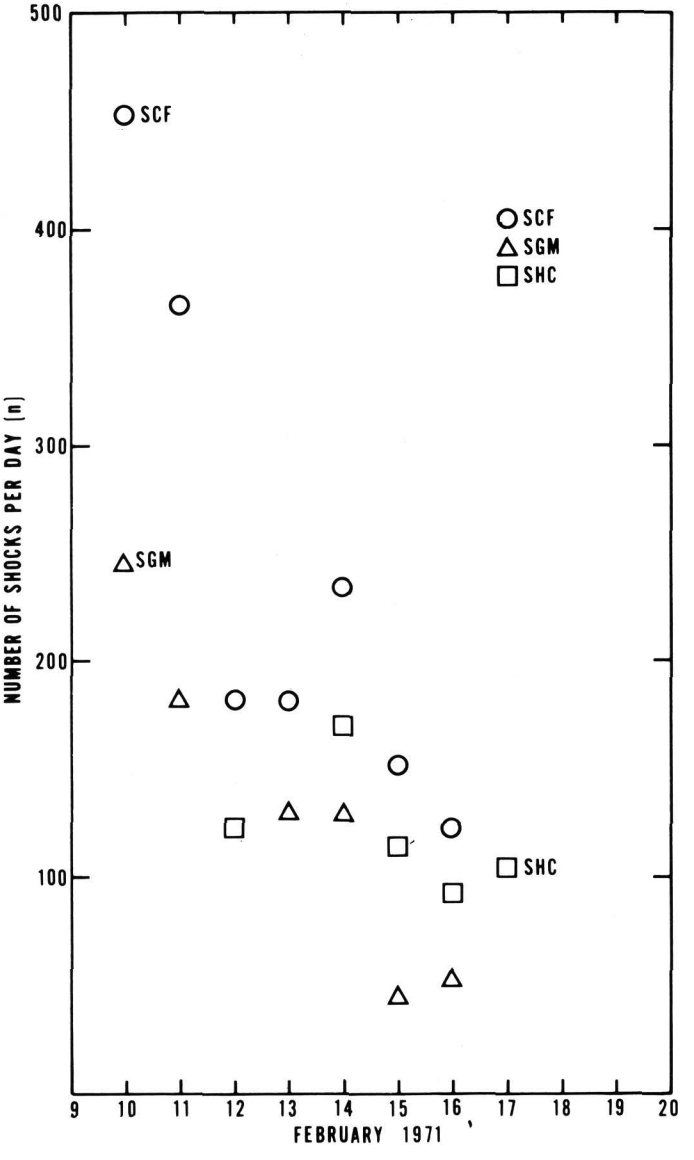

FIGURE 4.—Number of aftershocks per day, as a function of time, for the near-field stations SCF, SGM, and SHC.

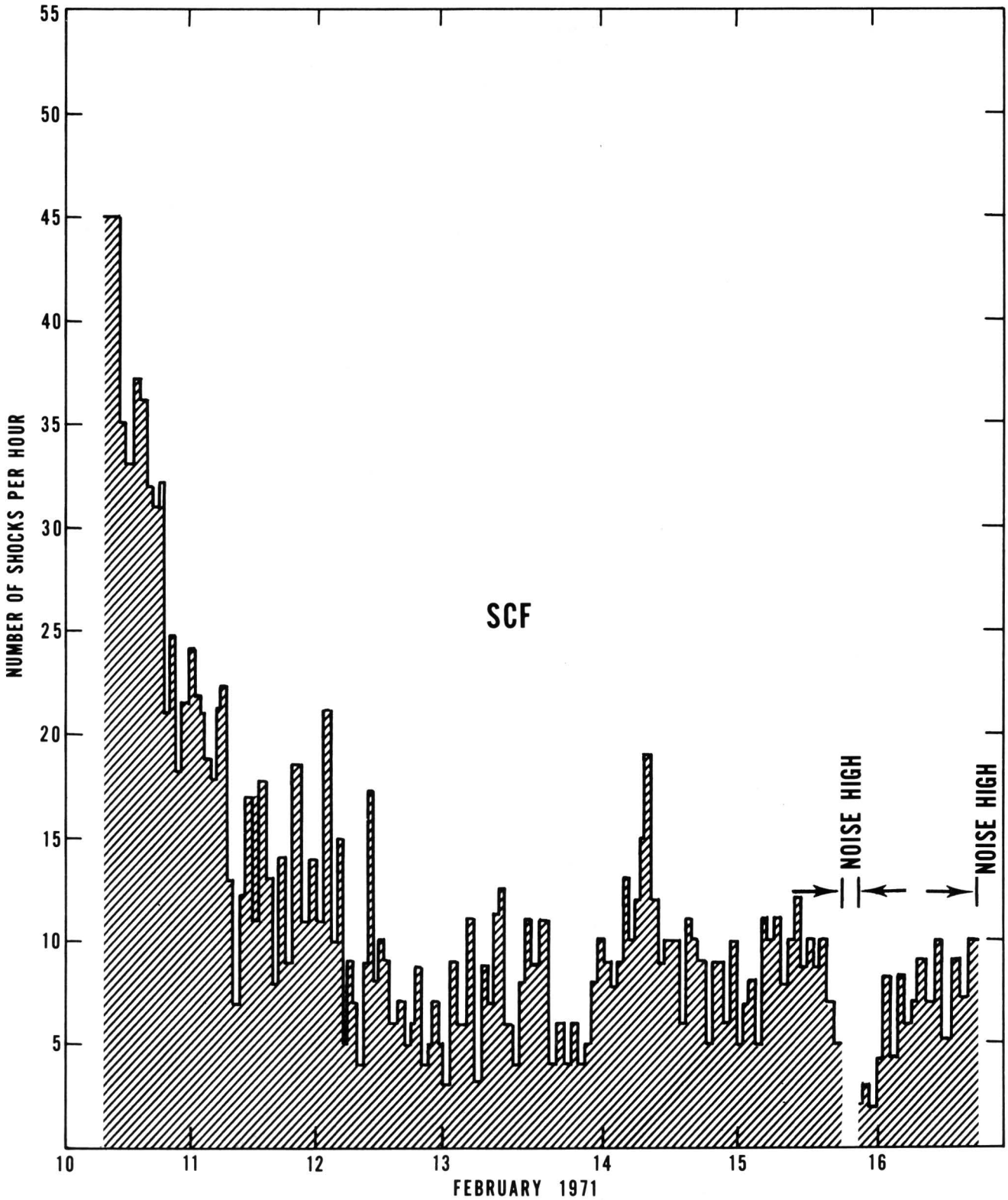

FIGURE 5.—Hourly frequency of aftershocks detected at station SCF, as a function of time (GMT).

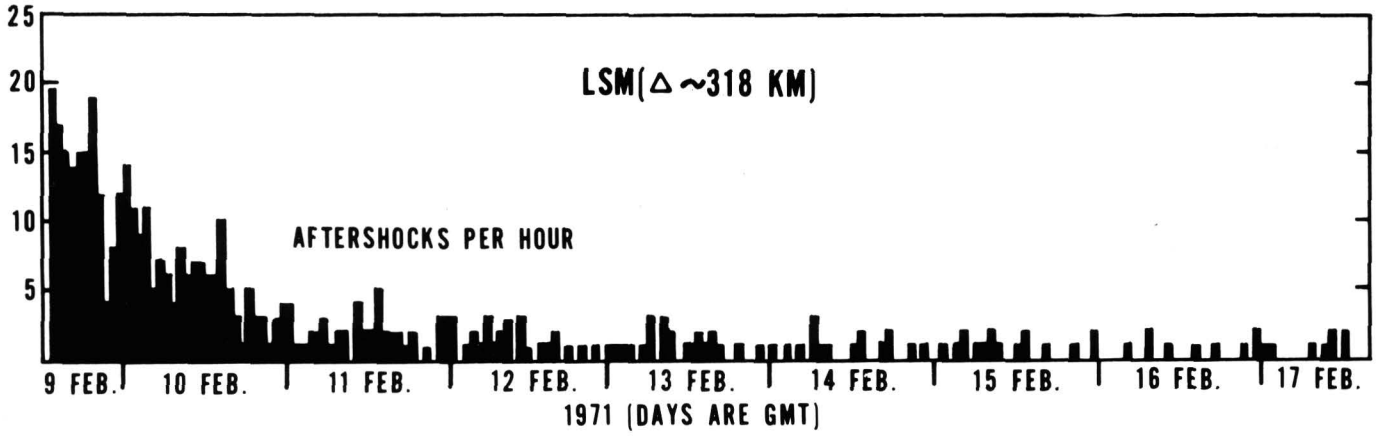

FIGURE 6.—Hourly frequency of occurrence of aftershocks, as a function of time (GMT), for station LSM, Nevada. Instrument gain at 1.0 Hz is 220,000, and at 10 Hz is approximately 2 million. Distance to the seismically active area is about 318 km.

PRELIMINARY FAULT-PLANE SOLUTION FOR THE SAN FERNANDO EARTHQUAKE

By W. DILLINGER and A. F. ESPINOSA
NATIONAL OCEAN SURVEY, NATIONAL OCEANIC AND ATMOSPHERIC ADMINISTRATION

The February 9, 1971, San Fernando earthquake, Richter magnitude 6.6, caused extensive damage in the Los Angeles and San Fernando areas. The National Ocean Survey (NOS) requested recordings for the main event from the Worldwide Network of Standard Seismographs (WWNSS) in order to evaluate the focal mechanism.

The preliminary hypocenter parameters for this earthquake, as reported to the NOS by California Institute of Technology, are:

Origin time: 14:00:41.5 GMT.
Epicenter: 34°24.0′ N. 118°23.7′ W.
Depth: 13 km.

A preliminary set of focal-mechanism solutions from P-waves recorded on short- and long-period seismograph systems is presented herein. In table 1 are listed the observed data covering an epicentral distance range from 0.3° to 134.7°. The azimuths in this table and all directions presented in this paper are measured clockwise, north through east. The last seven entries in this table are for PKP readings. The sense of motion is listed as read on the short-period (SP) and long-period (LP) recordings, and as reported by the NEIC of NOS. A quality-grading control is listed next to the SP and (or) LP sense of motion as read by NOS personnel; for instance: G=good, F=fair, P=poor, etc. The 132 short-period observations are used for the short-period solution and are plotted in an equal-area projection in figure 1. In the long-period solution, 47 observations are used, and are plotted in figure 3. Figures 1 through 4 represent the lower hemisphere of the focal sphere.

The procedure for finding the best fitting focal planes is incremental. Two orthogonal planes are incrementally rotated through three orthogonal angles to sample the focal sphere completely. For each position of the planes the number of observations in agreement with that orientation is computed as the score. The orientation of the planes which gives the highest score is selected as the best solution. These score values are then plotted at the positions of the poles of the planes and are contoured to show the approximate limits of the solution. A paper discussing these procedures was presented at the annual meeting of the Seismological Society of America in April 1969. (Focal Mechanism Determinations Using P- and S-Wave Data, by S. T. Harding, W. H. Dillinger, and A. J. Pope.)

The contours in figures 2 and 4 represent bounds on the poles of the planes. The contours that parallel the B plane limit the movement of the pole of the A plane. The contours in the vicinity of the A plane bound the pole of the B plane. If the limitation in accuracy caused by the incremental process is considered, then any pole that falls within a given contour may be selected and will give a solution which has a score represented by that contour. However, pairs of poles must be selected to give orthogonal planes. The edge of the contoured regions must be considered to be approximate owing to the incremental sampling. In the solutions presented here the increment used was 5°.

As can be seen from the solution diagrams, figures 2 and 4, the B plane is well determined by the P-wave data shown here, whereas the A plane is not. In figure 2 the inner contours represent solutions from the short-period data which have 90 percent of the observations in agreement, and the outer contours represent solutions with 88 percent agreement. These show that the pole and the strike of the A plane can vary over a range of about 60°. The dip of the A plane can vary over about 15° but not independently of the strike, as the pole of this

plane is confined to a narrow band shown by the contours parallel to the other plane.

Figures 3 and 4 show the P-wave fault-plane solution using 47 long-period observations. The solutions from these data for planes A and B are listed in table 2; however, they are only good representative samples and do not include all the possible solutions. The region of acceptable solutions is shown by the contours in figure 4. The inner contours show the approximate boundaries for solutions with 47 consistent observations. The outer contour is the approximate boundary for solutions which give 46 consistent observations from a total of 47.

Inspection of the long-period data and of the contours plotted for that solution shows that a plane striking 90° and dipping southward will also satisfy the data with all stations consistent.

The short-period data yield two solutions with 119 consistent observations from a total of 132. These results are as follows:

A plane			B plane		
Strike degrees	Dip degrees	Dip direction degrees	Strike degrees	Dip degrees	Dip direction degrees
120.0	40.0	210.0	120.0	50.0	30.0
90.48	43.96	180.48	120.0	50.0	30.0

The above discussion and the accompanying diagrams clearly show the limits of the solutions and the possible alternate solutions. The long- and short-period data available are generally in good agreement.

The direction of maximum shear obtained from geodetic surveys indicates an east-west direction near the Santa Susanna Fault and the Van Norman Reservoir. The maximum shear near Newhall has a northwest direction, which is close to the San Gabriel Fault. (See section by C. A. Whitten, this volume.) The B plane discussed in this paper is well determined and generally agrees with the strike directions of the San Gabriel Fault and the direction of maximum shear noted above. If an east-west plane is selected from those possible solutions given by our data, then it will be in agreement with the maximum shear direction in the vicinity of the Reservoir geodetic control station.

A tentative interpretation of the information currently available in our offices would seem to favor the preliminary short-period P-wave solutions, with an east-west strike and a plane dipping toward the south. This preferred solution is consistent with the long-period P-wave data and is shown pictorially in figure 5. However, the contours in figures 2 and 4 indicate that many interpretations are possible, and, indeed, the advantage of the contours is to show the various interpretations which will fit the data.

The results presented in this short note are subject to additional interpretation as further information becomes available and as the S-wave data are incorporated in the final fault-plane analysis.

ACKNOWLEDGMENTS

We are grateful to the Canadian, WWNSS, and the directors of the cooperating seismological stations who made their seismograms available for this study. The following also gave support for this report: L. M. Murphy, S. T. Algermissen, W. V. Person, E. R. Engdahl, G. J. Dunphy, R. Hansen, R. Robertson, and the Operating Branch of NOAA Computing Division.

TABLE 1.—*Observed data*

STA	Sense of motion					Delta degrees	Azimuth degrees	Focal angle degrees
	SP		LP		NEIC			
MWC					C	.3	121.1	96.33
PAS					D	.3	143.0	96.33
BLG					D	.6	243.5	88.7
ISA					D	1.3	356.7	56.7
SYP					C	1.3	276.4	56.8
GSC	C				D	1.6	54.6	56.7
LAC	C	G			C	1.6	89.4	56.7
PLM					C	1.6	128.6	56.7
PKF					C	2.2	312.4	56.6
PRI					D	2.6	313.8	56.7
BTY					C	2.8	27.5	56.6
MCV					D	2.9	40.3	56.5
SMN					C	3.0	25.2	56.5
CPX	C	G				3.1	36.1	56.5
BCN	D	G				3.3	60.4	56.1
GLA					C	3.3	113.2	56.1
SLD					D	3.5	320.1	56.1
TNP	D					3.8	14.0	56.1
TPH					C	3.8	14.0	56.4
JAS	D				D	3.9	335.5	56.1
MHC					C	4.0	319.0	56.1
MNV	D	G			D	4.0	2.6	56.4
MDC					C	4.5	321.6	56.1
BRK					C	4.7	319.0	56.0
OLC					C	5.1	316.9	55.5
KNB	D	G				5.2	58.3	55.5
NRR	D					5.3	347.7	55.5
REN			D			5.3	347.9	55.5
EUR					C	5.4	20.1	55.5
MMA			C	F	C	5.4	97.0	55.5
ORV			C	PF	C	5.7	335.1	55.5
BMN	D					6.1	8.4	55.7
GCA	D	PF				6.1	63.0	55.7
MIN					C	6.5	337.6	55.5
EKO	D					6.7	17.1	55.4
TUC			C	G		6.7	105.9	55.4
ELK	D	G			D	6.8	20.6	55.3
DUG	D	VG	D	VG	C	7.3	35.8	55.0
FHC					C	7.7	326.9	54.7
UBO	D	G	D	G		9.2	47.2	53.9
ALQ			C	G		9.8	83.4	53.6
BMO	D	VG				10.5	4.2	53.2
COR					D	10.9	341.0	53.0

TABLE 1.—*Observed data*—continued

STA	Sense of motion SP		Sense of motion LP		NEIC	Delta degrees	Azimuth degrees	Focal angle degrees
GOL	D	P	D	VG	D	11.7	59.2	52.5
DEN	D	P	D	VG		11.9	59.3	52.1
NEW	C	?	D	VG		13.9	3.5	50.3
HHM	D					14.3	11.8	50.1
NTI	C	?				14.3	3.8	50.1
VIC	D	P	D	G		14.6	346.6	49.9
LAO					D	15.4	33.2	49.7
JCT	C	G	C	G		16.2	98.8	48.2
SES	C	G	D	G	C	16.9	16.3	47.5
DAL	C	P	D	VG	C	18.1	88.8	47.7
FAY	C					19.8	78.1	40.6
FSJ					C	20.5	350.1	37.5
SLM	C	G	C	VG		23.0	71.1	34.9
DBQ	C	VG	C	VG		23.1	61.2	35.0
FFC	C	G	C	VG		23.4	24.4	34.5
OXF					C	23.9	81.4	34.5
NOL	C	P				24.3	92.6	34.8
CHI	C	G				25.2	63.6	33.5
LHC	D	G	C	VG		25.7	48.2	33.3
SHA	C	P	C	G		25.7	89.7	33.1
CPO	C	F				26.8	77.9	32.4
MLF	C	P				27.6	70.1	32.1
ATL	C	F	C	G		28.2	82.2	31.7
YKC	C	G	C	VG		28.2	3.8	31.7
FCC	C	G	C	G		29.2	26.0	31.9
CLE	C	F	C	VP		29.8	65.2	31.5
BLA	C	G	C	G		30.8	73.6	30.9
MRG					C	31.0	68.8	30.9
SCB			C	VG		31.6	61.0	30.9
KDC	D	F				32.7	326.1	30.5
BLC					C	32.9	17.7	30.5
LPS					C	33.1	119.9	30.7
WSC	C	G				33.2	69.7	30.7
GEO			C		C	33.3	69.9	30.6
PMR	C		C	G		33.5	333.7	30.5
OTT	C	G	C	VG	C	34.2	58.2	30.3
GWC					C	34.9	40.6	30.0
INK					C	35.0	350.7	30.1
COL			C	G		35.3	338.7	29.8
MNT					C	35.6	58.1	29.7
HVO					C	35.9	255.0	29.6
KIP	C	G	C	PF		37.1	260.1	29.4
BNH	C					37.3	59.7	29.4
WES	C		C	G		37.4	63.4	29.4
SFA	C	G	C	VG	C	37.6	55.6	29.4
GMA	C					40.1	333.8	28.9
SCH	C	VG			C	40.9	43.8	28.6
MBC					C	41.9	359.6	28.6
RES	C	G	C	VG	C	42.0	9.1	28.6
FBC	C	G	C	G	C	42.2	30.4	28.7
BHP	C	F	C	G	C	43.7	116.1	28.2
BEC			C	G		44.5	76.8	28.3
ADK	C					44.7	311.4	28.1
SJG	C	G	C	G	C	49.1	95.4	26.9
STJ	C	G	C	G	C	49.9	53.8	26.6
QUI					C	50.8	124.1	26.2
ALE	C	G	C	G	C	51.8	7.9	26.3
CAR					C	52.5	104.2	26.0
MDZ					C	52.5	104.0	26.0
CUM					C	54.4	102.1	25.3

TABLE 1.—*Observed data*—continued

STA	Sense of motion SP		Sense of motion LP		NEIC	Delta degrees	Azimuth degrees	Focal angle degrees
NOR					C	57.9	9.7	23.8
KTG					C	60.1	22.7	23.5
ARE					C	67.4	130.6	21.6
PNS					C	69.2	128.1	21.0
LPB					C	69.6	128.0	20.8
TRO	C					71.7	14.4	20.4
KEV	C	VG	C	VG		73.1	11.9	19.9
VAL	C	VG	C	VG		73.6	37.8	19.9
SOD	C	P				75.2	13.2	19.5
CPP					C	76.4	137.1	19.1
KJN	C	F	C	VG		78.2	14.4	18.7
UPP					C	79.3	20.8	18.4
NUR	C	G	C	VG		80.7	17.5	17.9
PEL					C	80.7	141.0	17.9
DBN					C	80.8	31.3	17.9
COP	C	G	C	G	C	81.0	25.7	17.8
PTO	C	G	C	VG		81.0	46.0	17.8
UCC	C	G	C	G		81.3	32.6	17.7
KRL					C	84.4	31.9	17.0
TOL					C	84.4	44.7	17.0
BUH					C	84.6	32.3	16.9
GRF					C	85.1	30.1	17.0
PRU					C	86.2	28.2	16.7
FUR					D	86.3	31.0	16.7
KHC					C	86.5	29.2	16.6
IFR					C	87.9	50.1	16.1
HNR	C	VG	C	VG	C	88.5	257.6	16.2
TRI					C	89.3	31.3	16.0
CMP					C	94.1	24.9	15.6
ESA					C	96.1	262.4	15.4
ANP					C	97.9	307.6	15.2
ATH					C	99.9	29.5	15.7
DAR	C	P				114.0	271.1	6.2
ASP					C	117.0	258.7	6.3
BNG					D	124.1	55.2	6.3
POO					C	126.1	345.5	6.2
KLG					C	130.1	256.5	6.3
MEK					D	130.9	262.8	6.3
MUN					D	134.7	257.0	6.3

TABLE 2.—*P-wave fault plane solutions long period data*

A			B		
Strike degrees	Dip degrees	Direction maximum dip degrees	Strike degrees	Dip degrees	Direction maximum dip degrees
120.0	40.0	210.0	120.0	50.0	30.0
160.0	50.0	250.0	118.07	48.44	28.07
180.0	60.0	270.0	116.57	52.24	26.57
145.0	45.0	235.0	117.76	48:36	27.76
152.55	51.13	242.55	120.0	50.0	30.0

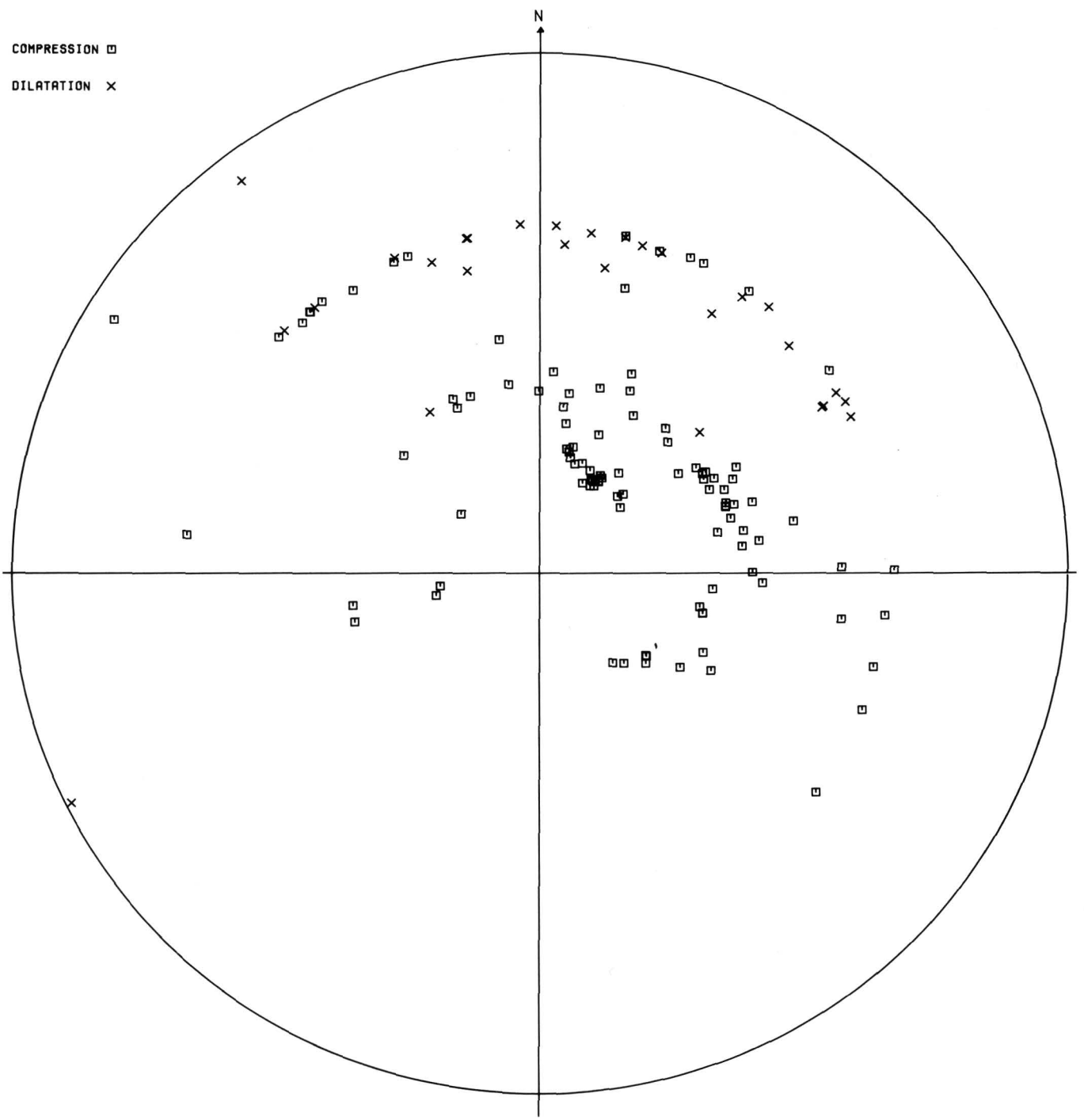

FIGURE 1.—P-wave sense of motion for the San Fernando earthquake short-period data.

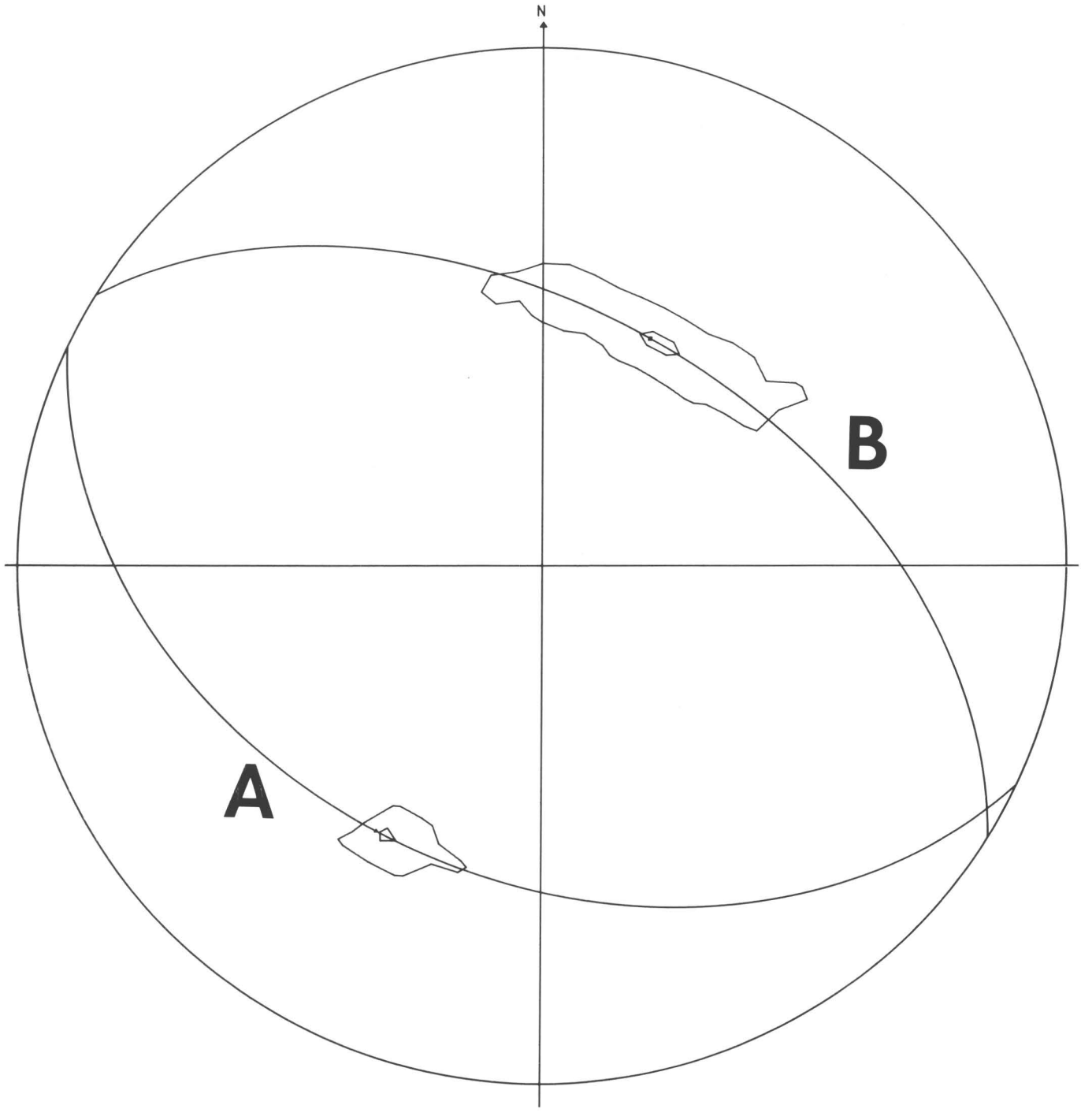

FIGURE 2.—Lower hemisphere of focal sphere. Fault plane solution from P-wave short-period observations.

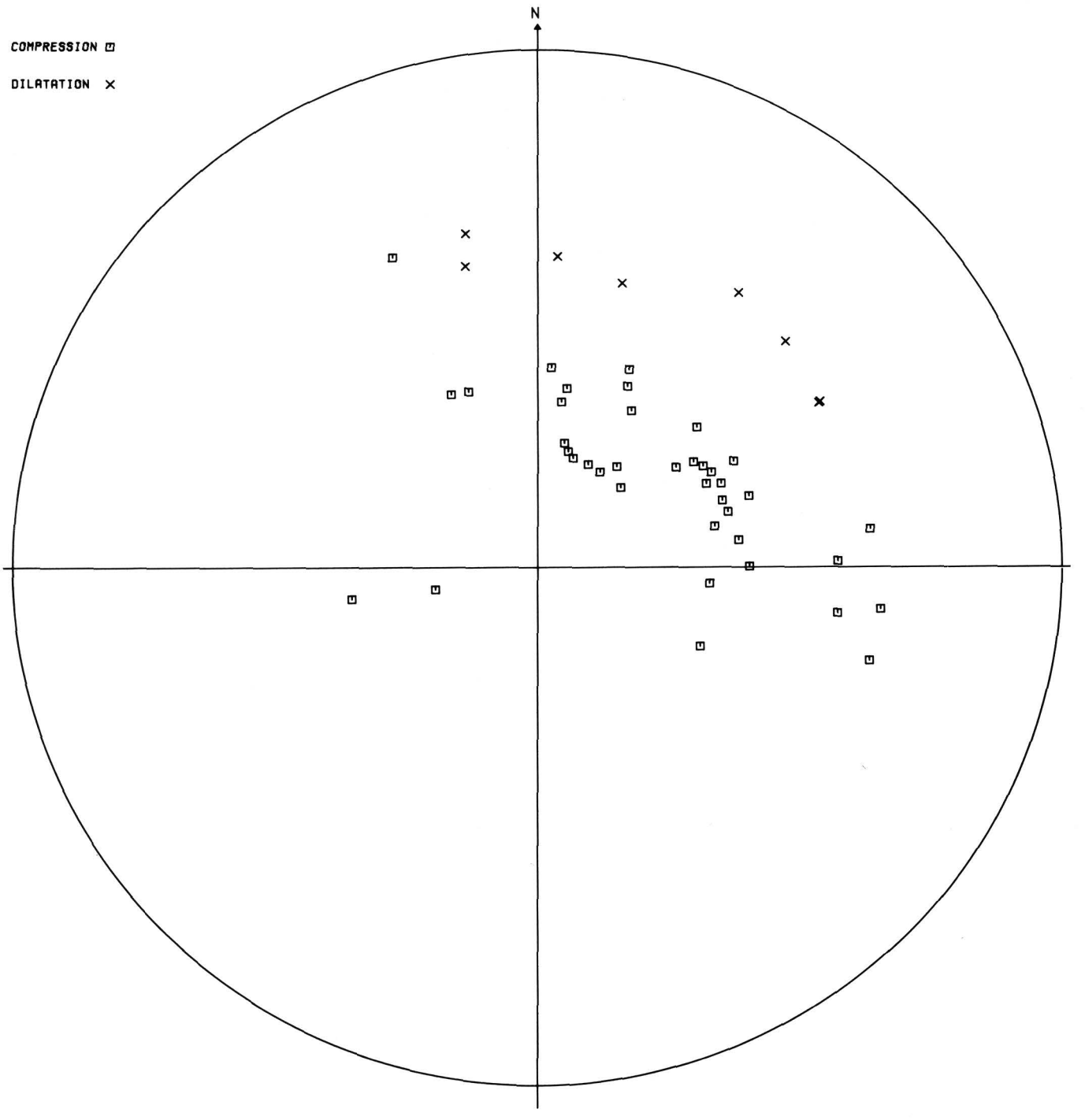

FIGURE 3.—P-wave sense of motion, long-period observations.

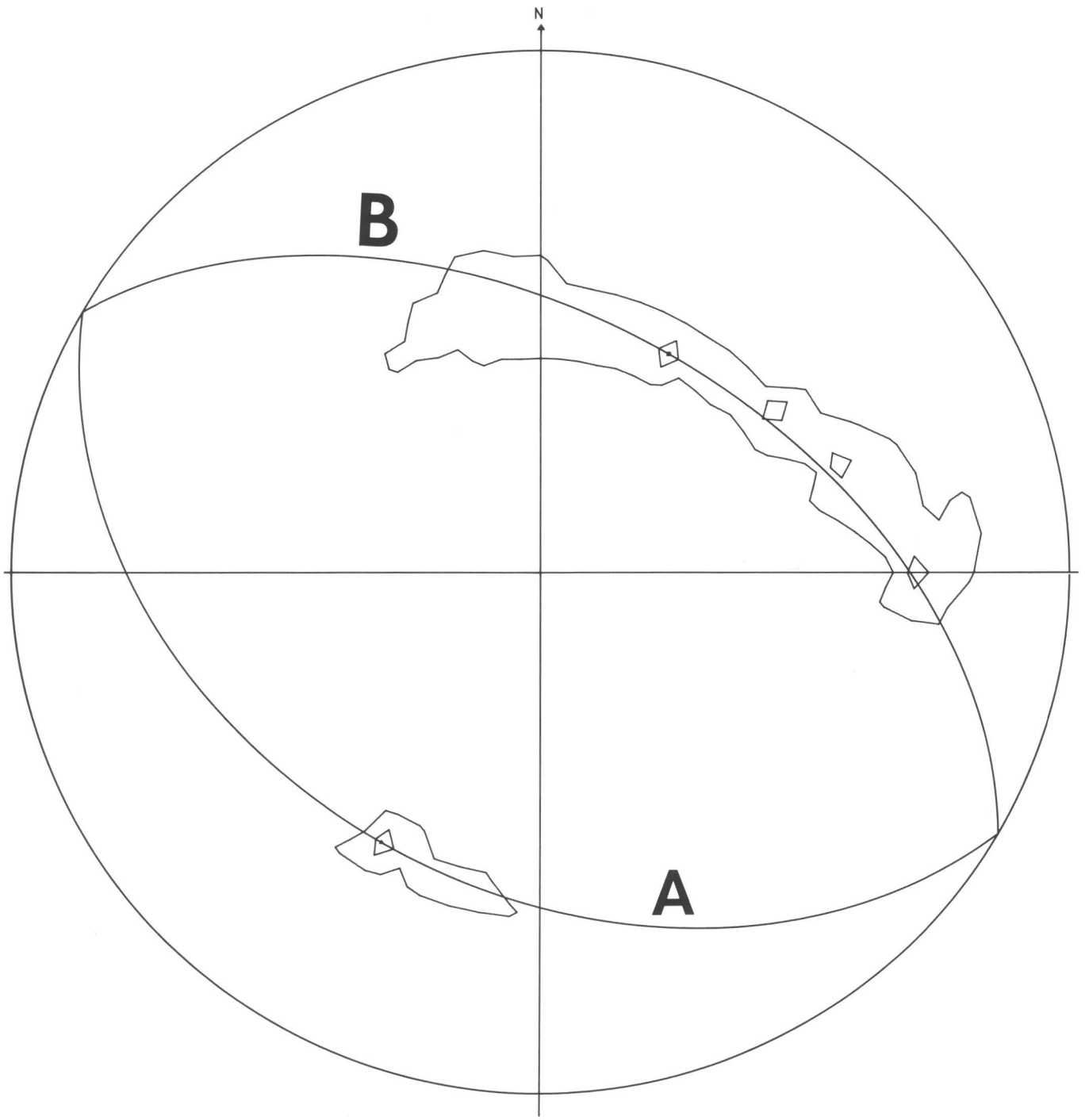

FIGURE 4.—Lower hemisphere of focal sphere. Fault plane solution from P-wave long-period observations.

FIGURE 5.—Perspective view of epicenter location and preliminary fault planes.

SOME OBSERVATIONS OF THE SAN FERNANDO, CALIFORNIA EARTHQUAKE WITH A LASER STRAIN METER

By JON BERGER
INSTITUTE OF GEOPHYSICS AND PLANETARY PHYSICS, UNIVERSITY OF CALIFORNIA, SAN DIEGO

A digital interferometeric laser strain meter has been operating on the surface at the Camp Elliott Geophysical Observatory of the University of California, San Diego, for the past 18 months. The device has a least count strain (LCS) of 4×10^{-10}, a frequency response that is flat from DC to 1 mHz

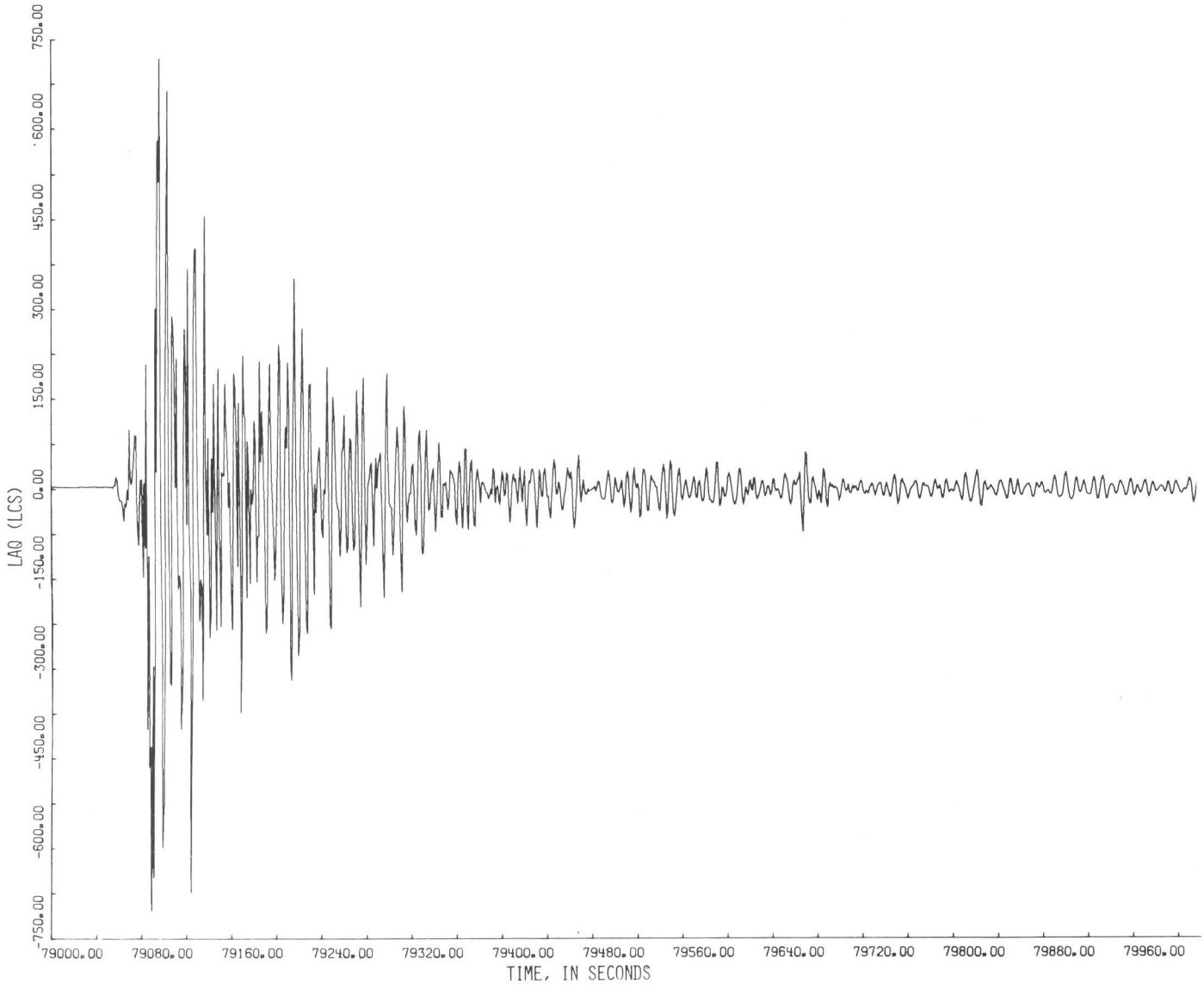

FIGURE 1.—A section of the record from the San Fernando earthquake. Strain is measured in units of least

and a dynamic range of better than 10^5 (i.e., it will accommodate relative motion of the two ends of a few centimeters). The estimated long-term stability is better than ± 1 LCS/month. These features make this instrument useful for recording both secular strain rates and seismic events.

The output from the digital fringe counter is recorded at one sample/second on magnetic tape. Figure 1 shows a section of the record from the San Fernando earthquake. The peak dynamic strains recorded were 6×10^{-7}, which occurred at a period of 8.6 seconds. The angle from the strainmeter direction to the epicenter is approximately 82°, and hence the sensitivity is near a minimum for both longitudinal and transverse waves.

In figure 2, 6 hours of data around the earthquake time have been lowpassed through a zero phase shift digital filter with a cut-off frequency of 2×10^{-3} Hz. The general concave appearance of data is due to the earth's tide. A clearly apparent offset occurred at the time of the earthquake in the source of compression and of a magnitude of 1.6×10^{-9}. Further examination of data from an extended period revealed a change in the secular strain rate from 4×10^{-9}/day to 8×10^{-9}/day at the time of the earthquake ± 8 hours. Changes in the secular strain rate of this magnitude, not coincident with earthquakes, have been observed before but such a sudden change is not normal.

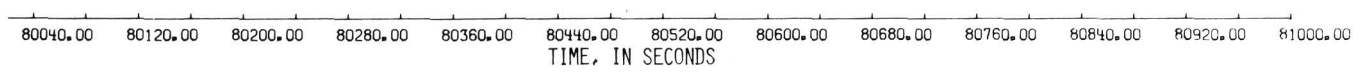

count strain (LCS). One LCS equals $4X10^{-10}$. Time is referred arbitrarily to the beginning of magnetic tape.

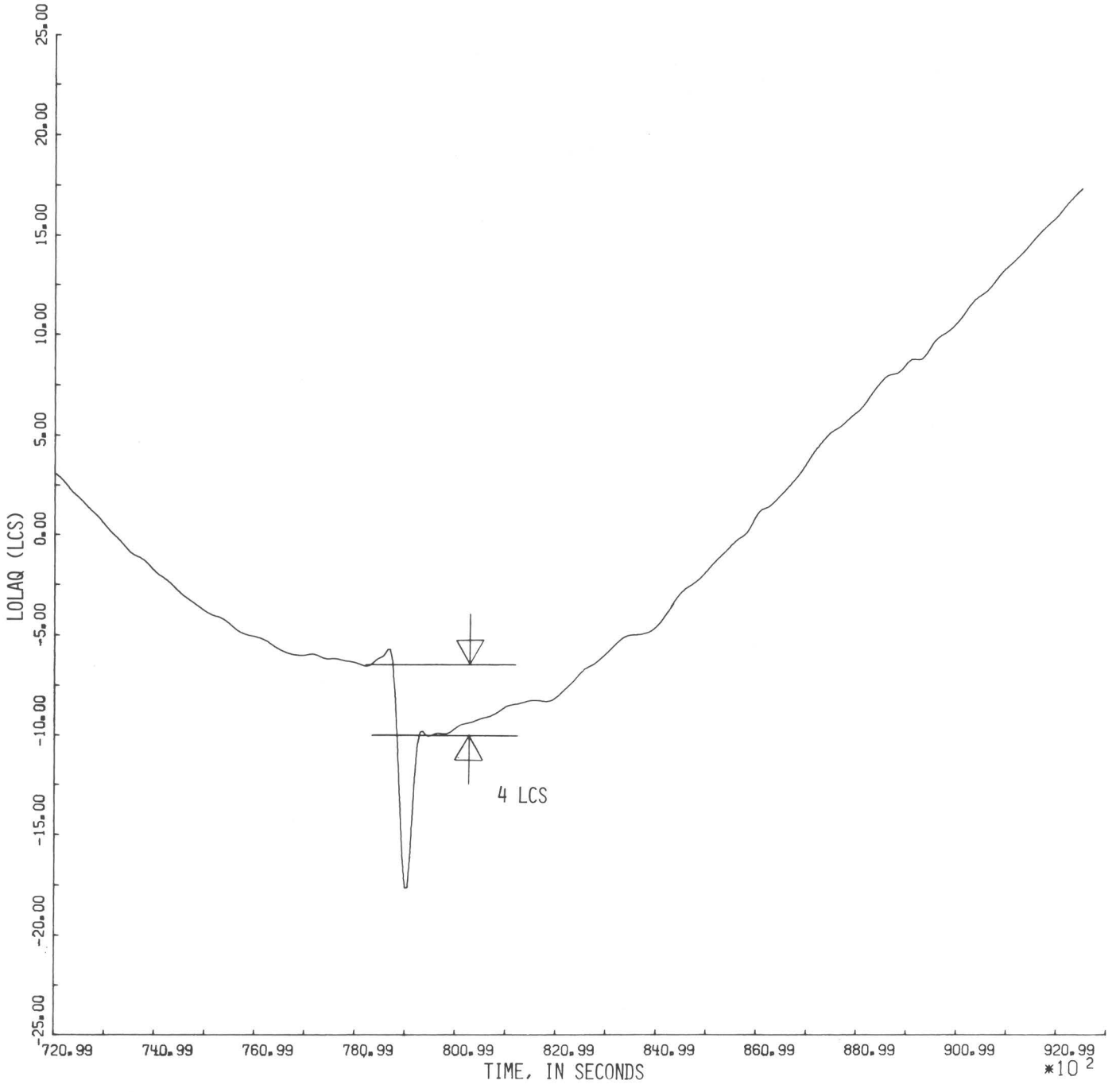

FIGURE 2.—A 6-hour section of the record has been lowpassed to reveal the strain offset.

PRELIMINARY REPORT ON FELT AREA AND INTENSITY

By NINA H. SCOTT
NATIONAL OCEAN SURVEY, NATIONAL OCEANIC AND ATMOSPHERIC ADMINISTRATION

This earthquake, the most destructive to occur in southern California since the Long Beach earthquake of March 10, 1933, was felt over approximately 80,000 square miles of California, Nevada, and Arizona; one observer at Beryl, Utah, reported the shock was slightly felt there (fig. 1).

The felt area was determined principally from the earthquake questionnaire card (Form NOS-680) canvass conducted by the National Ocean Survey. To date (March 4, 1971), 2,068 cards have been distributed—784 were distributed to postmasters and 1,284 to various other persons, including several hundred to structural engineers. To date, 1,860 reports have been received, and numerous requests for this form are being received daily.

A maximum intensity of VIII-XI has been assigned tentatively to a small area in the foothills of northern San Fernando Valley. This assignment is based on the catastrophic damage to the Sylmar Veterans Hospital, the Olive View Hospital, and the Holy Cross Hospital. Other effects in this high intensity zone were major damage to the Van Norman Dam, severe damage to water and power facilities, collapse of freeway overpasses, major ground ruptures, and bending of railroad tracks.

A report received from Robert E. Noel, reservoir keeper, Van Norman Dam, stated: "My wife and child were already up. She heard the quake coming. I was asleep. I tried to get out of bed but couldn't until the worst was over. I made a quick check of the family and a quick check of the house, then dressed and went to check the dam. We live on the reservoir at the bottom of the dam on the west end. When I got to the main road going to the top of the dam, I could see, through the dust, an irregularity of the crest of the structure below, looking to the top. I drove to the top of the dam and around the west abutment and saw the damage to the face. It was hard to believe what I saw."

Outside of the intensity VII zone (as shown in fig. 1), only slight to moderate damage was reported, principally cracked or fallen plaster and broken windows.

Nearly all observers remarked on the long duration of the earthquake.

The following reports are of interest regarding the direction of motion:

Fire Station No. 74 in Kagel Canyon.—"This building was moved approximately 12 inches off foundation and had to rise over sill at least 4½ inches to settle down without damaging the shingles."

Bear Divide Ranger Station (NW¼sec. 7, R. 14 W., Route 4, Box 303, Saugus).—"A great up-and-down motion, changing to north-south motion."

13706 N. Kagel Canyon Road (in area of Fire Station No. 74).—"My husband was awake and was thrown from north to south. Furniture was overturned from north to south, east-west, and west-east. Refrigerator was out of position from south to north about 18 inches. Kitchen cabinets were almost emptied both from north and south. Most violent action, from final position of furniture, seemed to be from east to west."

Valencia (just northwest of Newhall).—"Sensation was a violent rotary motion."

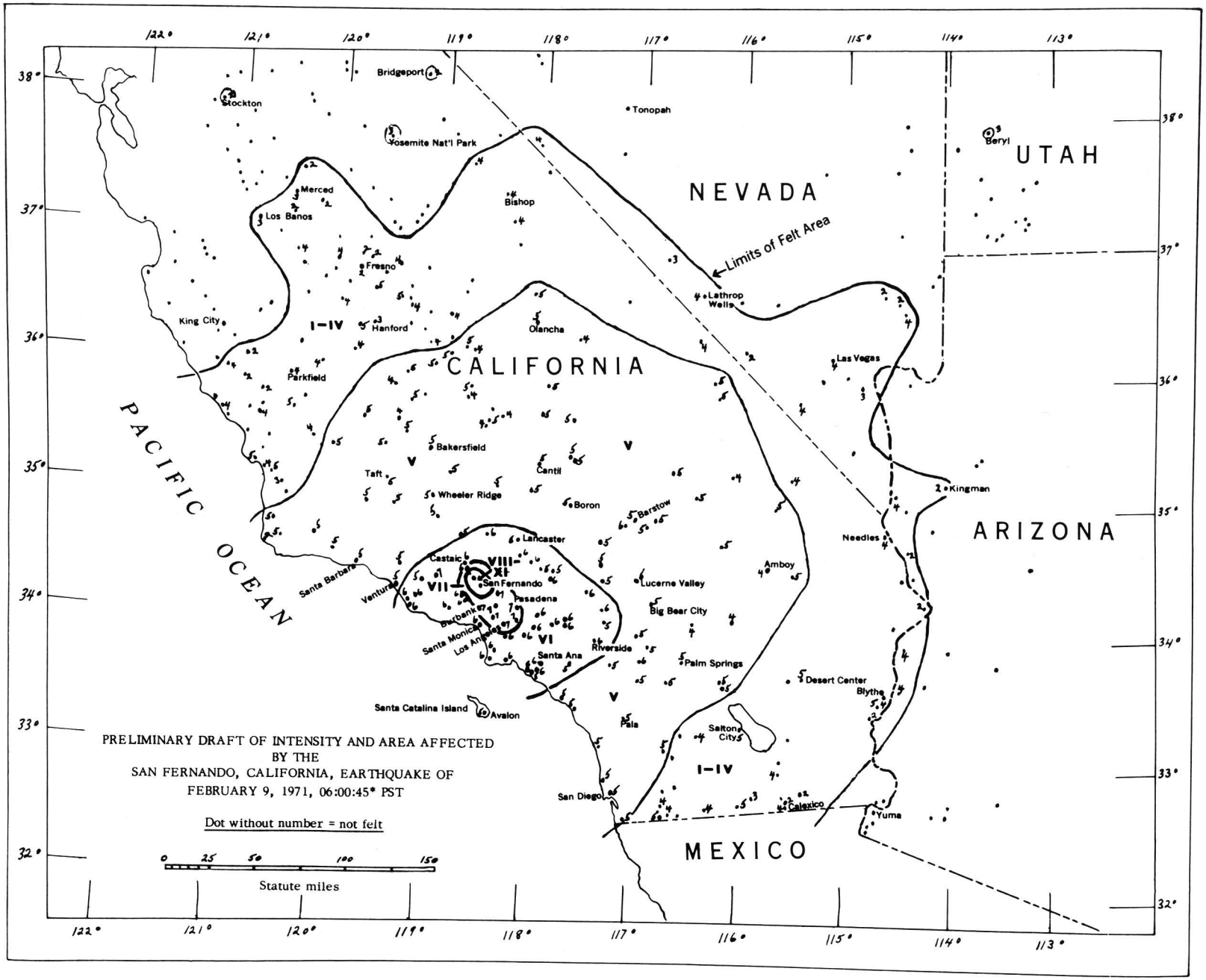

FIGURE 1.—Preliminary draft of intensity and area affected by the San Fernando, California, earthquake of February 9, 1971, 06:00:45 PST.

GROUND-MOTION AMPLIFICATION AND VIBRATION MEASUREMENTS

By KENNETH KING
NATIONAL OCEAN SURVEY, NATIONAL OCEANIC AND ATMOSPHERIC ADMINISTRATION

The Las Vegas Special Projects Party of NOS, in cooperation with the Atomic Energy Commission, installed and operated seismic instruments in California in the vicinity of the main epicenter of the San Fernando earthquake. The locations of the stations for the following programs are given in table 1.

BUILDING AND FREE FIELD SEISMIC MEASUREMENTS (PROGRAM NO. 1)

Several locations were instrumented with three-component velocity systems for seismic comparisons of aftershocks. The Van Norman Dam was instrumented to compare to an instrumented free field location, which was 100 yards from the Dam. The damaged Veterans Hospital was instrumented to compare with a free field station on bedrock in Loop Canyon. Ground plants were made near several schools to add to the Loop Canyon comparison. The stations recorded for approximately 2 days.

BANK OF CALIFORNIA PROGRAM (PROGRAM NO. 2)

The NOAA/NOS maintains three accelerographs in the Bank of California. The Special Projects Party installed additional three-component seismic systems near those three locations inside the building, plus one in the free field to study the building amplification and response characteristics to motion induced by aftershocks following the San Fernando earthquake. The seismic systems used were broad band and velocity sensitive systems and were recorded on magnetic tape. The four systems operated for about 5 days. The data have not yet been inspected or evaluated.

PACOIMA DAM COMPARISON (PROGRAM NO. 3)

The National Ocean Survey maintains an accelerograph station at the Pacoima Dam which recorded a high-level acceleration on the main San Fernando earthquake. To check the validity of the resulting strong-motion record, the NOS instrumented the accelograph location, the crest of the Dam, and a free field location in bedrock approximately 250 yards from the Dam with three-component velocity sensing systems. The stations recorded approximately 30 aftershocks that will be used for amplification and attenuation studies.

GROUND MOTION AMPLIFICATION (PROGRAM NOS. 4 AND 5)

The National Ocean Survey fielded two programs to study the seismic effects in the ground motion amplification study. Industrial and cultural seismic noise forced low-gain recordings which resulted in a limited number of recorded aftershocks. However, many events were recorded and can be used for the study. The portable seismic stations used on the programs consisted of three velocity sensing transducers, two horizontal and one vertical, which record broad spectrum from 0.1 to 30 Hz on magnetic tape.

Program No. 4 consisted of 23 three-component seismic stations located on a grid in the San Fernando Valley. Most stations were located in ground plants; a few were colocated at a preexisting seismic station, and one station was colocated with a Geological Survey seismic station. The stations recorded simultaneously for approximately 4 days.

Program No. 5 consisted of a similar network of 23 seismic stations located in the area of Glendale, Calif. The stations recorded for approximately 4 days.

BUILDING VIBRATION PROGRAM (PROGRAM NO. 6)

The Las Vegas Field Party measured the major structural periods of several buildings in the greater Los Angeles area. Data of induced and natural seismic disturbances in the horizontal planes of the high-rise structures were recorded

by temporarily installing velocity sensitive transducers at the uppermost accelerograph location in each of the buildings. The horizontal transducers were oriented to the short or minor and long or major axes of the building. The transducer/amplifier system is of the L-7 type, which has an essentially flat velocity response from 0.1 Hz to 100 Hz. The recording procedure was to record several minutes of ambient seismic background and then supplement this data with several short records of induced background. The induced force consisted of inertia created by a man swaying his body in synchronization with the building's natural period. The force was applied parallel to both major and minor horizontal axes of the building. The personnel who shifted their weight closed a contact, indicated on each seismogram at the stoppage of input. The refined method used has been developed through experience in Reno, Nev., Salt Lake City, Utah, and Las Vegas, Nev.

Phase I consisted of a quick test in 68 buildings. Phase II is a recheck and retest of buildings that gave questionable seismograms in Phase I. The seismograms were processed and scaled for preliminary information. The operation averaged six buildings per day. The following personnel recorded, scaled, and compiled data: Kenneth W. King, geophysicist; Louise Wuollet, geophysicist; John West, technician; and Eugene Sembera, technician.

TABLE 1.—*Station locations*

[Recorded on magnetic tape]

Station identification	Time on (P.s.t.)	Time off (P.s.t.)
Program 1		
Van Norman Dam (on the dam)	16 Feb 2100	18 Feb 1300
Van Norman Dam (free field)	16 Feb 2230	18 Feb 1415
Sylmar V. A. Hospital Chapel	17 Feb 1320	22 Feb 0900
Sylmar Loop Canyon	17 Feb 1500	22 Feb 1000
Alameney High School	17 Feb 1345	19 Feb 1200
Gridley Street School	17 Feb 1600	22 Feb 1100

TABLE 1.—*Station locations*—Continued

Station identification	Time on (P.s.t.)	Time off (P.s.t.)
Program 2		
Bank of California (roof)	18 Feb 1900	22 Feb 0200
Do (7th floor)	18 Feb 1700	22 Feb 2200
Do (basement)	18 Feb 1600	22 Feb 1130 [1]
Do (free field)	18 Feb 1500	23 Feb 1000
San Fernando Junior High	19 Feb 1300	23 Feb 1000
Gridley Street School	22 Feb 1100	23 Feb 1000 [1]
Sylmar V. A. Hospital Chapel	22 Feb 1000	27 Feb 1000 [1]
Sylmar Loop Canyon	22 Feb 1100	27 Feb 1000 [1]
Program 3		
Pacoima Dam (crest accelograph location, (free field)	24 Feb	Still running
Program 4 (San Fernando Grid)		
Golden State Freeway	26 Feb	2 Mar
Olive View Hospital	do	Do.
V. A. Hospital	do	Do.
Van Norman Lake (Upper)	do	Do.
Eldorado Avenue School	do	Do.
Gridley School	do	Do.
Olive Vista	do	Do.
Lower Van Norman Dam	do	Do.
Alameney School	do	Do.
Vaugan Street School	do	Do.
Pacoima Lutheran Hospital	do	Do.
Mission Hills Shopping Center	do	Do.
Mary Emaculate School	do	Do.
Jessup Park	do	Do.
Holiday Inn	do	Do.
Laurel High School	do	Do.
Sylvan Park School	do	Do.
Bel Air Presbyterian Church	do	Do.
Fire Station No. 108	do	Do.
Walter Reed Junior High School	do	Do.
Bank of California	do	Do.
Arminta Street School	do	Do.
Hubbard Street School	do	Do.
Program 5 (Glendale Grid)		
31, Dunsmore Street School	5 Mar	8 Mar
32, 3428 Prospect	do	Do.
33, Radio Tower "Free Field"	do	Do.
34, Casa Odobe de Son Rafael	do	Do.
35, Columbus School	do	Do.
36, Edison School	do	Do.
37, Atwater School	do	Do.
38, Verdugo Park	do	Do.
39, Nibley Park	do	Do.
40, Wilson Junior High School	do	Do.
41, Municipal Services Building	do	Do.
42, Glendale High School	do	Do.
43, Verdugo Recreation Center	do	Do.
44, Scholl Canyon Park	do	Do.
45, Griffith Manor Park	do	Do.
46, Griffith Park Headquarters	do	Do.
47, Brand Park	do	Do.
48, Roosevelt Park	do	Do.

[1] Also used in Program 5.

MAGNETIC FIELD SURVEY OF THE SAN FERNANDO EARTHQUAKE EPICENTRAL AREA

By J. E. O'DONNELL and H. E. KAUFMANN
NATIONAL OCEAN SURVEY, NATIONAL OCEANIC AND ATMOSPHERIC ADMINISTRATION

SEISMOMAGNETIC EFFECT

Recently the Japanese (Rikitake, 1968) and the Russians (Golovkov, 1969) have reported on conducting magnetic repeat field surveys in seismic areas in order to investigate the seismomagnetic effect. Their work suggests large changes in the magnetic field which could be related to earthquakes. Briener and Kovach (1968) have reported on work in the United States that consists of continuous monitoring of the magnetic field rather than running repeat magnetic surveys. They have an array of five rubidium magnetometers which have been operating in a differential mode, for the past few years, along a short portion of the San Andreas fault. Their work indicates that only very small changes (a few gammas) have been detected that could be correlated with creep and occasional small earthquakes along the San Andreas fault.

The San Fernando earthquake presented an opportunity in the United States to initiate an attempt to measure the seismomagnetic effect by magnetic field repeat surveys. A magnetic survey was made of the epicentral area between February 23 and March 4, 1971. A second survey will be necessary to detect any change, since we have no reports of the area being surveyed before the earthquake. A similar study was made by Kato (1940) when he conducted a magnetic field survey after a Japanese earthquake and then repeated it a year later. He found over a 100-gamma change, which he attributed primarily to the seismic activity in the area.

DESCRIPTION OF FIELD SURVEY

Thirty-two stations were established in the epicentral area, along with a base station which continuously monitored the magnetic field changes. The base station records were used to remove the diurnal and temporal variations from the survey. The recordings were made with a Schonstedt HMS-1 fluxgate magnetometer with a special sensor mount to allow alignment of the sensor in the total field direction. An ELSEC proton precession magnetometer (± 1.2 gamma) was used to take absolute measurements at this position during the survey, in order to establish a true base control. A 1-gamma drift per day was found at the base station, which could be due either to magnetometer drift or tilting of the sensor. The sensitivity and chart speed of this system were 0.9 gamma per mm and 1.2 minutes per mm, respectively. The sensitivity was computed from recorded calibration pulses obtained from energizing a calibration coil on the sensor.

The repeat stations were located on existing survey markers such as bench, triangulation, and reference markers whenever possible. These markers and other geographic positions were obtained from U.S. Geological Survey 7½′ topographic maps. The technique for making the measurements consisted of placing the sensor 60 inches above the marker on a tripod and observing five readings. The readings were repeated also at the four cardinal points located 20 feet from the marker. These cardinal-point values give an indication of the magnetic gradient in the vicinity of the marker. In some cases,, artificial magnetic anomalies, such as metal stakes and pipes, were noted in the station description. In a few cases, some of the cardinal points were not suitable for measurement. A file of complete station descriptions is being maintained at the Fredericksburg Geomagnetic Center. The observed and reduced data are presented in table 1, along with the gradient data, which indicate the better stations to be used for repeat work.

DISCUSSION OF DATA

The Sand Canyon station was occupied on three occasions during the survey, while Reynier Canyon and Sunland were occupied twice. The largest ob-

TABLE 1.—*Magnetic total field survey data for epicentral area of San Fernando earthquake of February 9, 1971*

Station name and location	Month and day	U.T.	Observed value (gammas)	Diurnal and temporal variation correction	Base station drift correction	Corrected value	Corrected gradient values	Remarks
Sand Canyon Fire Station (long 118°24'48.0" W., lat 34°23'05.4" N.)	2-24	17:04	49942	+8	+1	49951	49957S 49959W 49894N	Los Angeles County Fire Station No. 123.
	3-3	21:44	49901	+56	+8	49965	49986S 49980W 49912N	
	3-4	18:26	49930	+27	+9	49966	49984S 49975W 49914N	
Dillon Divide (long 118°20'5.0" W., lat 34°20'37.5" N.)	2-24	18:56	50333	+25	+1	50359	50408S 59287W 50202N 50383E	Former Forest Service monument, 1945.
Dillon Ranch (long 118°21'25.0" W., lat 34°20'50.0" N.)		19:58	49784	+53	+1	49838	50140S 50022W 49948N 49594E	U.S.G.S. bench mark.
Indian Springs (long 118°20'14.5" W., lat 34°19'21.0" N.)		21:09	49962	+52	+1	50015	49952S 50013W 50120N 49999E	U.S.G.S. bench mark. R68 1929.
Reese (long 118°20'10.5" W., lat 34°19'11.0" N.)	2-24	22:23	50131	+59	+1	50191	50269S 50230N 50249E	Forest Service marker 1940?
Camp No. 9 (long 118°23'43.5" W., lat 34°21'31.0" N.)	2-25	17:44	50827	+28	+2	50857	50808S 50807W 50913N 50840E	Measurements taken during 10γ bay activity of 20 min duration.
Little Tujunga Heli-pad (long 118°21'34.5" W., lat 34°17'45.0" N.)		19:31	50233	+39	+2	50274	50323S 50228W 50277N	
Reynier Canyon (long 118°25'04.5" W., lat 34°23'01.5" N.)		21:43	50011	+65	+2	50078	49967S 49962W 49968N 50017E	U.S.G.S. bench mark R8 1929.
	3-1	16:58	50051	+15	+6	50072	49970S 49965W 49970N 50015E	
Placerita (long 118°29'24.0" W., lat 34°23'46.5" N.)	2-25	22:55	50002	+43	+2	50047	50004E	U.S.G.S. triangulation station
Port (long 118°19'44.0" W., lat 34°23'11.0" N.)		19:50	49970	+36	+3	50009	50001S 50009W 50010N 50006E	Los Angeles County Port (reference mark No. 2.
Magic (long 118°19'03.0" W., lat 34°23'11.0" N.)		20:36	50029	+44	+3	50076	49637S 49514W 49372N	U.S.C.&G.S. triangulation station 1958. Sensor 8 in. above marker.
Cub (long 118°17'57.0" W., lat 34°23'28.5" N.)		21:45	49943	+42	+3	49989	50084S 49870W 49995N 50196E	Forest Service marker 1945.
Pacoima (long 118°24'20.0" W., lat 34°17'33'5" N.)	2-27	17:41	50274	+22	+4	50300	50046S 50041W 50034N 50023E	Pacoima triangulation marker 1935 RE 2177.
Sunland (long 118°22'51.0" W., lat 34°16'43.5" N.)	2-27	18:30	50237	+33	+4	50274	50207S 50260W 50212N	Forest Service reference marker No. 2.

TABLE 1.—*Magnetic total field survey data for epicentral area of San Fernando earthquake of February 9, 1971*—Continued

Station name and location	Month and day	U.T.	Observed value (gammas)	Diurnal and temporal variation correction	Base station drift correction	Corrected value	Corrected gradient values	Remarks
	3-1	20:44	50229	+46	+6	50281	50212S 50261W 50213N	
Pacoima E2 (long 118°27'40.0" W., lat 34°17'22.5" N.).		20:03	50304	+53	+4	50361	50239S 50215W 50184N 50190E	Los Angeles County control survey mark 2177.
Garfield (long 118°20'59.0" W., lat 34°22'02.0" N.).	2-28	18:43	50812	+31	+5	50848	50784S 50854W 50969N 50857E	Forest Service Garfield 4622 4622 1945. Sensor 10 in. above marker.
Trial Cyn. D1 (long 118°16'15.0" W., lat34°23' 45.5" N.).		19:47		+48	+5		49894S 49899W 49900N 49907E	Los Angeles County Trial Cyn. D1, 1962 steel post by marker.
Indian (long 118°15'19.0" W., lat 34°23'39.5" N.).	2-28	20:23	50201	+50	+5	50256	50250S 50281W 50245N 50249E	Forest Service indian 1945 marker.
Camp Ground 1 (long 118°16'32.0" W., lat 34°22'30.0" N.).		21:32	49669	+42	+5	42716	49560S 49477W 49451N 49600E	
Santa Clara Divide (long 118°17'06.5" W., lat 34°23'44.0" N.).		22:23	49779	+35	+5	49819	49725S 49854W 49852N 49767E	
Indian Canyon head (long 118°16'12.0" W., lat 34°25'04.0" N.).		23:00	50079	+30	+5	50114	50124S 50151W 50101N 50145E	
Soledad Camp (long 118°16'39.0" W., lat 34°26'17.0" N.).		23:31	49979	+27	+5	50011	50023S 50022W 50038N 50010E	
Aqua Dulce Bridge (long 118°20'07.5" W., lat 34°26'18.0" N.).		24:04	50118	+23	+5	50146	50148S 50123W 50147N 50143E	
Stone quarry (long 118°20'42.5" W., lat 34°26'02.0" N.).	2-28	24:46	50094	+20	+5	50119	50039S 50073W 49868N 50098E	U.S.C.&G.S. bench mark Q486 1955.
Placerita Canyon State Park (long 118°28'11.0" W., lat 34°24'40.0" N.).		17:33	50200	+18	+6	50224	50375S 50212W 50202N 50228E	
Mint Canyon (long 118°25'08.5" W., lat 34°27'50.5" N.).		18:41	50407	+25	+6	50438	50093S 50092W 50088N 50090E	
Vasquez Rocks (long 118°19'16.5" W., lat 34°29'20.0" N.).		23:30	50321	+14	+6	50341	50339S 50338W 50323N 50350E	
May (long 118°25'44.0" W., lat 34°21'08.0" N.).	3-2	19:38	51101	+33	+7	51141	51276S 50818W 50890N 51301E	U.S.G.S. marker.
Fernando 1 (long 118°25'03.5" W., lat 34°21'11.0" N.).	3-2	21:00	51121	+47	+7	51175	50841S 50818W 50738N 50869E	Los Angeles County survey marker 1955.

TABLE 1.—*Magnetic total field survey data for epicentral area of San Fernando earthquake of February 9, 1971*—Continued

Station name and location	Month and day	U.T.	Observed value (gammas)	Diurnal and temporal variation correction	Base station drift correction	Corrected value	Corrected gradient values	Remarks
Norman Reservoir (long 118°29'15.0" W., lat 34°17'30.0" N.). ------		24: 08	50089	+16	+7	50102	50115S 50107W 50105N 50131E	U.S.C.&G.S. triangulation reservoir 1932.
Big Tujunga (long 118°15'16.0" W., lat 34°18'49.5" N.). ------	3-3	18: 50	49840	+33	+8	49881	49786S 49759W 49680N 49649E	U.S.G.S. marker R 79 1929.
North Ball Park (long 118°17'30.0" W., lat 34°16'57.0" N.). ------		19: 54	49859	+61	+8	49928	49869W 49877N 49911E	
Silver Star Lane (long 118°24'43.0" W., lat 34°23'05.5" N.). ------	2-23 to 3-4							Base station continuous recording directly east of Los Angeles fire station 123.

served difference (14 gammas) at the Sand Canyon station is larger than the minimum error of 6 gammas involved in the magnetic reduction of the data. Two other possible errors not included in the reduction are the conductivity anomaly effect (Schmucker, 1970; and Elvert and others, 1970) and artificial magnetic gradients. The conductivity effect, we feel, would be negligible, since the magnetic activity recorded at the base station indicated only slight activity during a few measurements. The diurnal was less than 50 gammas but should be essentially uniform over the small area surveyed. The most likely source of error is in attempting to relocate the same position in a high magnetic gradient. The cardinal points at a station were not reoccupied precisely, while the center position was not off by more than 3 inches. Since a torroidal-wound sensor was used, with the ELSEC, it allowed measurements in a high gradient. It would be possible to have a high gradient 5 feet away (distance of sensor from ground), but to drop off substantially at 20 feet if the source were very localized. Consequently, we do not feel the Sand Canyon differences are of any significance at this time.

REFERENCES

Briener, S., and Kovach, R. L., 1968, Local magnetic events associated with displacement along the San Andreas fault (California): Tectonophysics, v. 6, no. 1, p. 69-73.

Elvers, D., Perkins, D., and Holbrook, R., 1970, A survey of anomalous geomagnetic variations in Puerto Rico: Operational Data Rept. C&GS DR 9, U.S. Department of Commerce, 1-44.

Golovkov, V. P., 1969, Anomalous geomagnetic field variations in a seismically active region: Geomagnetism and Aeronomy, v. 9, no. 6, p. 912-913.

Kato, Y., 1940, Investigation of the changes in the earth's magnetic field accompanying earthquake or volcanic eruptions: Tohoku Univ. Sci. Rept., ser. 1, v. 29, no. 3, p. 315-326.

Rikitake, T., 1968, Geomagnetism and earthquake prediction: Tectonophysics, v. 6, no. 1, p. 59-68.

Schmucker, U., 1970, an introduction to induction anomalies. Jour. Geomagnetism and Geoelectricity, v. 22, no. 1-2, p. 9-33.

CRUSTAL-MOVEMENT SURVEYS AND PREEARTHQUAKE STRAIN ANALYSIS

By C. A. WHITTEN
NATIONAL OCEAN SURVEY, NATIONAL OCEANIC AND ATMOSPHERIC ADMINISTRATION

The geodetic party assigned to California for monitoring crustal movement, and especially for repeating the fault-crossing surveys to detect fault slippage, had been working in the Los Angeles area for a few days immediately preceding the San Fernando earthquake. Recent preearthquake remeasurements of three of these fault-crossing surveys along the San Gabriel and San Andreas faults indicated no slippage. This seven-man party, with a few additional geodetic technicians, was assigned the task of reobserving the networks of geodetic control in the San Fernando region and the San Gabriel Mountains. Some of this control, which consists of triangulation and leveling, had been established by the Los Angeles County Engineer's Office. Personnel from that office are also engaged in reobserving portions of these networks. These cooperative efforts are fully coordinated by Ira H. Alexander, Division Engineer from Los Angeles, and Captain L. S. Baker, Chief, Geodesy Division of the National Ocean Survey. Several weeks will be required to complete the field surveys, reduce the measurements, and analyze the results.

The epicenters of the earthquake and major aftershocks are very near the southern end of one of the older arcs of triangulation established in 1932 as part of a broad program for detecting crustal deformation in California. This arc extended from San Fernando to Bakersfield in a dog-leg fashion with the axis of the arc perpendicular to the San Gabriel, San Andreas, and Garlock faults. This special survey was repeated in 1952 and again in 1962. The analyses of the resurveys in those years did not indicate any slippage along those major faults.

However, following the earthquake of February 9, the data from the extreme southern end of these three surveys were reanalyzed. Components of maximum shear were computed for the triangles in the network and the results are shown in figure 1. One of the triangles, with one of its vertices at the Van Norman Reservoir and the other two in the Mission Hills, shows an accumulation of strain of 41×10^{-6} units in the 30 years from 1932 to 1962. The direction of maximum shear for the triangles covering the general area of the Santa Susana fault is east-west. The direction of maximum shear for the triangles further north, near Newhall, and closer to the San Gabriel fault is northwest-southeast. In both cases, the direction of shear indicates right-lateral movement.

These components of shear, when considered collectively, provide some basis for interpretation of rates of accumulation of strain prior to the earthquake. However, it must be emphasized that the units are expressed in parts per million and are derived from conventional triangulation which could not be expected to be more accurate than 10 parts per million. Further, considering that the results depend upon comparisons of two surveys, the computed values may have an uncertainty of the order of 15 parts per million. The postearthquake program of reobservation includes the use of a laser geodimeter. Thus, any additional resurveys in the future would provide information with uncertainties not exceeding one or two parts per million.

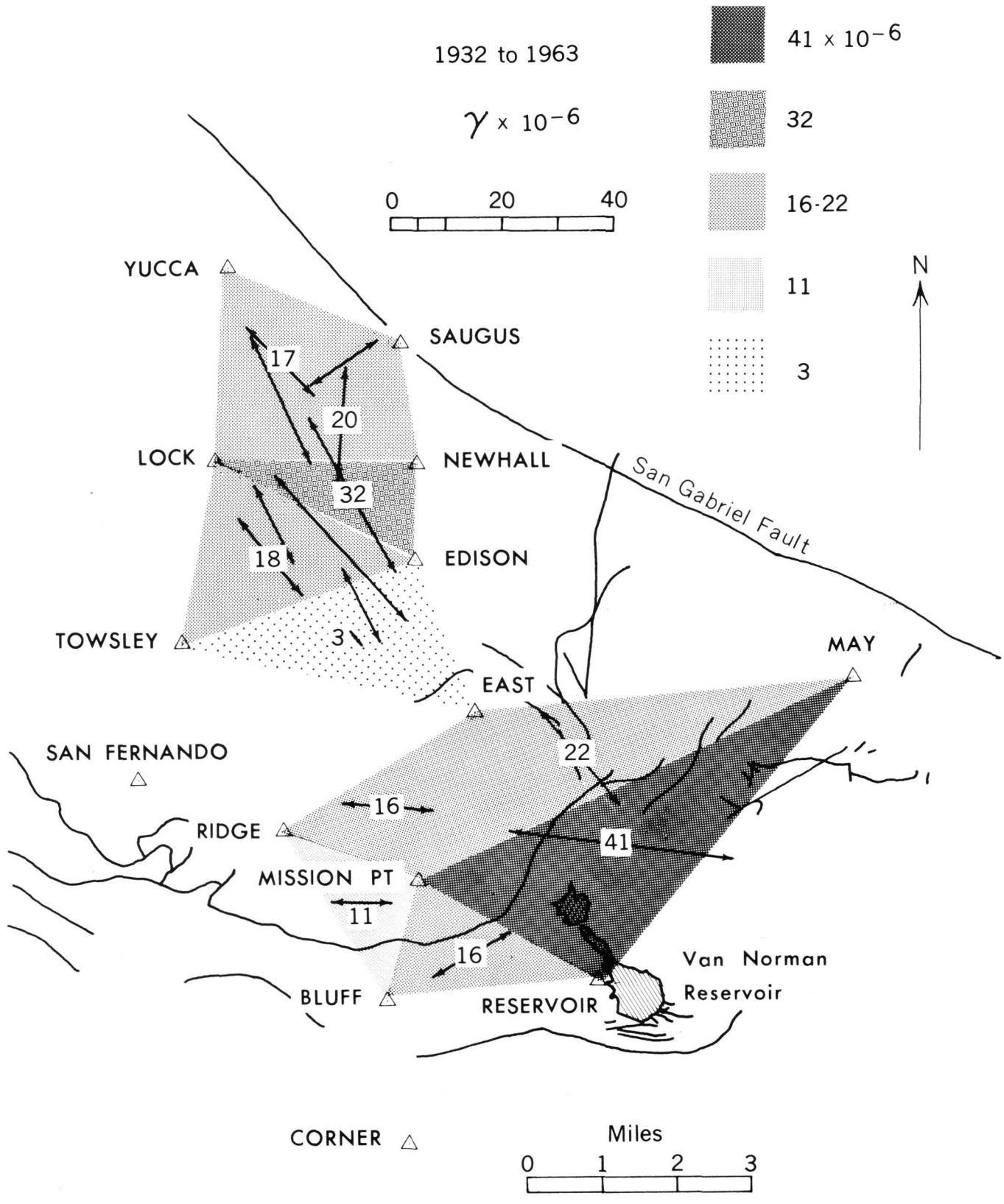

FIGURE 1.—Components of shear.

PRELIMINARY STRONG-MOTION RESULTS FROM THE SAN FERNANDO EARTHQUAKE OF FEBRUARY 9, 1971

By R. P. MALEY and W. K. CLOUD
NATIONAL OCEAN SURVEY, NATIONAL OCEANIC AND ATMOSPHERIC ADMINISTRATION

More than 250 strong-motion accelerographs were triggered in southern California by the magnitude 6.6 San Fernando earthquake of February 9, 1971. More than 200 of these are located in the Los Angeles area, primarily as a direct result of the inclusion in the building codes of Los Angeles and neighboring cities of a seismograph section requiring the installation of three accelerographs in buildings six stories and taller. In addition, approximately 120 seismoscope records were obtained within the strongly shaken area; these are almost equally divided between those located at damsites and those located on different geologic formations. Most of the strong-motion instruments are privately owned but are maintained by the Seismological Field Survey unit of NOAA's National Ocean Survey as part of a cooperative network.

The collection of records has nearly been completed; concurrently, the production of archival copies of the accelerograms and digitization of the important records are being done at the Jet Propulsion Laboratory in Pasadena. As record processing is completed, reproductions of the originals are being posted in the vibration laboratory at Thomas Engineering on the California Institute of Technology campus for public inspection. Detailed analysis of the strong-motion data is just beginning, although preliminary raw scaling of maximum accelerations is well underway. A sampling of those results has been included in this report.

PRELIMINARY STRONG-MOTION DATA

The locations of accelerographs outside the Los Angeles area are shown in figure 1. The individual stations are listed in table 1, which includes a selection of maximum ground-level accelerations recorded between 15 and 85 miles from the epicenter. Note that the spread of peak values measured at four sites in the Lake Hughes array, 15 to 19 miles distant, varies by a factor of more than two, ranging from 0.16 to 0.37 g, perhaps a consequence of the variation of rock types. The maximum accelerations of slightly less than 0.4 g observed at one Lake Hughes site and nearby Castaic are considerably larger than the ground-level records obtained at equivalent distances in the San Fernando Valley south of the epicenter.

The distribution of accelerographs in the Los Angeles area is shown in figure 2. At Pacoima Dam, 5 miles south of the epicenter, the earthquake accelerations were the highest ever recorded, i.e., in the 0.5 to 0.75-g range with several high-frequency peaks to 1 g (fig. 3). The initiation of strongest shaking began 1 to 2 seconds after instrumental triggering and lasted for approximately 12 seconds. The accelerograph, owned by the Los Angeles County Flood Control District, is located on a small ledge above the east abutment of the concrete arch dam situated in the deep narrow Pacoima Canyon above the Sylmar district of Los Angeles. Rock at the site is a gneissic granite-diorite complex, with prominent jointing trends parallel to the canyon. Figure 4*A* shows the relative location of the instrument housing and the massive spalling of bedrock that occurred below the station during the earthquake. In addition, some cracking, displacement, and subsequent tilting of the rock adjacent to the instrument housing were observed following the shock (fig. 4*B*). Tilting of the ledge was evidenced by a permanent displacement of the horizontal-triggering pendulum on the accelerograph, which caused all the paper to run off during the first 15 to 20 minutes following the earthquake.

A representative pattern of the maximum ground-

level accelerations measured in the Los Angeles area is listed in table 2, with the specific station locations keyed to the map of the metropolitan area (fig. 2). The largest values (>0.2 *g*) are generally observed at the stations nearest the epicenter, i.e., in the San Fernando Valley and at Pasadena. Dropoff of peak values, to 0.10 to 0.15 *g*, is noted in the high-rise area of central Los Angeles and along the Wilshire strip, although there are some deviations in this general trend. Ground records from the extended Los Angeles basin generally show about 10 seconds of higher-frequency strong shaking, followed by several cycles of longer-period waves in the 2-second period range.

Records were obtained in the upper levels of more than 60 buildings, six to 42 stories in height, ranging from 13 to 53 miles from the epicenter. These instruments are maintained by the Seismological Field Survey in cooperation with building owners in the cities that have incorporated the mandatory accelerograph provisions within the building code. Representative maximum accelerations recorded at the top level of a cross-section of structures are contained in table 3. Peak values in excess of 0.4 *g* were recorded as distant as downtown Los Angeles, nominally 26 miles, although the vast majority of measurements were in the 0.2- to 0.4-*g* range. From the sample thus far available, it is noted that taller structures (greater than 15 stories) tend to fall on the middle and lower end of this range, with the exception of identical twin towers (not included in table 3) located in central Los Angeles. The highest top-floor accelerations are approximately two to three times those measured at the ground level in the same structure.

Within a few days after the earthquake, five temporary accelerographs were installed at the following locations: Lower Van Norman Dam in San Fernando Valley, Pacoima Dam, the U.S. Forest Service Station in Soledad Canyon, the Los Angeles County Fire Station in San Canyon, and Acton. A number of aftershocks have triggered these instruments as well as several others at original stations, but the results are not yet available.

Excellent seismoscope records were obtained throughout Los Angeles and in adjacent strongly shaken areas to the north and northwest. Among these is a unique record from a Los Angeles Department of Water Power seismoscope originally located on the crest of Lower Van Norman earthfill dam. During the earthquake, this section of the crest partially failed and the instrument slid down into the lake. Undaunted by the apparent loss of the record, B. J. Morrill of the Seismological Field Survey pursued the recovery of the instrument in the belief a usable record could be obtained. When the lake level was lowered as a safety measure, the seismoscope was sighted and eventually appeared above water where it was retrieved by Morrill. Fortunately, the smoked glass plate was still in place, providing a record of the earthquake and the simultaneous dam failure (fig. 5). A second record was also recovered from the west abutment of Lower Van Norman Dam.

Another fine set of seismoscope records was obtained at Santa Felicia Dam, 22 miles northwest of the epicenter, where six instruments owned by the United Water Conservation District are located on the crest, east, and west abutments and below the toe of the dam. Large, strongly polarized amplitudes at an angle of approximately 40° to the axis of the dam were recorded at the two crest stations. When this prominent alignment was projected to the southeast on a map, the line fell substantially south of the instrumental epicenter.

SUMMARY

More than 250 accelerograph records and 100 seismoscope records on the San Fernando earthquake were obtained from the cooperative network maintained by the Seismological Field Survey unit of NOAA's National Ocean Survey. All records have been collected and are now being quickly scaled and duplicated; shortly they will be digitized prior to more comprehensive analysis.

Maximum ground accelerations were observed at Castaic and Lake Hughes, where values were slightly less than 0.4 *g*, and at Pacoima Dam, where there were a few peaks in the 1-*g* range, the highest ever recorded. Evaluation of the latter record may prove to be difficult because of facturing of rock adjacent to the station during the earthquake. Ground accelerations in the Los Angeles area were predominantly <0.2 *g*, except in the San Fernando Valley and Pasadena, while on the top floors of taller buildings maximum values occasionally exceeded 0.4 *g* but more often were in the 0.2- to 0.4-*g* range.

Five temporary accelerograph stations were established after the main shock between 1 and 10 miles from the earthquake epicenter. These included Pacoima Dam and Lower Van Norman Dam.

Among the significant seismoscope records obtained were two from Lower Van Norman Dam, including one from the crest that had slid into the lake during the earthquake, and a second set of six records from Santa Felicia Dam, located 22 miles northwestof the epicenter.

This earthquake has provided the largest collection of significant strong-motion data ever obtained and should prove to be of unprecedented value to the engineers, earth scientists, and public officials concerned with the problem of seismic hazards.

TABLE 1.—*Strong-motion accelerographs in southern California (exclusive of Los Angeles) with selected maximum ground-level accelerations*

Location	Number of instruments	Sampled maximum Acceleration (fraction of gravity)	Distance from epicenter (miles)
1. Point Concepcion	1	.....	.....
2. Cachuma Dam	2	.....	.....
3. Santa Barbara	2	.....	.....
4. Port Hueneme	1	0.03	49
5. Santa Felicia Dam	2	.....	.....
6. Castaic	1	.39	18
7. Lake Hughes array	4	.16-.37	15-19
8. Fairmont Reservoir	1		
9. Palmdale	1	.13	20
10. Pearblossom	1	.15	28
11. Wrightwood	2	.....	.....
12. Cedar Springs	2	.....	.....
13. Devils Canyon	2	.....	.....
14. San Bernardino	1	.....	.....
15. Loma Linda	1	.....	.....
16. Colton	1	.04	65
17. Desert Hot Springs	1	.....	.....
18. Puddingstone Dam	1	.08	39
19. San Antonio Dam	1	.....	.....
20. Carbon Canyon Dam	1	.....	.....
21. Whittier Narrows	1	.10	33
22. Santa Ana	1	.....	.....
23. Costa Mesa	1	.....	.....
24. Perris	1	.....	.....
25. San Onofre	1	.02	85
26. Hemet	1	.....	.....
27. Anza	1	.....	.....
28. Borrego Springs	1	.....	.....
29. Superstition Mountain	1	.....	.....
30. El Centro-Imperial	4	.....	.....
31. San Diego	3	.....	.....
32. San Juan Capistrano	1	.....	.....
33. Fullerton (building)	3	.04	45
34. Orange (building)	3	.....	.....
35. Gorman	1	.....	.....
36. Fort Tejon	1	.....	.....
37. Grapevine	1	.....	.....
38. Wheeler Ridge	1	.....	.....
Total number of instruments	56		

TABLE 2.—*Strong-motion accelerographs in the Los Angeles area with selected maximum ground level-accelerations*

Location	Number of instruments	Sampled maximum Acceleration (fraction of gravity)	Distance from epicenter (miles)
1. 111 N. Hope	3	.....	.....
2. 445 S. Figueroa	3	.14	26
3. 533 S. Fremont	3	.....	.....
4. 611 W. Sixth	3	.....	.....
5. 250 E. First	3	.13	26
6. 646 S. Olive	3	.....	.....
7. 808 S. Olive	3	.....	.....
8. 420 S. Grand	3	.....	.....
9. Santa Anita Dam	1	.....	.....
10. Cal Tech: Atheneaum and Millikan Library, Pasadena	3	.22	23
11. Jet Propulsion Lab., Pasadena	2	.....	.....
12. 633 E. Broadway, Glendale	1	.27	19
13. 1640 Marengo	3	.....	.....
14. 4814 Loma Vista, Vernon	1	.....	.....
15. 3663 S. Hoover	3	.....	.....
16. 3407 W. Sixth	3	.....	.....
17. 3470 Wilshire	3	.....	.....
18. 3710 Wilshire	3	.....	.....
19. 4867 Sunset	3	.....	.....
20. 4680 Wilshire	3	.12	22
21. 1025 N. Highland	3	.....	.....
22. 7080 Hollywood	3	.11	21
23. 120 N. Robertson	3	.....	.....
24. 1901 Ave. of Stars	3	.17	25
25. 945 Tiverton	3	.....	.....
26. UCLA Eng. bldg	1	.....	.....
27. 16055 Ventura	3	.....	.....
28. 8244 Orion	3	.28 (vertical)	13
29. Pacoima Dam	1	[1] .5-.75	5
30. Terminal Island, Long Beach	1	.....	.....
31. 215 W. Broadway, Long Beach	1	.03	45
32. 2011 Zonal	3	.....	.....
33. Pasadena Seismol. Lab	1	.....	.....
34. 3345 Wilshire	3	.....	.....
35. 750 Garland	3	.....	.....
36. 3440 University	3	.....	.....
37. 5260 Century	3	.....	.....
38. 9841 Airport Blvd	3	.....	.....
39. 15433 Ventura	3	.....	.....
40. 8639 Lincoln	3	.04	31
41. 6424 Sunset	3	.....	.....
42. 6464 Sunset	3	.....	.....
43. 3838 Lankershim	3	.18	18
44. 3411 Wilshire	3	.....	.....
45. 800 W. First	3	.....	.....
46. 222 Figueroa	3	.....	.....
47. 11661 San Vicente	3	.....	.....
48. 1900 Ave. of Stars	3	.....	.....
49. 234 Figueroa	3	.....	.....
50. 3550 Wilshire	3	.....	.....
51. 2070 Century Park East	3	.....	.....
52. Griffith Park	1	.18	21
53. Long Beach State College	1	.....	.....
54. 1150 S. Hill	3	.12	27
55. 1625 W. Olympic	3	.....	.....
56. Palos Verdes Estates	1	.04	43
57. 900 S. Fremont, Alhambra	3	.....	.....
58. 15107 Vanower	3	.....	.....
59. 16661 Ventura	3	.....	.....
60. 15910 Ventura	3	.....	.....
61. 15250 Ventura	3	.23	18
62. 15724 Ventura	3	.....	.....
63. 1760 N. Orchid	3	.....	.....
64. 930 Hilgard	3	.....	.....
65. 435 N. Oakhurst, Beverly Hills	3	.09	24
66. 450 Roxbury, Beverly Hills	3	.....	.....
67. 9100 Wilshire, Beverly Hills	3	.....	.....
68. 9450 Wilshire, Beverly Hills	3	.....	.....
69. 5900 Wilshire, Beverly Hills	3	.....	.....
70. 6200 Wilshire, Beverly Hills	3	.....	.....
71. 1177 Beverly Drive	3	.....	.....
72. 1880 Century Park East	3	.....	.....
73. 1800 Century Park East	3	.13	25
74. Century City Ground	1	.....	.....
75. 1888 Century Park East	6	.....	.....
76. 2500 Wilshire	3	.10	24
77. 616 S. Normandie	3	.....	.....
Total number of instruments	209		

[1] Several high-frequency peaks to 1 *g*.

TABLE 3.—*Representative maximum accelerations recorded on the top floors of Los Angeles area buildings*

[All stations are in Los Angeles unless otherwise noted]

Station	Distance from epicenter (miles)	Floor level	Maximum acceleration (fraction of gravity)
8244 Orion	13	8 (roof	0.39
15107 Vanowen	15	8 (roof)	.38
15250 Ventura	18	13 (roof)	.26
3838 Lankershim	18	21 (penthouse)	.23
Millikan Library—CIT, Pasadena	23	10 (roof)	.34
1880 Century Park East	25	17 (penthouse)	.27
4680 Wilshire	25	6	.30
1640 Marengo	26	8 (roof)	.43
611 W. Sixth	26	42 (penthouse)	.18
250 E. First	26	17 (roof)	.21v
8639 Lincoln	30	12	.12
4000 W. Chapman, Orange	53	19	.08

TABLE 4.—*Seismoscopes in southern California*

Location	Site
Altadena	Devils Gate Reservoir (crest).
	Devils Gate Reservoir (left bank).
	1972 Skyview Drive (residence).
Arcadia	Santa Anita Reservoir.
Arrowhead	U.S. Forest Service station.
Azusa	Cogswell Reservoir (crest).
	Cogswell Reservoir (right bank).
	San Gabriel Reservoir (crest).
	San Gabriel Reservoir (left bank).
Beverly Hills	Lower Franklin Canyon (west abutment).
	Lower Franklin Canyon (main dam, crest).
Burbank	Burbank High School.
Castaic	North Station.
	Old Ridge Routes.
Cedar Springs	Strong-motion station.
	Exterior.
Claremont	Live Oak Reservoir (crest).
	Live Oak Reservoir (left bank).
	Thompson Creek Reservoir (crest).
	Thompson Creek Reservoir (left bank).
Encino	Encino Reservoir (crest).
	Encino Reservoir (tower).
	Encino Reservoir (west abutment).
El Centro	Imperial Valley Irrigation District, strong-motion station.
	El Centro High School.
	El Centro steamplant.
	El Centro waterworks.
El Segundo	Hyperian treatment plant.
Eagle Rock	Eagle Rock Reservoir (west abutment).
	Eagle Rock Reservoir (main dam, crest).
Fairmount	Fairmount Reservoir (south abutment).
	Fairmont Reservoir (main dam, crest).
Glendale	Herbert Hoover High School.
Glendora	Big Dalton Reservoir (crest).
	Big Dalton Reservoir (left bank).
Goleta (2)	Two ------ ------ ------ ------
Hollywood	Hollywood Reservoir (west abutment).
	Hollywood Reservoir (main dam, crest).
La Jolla	Boquet Canyon Reservoir (west abutment).
	Boquet Canyon Reservoir (main dam, crest).
Lake Hughes	Array No. 2.
	Array No. 3.
	Array No. 4.
	Array No. 4A.
	Array No. 5.
	Array No. 7.
	Array No. 8.
	Array No. 9.
	Array No. 11.
	Array No. 12.
Long Beach	Municipal Bldg., strong-motion site.
	San Pedro High School.
	Terminal Island, strong-motion site.
Los Angeles	Baldwin Hills Reservoir (east abutment).
	E. Los Angeles Jr. College.
	Hancock Park.
	Taylor Residence.
	Colton, strong-motion site.
	Hollywood, strong-motion site.
	Tauxe Residence.
	Edison Bldg., strong-motion site.
	Vernon, strong-motion site.
	Leeds Residence.
	UCLA, strong-motion site.
	Duke Residence.
	San Marino City Hall.
	W. Los Angeles Public Library.
	Van Nuys High School.
	Southgate High School.
	Elysian Heights School.
	Playa Del Rey School.
	Windsor Hills School.
	Museum School Admin. Bldg.
	Huntington Park City Hall.
	Narbonne High School.
Monrovia	Sawpit Canyon Reservoir (right bank).
	Sawpit Canyon Reservoir (crest).
Mount Wilson	Cal Tech Seismograph Station.
Olancha	Haiwee Reservoir (east abutment).
	Haiwee Reservoir (main dam, crest).
Pacoima	Pacoima Dam.
Pasadena	Eaton Wash Reservoir (base).
	Eaton Wash Reservoir (crest).
	Gilman Residence.
	Millikan Library, CIT.
	Motta Residence.
	Muir High School.
	Washington Jr. High School.
	Seismological Laboratory.
	San Raphael School.
	Garfield School.
	Hale School.
	Cal Tech, strong-motion site.
Pearblossom	Pear blossom pumping plant.
Perris	Strong-motion station.
Riverside	Cal Tech Seismograph Station.
San Bernardino	Post Office, strong-motion site.
	Devils Canyon Site No. 1.
	Devils Canyon Site No. 2.
	Devils Canyon Site No. 4.
	Devils Canyon Site No. 5.
	Devils Canyon Site No. 6.
	Devils Canyon Site No. 7.
San Dimas	Puddingstone Reservoir.
	San Dimas Reservoir (crest).
	San Dimas Reservoir (left bank).
	Puddingstone Reservoir, strong-motion site.
San Fernando	Lower San Fernando Reservoir (east abutment).
	Lower San Fernando Reservoir (main dam, crest).
San Marino	1155 Shenadoah Rd. (residence).
Santa Ana	Strong-motion site.
Santa Barbara	Strong-motion station.
	University of California.
	Museum.
Santa Felicia Dam	Toe of dam.
	Outlet works.
	Right abutment.
	Right crest.
	Dam crest.
	Left abutment.
Saugus	Dry Canyon (east abutment).
	Dry Canyon (main dam, crest).
Sunland	Big Tujunga Reservoir (crest).
	Big Tujunga Reservoir (left bank).
Table Mountain	Tiltmeter station.
Westwood	Lower Stone Canyon Reservoir (east abutment).
	Lower Stone Canyon Reservoir (main dam, crest).

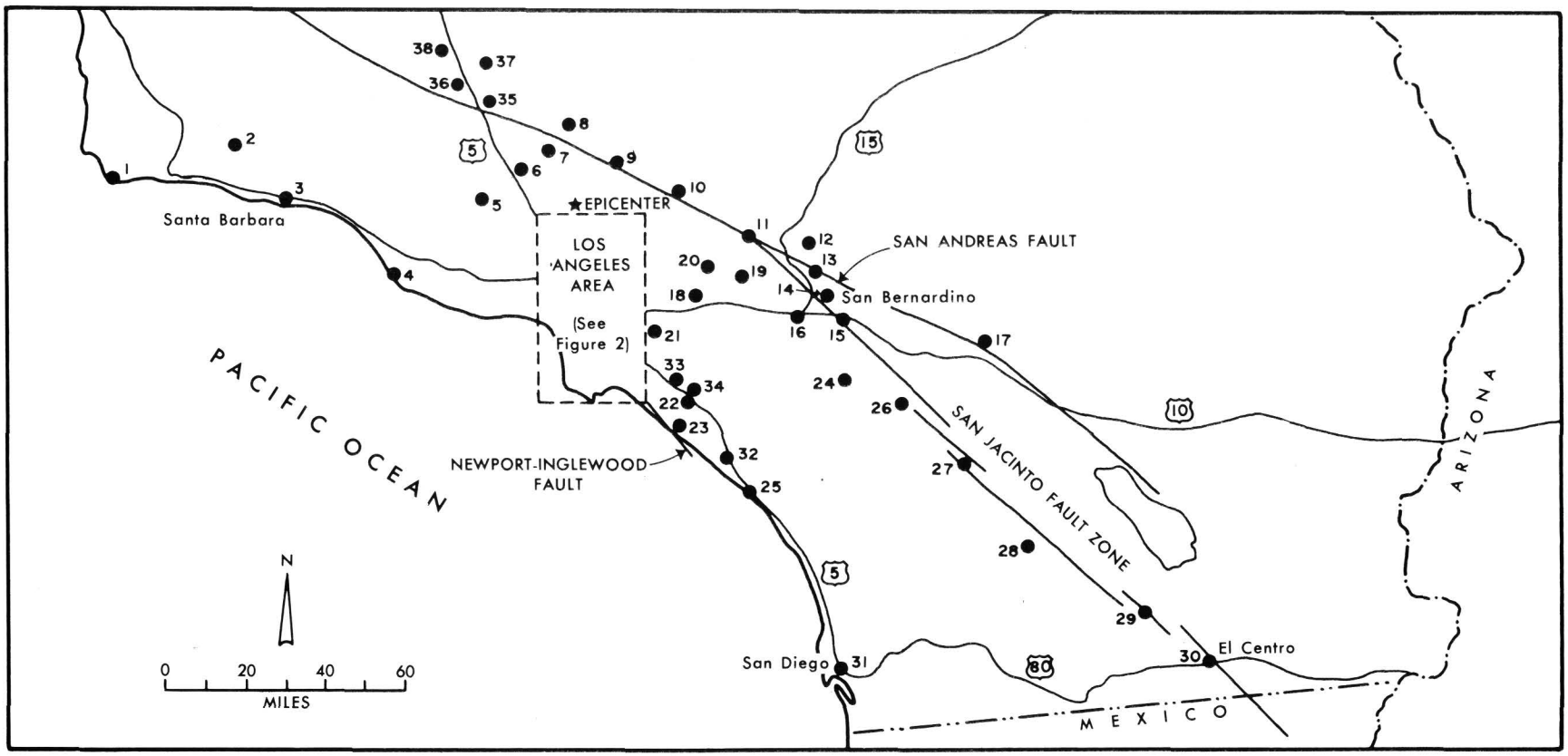

FIGURE 1.—Location of strong-motion accelerographs in southern California maintained by the NOS-NOAA as part of the cooperative network (February 1971).

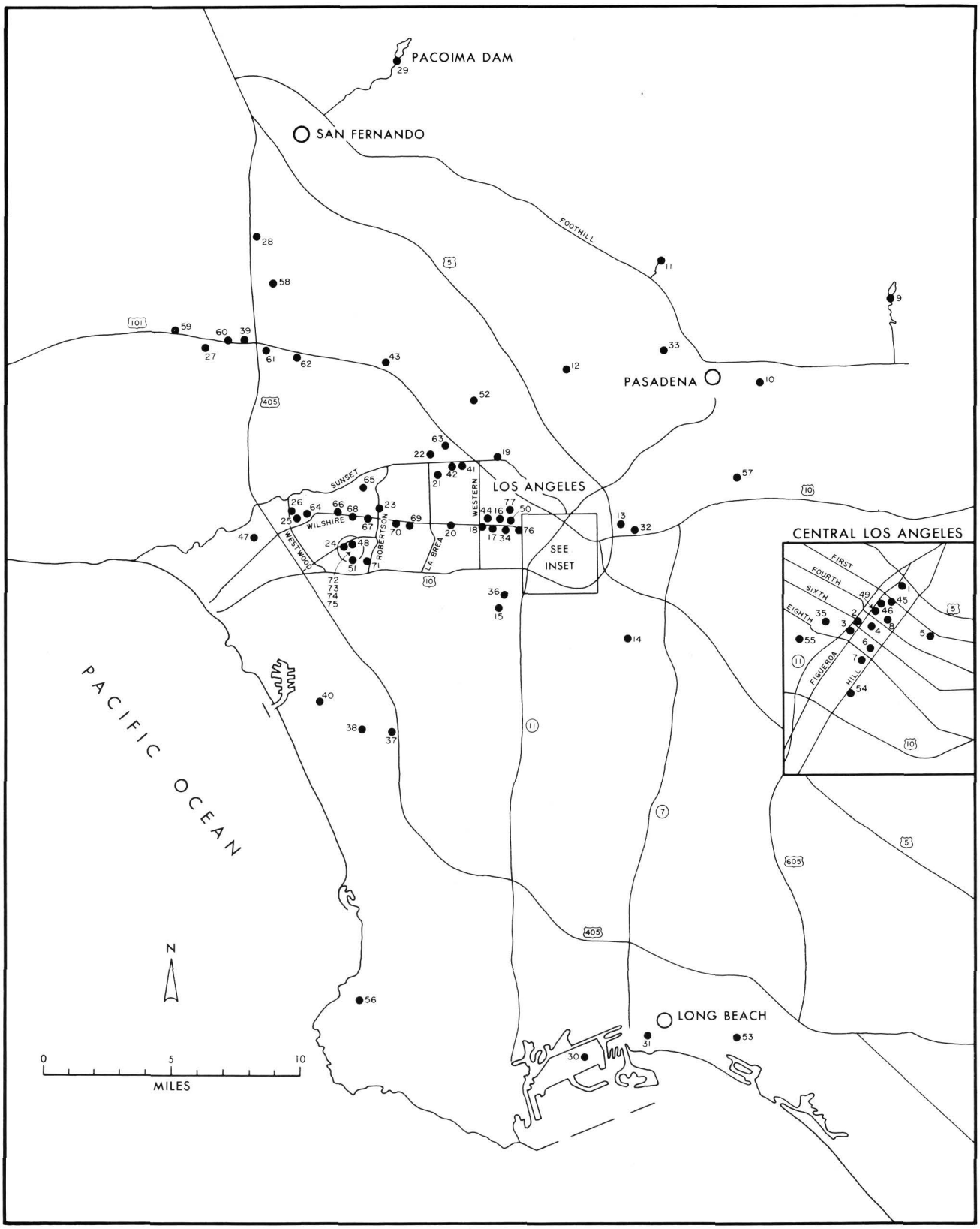

FIGURE 2.—Location of strong-motion accelerographs in the Los Angeles area maintained by the NOS-NOAA as part of the cooperative network (February 1971).

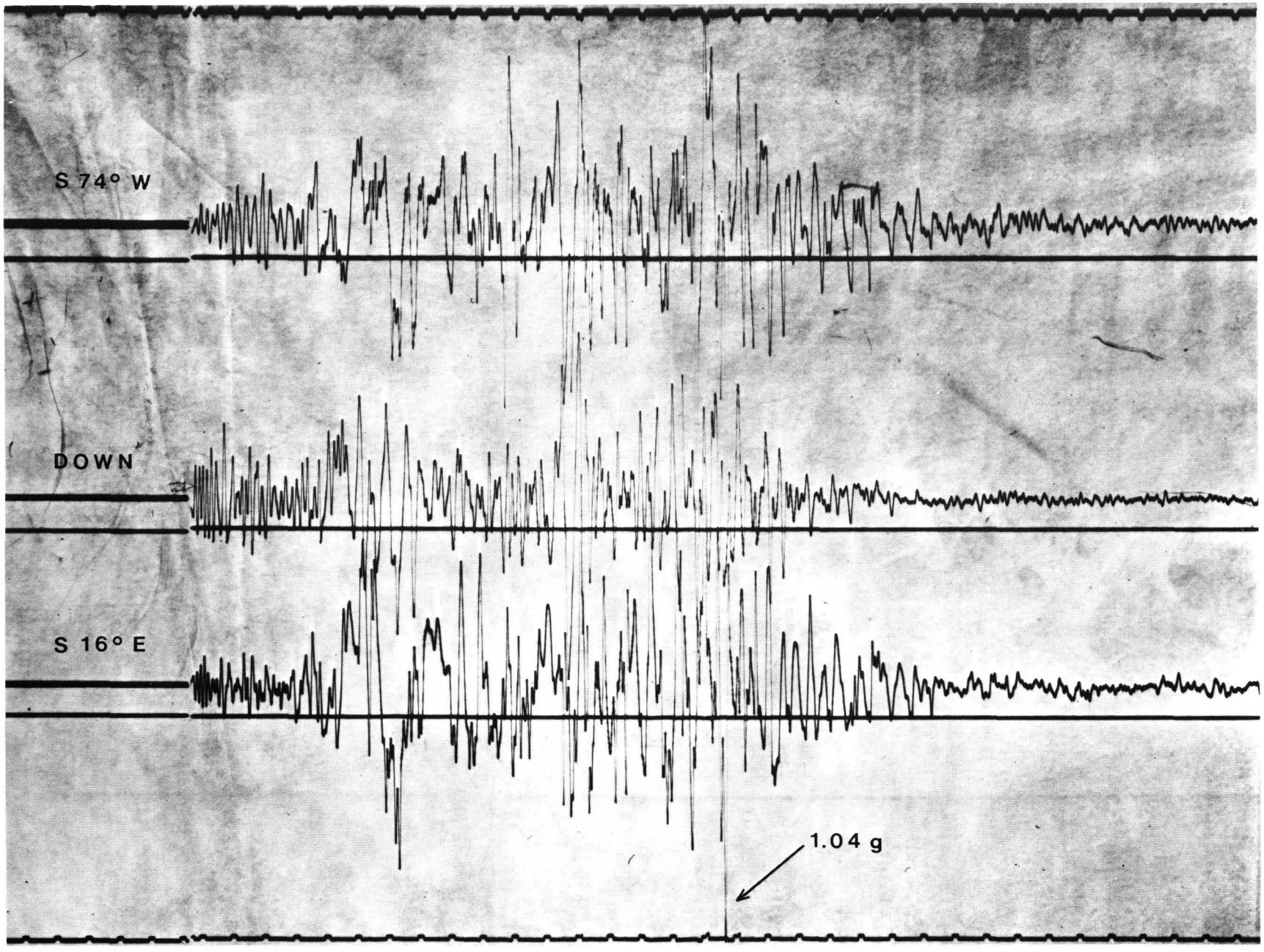

FIGURE 3.—Accelerograph record from the abutment of Pacoima Dam, a cooperative station with the Los Angeles County Flood Control District.

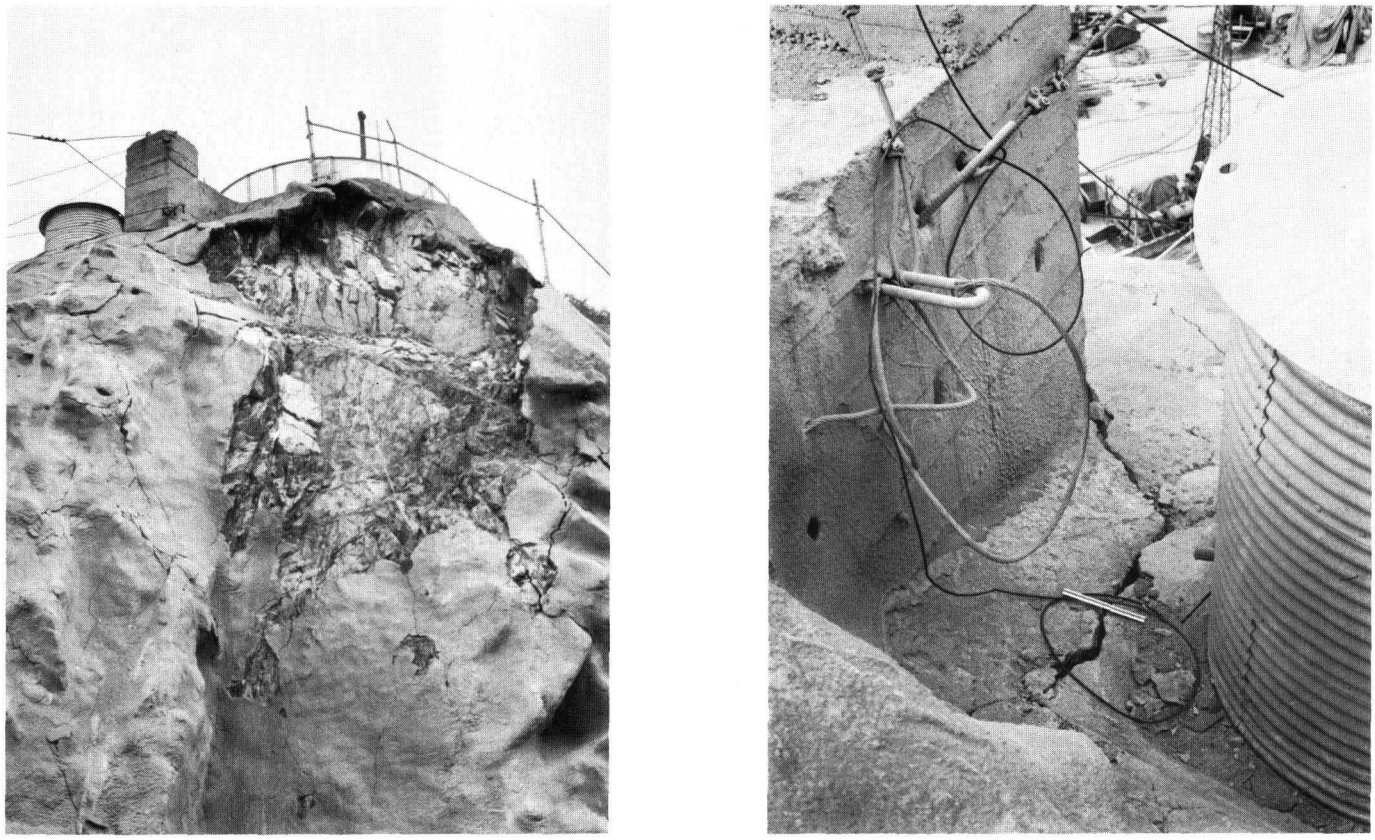

FIGURE 4.—Accelerograph site on the east abutment of Pacoima Dam. The instrument is located in the small silolike structure. Note (*A*) the massive spalling of bedrock and (*B*) the cracking and displacement adjacent to the accelerograph housing.

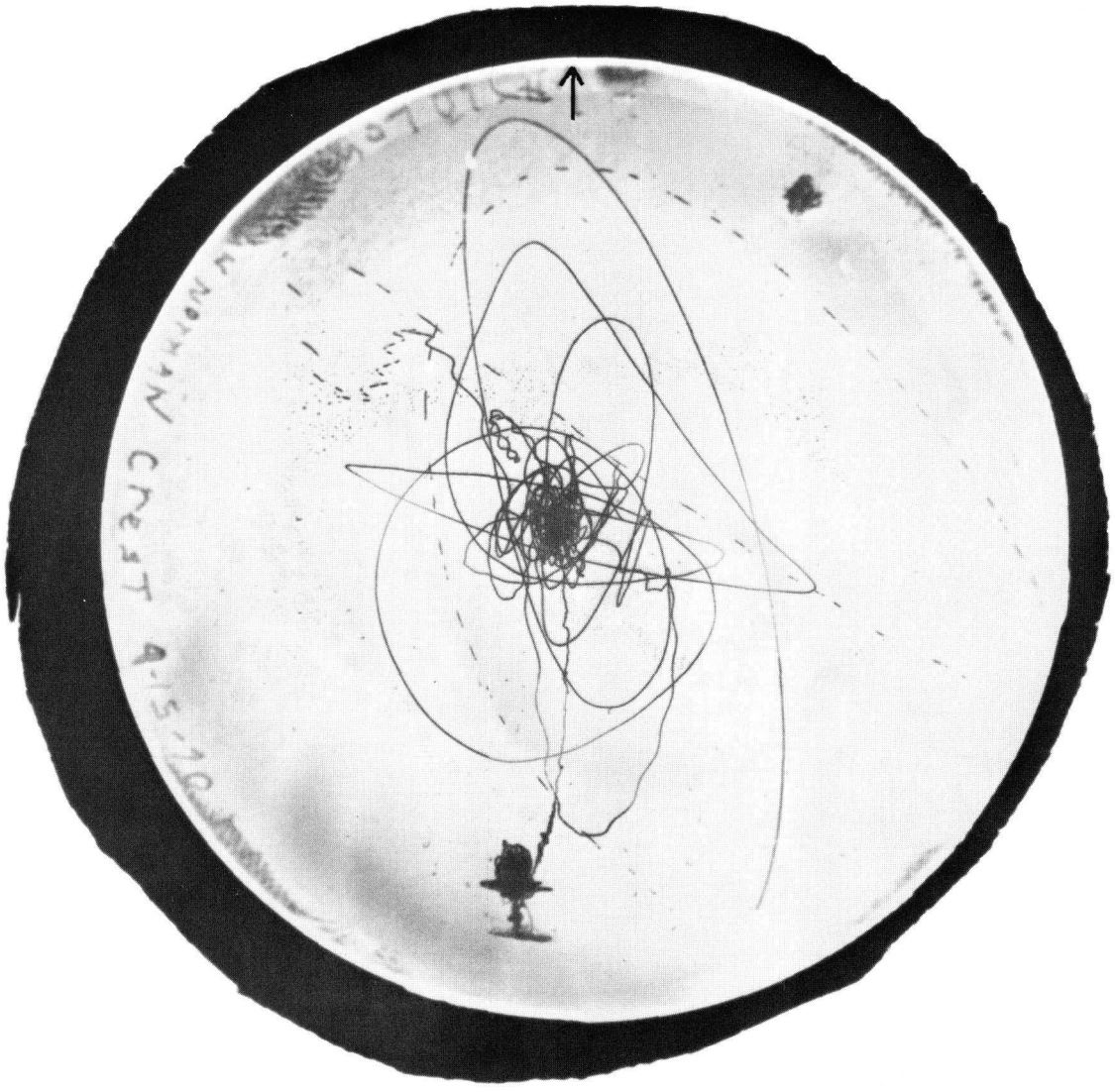

FIGURE 5.—Seismoscope record from Lower Van Norman Dam, a cooperative station with the Los Angeles Department of Water and Power. Arrow points north.

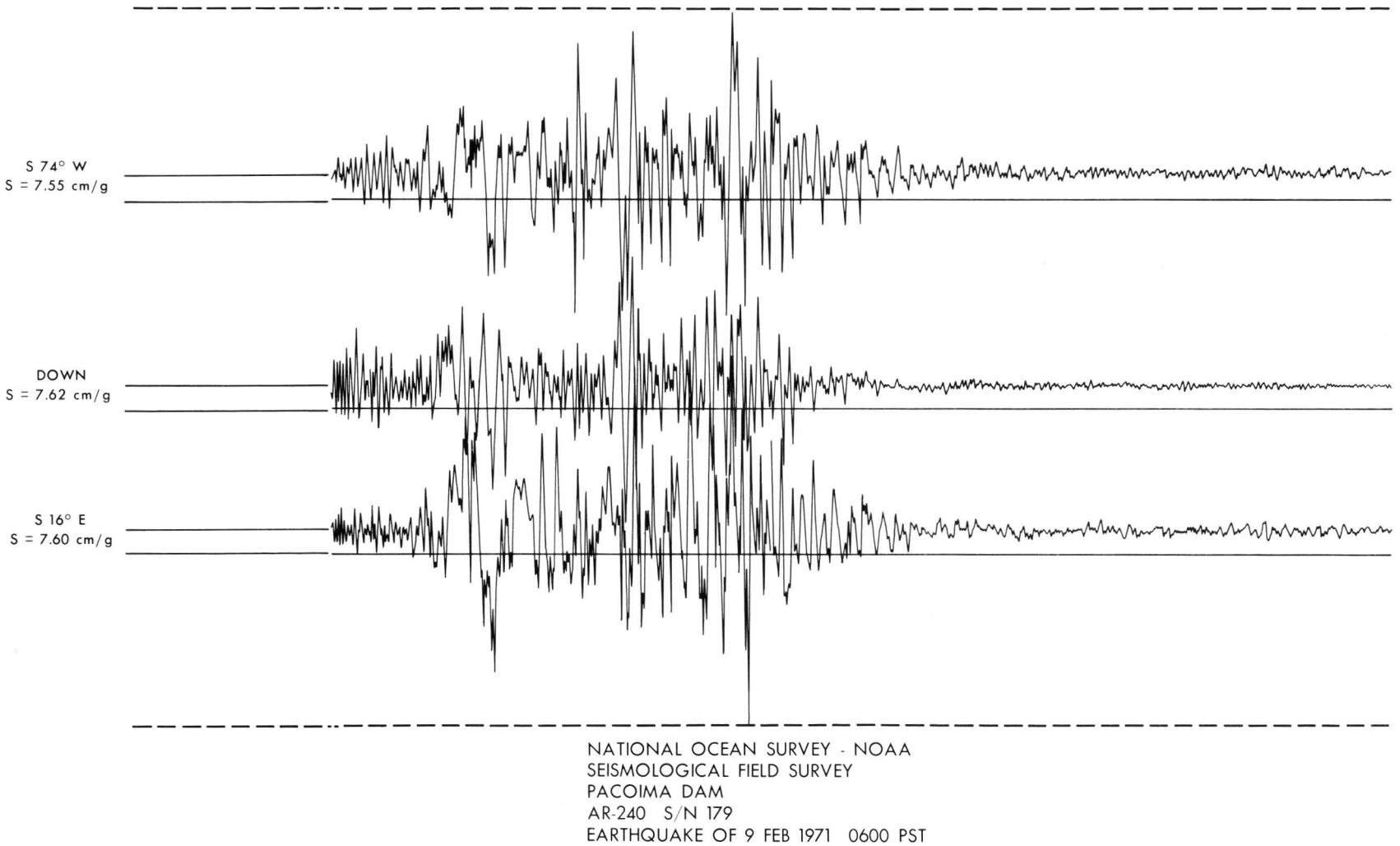

FIGURE 6.—Accelerograph record, Pacoima Dam.

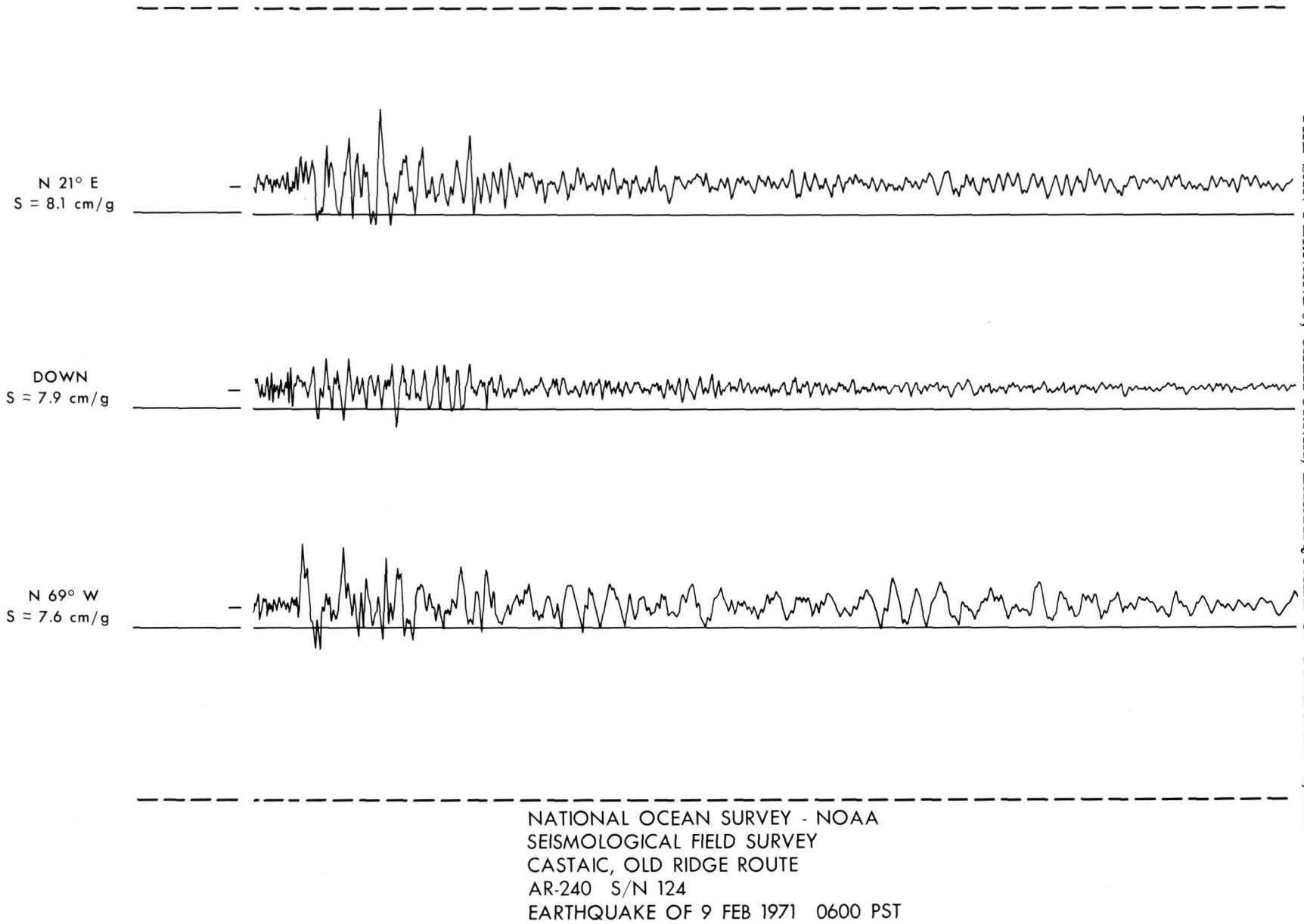

FIGURE 7.—Accelerograph record, Castaic, Old Ridge Routes.

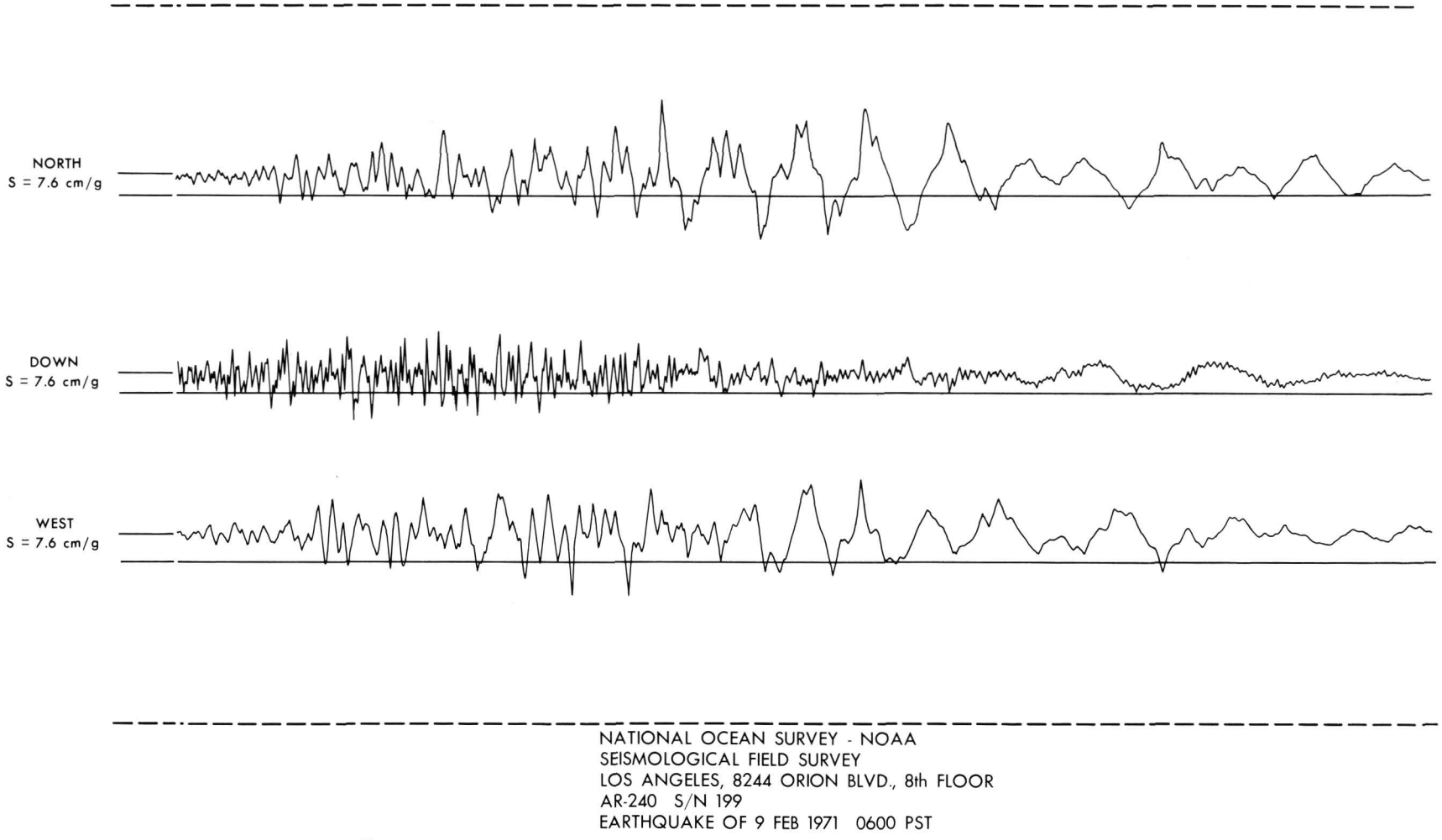

FIGURE 8.—Accelerograph record, Los Angeles, 8244 Orion, eighth floor.

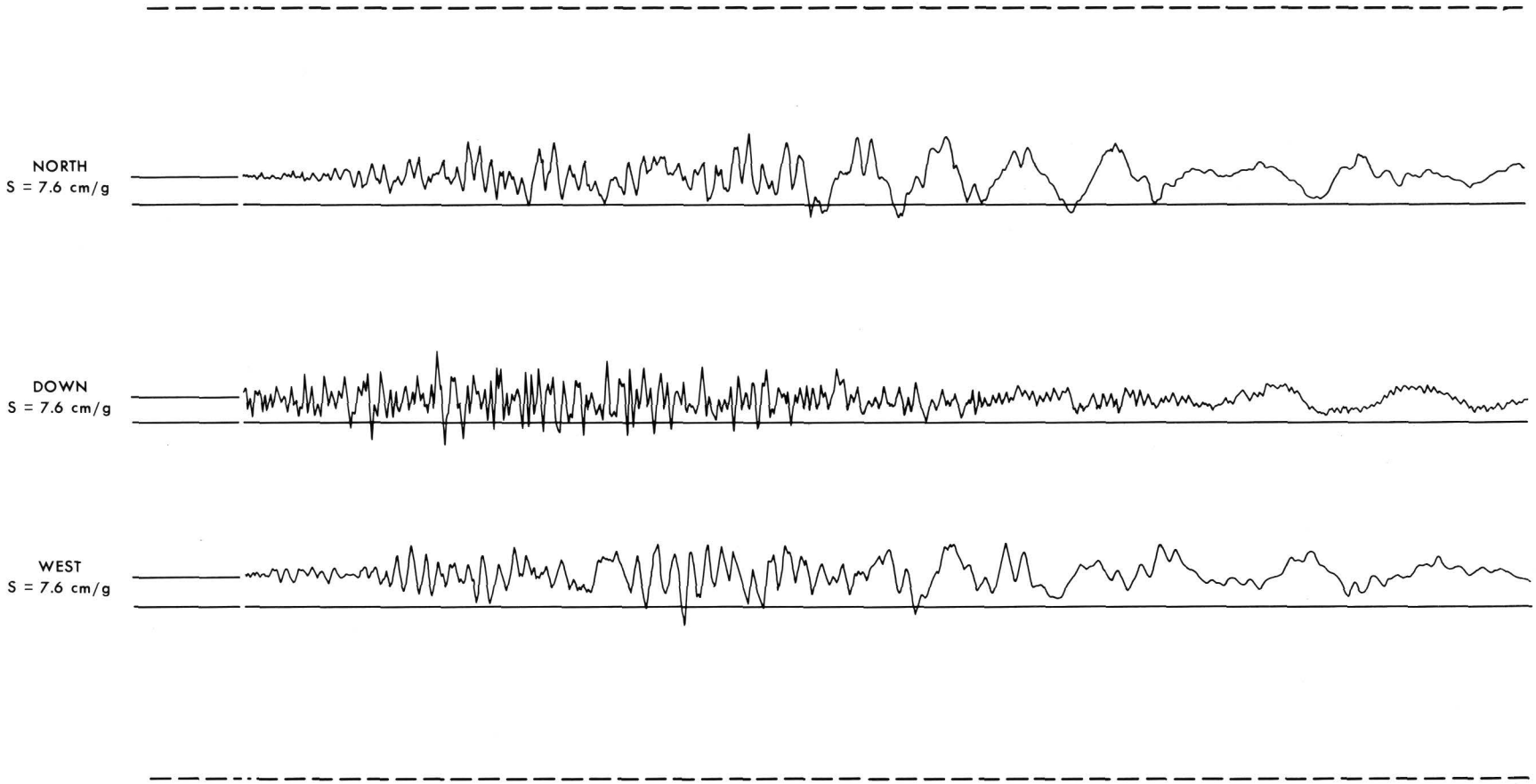

FIGURE 9.—Accelerograph record, Los Angeles, 8244 Orion, fourth floor.

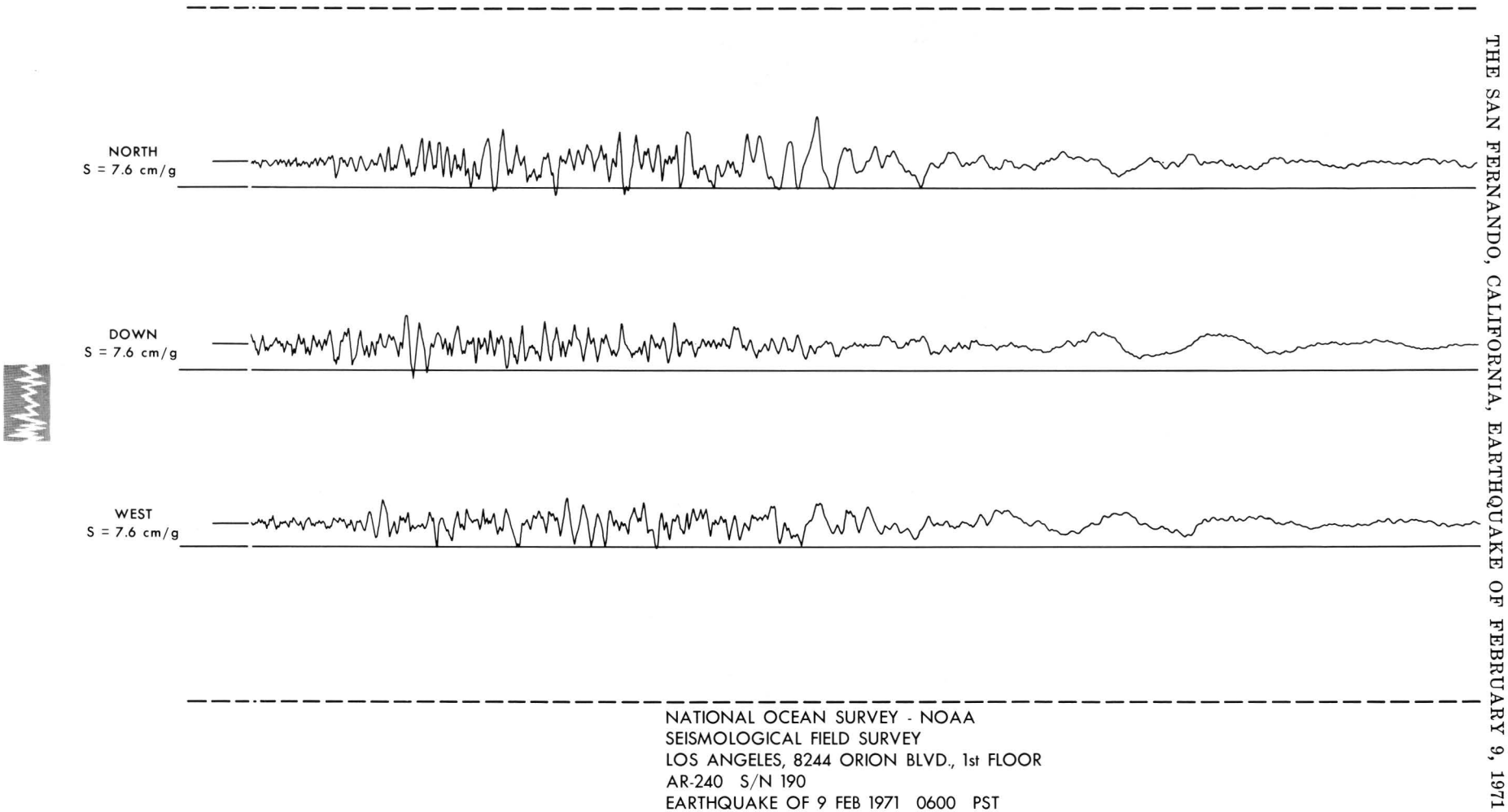

FIGURE 10.—Accelerograph record, Los Angeles, 8244 Orion, first floor.

EVIDENCE OF RECORD VERTICAL ACCELERATIONS AT KAGEL CANYON DURING THE EARTHQUAKE

By B. J. MORRILL
NATIONAL OCEAN SURVEY, NATIONAL OCEANIC AND ATMOSPHERIC ADMINISTRATION

The earthquake of February 9, 1971, which caused great damage in the foothills of the northern part of San Fernando Valley and which was felt throughout the greater part of southern California, produced evidence of vertical accelerations far in excess of any ever recorded instrumentally. The largest vertical accelerations recorded by a strong-motion seismograph during this quake were in the range of 0.5 to 0.75 g at Pacoima Dam, some 2.75 miles north-northwest of the Kagel Canyon Fire Station. Pacoima Dam is 5 miles and the Fire Station is 8 miles from the epicenter. The particular evidence was noted at the Los Angeles County Fire Station No. 74, 12587 North Dexter Park Road (Kagel Canyon), San Fernando, and it suggests that the vertical acceleration exceeded that of gravity and may have equaled or exceeded that of the great Assam earthquake of June 12, 1897 (Oldham, 1897) in very local situations such as described here. The questionnaire card shown in figure 1 indicates that the motion was extremely violent.

Firemen were resting in the wood-frame quarters building shown in figure 2. Mr. J. White, duty fireman, stated that he was tossed out of bed onto the floor, and the bed landed on top of him. Every object in the building was upset. Even the handset of a standard wall phone came off its hook. Loud cracking and thunderlike noises added to the general confusion. The building was shifted off its foundation. Outside, rocks were thrown off the ground, and large cracks appeared in both soil and rock. The rear view of the quarters building in figure 3 shows one of the many ground cracks that appeared throughout the area. The surface of a hill adjacent to the building exhibited the "shattered earth" effect reported (see section by R. Nason, this report) a few miles to the west. A nearby rock roadcut appeared to have exploded, and the adjacent road was offset in many places (figs. 4 through 6).

A 20-ton fire truck enclosed in the garage (figs. 7 and 8) moved 6 to 8 feet fore and aft, 2 to 3 feet sideways without leaving visible skid marks on the garage floor. The truck was in gear, and the brakes were set. Damage to the truck was a bent rear step, broken windshield, shattered red light, and siren broken off. Also, a ladder and a hook were broken. Marks which appear to have been made by the right rear tire were found on the door frame (fig. 9) 3 feet above the floor, while the metal fender was not damaged. The fender extends several inches out beyond the upper portion of the tire. Four feet above the floor the hose rack was broken by the rear step of the truck. The step was bent up while the hose rack was broken downward. The rear of the garage was pushed outward 6 to 8 inches, and the final position of the truck was about 4 feet out the front of the garage, with the garage door resting on the cab.

Figure 10 shows the northwest corner of the quarters building. Note that the bottom row of shingles is undisturbed. These shingles prior to the quake overlapped the foundation 4⅜ inches. Figures 11 and 12 show a plan and an elevation view of figure 10 with appropriate measurements taken shortly after the quake.

Figures 10, 11, and 12 suggest that the building accelerated upward, with respect to the ground, at a rate of at least 1 g for about 0.1 second; that is, if one assumes only 1 g and the given distance.

There is other evidence of catastrophic accelerations in the immediate area of the earthquake, of ground cracking and faulting. In Soledad Canyon, champagne glasses were broken at the base of the stems without unusual horizontal displacement. In

NOS FORM 680 (11-70)

U.S. DEPARTMENT OF COMMERCE
NATIONAL OCEANIC AND ATMOSPHERIC ADMINISTRATION
NATIONAL OCEAN SURVEY

OMB No. 41-R0013
Approval Expires June 30, 1975

EARTHQUAKE REPORT

1. An earthquake was felt [X]; not felt [ ]

Time 0601 A.M. _____ P.M.

Date of shock February 9, 1971

If felt, please supply information below *(Underline appropriate words or fill spaces.)*
If not felt, please sign and return card, which requires no postage.

2. YOUR LOCATION DURING EARTHQUAKE

a. City, County, State, and Township L.A. County, Calif.
Range, Section, Quarter Section, or Coordinates R-3N-14W. Sec. 32

b. Ground:
Rocky, gravelly, loose, compact, marshy, filled in, or _____
(Level) sloping, steep, or _____

c. If inside, type of construction
Wood, brick, stone, or wood frame

d. Quality of construction
New, (old), well built, poorly built, or _____

e. No. of floors in building	f. Observer's floor	g. Activity when earthquake occurred: Walking, (sitting), lying down, sleeping	h. If outside, you, others were: Quiet, active
Single	1st		

3. EFFECTS ON POPULATION

a. Felt by:
Very few, several, many, all (in your home) (in community)

b. Awakened:
No one, few, many, all (in your home) (in community)

c. Frightened:
No one, few, many, all (in your home) (in community) general panic

4. RELATED SOUNDS

a. Rattling of windows, doors, dishes, etc. All of above prior to shock

b. Creaking of building (Describe) Loud-snapping

c. Earth noises: Faint, moderate, loud Loud-similar to Jet

5. PHYSICAL EFFECTS AND DAMAGE

a. Outside:
(1) Trees and bushes shaken, vehicles rocked, etc. Yes
(2) Ground cracked; landslides; water disturbed, etc. All of these
(3) Chimneys, tombstones, elevated water tanks, etc., cracked, twisted, overturned All of these
(4) Other effects _____

b. Buildings:
(1) Hanging objects swung moderately, (violently) Direction East to West
(2) Small objects shifted, overturned, fell Yes
(3) Furniture shifted, overturned, broken Yes
(4) Plaster cracked, broken, fell Yes
(5) Windows cracked Yes
(6) Structural elements of brick, wood, or Wood
Damage slight, moderate, great Great

Signature and address of observer

Scott E. Franklin Eng. 74
Capt. LA County Fire Dept.

12587 N. Dexter Pk Rd
San Fernando
(Kagel Cyn.)

Additional information will be appreciated. Use space on reverse side.

FIGURE 1.—Earthquake report questionnaire indicates violent motion felt in Kagel Canyon.

many places transformers were lifted out of their brackets. Seismoscope records in some locations showed interruptions in their traces, which suggest that the styli left the smoke glass plates. Figure 13 shows one of these records.

ACKNOWLEDGMENTS

The patience and cooperation of the people of Kagel Canyon so soon after their disaster is very much appreciated.

Members of the Earthquake Mechanism Laboratory, NOAA, headed by Dr. Don Tocher, reviewed the manuscript.

REFERENCE

Oldham, R. D., 1897, Report on the Great Earthquake of June 12, 1897: India Geol. Survey Mem. v. 29 [1899].

FIGURE 2.—Quarters building of Los Angeles County Fire Station No. 74 (Kagel Canyon).

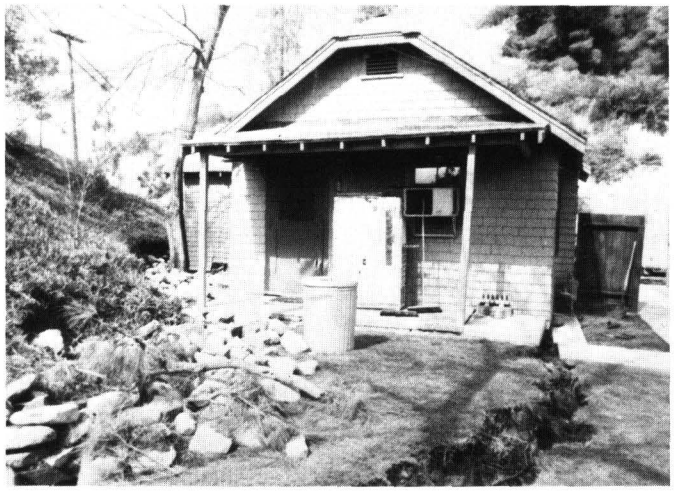

FIGURE 3.—Rear view of figure 2, showing one of the many ground cracks in the area.

FIGURE 4.—Tossed-earth effect noted at top of rock hill beside quarters building.

FIGURE 5.—Typical road cracking and offsets in immediate area.

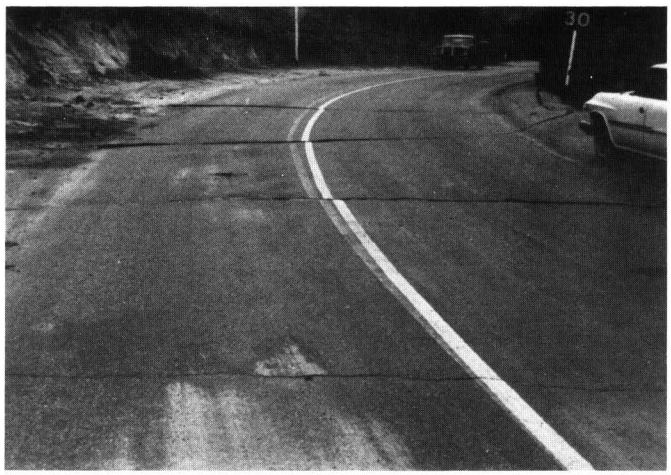

FIGURE 6.—Highway cracks and offsets. Rocks in face of road cut shattered with explosive intensity.

FIGURE 8.—Front view of fire truck shows broken windshield, damaged red light, and siren

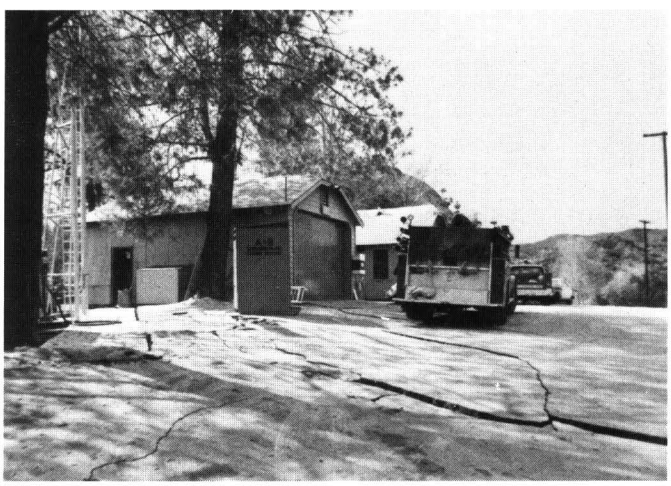

FIGURE 7.—Twenty-ton fire truck, located in garage at left, was moved several feet forward, backward, and sideways, without leaving visible skid marks on floor.

FIGURE 9.—Damage to garage interior. Rubber marks on door frame appear to have been made by rear tire of truck.

FIGURE 10.—Northwest corner of quarters building showing shingles which overlapped foundation. Shingles on opposite side of building also undamaged.

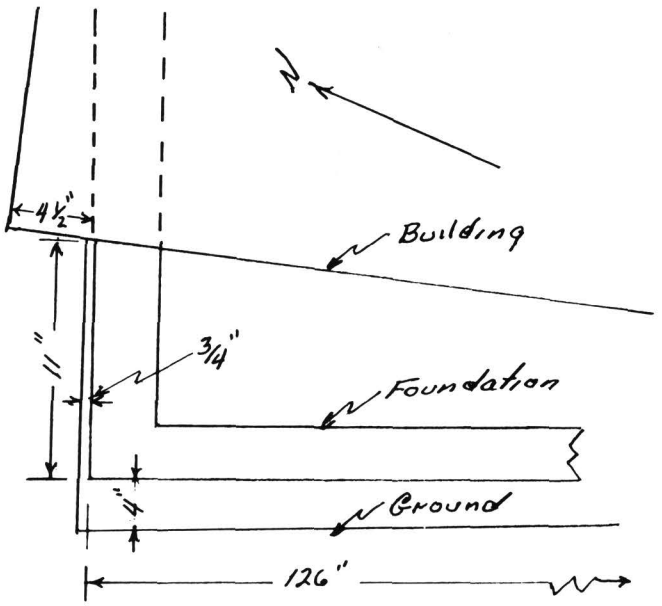

FIGURE 11.—Plan view of quarters building, northwest corner.

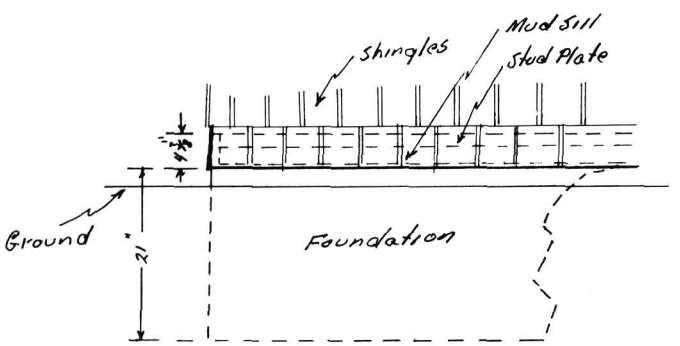

FIGURE 12.—Elevation view of quarters building, northwest corner.

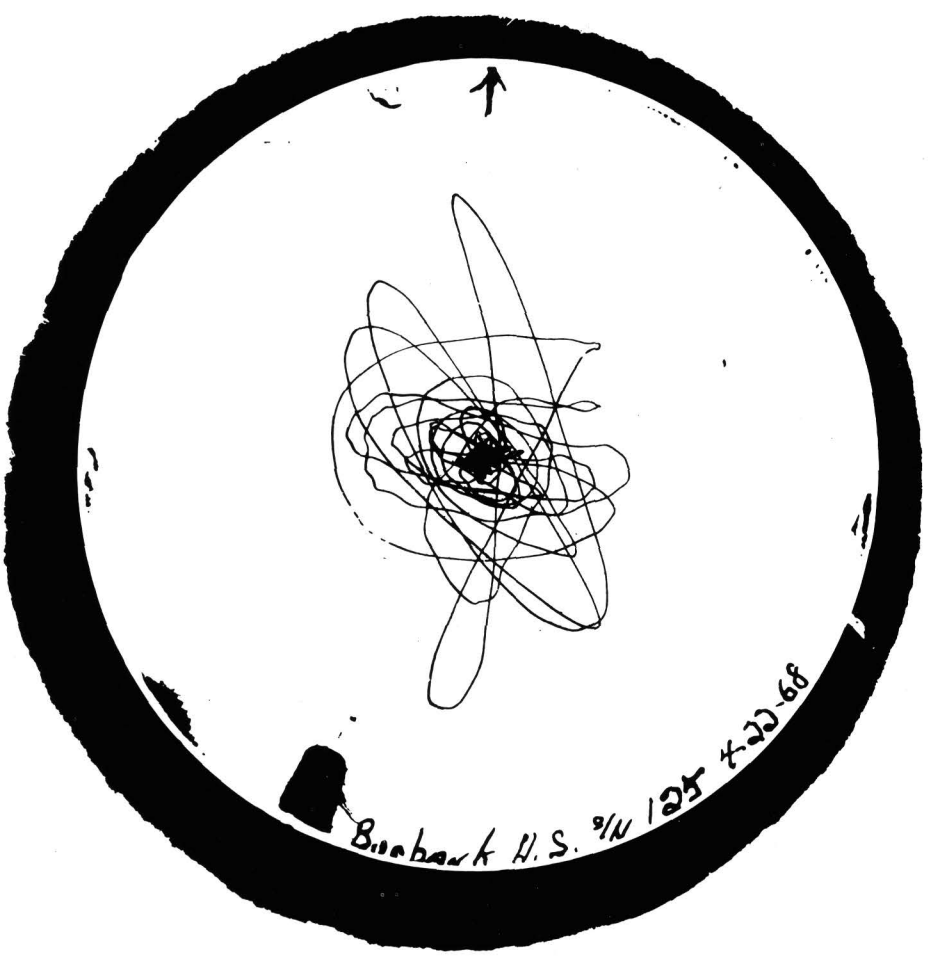

FIGURE 13.—Burbank High School seismoscope record. Vertical motion lifted stylus arm and interrupted trace.

PRELIMINARY REPORT OF AN ENGINEERING STUDY

This preliminary report on the engineering study of the San Fernando earthquake was prepared by the Earthquake Engineering Research Institute (EERI) under contract with the National Oceanic and Atmospheric Administration of the Department of Commerce. The EERI is a nonprofit organization composed of engineers and scientists from many earthquake-related disciplines. The membership is by invitation and is drawn from government, university, and private professional practice. The members of the EERI Committee are D. F. Moran, Chairman, Clarence Allen, W. A. Brugger, L. LeRoy Crandall, H. J. Degenkolb, C. M. Duke, J. F. Meehan, C. W. Pinkham, and Robert E. Wallace. Karl V. Steinbrugge provides liaison between the National Oceanic and Atmospheric Administration and the Earthquake Engineering Research Institute. A list of cooperating organizations is given at the end of the report.

INTRODUCTION TO THE ENGINEERING STUDY

By EARTHQUAKE ENGINEERING RESEARCH INSTITUTE COMMITTEE

The San Fernando earthquake of February 9, 1971, is very significant for several reasons.

Despite the moderate magnitude of 6.6, damage to structures, utilities, and transportation systems was severe over a small area. We must consider this earthquake as another warning. As in Long Beach (1933) and Alaska (1964), the off-hours timing (6:01 a.m.) was fortunate, and the resulting loss of life and injuries were only a small fraction of what might have resulted had the earthquake occurred 1 or 2 hours later.

The collapse of structures at the Olive View Hospital and the freeway bridges, combined with severe damage to roads and freeways, would have resulted in a large loss of life and many injuries. (See figs. 1 and 2 for maps of the area.) Collapse of old, unreinforced masonry walls would have caused additional deaths and injuries. Even so, 45 persons were killed by collapse of a portion of the Veterans Hospital in Sylmar.

We must learn important lessons from this earthquake which we can apply to improvement of our building codes, emergency procedures, and transportation facilities. We may not be so fortunate when the next earthquake occurs.

This shock is also significant because of the 200 records that were made by strong-motion instruments. In about each of 50 tall buildings three instruments were installed and operating, generally one in the basement or ground floor, one about midheight, and one on the roof. Records of all of these and other instruments will provide us with a wealth of data for evaluation of performance of all types of structures. This is easily the most instrumentally important earthquake which has ever occurred.

The earthquake also provided the first real test of earthquake-resistive construction as it is practiced in California.

Many structures failed the test. The three major multistory buildings in the area were hospitals, and all had to be evacuated owing to severe structural damage. Several freeway-bridge collapses caused closing of three major freeways and one railway north of Los Angeles.

Residential and apartment damage was heavy,

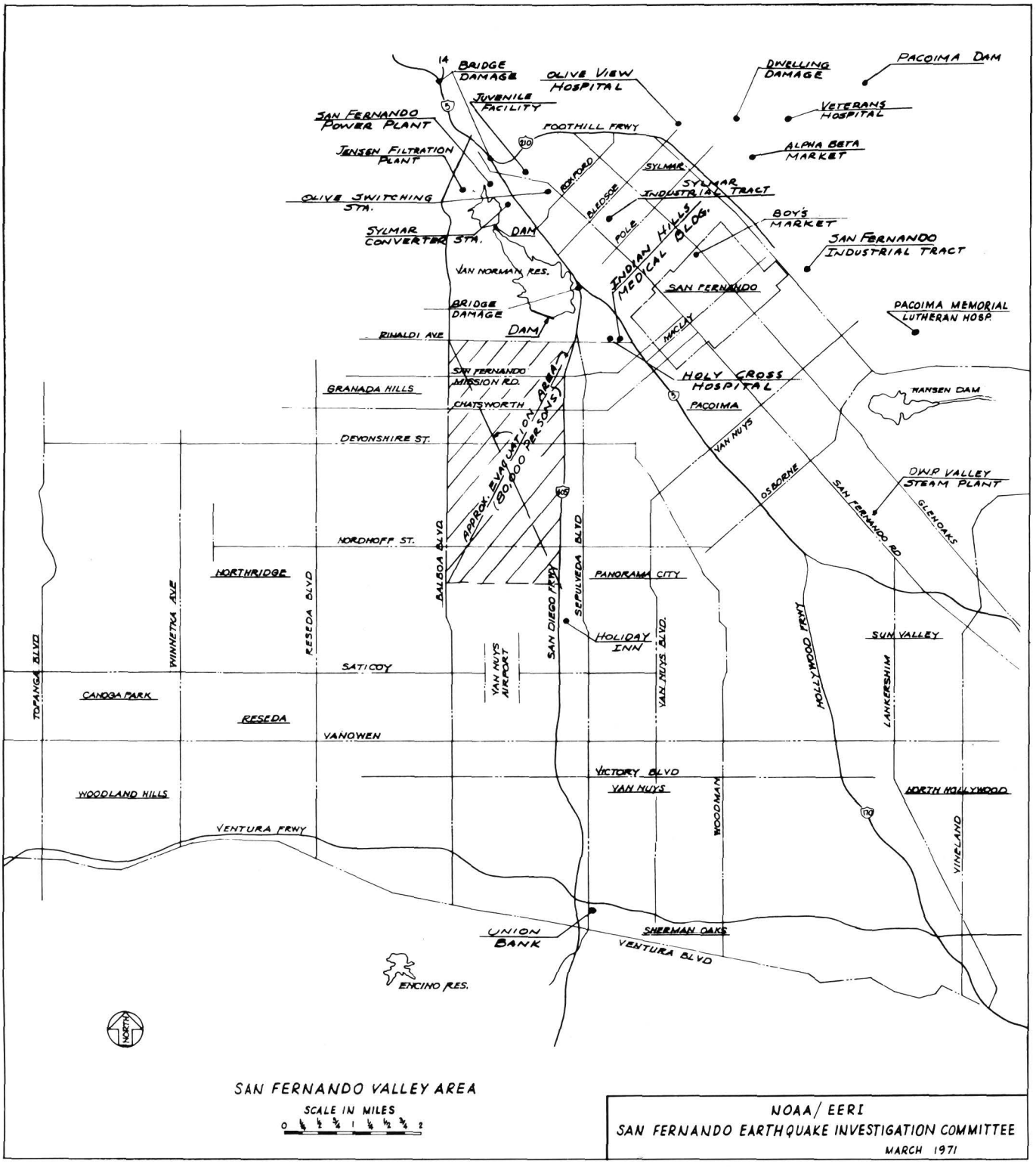

FIGURE 1.—San Fernando area.

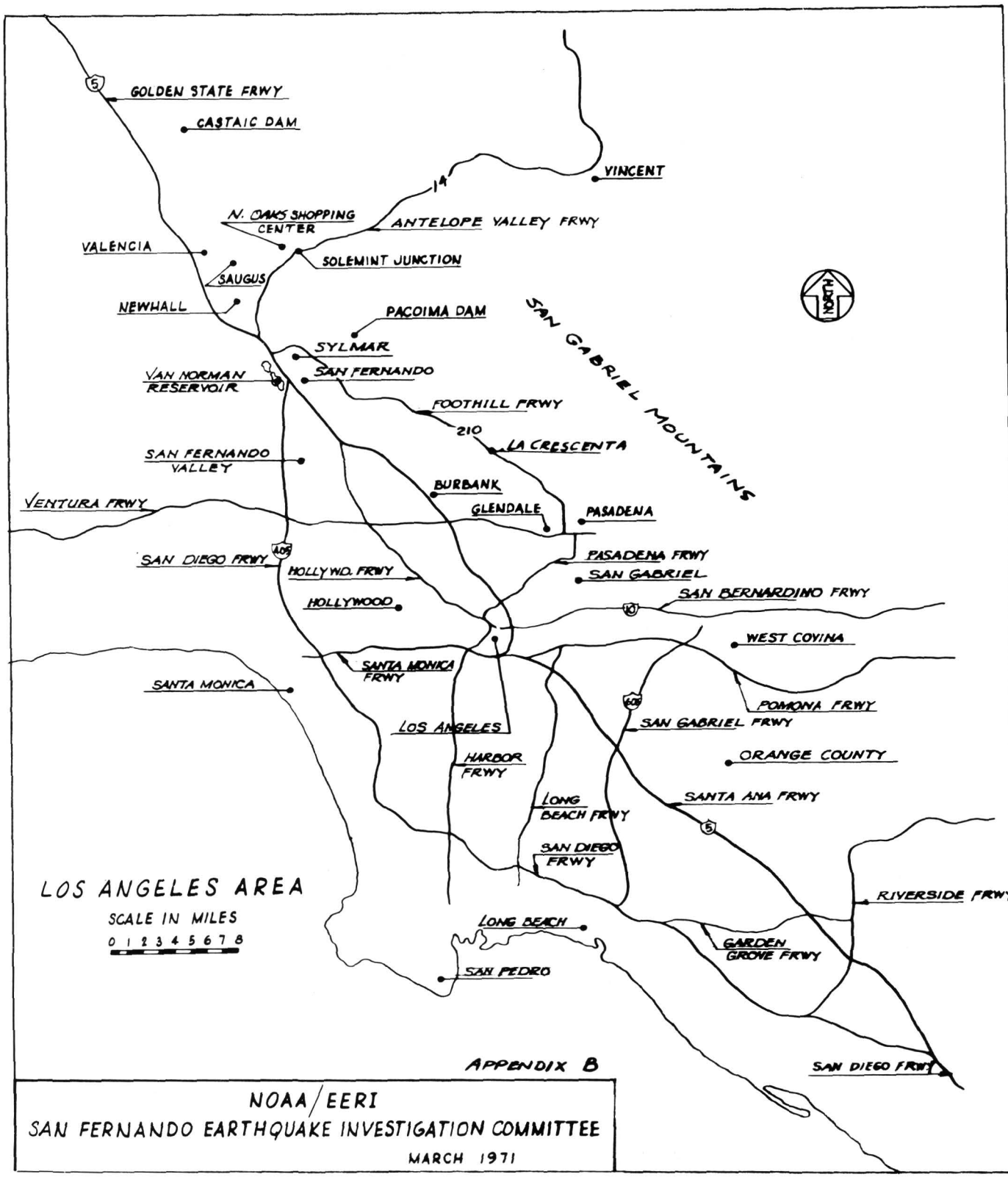

FIGURE 2.—Los Angeles area.

even to newer types. Undoubtedly, ground lurching, settling, and cracking contributed to the damage.

Detailed studies of perhaps 50 structures including buildings, bridges, dams, and dwellings will be be made.

Analysis of structures will be correlated with instrumental records. Included will be several high-rise structures which produced records.

The economic loss for this shock is estimated at one billion dollars, with about one-half for private and the other half for public properties.

Extensive studies must be made to determine the relative effects on damage of ground movements such as lurching, settling, cracking, and compression as compared with the effects of ground vibration.

The exact cause of damage to many structures may never be clearly known. There are strong evidences of severe vertical accelerations which could contribute to increased damage.

This preliminary report is necessarily brief and limited to descriptions of what was there and what happened to it. Many facts about damage and detailed statistical data are not available at this time. It is too early to reach conclusions and make significant recommendations.

The committee is convinced that the importance of this earthquake justifies a major investigation. We must learn as much as possible from this moderate quake before the next disastrous temblor comes.

We wish to acknowledge the valuable contributions of the various subcommittees and organizations. We are particularly grateful for the section on buildings which was provided by members of the Structural Engineers Association of California. Many structural engineers examined damaged structures and provided reports thereon as a service to their profession.

All organizations and agencies contacted have responded willingly and offered the committee their data, reports, and photographs for use in its investigation.

SOILS AND FOUNDATIONS

By L. LeRoy Crandall
L. LeRoy Crandall and Associates

With few exceptions, the buildings in the area of the greatest damage are underlain by a varying thickness of recent alluvial deposits. In the San Fernando portion of the San Fernando Valley, these alluvial deposits are relatively granular, consisting primarily of sands and silts. It is apparent that the bedrock motions during the earthquake were amplified several-fold, resulting in much larger ground-surface accelerations and amplitudes than might otherwise be expected from an earthquake of magnitude 6.6.

Although the surface accelerations were large, the greatest damage to structures and utilities may have been caused by ruptures and fractures in the earth's surface. Measurements of the permanent earth displacements are only in the preliminary stages as yet, but it is apparent that lateral and vertical offsets of several feet have occurred along some of the ruptures in the alluvial soils. The rupturing seems to occur in an east-west direction in several belts extending across the northern San Fernando Valley. Ruptures have also been observed in the hills to the north and east, but very few buildings are located on the relatively steep hillsides. Highways and transmission lines in those areas, however, suffered severe damage, particularly the bridge structures of the freeways. The cause of the extensive ground rupturing is one of the important aspects of the earthquake yet to be determined. While many believe the rupturing is a result of tectonic movements in the bedrock, there is the possibility that the permanent surface displacement resulted from extreme ground shaking.

Most buildings in the area are supported on conventional spread footings, although some of the taller structures are on drilled cast-in-place friction piles. Except where actual ground rupturing occurred beneath a building, the foundations of the buildings appear to have functioned satisfactorily. This observation is based on very limited investigation, however, and much study remains to be done before definite conclusions can be drawn. There is no doubt, however, that severe damage occurred to all buildings which were subjected to significant ground rupturing. Much thought needs to be given to methods of minimizing the effects of such permanent ground displacements, although it is doubtful that anything can be done to prevent serious structural damage in such cases. In passing, great praise should be given to the structural engineers whose buildings, for the most part, refused to collapse even though rent asunder by deformations of several feet. The fact that many of the buildings are standing at all should be heartening to those who occupy the structures and whose lives would be in jeopardy in less well-designed and less well-built structures.

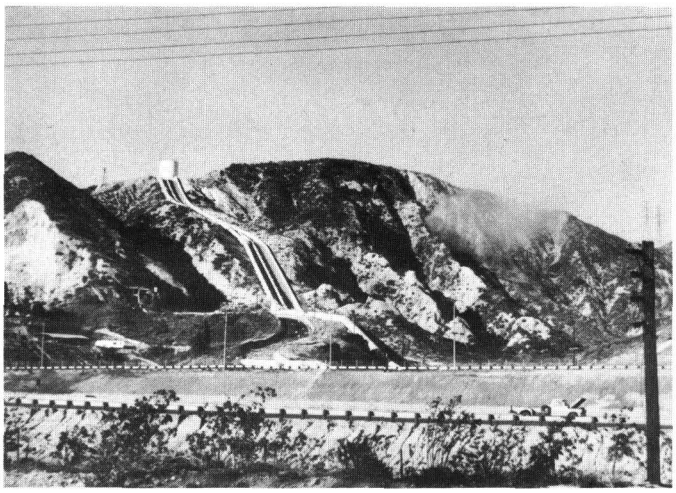

FIGURE 1.—Earthslide, afternoon of February 9, 1971, near intersection of Routes 5 and 14. J. F. Meehan, OAC photograph.

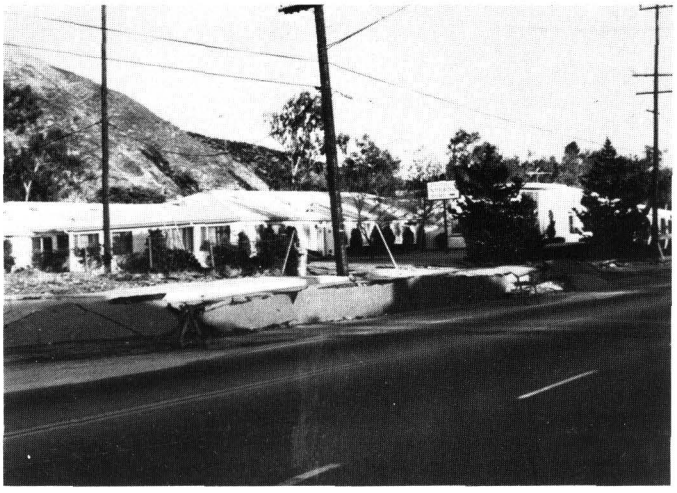

FIGURE 3.—Foothill Boulevard, east of Arroyo. Compression ridge in street, J. F. Meehan, OAC photograph.

FIGURE 2.—Surface expression of movement 2½ feet vertically, Lopez Canyon and Foothill Boulevard, J. F. Meehan, OAC photograph.

FIGURE 4.—Sidewalk, San Fernando Industrial Park. J. F. Meehan, OAC Photograph.

DAMAGE TO THE OLIVE VIEW HOSPITAL BUILDINGS

By EARTHQUAKE ENGINEERING RESEARCH INSTITUTE COMMITTEE

The Olive View Hospital is a new facility owned by the County of Los Angeles. There are five structures in the complex; a large five-story medical-treatment and care facility, a two-story psychiatric unit, power plant, assembly building, and small parking shelter (fig. 1).

Foundations are reinforced concrete, spread type.

The medical-care facility is a five-story reinforced-concrete structure over a basement area larger than the building above. Concrete is hardrock. The basement-floor level is at grade on the south and east sides but is buried at the north and west sides. The basement areas which extend beyond the structure above have dirt and planting supported on the basement-roof areas.

The plan is roughly cross shaped with four structurally-separated stair towers and recreation areas, located at the ends of each wing. Towers are supported over larger basement areas except for the tower located on the north side.

Construction is reinforced concrete. Generally, floor and roof are flat slabs with drop panels at columns. The lateral-force bracing system consists of reinforced-concrete shear walls for the top four stories and moment-resisting frames for the lower story and basement.

Ground breakage occurring in this area consisted of cracks in ground and paving and also compression ridges. An eyewitness describes the first and last movements as strongly vertical.

Areas of the basement collapsed, mainly outside of the structure supported above. Some perimeter basement columns punched through the slabs supporting earth and planting above (fig. 2). All towers except the north tower fell away from the main building and rested on their sides. The north tower is leaning but still standing. The collapsed towers pushed into the basement below and tore away vertically adjacent to the main building in some cases.

The main building suffered severe damage to the first-story columns above the basement and is leaning about 1½ feet to the north in the first story (fig. 3). Damage to the upper four floors is only moderate. Most first-story columns are square with round, spirally wrapped cores except for those at the corners, which are "*L*" shaped and tied. At the exterior walls, number 18 reinforcing bars extend from the basement columns up about 5 or 6 feet into the corners of the spirally wrapped columns above (fig. 4). These bars generally broke out of the corners. The round column cores were badly crushed, but concrete remained inside the spirals. Corner columns were badly fractured (fig. 5), many ties were broken, and some concrete fell from inside the vertical bars.

The assembly building is a one-story reinforced-concrete structure located just north of the medical care building (fig. 6). This structure is leaning about 18 inches toward the north (fig. 7).

The psychiatric unit was a two-story reinforced concrete structure. Floors and roof are pan-joist construction. Concrete above grade is lightweight. Lateral-force resisting system is by frame action for both floors. Columns are tied.

Columns in the first story failed (fig. 8), and the second floor is resting on the grade slab. Columns are badly shattered with broken ties, and much of the concrete is displaced from inside reinforcing bars. Direction of failure seems to be in a south and east direction (fig. 9).

The power station suffered severe damage to contents. Boilers were shifted as much as 4 feet. Piping and electrical and mechanical equipment were badly damaged (fig. 10). Steel flat-bar bracing in the north wall was stretched and broken (fig. 11). However, the reinforced-masonry shear wall at the south side was only slightly cracked.

The one-story parking shelter has a reinforced-concrete roof slab supported on columns. There are no walls. Columns failed, generally at the top, and the roof fell on several vehicles (fig. 12).

A special committee of members of the Structural Engineers Association of Southern California, with William T. Wheeler as chairman, has been appointed to study damage to this hospital facility for the County of Los Angeles.

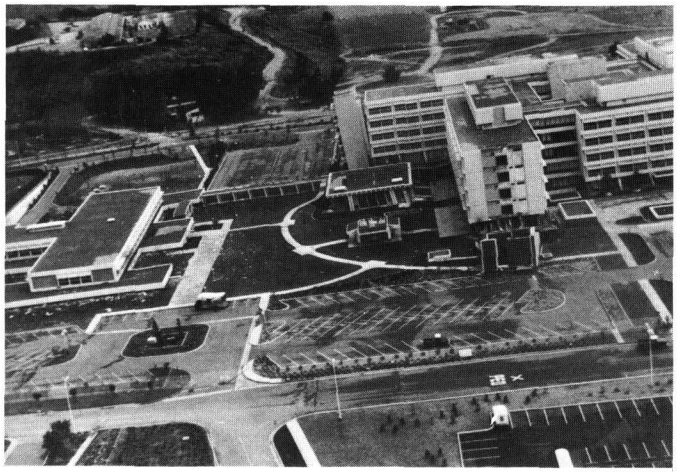

FIGURE 1.—Olive View Hospital. Medical Care Building on right, Assembly Building in center, and Psychiatric Unit at left.

FIGURE 2.—Olive View. South side of Medical Care Building. Columns punched through basement roof slab.

FIGURE 3.—Olive View, Medical Care Facility, north wall. Note shattered concrete in corner column.

FIGURE 4.—Olive View, Medical Care Facility. Spirally-wrapped column with number 18 corner bars.

FIGURE 5.—Olive View Medical Care Building. Corner column, first story.

FIGURE 6.—Olive View Medical Care Building. First-and second-story columns.

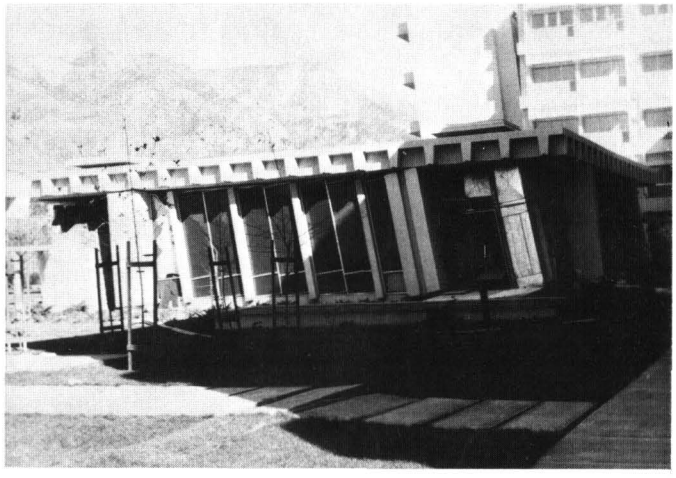

FIGURE 7.—Olive View Assembly Building.

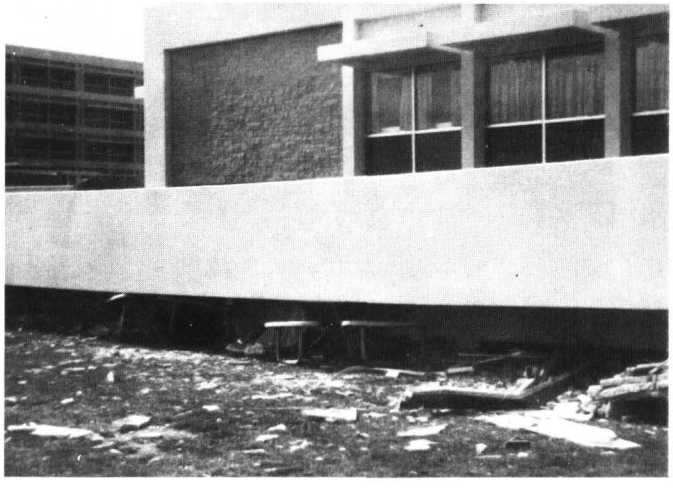

FIGURE 8.—Olive View Psychiatric Unit. Second floor rests on tables and chairs.

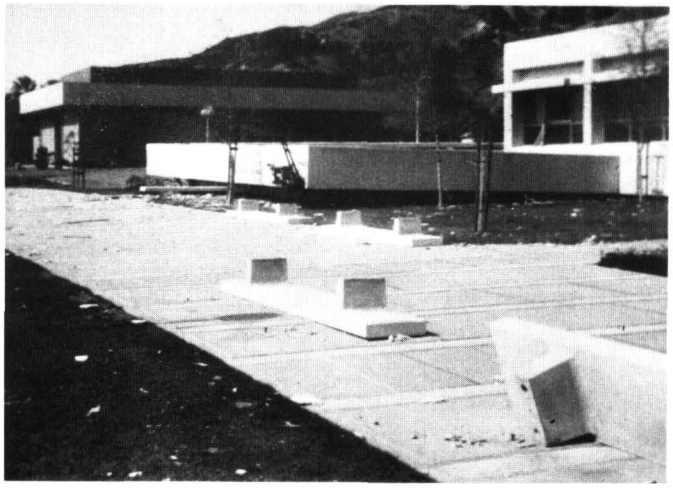

FIGURE 9.—Olive View Hospital. Overturned concrete benches. Psychiatric Unit in background.

FIGURE 10.—Olive View Power Building. Bent pipe hanger.

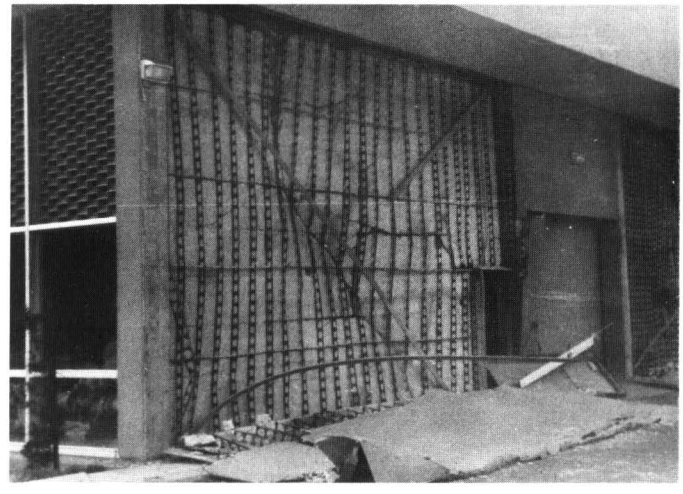

FIGURE 11.—Olive View Power Building. Flat-bar bracing broken in north wall.

FIGURE 12.—Olive View Parking Shelter.

DAMAGE TO THE LOS ANGELES COUNTY JUVENILE FACILITIES, SYLMAR

By JAMES H. THOMPSON
WILSON AND THOMPSON, CONSULTING STRUCTURAL ENGINEERS

The Juvenile Hall facilities comprise many one- and two-story buildings constructed of concrete floors and roofs with concrete frame or reinforced masonry bearing walls and in some cases nonbearing walls. Design is based on a modern building code with earthquake-resistive requirements.

The area was subjected to very heavy ground movement. Fissures opened that measured 18 to 24 inches wide at the top with a depth of 4 to 5 feet (fig. 1). Lateral differential movement occurred, causing pavement to rupture and slide as much as 1 to 2 feet over adjacent pavement. Vertical movement occurred, causing heaving up of large areas several feet high and depressions in other areas. Generally, movement was very large, resulting in permanent ground displacements and extensive damage to the building construction.

Damage to buildings was very heavy and extensive (fig. 2). Virtually every building received significant structural damage, except the gymnasium and one or two other buildings.

A portion of the two-story administration building (concrete frame) collapsed completely in the first story (fig. 3). Other one-story buildings have either collapsed or are nearing collapse. Many masonry walls were cracked and shattered or experienced heavy displacement (fig. 4). Hammering effects between adjacent buildings is evident in many places and caused significant structural damage along interface lines.

Preliminary estimates indicate that few, if any, of the damaged buildings can be saved.

FIGURE 1.—Juvenile Hall. Ground crack opening in girls dormitory. J. F. Meehan, photograph.

FIGURE 2.—Juvenile Hall. Detail of wall failure. J. F. Meehan, OAC photograph.

FIGURE 3.—Juvenile Hall. Cracks in pavement extend under collapsed administration building. J. F. Meehan, OAC photograph.

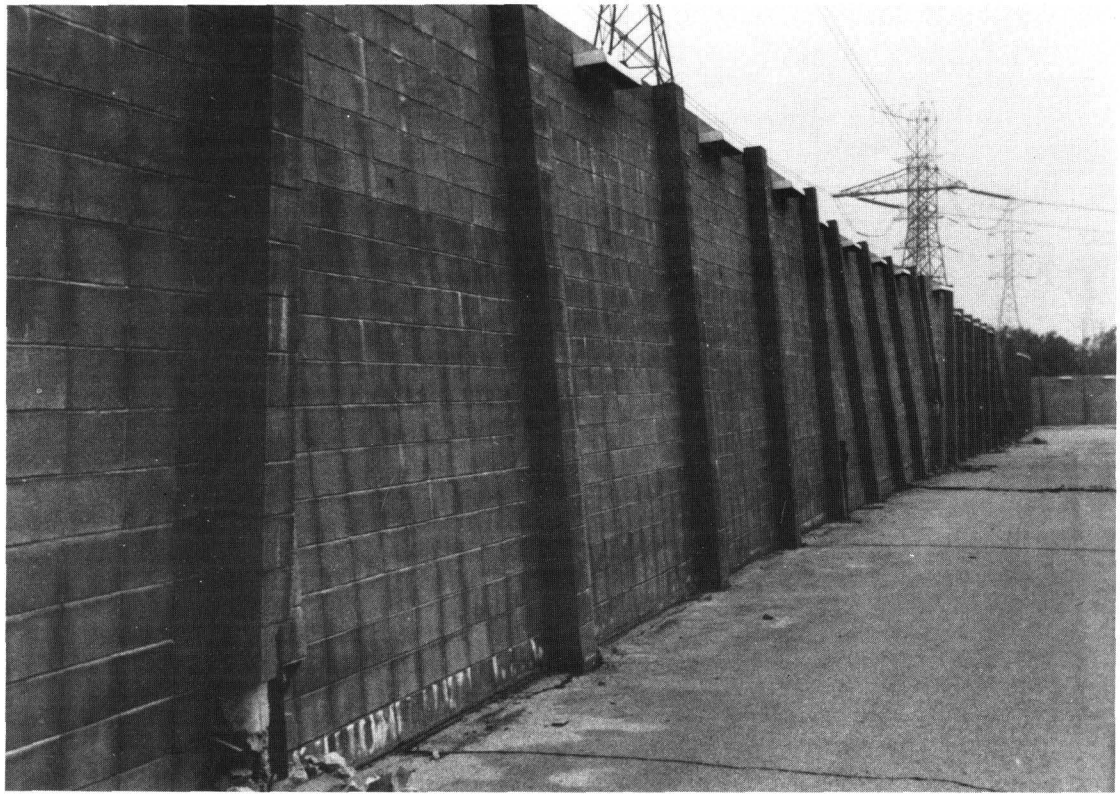

FIGURE 4.—Juvenile Hall. Cantilevered walls leaning. J. F. Meehan, OAC Photograph.

DAMAGE TO THE PACOIMA MEMORIAL LUTHERAN HOSPITAL

(11600 Eldridge Avenue, Pacoima)

By WILLIAM F. ROPP
DANIEL, MANN, JOHNSON, AND MENDENHALL, ARCHITECTS AND ENGINEERS

The building is composed of three sections isolated from each other by separation joints (fig. 1). The south section is one story in height, the north section is two and three stories in height, and the center section, or Nursing Tower, is four full stories in height with a mechanical penthouse.

The building is reinforced concrete and reinforced masonry. The floor and roof structures are reinforced concrete pan-joisted slabs supported by reinforced concrete beams. Shear walls for the south and center sections are reinforced concrete, while several of the shear walls for the north and south sections are reinforced brick masonry.

The building is supported by a foundation consisting of drilled concrete piles in clusters approximately 40 feet in length.

Damage to the building caused by the earthquake was massive. It is evident that the structure experienced sufficient seismic forces to cause actual uplift (fig. 2). The east end wall of the center section (fig. 3), which is a major horizontal load-resisting element of the structure, was cracked sufficiently to render it ineffective for further usage. The west end wall of the center section, also a major horizontal load resisting element, was badly cracked, though not as badly as the east wall. Some south wall piers of the center section, which act as both vertical and horizontal load resisting elements, are badly cracked near the second-floor level. Floor slabs of the second and third floors have sustained large diagonal cracks near the juncture with the end walls. This was caused by large horizontal forces being delivered to the end shear walls.

There is evidence of vertical misalignment of floor slabs which occurred during the rocking and apparent uplift of the structure.

A severe diagonal crack has occurred in the west wall of the cafeteria located in the south section (fig. 4).

This structure, built in 1959, was designed to, and did, comply with the requirements of the Los Angeles City Building Code in force at that time. The design and construction of the building was checked and approved by the Los Angeles Department of Building and Safety. In accordance with the requirements of the Building Code, the structure was designed to resist equivalent horizontal forces of approximately 10 percent of gravity. There is substantial evidence that the actual horizontal-force magnitude experienced was several times that amount.

The feasibility of restoration of the building has been considered. The north and south sections of the building could be restored with confidence, as the damage appears to be light. Restoration of the Nursing Tower, the four-story building, could entail the following:

1. Removal and replacement of the damaged east shear wall. This would require shoring of adjacent structure until replacement was complete.
2. Removal and replacement of west shear wall.
3. Removal and replacement of damaged wall piers on south wall.
4. Realignment of vertically displaced floor slabs.
5. Removal and replacement of damaged floor slabs at ends of building.
6. Exposure and repair, if required, of drilled pile footings at perimeter of tower.
7. Exposure and repair, if required, of interior bearing walls and columns.
8. Exposure and repair, if required, of interior block walls.

9. Replacement of slabs, floor finish, and ceilings removed for above noted exposure.
10. Restoration of wall finish, tile, door frames, ceilings, and other finish damaged during the earthquake.
11. Restoration of mechanical and electrical systems disturbed during rehabilitation.
12. The possible construction of additional shear-resisting elements.

The Department of Building and Safety will require that restoration include the bringing of the structure up to 1971 code requirements, including that for earthquake protection.

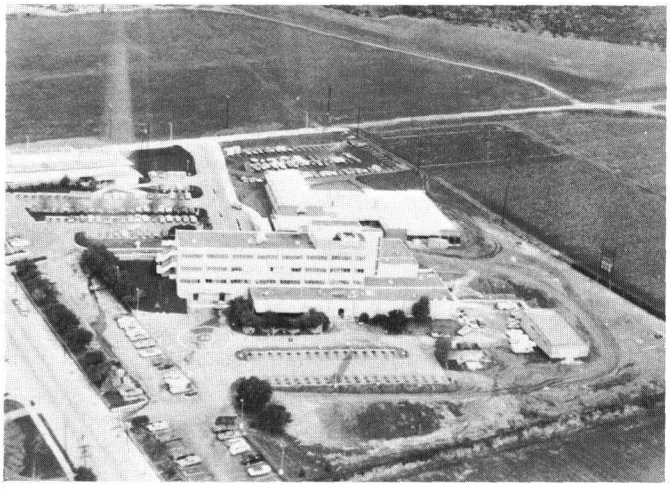

FIGURE 1.—Pacoima Memorial Lutheran Hospital. New addition in rear. J. F. Meehan, OAC photograph.

FIGURE 2.—Pacoima Memorial Lutheran Hospital ground cracks at north wall. Building raised about five inches relative to ground. D. F. Moran photograph.

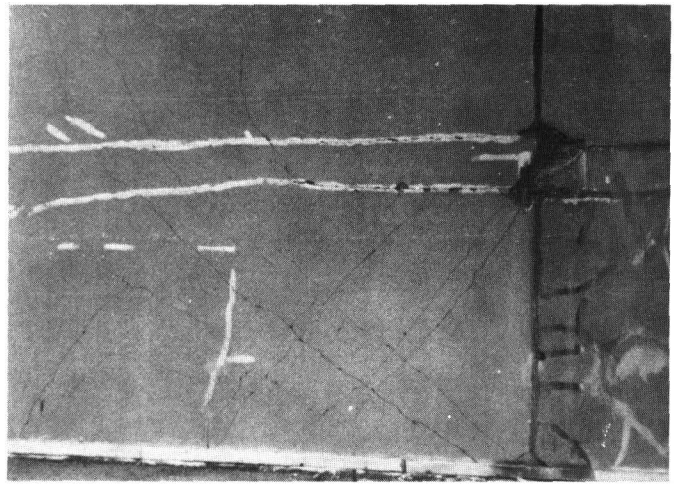

FIGURE 3.—Pacoima Memorial Lutheran Hospital, east shear wall diagonal cracks. White lines are patching before earthquake. D. F. Moran photograph.

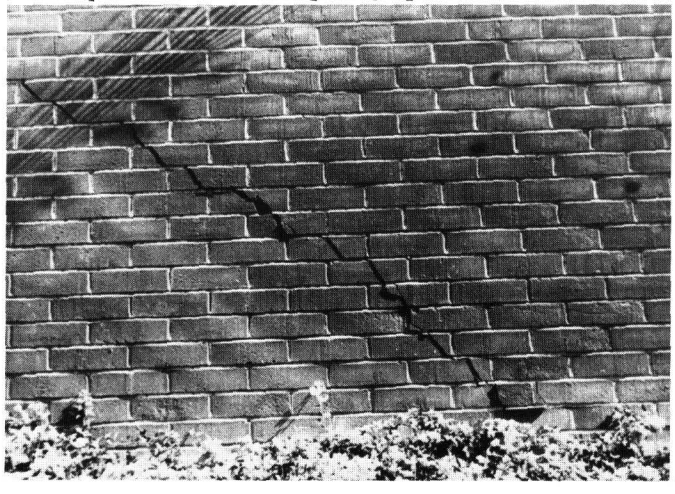

FIGURE 4.—Pacoima Memorial Lutheran Hospital cracked brick wall at west side of south section.

DAMAGE TO THE HOLY CROSS HOSPITAL

(15031 Rinaldi, Granada Hills)

By S. B. BARNES
S. B. BARNES AND ASSOCIATES

This hospital is a 10-year old seven-story building containing about 162 two-bed rooms plus necessary support units including administration, pathology, radiology, maternity, operating, kitchen, cafeteria, and laundry facilities. The basic seven-story tower has plan dimensions of about 89×184 feet, and its longitudinal axis extends approximately in an east-west direction (fig. 1). There is a three-story north wing and a one-story south wing (fig. 2). The wings are attached to the basic tower area. There is a basement under a portion of the tower area.

The framing system consists of lightweight concrete pan joist and beam floors supported by stone concrete columns and bearing walls. Foundations are drilled cast-in-place friction piles. Plans call for the ultimate compressive strength to be 3,000 psi for the lightweight concrete and 5,000 psi for the stone concrete in the tower area. Resistance to lateral loads is provided by a box system consisting of the floor and roof diaphragms supported by the concrete shear walls.

Damage to the structure was severe below the sixth floor. The most severe damage occurred in the second to fourth stories where shear walls underwent considerable diagonal cracking and some columns and beams failed (fig. 3). Horizontal cracks at pour lines are apparent in all shear walls. From the fourth floor downward, lateral loads due to the mass of the north wing appear to have contributed to the severity of damage in the second to fourth stories.

At the south end of the tower area is a pair of transverse shear walls interconnected by spandrel beams at floor lines and extending up from the second floor to the roof of the tower. The floor diaphragms at the third and fourth floors almost completely separated from this pair of shear walls. Columns on the same line as the pair of shear walls failed above the third floor. Beam failures occurred at both the third and the fourth floors where they spanned in a direction of 90° to the line of the shear walls. Floor diaphragms near this region sustained severe diagonal cracking at the second through fourth floors. Overturning moments in each of this pair of shear walls caused much spalling and crushing of concrete within the depth of the third-floor framing.

Distress in the transverse shear walls at the east end of the tower is also apparent (fig. 4). One of these walls which connects to the easterly corner column of the tower and extends from the third floor to the tower roof has severe diagonal cracking in the third and fourth stories. Crushing and spalling of the fourth-floor pour intrusion has occurred at the corner column resulting in column failure just above the floor pour as well (fig. 5).

Architectural columns of 16×32 inches spaced at 23-foot centers along the south and north sides of the tower have severe diagonal cracking and spalling within the third and fourth stories. Spandrel beams connecting these columns have medium intensity cracking, including horizontal cracks along the pour lines at the tops of floor slabs.

The third-floor diaphragm of the north wing has pulled away from the floor of the basic tower area. A crack about one-eighth of an inch wide extends the full width of the floor along the north edge of the tower area. There are no second-story shear walls in this north wing extending in a north to south direction. Second-story columns in the north wing have cracked and spalled as a result of motion in the south to north direction.

Longitudinal walls in the core area of the tower have cracked severely in the first to fourth stories. Of particular interest here are the lintels over doors, where concrete has cracked in an "X" pattern and,

in some cases, complete crushing has occurred. The diagonal cracking of lintels extends from the corners of openings to the soffit of the floor slab above, causing separation of the concrete slab from the stems of the joist in the local areas near the lintels.

Further study and detailed evaluation of failures in this building should yield much information concerning mechanisms of failure, effects of various structural details, and effects of construction methods upon the response of a building of this type to earthquake loading.

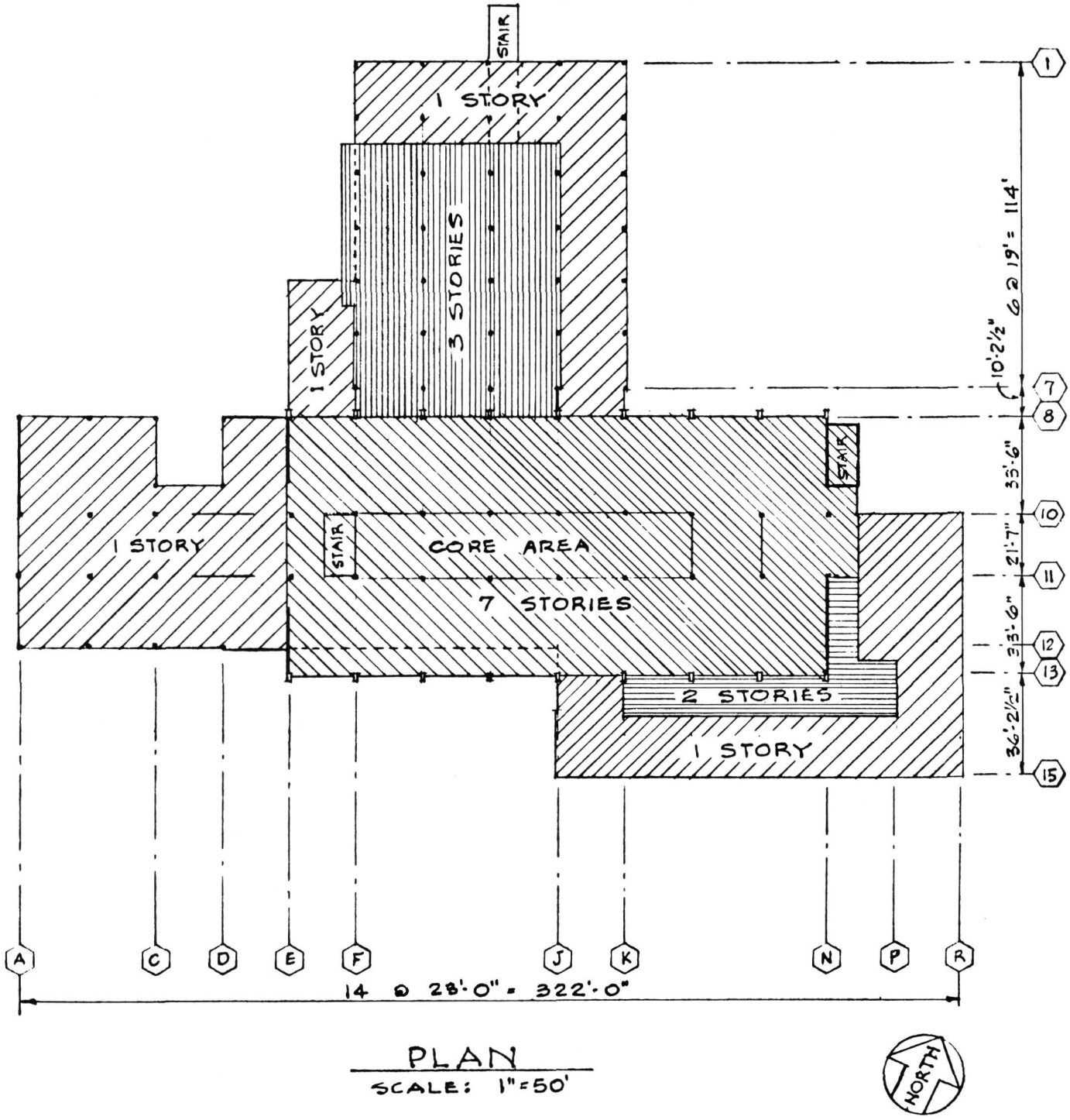

PLAN
SCALE: 1"=50'

S. B. BARNES & ASSOCIATES • CONSULTING STRUCTURAL ENGINEERS
2236 BEVERLY BOULEVARD • LOS ANGELES, CALIFORNIA 90057 • 382-2385

FIGURE 1.—Plan dimensions of seven-story tower, Holy Cross hospital.

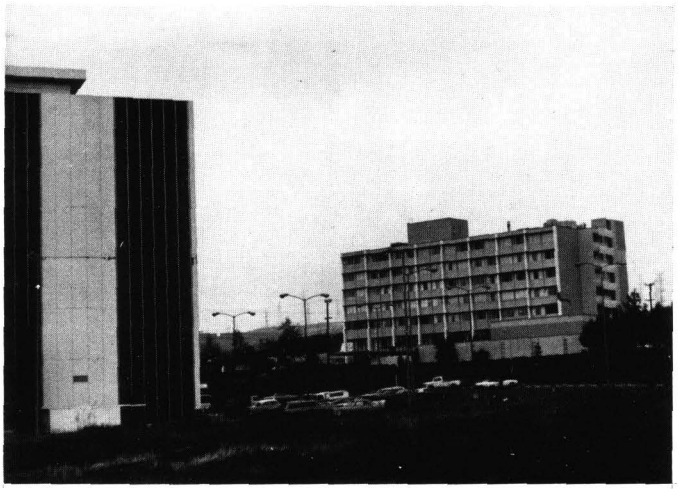

FIGURE 2.—Holy Cross Hospital right. Indian Hills Medical Center left.

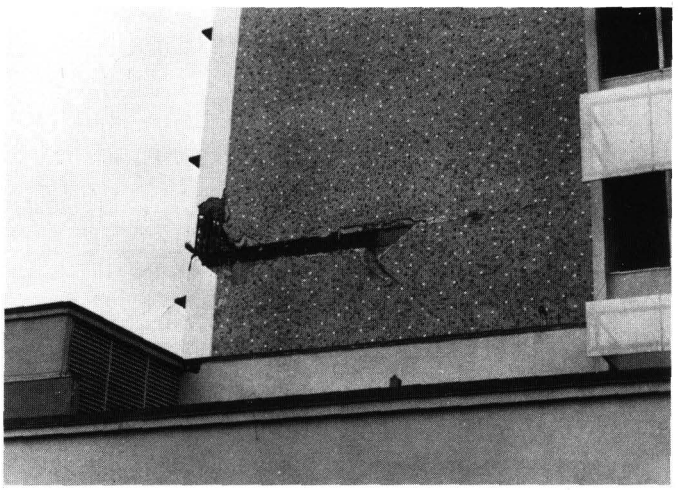

FIGURE 4.—Holy Cross Hospital, east wall. J. F. Meehan OAC photograph.

FIGURE 3.—Holy Cross Hospital, west wall. J. F. Meehan OAC photograph.

FIGURE 5.—Holy Cross Hospital, southeast corner column. J. F. Meehan OAC photograph.

DAMAGE TO THE INDIAN HILLS MEDICAL BUILDING

(14935 Rinaldi, Granada Hills)

By JAMES H. THOMPSON
WILSON AND THOMPSON, CONSULTING STRUCTURAL ENGINEERS
AND
JAMES KESLER
KAROTIS AND KESLER

The medical building is a six-story reinforced concrete structure, 64 feet by 172 feet in plan with a 17- by 85-foot projection on the south side. First-story height is 17 feet 6 inches, and the stories above are 13 feet 3 inches high. It has a reinforced concrete pile foundation and a light steel frame penthouse (fig. 1).

The building utilizes "frames in walls" for its lateral force bracing system; concrete beams and columns carry vertical loads elsewhere. Seismic design is based on the 1966 Los Angeles City Building Code (K=1.0).

Shear walls parallel to each of the main axes of the building had multiple diagonal cracks (fig. 2), and the concrete spalled along the vertical edges of the walls at the second, third, and fourth floors. Vertical reinforcing buckled in some instances.

Cracks also occurred at the beam and column connections (fig. 3). The ceilings, stairways, elevators, and mechanical equipment supports in the penthouse also suffered damage.

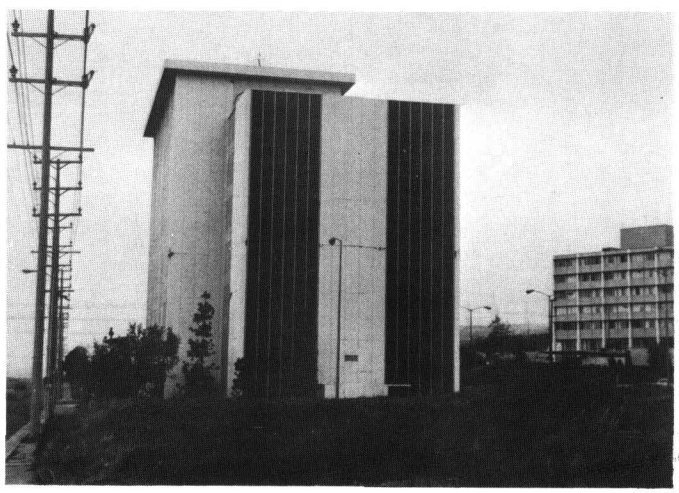

FIGURE 1.—Indian Hills Medical Center. Note horizontal crack in center shear wall. J. F. Meehan, OAC Photograph.

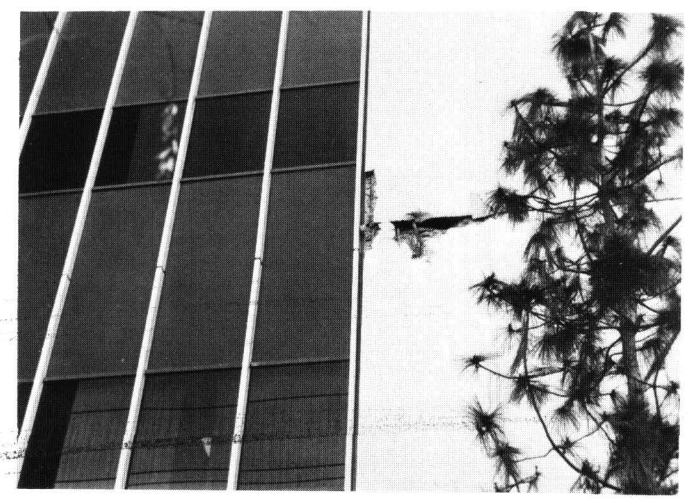

FIGURE 2.—Indian Hills Medical Center. Cracks in north wall. J. F. Meehan, OAC photograph.

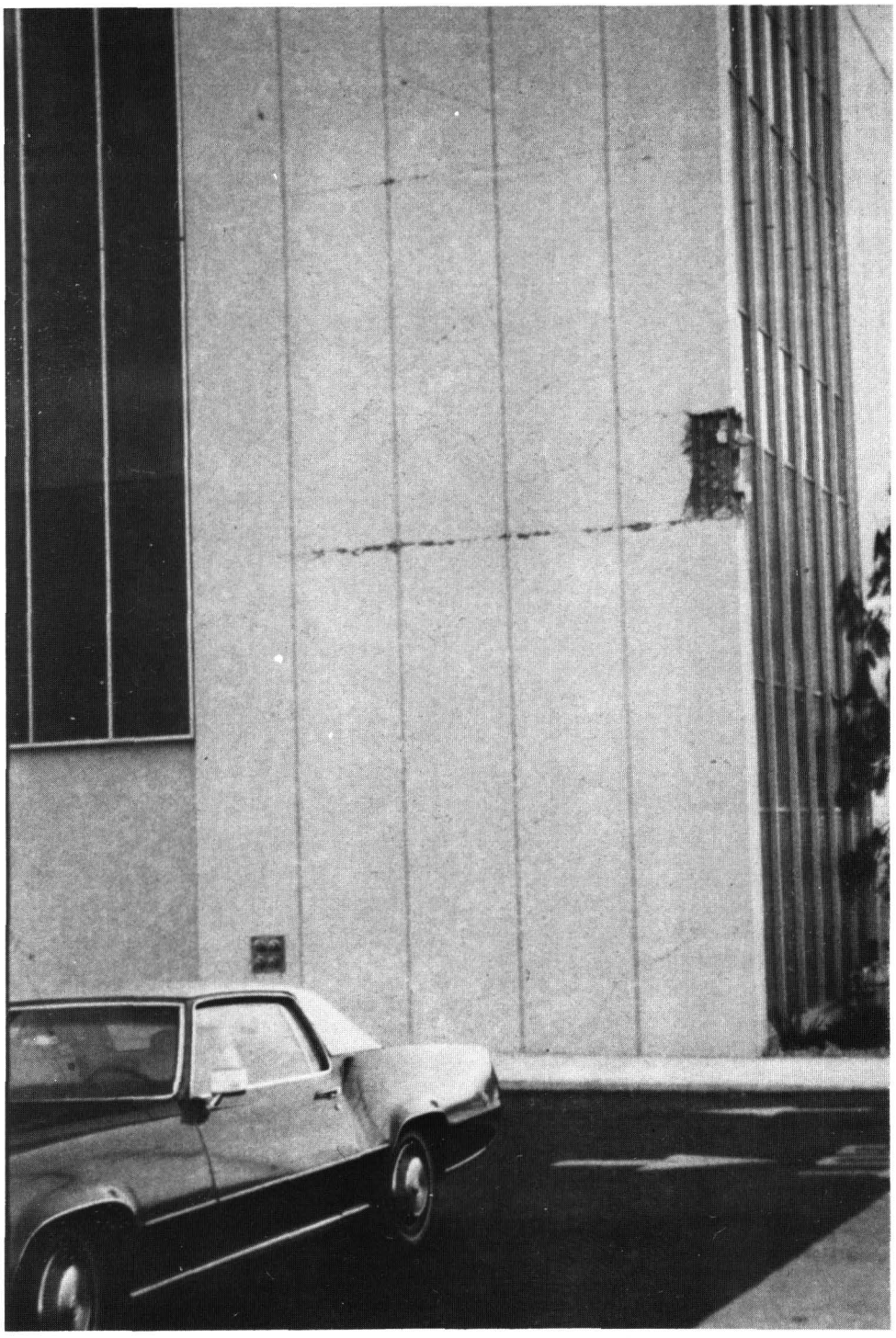

FIGURE 3.—Indian Hills Medical Center. Northwest corner. J. J. Kesler, photograph.

DAMAGE TO THE UNION BANK BUILDING

(Northeast corner of Sepulveda and Ventura, Sherman Oaks)

By PAUL GREENFIELD
ERKEL-GREENFIELD AND ASSOCIATES

The subject structure is 13 stories high over a two-level subterranean garage. The building above grade has floor-to-floor dimensions of 11 feet 9 inches, the first to second floor being 23 feet 6 inches. Total height of building is 164 feet 6 inches.

The longitudinal dimension (east-west) is seven bays at 27 feet 0 inch or 193 feet 0 inch. Transverse dimension (north-south) is two bays at 36 feet 0 inch or 72 feet 0 inch.

The mechanical penthouse is composed of light steel, framing, steel stud walls, and tufcor, zonolite concrete roof.

The building is composed of reinforced concrete columns, girders, and beams; a 4½-inch one-way concrete slab spans 12 feet 8 inches between east-west intermediate beams. All interior columns are 36 inches square while exterior columns are 24×36 inches. The 36-inch dimension is in the transverse direction. The four-corner columns are architecturally shaped 36 inches square having a 12-inch square corner notch which is the corner farthest removed from the center of the building. The remaining end-wall columns are 24×36 inches.

Typical spandrel girders are 18×41 inches, the second floor spandrel girders being 18×56 inches. The interior longitudinal girder is 24×32 inches, while the transverse frame girders are 24×33 inches.

The foundations consist of drilled cast-in-place friction piles.

Structural damage was limited principally to the four-corner columns. These columns are considerably stiffer than other exterior columns owing to an architectural configuration. The damage consisted of diagonal cracks at the second-floor joint. The southwest corner column cracked also at approximately 5 feet above ground level. The second-floor spandrel beam showed slight vertical hairline cracks above the colunms. A short concrete shear wall below grade indicated a diagonal hairline crack. This shear wall is between the ground floor and two sublevels.

Nonstructural damage was noted as follows:

1. The elevators were out of commission.
2. Several doors in the 2d, 3d, 4th, and 5th floors were slightly jammed, indicating some partition movement.
3. Considerable areas of ceiling tile over the second floor fell.
4. One dry-wall partition at the east end of the building buckled and showed horizontal movement.
5. Some steel stairlandings pulled away from their supports but were still functional.
6. Five large panes of glass in the first floor cracked or broke.
7. Marble veneer in the first-floor lobby cracked and fell away from the walls and had to be replaced.

The upper floors showed the least damage, and the penthouse showed no damage. The mechanical equipment in the penthouse was intact and securely mounted.

The building was designed under the 1964 Los Angeles City Code as a 100-percent frame using a K value of 0.67.

DAMAGE TO THE SAN FERNANDO INDUSTRIAL TRACT

By EARTHQUAKE ENGINEERING RESEARCH INSTITUTE COMMITTEE

The San Fernando industrial tract is located east of the intersection of Foothill Boulevard and Arroyo Street in the City of Los Angeles. Construction is one story and of moderate area with mostly tilt-up concrete walls. There are a few reinforced-masonry walls. Roofs are generally plywood sheathing.

A path of severe ground movement traverses the site consisting of compression ridges, cracks, and lurching. One reinforced-concrete block structure located at 12685 Foothill evidently suffered damage as a result of cracks extending directly under the building. The side walls were bowed outward.

A majority of the structures in this tract were posted as unsafe by the Los Angeles City Building Department.

Two apparently identical tilt-up structures are located about 100 feet apart at 12863 and 12885 Foothill. The one at 12885 suffered fracturing of the front-wall columns in the sash opening. Similar columns in the other building were only slightly cracked.

A reinforced-brick wall structure located at 12836 West Arroyo Street suffered collapse of the south wall (fig. 1) and the south-end bay of roof framing. The plywood sheathing was three-eighths of an inch thick, and most nails in the ledger pulled through the plywood in some cases (fig. 2). Some nails pulled out of the ledgers. Brick pilasters were spalled at beam seats (fig. 3).

The roof construction in this tract is typical of many structures in southern and other parts of California. This system is sometimes called "panelized." The plywood sheathing is supported on 2×4-inch joists at 2 feet on center. These are supported on 4-inch-thick purlins spanning 20 to 25 feet. Main roof beams are glued laminated wood on tapered steel beams.

Attachment to walls is by a 4-inch-thick ledger bolted to the wall. The plywood sheathing is nailed to the tops of the ledgers, and the purlins and joists are supported on the ledgers by metal joist hangers.

Most plywood diaphragm failures seemed to be by tension, causing nails to pull out of plywood or out of supporting ledgers and joists. The ledgers split horizontally along the bolt line, in some cases.

The east wall collapsed in a reinforced-concrete block structure at 12424 Gladstone. Plywood sheathing was one-half of an inch thick.

At 12460 Gladstone, a portion of the west wall collapsed (fig. 4). Walls are reinforced-concrete tilt-up construction. Roof sheathing is ½-inch plywood. Other walls were leaning out and cracked, and the east end roof bay collapsed. An interior portion of the roof also fell in this structure. This structure has a dock-height floor.

FIGURE 1.—12836 West Arroyo. South wall collapse. J. F. Meehan, OAC photograph.

FIGURE 3.—12836 West Arroyo. Damaged pilaster. J. F. Meehan, OAC photograph.

FIGURE 2.—12836 West Arroyo. Ledger on walls. Nails pulled through plywood sheathing. J. F. Meehan, OAC photograph.

FIGURE 4.—San Fernando Industrial Tract. 12460 Gladstone. Collapsed front wall. J. F. Meehan, OAC photograph.

DAMAGE TO THE SYLMAR INDUSTRIAL TRACT

By EARTHQUAKE ENGINEERING RESEARCH INSTITUTE COMMITTEE

In a large industrial building tract located in the city of Los Angeles just north of the city of San Fernando, a majority of the structures were posted as unsafe. Most of the construction is one story with precast concrete tilt-up walls and panelized plywood roofs. Some reinforced hollow concrete block walls were observed.

There was considerable evidence of ground movement in this area such as cracking and compression ridges.

Numerous failures occurred in the plywood roof systems. These were mostly direct tension failures, either at the exterior walls or in the general roof area. Severe wall damage and collapses resulted in many cases.

One new structure which had not been occupied was located at 12950 Bradley Avenue in this tract. Most of the glass on the west (front) wall was broken. The roof framing and sheathing was pulled away from the front wall but did not collapse. The east-end roof bay collapsed, and the east wall was cracked and leaning toward the east slightly.

Another tilt-up located at 12880 Bradley suffered collapse of the east-end roof bay and also wall collapse at the northwest corner.

A reinforced-concrete-block building wall collapsed at 12874 Bradley.

These and many other buildings in this tract deserve more careful analysis and evaluation of performance. This general type of construction is widely used in southern and other areas of California.

Loss of life and injuries could have resulted from collapses of these structures had the shock occurred 1 or 2 hours later.

DAMAGE TO A MARKET, GLENOAKS AND HUBBARD, SAN FERNANDO

By WALTER DICKEY
CONSULTING STRUCTURAL ENGINEER

This building was the westerly building of the complex at Glenoaks and Hubbard. It was about 150 by 180 feet square. The roof consisted of plywood paneled system on purlins carried by glued-laminated beams on pipe columns. Several cracks went through the floor slab of the building, showing a meandering cracking or slippage. These were not only quite open cracks but had differentials of elevation of as much as 6 or 8 inches.

The west end of the north wall and the west wall were open, on columns. The south wall had been a reinforced grouted brick wall, but at the time of inspection it had been removed because of having pulled away from the roof diaphragm system (figs. 1 and 2). It is possible that there had been considerable rotation of this rather eccentrically stiff building.

In addition, the easterly wall support had been lost as the glued-laminated beams had pulled off their supporting pilasters.

The southerly wall of the dock-height area had obviously been moved considerably to the south as shown by the tilted wall of the stairway (fig. 3).

The easterly wall had a crack right adjacent to it and had separated from an abutting wall toward its northerly end (fig. 4). It had also pulled away from the glued-laminated beams of this particular easterly wall, pulling off the anchors which had relatively small ties.

The large ceiling area had been rigidly attached to the exterior and, during the shake, had dislodged the fixtures which fell down on whatever was beneath.

The failure of the ties had probably been due to the great amount of ground movement, slippage, and cracking through the area.

FIGURE 1.—Market, Hubbard and Glenoaks. J. F. Meehan, OAS photograph.

FIGURE 2.—Market. East wall. J. F. Meehan, OAC photograph.

FIGURE 3.—Market. This portion of building moved southerly tilting the dock wall and fracturing the landing. Note the random cracks in paving in the background. Walter Dickey photograph.

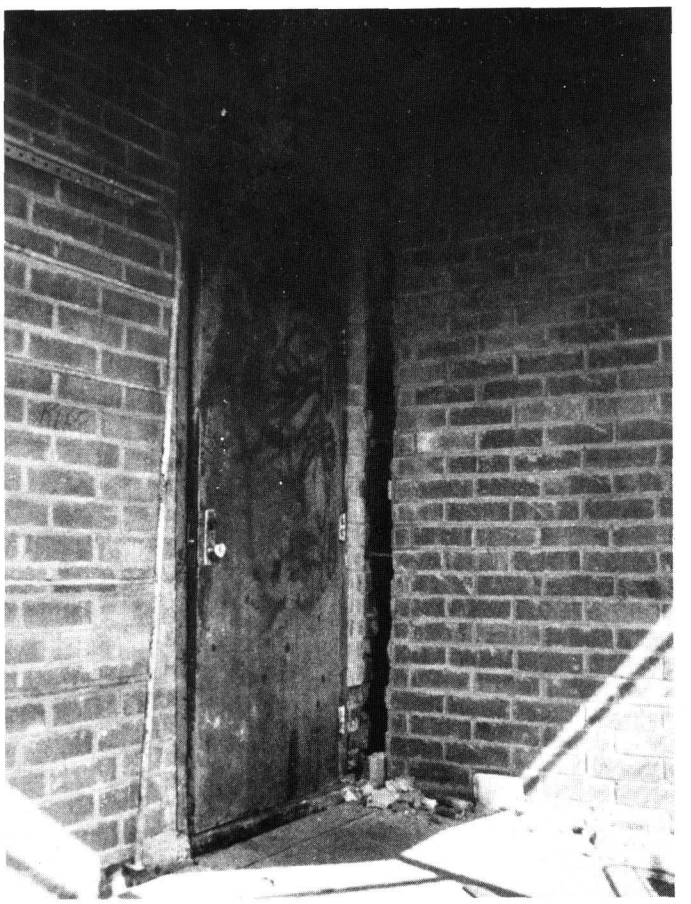

FIGURE 4.—Market. Separation of intersecting walls where crack passed through building. Walter Dickey photograph.

DAMAGE TO A MARKET, 13570 ELDRIDGE, LOS ANGELES

By EARTHQUAKE ENGINEERING RESEARCH INSTITUTE COMMITTEE

This market building was posted unsafe and has been vacated. It is a one-story reinforced-concrete building built with precast concrete tilt-up walls. Roof is plywood sheathing supported on inverted tapered steel girders.

A reinforced brick shear wall at the southwest corner was shattered. A canopy along the west side is supported on pipe columns on the outside but evidently was dropped several inches where it joins the main building. Most of the glass along the west side was broken.

A building located at 1132 Pico Street in the city of San Fernando has reinforced-concrete rigid frames supported concrete roof slabs and precast concrete walls. This structure was posted unsafe. The north wall panels broke loose from the frames and were leaning out. Some were shored.

DAMAGE TO TWO STORE BUILDINGS IN THE NORTH OAKS SHOPPING CENTER AND ONE BUILDING IN THE VALENCIA SHOPPING CENTER

By JAMES J. KESLER

KAROTIS AND KESLER

Department store—North Oaks Shopping Center (19419 Soledad Canyon Road).—The building is one story with brick exterior walls, glued-laminated beams, and panelized wood roof (fig. 1).

The rear wall of the building separated from the roof by about 9 inches in one area, and the adjacent roof section collapsed (fig. 2). Other sections of roof along the side walls also collapsed, and purlins were pulled out of their supports.

Building material store—North Oaks Shopping Center (19407 Soledad Canyon Road).—The building is one story with brick exterior walls, interior columns, and wood roof construction.

Brick piers spalled at connection to wood beams along front wall (fig. 3). Interior partitions cracked. Several main beams were pulled out from the masonry at their support along the front wall (fig. 4). Ledgers along masonry walls were pulled out, and parts of the roof structure collapsed. Cracks occurred in the paving of a nearby parking lot (fig. 5).

Store building—Valencia Shopping Center (24200 Lyons Avenue).—The building is a one-story brick masonry and wood roof construction. Masonry walls appear to be continuous on three sides of the building, but are reduced to relatively short walls on each side of the large glassed opening at the front. A large sign projects above the roof at one end of one of the short walls.

Large sections of the suspended ceiling collapsed; almost all the glass in the front wall broke. The brick walls at the front (fig. 6) spalled at ceiling level, and additional spalling occurred near ceiling level at the sign support.

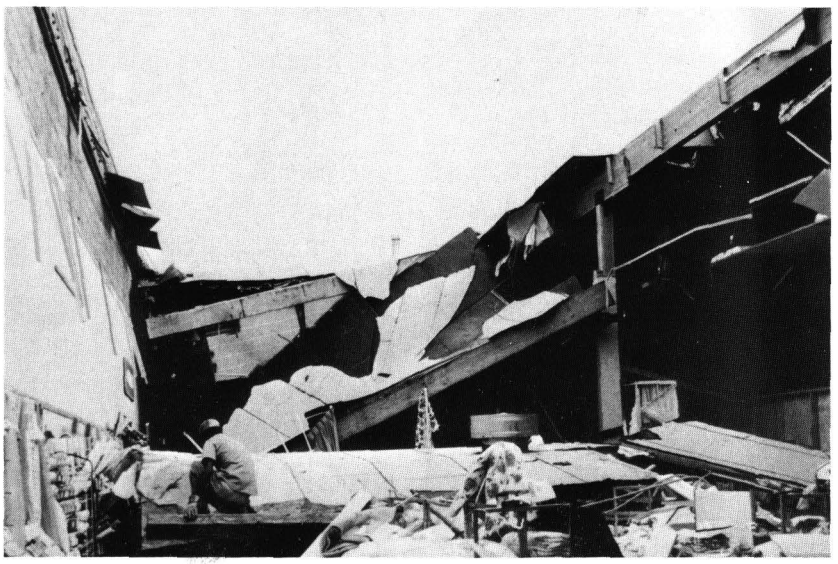

FIGURE 1.—North Oaks Shopping Center, 19419 Soledad Canyon Road.

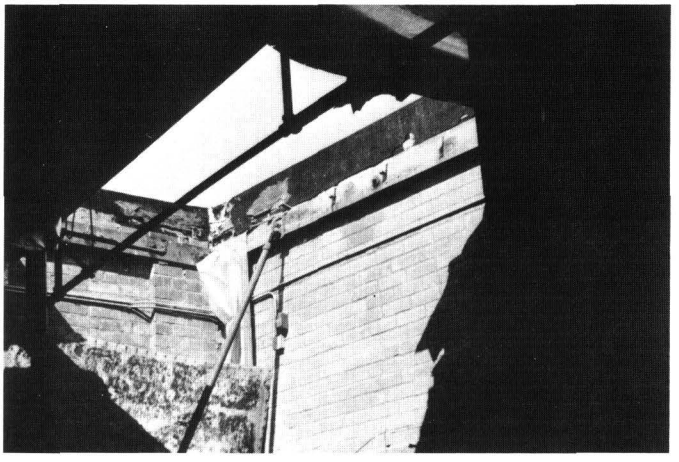

FIGURE 2.—North Oaks. Roof collapse. 19419 Soledad Canyon Road.

FIGURE 3.—North Oaks Shopping Center, 19407 Soledad Canyon Road. Front wall columns.

FIGURE 4.—North Oaks, Market. T-bar ceiling damage.

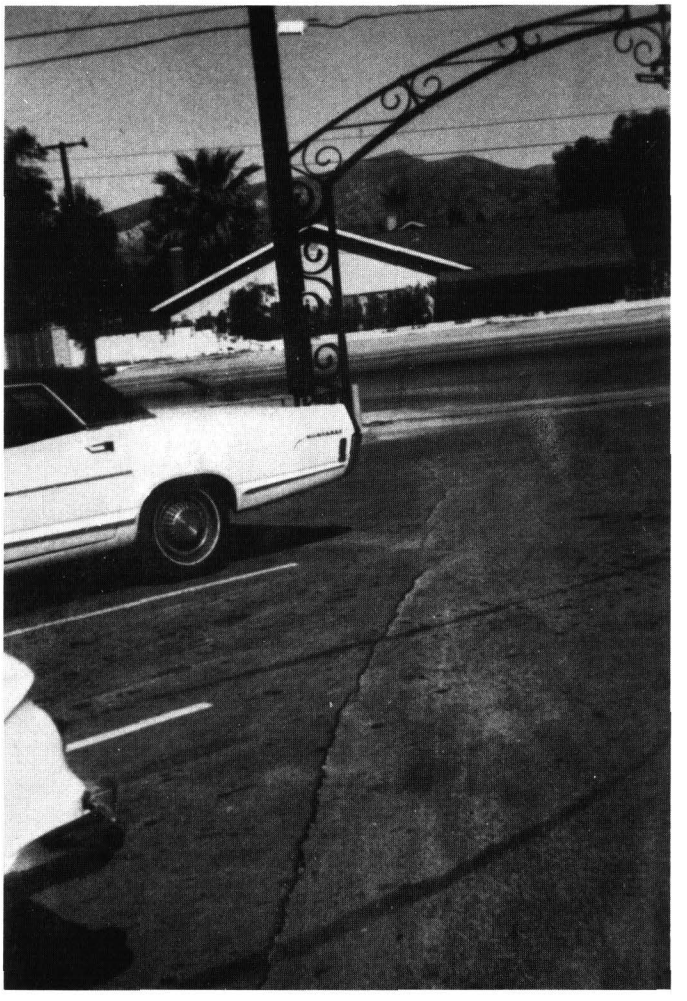

FIGURE 5.—Crack in paving. North Oaks Shopping Center.

FIGURE 6.—Store building, 24200 Lyons Avenue. Damage to front shear wall.

DAMAGE TO PUBLIC SCHOOL BUILDINGS

By J. F. MEEHAN
CALIFORNIA OFFICE OF ARCHITECTURE AND CONSTRUCTION

The author traveled to the epicentral area, which was then given as 34°26.4′ N. and 118°19.6′ W. This is about 1½ miles from the Agua Dulce Elementary School constructed in 1966. The observed damage to this school consisted of the fall of several plastic light diffusers from the fluorescent tube light fixtures and some light "cosmetic" damage (fig. 1). No other damage was observed. This building is of reinforced grouted brick masonry walls and wood frame roof with a plywood roof diaphragm. This building was sited in cut, and there was no ground cracking observed in the school grounds.

The Field Act was placed in the statutes by the California State Legislature about 6 weeks after the 1933 Long Beach earthquake. This act places the construction of public school buildings under the supervision of the State for the protection of life and property. Basically, it requires a California-licensed architect or structural engineer to prepare plans and supervise construction of public school buildings, the construction to be continuously inspected by an inspector acceptable to the architect, structural engineer and State; it requires the architect, structural engineer, inspector, and contractor to provide affidavits certifying that all work is in conformance with the approved plans and specifications; false statements on such certificates is a felony. The act provides other conditions, and the complete act can be found in Sections 15451 through 15465 of the California Education Code.

In 1967, the State Legislature required all public school buildings built prior to the enactment of the Field Act in 1933 to be examined for safety by June 30, 1970, and provided that if such buildings were found to be unsafe, they could not be used for public school use after June 30, 1975, unless they were rehabilitated to meet the requirements of the Field Act. The law absolved school board members of personal liability if steps were taken to alleviate the hazards.

Prior to 1967 there were no statutes on the siting requirements of public schools with reference to geologic hazards. In 1967, geologic siting requirements were added to the statutes but applied only to new school sites.

This earthquake tested a large number of pre-Field Act school buildings and an immense number of post-Field Act school buildings in the entire affected area.

The unrehabilitated pre-Field Act school buildings which received a modest amount of vibration were damaged as expected. It is the intent of the Los Angeles City School Board to demolish such pre-Field Act school buildings. Several pre-Field Act school buildings in the area were rehabilitated to meet the requirements of the Field Act and were not damaged to any significance. The plaster cracks will be repaired and the buildings will continue in use.

There were several thousand post-Field Act school buildings in the stricken area. Most of these suffered no damage of any kind. In areas where the site developed surface cracking, the building, too, developed comparable distress. Where the vibrations were strong, nonstructural damage occurred, usually in the form of damaged ceilings and light fixtures. Three buildings have been found to have suffered vibrational damage in the structure. The damage to these three buildings will be described.

STRUCTURAL VIBRATIONAL DAMAGE—FIELD ACT APPROVED

Clark Jr. High School, Glendale School District.—This site is located about 15 miles south of the epicenter. One of the buildings on this site is a partial three-story building of reinforced gypsum concrete on structural steel roof framing. The second floor is of reinforced concrete framing. The roof was laterally supported by reinforced grouted brick masonry construction exterior shear walls, and a steel

X brace was placed at the center of the roof diaphragm to resist the transverse lateral force shear for this double-loaded corridor classroom wing.

Roofing contained diagonal bulges at the shear walls, indicating possible cracks in the reinforced gypsum concrete diaphragm. Several reinforced grouted brick masonry shear walls contained hairline diagonal cracks. The flat bar diagonal X brace buckled sufficiently to warp the steel studs and thus damaged the gypsum lath fastened to the steel studs with sheet metal clips (fig. 2). Many light fixtures became displaced.

Crescenta Valley High School, La Crescenta.—This site is located about 16 miles south of the epicenter and about a mile from the Clark Junior High School. A double-loaded corridor classroom wing on this site, of three-story reinforced concrete construction, suffered structural damage. Two first-floor wall piers about 3 feet wide and 4 feet high in the administration portion were rather heavily X cracked. A horizontal construction joint between the wall and footing of the administration portion was exposed. The roof diaphragm contained light cracks under the roof overhang perpendicular to the wall approximately midway between the end walls. This is indicative of typical bending tension cracks of the roof diaphragm at midspan. Bolts were sheared off the floor beams of a third-floor walkway bridge between this classroom wing and an adjacent wing; however, the walkway was not damaged. The first floor was diagonally cracked across the building, which could have been the result of ground surficial damage. There was also considerable nonstructural damage in this wing. About 50 percent of the light fixtures on the third floor were damaged—many fell to the floor. Two such fixtures on the second floor were damaged. Several fusible link louvers over the classroom doorways fell to the floor. Furniture was overturned on the third floor. All third-floor map racks, hooked to eye-bolts in the walls, became dislodged and fell to the floor. Wall plaster in the administration office was cracked, and a piece of plaster 15 inches by 3 feet fell from the ceiling in the storage room.

No chemicals in the laboratory were lost because of a suggestion made and accomplished during a recent fire and panic safety check made at the site last year. All shelves in the chemistry laboratory were equipped with 4-inch railings to retain the chemicals in the event of an earthquake.

Glass was broken at a stairway exit in the girls' gymnasium.

The pedestals under the swimming pool filters became displaced and produced considerable piping damage.

Patrick Henry Junior High School, Granada Hills Area of Los Angeles.—This site is located about 16 miles southwest of the epicenter and had structural damage due to vibration. The four columns were damaged under the roof beams of a four-column reinforced-concrete two-story bridgeway between two classroom wings.

DAMAGE DUE TO SURFACE GROUND MOVEMENT

Several public school sites experienced damage when the ground cracking progressed through the school buildings. It is expected that building damage will result from such foundation activity or ground surface expression of the faulting, and the building codes do not and cannot provide for this.

Van Gogh School.—It was originally reported that the Van Gogh School (fig. 3), located west of the Upper Van Norman Reservoir and about 16 miles from the epicenter, would be demolished. However, this site is now under investigation by engineering geologists, and the extent of the structural damage is being investigated by structural engineers.

Sylmar High School.—This site, about 15 miles southwest of the epicenter, contained evidence of considerable ground surface expression of the fault (fig. 4)

San Fernando Valley Juvenile Hall.—This site, about 14 miles southwest of the epicenter, also contained evidence of considerable ground surface expressions of the fault. Several school buildings at this site were built under supervision provided by the Field Act.

Soledad Canyon School.—This school is located in Solemint, about 8 miles from the epicenter, and in the vicinity of Newhall. The reinforced grouted brick masonry walls were cracked about a foot around each end of the diagonal roof member. Note the typical diagonal cracks in the playground paving area. Such cracking was found throughout the school site. Extensive damage occurred to the T-bar ceiling construction and light fixtures in the multipurpose buildings (fig. 5).

Honby School.—This school site is located in Honby about 12 miles from the epicenter and had ground surface cracking throughout the site. One such crack passed through one of the buildings and produced a 1½-inch vertical displacement in the floor slab and cracked the roof concrete bond beam.

NONSTRUCTURAL VIBRATIONAL DAMAGE

Innumerable school buildings suffered nonstructural damage. The greatest single class of damage found in Field Act approved buildings was to the ceilings and light fixtures. The most common ceiling damage was of T-bar ceilings with lay-in panels. The damage always occurred at the perimeter of the ceiling where it adjoins the walls and partitions. Damage was frequently found within the central portion of the ceiling at the intersections of the T-bars and around the light fixtures.

At the Edison School and Bret Hart School in Burbank, T-bar ceilings were installed under the 1970-adopted ceiling requirements of the Schoolhouse Section of the Office of Architecture and Construction. No damage of any kind was observed to these ceilings. This new regulation requires that all ceilings must resist a lateral load of 1 pound per square foot or 20 percent of the weight of the ceiling.

Ceiling ventilating grilles fell to the floor at many sites throughout the area. Such grilles are frequently set in the ceiling with little or no anchorage connection.

Expansion joints provided at covered passage or arcade roof junctions with buildings frequently pounded together, causing ceiling plaster spalling.

PRE-FIELD ACT SCHOOL BUILDINGS

Morningside Elementary.—This site is located in San Fernando about 12 miles from the epicenter. There were two pre-Field Act classroom buildings of two-story construction on this site. One such building is a reinforced concrete building and was rehabilitated to meet the requirements of the Field Act and suffered no damage. The other, a brick masonry building, suffered damage to such an extent that it will be demolished.

Adult Education Center, Burbank.—This pre-Field Act school building is located about 19 miles from the epicenter.

Administration Center, Glendale.—This pre-Field Act school building about 21 miles from the epicenter was in the process of being rehabilitated. The entry brickwork was shaken from the building at the entry (fig. 6).

CONCLUSIONS

Although the investigation of the performance of public school buildings is incomplete at this time, there are several conclusions which can be drawn:

1. T-bar ceilings require engineering considerations to resist the dynamic forces of earthquakes.
2. All parts, including the anchorage, of light fixtures require engineering considerations to resist the dynamic forces of earthquakes.
3. All overhead objects such as grilles and fixtures, require particular attention to details and positive mechanical anchorage to prevent displacement during earthquakes.
4. Strong-motion earthquake records show the lateral loads experienced in many structures greatly exceed those required by present codes. Consideration will be given to this information as it applies to low, intermediate, and high buildings.

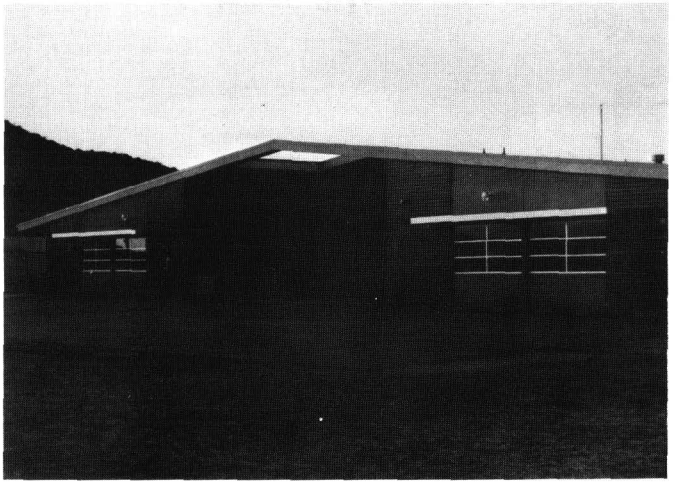

FIGURE 1.—Agua Dulce School, about 1½ miles from epicenter. Plastic lenses from several light fixtures fell to floor. J. F. Meehan, OAC photograph.

FIGURE 2.—Clark Junior High School. Steel flat bar diagonal bracing buckled and damaged plastered partitions. J. F. Meehan, OAC photograph.

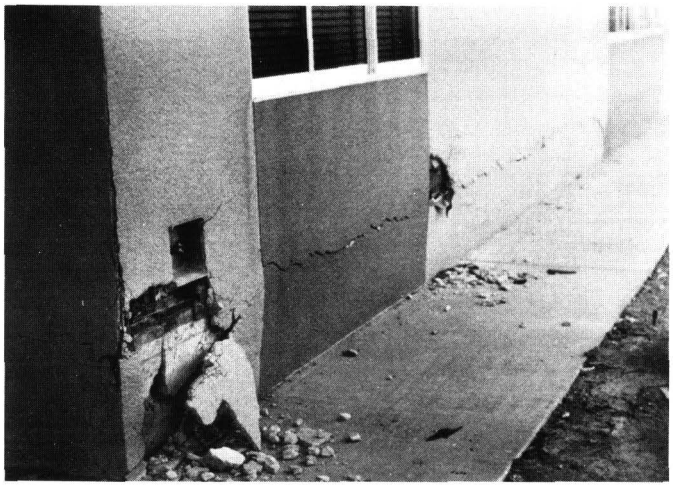

FIGURE 3.—Van Gogh School. Damage at junction of foundation and wood stud wall. J. F. Meehan, OAC photograph.

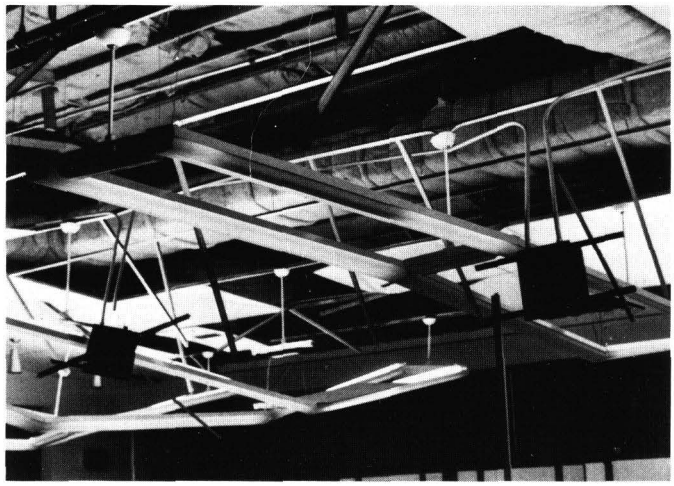

FIGURE 5.—Soledad Canyon School, T-bar ceiling, and light fixtures. J. F. Meehan, photograph.

FIGURE 4.—Sylmar High School. Arcade roof joints pounded. J. F. Meehan, OAC photograph.

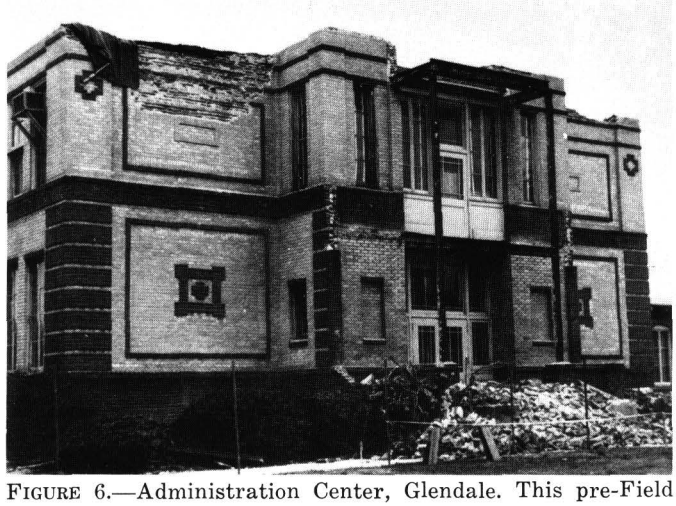

FIGURE 6.—Administration Center, Glendale. This pre-Field Act School was being rehabilitated. Brick work over the entry fell. J. F. Meehan, OAC photograph.

DAMAGE TO OTHER BUILDINGS

By WALTER BRUGGER

RESEARCH ENGINEER, LOS ANGELES CITY DIVISION OF BUILDINGS AND SAFETY

DWELLINGS

There were over 700 dwellings evacuated and declared unsafe and an additional 8,000 received varying degrees of damage (figs. 1 and 2).

A dwelling in the vicinity of Cometa and Fernmont was shaken off the foundation and moved approximately 2 feet forward (fig. 3). This building was in very close proximity to an earth fracture which has been identified as the Sylmar segment of the San Fernando fault. The damage to the rear stoop indicates a high intensity of ground motion in that area.

Many buildings that were slightly damaged lost fireplaces (fig. 4).

Numerous masonry garden walls fell over in the area (fig. 5).

APARTMENT HOUSES

There were approximately 60 apartment buildings evacuated and declared unsafe, which constituted 1,100 dwelling units. An additional 63 received damage in varying degrees (fig. 6).

OLD BRICK BUILDINGS—PARAPET REPAIR PROGRAM

In 1949 the city of Los Angeles initiated a parapet repair program for unreinforced masonry buildings. At the present time the program is approximately 85 percent complete.

Preliminary reports indicate that the parapets which were repaired under this program generally withstood the earthquake in good shape.

Many unreinforced masonry buildings were damaged in downtown Los Angeles (figs. 7 and 8). A large number of buildings of this type were also damaged in the city of San Fernando and the Sylmar section of the city of Los Angeles; however, the exact number is unknown at this time.

VETERANS HOSPITAL

An old hospital building at the Veterans Administration completely collapsed causing 45 deaths (fig. 9). This building had a skeleton concrete frame, concrete floors, and unreinforced hollow tile filler walls. The building which was five or six stories in height is reported to have been constructed before 1930.

TRAILER PARKS

Numerous house trailers fell off their supports (fig. 10).

GASOLINE STATIONS

Generally, gasoline stations performed well. At one modern station a decorative masonry chimney fell (fig. 11), and large rocks on the roof of canopies were thrown off (fig. 12).

FIGURE 1.—Almetz Street, between VA Hospital and Olive View. Los Angeles City Department of Building and Safety photograph.

FIGURE 2.—Older dwelling in the vicinity of 8th Street and Fernmont in San Fernando. Los Angeles City Department of Building and Safety photograph.

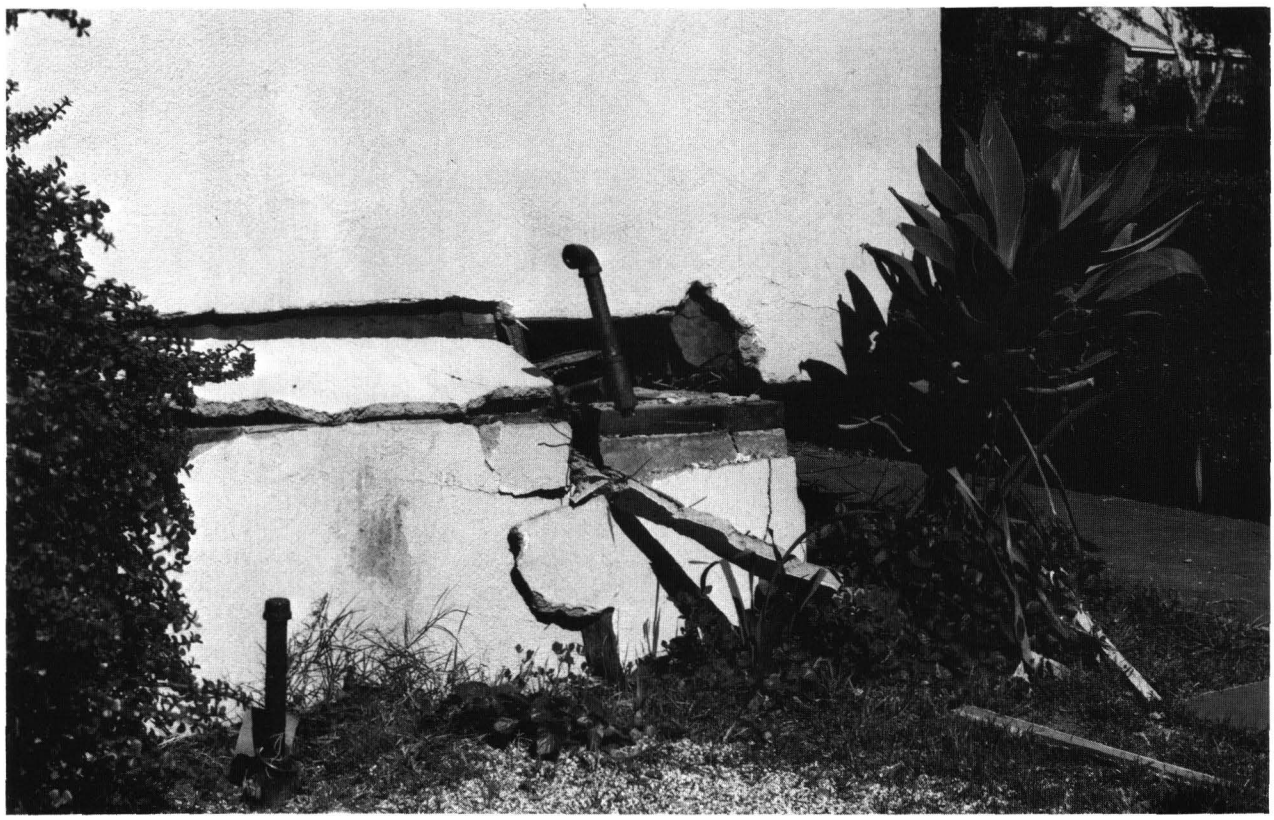

FIGURE 3.—Dwelling in the vicinity of Cometa and Fernmont, San Fernando. Building was shaken off foundation and moved 2 feet forward. Los Angeles City Department of Building and Safety photograph.

FIGURE 4.—Typical masonry fireplace damage. Los Angeles City Department of Building and Safety photograph.

FIGURE 5.—Typical concrete block masonry garden walls thrown down. Los Angeles City Department of Building and Safety photograph.

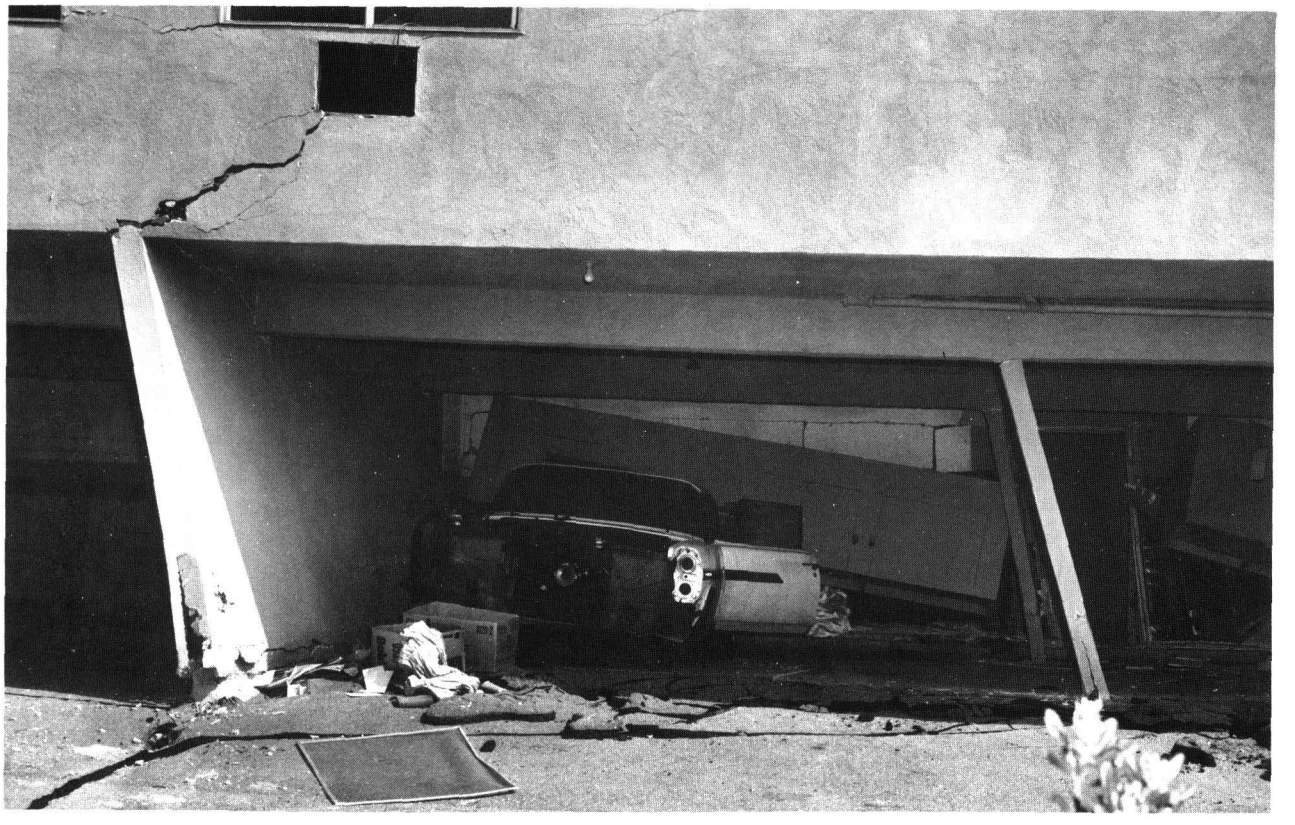

FIGURE 6.—Rear of apartment at Foothill Boulevard and Harding. Los Angeles City Department of Building and Safety photograph.

FIGURE 7.—Midnight Mission in downtown Los Angeles. Los Angeles City Department of Building and Safety photograph.

FIGURE 8.—Near 4th Street and Alameda, Los Angeles. Los Angeles City Department of Building and Safety photograph.

FIGURE 9.—Veterans Hospital rescue operations. Los Angeles City Department of Building and Safety photograph.

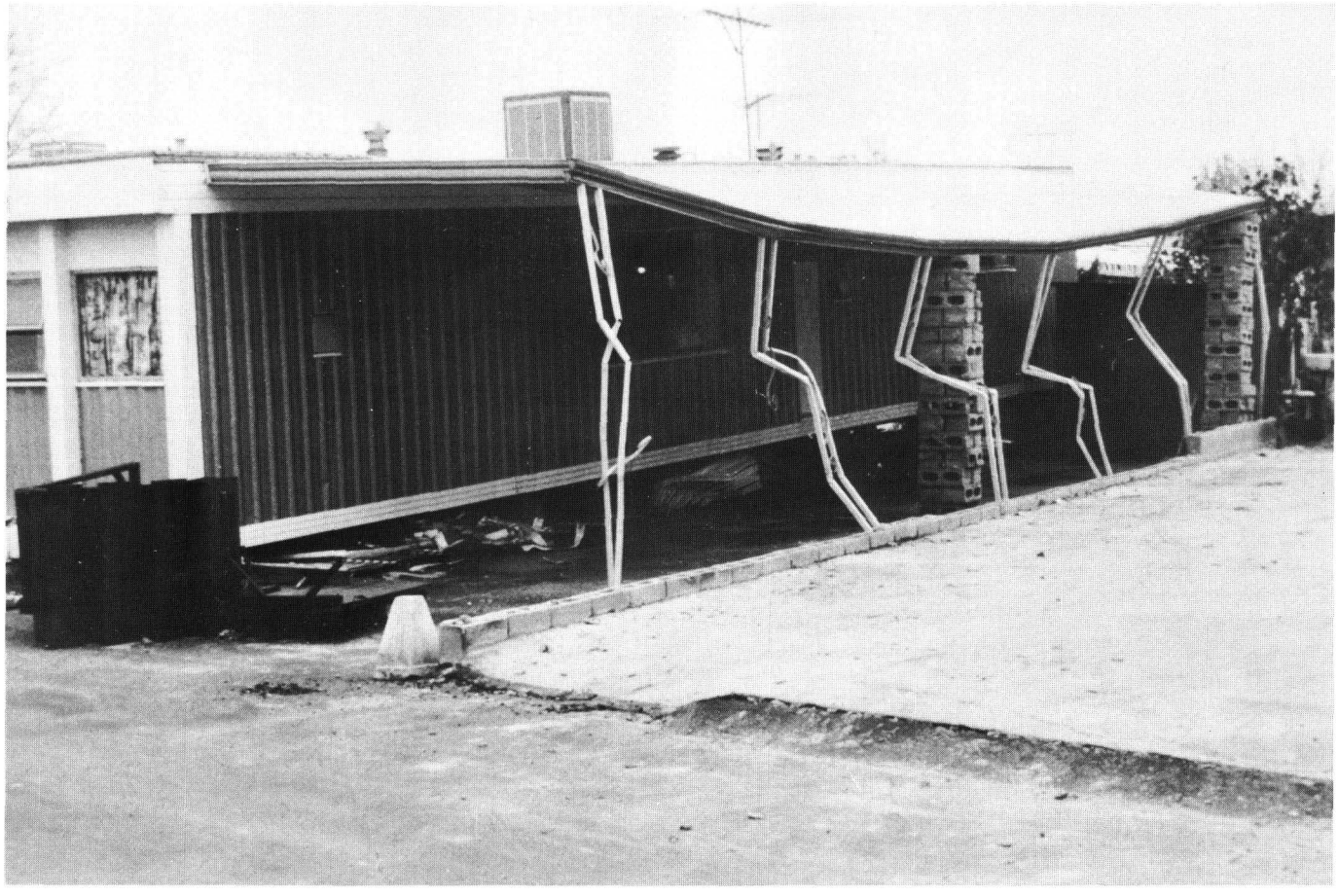

FIGURE 10.—House trailer off supports. J. F. Meehan, OAC photograph.

FIGURE 11.—Gasoline station, collapsed masonry chimney. Foothill and Van Nuys Boulevard. D. F. Moran, photograph.

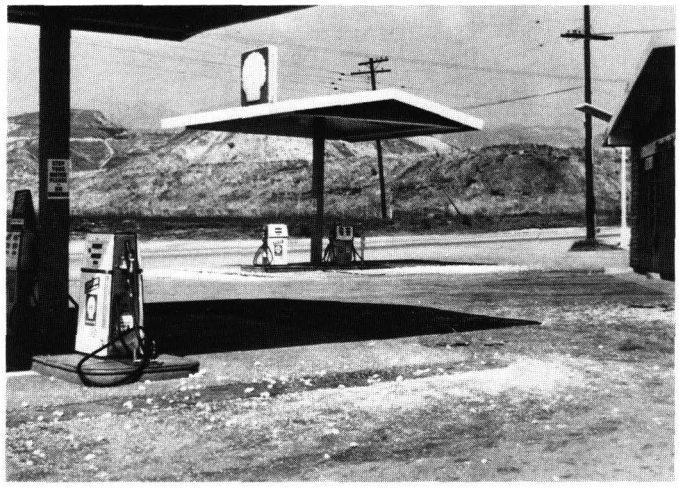

FIGURE 12.—Gasoline station. Rocks shaken off canopies. J. F. Meehan, OAC photograph.

DAMAGE TO BUILDING EQUIPMENT AND CONTENTS

By J. MARX AYRES

AYRES, COHEN, AND HAYAKAWA

We must modify our design philosophy that a building is safe if it survives an earthquake without damage to the structural system. The structural frame may absorb the earthquake forces without failures, but the movement of the building induces significant secondary damage to nonstructural elements.

A building is not safe if, during an earthquake, light fixtures and ceilings fall, elevators do not operate, emergency generators do not come on, loose objects block exits, and broken glass falls into the street. A building is not properly designed if an owner sustains huge losses due to nonstructural damage. The lessons learned by detailed studies of damage sustained by these earthquake-tested buildings must be carefully documented and widely disseminated.

The nonstructural damage observed to date appeared to follow that recorded in Anchorage, Alaska, during the March 27, 1964, earthquake.

Elevators.—Traction elevators were damaged when motor generator sets mounted on unrestrained vibration-isolation bases "walked around" the machinery rooms, and control panels fell over (fig. 1). Guide rails for counterweights were deformed, freeing the counterweights to swing about in the hoistways, resulting in snarled cables and in some instances, damaged cabs (fig. 2).

Light Fixtures.—Pendant-mounted light fixtures fell when supports tore loose at ceilings or the sheet-metal back of fixtures deformed (fig. 3). Lines of recessed fluorescent fixtures dropped from plaster ceilings.

Ceilings.—Ceiling tile was battered at perimeter walls as nonrestrained ceilings and light fixtures moved (fig. 4). Restrained fire-sprinkler piping and exposed heads tore ceiling tile as the unrestrained ceilings moved. Tile fell from perimeter runner strips that moved with the adjacent walls or partitions (fig. 5). At the Los Angeles County Courts Building, perimeter tile was damaged in most of the court rooms and corridors.

Glass.—Resilient rubber mounts in glass panels prevented excessive glass breakage (fig. 6). Tightly mounted glass panels failed.

Facades.—Excessive cracking of structural frame caused exterior plaster to fall.

Emergency Power.—Heavy emergency generators resting on unrestrained vibration-isolation spring mounts moved horizontally and fell to the floor, rupturing connections (fig. 7).

Mechanical Systems.—Pump motors were thrown from their pedestal mounts (fig. 8), and water chillers were torn from their tube bundles because they were not properly secured and tied together and to the floor (fig. 9). Heavy tanks not secured to floors shifted, and improperly designed legs collapsed (fig. 10). Central-station air-conditioning systems mounted on large unrestrained vibration-isolation springs shifted off their mounts (fig. 11). Large steam boilers shifted 3½ feet (fig. 12), damaging stacks, pipes, control panels and adjacent walls, because the boilers were not properly secured to the floor (figs. 13 and 14).

Storage Racks and Loose Objects.—Markets found their aisles filled with materials thrown from shelves. Library books were thrown to the floor (fig. 15), and in some instances, the book racks collapsed. Loose objects and carts blocked exits (fig. 16).

FIGURE 1.—Holy Cross Hospital. Elevator machinery-room generator sets were thrown off their mounts, and control panels were damaged. J. M. Ayres, photograph.

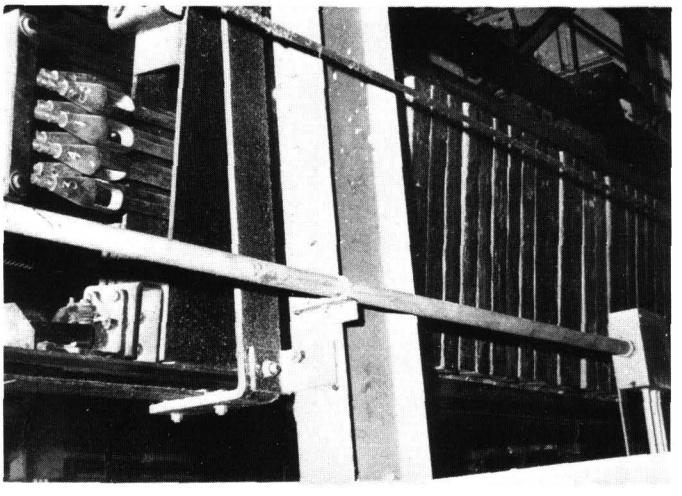

FIGURE 2.—Holy Cross Hospital. Elevator counterweights slipped out of their guide rails. J. M. Ayres, photograph.

FIGURE 3.—Olive View Power Plant. Light-fixture pendant mounts failed. J. M. Ayres, photograph.

FIGURE 4.—Olive View Hospital. Light fixtures slipped from support brackets as plaster ceiling moved. J. M. Ayres, photograph.

FIGURE 5.—Holy Cross Chapel. Marble veneer fell from wall. J. M. Ayres, photograph.

FIGURE 6.—Olive View Hospital. Glass light in rubber mount did not fail even though excessive frame deformation broke three adjacent lites. J. M. Ayres, photograph.

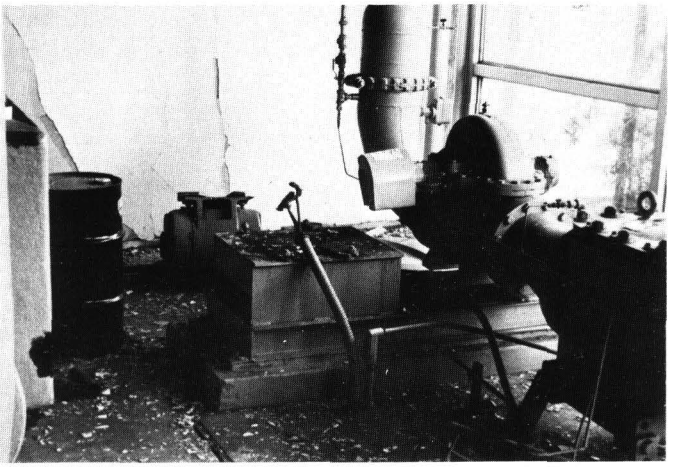

FIGURE 8.—Olive View Power Plant. Condenser water-pump motors were thrown from their pedestal mounts. J. M. Ayres, photograph.

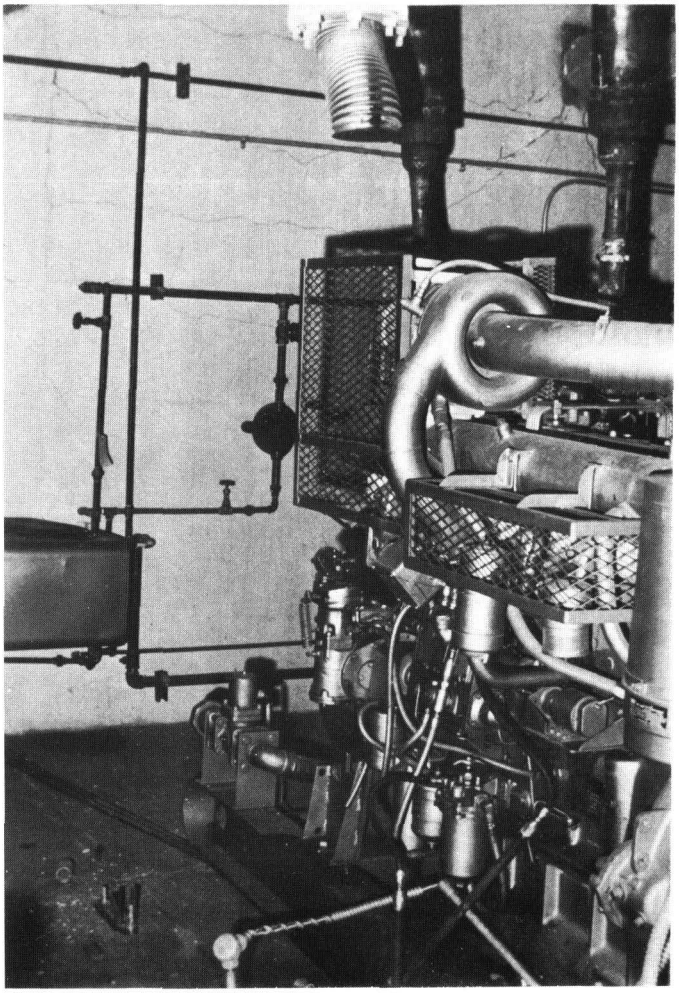

FIGURE 7.—Olive View Hospital. Emergency generators moved off of their vibration-isolation spring mounts. J. M. Ayres, photograph.

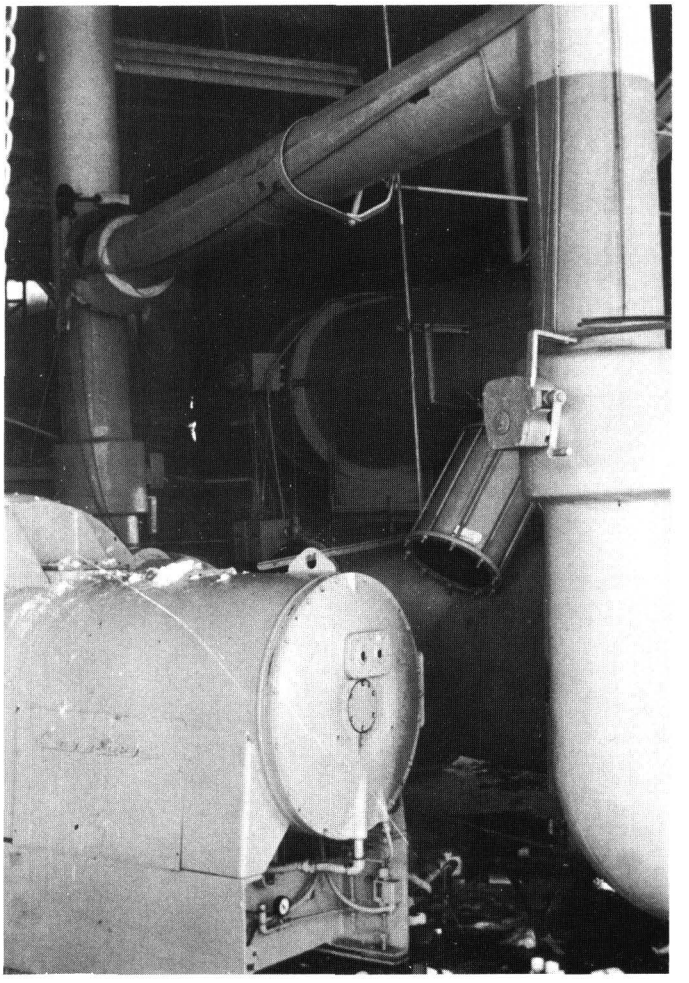

FIGURE 9.—Olive View Power Plant. Water chillers were torn from their adjacent tube bundles. J. M. Ayres, photograph.

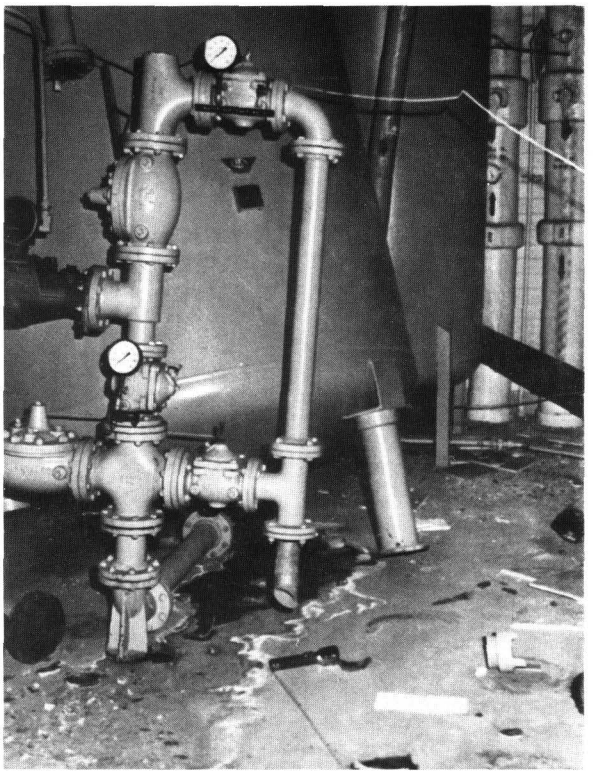

FIGURE 10.—Olive View Power Plant. Water softeners collapsed when screwed pipe legs failed. J. M. Ayres, photograph.

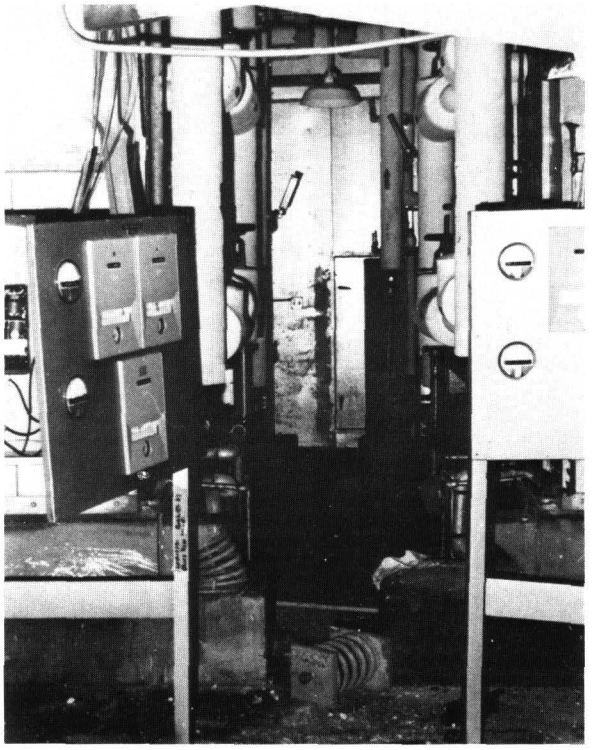

FIGURE 11.—Olive View Hospital. Large central-station air-conditioning systems moved off their vibration-isolation spring mounts. J. M. Ayres, photograph.

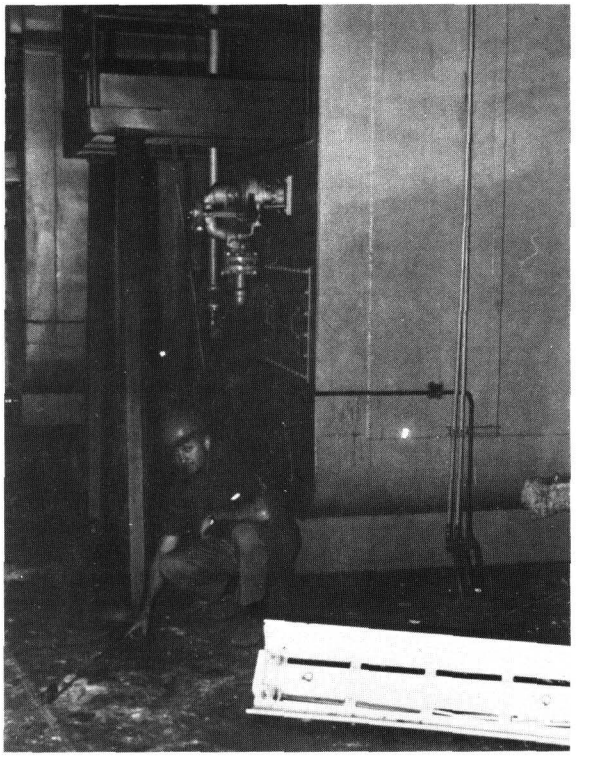

FIGURE 12.—Olive View Power Plant. Boilers shifted 3½ feet. J. M. Ayres, photograph.

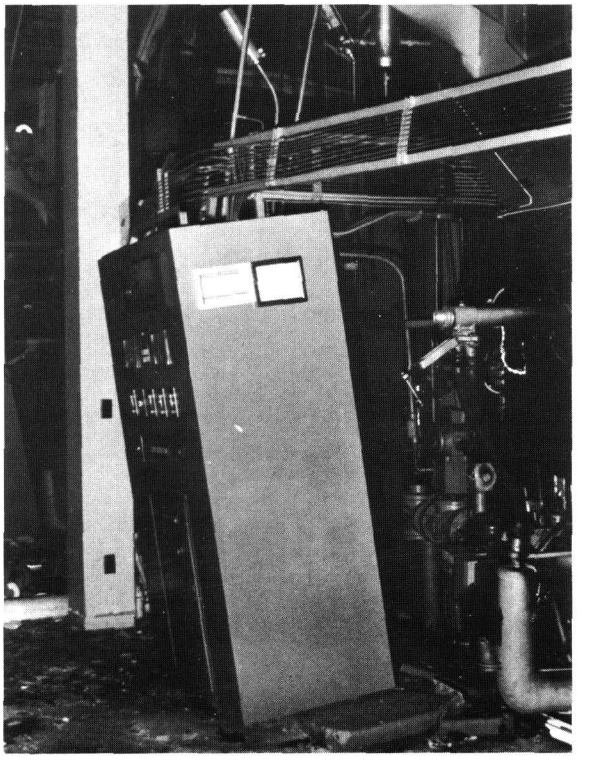

FIGURE 13.—Olive View Power Plant. Boiler control panels tilted and held up by tubing and conduits. J. M. Ayres, photograph.

FIGURE 14.—Olive View Power Plant. Roof-mounted cooling-tower intake louver damaged by racking, and adjacent boiler stacks twisted when boilers moved. J. M. Ayres, photograph.

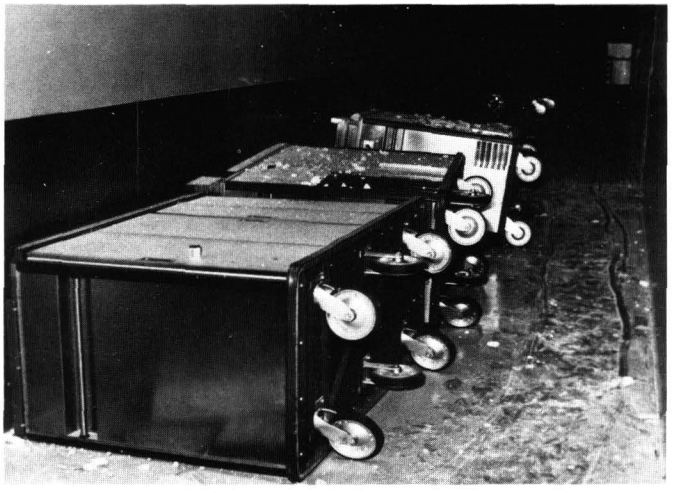

FIGURE 16.—Olive View Hospital. Corridor blocked by overturned carts. J. M. Ayres, photograph.

FIGURE 15.—Sylmar Elementary School. Books thrown from shelves. J. M. Ayres, photograph.

DAMAGE TO WATER SUPPLY SYSTEMS

By C. MARTIN DUKE

UNIVERSITY OF CALIFORNIA AT LOS ANGELES

The earthquake of February 9, 1971, did extensive damage to water-supply systems and their components. Most of this damage occurred in and around the most heavily shaken area, which included Sylmar, San Fernando, the Van Norman Reservoirs, and the Jensen Filtration Plant. Types of damage ranged from major dam failures to breakage of house connections for water and sewage, and included trunkline breaks, aqueduct and tunnel damage, and structural failures in a major filtration plant.

Strong-motion accelerographs and seismoscopes functioned at several dams.

STATEWIDE WATER SYSTEMS

Mr. Lawrence B. James, Chief Geologist of the California Department of Water Resources, reported on March 4 that there was no damage to any of the California Water Plant facilities, which extend from northern California across the Tehachapi Mountains, Antelope Valley, and to the vicinity of San Bernardino. Precise leveling is underway to assess possible changes in grade along the aqueduct.

Mr. Philip West, engineering geologist of the Southern California Edison Co., reported on March 4 that there had been no damage of any sort to the company's hydropower facilities, which are in the Sierra Nevada and San Bernardino Mountains.

FLOOD CONTROL FACILITIES

About $2,500,000 damage was done to Los Angeles County Flood Control District facilities. About half of this amount was due to breakage of reinforced concrete open channel and underground box channels (fig. 1) which appeared to be associated with surface fault displacement of major ground cracking. In one case, such breakage extended for the length of a city block.

Pacoima Dam, built in 1938 as a 370-foot-high concrete arch structure, is of interest because of the extremely large accelerations measured at one abutment, and because of rockslides in the earthquake near the west abutment which may require remedial measures (fig. 2). Water level behind the dam was quite low at the time of the earthquake. International Engineering Co. of San Francisco has been asked to study this case. The following summary was provided on March 8 by Omer D. Hall, Assistant Chief Deputy Engineer:

> No damage occurred to District flood control structures outside the San Fernando-Sylmar area, except for minor damage at a limited number of locations.
>
> The thrust of the earthquake caused substantial damage to portions of Wilson Canyon Channel, Mansfield Avenue Storm Drain, Pacoima Wash, Lopez Canyon Channel, and Storm Drain Bond Issue Project No. 256, Glenoaks Boulevard Drain, all in the San Fernando-Sylmar area. Damage occurred to other structures in the same area. Rubble channel side slopes cracked and small sections of concrete channel inverts were ruptured. There were some separations of concrete box culverts; many drain joints will need to be resealed; catch basins were damaged; there was extensive spalling of concrete; concrete channel walls were displaced; and in one case, a reinforced concrete box structure failed.
>
> Relatively minor damage occurred at the debris basins and a debris disposal area in the Sylmar area. Wilson, Schoolhouse, Stetson, Hog, and Sombrero Debris Basins will require repairs, and we are proceeding to make repairs as required.
>
> The only major District dam in the Sylmar area is Pacoima Dam. We have inspected it very carefully following the earthquake. Although massive rockslides occurred in the vicinity of the dam, and trails, roads, waterlines, and buildings in the camp area were damaged, there was no apparent structural damage to the dam. However, in view of our dam safety program, we are proceeding with a more detailed evaluation of the effects that the earthquake may have produced structurally to the dam.

Col. Robert J. Malley, Los Angeles District Engineer of the Corps of Engineers, reported on March 3 an absence of damage to the District's 11 dams and 20 debris basins, with one exception. This was the Lopez Debris Basin, north of Hansen Dam, which had serious damage. Hansen Dam was undamaged.

METROPOLITAN WATER DISTRICT OF SOUTHERN CALIFORNIA

The following nine paragraphs are quoted from a statement made on approximately February 16 by Mr. Henry J. Mills, General Manager of the district. Of special interest are the nearly completed Jensen Filtration Plant, Balboa Inlet Tunnel, San Fernando Tunnel, extensive ground cracking near the filtration plant, and the wash water tank.

The Metropolitan Water District's vast operating system of aqueducts, pumping plants, reservoirs, and treatment plants furnishing Colorado River water to Southern California came through the earthquake of February 9, 1971, with relatively little damage and there was no interruption of flow in any of its delivery lines. The 250-mile Colorado River Aqueduct with its five pumping plants continued to deliver a billion gallons of Colorado River water a day and the nearly 500 miles of distribution pipelines and tunnels continued to furnish water throughout Southern California to the District's 26 member agencies.

The Santa Monica Feeder and the Orange County Feeder each had one minor joint separation, both of which were repaired with no interruption of service. The L.A. Headquarters Building suffered superficial (non-structural) concrete and plaster damage along with a few broken windows. Certain earth slope and drainage system damage occurred on District property in the vicinity of the earthquake epicenter. This brief summation of damages reflects how relatively unscathed the District's existing facilities survived the major earthquake.

On the day of the earthquake the Metropolitan Water District had completed or had under construction about 500 million dollars worth of new facilities to be used for the distribution of State Project water when it becomes available next year from the California Aqueduct, also under construction. Most of these facilities, which have not yet been accepted by District, escaped serious damage with the exception of the 45 million dollar Joseph Jensen Filtration Plant and its inlet tunnel, which are located in the Sylmar area where the worst damage occurred. The main shock had a magnitude of 6.6 on the Richter Scale about 13 miles to the northeast of the Jensen Plant, and the acceleration at the ground surface of the plant was on the order of 0.4 g. Lateral earth movement of a foot or more occurred at the plant site.

The construction of the Jensen plant was about 85 percent complete on the ninth of February and all concrete work was completed. Damage to portions of the plant was extensive and the District's engineering staff, together with consultants George Housner, the firm of Converse, Davis and Associates, and H. B. Seed, are still in the process of assessing the damage and determining the cost and method of repairs. The finished water reservoir, a covered concrete structure approximately 500 feet square, was most severely damaged (figs. 3 and 4). About 300 feet of the concrete effluent box conduit between the filter beds and the reservoir is also severely damaged, and the chemical building and the influent conduit where it connects to the main control building received moderate to heavy damage. The 1¾ million gallon steel wash water tank (fig. 5) was half full of water, and while it was damaged sufficiently to pull its foundation bolts out of its concrete foundation, it did not lose any water. Minor damage occurred at other places such as in the mixing basins and to the traveling bridges with their sludge removal equipment.

The rest of the plant shows surprisingly little damage, including the main control building, the settling basins, filters, wash water reclamation units and chemical storage area. There is minor damage at some construction joints and some structures show indications of movement, but on the whole the major portion of the plant is in good condition.

The Balboa Inlet Tunnel, 14 feet in diameter, which will bring the water from the Foothill Feeder at Magazine Canyon to the Jensen Plant, received some damage about 1,500 feet in from its downstream portal. For a distance of about 100 feet at the fault crossing, the tunnel lining is badly damaged (Fig. 6). Other tunnels and pipelines along the Foothill Feeder and the Sepulveda Feeder leading from the Jensen Plant to the Palos Verdes Reservoir apparently escaped any serious damage. The San Fernando Tunnel, 18 feet in diameter and 29,000 feet in length, extending from Magazine Canyon to Pacoima Wash, was about two thirds excavated, being driven from the east portal. There was some vertical displacement along this tunnel and minor damage to the tunnel supports. District surveyors are presently checking the tunnel for line and grade.

One of the District's primary activities during the aftermath of the earthquake was to assist the City of San Fernando in restoring water service to many of its 17,000 residents. In cooperation with Calleguas MWD and the cities of Pasadena, Burbank, and Long Beach, District crews worked around the clock for several days making temporary service installations and initiating pipeline repairs so that the City of San Fernando could again meet water demands in most of its service area. The Corps of Engineers has now taken over the responsibility of permanently restoring the City's system.

It will be some time before the total extent of the earthquake damage is known, as well as what steps will be necessary to repair the damage. It appears, however, from all information presently available, that the Metropolitan Water District should be able to accept, treat, and deliver State Project water not later than the summer of 1972.

Mr. Munson Dowd, Chief Design Engineer, on March 3 reaffirmed the foregoing statement and added that the San Fernando Tunnel had experienced a 6½-foot vertical displacement between its portal and a point 4½ miles into the tunnel.

LOS ANGELES DEPARTMENT OF WATER AND POWER

Most dramatic of the department's water system damage was the failure of two old hydraulic-fill earth dams. The larger of these, Lower San

Fernando Dam, was in danger of imminent sudden release of the waters of Lower Van Norman Reservoir into a downstream residential area of 80,000 people. Immediate and effective action of the Department, with the aid of several other agencies, prevented such a disaster. The actions included reservoir drainage and reinforcement and evacuation of the imperiled area. The dams will be discussed in more detail below.

Also damaged were the First and Second Owens River Aqueducts. The First Aqueduct, the larger of the two, was restored to working order within 2 days. The Second, completed in 1970, was damaged in its Saugus pipeline portion between Terminal Hill and Magazine Canyon, but should be returned to service within a month. The damage consisted of buckling of the pipe and movement of its supports.

Water service to the Granada Hills, Porter Ranch, Sylmar, and other high-elevation areas in the San Fernando Valley was interrupted when the Susana, Granada, and Maclay trunklines were broken in many places by permanent differential ground displacements (fig. 7). On the Granada line, most of the 10 or 12 breaks were in the Jensen Filtration Plant area.

The wood roof collapsed at the small Maclay Reservoir, on the Maclay High Line, and cracking occurred at the sides and corners of the basin. Rapid repairs are under way.

Table 1 provides a summary of the damages to the water system facilities of the department. The two dams constitute the greatest loss, followed by the Saugus pipeline and the trunklines.

The failed dams were constructed in approximately 1915 by the hydraulic-fill method. This involves sluicing earth and rock from the reservoir bottom and nearby hills into a pond in the dam area and draining off the excess water. In contradistinction, modern good practice calls for careful placing of all earth materials, with compaction by sheepsfoot or pneumatic rollers under controlled moisture content and density.

Upper San Fernando Dam, retaining Upper Van Norman Reservoir, had a crest elevation of 1,218 feet (U.S. Geol. Survey), a spillway elevation of 1,210 feet, and a maximum dam height of about 60 feet. Side slopes were approximately 2.4:1 on the upstream face, with a slope-berm-slope configuration averaging approximately 4:1 on the downstream face (fig. 8). At the time of the earthquake, the lake was full to the spillway level.

TABLE 1.—*Estimated total costs of temporary and permanent restoration of facilities damaged in earthquake of February 9, 1971*

[Los Angeles Department of Water and Power. Effective Feb. 14, 1971, approximately. Preliminary and subject to revision]

	Immediate repairs	Permanent Reconstruction	Total
Deadman siphon	$20,000	$.....	$20,000
Cascades	45,000	.....	45,000
Various First Aqueduct locations	100,000	.....	100,000
High-speed channel	57,256	225,045	282,301
Bypass channel	75,200	262,520	337,720
Saugus pipeline (Terminal Hill)	100,000	1,810,300	1,910,300
First Aqueduct penstock	80,000	257,000	337,000
Terminal pad and structure	95,000	.....	95,000
Powerhouse bypass	84,000	.....	84,000
Tujunga trunkline	.....	1,543,000	1,543,000
Granada trunkline	150,000	.....	150,000
Susana trunkline	50,000	.....	50,000
Maclay High Line	50,000	769,000	819,000
Susana-Tujunga connector	12,000	.....	12,000
Stone Canyon line blowoff	6,000	.....	6,000
Upper Van Norman Bypass	40,000	.....	40,000
Lower Van Norman Bypass drain	6,000	.....	6,000
Olden street line	37,500	.....	37,500
Chatsworth high line connections	30,000	.....	30,000
Van Norman pumping station suction line	45,000	.....	45,000
Maclay Reservoir	25,000	500,000	525,000
Upper Van Norman Reservoir	100,000	8,000,000	8,100,000
Lower Van Norman Reservoir	350,000	25,000,000	25,350,000
Van Norman Bypass Reservoir	30,000	.....	30,000
Second Upper Van Norman Reservoir Bypass line	.....	500,000	500,000
Sesnon Inlet-Outlet line	40,000	235,000	275,000
Granada Hills inlet-outlet line	15,000	13,000	28,000
Alta Vista inlet-outlet line	15,000	.....	15,000
Various pumping stations	11,000	.....	11,000
Turbidity control at reservoirs	119,458	.....	119,458
Ducommun yard buildings	1,000	.....	1,000
Tank trucks	3,000	.....	3,000
Distribution mains and trunk lines	1,150,000	.....	1,398,000
Meters and service connections	645,000	.....	645,000
Operation of source and pumping facilities	30,000	.....	30,000
Lost water	5,875,000	.....	5,875,000
TOTAL	$9,492,414	$39,114,865	$48,855,279

The failure mechanism appears to have been a downstream sliding on a curved surface, extending under the dam to or beyond the downstream toe, from an area of extensive longitudinal cracking on the upstream face. The dam crest displaced

about 3 feet downward and about 5 feet horizontally downstream. Other phenomena are consistent with this hypothesis, including longitudinal cracks on the upper part of the downstream face and joint separations and compressions located, respectively, in the upstream and downstream portions of the outlet tunnel. The sink hole seems due to such a joint separation. Continued operation of this dam, at a sharply lowered water surface elevation, is essential for water-supply purposes, and the department is proceeding with interim repairs pending reconstruction in the near future.

Lower San Fernando Dam was a much larger structure than the upper dam. Its crest elevation was 1,143 feet (U.S. Geol. Survey), with maximum water-surface elevation not allowed to exceed 1,135 feet, and a maximum dam height of about 142 feet. The dam rests on some 35 feet of alluvium overlying bedrock. Side slopes were 2.5:1 upstream, with a slope-berm-slope arrangement having an average slope of about 4:1 downstream. At the time of the earthquake, the water-surface elevation was 1,109.4 feet.

The failure mechanism of the lower dam appears to have been a sliding of the top of the dam into the reservoir on a curved surface extending upstream from a zone of major longitudinal cracking that appeared on the upper (2.5:1) slope of the downstream face (figs. 9, 10, and 11). This hypothesis is supported by soundings taken in the reservoir to establish the top of the sliding mass and by an absence of cracking or other deformation below the downstream berm.

Residents of the 12-square-mile evacuated corridor between the San Diego Freeway and Balboa Street were permitted to return at 4 p.m. on Friday, February 12. This action was taken based on the judgment of officials that the Lower Van Norman water surface had been sufficiently lowered (by 13 feet) to reduce to an acceptable level the hazard due to a major aftershock. Water had been discharged at its maximum rate since minutes after the earthquake. The Corps of Engineers added about 10 percent to the rate by means of 11 pumps.

The lower dam has been taken out of circulation and essentially emptied. Plans for removal and reconstruction are indefinite at this point. The Department of Water and Power, the Department of Water Resources, and Prof. H. B. Seed will perform a major investigation of the failure.

Several cases of damage to large water-storage tanks have occurred. One is the Sesnon Tank of LADWP in Granada Hills which developed a donut-like wrinkle in its top third. A tank at Olive View developed such a wrinkle at its bottom. A MWD tank near the Jensen plant pulled out its anchor bolts but did not lose its water.

Appreciation is expressed to Mr. Robert V. Phillips, Chief Engineer of Water Works and Assistant Manager of the Los Angeles Department of Water and Power, for authorizing access to the water system damage data given herein.

CITY OF SAN FERNANDO WATER SUPPLY

San Fernando, with a population of 17,000, had its water-supply system devastated by the earthquake. The sole supply was from wells north of the city. Whether the wells themselves were ruptured by ground cracking is not yet known, but the delivery conduit from the well field was shattered. The distribution system was so fractured by ground cracking, as well as by the violent shaking, as to require practically a completely new water system for the city (fig. 12).

All the city's reservoirs were leaking, two of them not being repairable. A new 3-million-gallon reservoir is being planned.

Besides the water-supply problem, San Fernando had massive damage to the sewage system, gas system, street paving, street lighting, homes, and small businesses.

Emergency assistance to the populace was provided by the city with extensive support of the Metropolitan Water District, the Cities of Pasadena, Burbank, and Long Beach, the Corps of Engineers, Salvation Army, and the Red Cross, among others. The Calleguas Water System and some Los Angeles water were connected into the San Fernando fire hydrants, with fire hose and 10-inch pipelines run down street gutters. Some 250 portable toilets were set up. The MWD reported the repair of some 45 leaks found upon repressuring the water system. The Corps of Engineers has now taken over the overall utilities reconstruction task, and has contracted with Morrison-Knudson Corp.

CONCLUSIONS

Detailed analyses must be made of the behavior of the following structures:

Lower San Fernando Dam
Upper San Fernando Dam
Jensen Filtration Plant
Saugus Pipeline
San Fernando Tunnel
Pacoima Dam

Flood Control District Box Culvert
Lopez Debris Basin
Balboa Inlet Tunnel
LADWP Granada Trunk Line
Sesnon Water Tank
MWD Wash Water Tank

A case study should be made of the San Fernando water, sewage, gas, and street systems. Another case study should be made of the sociological aspects of the evacuation below Lower San Fernando Dam.

Many of the above structures and systems were designed in accordance with the criteria and procedures of modern good practice. However, instrumental records obtained a few miles from the zone of heaviest damage appear to contain more severe ground motions than those that have been used as a basis for design up to now. Furthermore, widespread surface fault breaking and ground cracking, such as obviously played a major role in much of the damage here, has not in the past been incorporated systematically into the design of most structures.

The explanation for much of the damage to hydraulic structures designed according to modern good practice should evolve in context with the studies now being undertaken.

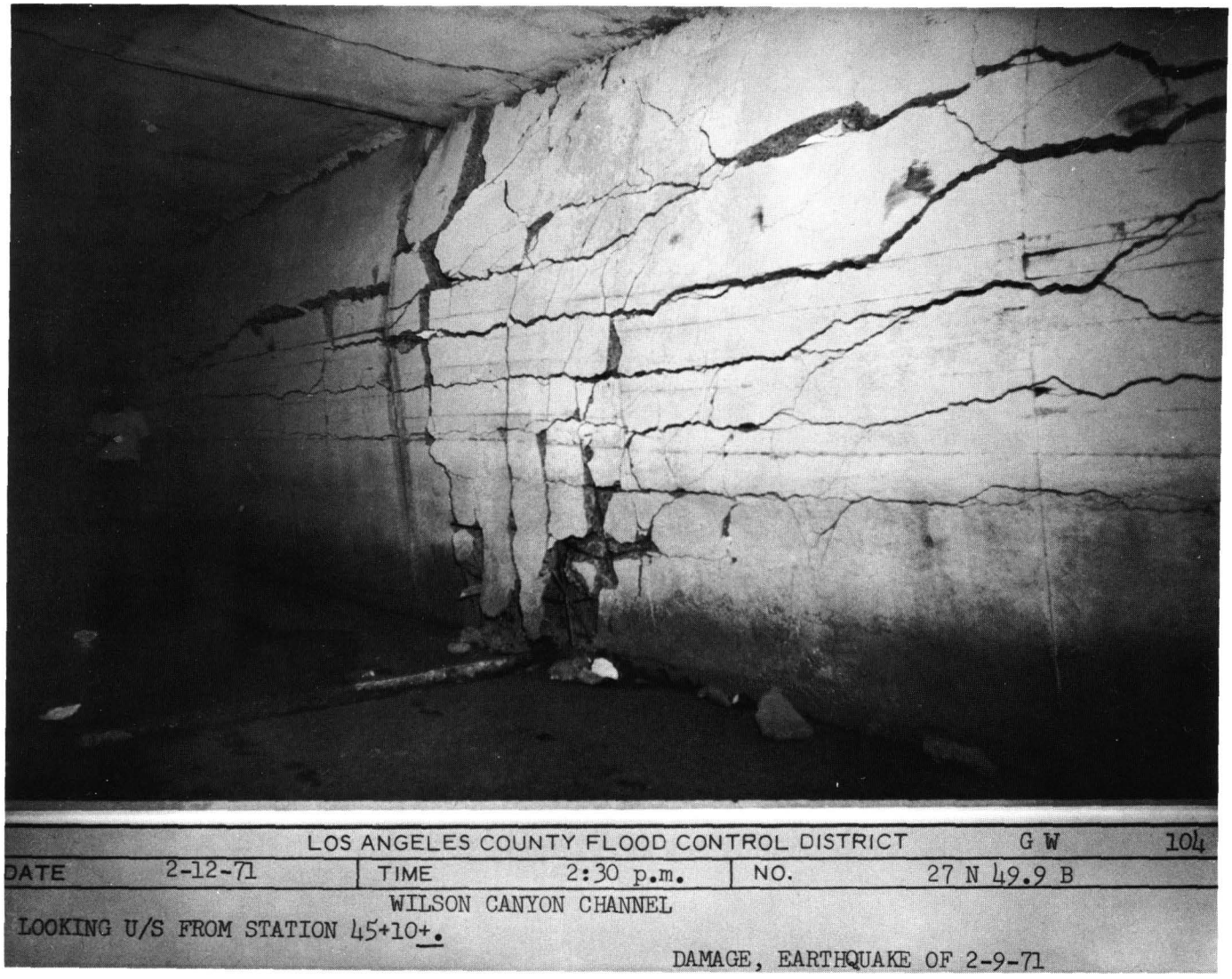

FIGURE 1.—Inside of Box Culvert at Wilson Canyon Channel. Los Angeles County Flood Control District photograph.

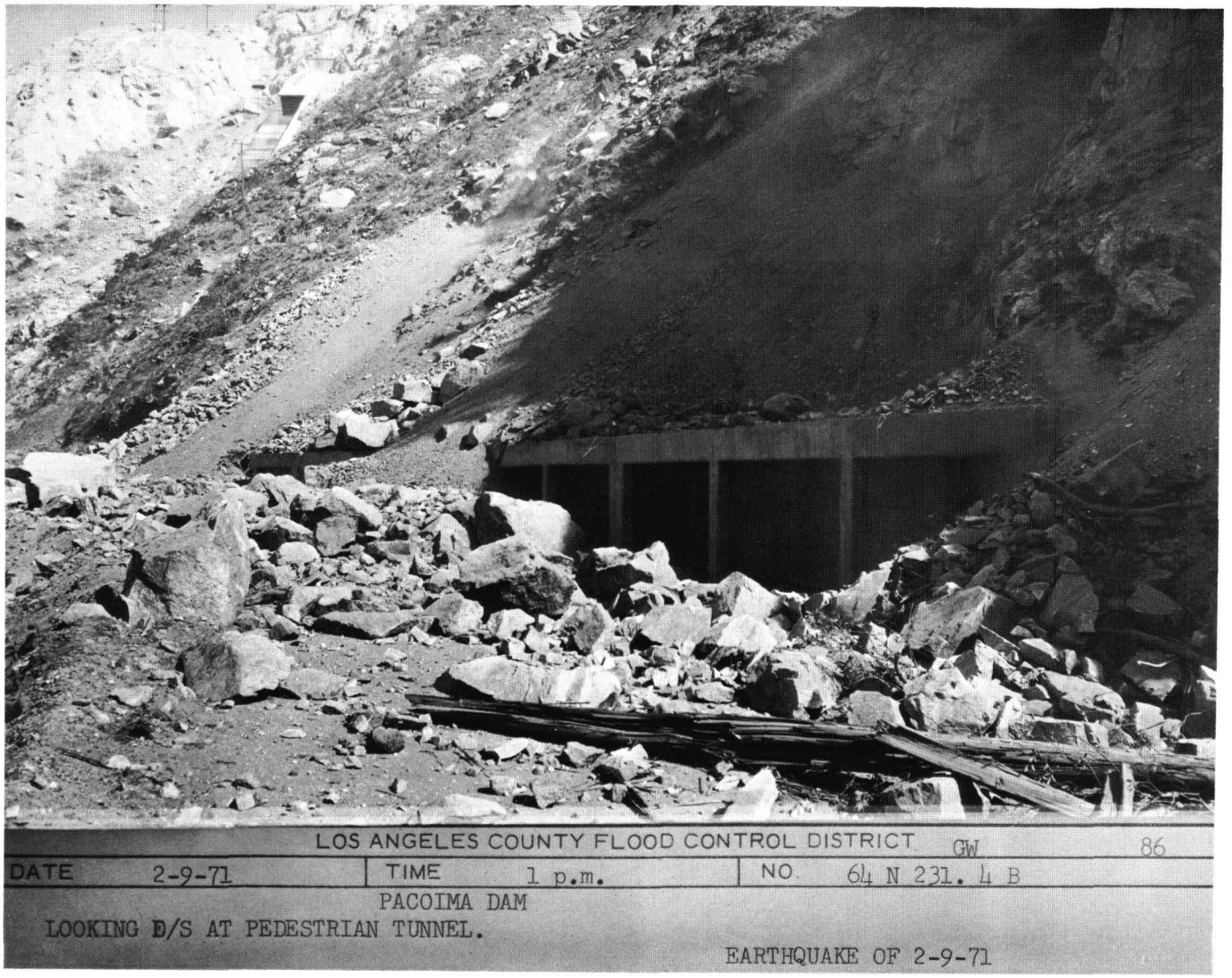

FIGURE 2.—Rockslides at west abutment of Pacoima Dam. LACFCD photograph.

FIGURE 3.—Metropolitan Water District, Joseph Jensen Filtration Plant, Interior of finished water reservoir. MWD photographs.

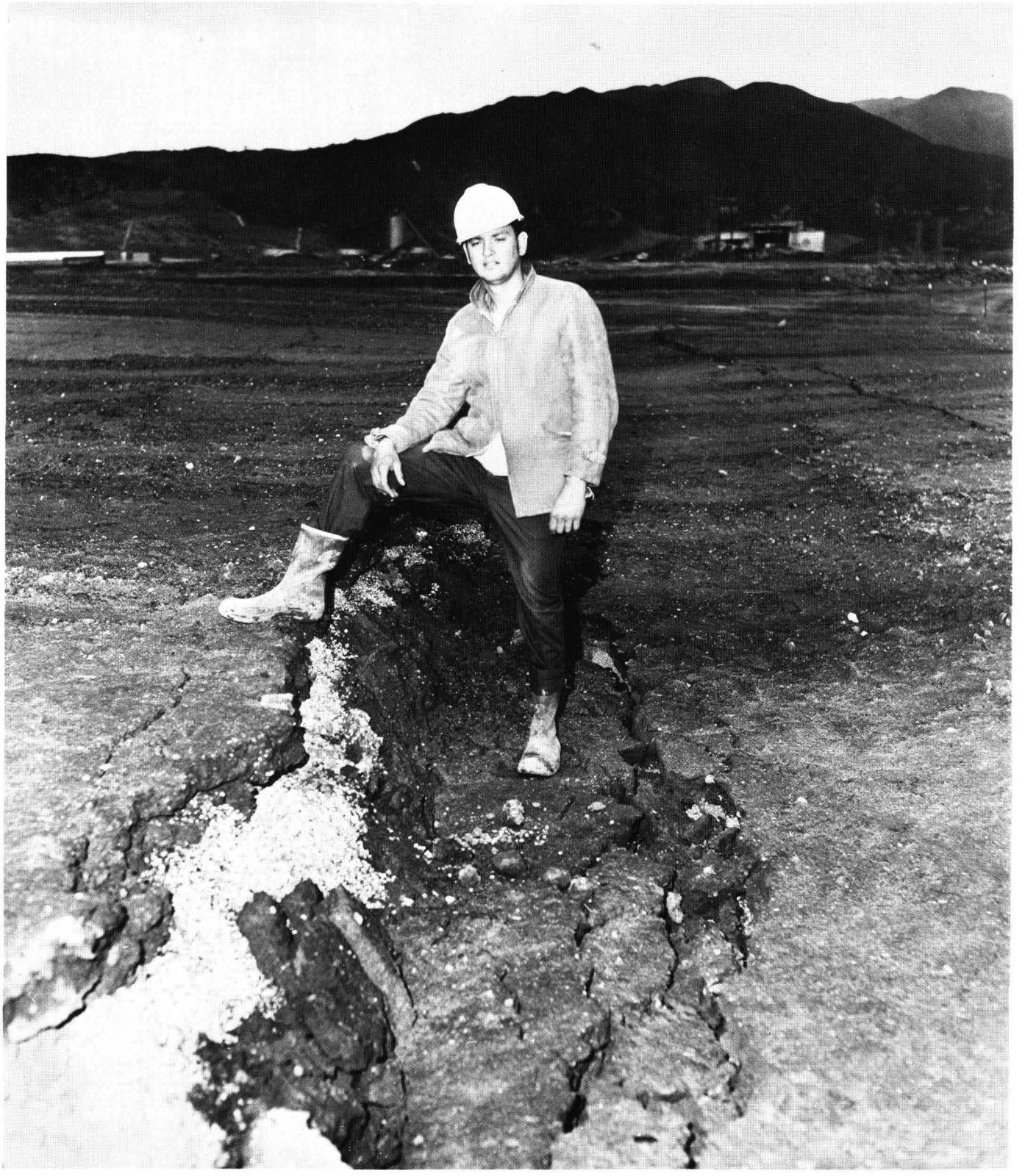

FIGURE 4.—Metropolitan Water District, Joseph Jensen Filtration Plant. Looking north along the east perimeter of the finished water reservoir showing cracks in the compacted fill adjacent to the reservoir. MWD photograph.

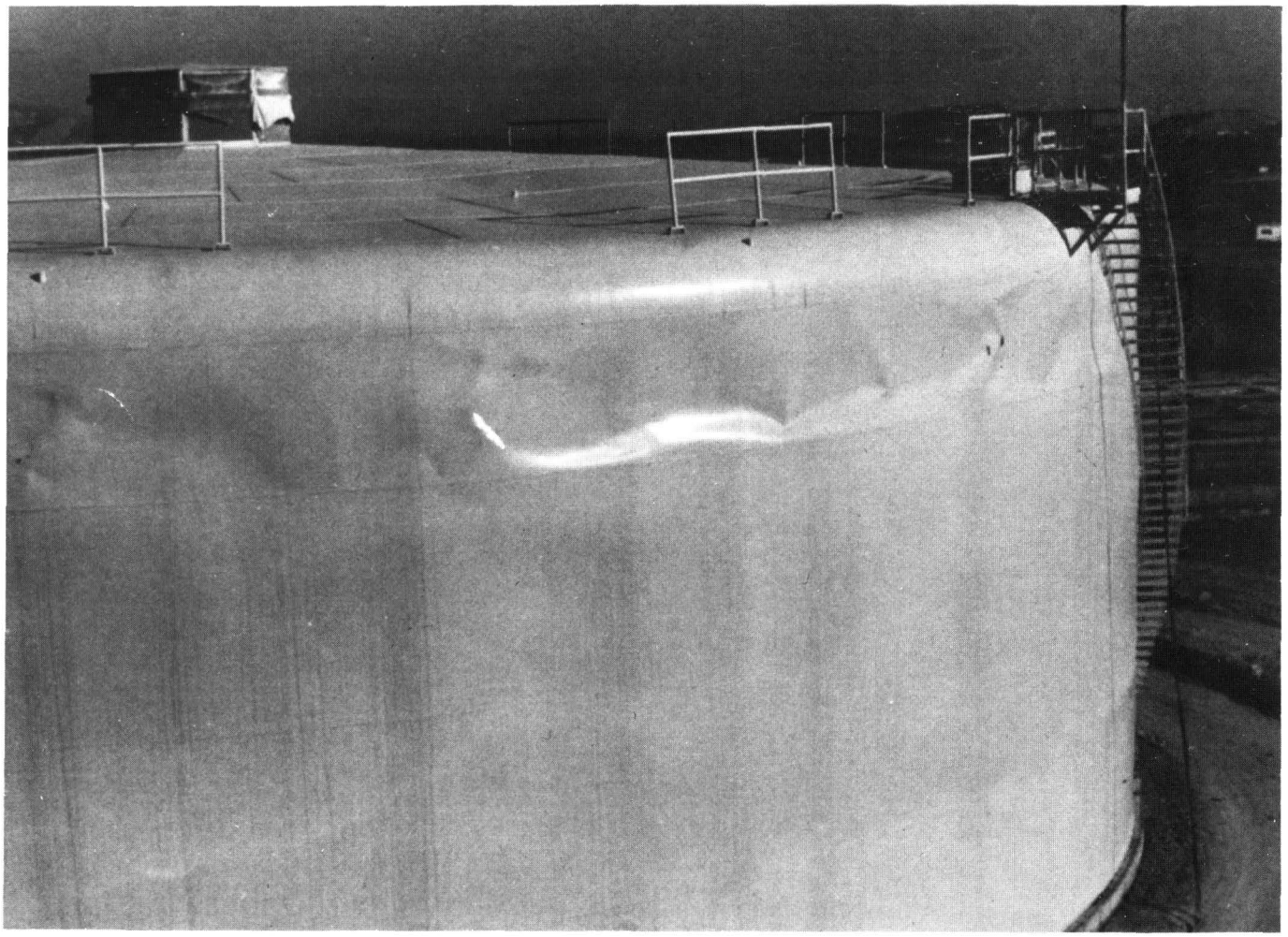

FIGURE 5.—1,750,000 gallon wash water tank, Jensen Filtration Plant. J. F. Meehan, OAC photograph.

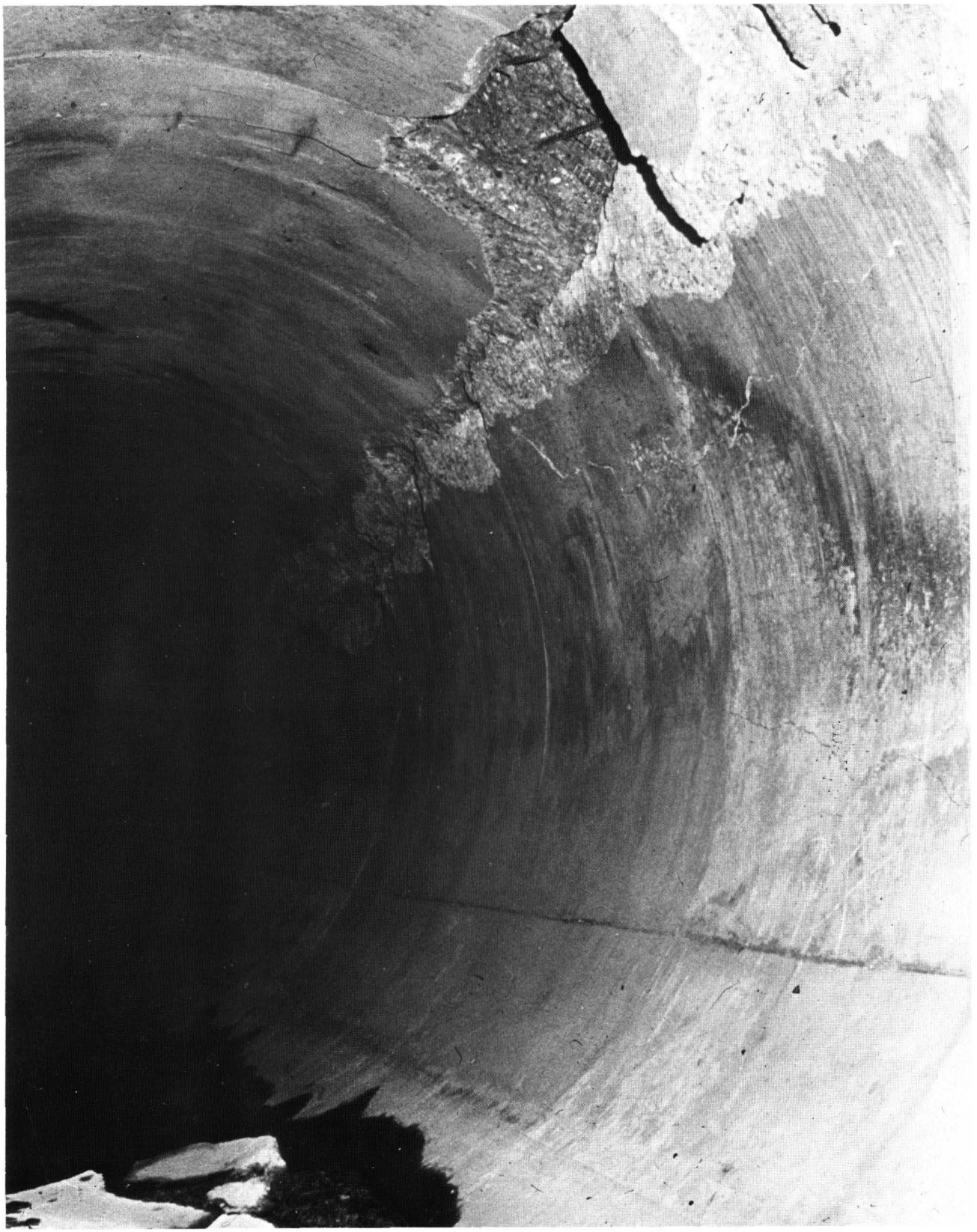

FIGURE 6.—Metropolitan Water District, Balboa Inlet Tunnel. View from inside the tunnel approximately 1600 feet from the south portal showing damage to the tunnel lining. MWD photograph.

FIGURE 7.—Water trunk line break under repair. DWP photograph.

FIGURE 8.—Looking downstream from the berm of Upper San Fernando Dam. Sink hole in foreground. DWP photograph.

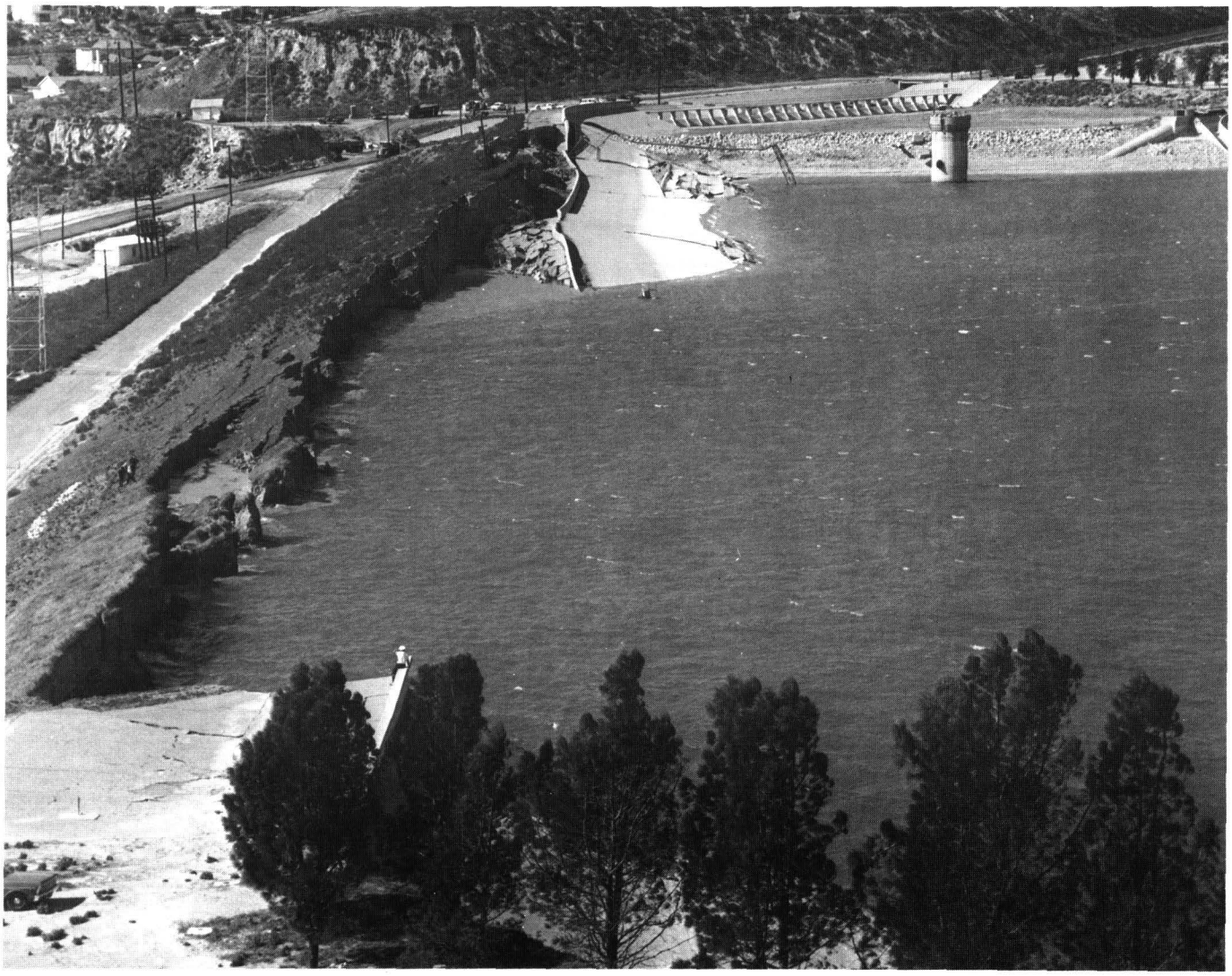

FIGURE 9.—Lower San Fernando Dam. February 9, 1971. DWP photograph by Max Gould.

FIGURE 10.—Lower San Fernando Dam, near east abutment, February 9, 1971. DWP photograph by Max Gould.

FIGURE 11.—Lower San Fernando Dam, lowest point in dam after failure. February 9, 1971. DWP photograph by Max Gould.

FIGURE 12.—Residential water meter exhibiting leakage. DWP photograph by Roy Collins.

DAMAGE TO TRANSPORTATION SYSTEMS

By J. F. MEEHAN

CALIFORNIA OFFICE OF ARCHITECTURE AND CONSTRUCTION

HIGHWAYS AND BRIDGES

Structural damage which resulted from the earthquake of February 9 centered in an area north of San Fernando which includes the Route 5/210 Interchange (fig. 1) and the Route 5/14 Interchange (fig. 2).

Most of the major damage was within the general area of the two interchanges, which are about a mile apart along Route 5.

Five structures must be entirely replaced. Three of these structures totally collapsed during the earthquake. The other two partially collapsed and were so badly shattered as to require the removal of the entire structure (fig. 3).

In addition, at the 5/14 Interchange, two spans of a nine-span bridge collapsed. Also, at the crossing of the Los Angeles Aqueduct and Route 5, a portion of the structure which carries the aqueduct channel under Foothill Boulevard collapsed and must be replaced.

In addition to these structures which will require total or partial replacement, almost all the remaining structures in the general vicinity of the interchanges (possibly including as many as 70 structures) sustained some degree of damage (fig. 4). Many of these structures will require extensive repair.

The total estimated cost of all structure damage resulting from the earthquake is $9.5 million.

The opening of Route 5 through the interchange area will require the construction of one temporary bridge over San Fernando Road and the Southern Pacific tracks to detour Route 5 traffic around the site of the San Fernando Road Overhead, which partially collapsed and must be entirely removed.

A preliminary investigation by our engineering geologists indicates that movement occurred on the Santa Susana thrust fault, which passes through the interchange areas.

In general, the footings at the 5/210 Interchange are on piles in about 40 feet of granular alluvial material which overlays harder material in this area, while the footings at the 5/14 Interchange consist of drilled caissons in rock. According to the geologists, this accounts for the greater movement at the 5/210 Interchange resulting in greater damage to the structures (figs. 5 and 6).

Some of the preliminary recommendations for improved performance in bridge structures during an earthquake that have been proposed by the Bridge Study Team are—

1. Use anchored ties or spirals.
2. Use added ties at tops and bottoms of columns.
3. Use intermediate crossties in large columns.
4. Use 135° hooks on column hoops and crossties.
5. Prohibit splices in reinforcement at maximum moment locations.

It is proposed to anchor columns more effectively into footings by—

1. Putting column bar hooks under the bottom mat.
2. Putting top mat and stirrups in footing slabs.

Numerous slides in the San Gabriel Mountains blocked several highways. Many streets were damaged by water and gas leaking from ruptured pipes. Some were damaged by ground cracks and compression ridges.

RAILROADS

The railroad line adjacent to San Fernando Road was closed by collapse of freeway structures at the intersection of Routes 5 and 210. Rails were also bent just west of the Juvenile facility (fig. 7).

HARBORS

Los Angeles and Long Beach reported that the harbor areas did not suffer any significant damage.

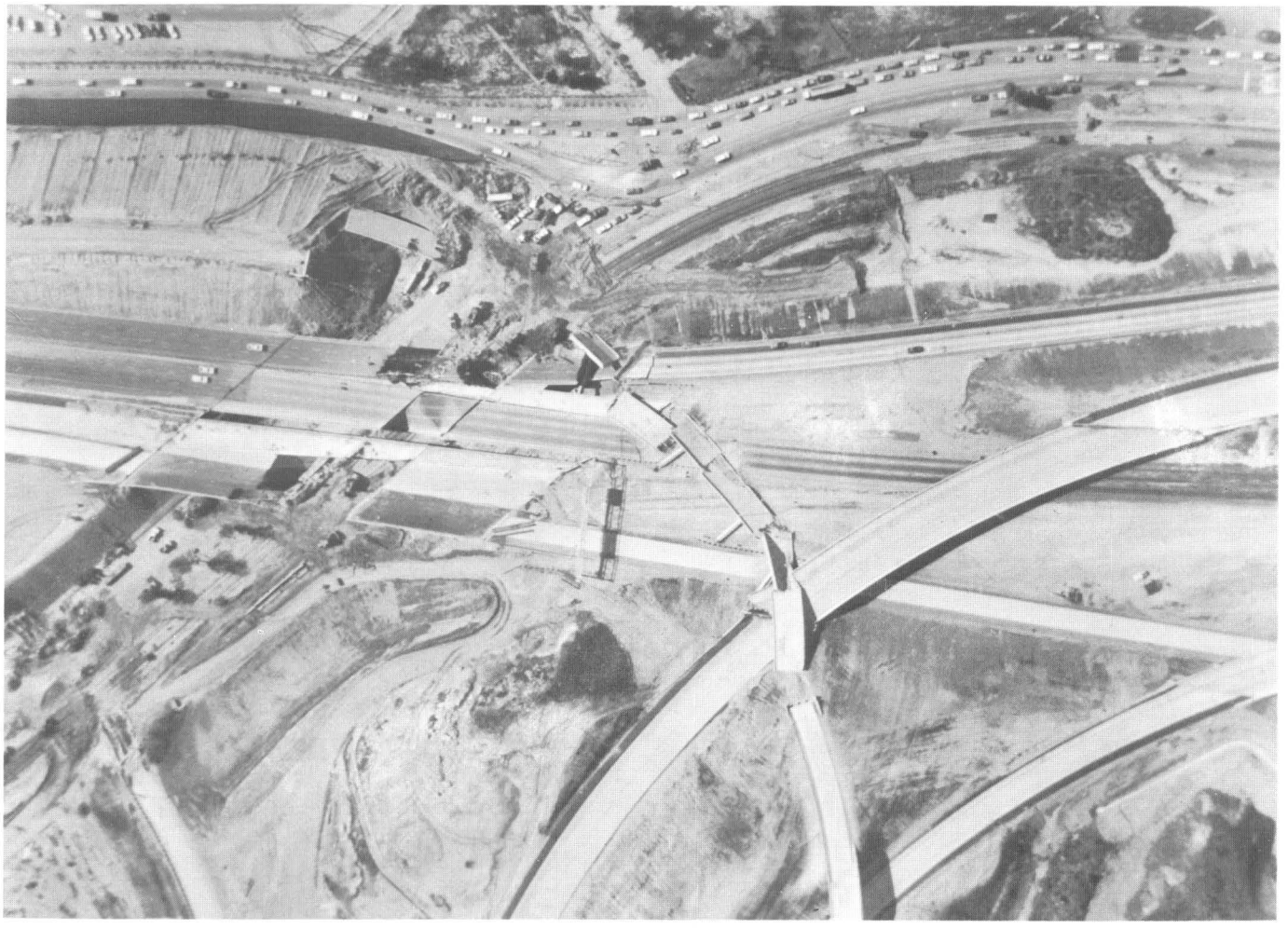

FIGURE 1.—Interchange at Route 5/210. Looking west. Overpass and bridge collapses. California Division of Highways photograph.

FIGURE 2.—Interchange at Routes 5/14. Looking north. Overpasses under construction collapsed. California Division of Highways photograph.

FIGURE 3.—Freeway overpass collapse. At interchange of Routes 5/210. J. F. Meehan, OAC photograph.

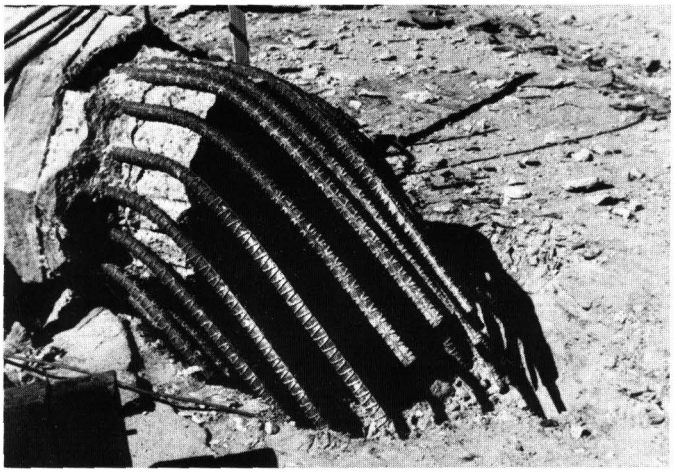

FIGURE 5.—Freeway overpass collapse. Routes 5/210. Column bores pulled from footing. J. F. Meehan, OAC photograph.

FIGURE 4.—Freeway compression, about 27 inches. South of interchange of Routes 5/210. J. F. Meehan, photograph.

FIGURE 6.—Freeway Interchange 5/210. Column movement in soil. J. F. Meehan, OAC photograph.

FIGURE 7.—Railroad west of Juvenile Facility. J. F. Meehan, OAC photograph.

DAMAGE TO ENERGY AND COMMUNICATION SYSTEMS

By D. F. MORAN

CONSULTING STRUCURAL ENGINEER

ELECTRICAL

GENERATING FACILITIES

The Los Angeles Department of Water and Power Valley Steam Plant is located in the San Fernando Valley, about 6 miles south of the epicentral area. There are four steam electric-generating units with four 250-foot-high concrete stacks.

Boilers are hung from and enclosed by braced steel frames. Boilers are anchored laterally to the steel frames. The boilers must expand laterally and downward owing to operating temperatures and pressures. The lateral anchorages between the boiler frame and the supporting steel frame must then allow these movements but resist lateral forces due to earthquakes. Two systems are used in this plant. These are link and sliding type.

The electric-generating units are supported on heavy reinforced-concrete portal-frame-type pedestals which are very rigid to prevent excessive deflections.

The entire plant was designed for lateral forces equivalent to 20 percent of gravity.

The only damage in the plant was a broken lightning rod insulator on one of the large transformers. There were evidences of heavy lateral forces at the bracing connections between the boilers and steel frames. Some of the large piping moved and mashed the insulation at supports. The oil-storage tanks and stacks did not suffer damage. No evidence of damage to the electrical generator has been detected.

A small 50-year-old hydroelectric plant is located just northeast of the Upper Van Norman Reservoir and is powered by the Owens Valley aqueduct. The earthquake caused the aqueduct pipe to fracture at the scroll case of the turbine. This caused severe undermining of the structure. However, structural damage to this old reinforced-concrete structure was only moderate.

TRANSMISSION LINES

There were no reported failures of completed large electrical transmission lines or towers as a result of this earthquake. Ground cracks occurred near some towers in the San Gabriel Mountains. Two towers under construction were reported to have fallen.

TERMINALS

Sylmar Converter Station

There was extensive damage to this station where the 800,000 volt d.c. line from the Pacific Northwest terminates. The loss of the Pacific Intertie, which was dedicated in September 1970, means power from the Northwest—around 525,000 kilowatts—will not be available this summer when peak demands for power occur. However, power from steamplants in the area is sufficient to meet the present electrical demands, while other sources of power to help meet the peak summer load are now being obtained by negotiation.

Damage to this plant was in excess of $28 million and involves mainly electrical equipment and underground conduit. Evidences of severe ground movement in this area exist. There are many cracks and separations of concrete walls in the yard area.

The building has a steel frame with metal deck roof and walls. A partial basement occurs under the service area. A structural separation divides the valve bay to the north from the service area to the south. This separation stops at the first floor, where the separate steel columns above rest on common-reinforced-concrete columns.

The steel frames have vertical "X" bracing to resist earthquake forces. The steel frame and bracing performed well.

Damage occurred in the basement in the vicinity of the separation joint.

Two large, 50-foot-high steel-framed radio-shielded areas adjoin the main building on the east and west sides. These frames are covered with wire mesh and have horizontal and vertical steel "X" bracing. Loading of these frames is small, consisting of conductors and insulators.

Numerous braces were buckled and stretched or broken. Many columns are bent and some lean. Ground cracks occur in these areas, and there is evidence of stretching of the ground. There may also be some differential vertical movements. It is estimated that these structures could resist more than 50 percent gravity owing to their light weight and wind-design loads. It is felt that the majority of this damage is due to ground lurching and settlement in these areas.

Severe damage to electrical equipment occurred in the valve bays.

Outdoor electrical equipment was heavily damaged. Most of this equipment was supported on insulators which failed during the earthquake (fig. 1). Some heavy pieces of equipment overturned owing to failure of their anchorage to foundation pads (fig. 2). Extensive damage was caused by swinging of heavy conductors which broke supporting insulators.

Anchorages of very large (200 ton) transformers performed well.

Olive Switching Station

This station is located about 1 mile southeast of the converter station. Severe damage was suffered by the electrical equipment in this yard (fig. 3).

Insulator-supported equipment collapsed and several large transformers fell over.

The Vincent Intertie Station

The Vincent Intertie Station has some equipment similar to the Sylmar Converter Station but suffered only minor damage.

Distributing Stations

Two modern distributing stations in the Sylmar-Granada Hills area suffered damage to the cantilevered walls surrounding the plants, but electrical equipment performed well.

One distributing station in Sylmar has 20-foot reinforced-concrete-block cantilever walls. These walls were designed for 20 percent gravity. Vertical concrete-block pilasters supported on drilled concrete piles support these walls. The performance of these walls was good considering the probable severity of ground motion. Many of the pilasters were cracked and spalled near their bases, and walls were leaning both in and out 1 to 2 feet at the top. However, none collapsed.

Another station in Granada Hills had precast-concrete cantilevered walls supported by vertical steel beams. These were designed for 20 percent of gravity. Many of the steel columns were bent, and some ruptured in the webs. Concrete-panel-to-steel-column connections failed in some cases, but no panels fell down.

Several old distributing stations in downtown Los Angeles suffered cracks in their unreinforced brick walls.

Distribution Systems

Many pole transformers were thrown down in the Sylmar area. Insulators and crossarms were broken, and wires and poles were knocked down. Cables sheared off in underground ducts.

By Friday, February 12, all feeders were restored, downed transformers were replaced, and all power to customers was back in service.

Careful studies must be made of the performance of electrical equipment. Designs must be developed by structural engineers working together. Full-scale tests of some equipment under simulated earthquake loading would be desirable.

GAS

The Southern California Gas Co. reports that, in general, the distribution piping system withstood the stresses of the earthquake remarkably well. This is borne out by the fact that in many areas where buildings obtained appreciable damage, the system remained intact.

The major transmission lines from out-of-State, 30 inches in diameter or more, did not suffer any apparent damage. Service to the great majority of the company's 3.1 million customers was little affected.

The only area where the distribution piping system was seriously damaged occurred within a 11- to 12-square-mile area in the northeast section of San Fernando Valley, including Sylmar and the city of San Fernando. This region suffered widespread damage to all types of buildings and underground structures, as well as utility services. The somewhat diagonal area is bounded by the Golden State Freeway on the west, the Pacoima Wash on the south, and the San Gabriel Mountains on the north.

The transmission system handling the deliveries of California gas from the San Joaquin Valley to the Los Angeles basin was damaged to the extent that four lines had to be shut down in the San Fernando area. Damage to the four lines, which range from 12 to 26 inches in diameter, occurred between Newhall and San Fernando and resulted in the loss of supply to the distribution system in the Sylmar-San Fernando area.

The distribution system in this hard-hit area consists principally of a network of 2-, 3-, and 4-inch welded steel mains serving approximately 17,000 customers. The violent earth movement there pulled, compressed, and twisted the piping system, resulting in broken mains, valves, and service risers. Approximately 450 breaks have been discovered.

There were two or three gas fires within streets at broken lines. We are not aware of any specific damage to buildings due to fires associated with gas.

In general, all utility facilities were out of service in the critical San Fernando area—gas, electric, water, telephone, and sewer.

Damage to the remainder of the company's distribution system was confined to isolated fractures or pipe separations that did not result in serious impairment of service to customers.

Repairs to the damaged gas mains in San Fernando area were commenced almost immediately after the earthquake. Gas service to customers was restored commencing Sunday, February 14, and completed for the most part by Saturday, February 20th.

TELEPHONE SYSTEMS

The General Telephone Co. reports that all the telephone equipment in the Sylmar central office was totally destroyed by the earthquake. Damage to the building and equipment is estimated at $4.5 million. The 9,500 customers in Sylmar were completely without telephone service.

Around-the-clock work began at once to rebuild the central office. On February 27, just 18 days after the earthquake enough equipment was installed to place more than 1,000 Sylmar customers back in service.

Attention must be given to the anchorage and bracing of critical telephone equipment.

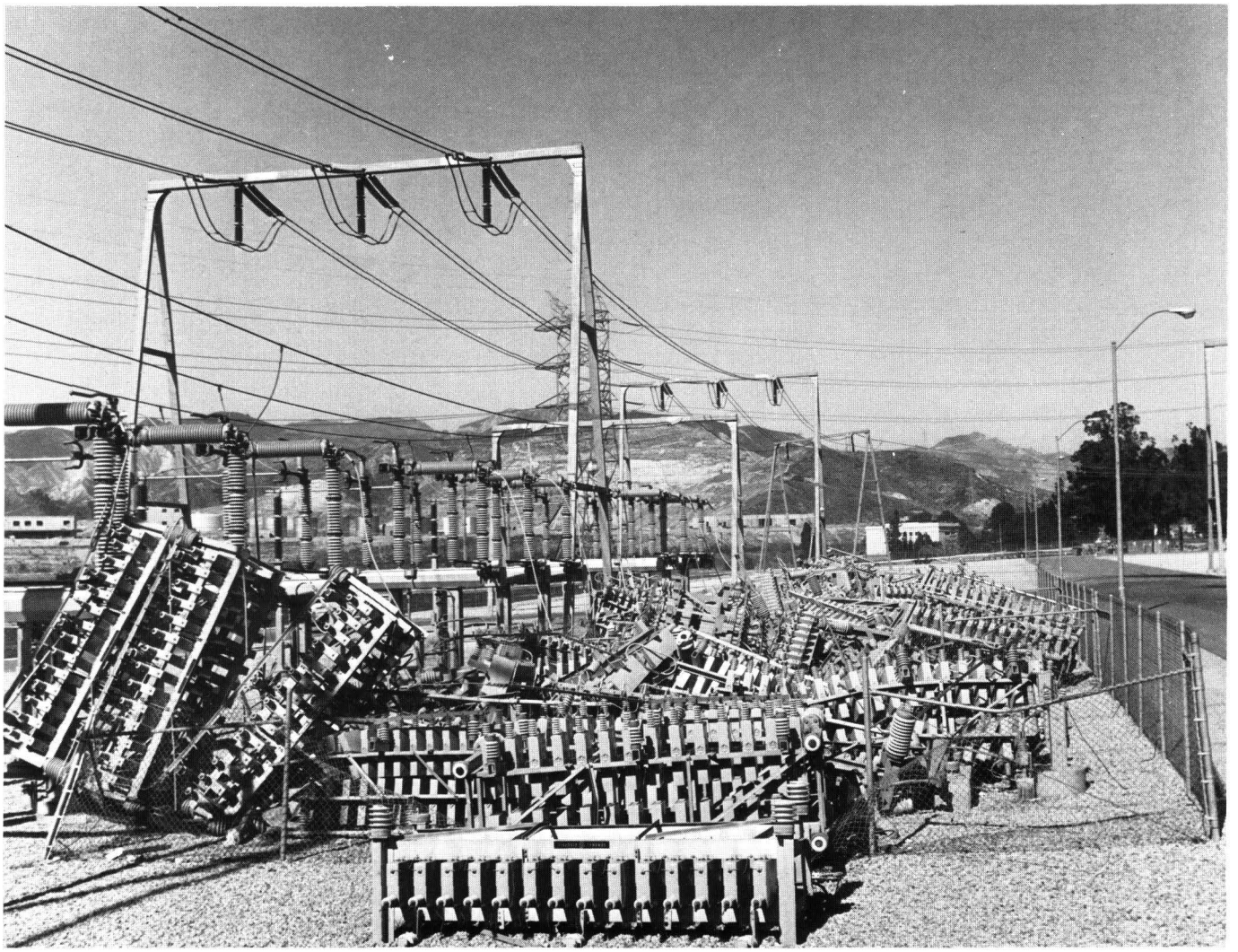

FIGURE 1.—Sylmar Converter Station collapsed condenser banks. DWP photograph.

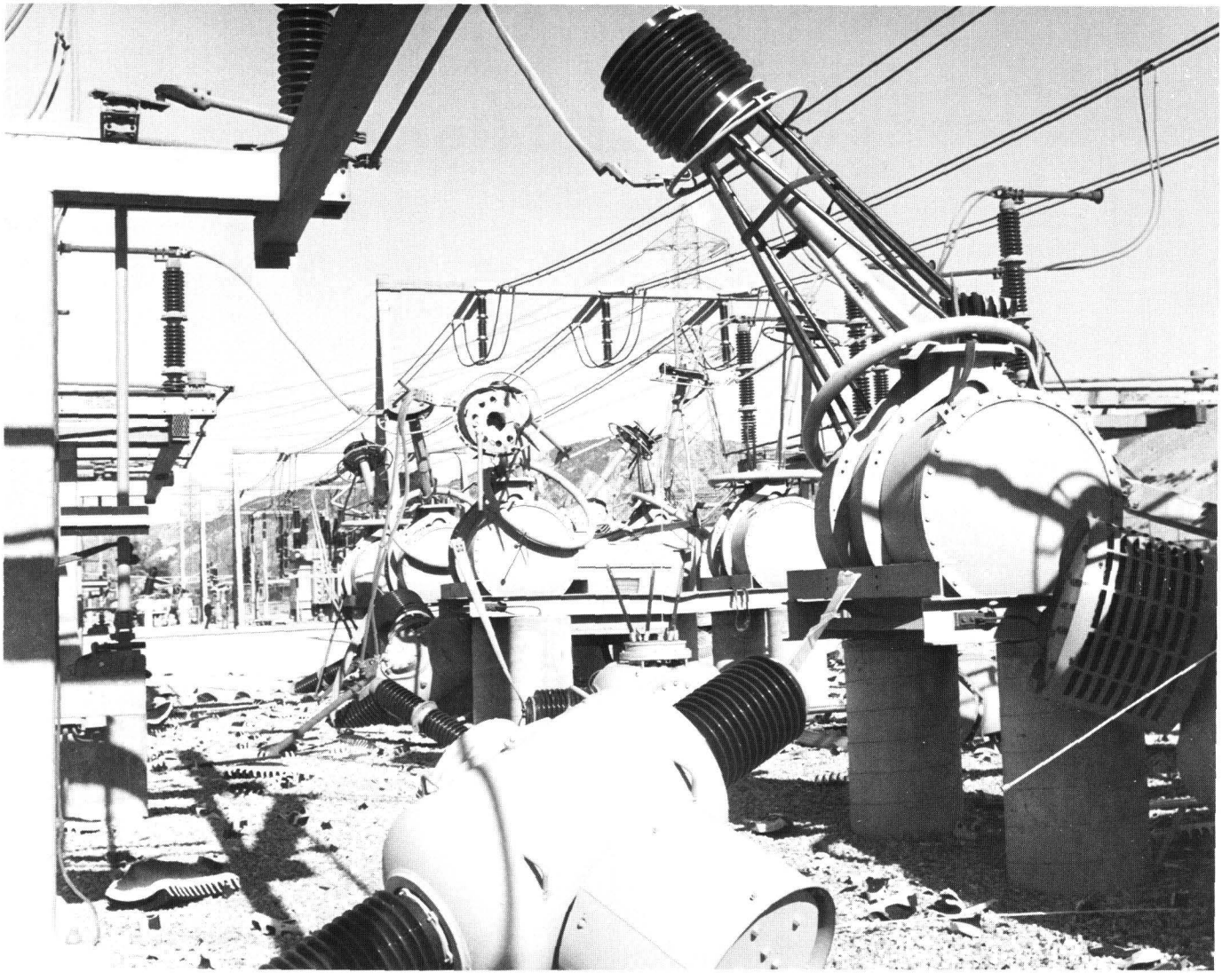

FIGURE 2.—Sylmar Converter Station air switches. DWP photograph.

FIGURE 3.—Olive Switching Station overturned transformers. DWP photograph

SOCIOLOGICAL ASPECTS OF THE EARTHQUAKE

By EARTHQUAKE ENGINEERING RESEARCH INSTITUTE COMMITTEE

In general, emergency measures worked well in this earthquake. Many fires were started but were quickly extinguished by the fire departments. Some fires in streets due to ruptured gaslines burned for some time.

Efficient action by the police department, aided by television and radio announcements, resulted in the orderly evacuation of some 80,000 persons below the threatened Lower Van Norman Dam. Police then patroled the vacated area to prevent looting.

Emergency actions to rescue persons trapped in the collapse at the Veterans Hospital in Sylmar were initiated shortly after the shock, following a delay due to communication difficulties. The U.S. Corps of Engineers provided heavy equipment and fire departments were on the scene.

Prison labor helped in the rescue effort, which went on for some 100 hours. Many persons were trapped between collapsed concrete floor slabs which were stacked directly on top of each other. The rescue work was slow and painstaking for this reason.

Traffic lanes on the damaged freeway systems were opened to thru traffic within a few days. Numerous pavement cracks and settled abutment fills at bridges had to be filled in with asphalt, and bypasses were built around the overpass collapse areas.

Emergency evacuation of patients from the four damaged hospitals in the area was orderly. Patients were carried down stairways because elevators were inoperative.

About 80 inmates of the Los Angeles County Juvenile facility in Sylmar escaped when a part of a wall collapsed. All inmates were later evacuated from this heavily damaged facility.

Many areas were without power, water, gas, and telephone service for several days after the earthquake. Restoration of these utilities is a slow and expensive process, particularly when facilities are underground. In the city of San Fernando, a temporary water system was installed above grade.

Red Cross and Salvation Army units were effective in mass care actions.

In all cases, repair crews are working around the clock to restore services.

A severe water shortage was alleviated somewhat by providing large tanker trucks in shopping-center parking lots. Some grocery stores which suffered heavy damage held food sales in their parking lots.

All residents were requested to turn off their gas supply to prevent leakage and possible explosion.

Severe damage to telephone-exchange equipmnt will result in impaired service in the heavily hit area for several months.

Total damage to sewer and storm-drain facilities is not known at this time.

The local building departments quickly sent inspection teams into the field to check structures for safe occupancy. Numerous structures were posted as unsafe after a cursory examination disclosed some damage. Later, crews were sent around to make more complete checks and specify to the owners what the extent of damage actually was.

Repair of damage is proceeding rapidly, particularly in commercial and industrial construction. In one case it was observed that an occupant of an industrial building had erected a temporary wood wall to replace a collapsed wall and was proceeding with "business as usual," although his structure was posted as "unsafe" by the Building Department.

The loss of life associated with this earthquake is 63. Nine of these deaths were as a result of heart attacks, and 45 died as a result of the collapse at the Veterans Hospital. One person was killed in the collapse at the Olive View Hospital. One person died owing to partial collapse of the old Midnight Mission in downtown Los Angeles. Two persons were killed in a truck under a freeway overpass collapse.

Over 1,000 persons were injured; many by broken glass.

It should be pointed out that the loss of life and injuries would have been much greater had the shock occurred even 1 hour later, when many persons would have been traveling to work on crowded freeways and would have been occupying areas of buildings which collapsed.

Total restoration costs have been estimated at $1 billion. About one-half of this is for public and the other for private damage. The U.S. Corps of Engineers is proceeding with restoration work in the city of San Fernando and other areas. They will be rebuilding public facilities, as requested, to fully conform to current codes.

The amount of loss covered by insurance is small, probably less than $50 million with very little of this on dwellings.

Many dwellings are total losses, and this is a serious blow to the owner who already has a large mortgage and must borrow more money to rebuild. Some owners have abandoned their heavily damaged homes.

The overall effect of this earthquake on employment is not known at this time. Certainly it will provide many jobs in the construction industry, but some manufacturing and service jobs may be curtailed during the rebuilding program.

Severe psychological traumas to individuals have been reported.

PRELIMINARY CONCLUSIONS AND RECOMMENDATIONS BASED ON ENGINEERING STUDIES

By EARTHQUAKE ENGINEERING RESEARCH INSTITUTE COMMITTEE

The committee has arrived at the following preliminary conclusions and recommendations:

1. The hazard of non-earthquake-resistive construction was reemphasized. Old structures, particularly unreinforced masonry bearing wall type with weak mortar, performed poorly. Collapse of non-earthquake-resistive skeleton concrete frame buildings with unreinforced hollow tile walls at the Veterans Hospital resulted in the greatest single loss of life.

2. Modern high-rise construction survived this shock well. However, most were not fully tested owing to their distance from the epicenter. We must learn as much as possible from correlation of strong-motion records with design criteria.

3. Surprisingly large ground motions were recorded. They exceeded, at some places, the El Centro and Taft records which have guided earthquake-resistive design for 30 years. The high vertical accelerations recorded on instruments and reported by witnesses probably contributed to increased damage to structures.

4. Reassessment of some design criteria and methods are indicated for bridges, overpasses, buildings, and earth dams containing hydraulic fills. Particular attention should be focused on the poor behavior of many one-story industrial and commercial structures, since they comprise the majority of construction, other than residences. Plywood diaphragms must be studied and tested. Reinforcing and joinery details must be improved.

5. Desirability of designing important buildings for differential foundation movements must be considered. Also, overall increased seismic safety of important structures such as hospitals, utilities, and those housing emergency operations must be examined.

6. Greater caution is required relative to building in the zones of larger faults, and effort is required to map the fault locations better and to understand their degree of activity. Ground movements such as lurching, settling, cracking, and compression in many areas undoubtedly contributed significantly to damage to structures in these areas.

7. Confidence increased in California public-school design criteria and methods. However, non-earthquake-resistive school buildings performed poorly.

8. This is the most important earthquake in history from the standpoint of instrumental data and real testing of earthquake-resistive construction.

9. Modern one-story wood-frame and stucco dwellings performed reasonably well considering the high ground accelerations and movements. However, reconsideration of code provisions and enforcement is indicated, particularly for two-story construction and masonry chimneys.

10. New efforts are needed to safeguard important electrical, mechanical, and communication equipment. New design criteria and methods must be developed.

11. Greater attention to the hazard of broken glass is needed.

12. Disaster-relief activities were effective but should be improved relative to organization and communication.

13. The Earthquake Engineering Research Institute is convinced that this important earthquake must be the subject of a major investigation and report.

COOPERATING ORGANIZATIONS

American Society of Civil Engineers—Los Angeles Section
California Department of Aeronautics
California Department of Navigation and Ocean Development
California Department of Water Resources
California Division of Highways
California Division of Mines and Geology
California Institute of Technology
General Telephone Company
International Conference of Building Officials
Lamont-Doherty Geological Observatory of Columbia University
Long Beach Harbor Department
Los Angeles City Building Department
Los Angeles City Engineer
Los Angeles City Fire Department
Los Angeles City Police Department
Los Angeles County Engineers Office
Los Angeles County Flood Control District
Los Angeles County Road Department
Los Angeles Department of Airports
Los Angeles Department of Water and Power
Los Angeles Harbor Department
Metropolitan Water District of Southern California
Pacific Telephone Company
Southern California Edison Company
Southern California Gas Company
Southern Pacific Railroad
Structural Engineers Association of California
U.S. Army Corps of Engineers
U.S. Atomic Energy Commission
U.S. Bureau of Public Roads
U.S. Office of Emergency Preparedness
University of California, Los Angeles, Berkeley, and Davis

☆ U. S. GOVERNMENT PRINTING OFFICE : 1971 O - 420-813

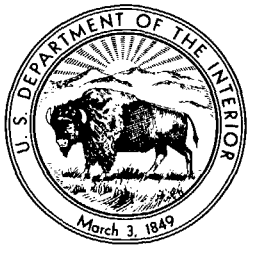
U.S. DEPARTMENT OF THE INTERIOR
March 3, 1849


DEPARTMENT OF COMMERCE
UNITED STATES OF AMERICA